"Macrocycles, macrobicycles: a study"

Thesis

"MACROCYCLES, MACROBICYCLES: A STUDY"

A Thesis Submitted for the Degree
of
Doctor of Philosophy
by
Deborah Jane Marrs, B.Sc

Faculty of Science
The Open University, Milton Keynes

April 1990

Date of submission: 23 March 1990

Date of award: 30 April 1990

To my parents -
thank you.

DECLARATION

The work described in this thesis was carried out in the Department of Chemistry, The Queen's University of Belfast on behalf of the Open University, Milton Keynes, between October 1986 and September 1989. The work has not been submitted for any other degree and is the original work of the author, except where acknowledged by reference.

D.J. Marrs
April 1990

ACKNOWLEDGEMENTS

I would like to thank my supervisor Dr. Jane Nelson for her encouragement and inspiration over the last 3 years. Her constant interest and enthusiasm has brought the area of macrocyclic chemistry to life for me, making the last 3 years a pleasurable and stimulating experience. And who could have asked for a better and more supportive co-supervisor than Dr. Charlie Harding. His low temperature esr spectra are greatly appreciated (his jokes about helium time bombs less so!) as is his ability to mend the fibres for the Faraday balance!

I am indebted to many people who made more out of the compounds than I could have hoped for. Firstly I would like to thank Dr. Vickie McKee for the X-ray analyses and to Dr. Mike Drew for X-ray analyses and modelling studies. The S.E.R.C mass spec. service provided the F.A.B spectra and the S.E.R.C Highfield nmr service at Edinburgh (I. Sadler) and at Warick (O. Howarth) provided many of the nmr spectra shown in the thesis. My thanks are due to the Queen's University of Belfast for use of facilities in the Department of Chemistry where this research was carried out. In particular I would like to thank Dr. J. Hamilton and Dr. B. Hamilton for 90MHz nmr spectra, Dr. P. Stevenson for 500MHz spectrum and members of staff who gave advice and encouragement along the way. I would also like to thank the analytical services for elemental analyses.

The award of Higher Degrees matched studentship by the Open University, Milton Keynes and Du Pont is gratefully acknowledged.

To my friends at Queen's, the "alternative tea club" members, a word of thanks. The "crack" has been great and will be sorely missed as we all go our separate ways - Good Luck to you all.

A special mention must go to my family. Mum and Dad - I will always give thanks for your love, support and example over the years but especially over the last few months - I therefore dedicate this work to you. Judy and Brendan - my thanks just for being there when I needed you.

Rachel - you're a gem. My scribbled notes actually made it to this stage with your help - thanks. Thanks also to mum^2 - over 600 references later and we are still speaking.

Finally, to David - thankyou for your patience, encouragement and hard work.

I never notice
what has been done,
I only see what
remains to be done.

Madame Curie.

CONTENTS

SUMMARY

A template directed [2+2] Schiff base condensation of 2,6-diformyl pyridine and 1,3 diaminopropane afforded the 20 membered N_6 macrocycle "WT". The X-ray structure of the barium templated WT has been determined (M.G.B. Drew, at the University of Reading). Complexes of first transition series ions, obtained by transmetallation, have been characterized using electronic, infrared and esr spectroscopy. Results indicate that WT provides a cavity suitable for single atom bridged binuclear assemblies.

The Schiff-base strategy was further used to yield macrobicyclic cyclophanes from the [2+3] condensation of tris(amino ethyl) amine ie tren, with a series of aromatic dicarbonyls. X-ray structures and 'Hnmr studies show that these macrobicycles have very different conformations in their complexed and uncomplexed forms.

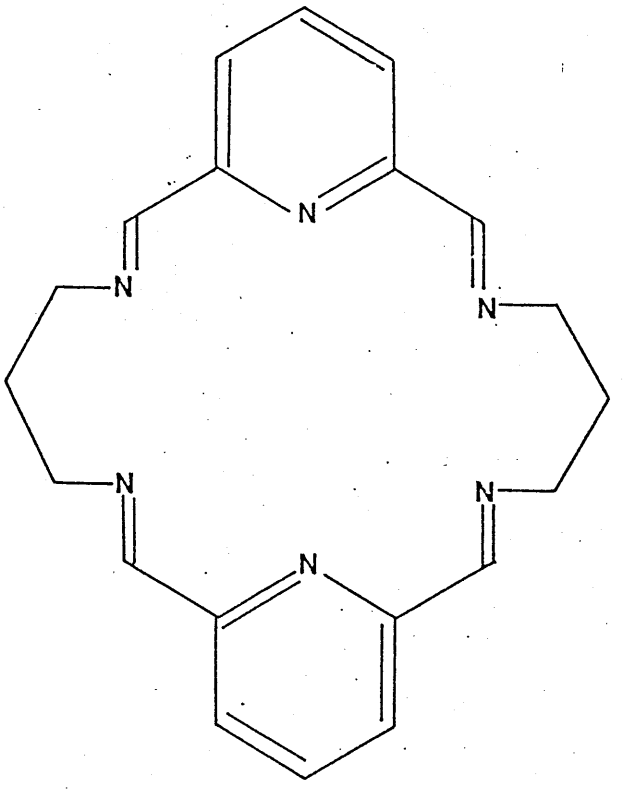

LIGAND WT

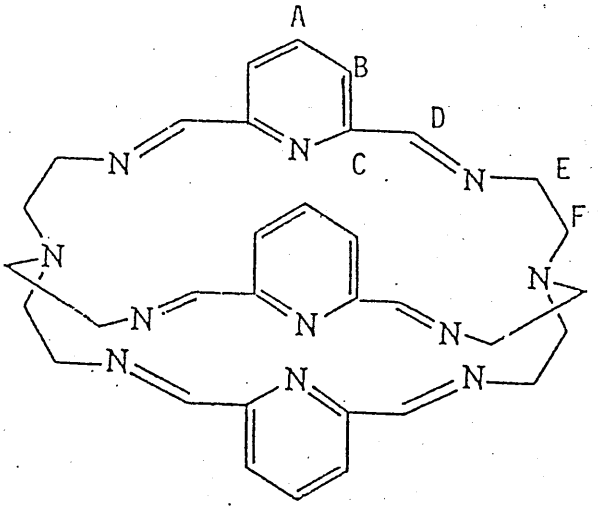

LIGAND 3P

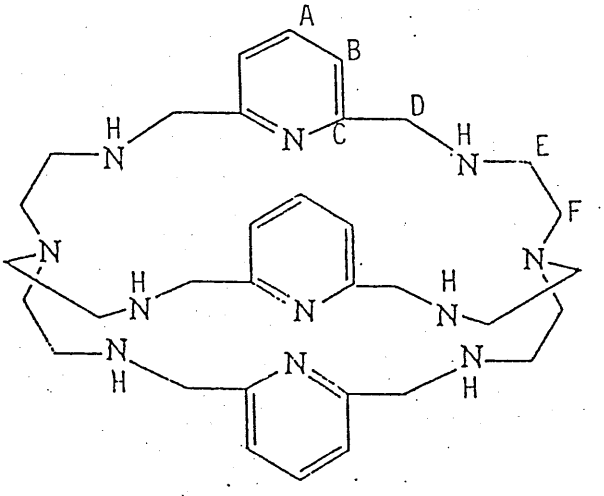

LIGAND R3P

INTRODUCTION

The work described in this thesis is in two separate but related sections - a macrocyclic study and a macrobicyclic study.

The macrocyclic study involved the Schiff base ligand "WT". Binuclear complexes of this ligand were prepared and the mode of bridging, and hence the magnetic properties of the single atom azide, thiocyanate and hydroxide bridging group investigated to determine which group mediated the strongest interaction. Intermolecular interactions complicated the magnetic behaviour of some of the macrocyclic complexes and prompted the move to macrobicyclic systems. Thus the N_{11} polyaza macrobicyclic ligand 3P was prepared in an attempt to find a ligand that would offer increased steric protection to the binuclear bridged assembly thus allowing a better environment for magnetic interaction.

The success of the synthesis of both templated and uncomplexed forms of 3P prompted us to try the condensation of tren with other dicarbonyl groups. These included terephthalaldehyde, isophthalaldehyde, 2,5 diformyl furan and 2,5 diformyl thiophene, which gave 3Bp, 3Bm, 3F and 3S respectively. All could be formed in both complexed and uncomplexed form except for 3S which could not be formed as the metal free derivative.

All the ligands were successfully reduced (using sodium borohydride) to their octaamine derivatives R3P, R3Bp, R3Bm, R3F, and R3S.

Many of the above ligands show fluxional behaviour in their ^{1}Hnmr spectra, and discussion of the macrobicyclic ligand series is centered on this aspect of the study. Several bridged structures have been prepared and one magnetic study is reported.

Ligand 3P gave an interesting, if irreproducible - pendant armed species, 2P, in its reaction with silver.

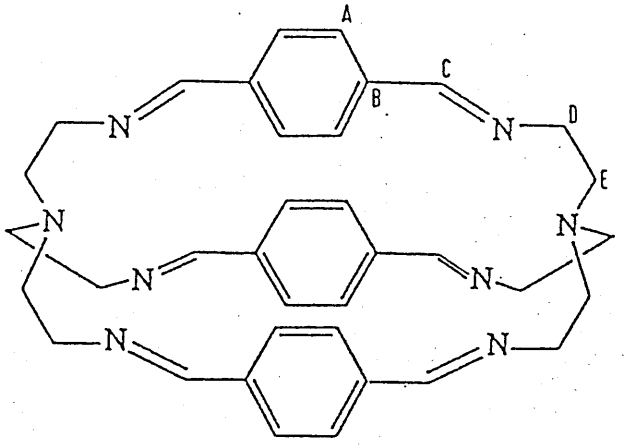

LIGAND 3Bp

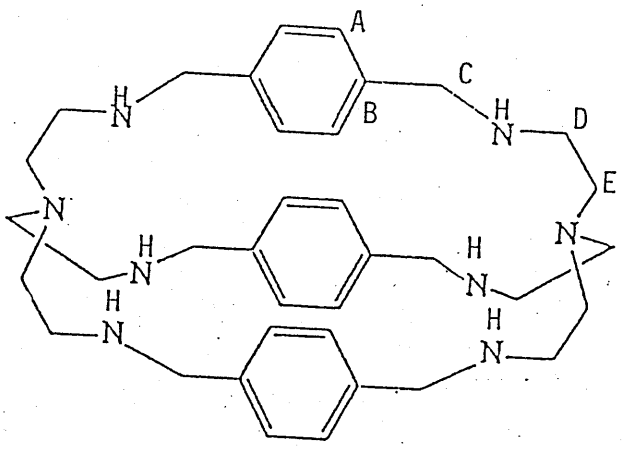

LIGAND R3Bp

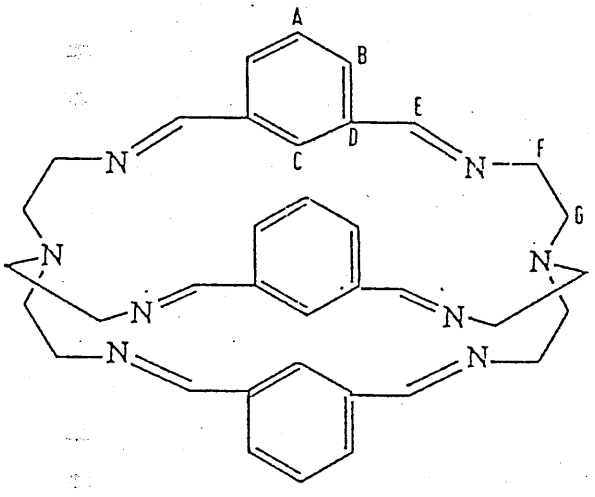

LIGAND 3Bm

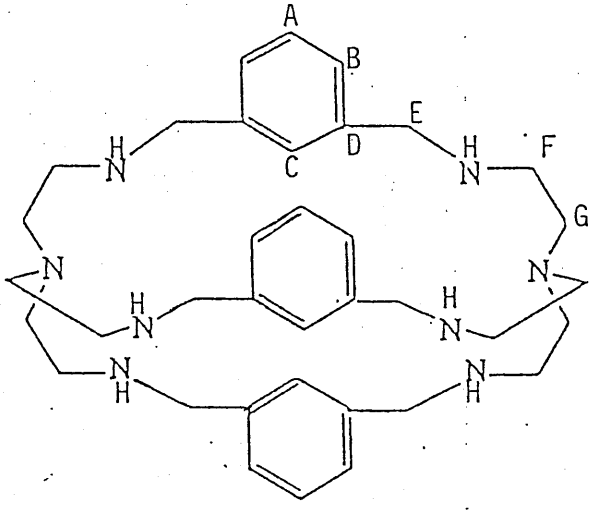

LIGAND R3Bm

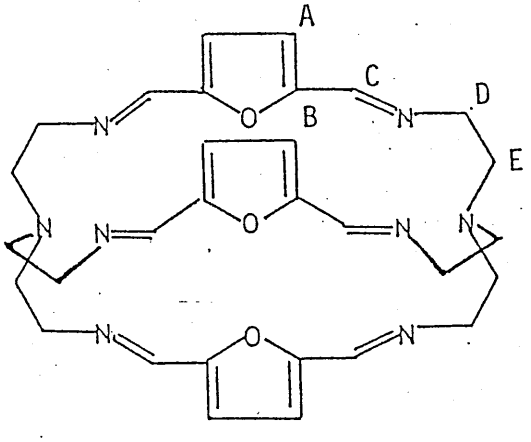

LIGAND 3F

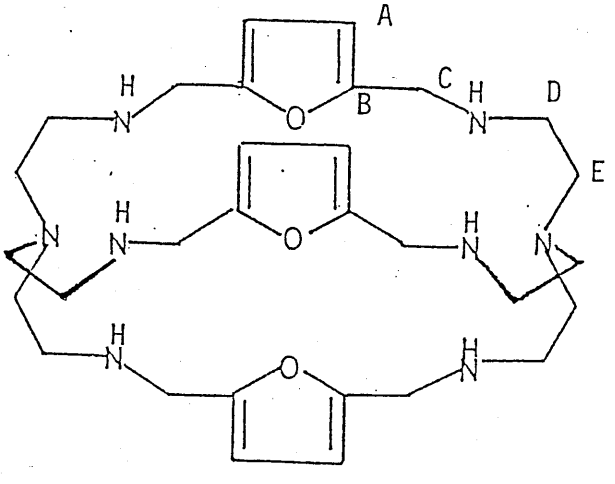

LIGAND R3F

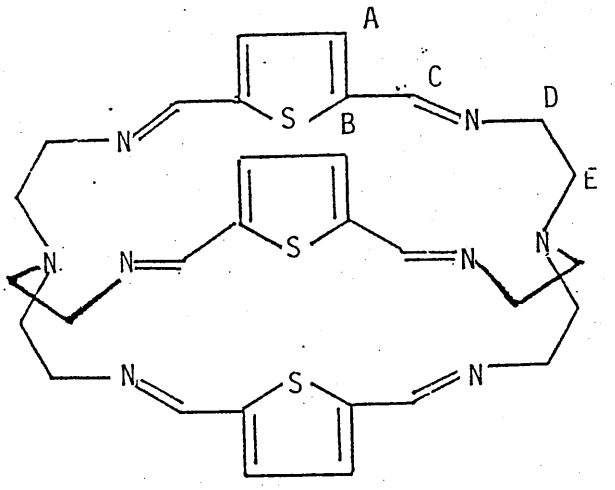

LIGAND 3S

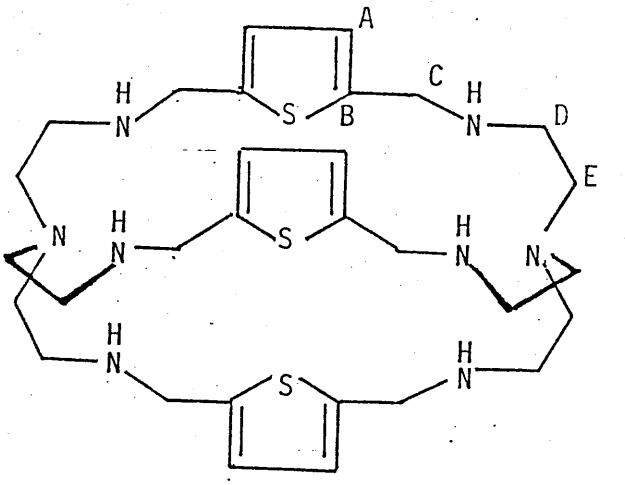

LIGAND R3S

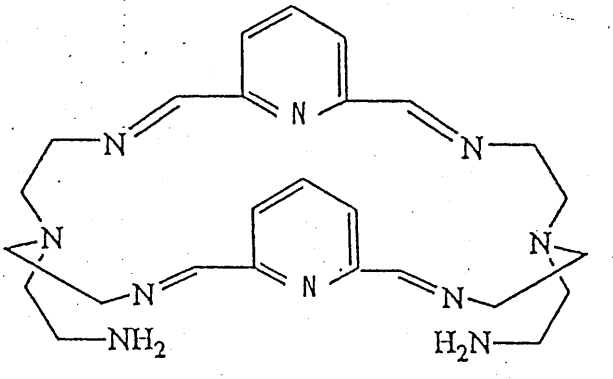

LIGAND 2P.

The work described in Chapter 2 (experimental), Chapter 3 (macrocyclic discussion) and Chapter 4 (macrobicyclic discussion) is preceeded in Chapter 1 by a review of literature covering particularly the area of transition metal molecular hosts. Four appendicies cover the areas of electronic absorption spectroscopy, electron spin resonance, magnetism and spin relaxation effects.

CHAPTER 1

REVIEW

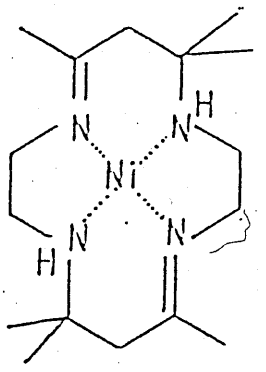

FIG.1-1

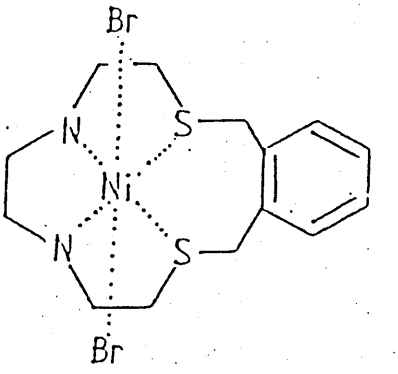

FIG.1-2

FIGURE 1. EARLY MACROCYCLIC LIGANDS.

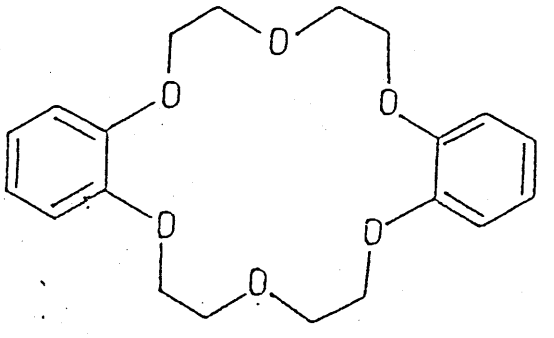

CROWN ETHER

FIG.2-1

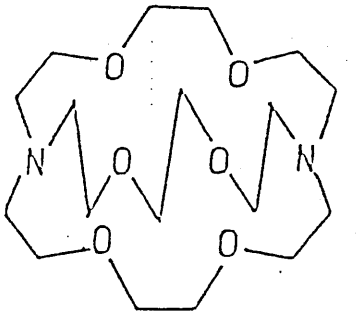

MACROCYCLE

FIG.2-2

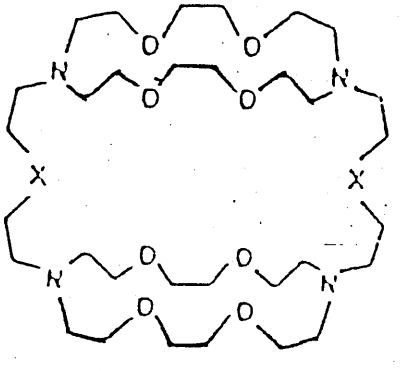

MACROTRICYCLE

FIG.2-3

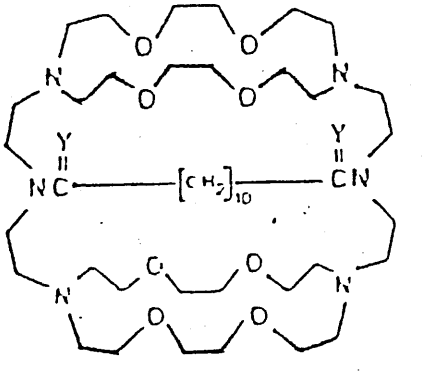

MACROTETRACYCLE

FIG.2-4

FIGURE 2.

MACROCYCLES and CRYPTANDS - a brief history.

Over the last 25 years the chemistry of macrocyclic coordination compounds has grown rapidly and the literature output of this area has developed from the few scattered reports prior to 1960[1-5] to the current situation, where there are many sub-divisions within this class of molecule. A major reason for the recent interest has been the realization that metal ions encapsulated in macrocycles could have novel and potentially useful properties. Also many important natural products are cyclic or cavity based. There is the possibility of commercial use for macrocyclic complexes as dyes, optical and electrical materials and catalysts.

The earliest relevant studies on coordination compounds of the synthetic macrocycles emerged from New Zealand by Curtis in 1960[6] (Fig.1-1) although it was Thompson and Busch in 1964[7] who achieved the first deliberate synthesis of a new macrocyclic ligand (Fig.1-2).

In 1967 Pederson[8] introduced a new class of macrocycle of which Fig.2-1 is a typical example. These cyclic polyethers became known as "Crown" ethers because with them "cations could be crowned and uncrowned without physical damage to either, just as the heads of royalty." Their capacity to form stable complexes with the transition metals was limited[9] but this was compensated for by their interesting ability to form isolable crystalline complexes of the alkali and alkaline earth metal ions[8] and also by their ability to encapsulate small non metallic molecules or ions [8]. The importance of these compounds is acknowledged but will not be discussed further except where relevant to the area under consideration.

Lehn et al.[10] made a major advance in synthesizing the cryptands. These macrocyclic ligands represent an extension of the crown ether synthesis into the third dimension by utilizing tripod bridgehead nitrogens joined via polyether strands (Fig.2-2). Such ligands can totally encapsulate a metal ion that fits into its 3-dimensional cavity and in doing so forms an inclusion complex or cryptate. Lehn has extended the macrobicyclic ligand

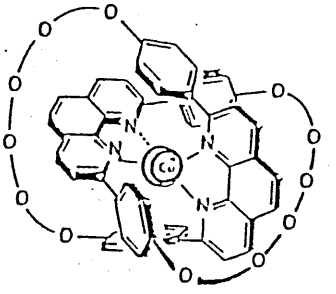

CATENATE

FIG.3-1

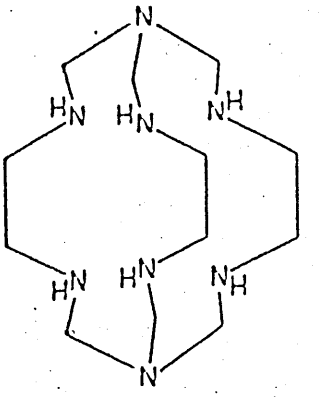

SEPULCHRATE

FIG.3-2

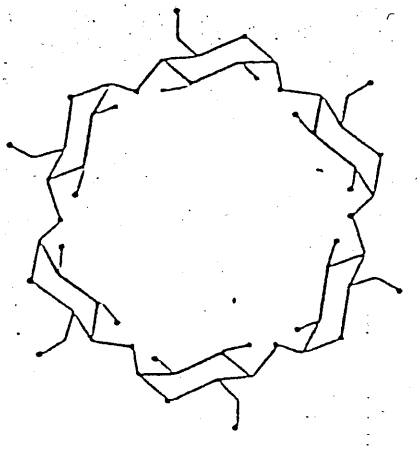

CYCLODEXTRIN

FIG.3-3

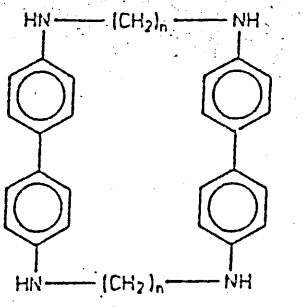

(n = 2, 3, 4)

CYCLOPHANE

FIG.3-4

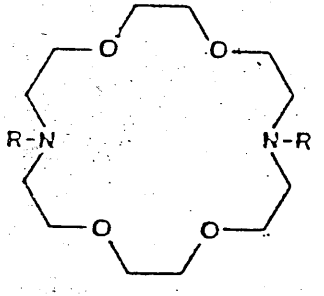

(2,2)

FIG.4-1

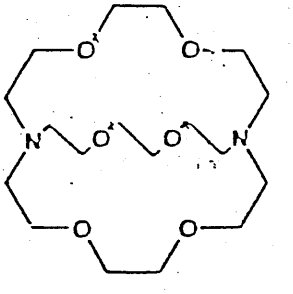

(2,2,2)

FIG.4-2

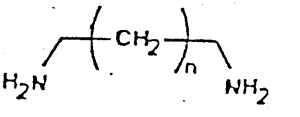

FIG.4-3

LOG Ks

	(2,2)	(2,2,2)	Δlog Ks
K^+	2.0	10.8	8.4
Ba^{2+}	5.9	12.9	7.0
Ag^+	10.0	12.2	2.2

FIGURE 4.

series to include purpose built macrotricycles and macrotetracycles[11,12] (eg.Fig.2-3,2-4)

From these beginnings the areas of bridged supramolecules, catenates, sepulchrates, cyclodextrins, cyclophanes, to name but a few classes have developed. Fig.3. Apart from the chemical properties of macrocyclic complexes, spin offs from this chemistry have included organic synthesis in the presence of metal ions and rationalization of the unusual behaviour of many metalloproteins. Synthetically 'tunable' environments of the macrocyclic type also have been used in (occasionally successful) attempts at generating metal ion catalysts. Biochemistry is itself all about catalysis on a major scale and it is clear that modelling/mimicking biochemistry is an important objective for the inorganic chemist.

THE MACROCYCLIC AND CRYPTATE EFFECT.

From the earliest studies it was realized that macrocyclic ligands could impart unusual properties to the complexed metal ions. Examples include slow rates of formation and dissociation of the complex[13], high ligand field strengths[14] and large stability constants for macrocyclic complexes when compared with the corresponding open chain ligands[15]. The term 'macrocyclic effect' was coined in recognition of these properties. It is a collective term incorporating both kinetic[13,14] and thermodynamic factors[16,17]. An extension of the macrocyclic effect - the cryptate effect [18] is used to describe the analogously enhanced stability of macrobicyclic systems over macrocyclic systems.

Cox [19] compared the stability constants of the silver, barium and potassium complexes of macrocycle (2.2) with the macrobicycle (2.2.2) (Fig.4). The small change in the silver ion value is due to the selectivity of silver with nitrogen. Buschmann [20] has also used the above systems and compared them with the noncyclic analogue Fig.4-3 and studied their complex formation with Co(II) and Ni(II)cations.

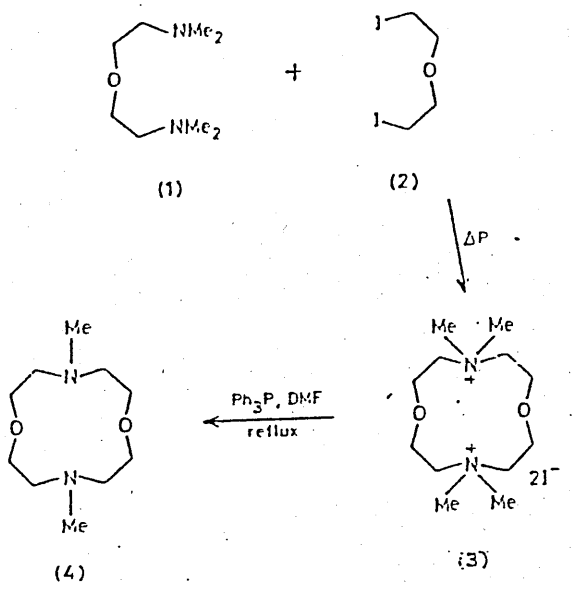

FIGURE 5.

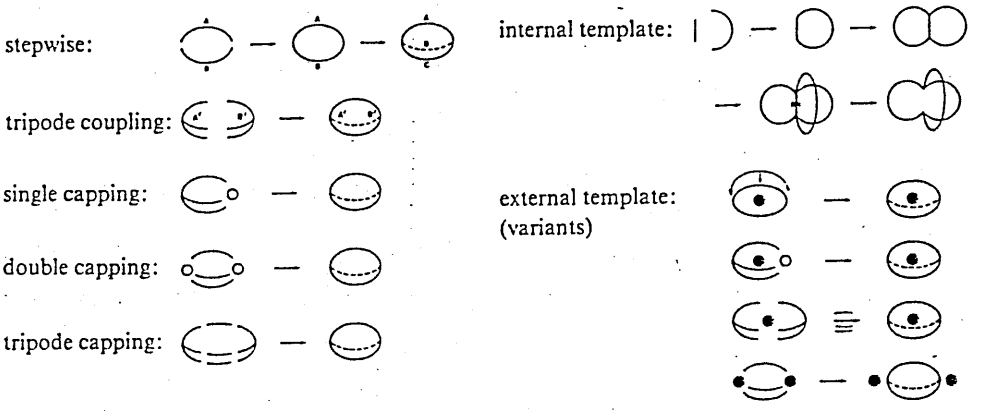

FIGURE 6.

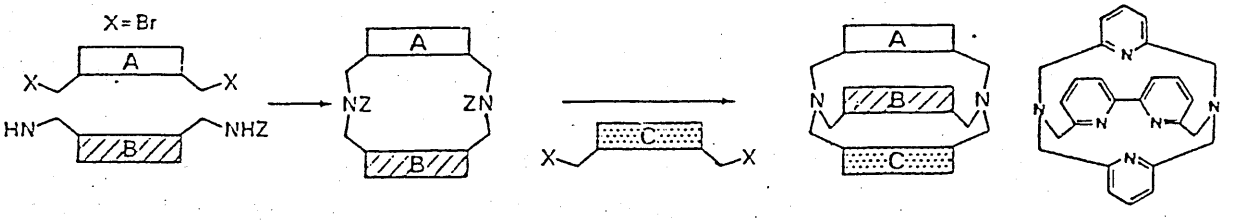

FIG.7-1

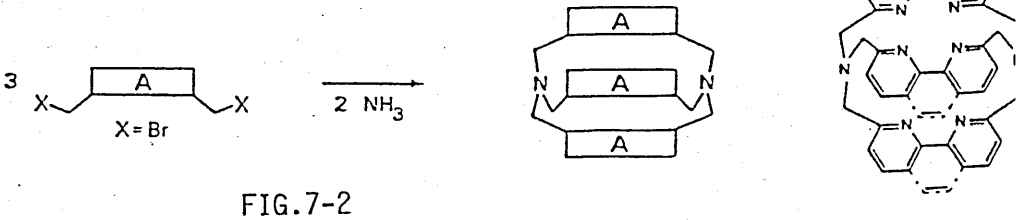

FIG.7-2

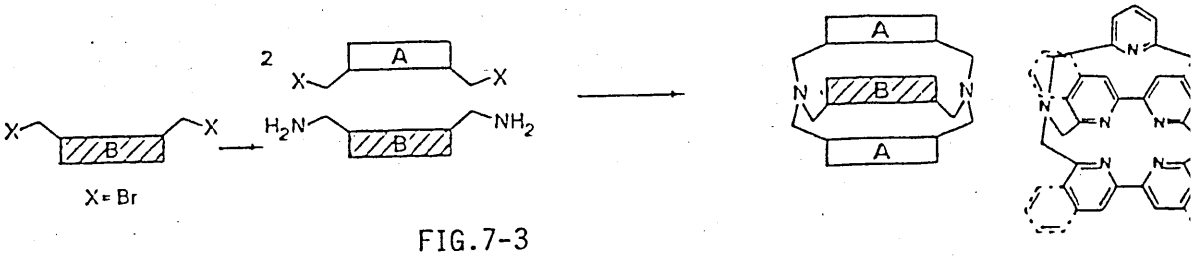

FIG.7-3

SYNTHESIS.

The synthetic routes to macrocyclic ligands fall into 2 main categories;

(1) **DIRECT SYNTHESIS** by conventional organic chemistry. This has been extensively employed in the preparation of cyclic tetraamines, crowns[8] and cryptands [21]. Yields for directly synthesized macrocycles are frequently very low because of competing intermolecular polymerization reactions. This problem is usually controlled by completing the final ring-closure step under conditions of high dilution. Several cyclic amines have been prepared in high yield by direct synthetic routes [22-25].
High pressure techniques [26,27] are providing an alternative to the high-dilution techniques, providing the compounds do not contain reducible groups. Recently Jurczak et al [28] reacted α-w-tertiary diamines with α,w-di-iodo compounds to give the cyclic bis-quaternary diazacoronand salts in high yield (≈80%) Fig.5.
(2) **IN SITU SYNTHESIS** involves cyclization in the presence of a metal ion. Cyclic polyethers excepted, the template or in situ synthesis[29-31] is the most frequently used method of forming macrocycles. However in some cases Group I and II metal ions can be used as template agents in forming crown ethers[32]. The template effect is believed to arise from the ability of the metal ion to organize the open chain reactants in a conformation favourable to ring closure [30,33,34].

Cryptands can be prepared by direct synthesis or by template synthesis, and extension into the macropolycyclic manifold requires consideration of synthetic strategies for the construction of such multibridged frameworks [35]. Fig.6 shows the various approaches to the synthesis of cryptands. The stepwise process requires two cyclization reactions (each forming two bonds) but generates an intermediate macrocycle which may also present interesting properties and allows the introduction of 3 different bridges A,B and C Fig.(7-1). The tripod coupling process is a "one pot" procedure but can suffer from extensive side reactions since it requires formation of 3 bonds in a single condensation step; Fig.7-2. This method also gives access to 'left-right'-dissymmetric macrocycles when 2 different tripodal subunits A and B are employed Fig.7-3; these compounds conserve a three

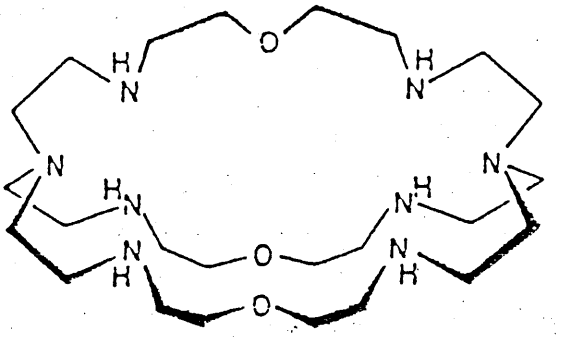

FIG.7-4

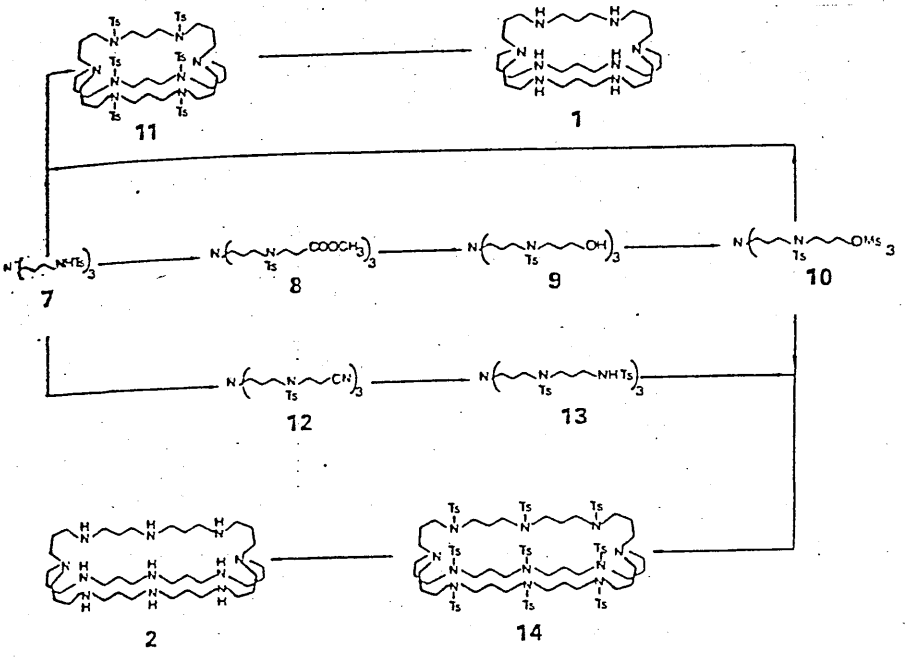

FIGURE 8.

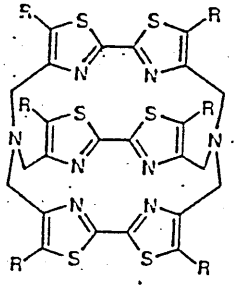

FIG.9-1

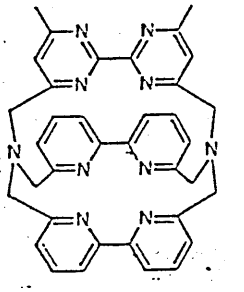

FIG.9-2

FIGURE 9.

Macrobicyclic Cryptates incorporating Bithiazole, Bisimidazole and Bipyrimidine Binding Subunits.

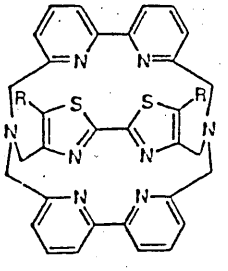

FIG.9-3

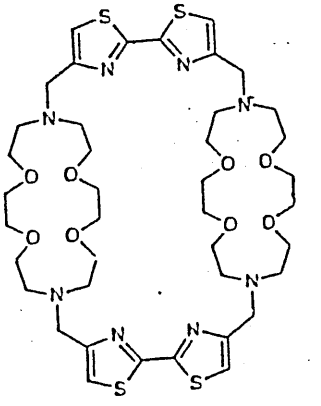

FIG.9-4

fold symmetry axis through the bridgehead atoms. The synthesis of triply bridged cyclophanes [36-40], triphenylmethane [41] and 1,3,5 triazine [42] involve the 'tripode' coupling mechanism. Compound O-BISTREN has been synthesized using a step wise manner [43] Fig.7-4.

Twelve centre reactions involving the near simultaneous formation of 6 bonds in a single step which belong to the 'tripode capping' type Fig.6 afford macrocyclic cryptands [44] Fig.8 and templated capping gives sepulchrates[45] Fig.3-2. Triple bridging of C_3 cyclotriveratrylene (CTV) derivatives leads to bis-CTV[46] and speleand[47] macrocyclic cages.

Lehn[21] has synthesized macrobicyclic polyamines by direct macrobicyclization via tripode-tripode coupling. This involves simultaneous formation of 3 C-N bonds via a (C-X and tosylamine) reaction and without recourse to high dilution conditions Fig.8. More recently[48] he has directly linked bis-heterocyclic rings, in a single step synthesis Fig.9(1-4) the products of which are of special interest as metal binding sites for macrocyclic ligands. Indeed they have formed 1:1 inclusion complexes with the luminescent lanthanide ion Eu(III) and so may function as light conversion molecular devices[49,50]

Schiff-base Macrocycles and Cryptands.

Condensation of amines and carbonyl functions to give Schiff-base products has been important in the development of coordination chemistry[29,51], and has been widely exploited in the synthesis of nitrogen donor macrocyclic and chelating ligands[29,30,33]. The template method of synthesis is particularly useful in the formation of such Schiff-base macrocycles. Schiff-base condensations Fig.10 are known to proceed by way of nucleophilic attack by the amine group at the carbon atom of the carbonyl function to yield a carbinol amine intermediate (seldom isolated) followed by elimination of water to generate the imine[52]. Normally the reaction is acid catalysed but this role may be taken by a metal ion, which functions as an acid by drawing electron density away from the coordinating carbonyl

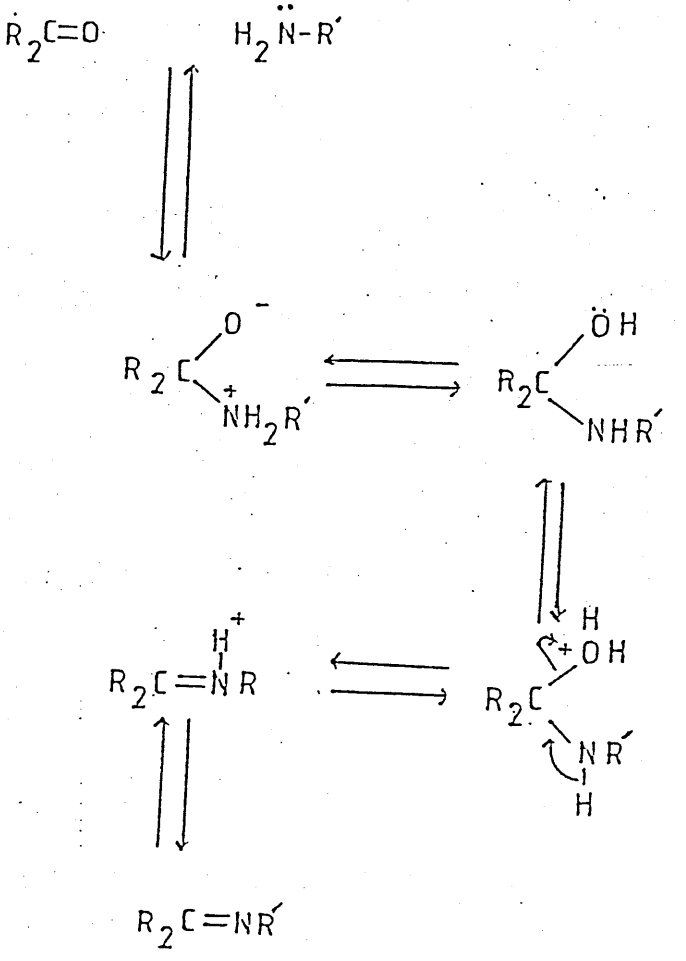

THE MECHANISM OF SCHIFF-BASE CONDENSATION.

FIGURE 10.

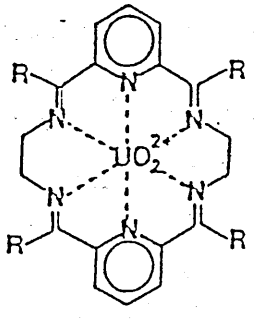

METAL-TEMPLATED SYNTHESIS OF MACROCYCLIC COMPLEXES OF THE URANYL ION.

FIGURE 11.

function. In this case the imine product is generally isolated as the metal complex.

Two template effects may be recognized : **the kinetic template effect** in which the metal ion controls the steric course of stepwise reactions so as to lead, for example, to cyclic rather than polymeric products; **the thermodynamic template effect** where the metal ion disturbs an existing equilibrium so as to increase the yield of the desired product. It is often difficult however to separate the two effects and it is probable that both are simultaneously operative in very many synthesis.

Where Schiff-base ligands are concerned the use of templates is widespread although several Schiff-base systems have been isolated in the absence of metal ions [53,54]. This may result from a low solubility of the macrocyclic product as against other non- macrocyclic species present or to a special stabilization of the macrocycle arising from the presence of intramolecular hydrogen bonds[39,40,41]. For a full discussion of the mechanistic aspects of template synthesis and the role of the metal ion control in macrocyclic synthesis consult references 30,33 and 34.

For many templated species, the Schiff-base is stable only when coordinated, and attempts to liberate the free ligand from the complex often leads to ligand decomposition. An exception to this is the series of cryptands including the O_3N_8 bicyclic structure described later in this thesis which can be made metal free (≈30% yield) and templated on Ba(II) (75% yield). Template ions most commonly used for Schiff base macrocycles are the Group II metals, Pb(II) or Ag(I) which are large and sterically non-demanding. It is only within the last few years that lanthanides[55] and actinides[56] have been used successfully as templating agents. Fig.11 shows the first six N donor macrocyclic complex reported for any of the actinides[57]. It is exceptionally inert towards release of UO_2^{2+} even in the presence of acids or strongly competing ligands, suggesting systems of this type may be used advantageously when effective sequestering of the actinide ion is an important requirement.

The choice of template metal ion can control the product obtained via its geometric coordination preferences. The size of template ion chosen can be

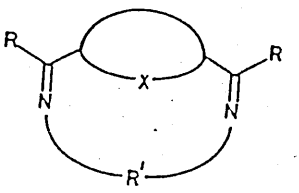

1 + 1

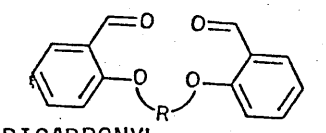

DICARBONYL

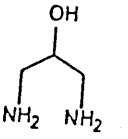

DIAMINE
(ref 63)

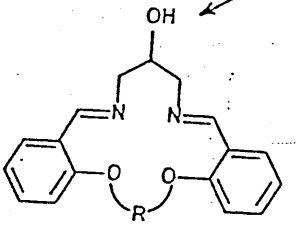

SCHIFF-BASE

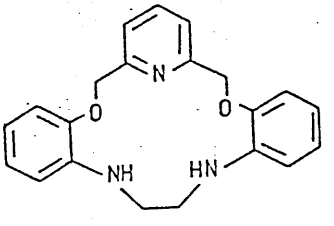

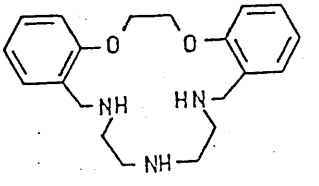

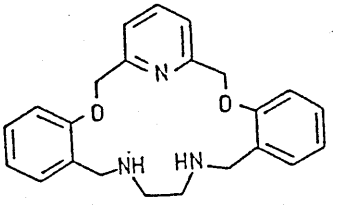

(ref 65a)

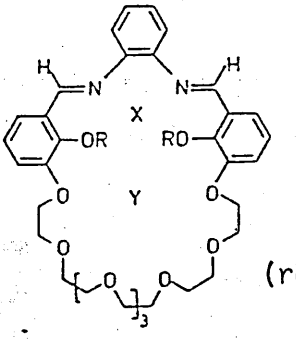

(ref 65b)

1: R = H; X = –; Y = –
2: R = H; X = –; Y = $Ba(ClO_4)_2$
3: R = –; X = Ni; Y = urea
4: R = –; X = UO_2; Y = $7H_2O$
5: R = –; X = UO_2; Y = urea

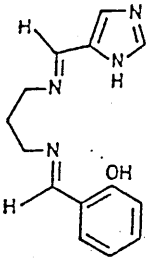

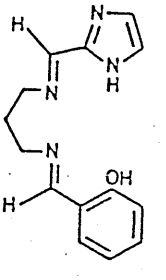

(ref 65c)

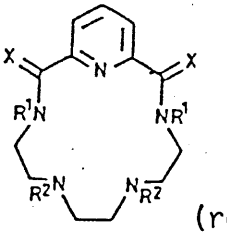

(ref 65d)

L^1: X = O; R^1 = H, R^2 = Me
L^2: X = H_2; R^1 = H, R^2 = Me
L^3: X = H_2; R^1 = R^2 = Me
L^4: X = Me, H; R^1 = R^2 = H
L^5: X = H_2; R^1 = R^2 = H

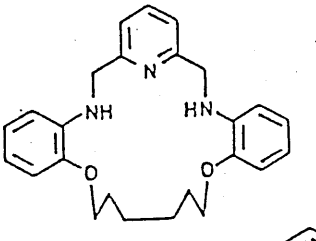

(ref 65e)

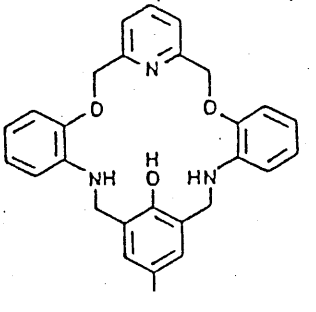

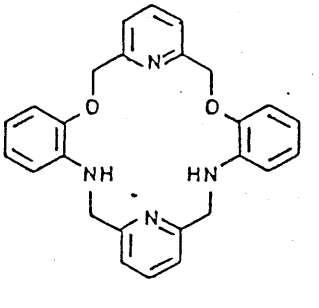

EXAMPLES OF 1+1 SCHIFF-BASES.

FIGURE 12.

used to direct the condensation e.g. between one molecule of dicarbonyl and one molecule of diprimary amine versus 2 molecules of each reactant [58-60] or more [61] thus forming [1+1],[2+2] or [4+4] macrocyclic products respectively. 2,6 diacetyl-pyridine (DAP) and 2,6 diformyl-pyridine (DFP) have prooved to be particularly useful precursor dicarbonyls with their strongly donating pyridine 'anchor' which serves to hold and activate the carbonyl towards nucleophilic attack [62]. However 2,5 diformylfuran, (DFF) 2,5 diformylthiophene (DFT) and pyrrole based macrocycles are also well documented.

There are many examples of [1+1] condensations giving tri, tetra, penta and hexadentate closed cyclic systems. Fenton[63] and Lindoy[64] have recently employed [1+1] condensations to give oxa-aza macrocycles capable of metal ion recognition. A collection of examples of Schiff base polyaza and mixed-donor [1+1] ligands are shown with references[65] in Fig.12. Many open chain [1+1] condensation products have also been reported but will not be discussed here.

Whether a [1+1] or [2+2] cyclic condensation occurs depends, at least in part, on the size of the metal ion used in the template process. Thus while Ni(II) affords the 14 membered 'N_4' [1+1] macrocycle L' Fig.13-1. the larger Ag(I) cation produces the binuclear complex $[Ag_2L]X_2$ (X=(ClO_4, BPh_4) Fig.13-2 in which the ligand is a 28 membered macrocycle derived from a [2+2] condensation [60]. The relatively large size of the Ag(I) ion appears to be responsible for directing the course of the reaction towards the [2+2] rather than the [1+1] product.

Application of this principle to other systems has resulted in the synthesis of [2+2] macrocycles of various sizes, which differ in number, nature and disposition of the donor atoms. The alkaline earth metal cations have proved particularly effective templating agents in these systems and from these, by transmetallation (see later discussion), a range of mono and binuclear complexes have been prepared [30]. Selected examples of [2+2] Schiff-base macrocycles are shown with references in Fig.14[66] and comprehensive accounts of Schiff-base macrocycles are found in references 30,33.

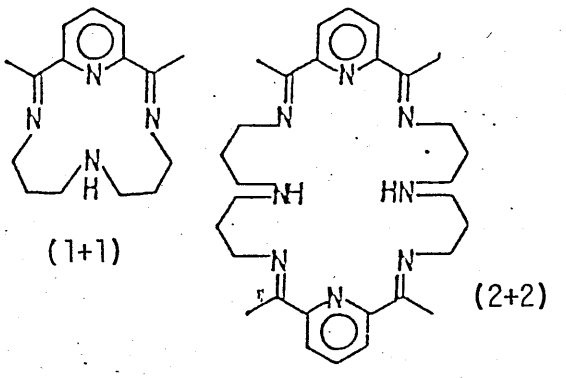

FIGURE 13.

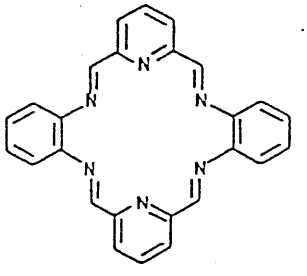

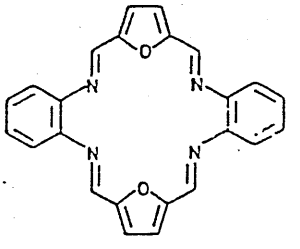

(ref 66a)

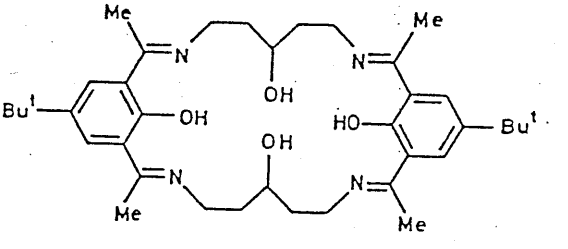

(ref 66b)

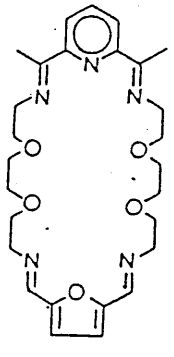

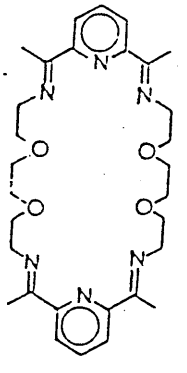

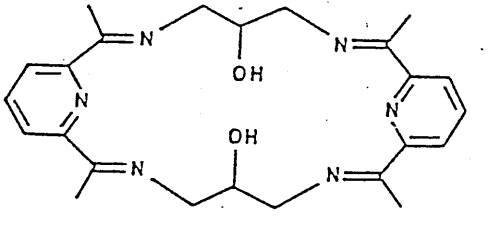

(ref 67)

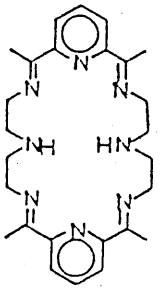

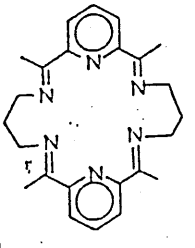

(ref 30)

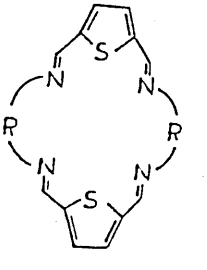

(ref 33)

FIGURE 14. EXAMPLES OF (2+2) SCHIFF-BASES.

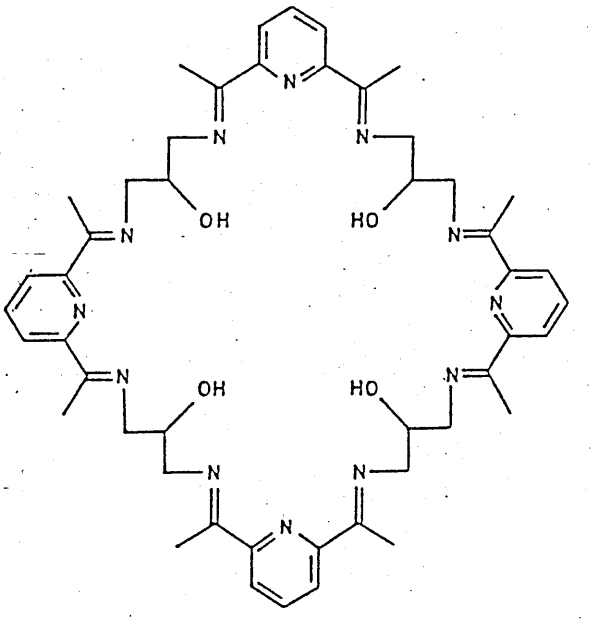

H_4L'

FIGURE 15.

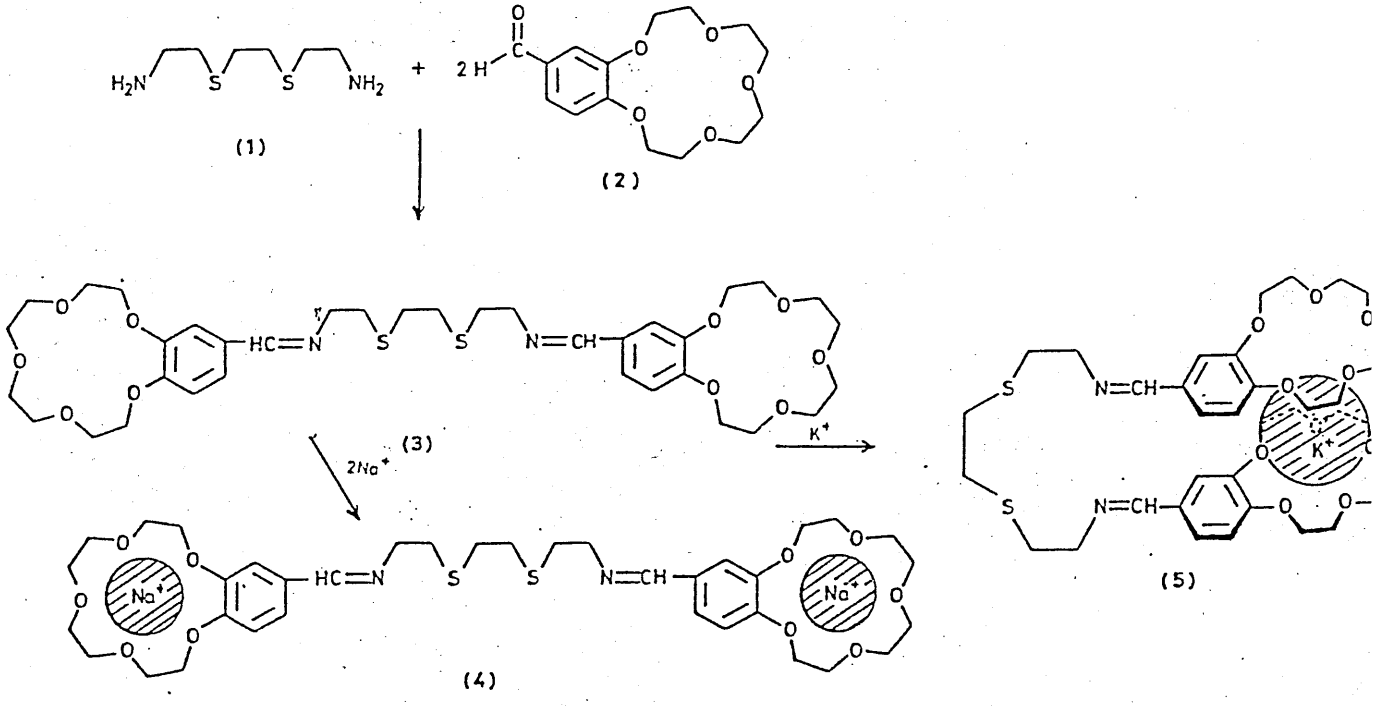

FIGURE 16. (1+2) DIAMINE, CARBONYL SCHIFF-BASE.

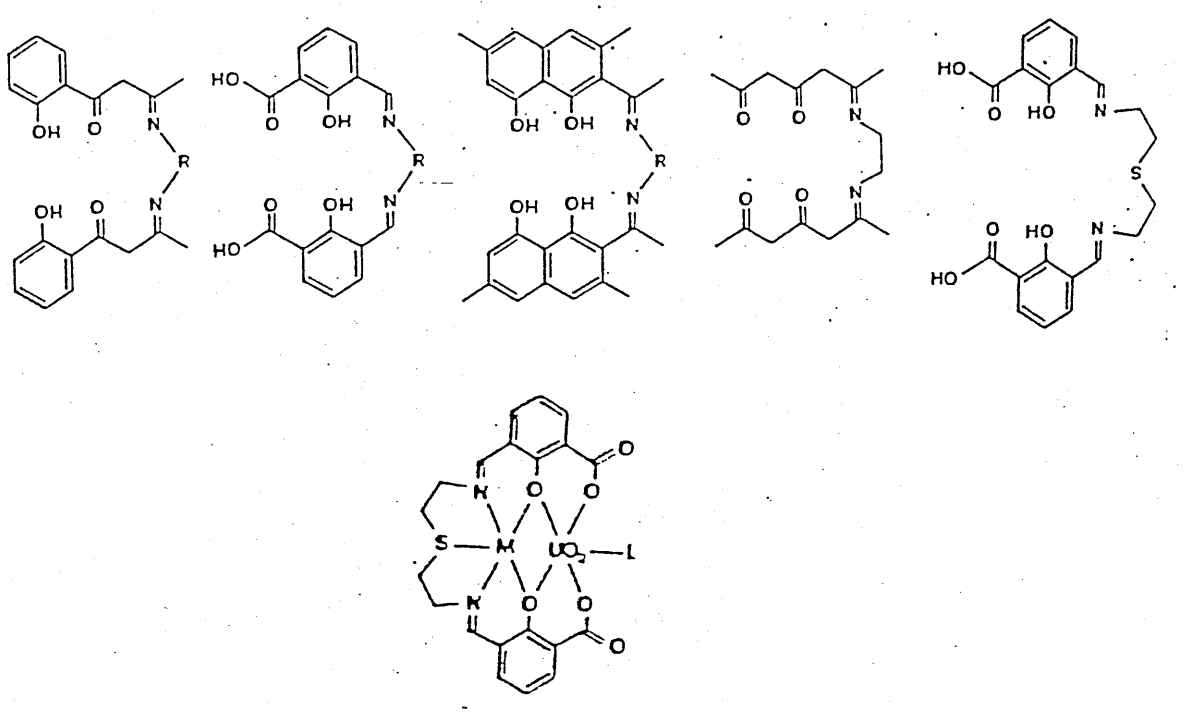

FIGURE 17 COMPARTMENTAL LIGANDS CAPABLE OF FORMING HOMO- AND HETEROBINUCLEAR COMPLEXES

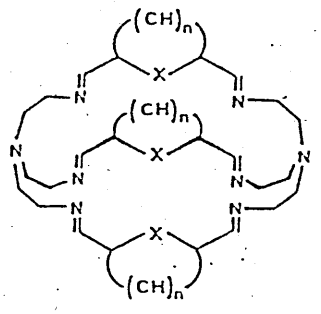

1^{73} x=CH n=3
$2^{73,72}$ x=N n=3
3^{73} x=O n=2
4^{73} x=S n=2

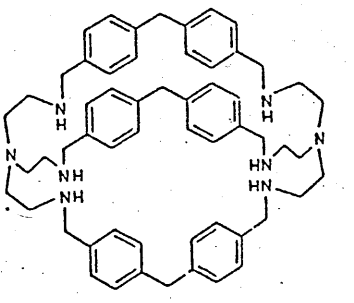

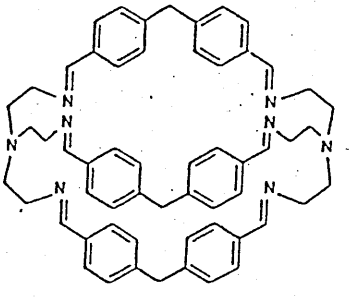

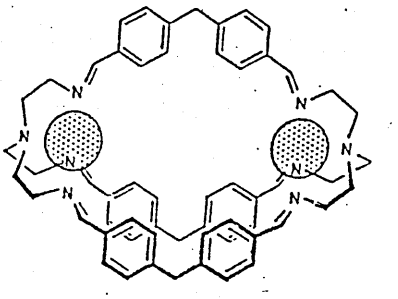

FIGURE 18 (2+3) SCHIFF-BASE MACROCYCLES.

A [4+4] [67,68] condensation has been reported. This was observed by McKee in a Mn(II) derivitive of the ligand shown in Fig.15. The 40 membered macrocycle is found wrapped around a tetrahedral Mn(II) core in which each endogenous alkoxide group is in contact with 3 Mn(II) ions.

Novel chelating ligands have been prepared by Beer[69] who used a [1+2] diamine, carbonyl Schiff-base condensation to give the bis (crown ether) ligand Fig.16 which contains a pair of recognition sites for alkali and transition metal guest cations. These multisite receptors may exhibit allosteric properties [70] by binding sequentially 2 or more guest metal cations. The resulting polynuclear complexes may facilitate electron transfer studies and serve as models of relevance to biological redox processes.
Fenton[71] also using a [1+2] diamine, carbonyl reaction produced a series of compartmental ligands Fig.17 which can form complexes with UO_2^{2+}, Ni(II) and Cu(II). Fig.17-5 is capable of forming homo and heterobinuclear complexes. Fig.17-6. Lehn[72] and Nelson[73] have used a [2+3] condensation method of synthesis to give a series of macrobicycles Fig.18.

TRANSMETALLATION.

Such templated Schiff base macrocyclic compounds are potentially capable of forming binuclear complexes with transition metal ions because the template ion may be replaced in the complex by treatment with a salt of another metal ion which is itself ineffective as a template for the ligand synthesis. This metal ion exchange or transmetallation Fig.19 [30] occurs readily when a larger alkaline earth metal is to be replaced by a smaller transition metal or other metal likely to form stronger bonds with the ligand donor atoms. In this way the macrocycle, macrobicycle or other Schiff-base ligand is 'captured' and stabilized by the 2nd metal ion before decomposition sets in. Although the precise mechanism of the transmetallation reaction is unknown it seems likely that it involves a concerted process in which the incoming metal ion becomes partially bound to the ligand before the outgoing (template ion) is fully released. In this exchange process a single alkaline earth metal template ion may be replaced

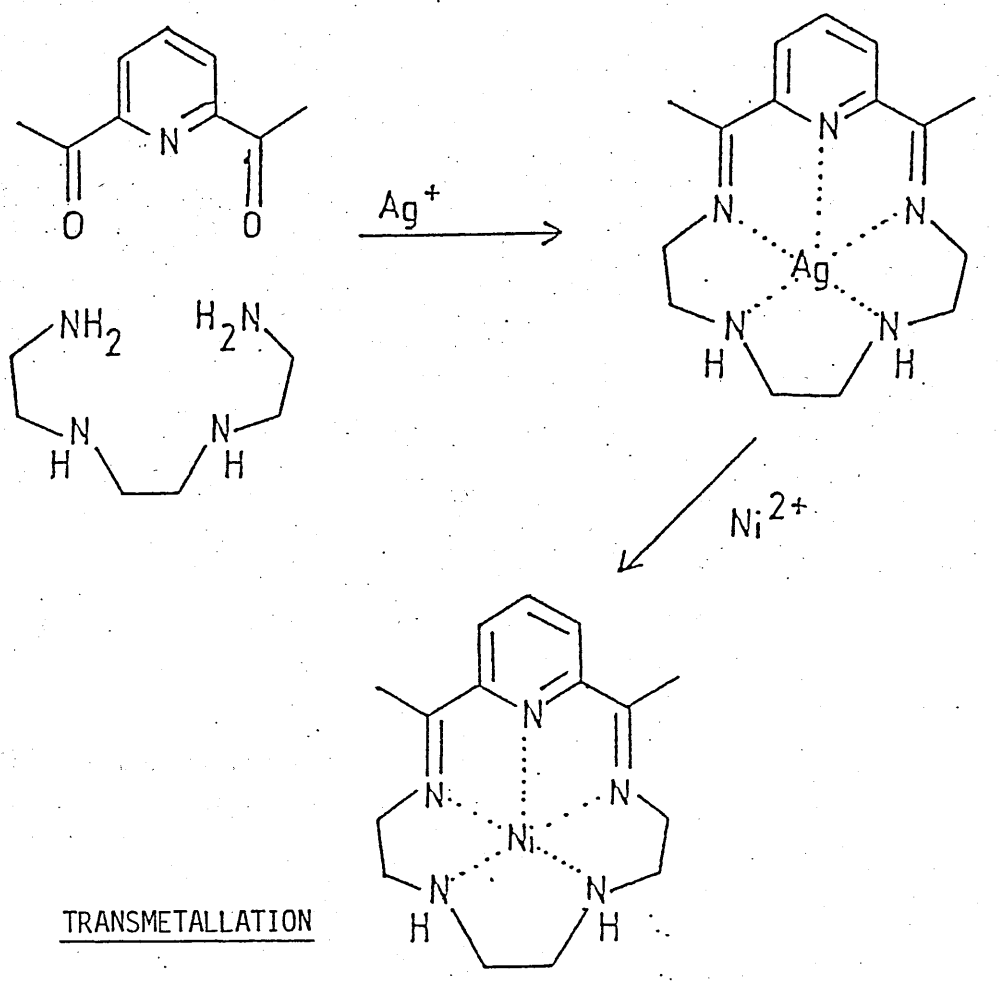

FIG.19-1

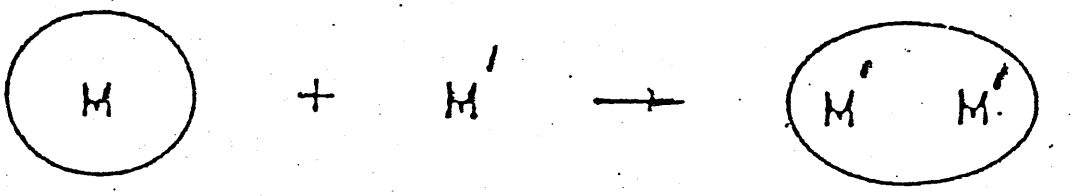

Binuclear Complex

Formation of a binuclear from a mononuclear complex of a macrocyclic ligand via transmetallation.

FIG.19-2

by 1 or 2 transition metal ions Fig. 19-2. In this way a series of binuclear complexes can be prepared.

POLYAZA MACROCYCLIC LIGANDS & COMPLEXES.

Polyaza macrocyclic and macrobicyclic complexes have attracted much attention for the unusual properties they display which are not always encountered with their open chain analogues: an extreme kinetic stability, high thermodynamic stability and frequent stabilization of unusual oxidation states (eg. +3 state of the normally divalent Ni(II) and Co(II)) enforced on the metal ion via the electron-donor properties of the so-constrained donor atoms. The macrocyclic polyamines are basic and thus in their protonated form are useful as anion complexons whereas they behave as good cation receptors (especially the transition metals) in the unprotonated form. Because of their ability to encapsulate 2 transition metal ions in close proximity there is much interest in these complexes as bio-models. Often, however, the basic macrocyclic structure cannot include all the required functional groups within its framework to mimic the natural system. However additional functional features may be introduced into the system by means of elegant synthetic work to incorporate the required functionality or by means of pendant arms. The incentive for attaching functionalized pendant arms to the macrocyclic polyamines, arises because some biological macrocyclic tetraamines (eg. porphyrins and corrin) are functionalized for their specific activities by having proximate donor ligands such as imidazole, phenolate or cysteine at an axial position. Therefore it is hoped that incorporation of intramolecular axial donor groups into macrocyclic polyamines might confer various enzyme functions upon the metal complexes.

Thus, over the last decade funtionalization of the established systems shown in Fig.20 has become an interesting and often rewarding area of work, leading to many new systems which show a diverse range of uses and properties. Fabbrizzi has looked at the temperature dependance of the Ni^{III}/Ni^{II} redox couple in aqueous solutions of the above systems [74]. Trapping of the metal centre within the cyclic coordinating framework, with

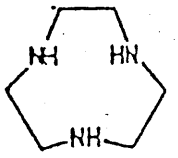

FIG.20-1

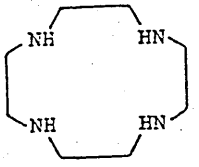

(12)aneN$_4$

FIG.20-2a

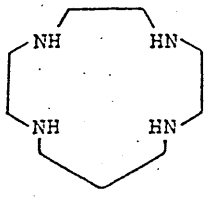

(13)aneN$_4$

FIG.20-2b

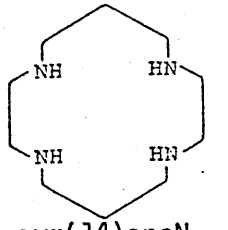

sym(14)aneN$_4$

FIG.20-2c

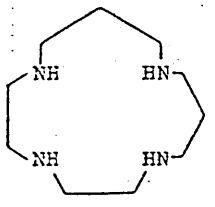

asym(14)aneN$_4$

FIG.20-2d

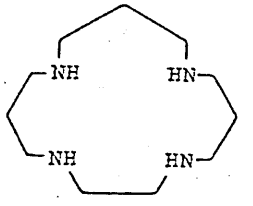

(15)aneN$_4$

FIG.20-2e

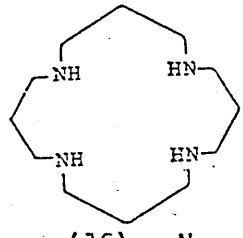

(16)aneN$_4$

FIG.20-2f

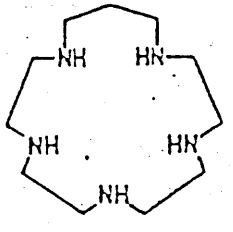

FIG.20-3

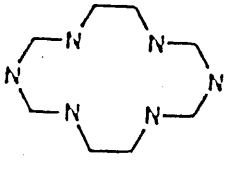

FIG.20-4

closely bound saturated amino groups stabilizes the Ni^{III} oxidation state. The solution stability of the trivalent complex relevant to the divalent one is expressed by the value $E_{\frac{1}{2}}(Ni^{III}/Ni^{II})$, a quantity that can be modulated over a substantial range of potentials through structural modifications on the ligand :

i - nature and number of donor atoms [81]

ii - size of the macrocyclic cavity [76]

iii - the degree of unsaturation [83]

iv - the presence of substituents on the N atoms [78] or(v on the carbon backbone[79])

The work on the thermodynamic [74] aspects of the Ni^{III}/Ni^{II} couple showed that the attainment of the trivalent nickel in solution depends on (1) solute-solvent interactions controlling access to the Ni(III) state (which is favoured in processes involving less pronounced uptake of water molecules) (2) steric effects - coordination geometry preferences for different oxidation states. Thus the nature of the ligand and its degree of delocalization will influence the oxidation state - delocalization favours low oxidation states.

Entry of metal ions into cavities of unfunctionalized macrocycles is often rather slow, partly because of the ligand conformational changes which can occur following initial metal cation binding [80-83]. Studies indicate that functionalized macrocycles with pendant coordinating arms may allow entry of a metal ion into the macrocycle cavity at a more rapid rate than is possible with the unfunctionalized parent molecule. The proposed mechanism involves initial capture of the metal ion by the pendant arm followed by transfer to the macrocyclic cavity [84-87]. Therefore not only would the pendant arms enhance the stability of the final products but they would also be beneficial in aiding the kinetics of the overall formation process.

FIGURE 21.

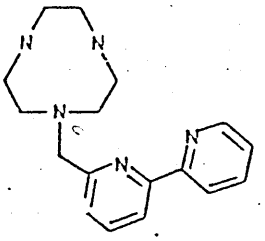

FIG.21-1

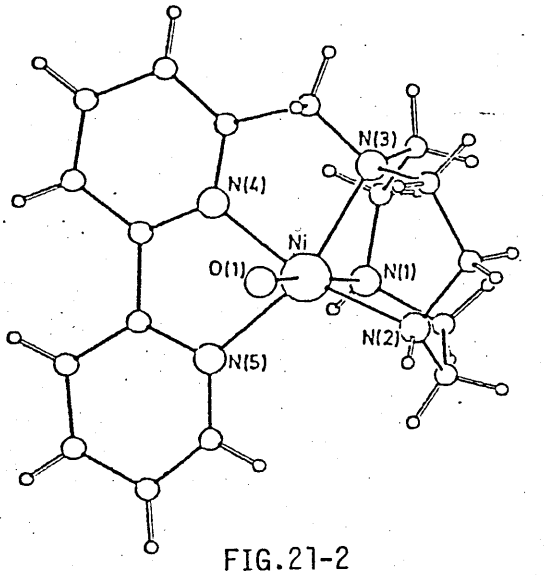

FIG.21-2

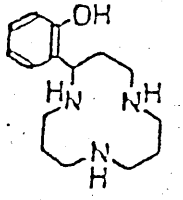

FIG.21-3

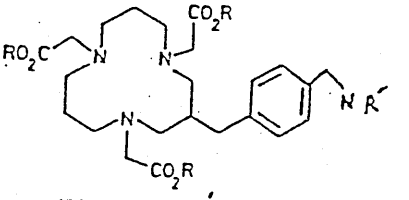

(3) a; R = Et, R' = Ac
b; R = R' = H

FIG.21-4

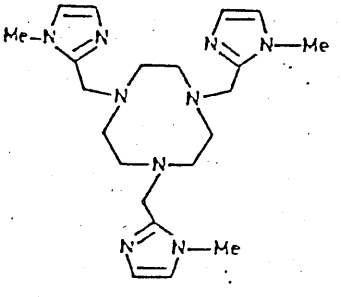

FIG.21-5

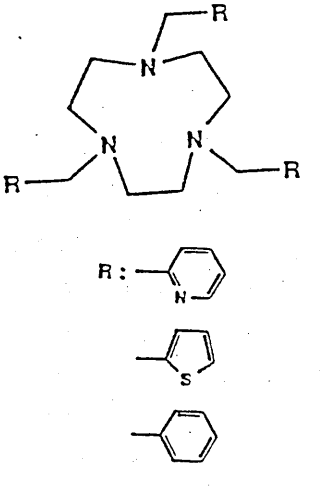

FIG.21-6

TRIAZAMACROCYCLES.

Cyclization of saturated triamine ligands has remarkable thermodynamic and kinetic effects on complex formation and a recent review [87] shows the considerable current interest in the coordination chemistry of triazamacrocycles. Early studies [88] were limited to unsubstituted triamines of various ring sizes which coordinate with transition-metal ions only facially for 3 coordinate 1:1 complexes with the remaining sites unoccupied (or solvated) in solution or for 6-coordinated 2:1 complexes [88f,88g]. The triamine ligands that posses a potential fourth donor covalently attached to the macrocyclic ring can greatly affect the structure and properties of the complex.

Moore has reported the synthesis of N-functionalized tri-(and tetra) aza macrocycles with a single pendant co-ordinating 2,2'-bipyridal-6-yl methyl arm [89,90] Fig.21-1. From an X-ray structure of the Ni(II) complex Fig.21-2 it is seen that the metal ion is pseudo-octahedral with a coordinated water molecule in a trans position to N(I) and with the coordinated N-atoms of the pendant bipyridyl group in trans positions. The tetra aza species binds through all 6 N atoms and gives 6 coordinate complexes in compounds studied so far [89]. Moore has used stop-flow spectrophotometry to establish the 2 stage mechanism of the ligands with metal ions [90] as shown in the scheme below:-

$$[M\text{-}(dmso)_6]^{2+} + L \underset{k_2}{\overset{k_1}{\rightleftharpoons}} \text{intermediate} \longrightarrow \text{products}$$

ie. an initial rapid second order process is followed by a much slower first order rate equation . The rate constant (k_1) and equilibrium constants (k_1/k_2) were similar for the tri and tetraaza substituted ligands. This is significant since it reveals that the intermediates involved in the initial coordination must involve only the metal and pendant arms and that the bonds to the nitrogen atoms of the macrocyclic rings must form during the slower second stage. Moore has also used

$Me_2NCH_2CH_2$ to N-functionalize the triaza species and observed coordination of the pendant arms[91].

Kimura has synthesized metal complexes of macrocyclic triamines bearing a phenol pendant [92] Fig.21-3. The phenolic O-donor in general shows strong interactions with Cu(II), Ni(II), Zn(II) and Co(II) as supported by perturbed UV spectra of the phenol. As a result of this coordination their 1:1 complexes are more stabilized with respect to their parent [12]ane N_3 complexes. The phenolate interactions are generally stronger in the triamine compared with the tetraamine complexes.

When tumor-localizing monoclonal antibodies are radiolabelled for use in tumor imaging, it is essential that the radiolabel does not dissociate from the antibody conjugate over a period of several days. Presently Parker et al [93] are using macrocyclic complexes to bind the γ emitting radiolabel ^{111}In ($t_{½}$ 2.83 days), taking advantage of their slow rate of metal dissociation. They used a hexa-coordinating ligand with 3 ionizable groups to reduce the effective nuclear charge at the tripositive indium centre Fig.21-4. The overall complex is then electrically neutral and is therefore much less sensitive to acid-catalyzed dissociation. By then C-functionalizing the ligand it can be covalently attached to an antibody which selectively binds to tumor associated glycoprotein found in human colorectal and breast cancers.

Di Vaira [94] has been successful in arming tri and tetraaza macrocycles with coordinating imidazole groups Fig.21-5, while Tsukube [95] has recently reported a new series of "pyridine-armed" aza macrocycles. Fig. 21-6. Pyridine-armed triaza macrocycle selectively and efficiently transported Na^+ while the analogous thiophene and benzene armed species could not act as effective carriers for any examined cations. The tetraaza analogues showed lower transport abilities as did the crown and hemispherand type ionophores. Thus the triaza macrocycle armed with a pyridine pendant arm clearly offers a new and effective ionophore for hard metal cations.

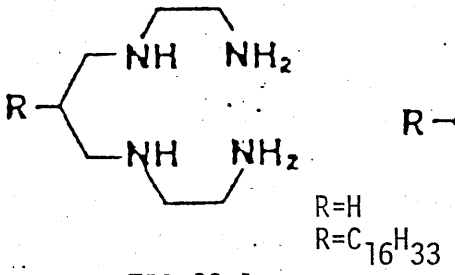

FIG.22-1

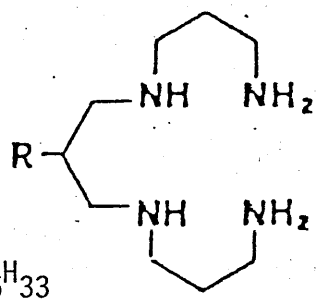

FIG.22-2

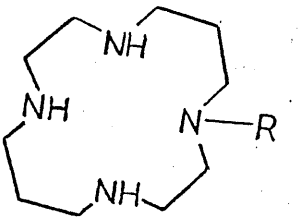

FIG.22-3

THREE-PHASE TREATMENT OF A CONVENTIONAL AQUEOUS REDOX PROCESS

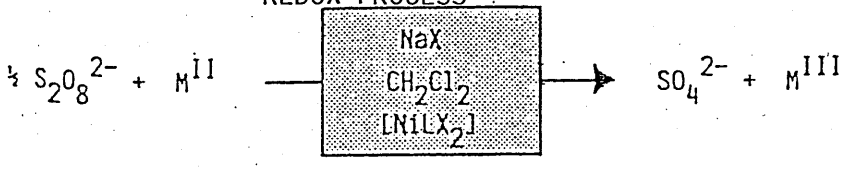

THERMODYNAMIC CONTROL: appropriate choice of the background electrolyte NaX makes the process to occur or not to occur.

KINETIC CONTROL: nature of the reducing agent determines the rate of the redox process . (SELECTIVITY)

FIG.23

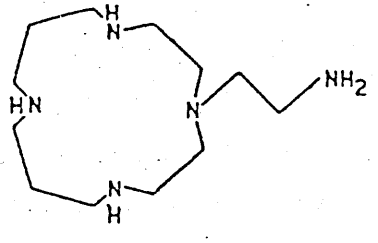

FIG.24-1

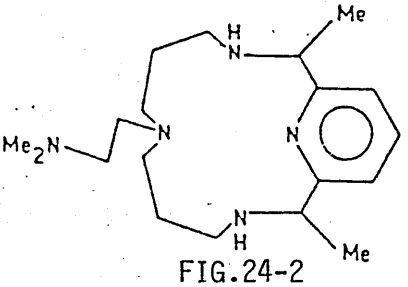

FIG.24-2

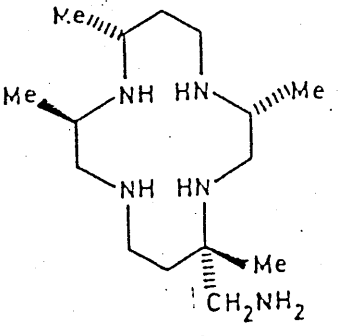

FIG.24-3

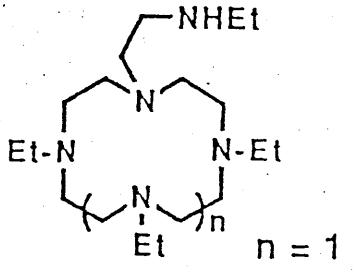

FIG.24-4

TETRAAZA MACROCYCLES.

Tetraaza macrocycles were developed in the early 1960's due to the pioneering independant contributions of Curtis and Busch [29]. Among synthetic tetraaza macrocycles, the most popular is surely cyclam, Fig.20-2c whose simple and convenient synthesis was described by Barefield[96]. Paoletti found using a series of 12-16 membered tetraaza macrocyclic rings Fig.20-2(a-f) that the 14 membered saturated macrocycle cyclam is able to exert extremely strong coordinative interactions with 3d metal cations compared to the analogues of higher and lower atomicity [97] while Fabbrizzi [98] observed that the complexes of cyclam were more stable than those formed by the other 14 membered tetraaza iso cyclam Fig.20-2b.

In an attempt to determine the steric effects on the stabilization of the high oxidation states of encircled ions Fabbrizzi N-mono-functionalized cyclam with a methyl group [75]. This caused a destabilization of the trivalent state indicating that apical solvent molecule/methyl group repulsion plays a minor role in the oxidation of the divalent metal. A far more important factor is the N-methyl induced weakening of the metal-N bond which is greater for the trivalent than the divalent cation.

Fabbrizzi has long been interested in the transport of 3d metal ions across a bulk liquid membrane by lipophilic carriers. To this end he designed the open chain tetraaza [99] systems shown in Fig. 22-1 and 22-2 which can transport metal ions across a bulk liquid membrane. The process is controlled by a concentration gradient and extraction yields for a given metal are affected by the pH of the aqueous layer and by the nature of the counter ion. However more recently he has designed a mono-N-functionalised cyclam to act as a carrier able to perform selective electron transport across liquid membranes [100]Fig.22-3. The system behaves as a 3 phase device that allows oxidation of the metal centered redox agents with aqueous peroxydisulphate according to the scheme in Fig.23. In the reaction conditions electron transfer from Red(aq) to $S_2O_8^{2-}$ (aq) does not take place directly but is mediated by a carrier - the lipophilic Ni(II) tetraaza macrocyclic complex dissolved in the organic layer which separates the 2 aqueous (oxidizing and reducing) compartments.

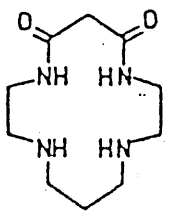

Dioxocyclam

FIG.25-1

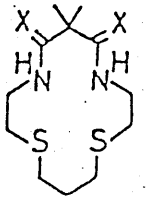

X = O

X = H_2

FIG.25-2

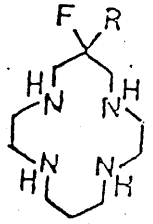

FIG.25-3

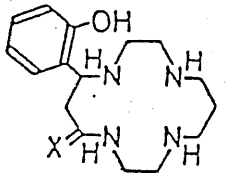

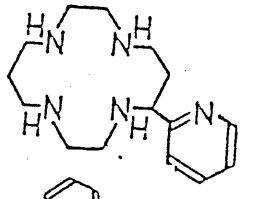

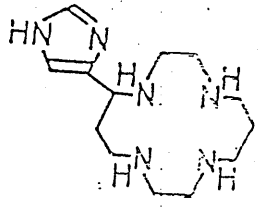

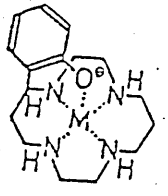

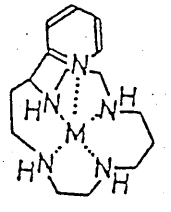

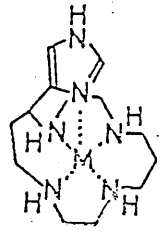

C-Pivot Pendant

FIG.25-4

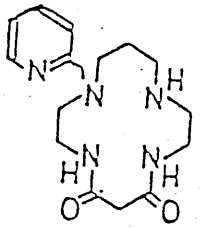

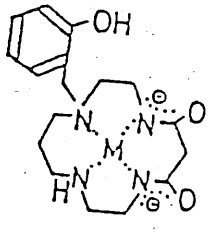

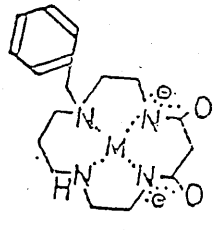

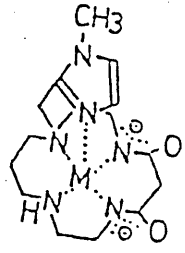

N-Pivot Pendant

FIG.25-5

FIGURE 25.

Fabbrizzi has constructed a novel functionalized N-(aminoethyl) cyclam in which a NH_2CH_2-CH_2- chain is appended onto the ring [101] Fig.24-1. The tail can coordinate to a metal centre held within the ring and thus the ligand can behave as a quinquedentate ligand. The first example of ligands of this type were described by Kaden [102] Fig.24-2. The Ni(II) complexes of this ligand type behave as acid-base indicators because when the side chain is coordinated (low pH) the species are a blue colour (high spin) but when the side chain is protonated (high pH) it is uncoordinated and the complex is yellow due to the low spin configuration of the Ni(II) metal centre Fabbrizzi has termed such ligands -"Scorpiands". Hay [103] has prepared a C-functionalized cyclam derivative containing a $-CH_2NH_2$ appendage Fig.24-3. The addition of acid to the Ni(II) complex caused the blue to yellow colour change due to protonation of the aminomethyl group. Hay has also functionalized all 4 nitrogen donor atoms with 2-hydroxyethyl [104] and 2-cyanoethyl groups [105].

Krakowiak [106] has prepared several monofunctionalized cyclams (and triaza crowns) containing a secondary amine group on a side chain Fig.24-4. An X-ray structure of the silver complex shows that the N atom of the side chain interacts strongly with the silver ion.

Kimura has renovated the classical cyclam structure (and other polyamines) in 4 ways [107] :-

-1- conversion of amines into amides (ie. dioxocyclam) [108] Fig.25-1
-2- replacement of N donors for S donors [107] Fig.25-2
-3- replacement of skeletonic C-H for C-F [109] Fig.25-3
-4- attachment of intramolecular pendant donors which may be C-pivot donors [123,110-113] Fig.25-4 or N-pivot donors [107] Fig.25-5.

Kimura studied the complexation of the dioxo tetraaza macrocycle with the oxo groups cis to each other [114-115] whereas Fabbrizi studied the equilibrium measurements of complexation of the dioxo macrocycles bearing trans amide groups [116].

Meares [117] has prepared a bifunctional ^{64}Cu 6-[p-(bromo-acetamide)benzyl]-1,4,8,11 tetraaza cyclotetradecane -1,4,8,11 tetra acetic acid complex

FIGURE 26

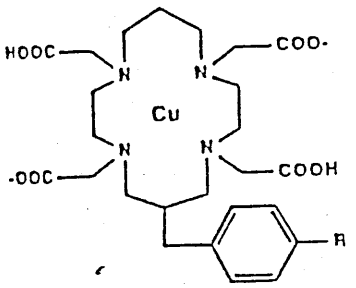

MoAb = monoclonal antibody.

FIG.26-1

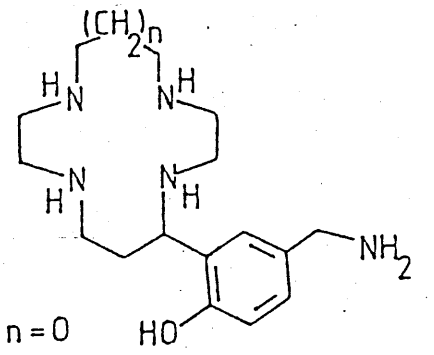

FIG.26-2

Implementation of macrocycle conjugated antibodies for tumour-targetting

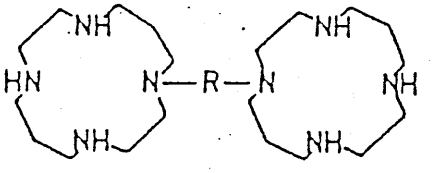

ref 124a

R: $-CH_2CH_2-$; $-CH_2CH_2CH_2-$; $-CH_2CH_2CH_2CH_2-$; $-CH_2-C_6H_4-CH_2-$ (p) ; $-CH_2-C_6H_4-CH_2-$ (m)

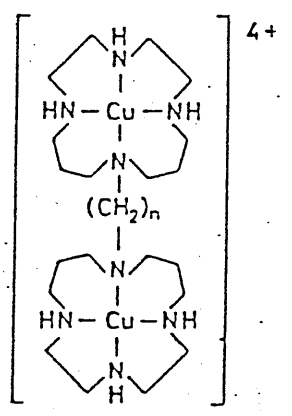

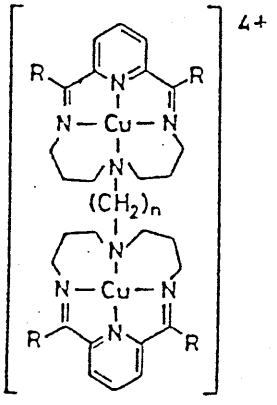

ref 124b

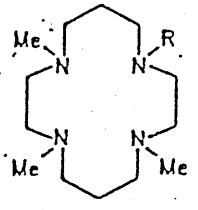

ref 125

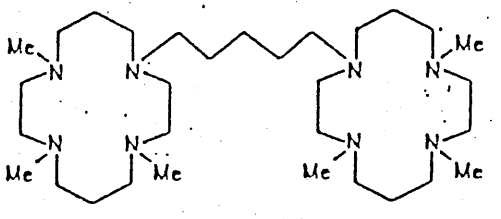

FIGURE 27

FIGURE 27 contd. C,C′-bis(macrocycles)

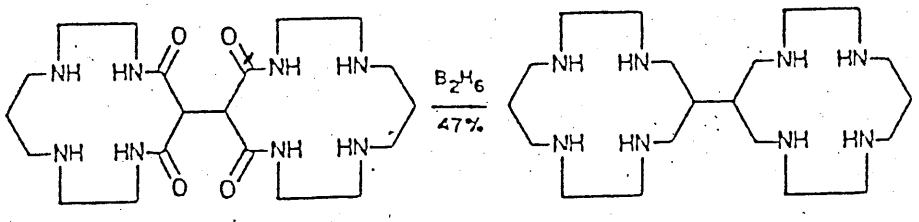

ref 127

FIGURE 28

A TETRAAZA MACROCYCLE OF THE CYCLOPHANE TYPE.

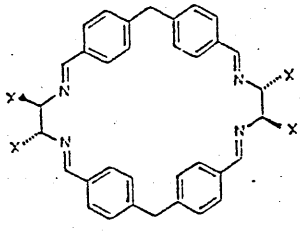

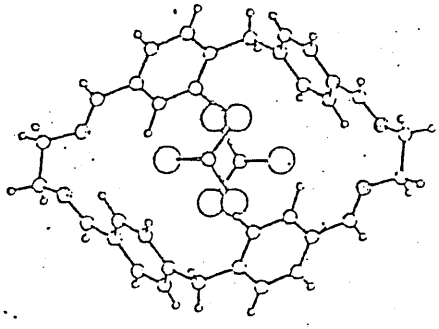

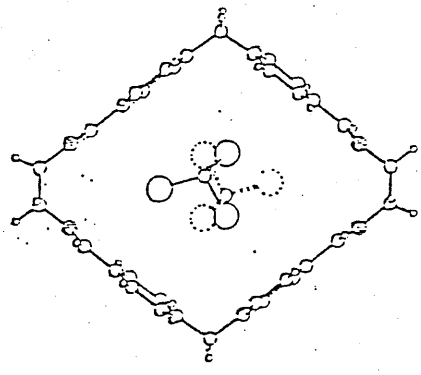

FIGURE 29.

EXAMPLES OF PENTAAZA.

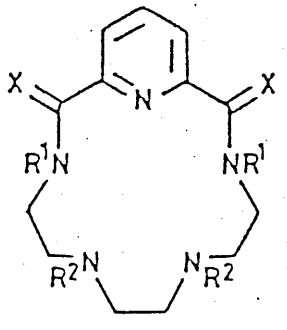

L^1; X = O; R^1 = H, R^2 = Me
L^2; X = H_2; R^1 = H, R^2 = Me
L^3; X = H_2; R^1 = R^2 = Me

FIG.29-2-4 ref 130b

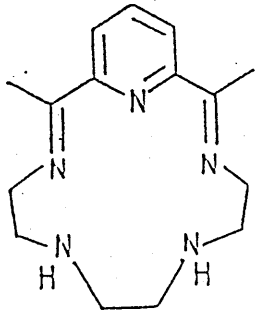

FIG.29-1 ref 130a

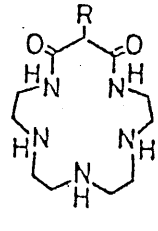

FIG.29-5 ref 130

Fig.26-1 for use as a tumor imaging and tumor therapeutic agent. Parker who has functionalized the triaza ligands [93] has also prepared $^{64}Cu(II)$ tetraaza macrocyclic systems [118,119] Fig.26-2 that can attach to an antibody. Here the side arm is a primary amino group.

Kaden [120] has used functionalized tetraaza macrocycles to see if the metal ion modifies the properties of the functional groups in side chains in the same way as the side chain modifies the properties of the coodinated metal ion using visible spectroscopy and redox potentials.

The bis (macrocycles) in which two cyclic polyaza subunits are linked together either through an aliphatic chain joining 2 macrocyclic N-atoms (N,N'-bis(macrocycles)[121-125] or by a chain joining 2 macrocyclic carbon atoms (C,C' bis(macrocycles))[126-128], are ligands capable of strongly coordinating pairs of metal ions. Some of these dinuclear assemblies display redox activity in solution disclosing two consecutive one electron redox steps. Communication between the 2 metals may be through 2 main pathways (1) electronic-direct interaction or delocalization through a bridging coordinating group, and/or (2) electrostatic. Fig.27 gives some examples (with their references) of the bis(macrocycle) ligands.

Lehn [129] has synthesized a tetraaza macrocycle of the cyclophane type Fig.28-1. The tetramine forms a chloroform inclusion complex and the protonated species Fig.28-2 binds the dicarboxylate anion.

PENTAAZA MACROCYCLIC COMPOUNDS.

Reports of work involving pentaaza macrocyclic compounds fall in the shadow of the highly successful tetraaza cyclam models. Also many pentadentate macrocycles offer a mixed donor set or else have been functionalized by means of endogenous bridges or groups (both will be discussed in later sections). However some examples of pentaaza ligands are shown in Fig.29[130].

FIGURE 30.

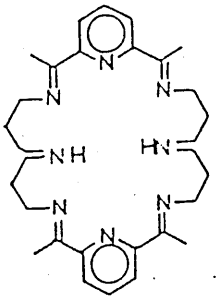

ref 30

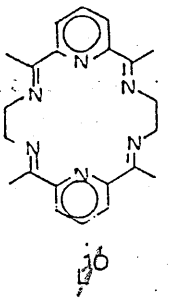

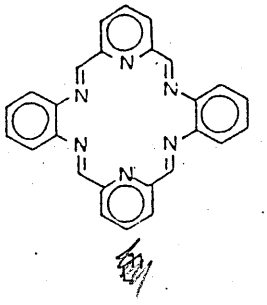

(Co^{2+}, Sr^{2+}, Ba^{2+}, Pb^{2+})

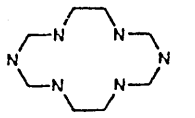

ref 131a

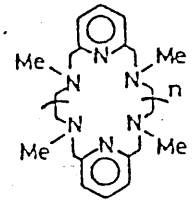

I (n=1)

II (n=2)

ref 131b

FIGURE 31.

LARGE POLYAZA CYCLOALKANES.

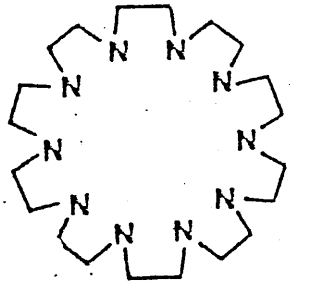

FIG.31-1

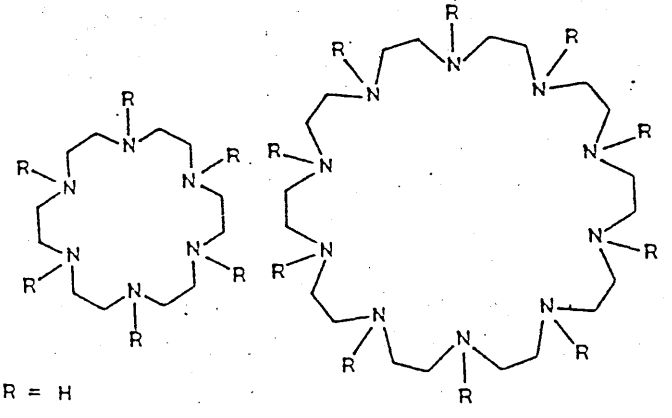

R = H

R = n-$C_{11}H_{23}CO$-

R = n-$C_6H_{17}O$- 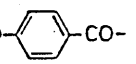 -CO-

R = n-$C_{12}H_{25}O$- 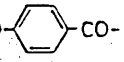 -CO-

FIG.31-2

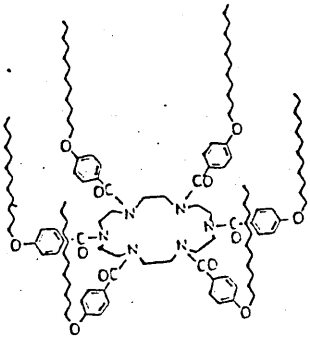

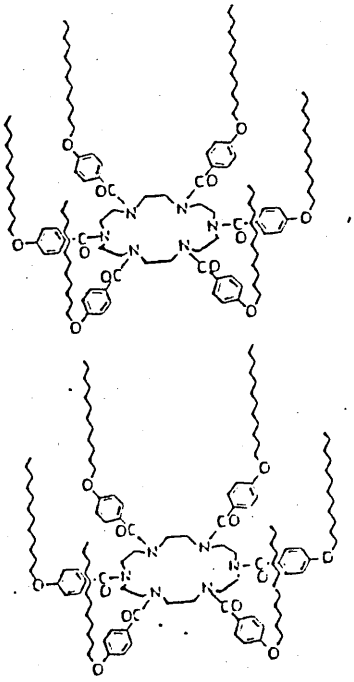

Busch obtained the saturated pentaaza macrocycle, which is the cyclam structure adapted to include the pyridyl group, Fig.29-1 by reducing the Mn(II) templated Schiff base product with an $Ni^{(III)}/Al^{(III)}$ alloy in basic aqueous solution [130a]. Moore [130b] has functionalized this system using methyl groups to give 3 related pentaaza ligands Fig.29(2-4). However all complexes formed with the functionalized ligands are less stable than the analogous tetraaza systems.

Kimura has developed his oxo polyamines to include the dioxo pentaaza ligands [130c] Fig.29-3 and has made an X-ray study of the redox behaviour of the Ni^{II}/Ni^{III} oxidation which involves significant ligand distortion.

HEXAAZA MACROCYCLIC LIGANDS.

The number of hexaaza macrocycles is ever increasing and it is difficult to review such a large area of work. Fig.30 gives a number of examples (with their references) [131]. It is also noted that these hexaaza ligands are capable of forming many binuclear complexes which can be useful in biomimicry studies where a bridging group between 2 closely held ions is required.

Acknowledgement of Sargeson's macrobicyclic sepulchrates and sacrophagines and Martell's macrobicycles O-BISTREN/BISTREN ligands is noted and these will be discussed later.

LARGE POLYAZACYCLOALKANES.

The adjective 'large' has been used to describe polyaza cyclo-alkanes having more than 6N donor atoms [132]. They are interesting ligands because owing to the greater number of donor atoms they can form polynuclear metal complexes in which the M^{+}-M^{+} interactions can be studied and because they are polybasic making the protonated forms suitable for anion coordination.

Paoletti has synthesized [24ane N_8][132], [27ane N_9][133], [30ane N_{10}][134], [33ane N_{11}][135] and [36ane N_{12}][136] containing 8,9,10,11 and 12 N donor atoms respectively. Fig.31-1 shows the general structure of

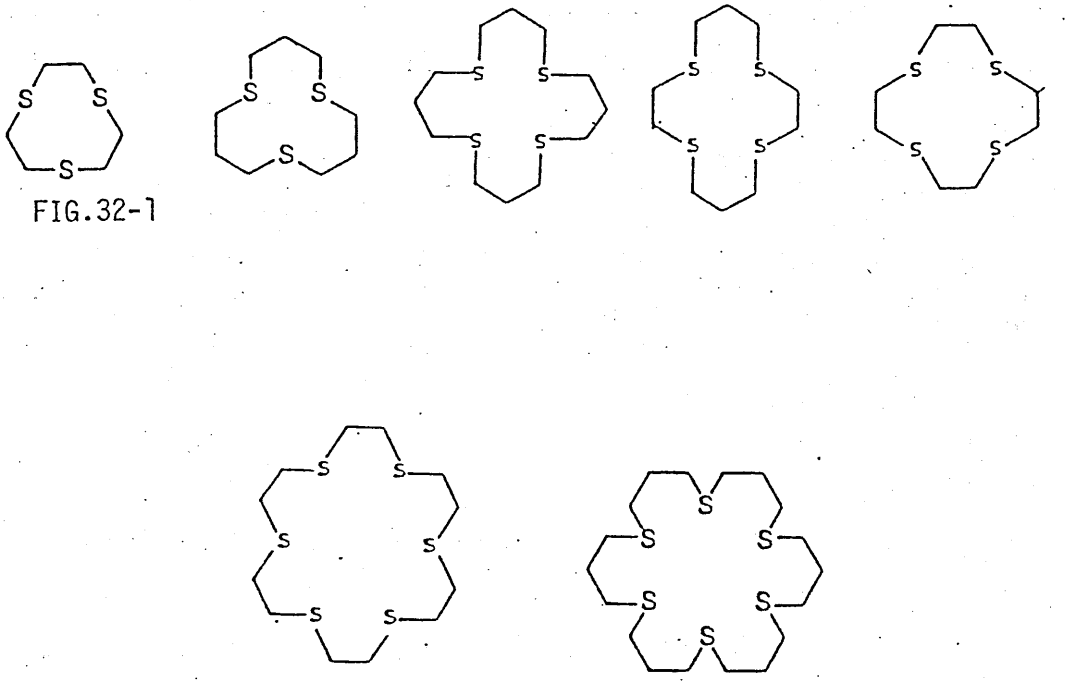

FIGURE 32. THIOETHER ANALOGUES OF THE POLYAZA SYSTEMS.

these systems. The basicity constants show that the macrocycles behave as relatively strong bases in the first protonation steps and as a weaker base in the later steps which can be explained in terms of charge repulsion effects [137,128]. Stable binuclear complexes with Cu(II) are obtained for N_8, N_9 and N_{10} ligands while the 2 higher members of the series form stable trinuclear species. Their complexation of the anions $[Fe(CN)_6]^{4-}$ and $[Co(CN)_6]^{3-}$ did not give evidence of selectivity with respect to the size of the macrocyclic cavity. This is consistant with strong interaction, mainly coulombic in nature, between the anion and the protonated second sphere ligand.

Lehn [139] has poly-N-acetylated macrocyclic polyamines [18]-N_6 and [30]-N_{10}, Fig.31-2, the products of which form Langmuir monolayers in which the macrocycle lies flat on the water surface while the alkane chains sit upright in the compressed film.

There are various analogues of the polyaza systems. The crown ethers are the oxygen analogues which are well known and established. Fig.32 shows the thioether anologues which due to the π acidity of the sulphur donors have tended to favour lower oxidation states often stabilizing M^+. Indeed Cooper [140] found that the $9S_3$ ligand, Fig.32-1 was able to stabilize monomeric Rh(I) that had prooved elusive by virtue of the tendancy of the Rh(II) complexes to dimerize and/or disproportionate to Rh(III)/Rh(I). Schroder [141] has studied the tetrathia systems with respect to Pt(II) and Pd(II) binding and their subsequent carbon monoxide and hydride insertion reactions at the metal template.

FIGURE 33.

THE DEVELOPMENT OF MIXED DONOR MACROCYCLIC SYSTEMS FOR METAL-ION DISCRIMINATION

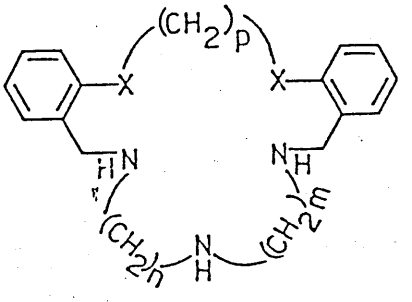

(1)

X	m	n	p
C	2	2	1
O	2	2	2
C	2	3	2
O	3	3	2
O	2	2	4
S	2	2	1
S	2	2	2
S	3	3	2

FIGURE 34.

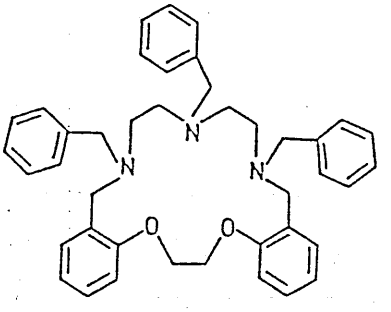

MIXED DONOR SYSTEMS.

The systems discussed thus far have been homoleptic macrocycles however the interactions of metal ions with O-N mixed donor macrocycles has been the subject of a range of recent studies. Systems having endogenous groups represent a large group of these mixed donor macrocycles and will be discussed in a later section.

Lindoy has taken 3 approaches in developing mixed donor macrocycles for metal ion discrimination.

Firstly **Dislocations**[142] occur when the gradual change of properties along a ligand series induces a sudden change in the coordination geometry for the complexes of adjacent molecules. The occurrence of such a dislocation can form the basis for discriminating between these ions. Using the ligand series shown in Fig 33 Lindoy examined the complexation behaviour of Ni(II), Zn(II) and Cd(II) and for both Zn(II) and Cd(II) dislocation behaviour (i.e. discrimination) was observed [143]. Other such studies have been carried out [65a,144].

Secondly he has investigated metal ion complexation across a matrix of related mixed donor macrocycles such as those in Fig.33, searching for stability maxima at different points of the matrix. A typical 3-dimensional matrix might exhibit variation of macrocyclic hole size along one direction, increasing macrocyclic ring substitution along another and variation of donor atom type along a third. He has used the matrix approach to achieve high discrimination for Ag(I) over Pb(II) [143].

Thirdly he has N-functionalised an O-N macrocycle with benzyl groups [145] Fig.34. The stability of the complexes formed with this sterically hindered ligand tend to be much lower than those of the respective unsubstituted parent macrocycle and only in the case of Ag(I) was there any observed enhanced stability. A study of space filling models led to the proposal that Ag(I) induces a major conformational change in the macrocycle i.e. Ag(I) alone can act as a 'trigger' for the conversion of the macrocycle to

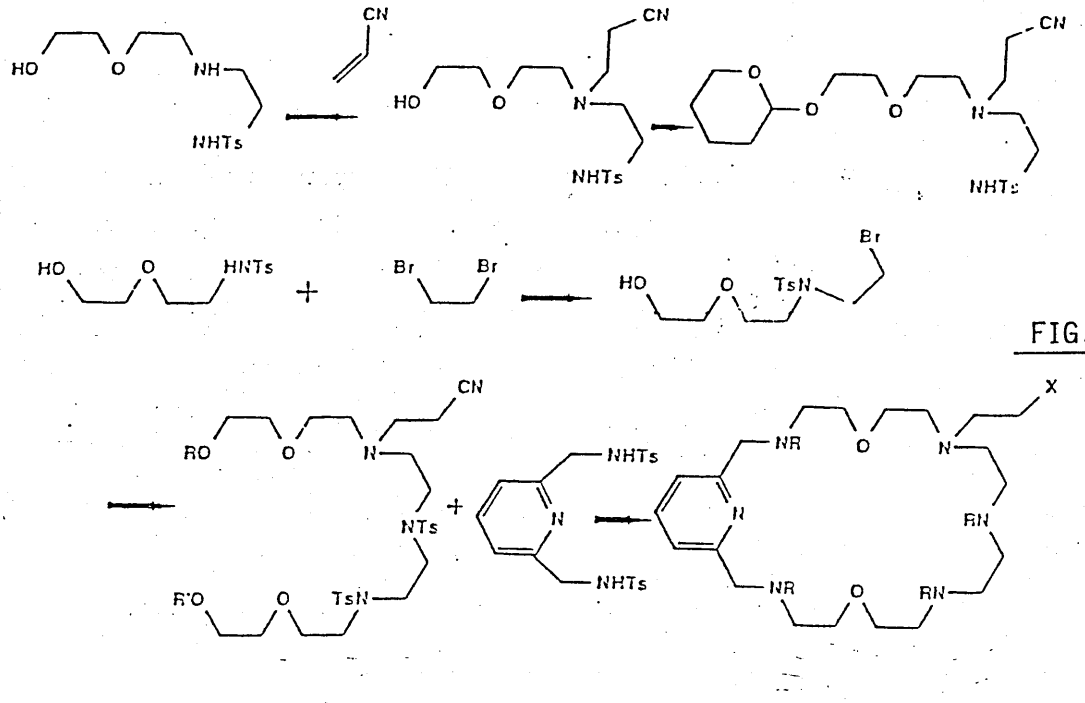

FIG.35-1

FIG.35 : A "CONVERGENT ROUTE" TO UNSYMMETRICAL N-FUNCTIONALIZED MIXED DONOR MACROCYCLES.

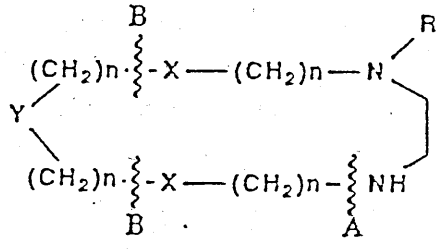

FIG.35-2.

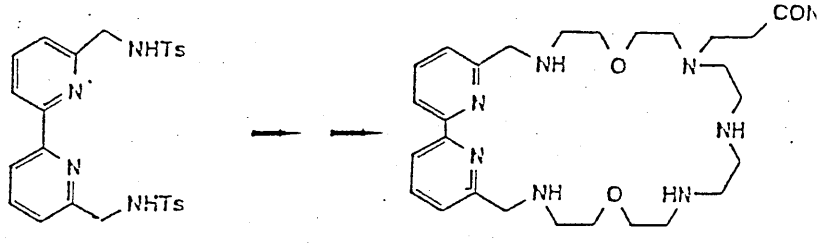

FIG.35-3

FIGURE 36.

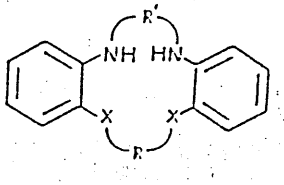

FIG.36-1

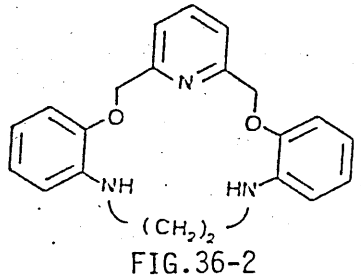

FIG.36-2

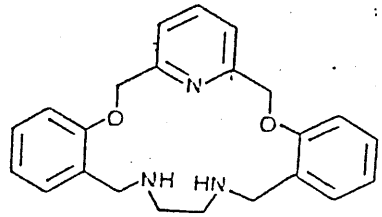

FIG.36-3

X = O,S,NH

R = various

R' = 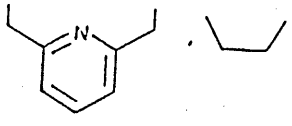

a sterically locked conformation ideally suited to this ion. If this interpretation is indeed the case, then such behaviour represents a new and potentially important mechanism for achieving metal ion discrimination which does not appear to have been investigated previously. Hancock has also examined N-O donor systems with respect to metal ion selectivity on the basis of size [146] using molecular mechanics.

Nelson has studied many examples of macrocyclic complexes from the O-N mixed donor category as part of a wider investigation of the role of the metal ion in template synthesis of such macrocyclic Schiff base systems [30,147]

Mertes [148] has recently described a "convergent route", Fig. 35-1, for the synthesis of unsymmetrical N-functionalized mixed donor macrocycles that is potentially applicable for the synthesis of a wide variety of macrocycles of differing ring size and heteroatom substitutions. The bond disconnection shown in Fig.35-2 highlights two advantages of the method. The western half of the macrocycle can be varied in the cyclization (step 8) leading to a variety of ring sizes and substituents X. The eastern half is prepared conveniently in a convergent sequence (A) that employs, in the examples given, the cyanoethyl group as the pendant functionality. Furthermore, the length of the eastern section can be readily varied to give different ring sizes and heteroatom substitutions (Y) e.g Fig. 35-3.

Fenton has contributed to the development of metal ion selective ligands via mixed donor macrocycles , and has studied the selectivity of the ligands in Fig.36(1-3). The inclusion of both strong and weak donors coupled with various chelate ring sizes and flexibilities in macrocyclic systems is likely to effect discrimination between metal ions. Such discrimination is usually structurally based, there being one or more donor atoms nonbonded and/or a different complex conformation of the ligand. This can result in an energy difference between the complexes, hence one metal complex is stabilized thermodynamically with respect to another.

Some metal ion discriminization has been observed with ligand 2 in Fig.36. The Ni(II) complex is destabilized relative to the copper (II) complex due

FIGURE 37 MIXED DONOR MACROCYCLES PROVIDING THE SOFT "S" ATOM DONOR.

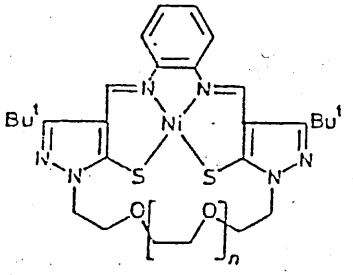

$n = 1$
$n = 2$
$n = 3$
$n = 4$
$n = 5$

FIG.37-1

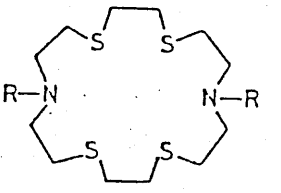

FIG.37-2 : R = H

FIG.37-3 : R = Me

N_2S_4-Donor Macrocycle

FIGURE 38.

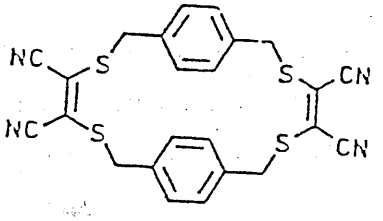

FIG.38-1

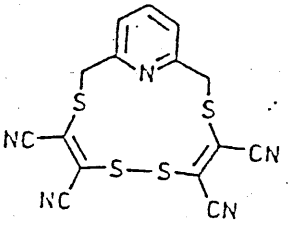

FIG.38-2

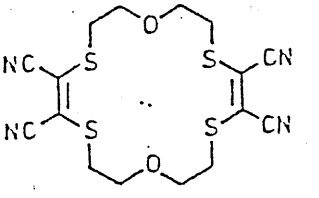

FIG.38-3

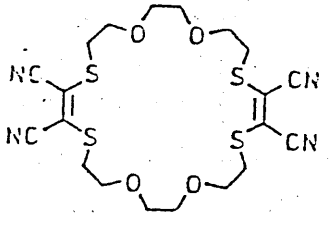

FIG.38-4

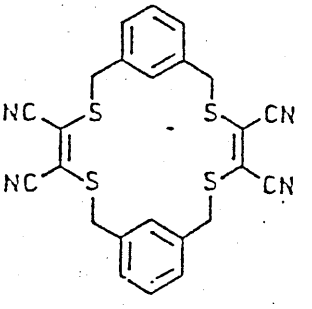

FIG.38-5

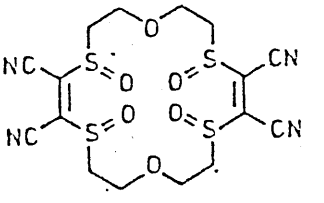

FIG.38-6

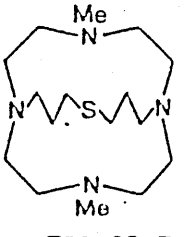

FIG.38-7

to the non-coordination of one of the ether-oxygens; there is also a difference in the macrocycle conformation [65a].Ligand 3, which has a larger cavity and is more flexible than 2 (Fig.36), can form complexes with Mn(II), Co(II), Ni(II), Cu(II), Zn(II) and Cd(II). Solution studies indicate a variety of available coordination modes dependant upon both the metal and anion present - these results are supported by X-ray crystal structures [149].

Many of Lehns early cryptands were all N-O donor systems and there is a recent review article on the synthesis of these aza-crown macrocycle systems [150]. However there are now various other mixed donor systems offering, N-S, N-S-O and N-P donor atoms.

The macrocyclic ligands containing thiolato functions are still rare. However because the thiolato function can be expected to be an effective mediator of steric and electronic effects these systems have promising applications as chemical sensors.

Becher [151] has reported an efficient synthetic route to a series of ligand systems in which a soft donor site is combined with a hard polyether site via 2 hinging central thiolato functions Fig.37-1. Where n=2 a heterobinuclear Ni(II)/Th(I) complex has been formed.

Schroder and Lavery [152,153] have developed a series of S_4N_2 ligands Fig.37(2,3) which balance the redox properties of the 2 opposing donor types i.e. N donors stabilize higher oxidation states of transition metal ions probably due to the largely σ donor nature of the bonding effectively stabilizing the large +ve charge on the metal centres. The π acidity of the thioether donors has tended to favour lower oxidation states often stabilizing M^+. Both mononuclear and binuclear species can be generated with Pt(II) and Pd(II). Mononuclear complexes are formed with the 1st row transition metals Mn(II) to Zn(II) by 37-2. The Cu^{II}/Cu^{I} reversible redox change was at $E_{½}$ = -0.31V and no Cu^{I} complexes with 37-2 were isolated . The Cu^{II} complexes of the methylated ligand had a reversible change at $E_{½}$=0.06V assigned as the Cu^{II}/Cu^{I} couple by esr. The large differences in the reduction potential for the nonmethylated and methylated ligands

FIGURE 39 HETEROTOPIC LIGANDS.

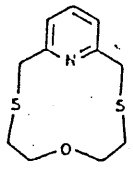

FIG.39-1

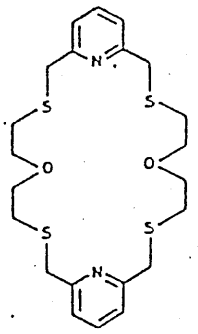

FIG.39-2

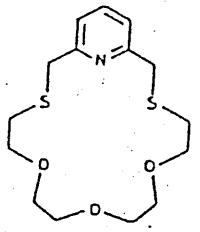

FIG.39-3

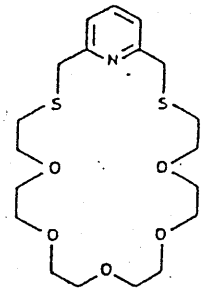

FIG.39-4

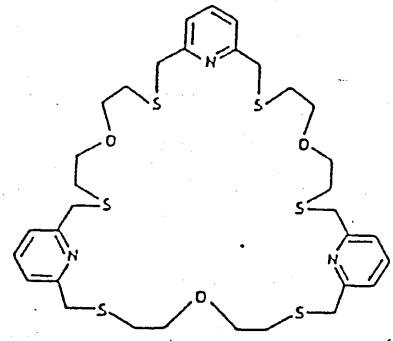

FIG.39-5

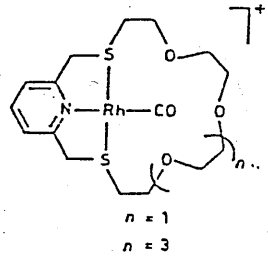

FIG.39-6

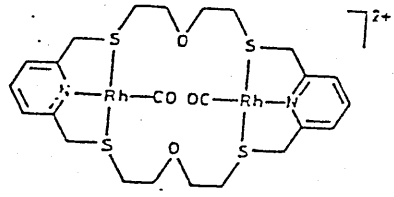

FIG.39-7

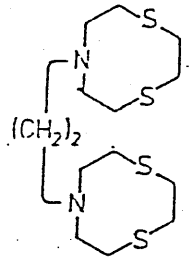

FIG.39-8

FIGURE 40 AZA- AND OXAPHOSPHANDS.

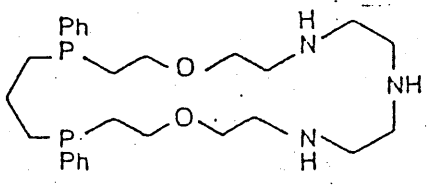

[22]$P_2O_2N_3$

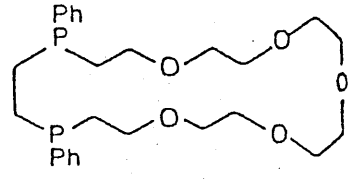

[21]P_2O_5

Cu^{II}/Cu^{I} couple is due to unfavourable steric interactions in the latter, which increases the C---N distance so reducing strain. This allows for a closer approach of the 4 thioether groups increasing the sulphur coordination to the Cu^{II} and so provides greater stability for the Cu^{I} oxidation state. This stability is reflected in the isolation of a stable binuclear Cu^{I} complex for the methylated ligand in which each Cu^{I} is bound by an N_2S_2 donor set similar to that in type 1 copper proteins.

Markl ‹154› has reported various mixed donor systems and novel tetra thio species Fig.38(1-6), while Micheloni has expanded his work on substituted tetraaza macrocycles ‹155›, to give a macrobicyclic ligand containing a sulphur atom in the added chain ‹156› Fig.38-7. This cryptand forms an extremely stable mononuclear Cu^{II} complex.

Parker ‹157› has recently synthesized heterotopic ligands containing 2 distinctly different binding sites which can co-complex 2 different metals Fig.39(1-7). Ligands 1-4 formed rhodium-carbonyl complexes e.g. 39-6 while 39-2 is sufficiently large to permit co-complexation of a coordinatively unsaturated d^8 metal centre and a Group 1 or 2 metal cation or a neutral small molecule such as CO Fig.39-7. He has also synthesized the N,N^{I} bridged bis-[9] NS_2 macrocyclic ligand 39-8 which has been prepared via a six step synthetic route - the 1:1 silver(I) sandwich of this ligand has been characterized ‹158›.

Lippard ‹159› has developed heterobinucleating oxa-aza-phospha and oxo-phospha macrocycles - [22]$P_2O_2N_8$ and [21] P_2O_5 respectively Fig.40. He has called these ligands, based on the tropocorand structures - phosphands.

INCLUSION COMPLEXES OF MOLECULAR TRANSITION METAL HOSTS. (PLUS A LITTLE EXTRA)

The analogy between host-guest complexes and enzyme-substrate complexes has directed much attention to host-guest chemistry. The term 'host-guest' was coined by Cram and Cram in the early 70's and a 'host-guest' complex may be defined simply as a complex between organic compounds that simulates the

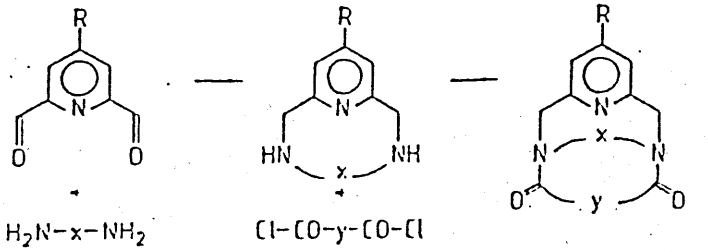

FIGURE 41 CONCAVE PYRIDINES.

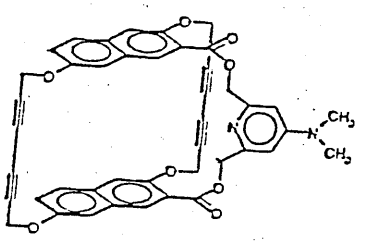

FIG.42-1

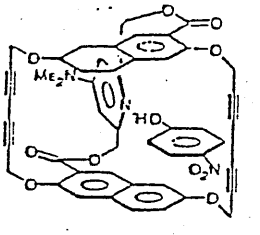

FIG.42-2

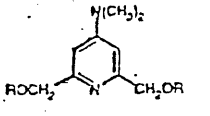

FIG.42-3

FIGURE 42 CONCAVE FUNCTIONALITY : DESIGN OF A PHENOL STICKY HOST.

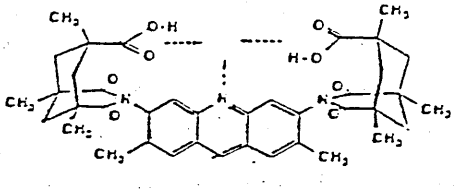

FIG.43-1

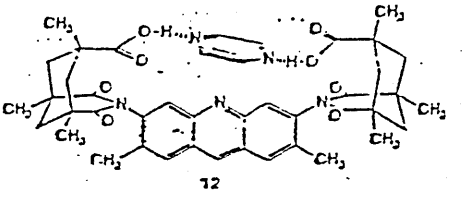

FIG.43-2

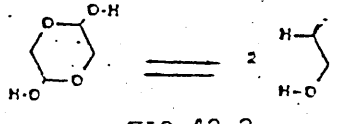

FIG.43-3

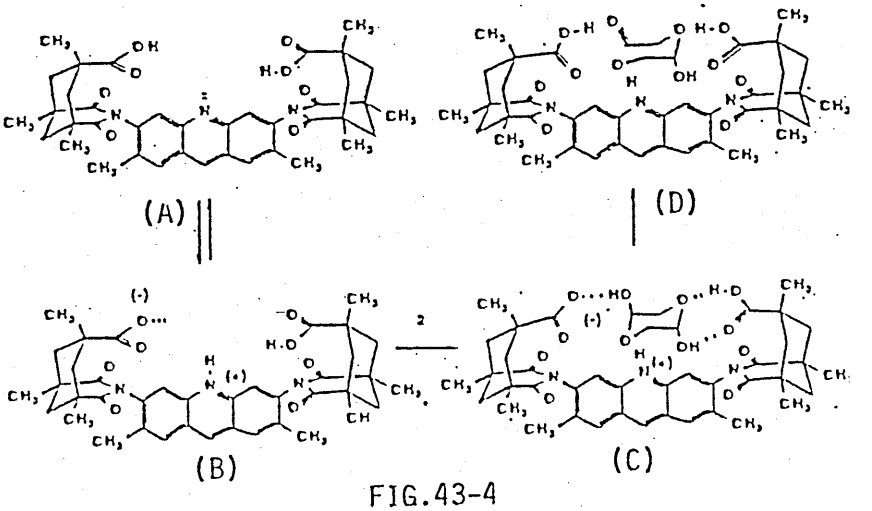

FIG.43-4

substrate selectivity of enzymes [160]. Such interactions imply a phenomenon described as molecular recognition. Since the guest assumes a site within the host during host-guest complexation, the concave surface of a host complements the convex surface of a guest [161] or as Cram has stated " a host is characterized by its employment of converging binding sites while a guest incorporates diverging binding sites."

Coordination chemists have been aware of the importance of convergent binding sites for many years and so many groups have taken up the challenge of designing molecules with the reactive centre, e.g. a basic centre, on the inside. Luning has synthesized macrobicyclic concave pyridines [162]. Fig.41. Their basic properties are determined by the whole molecule and the macrobicyclic pyridines showed larger basicities than the macrocyclic or open chain compounds. Whitlock constructed a host molecule [163] Fig.42-1 possessing a phenol sticky [164] cavity. The host was designed to test the idea that a concave (inwardly pointing) functionality, e.g. 4-(dimethylamino) pyridine, would exhibit guest "stickiness" in non aqueous media. The host is formed as a 2:1 mixture of di-host and its meso isomer, and the former binds certain phenols e.g. p-nitro phenol very tightly Fig.42-2 due to a high degree of cooperativity between hydrogen binding and intercavity interactions. The prehost species Fig.42-3 exhibits no complexation behaviour. J.Rebek [165] has examined a series of rigid structures in which 2 carboxylic acid groups converge to define a molecular cleft. Using nmr methods he was able to show that only where molecules were of complementary size, shape and functionality, would they bind within the cleft Fig.43. When pyrazine was accepted as a guest (Fig.43-2) into the molecular host, the interior protons moved upfield by >0.5ppm. These shifts were rationalized by the 2 point binding of pyrazine postulated in Fig.43-1 in which the ligands interior protons protrude into the strongly shielding regions of the pyrazine aromatic moiety. Using various benzo derivatives of pyrazine the recognition of molecules having appropriate size,shape and complementary functionality was clearly demonstrated. This molecule has been shown to catalyse a hemiacetal cleavage of the type shown in Fig.43-3 by the mechanism shown in Fig.43-4. Binding of the hemiacetyl function to a carboxylic acid of Fig.43-4a brings the other hemiacetyl into contact with both acidic and basic groups. The latter are poised for general acid-base

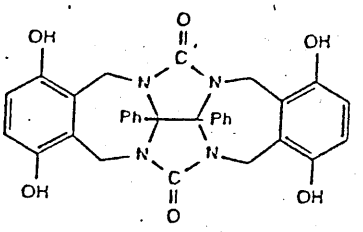

FIG.44-1

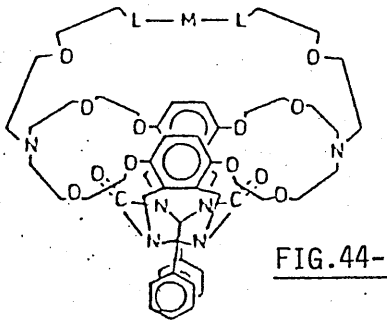

FIG.44-2

FIGURE 44 BASKET-SHAPED HOSTS

catalysis in the concerted sense suggested in Fig.43-4c,43-4d.[166]. The use of a molecular cleft offers the advantage of efficient assembly and the unique feature of convergent functional groups introduces, at least to model systems, a high degree of directionality [167] in host/guest (receptor/substrate) interactions. In large part, the directionality is due to the nature of the binding forces involved.

Noite [166] has designed the concave building block Fig.44-1 which by attaching oxa and azamethylene bridges to the 3,6 and 3'6'-positions of the xylene rings and complexing this to a metal centre gives basket shaped (Fig.44-2) complexes.

Inclusion complex formation may be thought of as occurring when a host includes a guest without covalent bond formation [169,170]. The binding forces that are present in such complexes are recognized as van der Waals attractions, ion pairing, hydrogen bonding, metal ion to ligand attractions, and/or π acid to π base attraction along with hydrophobic and solvent liberation driving forces. Many reviews exist on this area including (161,171-174).

The clathrates, zeolites, intercalcated derivatives of graphite, and transition metal chalogenides are examples of solid state inorganic host molecules while the cyclodextrins, crown ethers, ionophores, cyclophanes, cryptands and their many related structures are the molecular organic hosts.

Host guest complexes provide the opportunity to study the various possible modes of interaction and to learn about the regio- and stereoselective interactions that may accompany inclusion complex formation. The roles of such interactions in catalytic rate enhancement are also of vital interest in such studies.

The traditional approach to host-guest chemistry lacks the ability to model metalloenzymes in which the metal atom is critical to the enzyme function. However interest in the field of molecular host-guest chemistry for those systems in which a transition metal ion is incorporated into the host

molecule is growing as it may open the door to many new areas of chemistry: modelling of metalloenzyme active sites may lead to the development of new kinds of transition metal catalysts. Recalling that the host accomodates the guest without covalent bond formation, the transition metal can therefore be left coordinatively unsaturated leaving sites available for coordination to other molecules such as dioxygen i.e. the presence of the transition metal exerts an effect on the binding of further substrates by its host. When it functions in this way, the transition metal ion confers a sort of 'double recognition' capability on the host compound. This is known as the cascade effect <175>. It follows that the metal ion may affect both the fundamental process of inclusion complexation and the catalytic action of these hosts. Different metal ions can offer different properties (magnetic, uv-vis interactions etc) and this allows for varying abilities of participation in redox reactions of a catalytic nature. In the limit we can visualize doing highly oxygen and moisture sensitive chemistry within a protected cavity of a complicated host molecule that is otherwise exposed to ambient conditions.

After a brief consideration of some of the essential elements of designing host-guest complexes and the methods of studying them, I intend to review some of the more common families of transition metal molecular hosts followed by a discussion of anion and cation receptor systems.

ESSENTIAL ELEMENTS OF DESIGN / DESIGN CONSIDERATIONS.

Selectivity, thermodynamic stability and the kinetics of complexation are important receptor features. So too are the solubilities of substrate, receptor and complex. All of these can be controlled, to some extent, by structural and electronic effects and it is therefore important to optimize the conditions which achieve the design goal.

In order to design a molecular host/receptor capable of selectivity it is necessary to consider which functional group(s) can help bring about the required discrimination. It is then important to be able to build that functionality into the basic receptor framework. The need for selectivity

FIG.45 A SUMMARY OF THE CONSIDERATIONS AND FACTORS THAT INFLUENCE THE DESIGN OF A SPECIFIC FUNCTIONAL RECEPTOR.

DESIGN CONSIDERATIONS.

(1) BINDING AND ENVIRONMENTAL FACTORS.

(A) ELECTRONIC EFFECTS - interactions - nature of which gives measure of control over substrate type that can bind.
e.g. ion-ion, ion-dipole, ion-induced dipole.

- substrates - - must consider size, charge density, hardness.

- types of binding site -

- number of binding sites - impose a minimum cavity size - therefore distinguish between various sized substrares.

(B) STRUCTURAL EFFECTS - shaping groups - to impose conformational and steric barriers that affect complexation, stability and selectivity.

- conformational mobility - rigidity of cavity, discrimination and kinetic stability.

- external control of conformation - using switches e.g. photocontrol (*) redox control to bring about conformational transformation to effect selective binding.

- binding site topology -

- binding site access - steric exclusion.

- layer properties - solubility in aqueous or organic media.

(C) COUNTER ION AND MEDIUM EFFECTS - counterions -

- solvent - weaker donor solvents allow higher complex stabilities and slower exchange dynamics.

varies according to the receptors end use. The more selective a receptor needs to be towards a member of a group of similar substrates, the higher the degree of complementarity between substrate and receptor there needs to be. The design process will often then become limited by synthetic feasibility.

Considerations and factors influencing the design of a specific functionalized receptor are given in Fig.45. For a fuller discussion on the design of receptors useful review references include 175,176.

METHODS FOR STUDYING TRANSITION METAL, HOST GUEST COMPLEXES.

The methods for studying transition metal host-guest complexes are the same techniques used in studying organic host molecules <177> and include nmr, uv and vis absorption, fluoresence spectroscopy esr, spin labels, titrations, polarographic measurement, cyclic voltametry, circular dichroism and X-ray.

NMR has been used extensively in the detection of the formation of inclusion complexes as well as measurements of their binding properties. The host protons directed into the cavity will be affected by inclusion of a guest and their signal will be shifted as the guest molecules are encapsulated by the host. The technique has proven extremely useful in a number of studies with several different host molecules <178-180>.

Fluoresence measurements have been widely used in the study of host-guest complexing e.g. when simply dissolved in an aqueous solution, 1,8-ANS exhibits only weak fluoresence but marked enhancement is observed when complexed within the cavity of the host molecule <181>. These results suggest <182> that the guest has been moved from the external polar medium into the relatively non polar environment of the cavity within the host. It has also been used extensively for studying inclusion of the lanthanide ions, especially Eu^{III}, by cryptands - this is discussed later.

Electronic absorption spectra have also been used to detect transition-metal, host-guest interactions in solution and such measurements have been widely used in the determination of the related reaction rates and dissociation constants. Circular dichroisim spectra have revealed conformational changes upon addition of a guest into a solution containing a cyclodextrin having an appended porphyrin.

In the interesting cases where a guest is coordinated between two metal centres within a host molecule, esr spectra are uniquely informative, showing the presence or absence of antiferromagnetic coupling between 2 paramagnetic centres. X-ray studies provide the ultimate demonstration of the presence of guests within hosts in the solid state and thus has been of particular significance for systems involving guest molecules bridging between pairs of metal atoms as is discussed later.

CRYPTANDS.

The cryptands, developed by Lehn [11,12], are selective in the formation of inclusion complexes, and these inclusion complexes, called cryptates, are very stable. The selectivity and stability of the complex may be intimately controlled through the ligand structure by increasing or decreasing the size of the cavity and by regulating the number and nature of the binding sites. A number of reviews deal exclusively with cryptand/cryptate (macrobicyclic) systems [174,183,184].

The synthesis of the cryptands is often more difficult than the closely related crown ethers because of their bicyclic structure and the increase in the number of required synthesis steps [18,21,48]. The coordination chemistry of the cryptands show important properties of the host. Thus the early cryptands with their polyether strands linked at a nitrogen bridgehead gave very stable complexes with the alkali and alkaline earth metal cations [18,185], with the inclusion of the ion right into the molecular cavity of the cryptand [186,187].

There are now many polyaza cryptand ligands which, unlike the crown ethers, are able to form stable mono and binuclear complexes with the transition

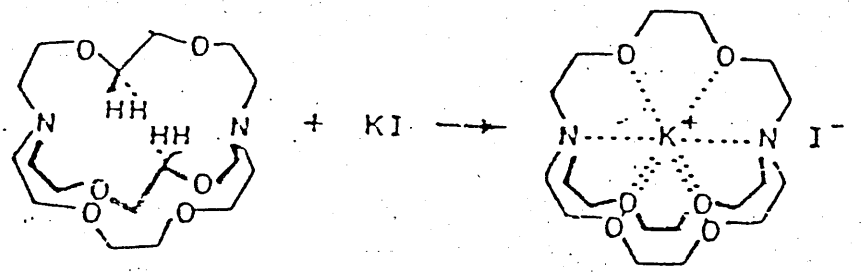

FIG.46 REORGANISATION OF A CRYPTAND UPON COORDINATION TO POTASSIUM ION.

metal ions. This is particularly relevant in the area of biomimetic studies because of the number of natural compounds whose correct functioning relies on the presence of a metal ion or pair of metal ions in a nitrogen donor environment.

The X-ray structures of these hosts do not usually show the presence of a cavity in the absence of a metal ion or guest. Instead these cavities are produced by the folding outward of their inward parts during complexation of a guest [188] (Fig.46) and the overall geometry of these molecules has a pronounced effect on the stabilities of the host-guest complexes and coordination complexes due to the cryptate effect [184].

Those macropolycyclic structures that possess two receptor sites and which can therefore include 2 metal cations or guest molecules are known as dinuclear cryptates. Again, these metal species are included without covalent bond formation, leaving them coordinatively unsaturated and so able to accept small bridging anions or molecules.

There is much interest in dioxygen carriers for the chemical separation of oxygen from the air and other gaseous mixtures. Dioxygen carriers considered good candidates for oxygen separation and transport (which require repeated recycling between the oxygen free complex and its oxygen adduct) are generally those that have low oxygenation constants.

Martell and Lehn have developed a series of transition metal cryptates, using the ligand O-BISTREN [189-192] Fig.47-1, which are stabilized by coordination of μ-hydroxo groups [192] and in the case of Co(II) by the formation of (μ-hydroxo) (μ-peroxo) bridged species [191] Fig.47-2. The binding of an OH^- group to the bimetallic Co(II) centre is larger, at $10^{11.56}$, then the chloride ion. The unusual stability of the binuclear hydroxide complex can be appreciated by comparison with the hydroxide binding constant of the mononuclear cryptate $[CoL]^{2+}$, which at $10^{3.36}$, is 8 orders of magnitude lower. This is an example of cascade binding [175] i.e. where the primary ligand O-BISTREN binds 2 Co(II) ions in such a way as to induce secondary binding of dioxygen between the metal ions.

FIGURE 47.

Dicobalt–O-BISTREN Cryptate as a Reversible Dioxygen Carrier for Oxygen Separation and Transport

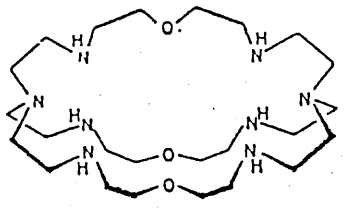

FIG.47-1

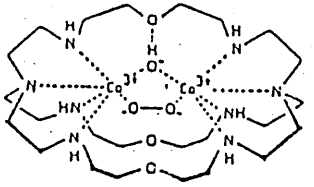

FIG.47-2

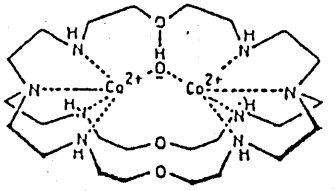

FIG.47-3

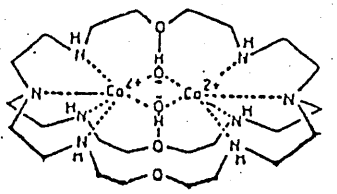

FIG.47-4

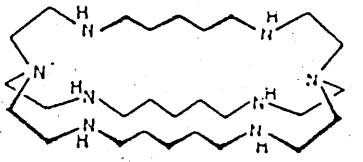

FIG.47-5

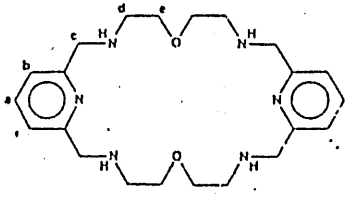

BISBAMP

FIG.47-6

BISDIEN

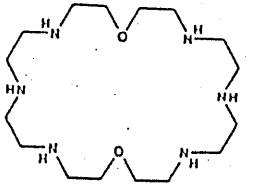

FIG.47-7

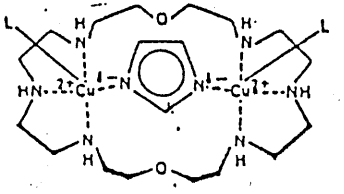

FIG.47-8

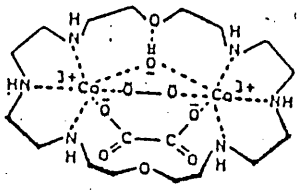

FIG.47-9

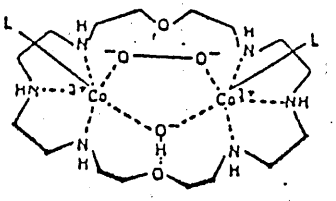

FIG.47-10

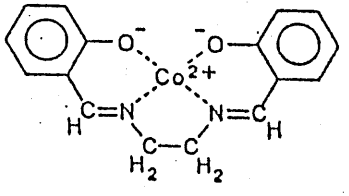

FIG.47-11

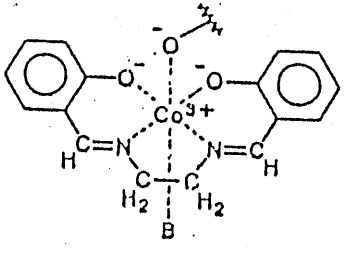

FIG.47-12

More recent studies [193] show that the simple binuclear complex $[Co_2(O\text{-}BISTREN)]^{4+}$ is never more than a minor species in aqueous solution but stabilization by hydroxide ion bridging results in its conversion to the major hydrolyzed species. $[Co_2(OH)(O\text{-}BISTREN)]^{3+}$ and $[Co_2(OH)_2(O\text{-}BISTREN)]^{2+}$ at neutral and high pH Fig.47-3 and Fig.47-4 respectively. The dioxygen complex formed from these latter species is the dibridged μ-(hydroxo)-μ(peroxo) type $[Co_2(OH)(O_2)\text{-}(O\text{-}BISTREN)]^{3+}$ Fig.47-2 which has an unexpectedly low oxygenation constant ($K_{O2}=47[2]/47[4]$ $\rho_{O2}=10^{1.2}$ atm^{-1}) compared to Co(II) complexes of comparable polyamines such as tren itself [194]. This observed low stability is rationalized by steric crowding of the dioxygen in the cryptate cavity.

It was suggested [192,195] that the special nature of the OH bridge could be due to stabilization through hydrogen bonding to one or more ether oxygens of the cryptand. This hypothesis was tested by measuring the OH binding constants for the macrobicyclic cryptand having a structure similar to that of O-BISTREN but without the bridging ether oxygen i.e. C-BISTREN [196] Fig.47-5. The OH binding constant of the binuclear C-BISTREN copper cryptate with a log value of 6.2 is about 4 orders of magnitude weaker than that of O-BISTREN and is a more reasonable value for a bridging hydroxide between two closely spaced Cu(II) ions. This superior stabilization of the bridging hydroxide group is likely to be due to hydrogen bonding to one of the bridging ether groups.

It has been proposed that type III copper proteins contain 2 Cu(II) ions bridged by a hydroxo bridge [197]. The X-ray structure [198] of deoxyhemocyanin shows that the 2 copper ions are each surrounded by 3 histidine ligands. The bridging oxygen ligand is inferred from the magnetic interaction while a charge transfer band [199] indicates the presence of the peroxo group. In bovine superoxide dismutase an imidazolate ion acts as a bridge between Cu(II) and Zn(II) [200]. Synthetic ligands with an appropiate arrangement of donor atoms have been prepared to mimic the structure of these proteins and it has been possible to show the presence of hydroxo, imidazolato, azido, and alkoxo bridges between metal ions. (These are discussed later) Martell has synthesized 2 structurally related macrocycles BISBAMP [201] and BISDIEN [202] Fig.47-6, Fig.47-7

respectively. In all cases the complexes of BISBAMP were less stable than BISDIEN which is attributed to the lower basicity of the former ligand [201].

The binucleating tendancy of BISDIEN is relatively weak compared to O-BISTREN due to the latters higher degree of preorganization. However the tendency of BISDIEN to form binuclear complexes is greatly strengthened by a combination of its metal complexes with appropriate bridging groups, such as imidazole with Cu(II), to form the complex shown in Fig.47-8 and dioxygen with Co(II) to form the peroxo bridged complex 47-9. The oxygenation constant of the dicobalt (II)-BISDIEN complex is nearly 3 orders of magnitude greater than that of O-BISTREN in spite of the large number of basic nitrogen donors in the latter complex (log k's for oxygenation of Co(II) complexes usually vary linearly with the basicities (Σpk's) of the donor groups coordinated to Co(II) [194]). This unexpected result was attributed to steric crowding of dioxygen in the cavity of the binuclear Co(II)-O-BISTREN cryptate [189,203]. Martell used this dioxygen complex of BISDIEN to study the rate of oxidation of the oxalate anion by the coordinated dioxygen[204,205] Fig 47-10 shows the resulting (μ-oxalato)-dicobalt(11)-BISDIEN-dioxygen complex. From the results they proposed a mechanism for the oxidation of bound oxalate by dioxygen involving electron transfer through the metal ions which have low energy orbitals capable of accepting the electron, thus providing pathways for the electron transfer process. Direct electron transfer from oxalate to peroxide is not considered likely because of their negative charges leading to coulombic repulsions which would space them far apart in the macrocyclic complex.

Martell has not only considered cryptand and macrocyclic structures but he has also investigated the stabilities of the Co(II) complexes of open chain polyamine Schiff bases and their dioxygen adducts[206,207] Fig 47-11,47-12. Four coordinate Co(II) chelates, Fig 47-11. do not by themselves bind oxygen strongly, but their adducts with suitable monodentate Lewis bases readily bind oxygen under suitable conditions of temperature and oxygen pressure. This results from the additional stablization of the Co(11)-dioxygen bond through increased electron density at the metal centre

FIGURE 48 SARGESON'S SYSTEMS.

STABLE HEXAMACROBICYCLIC CAGE LIGANDS.

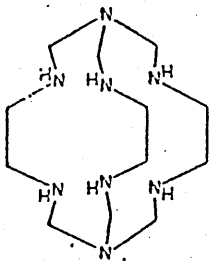

SEPULCHRATE

FIG.48-1

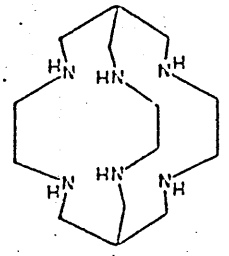

SARCOPHAAINE

FIG.48-2

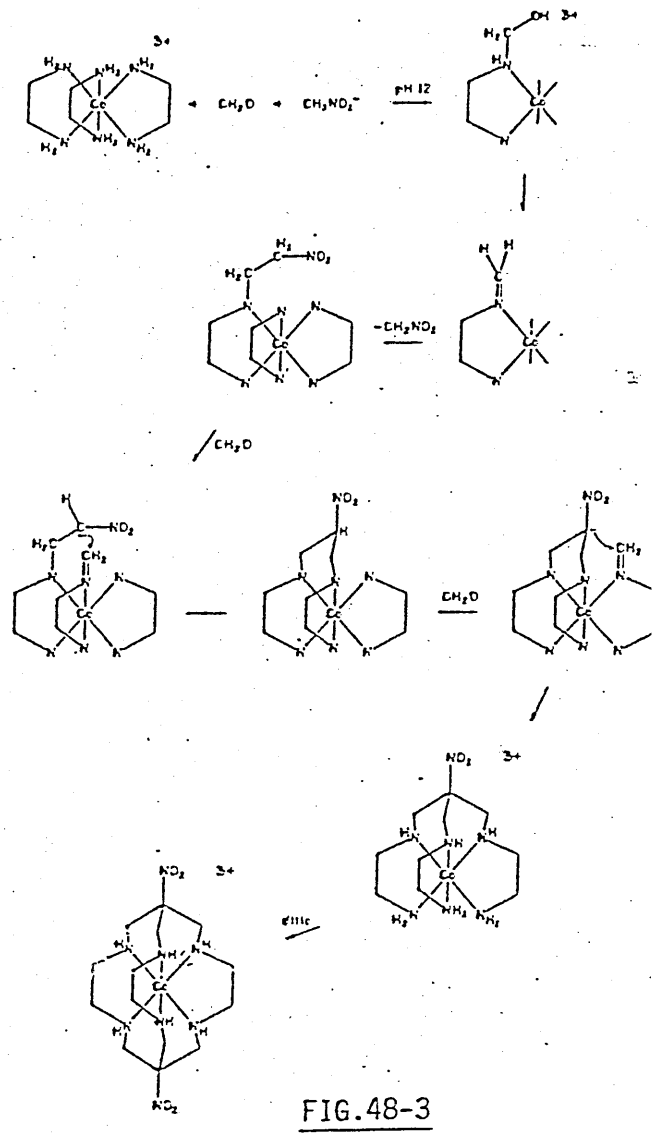

FIG.48-3

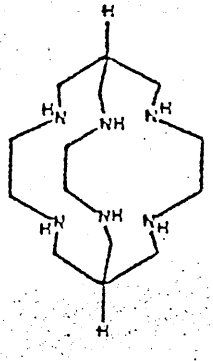

FIG.48-4

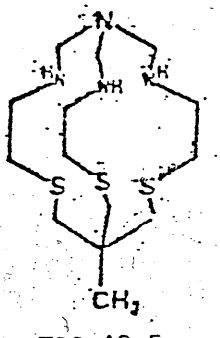

FIG.48-5

provided by the axial base. The dioxygen ligand binds in a position trans to the axial base. 47-12. The axial bases (B) that promote oxygenation of 47-12 may be aliphatic or aromatic amines. Pyridine and substituted pyridines are most frequently employed.

Sargeson has developed a class of polyazamacrocycles which have the capacity to encapsulate metal ions, and in particular, transition metal cations[208-210]. They are generally hexaaza macrobicyclic cage ligands and fall into 2 main groups-the sepulchrates (having a tertiary nitrogen bridgehead) Fig 48-1 and the sarcophagines (having a tertiary carbon bridgehead)Fig 48-2. The cage molecules are constructed about the metal ion by using it as a template to hold the reacting organic molecules[210,211] Fig.48-3. The templating metal can be extracted using conc. HCl or HBr at high temperatures to give the free ligands and a variety of mononuclear metal complexes have thus been able to be prepared[212]. Numerous variations for substituents can be incorporated in the apical position and these include - NO_2, NHOH, -NO, $-NH_2$, $-NH_3^+$, $-N(CH_3)_3^+$, -OH, -Cl, -Br, -I, -COOH, -COOR, $-NHCOCH_3$, -CN, $-CONH_2$, -CN, $-CONH_2$, $-CH_2OH$. These substituents give a wide range of redox potentials and other properties to the molecules. The total redox span is ≃2V which gives an impressive array of redox reagents although not all are readily accessible. For the Co(II)/Co(III) couple a span of)0.6V is observed [213], which despite the insulating organic coat, implies an electron self exchange rate of $\simeq 10^5$ fold greater than that for the parent $[Co(en)_3]^{2+/3+}$ ions [214]. This is due to the strain generated in the ligand by the encapsulation of the ion [210]

By using the broad capping strategy[215], and using tri (1,3,propanediamine) they increased the cavity size of the ligand. This species formed a Rh(II) complex giving a (III)/(II) redox potential that was substantially altered (≃+0.4V) relative to the equivalently capped, 1,2, ethanediamine based ligand [216]. The Rh(II) ion presumably is more readily tolerated in the larger cavity size of the sexidentate ligand where all the rings are 6-chelate and the Rh(II) complex therefore becomes more accessible and presumably more stable using the 2 ligands, 48-4 and 48-5 [217]. Sargeson investigated whether there was any systematic dependence of the rates of metal couple self-exchange upon the symmetry of the donor and

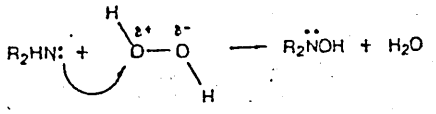

FIG.48-6

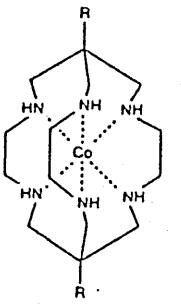

R = NO_2, Cl

FIG.48-7

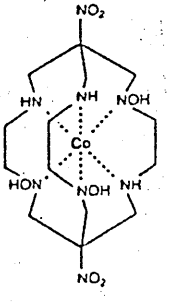

C - 3NOH

FIG.48-8

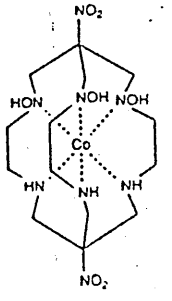

B - 3NOH

FIG.48-9

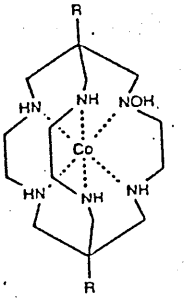

II. R = NO_2

III. R = Cl

FIG.48-10

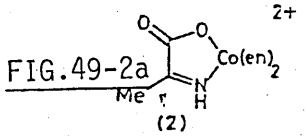

FIG.49-2a

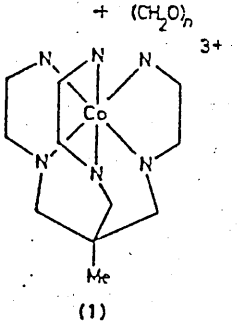

FIG.49-2b

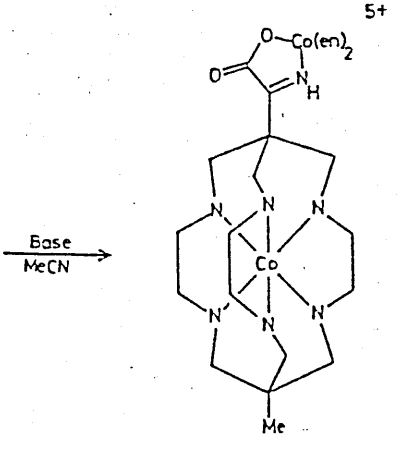

FIG.49-1

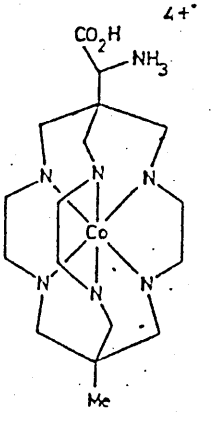

FIG.49-3

of the acceptor orbitals. Results indicated that this was not the case and that the exchange rates follow closely those predicted by the adiabatic theories of Marcus [218] and Hush [219] and that no discrepancies were detected that indicated nonadiabatic behaviour.

Secondary alkylamines are readily oxidized to hydroxylamines by hydrogen peroxide in aqueous solution (Fig.48-6) but yields of hydroxylamines are usually low due to further oxidation. Placing an electronegative substituent on the cap of the cages [220] considerably lessons the pka of the coordinated amines, while rendering them more susceptible to attack by H_2O_2 in basic solutions. Thus Fig.48-7 gives a mixture of products when treated with H_2O_2 and base. These are shown in Fig.48-8,48-9 and 48-10 and are stable at room temperature because geometry of the cage complexes allows for no further oxidation of the hydroxylamine groups which would result in the breaking of the cage structure.

Recently Sargeson has reported the synthesis of a pyruvate imine Co(III) complex [221] from which a variety of new cages have become available. Fig.49-1. In the synthesis the metal ion both activates the methyl group of the pyruvate imine, Fig.49-2a to reaction with a carbonyl function Fig.49-2b and protects the pyruvate imine functionality. The product of the reaction, Fig.49-1 contains an imine function which can undergo reduction to give a novel cage substituted amino acid Fig.49-3.

A striking example of purposeful ligand design was carried out by Busch and coworkers who designed and synthesized a new family of host molecules, called vaulted complexes, for the purpose of mimicking the ternary (enzyme:dioxygen:substrate) complex of cytochrome P_{450} [222-224]. Whilst not strictly cryptands in that they possess a permanent void/cavity they are macrobicyclic in nature and will therefore be discussed at this point Fig.50-1 represents the structure as a flat projection while Fig.50-2 represents its 3-dimensional structure. These species are cationic and contain the positively charged metal ion, coordinated to four N donor atoms, incorporated into one wall of the permanent void provided to accomodate a substrate molecule. These structures were derived from an intensely studied family of the laccunar (from Latin meaning hollow, gap)

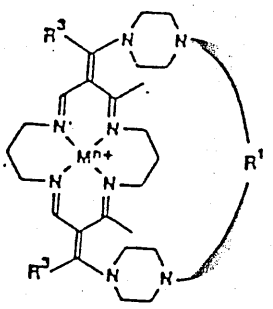

FIG.50-1

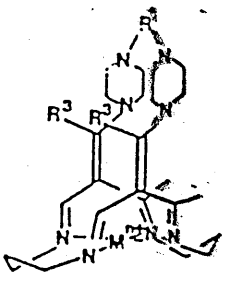

FIG.50-2

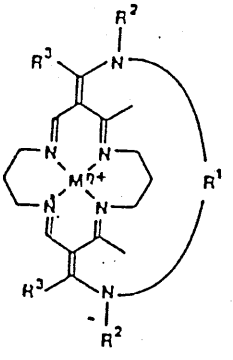

FIG.50-3

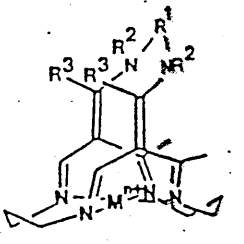

FIG.50-4

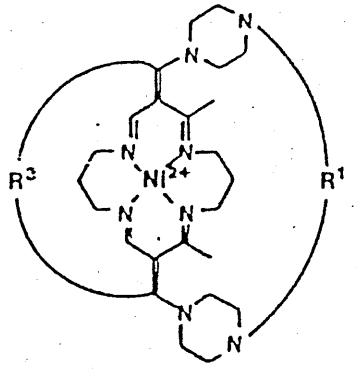

FIG.50-5

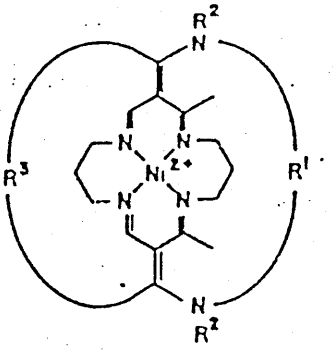

FIG.50-6

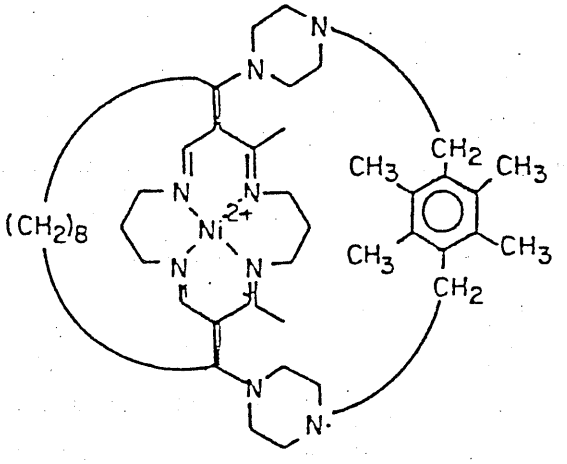

FIG.50-7

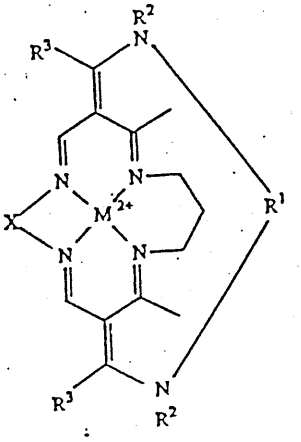

FIG.50-8

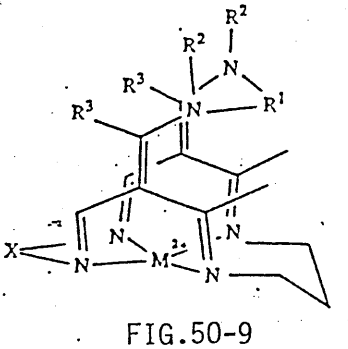

FIG.50-9

dioxygen complexes [225], Fig.50-3 and Fig.50-4, in order to provide a coordination environment that would guarantee the ability to bind oxygen. The deep saddle shape that was well established in studies of the laccunar complexes has been preserved in the structures of the vaulted complexes.

X-ray crystal structures [222,225c] of the vaulted complex having R_1 = anthracene show a cavity having dimensions from 8.24 x 8.95Å at the grand opening to 7.26x6.57Å at the opposite smaller entry. A guest molecule - acetonitrile, has been accomodated. The host provides a hospitable environment for the guest by rotating its piperazine rings so that the N atom of the acetonitrile can enjoy six nearly ideal van der Waals contacts with hydrogen atoms while aligning the π system of the nitrile group with that of the anthracene ring.

The ligands form iron and cobalt complexes that can bind oxygen. The design incorporates a "dry-cave" bound by bulky hydophobic groups on one side of the metal complex, the other being blocked by monodentate ligand or solvent. As in Martells' Schiff base polyamines [205,206] the nature and concentration of this axial ligand plays an important role in the affinity of the complex towards oxygen and so it can provide a means of regulating the uptake of oxygen [226,228]. It is the built in dry cave which permits the oxygen to bind but not oxidize the metal centre.

In a further extension of the molecular design, doubly bridged structures giving tricyclic species were synthesized Fig.50-5 to 50.7. This was achieved by combining 2 bridging processes [222]. Earlier studies with vaulted complexes have fully characterized their hydrophobically driven inclusion complexation with alcohols and phenols in aqueous media [222,229-231]. The doubly bridged designs show several advantages:-

(1) each bridging group plays a distinctive role in moderating the binding of an included species while they act in concert to increase the fractional area of the void that is bonded by hydrophobic groups.

(2) the enhanced hydrophobic nature of the guest site substantially increases the equilibrium constant for host guest binding.

(3) the reterobridge places steric constraints on the axial binding site inside the void so favouring coordination of large ligands at the external

FIGURE 50 CONTD

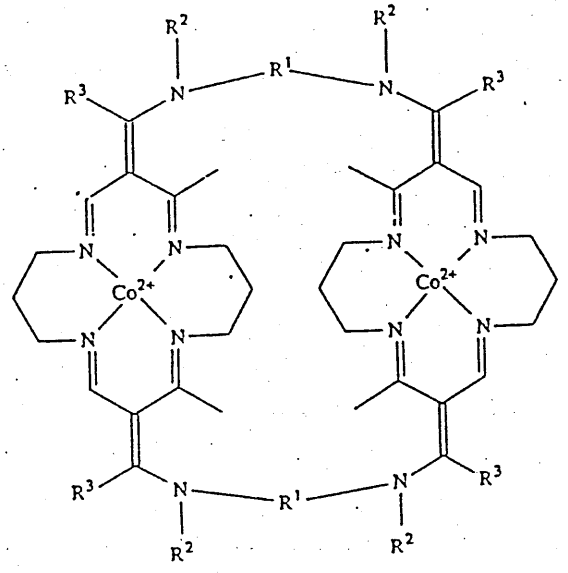

FIG.50-10

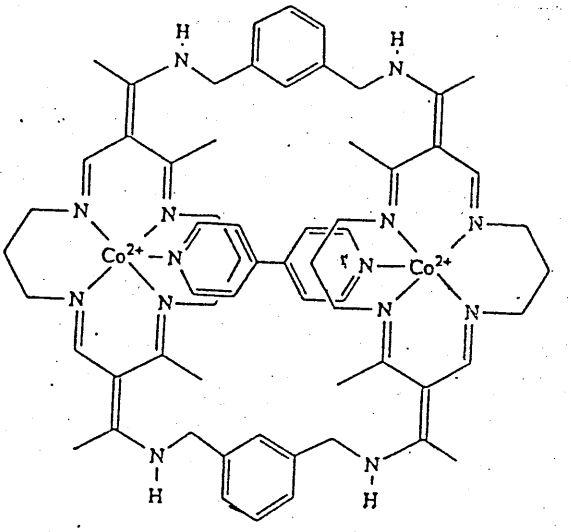

FIG.50-11

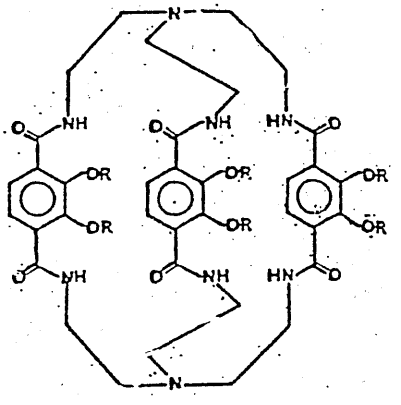

FIG.51-1

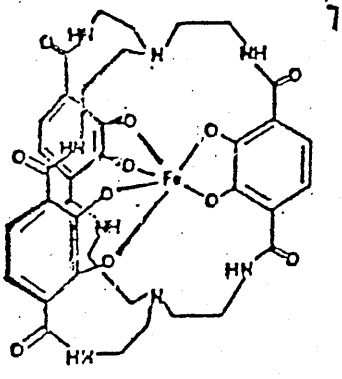

FIG.51-2

FIGURE 51 NEW MACROBICYCLIC Fe(III) SEQUESTERING AGENTS

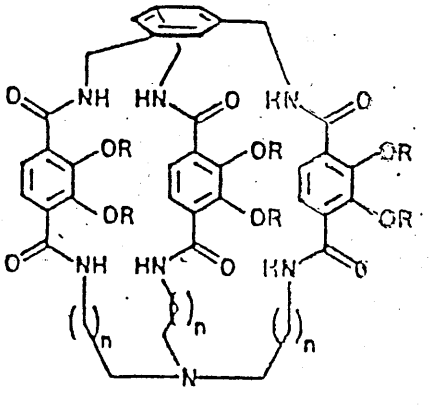

FIG.51-3

side. This helps maintain the 5 coordinate structure in the absence of dioxygen and other similar small ligands. This is obviously important since a ternary complex of the desired kind (metal chelate - substrate - O_2) requires a vacant binding site inside the void that can be used for O_2 binding.

All of the cyclidene complexes discussed so far are based on the well known 16-membered macrocyclic ligand first reported by Jager [232]. Busch has now formed the 15 membered ligand [233] Fig.50-8,9. ESR has been used to show the formation of a 1:1 dioxygen adduct. The K_{O_2} values of the 15 membered Co(II) complex (where $(CH_2)_n$: n>6) are greater with the 16 membered analogues [225a]. These results contradict the electrochemical data where the $E_{1/2}$ values of the 15 membered macrocycles are more anodic than the corresponding 16 membered macrocycle which suggests a higher K_{O_2} value for the latter. This is rationalized by the fact that the Co^{III}/Co^{II} couple is sensitive to bridge length - a relationship attributed to the importance of binding a ligand within the cavity of the oxidized member of the couple [234]. However a larger bridge is required to produce the equivalent lacuna for the derivatives of the 15 membered cyclidene. Consequently for a given bridge size the cavity is more available to the 6th ligand in the case of the 16 membered cyclidene and this stabilizes the oxidized state.

When the bridging diamine is primary, i.e. R^2=H, then a competing dimerization reaction can occur resulting in the face-to-face bis-(cyclidene) complexes [235,236] Fig.50-10. The dimers contain 2 identical metal ions separated by an intramolecular void. These dinuclear bis-(cyclidene) complexes of Co(II) react with dioxygen in 2 ways, -adduct formation and autoxidation. In the di-cobalt (II) complexes the intermetallic separation is greater than 8Å : relatively little metal-metal interaction is found (1.90-2.09 μβ/Co(II)) although the absence of hyper fine splitting in the esr spectra, observable in the mononuclear laccunar complex due to the presence of the axial nitrogen donor, may be associated with some metal-metal interaction. These face-to-face bis-(cyclidene) complexes have characteristic molecular cavities between the two metal sites that are of potential importance in various classes of inclusion chemistry. Indeed the bridging ligand 4,4'-bipyridine has been included

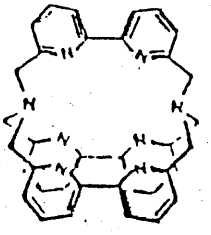

FIG.52-1

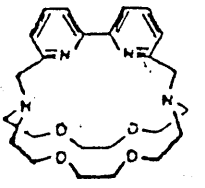

FIG.52-3

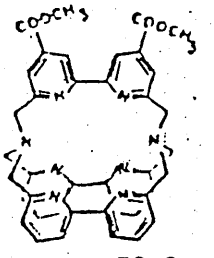

FIG.52-3

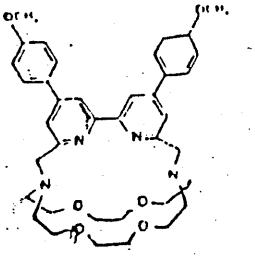

FIG.52-4

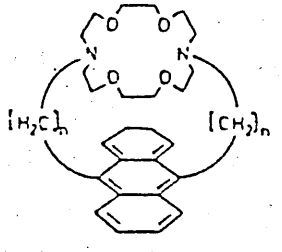

n=2 ; A22

n=3 ; A33

FIG.53-1

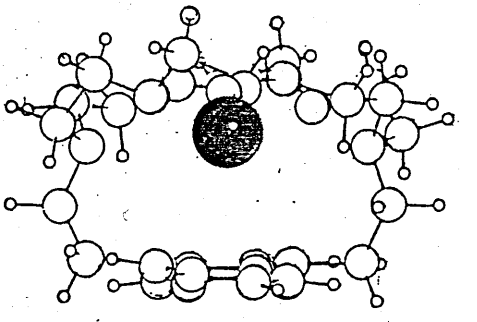

A22Tl^{+}

FIG.53-2

within the cavity of the m-xylene-bridged dicobalt bis-(cyclidene) complex Fig.50-11. This bridging group allows a small mediation of exchange coupling which is thought to be via a σ pathway. Magnetic moments gave results (2.05-2.15 μ_B/Co(II)) slightly but definitely higher than those for the host alone.

The synthesis of ligands that specifically sequester a given metal ion under physiological conditions presents a challenge to the coordination chemist. Raymond has reported the synthesis of siderophore analogues with linear [237-239], tripodal [240,241] and macrocyclic [242] topologies [243] some of which are promising candidates for the <u>in vivo</u> removal of iron as well as actinides [244,245]. In 1987 he reported the synthesis of a new macrobicyclic catechoylamide ligand [246], bicapped TRENCAM [247] Fig.51-1 synthesized by high dilution techniques (3.5-27%) or by template synthesis (70%). The simplicity of the nmr reflects the idealized D_{3h} symmetry of the molecule. They have since developed the synthesis to give unsymmetrical macrobicycles via a "half-cage" template reaction [248] Fig.51-2. Electrochemistry on the ferric complexes of these ligands demonstrates that overall selectivity for the ferric ion is retained.

Luminescence is an important phenomenon for fundamental and practical applications (lasers, electric display devices, molecular labels, solar energy conversion etc) and Lehn has prepared Eu^{3+} and Tb^{3+} cryptates [249] Fig.52(1-4), in search for synthetic luminophores i.e. where the energy transfer between the absorbing and the emitting species is high [250]. Data shows that excitation in the spin allowed ligand centred bands is followed by transfer to the emitting level of the lanthanide ion. The largest amount of emitted light is obtained with $[Eu\ 1]^{3+}$ and $[Eu\ 2]^{3+}$, complexes which may be considered efficient molecular devices for the conversion of uv-light into vis-light. Recently Lehn[48] has synthesized a range of macrobyclic cryptates incorporating bithiazole, bisimidazole and bipyramidine binding subunits (Fig.9). The luminescence properties of their Eu^{III} complexes have yet to be reported.

The anthracenocryptands [251] Fig.53-1 are designed to combine the specific complexing ability of cryptands with the photophysical behaviour of the

Lanthanide Amine Cage Complexes

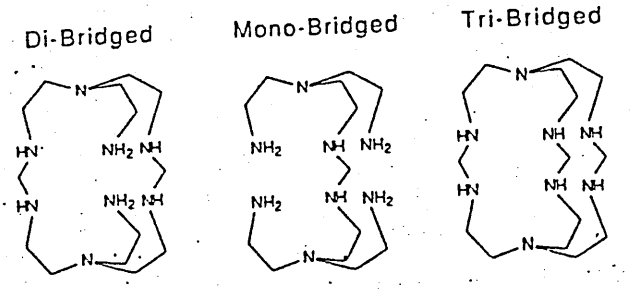

FIG.54

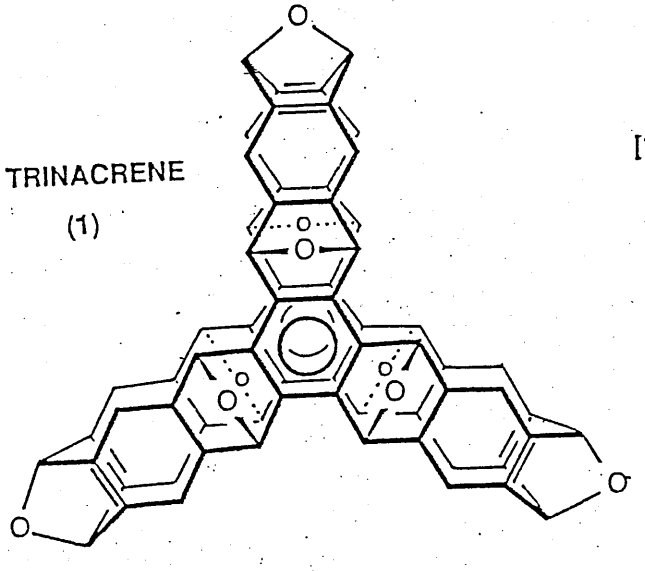

[12]Collarene
(2)

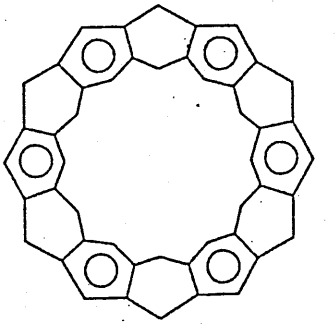

[12]Beltene
(3)

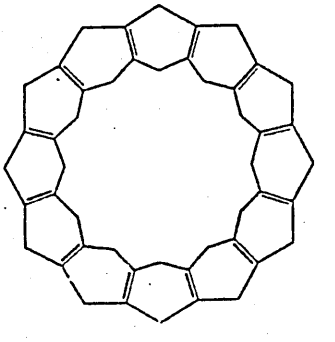

FIG.55

anthracene ring. The formation of inclusion complexes with K^+, Ag^+, Tl^+ Fig.53-2 result in a very sensitive photophysical response of the anthracene bound to an efficient ligand.

Raymond has used a template approach (using the lanthanide triflate salts) to give a fully encapsulated lanthanide amine complex [252-254]. Depending on the size of the metal cation used (M^{3+}= Ce, Pr, Eu, Nb, Y) partial cages or macrocyclic cage products were obtained [254] (Fig.54).

A novel bicyclic structure has recently been published by Stoddart. Trinacrene, a 3-dimensional molecular barrel [255], Fig.55-1 has been synthesized using a Diels Alder approach to the synthesis. Its large rigid molecular cavity could play host to a variety of organic, organometallic, metallorganic and inorganic guest species - both neutral and charged. Chemical modification should permit useful steric and electronic manipulation of the structure. The synthesis of trinacrene with its 24 chiral centres and 6 pseudochiral centres in 2 steps establishes the principle of structure-directed synthesis in the realm of unnatural products [256]. He has also used this method to produce 2-dimensional molecular belts and collars [255,257,258] Fig.55-2 and 55-3.

Lehn has defined a new subclass of cryptands called speleands [47]. Described as polar binding subunits operating in conjuction with hydrophobic-shaping components, they are 'hollow' in nature and have flexible bridges which permits adjustment of cavity height. Fig.56. Thus Busch's vaulted cyclidenes could be included in this area of chemistry.

MACROTRICYCLIC & MACROTETRACYCLIC MOLECULES.

Macropolycyclic systems are molecules of intermediate size - meso molecules[259] - lying between the usual molecules of organic chemistry and macromolecules. They define regions of space, cavities of various shapes, sizes and properties. Previous discussion has been restricted to macrocycles (coronands) and macrobicyclic cryptands (podands). However elegant synthetic work by Lehn and co-workers extended the macrobicyclic series to the purpose built macrotri- and macrotetra cycles [11,12]

FIGURE 56

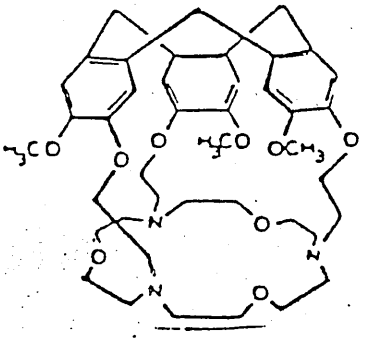

FIG. 56-1

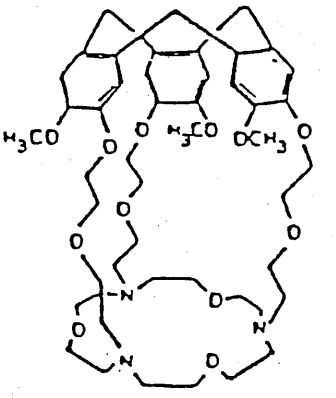

FIG.56-2

FIGURE 57 MACROTRICYCLIC AND MACROTETRACYCLIC MOLECULES.

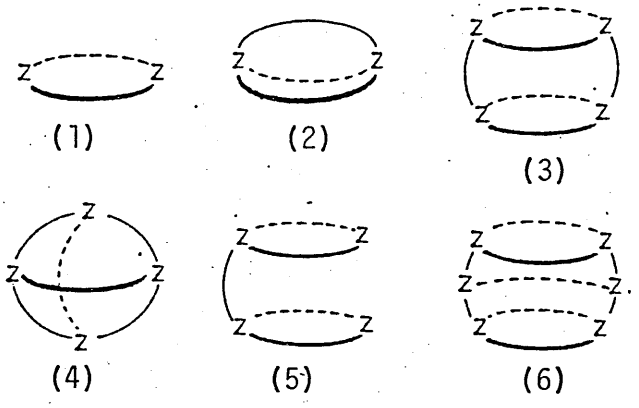

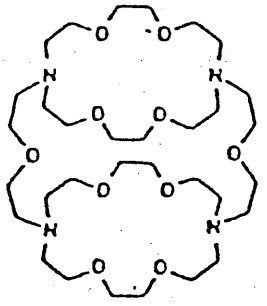

FIG.57-7
(ref 260a)

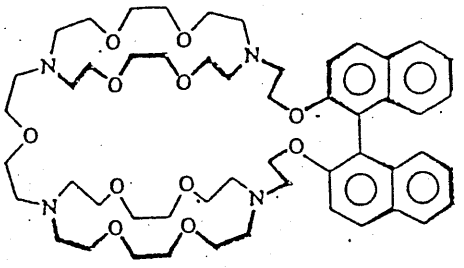

FIG.57-8
(ref 260b)

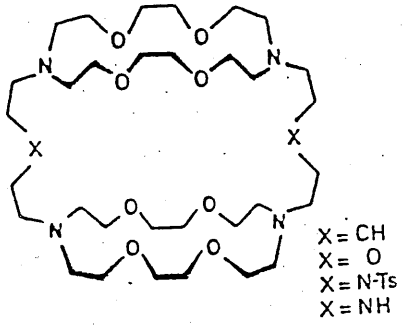

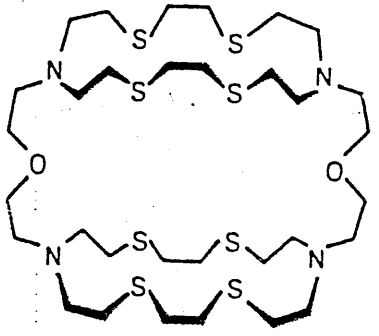

FIG.57-10
(ref)

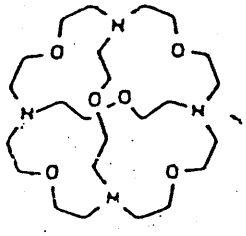

FIG.57-11
(ref 260a)

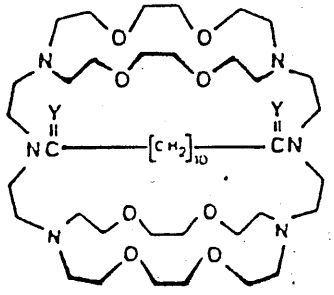

FIG.57-12
(ref 11)

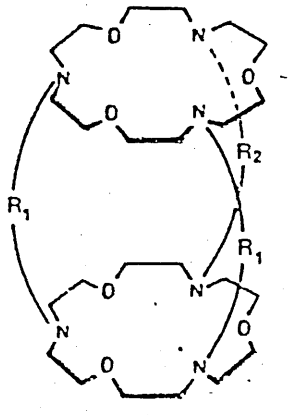

FIG.57-13
(ref 12)

Fig.57(1-6). Macrotricyclic molecules may present two types of topologies of high symmetry - cylindrical Fig.57-3 and spherical Fig 57-4. Cylindrical ligands like 3 (D^{2h} symmetry) are constructed by two rings and two bridges linking the rings. They show new features with respect to the macrocyclic Fig.57-1, the macrobicyclic structure Fig.57-2 or the spherical macrotetracycle Fig.57-6 which all contain one central cavity. Cylindrical systems, on the other hand, define three regions: two lateral bidimensional cavities inside the 'top' and 'bottom' rings of the cylinder, and the central, tridimensional cavity limited by the rings and bridges between them. A double structural control is therefore possible: modifying the branches of the rings changes all three cavities (size, binding properties etc) whereas modification of the connecting branches changes only the nature of the central cavity. Fig.57(7-11) shows examples with references[260], of various macrotricyclic systems.

The bis-macrocycles represented in Fig.57-5 are 'open' analogues of Fig.57-3 lacking the central cavity. Examples of these have already been discussed [69] Fig.16.

Adding a further bridge across the two bridges of the macrotricycles Fig.57-3 leads to a macrotetracycle Fig.57-6 in which the large central cavity of the macrotricycle is now closed up in one direction so as to leave only one side open. Thus ligands of this type define molecular pockets which might be able to take up substrates Fig.57-12 and 57-13.

These systems will be considered in more detail with respect to their cation and anion binding properties in a later section.

CYCLODEXTRINS.

The cyclodextrins were the first host compounds to be recognised as possessing selective molecular recognition capabilities [261] and thus have been intensively studied [170,262]. They are a class of cyclic oligomers of glucose Fig.58-1 which are very soluble in water usually forming 1:1 host-guest complexes although some 1:2 host-guest complexes are known[263-266]. Although there are many various proposed binding forces involved in

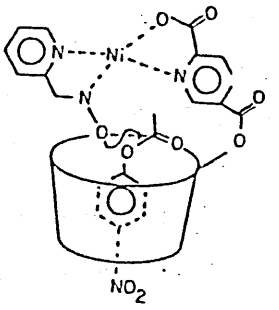

The catalyst-substrate interaction for an artificial enzyme based on a substituted cyclodextrin chelated to ametal ion

FIG.58-2

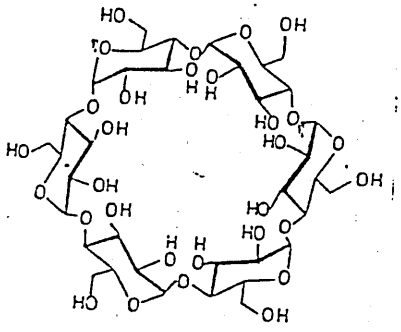

FIG.58-1

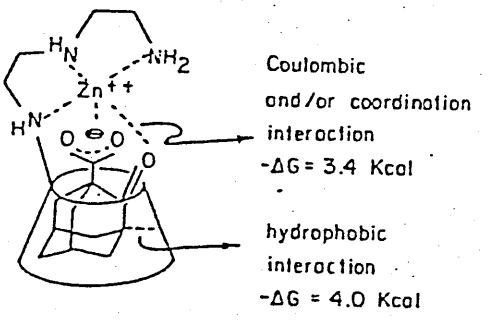

FIG.58-3

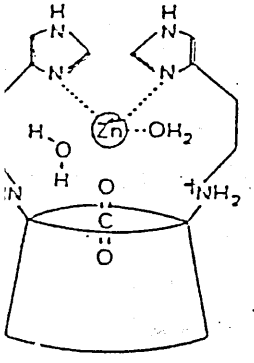

FIG.58-4

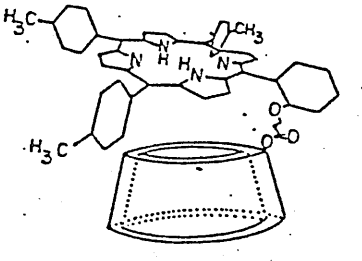

FIG.58-5

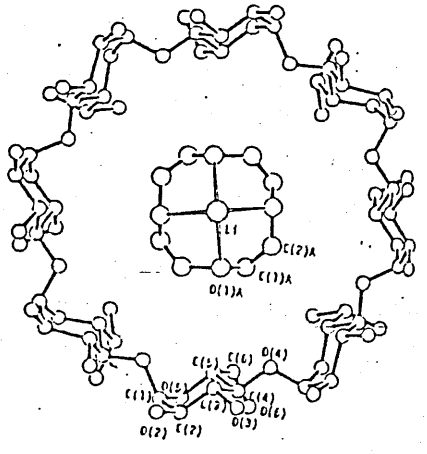

FIG.58-6

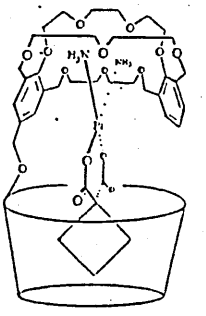

FIG.58-7

inclusion complex formation by cyclodextrins the most significant may be due to van der Waals and hydrophobic interactions [266-268] due to the fact that interaction takes place in aqueous medium. On inclusion complex formation with a guest, water molecules are displaced from the cavity. [269] The complexation of organic molecules by cyclodextrins in water solution is reviewed in reference 268, some recent references include (270-273) and chiral selection by modified cyclodextrins is considered in 274.

Disappointing results were obtained in attempts to mimic enzyme functions with cyclodextrins; however addition of a transition metal ion has yielded more promising results. Breslow [275] combined the catalytic ability of the nickel solvolytic catalyst with the regioselective substrate binding of the hydrophobic cavity of an α - cyclodextrin Fig.58-2. The compound was an effective catalyst for the hydrolysis of certain esters e.g. p-nitrophenol acetate was hydrolysed by the Ni(II) complex with a rate of acceleration of greater than 10^3 times that of the uncatalysed rate.

Tabushi modified cyclodextrins with flexible caps[276] Fig.58-3. Hydrophobic anionic guests are especially strongly bound because of the combined effect of the hydrophobic interaction and the electrostatic attraction of the anion for the cationic cap [181]. This structural design has been used to produce polymeric cyclodextrins which can be attached to a polystyrene support by polyalkyleneamines [277]. The cyclodextrin polymers form metal complexes when treated with aqueous solutions of metal salts. The product is especially useful for extracting organic anions from aqueous solutions.

A bifunctional cyclodextrin has been equipped with a transition metal ion in order to produce a novel carbonic anhydrase model [278] Fig.58-4. This complex incorporates the following recognized features of carbonic anhydrase : a hydrophobic pocket, Zn(II) bound to imidazole and located at the edge of the hydrophobic pocket and additional favorably placed basic groups.

Several reports [279-281] have appeared on attempts to combine the oxygen carrying ability of the porphyrins with the host-guest capabilities of the

FIGURE 59 CALIXARENE-BASED URANOPHILES

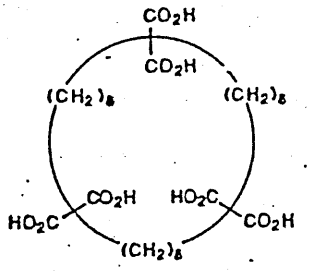

FIG.59-1

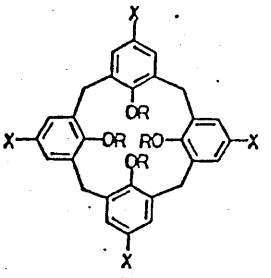

FIG.59-2

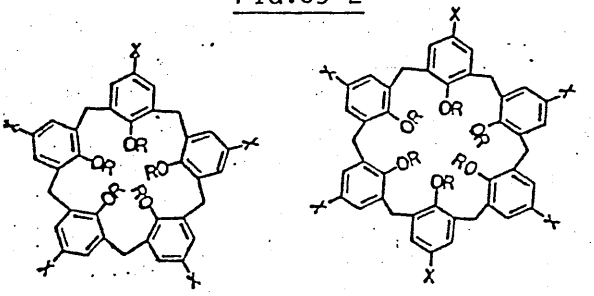

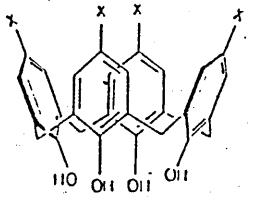

"cone" structure

FIG.59-3

DOUBLE-CALIXARENES

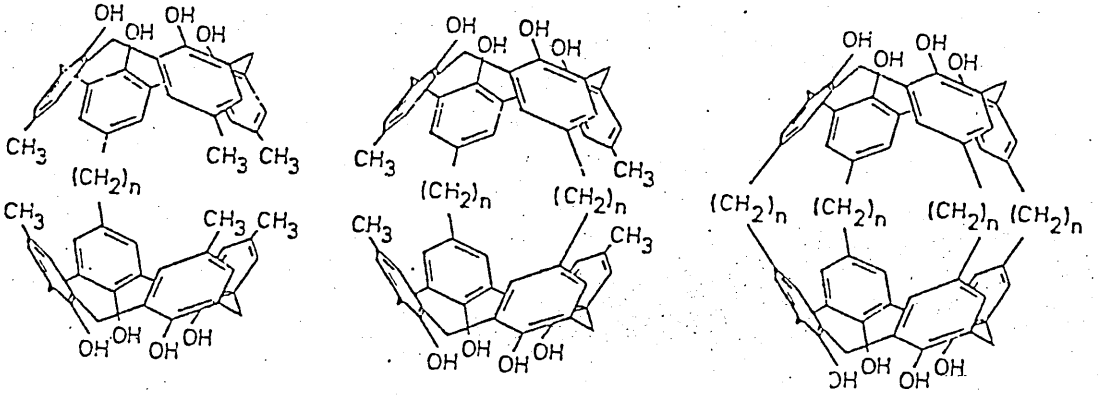

FIG.59-4

water-soluble cyclodextrins Fig.58-5. The products are interesting models of the natural oxygen carriers and help overcome the water solubility problem of the obvious hemoglobin models such as picket fence or capped porphyrins.

Hirotsu has reported the inclusion of 12-crown-4 LiSCN and 12-crown-4 KCl in γ cyclodextrins to give double macrocyclic inclusion complexes ‹282,283› Fig.58-6, while Stoddart has modified the cyclodextrin structure using a macrobicyclic polyether to form a ditopic receptor Fig.58-7. This receptor can bind the anti-tumor drug carboplatin and other transition metals as diammines ‹284› Fig.58-8.

'Calixarenes' are cyclic oligomers made up of benzene rings in a similar way to that in which cyclodextrins are made up of glucose units. However, only when suitably functionalized can they form inclusion complexes in solution ‹285›. Tabushi et al‹286› have functionalized calix-[6]arene with 6 carboxylate groups, Fig.59-1 which makes the host molecule a useful uranophile. The inclusion complex shows a high stability. Shinkai remodified the system ‹287› Fig.59-2 to provide a more selective system for UO_2^{2+} over other cations. Shinkai has also synthesized the water soluble ρ-sulfonatocalix [4] arene,- the cone structure Fig.59-3 is stabilized by cationic guests e.g. the alkali metals ‹288›. Ungara ‹289› has used chloromethylation to achieve water solubility while Reinhoudt et al ‹290,291› have selectively functionalized the upper rim of the calixspherand leading to complexes, notably the alkali salts, complexed in the upper rim cavity.

Recently Bohmer et al ‹292› have reported the synthesis of a face to face "double" calixarenes Fig.59-4 i.e. two calix [4] arene moieties connected in the para position by 1,2 or 4 aliphatic chains of various lengths. Inclusion studies are in progress.

Some lanthanide complexes of the p-t-butylcalix [n] arenes (n=4,6,8) are known ‹293›.

FIGURE 60 CYCLOPHANES.

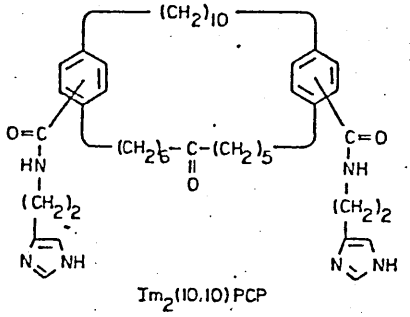

FIG.60-1

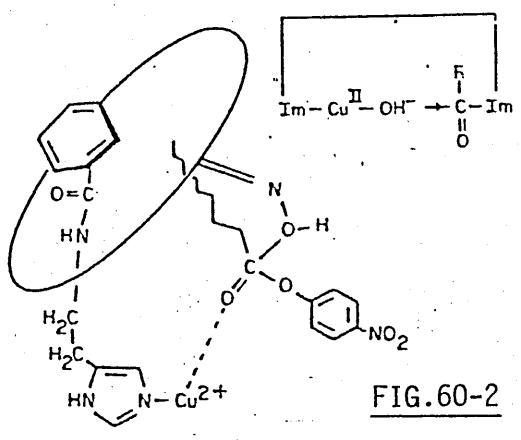

FIG.60-2

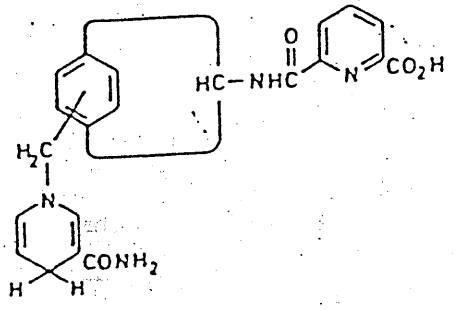

FIG.60-3

CATALYTIC CYCLOPHANES: A HIGHLY EFFICIENT MODEL FOR PYRUVATE OXIDASE

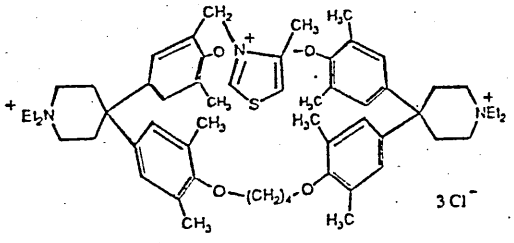

FIG.60-4

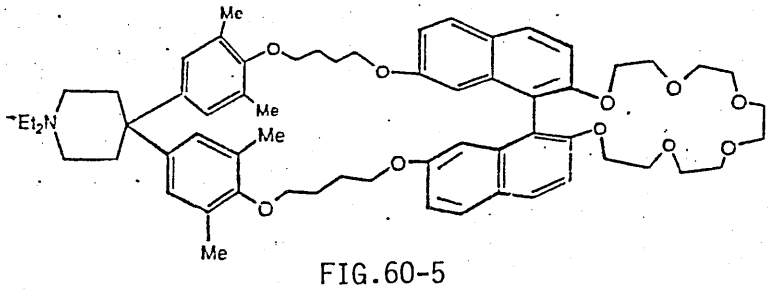

A DITOPIC CYCLOPHANE HOST

FIG.60-5

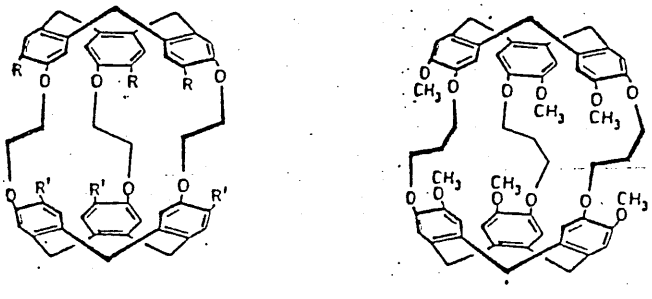

FIG.60-6

CYCLOPHANES.

Cyclophanes are simply 'bridged' aromatic compounds and are more commonly associated with inclusion of organic or uncharged guests. Useful reviews include (294-298).

Cyclophanes are insoluble in water but solubilization can be effected by achieving a hydrophobic-hydrophilic balance in their design. Using appended imidazole groups Fig.60-1 Murakami [299] has synthesized derivatives of [20] and [10.10] paracyclophanes with coordinated Zn(II) and Cu(II) which showed enzyme- like activity in the catalysis of ester hydrolysis [299-301] Fig.60-2. Using a modified [20]paracyclophane skeleton a model of NAD-dependant alcohol dehydrogenase has been prepared [299]. Fig.60-3. This enzyme catalyses the conversion of carbonyl compounds into alcohols and the above model has been tested using the activated ketone, hexachloro acetone, as a substrate. The Zn(II) complex of the substituted cyclophane catalyses the reaction with a maximum acceleration factor of 7.

Diederich [302] has reported a thiazolium ring, functionalized cyclophane Fig.60-4 which in the presence of potassium ferricyanide is an efficient catalyst for the oxidation of aromatic aldehydes to carboxylic acids i.e. it is a highly efficient model for pyruvate oxidase. He has also recently reported a ditopic cyclophane host [303] Fig.60-5 which under suitable conditions is a good binder of potassium ions despite having to undergo considerable conformational changes on binding.

Face-to-face cyclophane molecules exist -the cryptophanes- which have already been considered under their synonym -double or face-to-face - calix (n) arenes. Some 'cryptophanes' are shown with references in Fig.60-6 [304].

There are a large number of 'cyclophanes' that form inclusion complexes with metal ions in organic solvents, although most of these are members of the classes of host compounds in which the donor heteroatoms (O,N,S etc) are the major binding sites (crown ethers, cryptands or their analogues having aromatic rings). In these hosts the aromatic rings act as auxillary

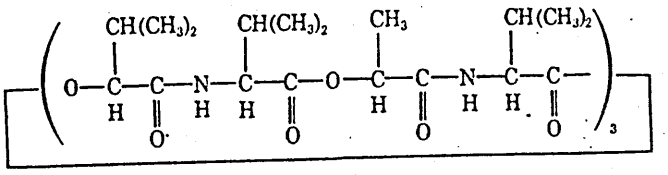

VALINOMYCIN

FIG.61-1

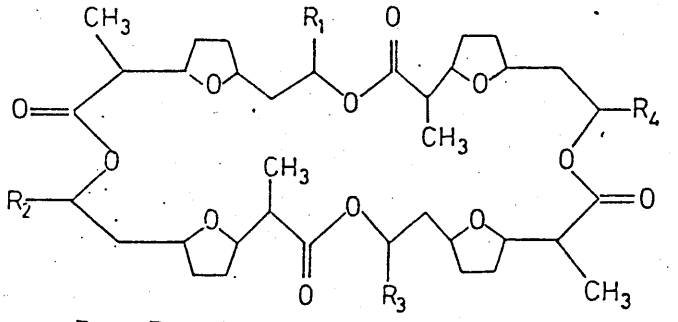

$R_1 = R_2 = R_3 = R_4 = CH_3$	Nonactin
$R_1 = R_2 = R_3 = CH_3, R_4 = C_2H_5$	Monactin
$R_1 = R_2 = CH_3, R_3 = R_4 = C_2H_5$	Dinactin
$R_1 = CH_3, R_2 = R_3 = R_4 = C_2H_5$	Trinactin
$R_1 = R_2 = R_3 = R_4 = C_2H_5$	Tetranactin

FIG.61-2

FIGURE 62 EXAMPLES OF CROWN ETHERS.

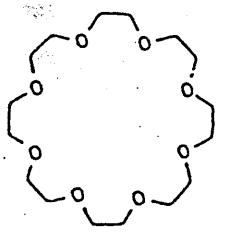

FIG.62-1
(ref 8)

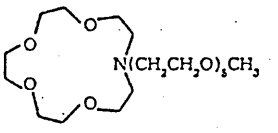

FIG.62-2
(ref 306a)

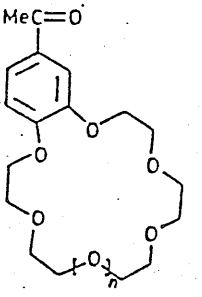

FIG.62-3
(ref 306b)

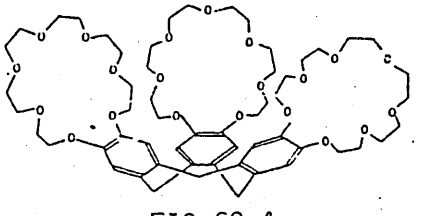

FIG.62-4
(ref 306c)

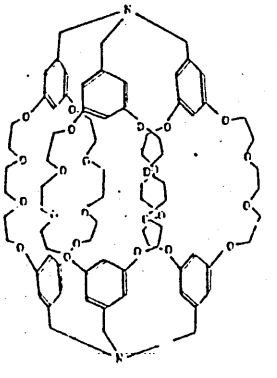

FIG.62-5
(ref 306d)

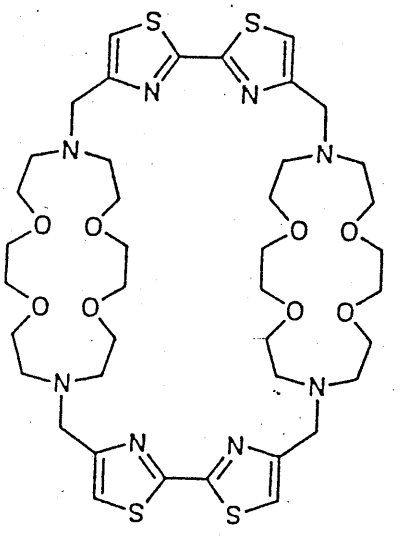

FIG.62-6
(ref 48)

binding sites or rigid structural units. These compounds are discussed where relevant.

CROWN ETHERS.

A fourth class of organic host complexes involves the crown ethers- an area that is well reviewed [70,188,305]. The crown ethers and cryptands are related in structure, properties, and chemical behaviour to the natural and neutral ionophore antibiotics exemplified by valinomycin Fig.61-1 and nonactin Fig.61-2. These antibiotics affect the uptake and transfer of ions through a lipophilic medium.

Due to the hard nature of the 'O' donor atoms the crowns are much better suited to hosting alkali and alkaline earth metals. Over the years the 'crown' ethers have undergone significant developments from the simple macrocyclic polyoxo systems to the substituted N,S,O mixed donor systems, to the highly complex macrobicyclic systems containing one or more crown ether moieties, to the chiral crown ethers. Fig.62 gives examples and references[306].

Stoddart [307,308] has constructed macrobicyclic polyethers as second sphere ligands for tetraamine platinum (II) Fig.63-1. This is mainly due to hydrogen bonding of the amine ligands to the carbonyl function of the two pairs of amide linkages that characterize the entrance of the receptor cavity of the molecule.

Beer [309] has recently constructed the bis-benzo crown-ethers which contain the recognition sites for transition metals Fig.64. Chelation of Ru(II) occurs at the bipyridyl nitrogens forcing the bipyridyl function towards coplanarity restricting the conformational freedom of the 2 benzo-15-crown-5 binding units in such a way as to favour the formation of an intramolecular sandwich complex with sodium.

Pietraszkiewicz [310] combined the fluorescent unit, fluoresceine- with the macrocyclic 18-N_2O_4 crown Fig.65. The latter forms strong complexes with

FIGURE 62. EXAMPLES OF CROWN ETHERS.

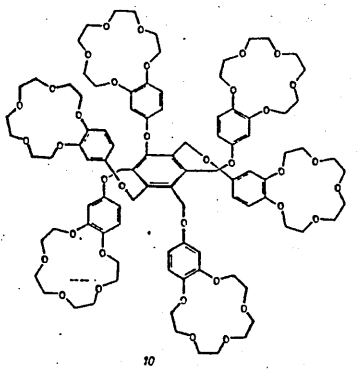

FIG.62-7

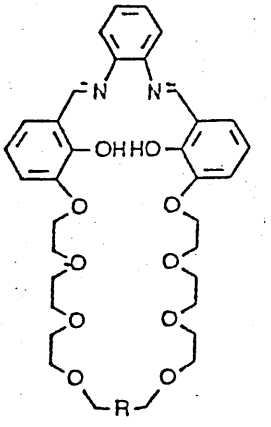

FIG.62-8

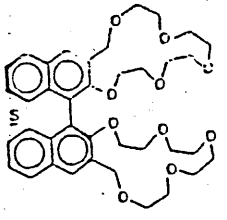

FIG.62-9

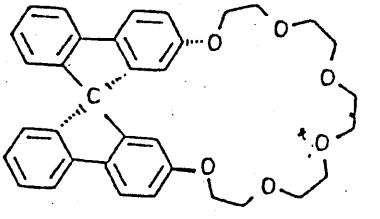

FIG.62-10

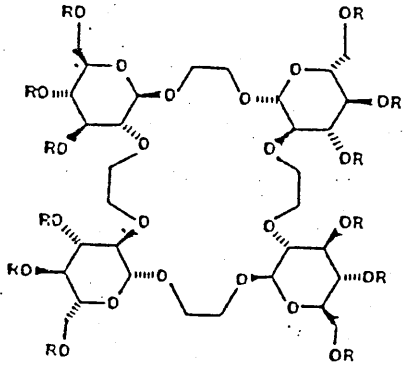

FIG.62-11

FIG. 63 MACROPOLYCYCLIC CROWN ETHER BISAMIDE RECEPTOR.

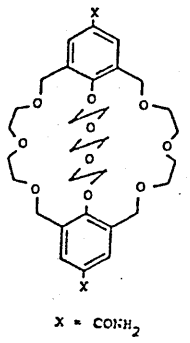

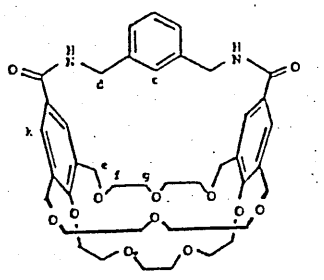

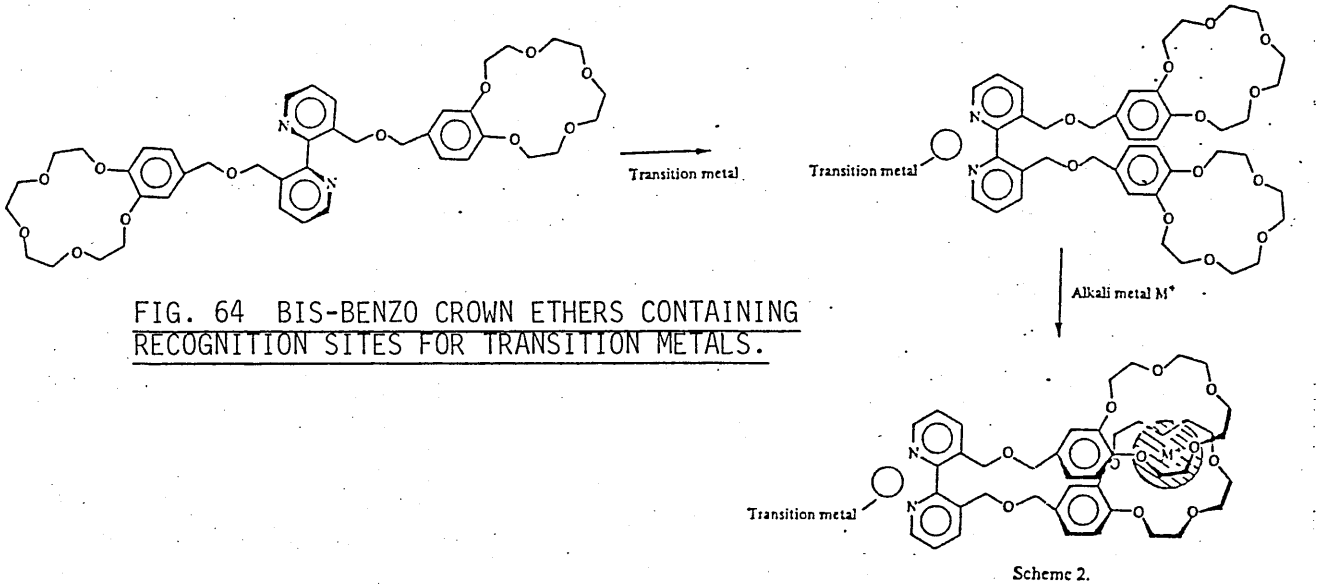

FIG. 64 BIS-BENZO CROWN ETHERS CONTAINING RECOGNITION SITES FOR TRANSITION METALS.

Scheme 2.

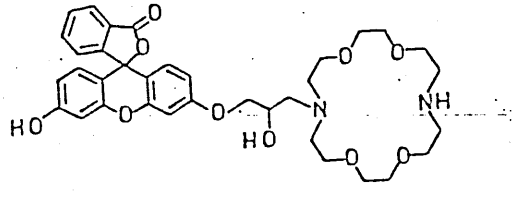

FIG.65 FLUORESCENT SENSORS FOR HEAVY METAL IONS

Basic prophyrin structure

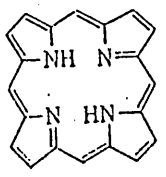

FIG.66-1

Picket fence

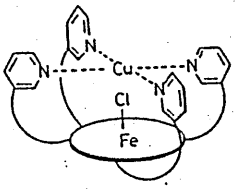

FIG.66-2

(ref 311)

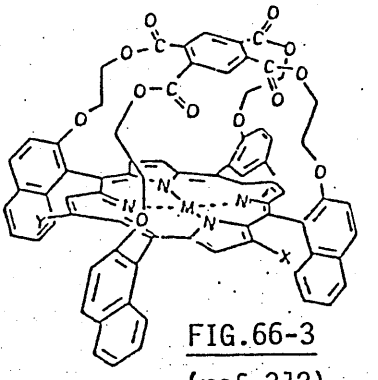

FIG.66-3

(ref 312)

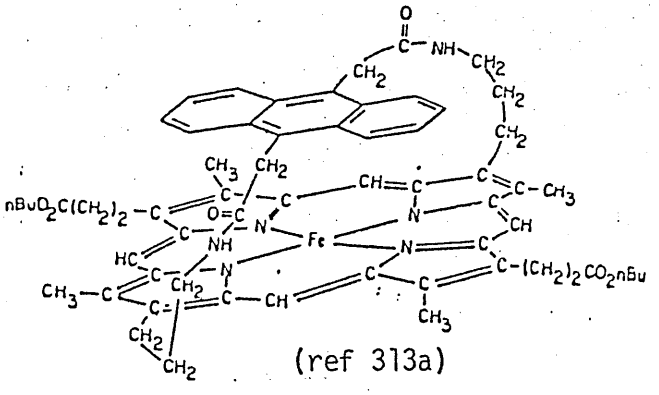

(ref 313a)

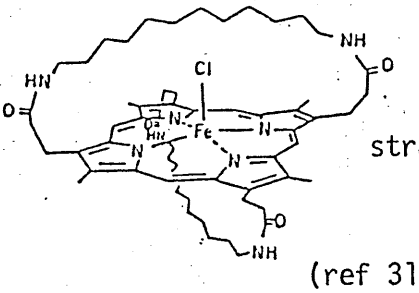

strapped

(ref 313b)

FIG.66-4

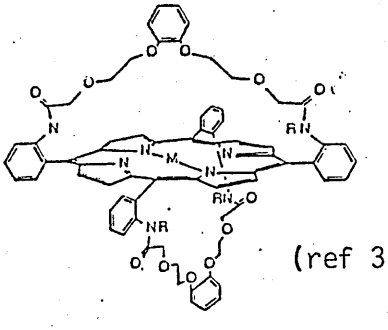

(ref 313c)

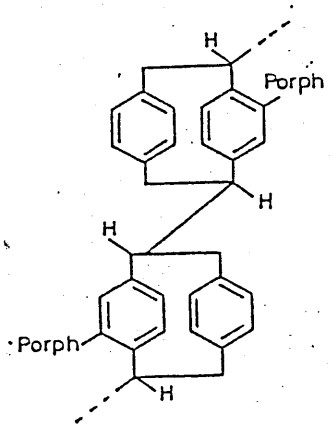

FIG.66-5

(ref 314)

heavy cations e.g. Cd(II), Hg(II) or Pb(II) which showed effective fluorescent quenching when present in suitable concentrations. Similarly Shirai has studied the effects of cation binding on the phosphorescence properties of acetophenone derivatives with a crown ether moiety.

PORPHYRINS.

Busch's complexes, already discussed, represent a family of totally synthetic non-porphyrin macrocyclic complexes which model several main features of natural hemoprotein systems . However many groups have designed model porphyrin systems in an attempt to mimic the local environment of the hemoprotein binding site i.e. steric encumbrance about the oxygen binding site in a cobalt or iron complex. Thus there are many structural modifications of the basic porphyrin structure Fig.66-1. These include picket fence[311] Fig.66-2, capped[312] Fig.66-3 bridged/strapped/basket handled [313] Fig.66-4 cyclophane [314] Fig.66-5 and gable porphyrins [315] Fig.66-6, all of which provide a sterically hindered face at which small molecules may coordinate with varying degrees of difficulty. The porphyrin model systems generally base themselves on polar effects rather than distal side steric effects used in Buschs models [226-228].

Face-to-face porphyrins Fig.66-7 and 66-8 serve as models for the hemoproteins if they are regarded as bridged systems or as models for binuclear systems such as cytochrome C. The linkages between the 2 rings can be between 2 meso positions [316a] Fig.66-7 or between substituents on the pyrrole rings [316b] Fig.66-8. The face-to-face systems were investigated as possible catalysts for the electrochemical reduction of oxygen to water. The bis-Co(II) complex of Fig.66-7, where m=n=1, when attached to the surface of a graphite electrode was found to be an efficient catalyst for this reaction. Where m and/or n>1 the systems were less efficient.

Although there has been reasonable success at combining the porphyrins and cyclodextrins [279,281] it was only in 1987 that the related synthetic phthalocyanine were combined with crown ether units [317] Fig.67-1. In attempts to obtain a high yield synthesis of 2 closely bonded porphyrin

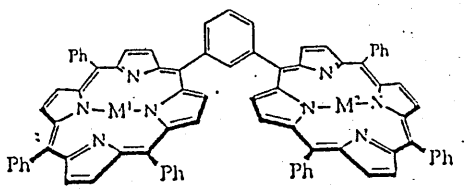

(ref 315a)

FIG.66-6

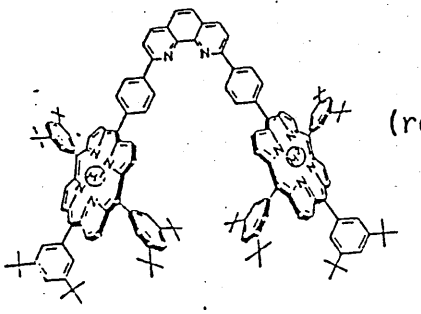

(ref 315b)

Gable porphyrin

FIG.66-7

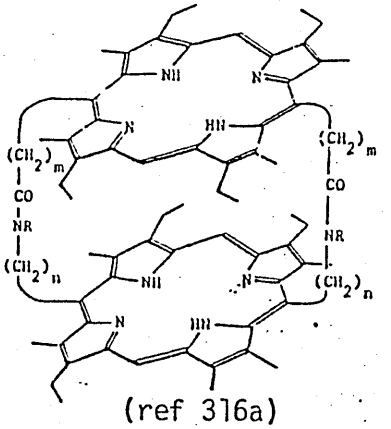

(ref 316a)

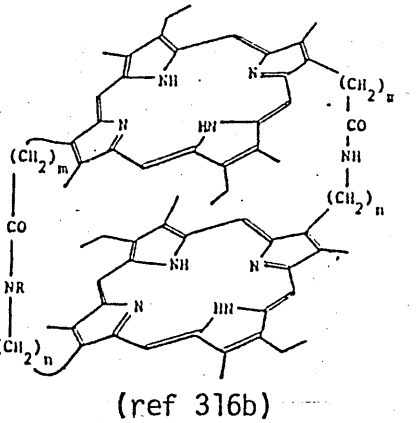

(ref 316b)

Face to face porphyrins

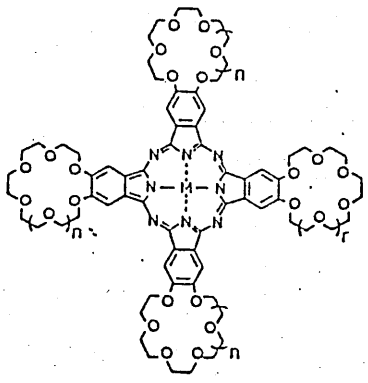

FIG.67-1

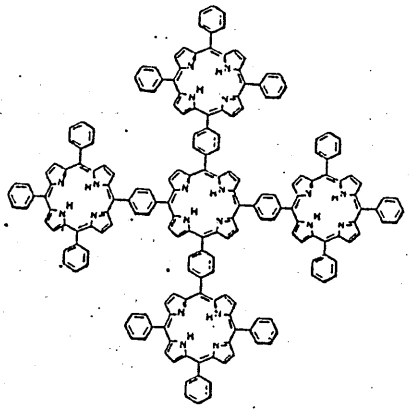

FIG.67-2

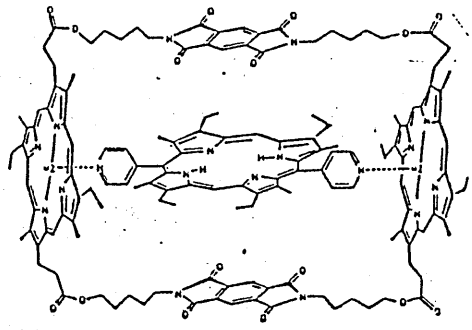

FIG.67-3

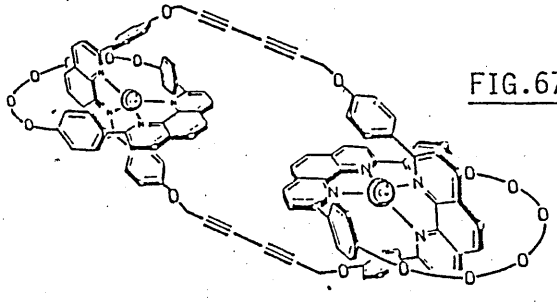

FIG.67-4

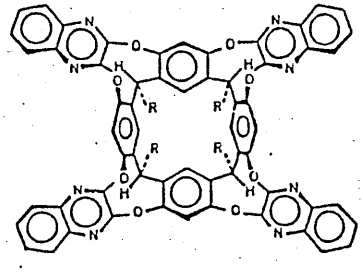

FIG.68-1

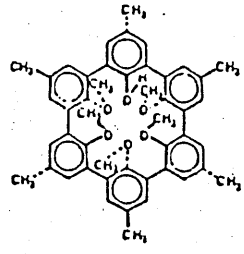

FIG.68-2

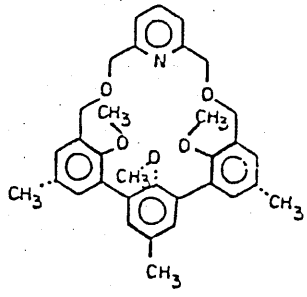

FIG.68-3

FIGURE 68 CAVITANDS.

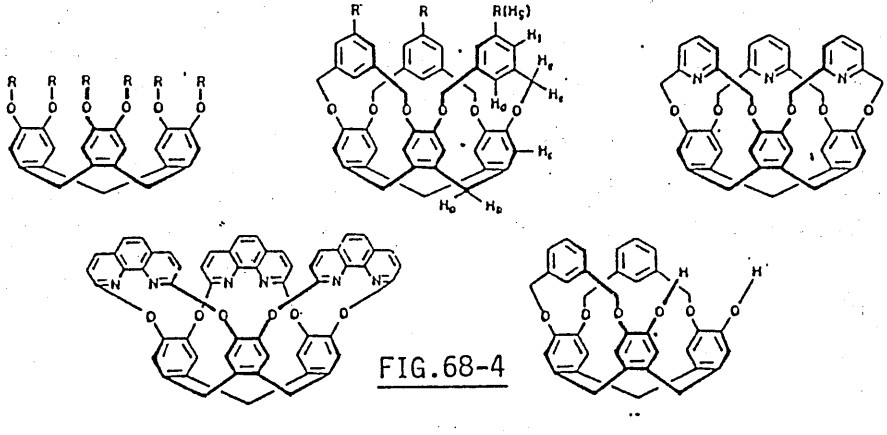

FIG.68-4

products, Wennerstrom synthesized a macrocycle with 5 covalently linked porphyrin units [318] Fig.67-2, while Sanders has developed a photoactive supramolecule using porphyrin coordination chemistry [319] Fig.67-3.

Catenates are a class of compound that are composed of interlocked macrocyclic structures. The first metallocatenate was that produced by Sauvage et al[320,321] of a highly stable Cu^{I} complex of a catenand of 2 interlocking crown polyether type ligands. In 1987[322] he reported the [3]catenate of a dicopper(I) complex which contained 2 peripheral 30 membered rings separately interlocked with a central 44 membered ring Fig.67-4.

CAVITANDS.

It is useful to make a distinction between those complexes which undergo significant host reorganization upon complexation with a guest (crown ethers, cryptands cyclophanes etc) and those that have permanent or preorganized cavities. Cram has developed synthetic organic hosts that possess enforced cavities large enough to accomodate simple molecules and ions. They are called "cavitands" to describe their unique properties [323-325] Fig.68-1. Spherands are cavitands with fixed cavities and relatively rigid walls Fig.68-2, while hemispherands are cavitands with partially rigid walls Fig.68-3.

Cram [326] has recently reported a new family of cavitands Fig.68-4 - however they have more potential in hosting organic or neutral molecules than transition metal cations.

CATION AND ANION RECEPTORS.

Macrocyclic polydentate complexing ligands can be used for the complexation of anions and cations, or of neutral molecules. Supramolecular chemistry [35] is the term used to describe the association of 2 or more species through non-covalent bonds and this chemistry is to the molecule and the intermolecular bond what molecular chemistry is to the atom and the

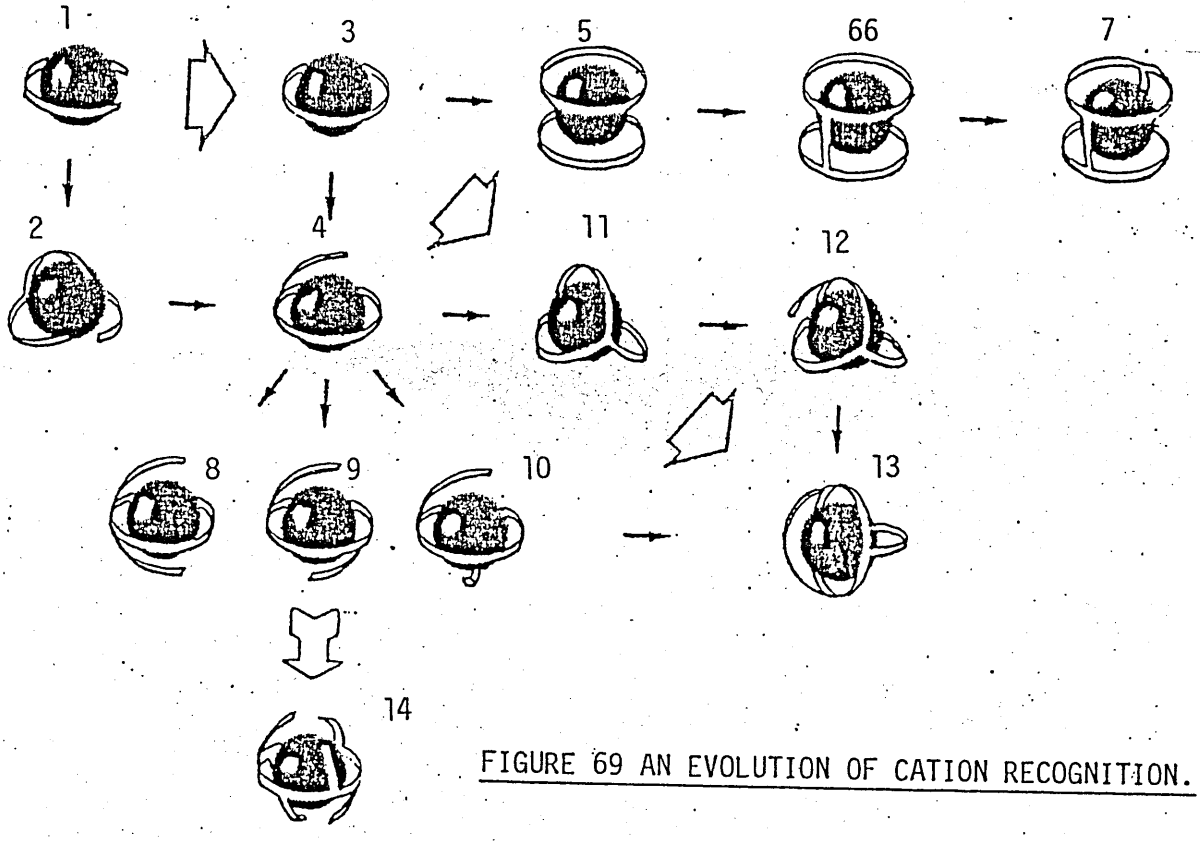

FIGURE 69 AN EVOLUTION OF CATION RECOGNITION.

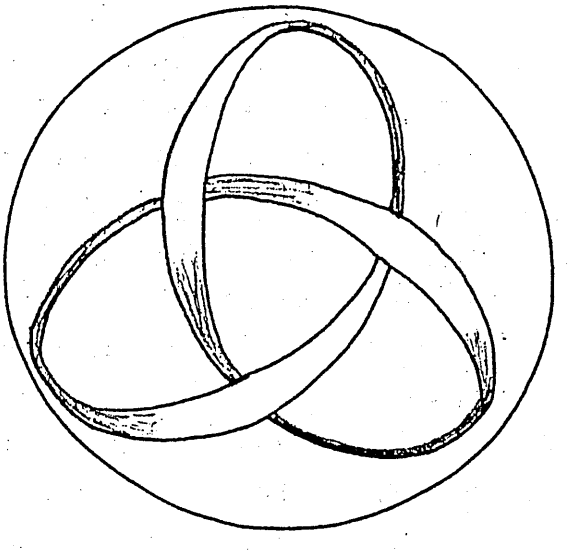

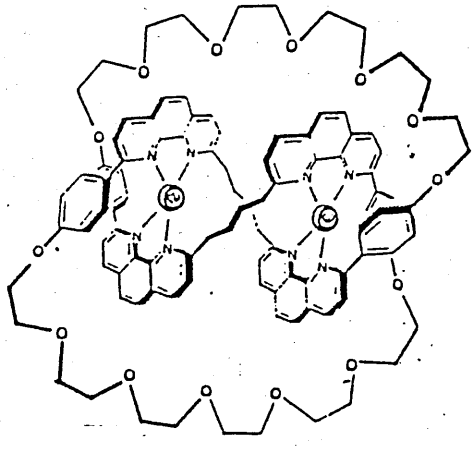

FIGURE 70 THE TREFOIL KNOT.

covalent bond. The individual component bonds forming the intermolecular bonds are much weaker than covalent bonds and are more properly considered as interactions. We can therefore speak of complexation whenever 2 or more species interact attractively with little or no covalent character in the binding interactions. Such a complex may be termed a supermolecule. Some authors prefer the receptor-substrate terminology to the host-guest termiology since the latter covers all kinds of intermolecular associations and the former conveys the flavor of the highly specific biological receptor-substrate interactions.

Many metal cationic hosts have already been discussed and these systems can act as anionic receptors. However inclusion of organic cations e.g. NH_{4+}, or protonation of amine function of an 'N' donor system can also result in the modified host behaving as an anion receptor <327,175,176>.

Fig.69 shows how the increase in topological complexity of cation complexes starting with the simple bidimensional bi and polydentate chelates Fig.69-1 leads to macrocycles Fig.69-3,69-4 to tridimensional (3) cryptates Fig.69-7 (cylindrical) and Fig.69-13 (spherical). Only recently has Fig.69-12 - the trefoil knot - been synthesized <328> by Sauvage Fig.70. Such a topology is seen in the DNA structure which can be converted into highly knotted forms making the synthesis of knots an even more challenging problem for the chemist.

Many receptors play host to many varieties of organic cations or neutral species and in this text only one class of host for one type of organic cation - NH_4^+ the ammonium ion - will be considered. The cylindrical macrotricycles are ditopic in nature, Fig.71-1 and can form stable ammonium cryptates in 2 main ways : by dinuclear monohapto binding Fig.71-2 to 71-4 or mononuclear dihapto binding Fig.71-5. The former displays the 3 isomers shown in the figure i.e.endo-endo, exo-endo or exo-exo (both groups lying outside the molecular cavity). To bind NH_4^+/RNH_3^+, macrocyclic subunits must be able to bind primary ammonium groups e.g. 18-O_6 polyether macrocycles [18]N_2O_4 or [18] N_3O_3 oxoaza macrocycles. The latter two are especially well suited for complexation of R^+NH_3 ions because of the formation of $^+$N-H....N hydrogen bonds <329>. Orientation of the bridgehead

dinuclear monohapto

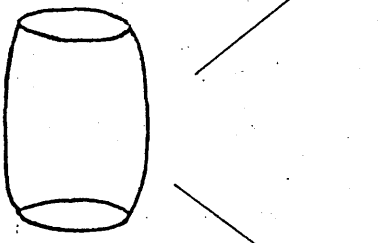

FIG.71-1

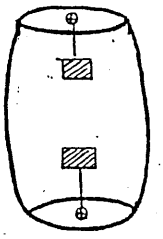

FIG.71-2

endo endo

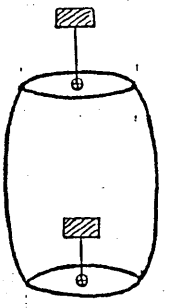

FIG.71-3

endo exo

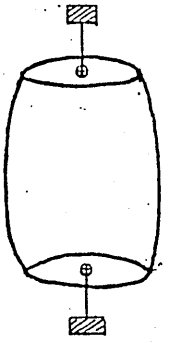

FIG.71-4

exo exo

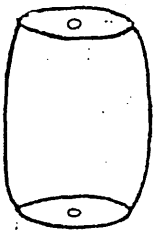

FIG.71-5

mononuclear dihapto

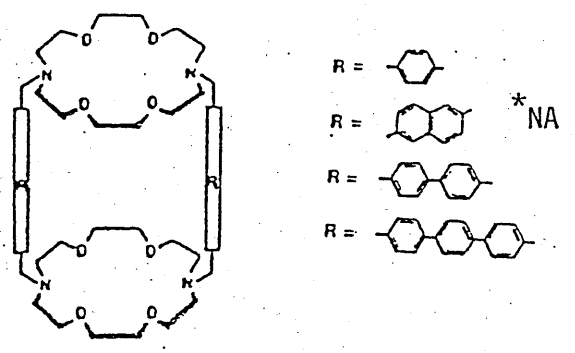

FIGURE 72

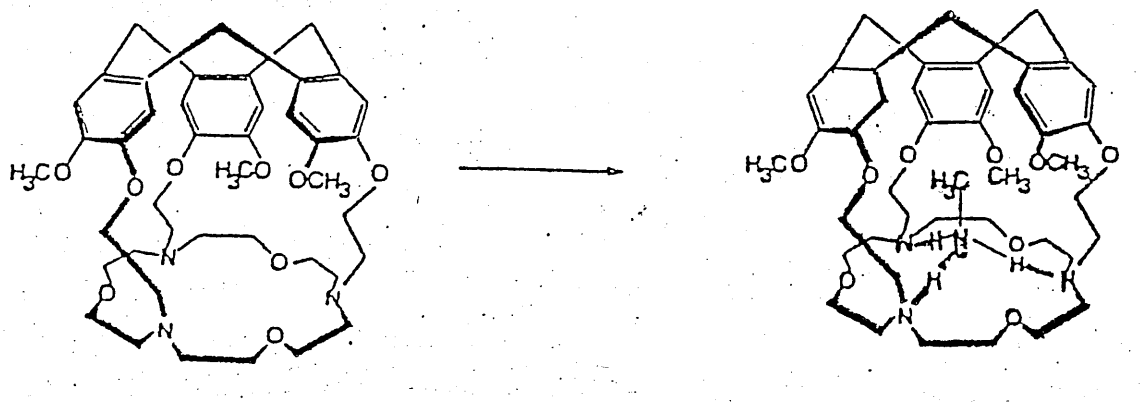

FIGURE 73.

N sites and the O sites towards the interior favour binding in an endo form i.e. into the central molecular cavity. Complexation of NH_3^+ into the intermolecular cavity is detected by ^{1}Hmmr fluorescence studies, and ultimately by X-ray.

The results of such studies have shown that when forming mononuclear dihapto cryptates with diammonium cationic species the preferentially complexed substrate is that whose length corresponds to the length of the molecular cavity Fig.72 ‹330,331›. Thus where R=NA, the system can discriminate between the biologically important cadaverine N^+H_3-$(CH_2)_5$-N^+H_3 and putrescine (N^+H_3-$(CH_2)_4$-N^+H_3) ‹332-334›. These reults form the basis for structural receptor-substrate complementarity in linear molecular recognition. Complementarity between components expresses itself in both structural and dynamic properties of the supramolecular species.

The speleands, in which the polar binding subunits are connected with large concave, more or less rigid hydrophobic shaping components ‹47› are useful receptors for organic ammonium cations. On combining the symmetric [18]-N_3O_3 macrocycle with derivatives of racemic cyclotriveratrylene (CTV) tris methyl esters, the speleands, in Fig.73 are obtained. Fig.73 binds $CH_3NH_3^+$ yielding a mixture of slowly exchanging endo-exo isomeric complexes Fig.73-2. Where R is larger than the methyl group endo binding is prevented and thus Fig.73-1 is a highly selective ammonium host.

The various ways in which a cylindrical (3) cryptand can be transformed into polytopic receptors is shown in Fig.74-1 to 74-6. Inclusion of binding sites along one or both linking arms may afford tri- or tetratopic structures Fig.74-2 and 74-4 respectively. Schematic elongation of one or both macrocyclic subunits, affords tri or tetratopic receptors Fig.74-5 and 74-6, where one or two pairs of ions are side by side. Still another variation is the macrotetracycle Fig.74-3 which may form as a side product of (3)-cryptand synthesis, corresponding to the 3+3 coupling product ‹327›. In these cases all 3 macrocyclic subunits are identical. Modification of synthetic procedures can lead to the macrotetracycles as the main products ‹327› and dissimilar subunits can be built in using protection and deprotection steps. The receptor shown in Fig.75-1 ‹335› resembles

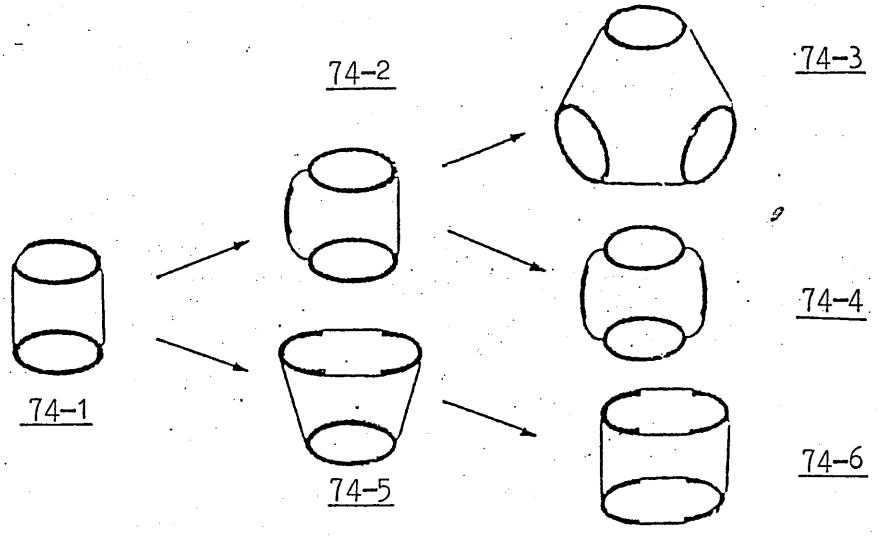

FIGURE 74 TRANSFORMATIONS OF A CYLINDRICAL (3)-CRYPTAND POLYTOPIC RECEPTORS.

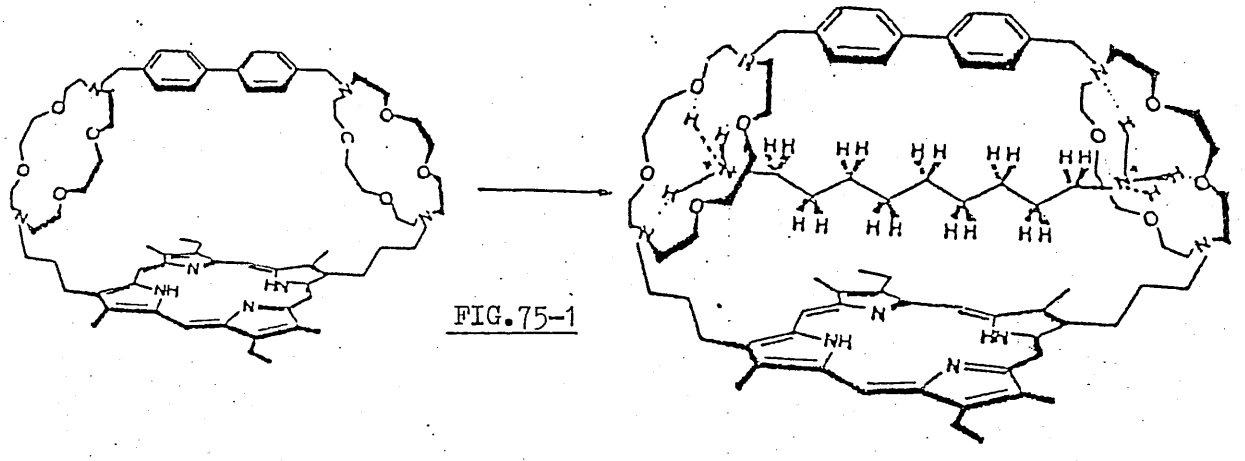

FIG.75-1

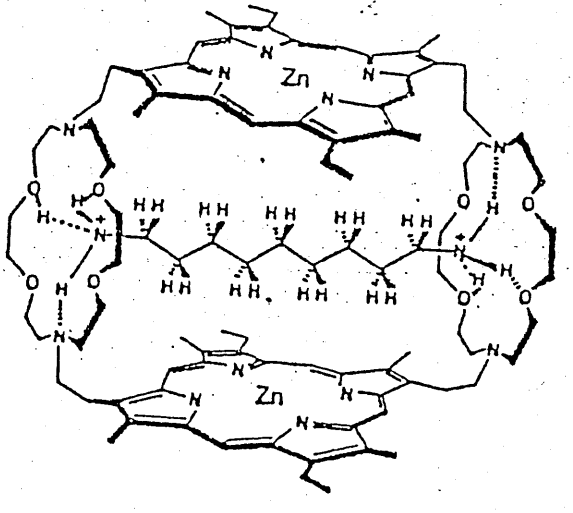

FIG.75-2

FIGURE 75

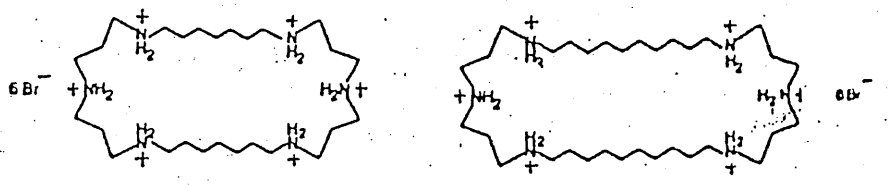

FIGURE 76.

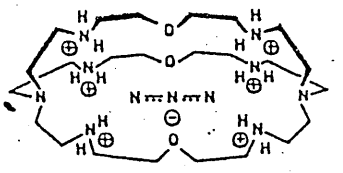

FIGURE 77.

macrotricycle Fig.74-2 except that the third site happens to be a porphyrinic macrocycle. A second porphyrin has also been fitted between 2 macrocyclic units in Fig.75-2 and as shown both can form inclusion complexes with linear diammonium ions [335].

Compared with cation receptor molecules, the field of anion coordination is relatively new [35,260a,336,337]. It has evolved in parallel to macrocycle polyamine chemistry because almost any amine-containing cation receptor can be transformed into an anion receptor after protonation although endo protonation reduces cavity size somewhat. The strongest binding makes use of H^+-bonding in combination with electrostatic attraction, although the latter may suffice in some cases. The first anion ligands were the catapinands which when diprotonated and of a suitable size are able to enclose halide ions [338-340]. The highly ionized polyammonium and polyguanidium receptors can only be studied in aqueous solution and complexation of monoanionic substrates is feeble in this medium. However di,tri and tetraamines display much larger complexation constants [327]. The protonated polyazamacrocycles display weaker selectivity patterns with anions, in terms of size and charge, than the polyoxomacrocycles do with cations, but size and geometrical selectivity is found in the available data [341]. Fig.76 shows 2 elongated ditopic polyazamacrocyclic receptors. They exhibit a peak selectivity for length with aliphatic dicarboxylates, with Fig.76-1 peaking with pentanedioate and Fig.76-2 with heptanedioate [342].

The protonated polyaza-(2)-cryptands [343-345] have ellipsoidal cavities which are best complemented by ellipsoidal substrates. Consequently N_3^-, binds quite strongly to the BISTREN receptor, $[2_{NON}.2_{NON}.2_{NON}].6H^+$ [346] Fig.77 whereas NO_3^-, ClO_4^-, HCO_2^- and the halides are more weakly bound. The ditopic polyaza 2 cryptands can be elongated by the tripod-tripod coupling procedure Fig.6. These have displayed a peak selectivity for length with dicarboxylates in line with the expected cavity lengths. [347].

The protonated forms of (3)-cryptands display a spherical recognition of anions Fig.78-1 [348]. The quaternized (3) cryptands which cannot participate in H^+ - bonding can complex Cl^- and Br^- reasonably well due to

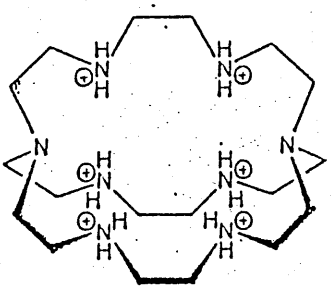

FIG.78-1

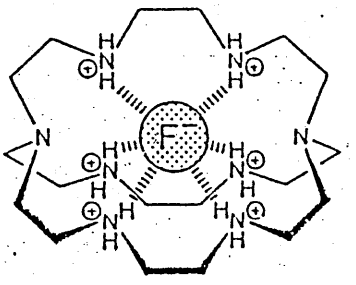

FIG.78-2

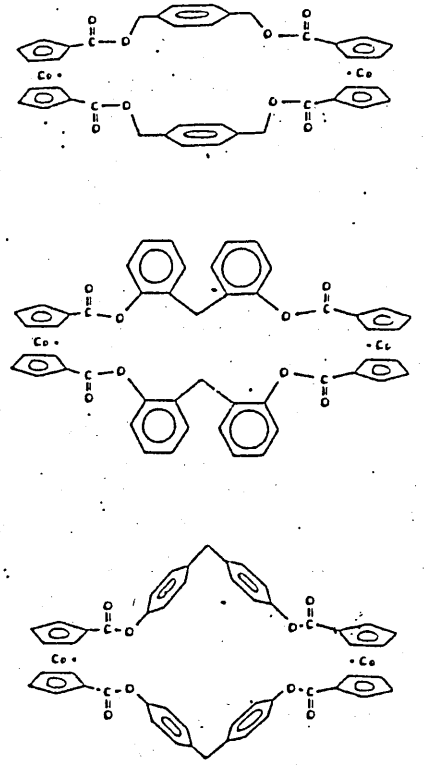

FIGURE 79

electrostatic interactions [349]. Larger similar cavities have been developed [350] which effect a more efficient complexation of Br^- and I^-.

Lehn has recently [351] prepared an octaaza-cryptand that binds fluoride anions. The cryptate is a quasi-trigonal prismatic array of six $F^-.....H-N^+$ hydrogen bonds Fig.78-2 The protonated polyamines represent the most extensively studied anion ligands and Lehn has previously studied the anion complexation features of a number of macrocyclic [352], macrobicyclic [196,343,353-355], and macrotricyclic [356] molecules bearing ammonium groups as binding sites.

In as much as exposed faces of cations constitute binding sites for ligating anions, all macrocycles hosting cationic species can be considered as anion receptors. Strongest binding is observed with dinuclear metal complexes which present an intermetallic region of high charge density where, structure permitting, anions can be shared by both metal ions. The strength of selectivity of such anion binding is not always readily accessible although as in the case of the bridged hydoxo species in dinuclear BISTREN complexes Fig.47-4,47-5, potentiometric titrations were used [213,214].

Beer [357] has synthesized a series of macrocycles containing the redox active cobaltinium Fig.79. The metal complex carries a single positive charge which is independant of pH. It is also coordinatively and electronically satisfied and so anion binding forces are electrostatic and reversible. In addition, the incorporation of the redo-active unit into these macrocycles makes the electrochemical study of the anion complexation process possible. 1:1 complexes with halide ions have been observed for all three macrocycles shown.

Newcomb has developed macrocyclic [358] and macrobicyclic [359] hosts Fig.80-1 and 80-2 that contain Lewis acidic tin atoms as anion binding sites. Low size selectivity was observed in chloride binding by macrocyclic hosts containing 2 sites but substantial size selectivity in halide binding was found in the ditopic macrobicycles. Solution [119] Sn nmr studies of bicyclic hosts binding anions in halogenated solvents, X-ray

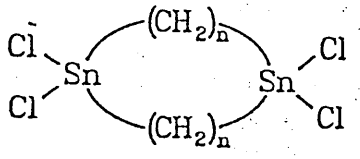

FIG.80-1

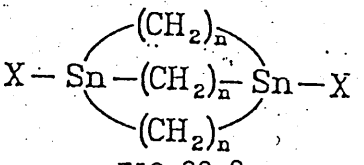

FIG.80-2

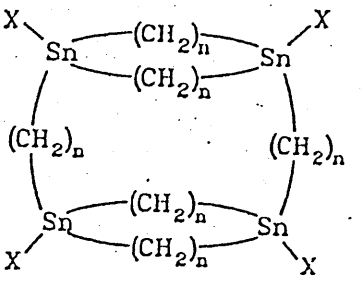

FIG.80-3

MACROCYCLES CONTAINING TIN.

FIGURE 80

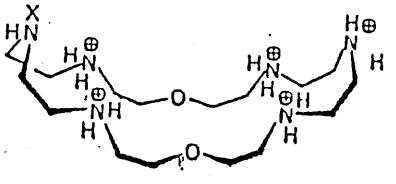

FIG.81-1

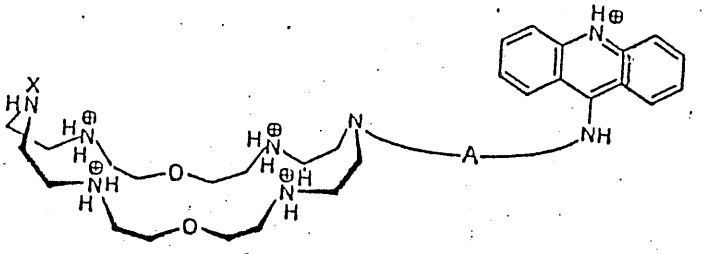

FIG.81-2

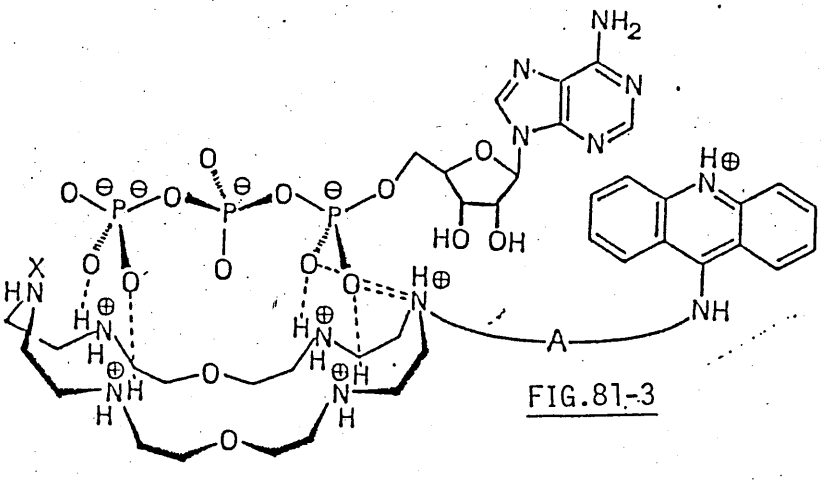

FIG.81-3

FIGURE 81 MULTIPLE MOLECULAR RECOGNITION.

crystallography data and solid state ^{119}Sn nmr studies demonstrate that the anions are held in the cavities of the hosts; the selectivity originates from the fit of the encrypted anion in the cavity. He has recently [360] reported di-topic macrotricyclic structures containing 4 tin atoms, Fig.80-3, which due to the incorporation of additional binding sites results in stronger binding and higher selectivity.

MOLECULAR RECOGNITION.

Discussion thus far has presented the idea of selectivity of the host (receptor) for a particular guest (substrate). Selectivity depends, to some extent, on the host recognizing the guest to be included. Just how far this process has been developed by the synthetic chemist is demonstated by the following examples.

The design of specific probes for biologically important compounds may be achieved with polytopic receptors containing subunits which should be complementary to the different functional groups present in the substrate [361]. Nucleotide polyphosphates, in particular adenosine triphosphate (ATP), are of fundamental significance as a source of energy in living organisms. Lehn has developed protonated macrocyclic hexamines in particular Fig.81-1, which can bind nucleotide polyphosphates by electrostatic interactions [362] and which can catalyse their hydrolytic reactions [363,364]. Connection of the anacridene derivative to Fig.81-1 yields polyfunctional receptor molecules Fig.81-2 which combine a macrocyclic polyamine as anion binding site, an acridine side arm for stacking interactions, and catalytic amino groups on the macrocycle for facilitating hydrolytic reactions [365]. A schematic representation of ATP binding is given in Fig.81-3. Both Fig.81-1 and 81-2 catalyse the ATP and ADP (adenosine diphosphate) hydrolysis but the latter system shows greater selectivity between ATP and ADP. The mechanism of the supramolecular catalysis of ATP by the macrocyclic polyamines is discussed in references 363 and 366.

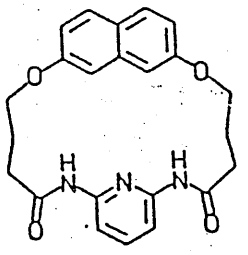

FIG.82-1

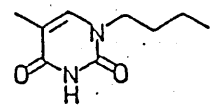

FIG.82-2

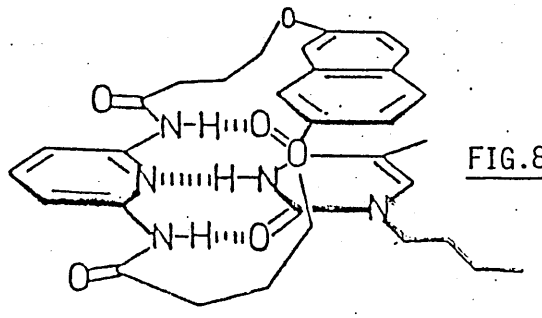

FIG.82-3

FIGURE 82

FIG.83-eqn1

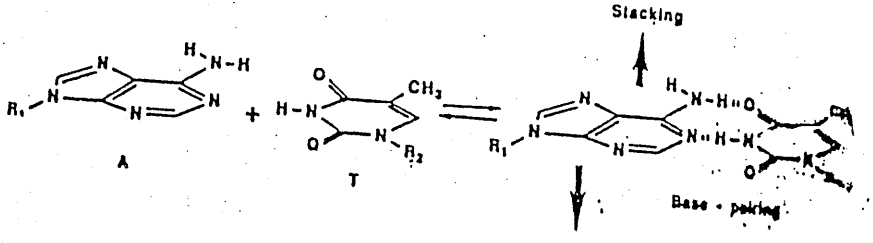

FIG.83-eqn2

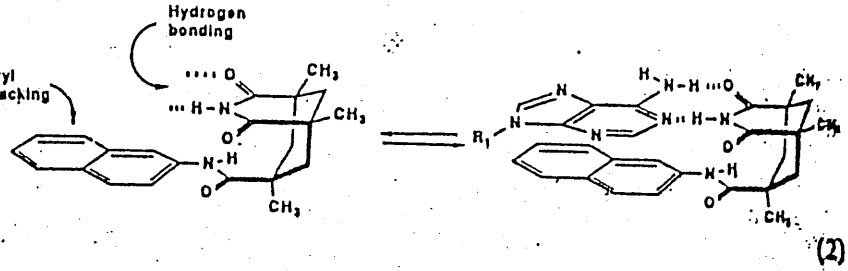

Molecular recognition: Watson-Crick and Bifurcated Hydrogen Bonding in a Model for Adenine Recognition.

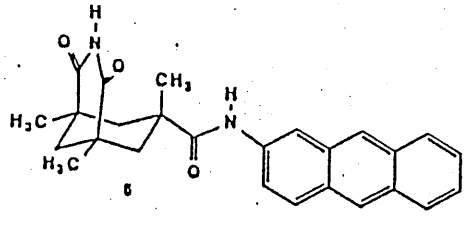

FIG.83-3

Hamilton ‹367› has incorporated multiple recognition sites into a new class of nucleic acid binding molecules. He assembled hydrogen binding and hydrophobic groups within a macrocyclic structure that could form a cavity complementary to a nucleotide base substrate Fig.82-1. Treatment of the host with 1-butyl thymine Fig.82-2 gives the triply hydrogen bonded complex shown in Fig.82-3. On substrate complexation the host acts as a molecular hinge which swings the naphthaline unit through an arc to within van der Waals distance of the thymine ring. This induced fit behaviour in a synthetic molecule directly mimics the recognition of nucleotides by ribonuclease t_1 in which a tyrosine residue moves into place above the bound guanine .

Rebek's concave systems have already been discussed ‹166› Fig.43 and these represent systems that are able to recognize smaller molecules of complementary size, shape and functionality. For double stranded nucleic acids the principal stabilizing intermolecular forces involve Watson-Crick hydrogen bonds in a base-pairing sense and aryl stacking interactions between adjacent base pairs Fig.83-eqn 1. Rebek introduced a model system ‹368,369› Fig.83-3 in which stacking and hydrogen bonding converge from perpendicular directions to recognize and complex adenine derivatives Fig.83-eqn 2.

Stoddart has synthesized cyclophane - like macrocyclic polyethers Fig.84-1-84-4 in order to achieve discrimination and selective complexation of paraquat $[PQT]^{2+}$ Fig.84-5 over Diquat $[DQT]^{2+}$ Fig.84-6. Fig.84-1 binds $[DQT]^{2+}$ with high selectivity ‹370,371›, whereas Fig.84-2 shows modest selectivity towards $[PQT]^{2+}$ ‹372› Fig.84-3 and 84-5 have been shown to bind $[PQT]^{2+}$ in the solid state.

Diederich has synthesized a series of cyclophane hosts capable of selective molecular recognition of neutral substituted benzene groups ‹296› Fig.85-1. Complexation is driven by very strong enthalpic hydrophic effects ‹303›. He has also synthesized ‹373› Fig.85-2 and 85-3 which both serve to recognize naphthalene. Comparative studies on Fig.85-2 and 85-3 demonstrate a negative heterotopic allosteric effect in complexation. The stability of the naphthalene complexes of Fig.85-2 does not change upon addition of

FIG.84 MOLECULAR RECEPTORS FOR DIQUAT AND PARAQUAT

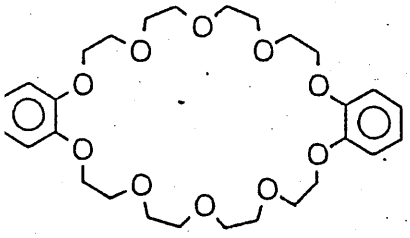

FIG.84-1

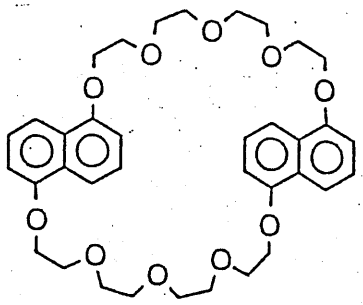

FIG.84-2

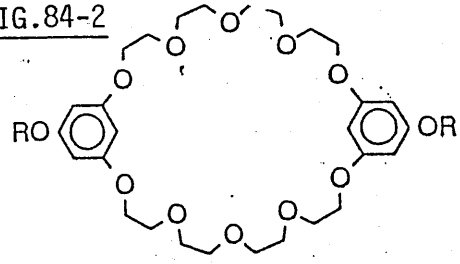

FIG.84-3

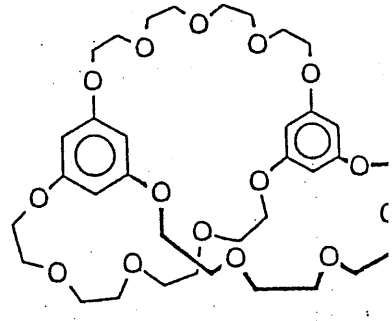

FIG.84-4

[PQT]$^{2+}$

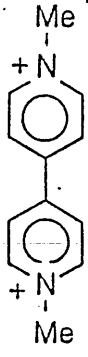

FIG.84-5

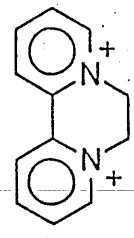

[DQT]$^{2+}$

FIG.84-6

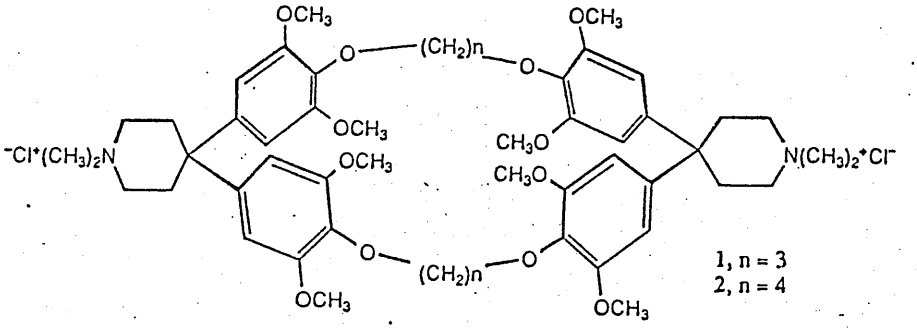

FIG.85-1

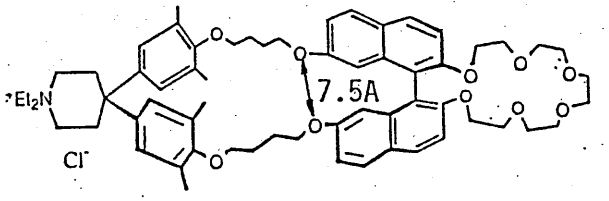

FIG.85-2

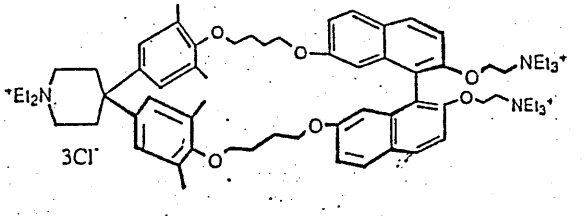

FIG.85-3

potassium salts whereas the stability of the naphthalene complexes of Fig.85-3 are significantly reduced as a result of cation binding to the crown.

CHAPTER 2
EXPERIMENTAL

SAFETY NOTE

Perchlorates(notably Ag^{+}, Pb^{2+} and Fe^{2+})are potentially explosive and c
should be taken whilst working with them.

1.The wearing of safety glasses, lab coat and heavy shoes are obvious precautionary steps.

2.Never reflux a perchlorate: if necessary reflux as the nitrate and ad the perchlorate salt after! When warming a solution containing the perchlorate counter ion always use a condenser connected to a water swi to prevent the solution boiling dry.

3.Never dry a perchlorate product using heat; either dry in vacuo or le to air dry.

4.If the product has been collected on a frit never scrape it off as th friction can create the heat that causes the heat that causes the produ to explode.

THE LIGAND 'WT' AND ITS COMPLEXES.

1,3-diamino propane. $H_2N(CH_2)_3NH_2$

This was obtained from the Aldrich Chemical Company Ltd, and used without further purification.

2,6-Diformyl pyridine (DFP).

The procedure used by Jerchel[1] was followed throughout this preparation.

2,6-pyridine dimethanol (19g) and selenium dioxide (15.15g) were dissolved in dry dioxan (300cm^3) and refluxed for 4 hours. The solution was filtered and evaporated to dryness to give the crude product 2,6-diformyl pyridine. This was crystallized using a chloroform/pet.ether (40°-60°) mixture. The cream coloured powder was stored in the freezer. (YIELD = 77%).

INFRARED SPECTRUM.

Inter alia. 3080 (aromatic C-H) 2860 (aliphatic C-H) 1715 (C=O) 1580, 1350, 1260, 1290, 810, 799.

TEMPLATE SYNTHESIS OF 'WT'.

DFP [2.025g] and $Ba(ClO_4)_2$ [2.7g] were dissolved in EtOH (300ml) and brought to reflux. Diamino,1,3-propane (1.1g) in EtOH (15ml) was added in a dropwise fashion over 15 minutes. The mixture was then refluxed for 1 hour with stirring. On cooling a white fine precipitate formed which was collected and washed with EtOH and dried in vacuo. A second batch was obtained from the filtrate after 24hrs at -20°C. On recrystallization, using ethanol and acetonitrile, crystals of X-rayable size were obtained (Yield 58%)

INFRARED SPECTRUM.

Inter alia. 3080 2920 1635m C=N 1583cm^{-1} (pyridine) 1130 1100 1050vs, 627, 625, 618, ms ($V_{ClO_4^-}$)

ANALYSIS : $BaWT(ClO_4)_2$

calc :	C	35.1	H	3.2	N	12.3
found :	C	35.4	H	3.2	N	12.2

Ω = 212 $Scm^2\ mol^{-1}$

On recrystallization, using an acetonitrile/ethanol mixture, crystals of X-rayable size were isolated.

ANALYSIS. $BaWT(ClO_4)_2.2EtOH$

calc :	C	35.4	H	3.7	N	11.2
found :	C	35.6	H	3.6	N	11.3

TRANSMETALLATED COMPLEXES.

$MnWT(SCN)_2.2MeOH$.

$BaWT(ClO_4)_2$ (.001 mole .6830g) was suspended in MeOH (100ml) and heated to 60°C. Solid $Mn(ClO_4)_2.6H_2O$ (0.0025 mole) was added. The $BaWT(ClO_4)_2$ gradually dissolved forming a yellow cloudy solution. This was filtered before NaSCN (.008 mole .6486g) in MeOH (50ml) was slowly dripped in. The resulting solution was heated for one hour at 60°C. It was reduced in volume to ≃40ml and an equal volume of ether added. This was left at room temperature for 1½ weeks at which stage, a yellow powder had formed leaving a colourless supernatant. (YIELD 49%).

INFRARED SPECTRUM.

Inter alia 3060, 2920, 2085sh, 2075sh, 1642m, 1592(pyridine)

ANALYSIS. $MnWT(SCN)_2.2MeOH$

calc :	C	49.56	H	5.20	N	19.26
found :	C	49.57	H	4.69	N	19.13

Ω = 90 $Scm^2\ mol^{-1}$

$Fe_2WT(SCN)_4(.xH_2O)$.

$BaWT(ClO_4)_2$(0.5 mmole, .3300g) was dissolved in dry and deoxygenated MeCN(≈100ml). On addition of solid $Fe(ClO_4)_2.6H_2O$ (1 mmole, .3507g) there was an instantaneous colour change (colourless to red to deep purple). NaNCS (0.010 mole, .3134g) in dried and deoxygenated CH_3CN (50ml) was added over 15 minutes and the resulting solution filtered. Nitrogen was bubbled through the solution until the first signs of solid at which point the flask was placed in an ice bath. A deep purple solid was filtered off and dried in vacuo. (59%)

INFRARED SPECTRUM.

Inter alia (3400-3300 (br-H_2O))* 2070cm^{-1}, 1990, 1640vw,1588cm^{-1}

ANALYSIS

$FeWT(SCN)_4$						
calc :	C	41.75	H	3.21	N	20.29
found :	C	39.81	H	3.25	N	19.46**
$Fe_2WT(SCN)_4.H_2O$						
calc :	C	39.67	H	3.61	N	19.28

$Ni_2WT(SCN)_4$

$BaWT(ClO_4)_2$(.001 mole, .683g) was dissolved in hot MeCN (150ml). A solution of NaSCN (.006 mole, .324g) in MeCN (20ml) was added and a small amount of white precipitate ($Ba(SCN)_2$) was filtered off before a solution of $Ni(ClO_4)_2.6H_2O$ (.002 mole, .7314g) in MeCN (20ml) was slowly added. The resulting solution was warmed at 50°C until there was no further colour change (30min) and the flask was then cooled in ice. A bright green precipitate formed which was filtered, washed in ice cold EtOH and dried in vacuo. (YIELD=68%)

* Some IR's showed water and some didn't. Unfortunately those that showed water did not fit analysis.

** IR did not indicate water.

INFRARED SPECTRUM.

Inter alia 3045, 2920, 2105ms, 1985vs(Vas NCS^-), 1623m (VC=N), 1580, 1050, 820, 760, 468,

ANALYSIS. $Ni_2WT(SCN)_4$

calc :	C	41.40	H	3.18	N	20.12
found :	C	41.39	H	3.38	N	20.31

μ_{eff} 293k=3.11Bm 93k=3.10Bm

$Ni_2WT(SCN)_2(Ph_4B)_2.2MeCN$.

$BaWT(ClO_4)_2$ (0.5 mmole, .3413g) was warmed to 50°C in MeCN(100ml). Solid NaNCS (.001 mole, .0811g) was added and the resulting solution stirred for 5 minutes. After filtering, $Ni(ClO_4)_2.6H_2O$ (.001 mole, .3657g) was added again in solid form. After 15mins, $NaPh_4B$ (.002 mole, .6845g) in MeCN (50ml) was added over 1hr. The resulting olive green solution was stirred for ½hr at 50°C, filtered hot, and placed in an ice bath. A green crystalline product separated out of solution. This was collected and air dried. (YIELD=75.5%)

INFRARED SPECTRUM

Inter alia 3050cm^{-1}, 2940, 2310, 2280 (VMeCN), 1975vs(VasNCS^-), 1627mwC=N, 1580cm^{-1}, 740 713 (BPh^-_4), 472

ANALYSIS $Ni_2WT(SCN)_4$

calc :	C	68.2	H	5.2	N	10.7
found :	C	68.1	H	5.2	N	10.5

$Co_2WT(NCS)_4$.

$BaWT(ClO_4)_2$, (0.5mmol) was dissolved in MeCN(50ml) and $Co(ClO_4)_2.6H_2O$ (1mmol) added. The resulting solution was refluxed for ≈30min before 2-3mmol of NaNCS dissolved in EtOH (20ml) was added. After 10mins, the solution was allowed to cool to room temperature before being concentrated using a rotary evaporator to ≈30cm^3. After filtering, the solution was left

to crystallize in a freezer at -20°C. A light brown microcrystalline powder was collected (YIELD 72%).

INFRARED SPECTRUM.

Inter alia. 3043, 2842, 2090ms, 1985vs, 1628, 1582cm^{-1}

ANALYSIS $Co_2WT(NCS)_4$

calc :	C	40.3	H	3.1	N	19.6
found :	C	40.8	H	3.0	N	19.1

μ_{eff} 293k; 4.63 93k 4.30

NOTE: Despite much effort no other pure (with respect to acceptable microanalysis) was obtained. Crude $Co_2WT(N_3)_2(Ph_4B)_2$ showed both the high frequency (2080cm^{-1}) and low frequency (2000cm^{-1}) N_3^- signals so it is possible this is a candidate for a single end-on azide bridge!

$Cu_2WT(ClO_4)_3\mu OH$.

Copper perchlorate hexahydrate (.008mole, 2.964g) was dissolved in hot ethanol (20ml) and added to a hot suspension of $BaWT(ClO_4)_2$ (.002 mole, 1.365g) in EtOH (200ml). The suspension was refluxed for 1hr during which a light blue to dark blue colour change occurred. After cooling a sky blue powder was collected. (YIELD 40%)

* No more product was obtained from the filtrate.

INFRARED SPECTRUM.

Inter alia 3547(ν_{OH}), 3041(aromatic C-H), 2943(aliphatic C-H). 1630(C=N), 1585(pyridine), 1165, 1091vs, 623ms(ClO_4),

ANALYSIS $Cu_2WT(OH)(ClO_4)_3$

calc :	C	30.5	H	2.9	N	10.7
found :	C	30.5	H	3.1	N	10.5

Ω=409 Scm^{2}mol^{-1}

μ_{eff} 293k, 1.60βm, 93k, 0.90βm.

$Cu_2WT(ClO_4)_2(SCN)_2$

$Cu_2WT(ClO_4)_3(OH)$ (0.5 mmole, .4144g) was warmed to 50°C in MeCN (80ml) before NaNCS (.0012 mole, .0843g) in MeCN (20ml) was slowly dripped in over ≈20mins. The flask was placed in ice to cool it quickly, and a small amount of green precipitate formed. This was removed before the solution was concentrated to ≈20ml. It was then left in a freezer at -20°C for 16hrs. A green microcrystalline product was collected and washed with ice cold MeCN. (YIELD 52.%)

INFRARED SPECTRUM.

Inter alia 2070s, 1625, 1589, 1090vs, 629ms

ANALYSIS $Cu_2WT(SCN)_2(ClO_4)_2$

calc :	C	33.5	H	2.8	N	14.2
found :	C	33.5	H	3.0	N	14.0

μ_{eff} 293k=1.67βm 93k=1.51βm

$Cu_2WT(SCN)_2(Ph_4B)_2$

$Cu_2WT(ClO_4)_3(OH)$ (0.4 mmol, .3300g) was dissolved in MeCN (300ml) and a solution of NaNCS (0.25 mmol, .0203g) in MeCN (150ml) was dripped in over 1½hrs. The experiment was carried out at room temperature. An excess of Ph_4BNa (.0012 mole, .411g) in MeCN (100ml) was dripped in over 1hr once all the NaNCS solution had been added. With both solutions added, the resulting green solution was stirred at RT for ½hr. The volume was reduced by ½ and the remaining solution left in a freezer at -20°C for 48hrs. A green crystalline product was obtained. (Yield 48%)

INFRARED SPECTRUM

Inter alia 3028, 2780, 2029s, 1623 mw, 1582, 740 715ms (Ph_4B)

ANALYSIS: $Cu_2WT(NCS)_2(Ph_4B)_2$

calc :	C	68.4	H	5.1	N	9.1
found :	C	68.3	H	5.0	N	9.2

Ω = 170 $Scm^2\ mol^{-1}$ (10^{-3}M MeCN)

μ_{eff} 293K = 1.71 Bm 93K = 1.70Bm

NOTE When this reaction was tried with smaller volumes the yield was significantly lower. When the reaction was carried out at 40°C an oily product was obtained.

$Cu_2WT(N_3)_2(ClO_4)_2$

This experiment was carried out at room temperature throughout. NaN_3 was dissolved in EtOH (30ml) to which a small volume of water (10ml) had been added. This was diluted with MeCN (160ml). This solution was slowly dripped into a solution of $Cu_2WTOH(ClO_4)_3$ in MeCN (100ml) and the resulting solution stirred for 2½hrs. It was then reduced to ≃ 30ml and left at -20°C for 72hr. Dark green crystals were collected and air dried. (32% Yield)

INFRARED SPECTRUM

Inter alia 3065, 2940, 2075s, 1645, 1580, 1340ms ($V_{as}N_3^-$)
1623mw, 1090vs, 628ms

ANALYSIS $Cu_2WT(N_3)_2(ClO_4)_2$

calc :	C	31.7	H	2.9	N	22.2
found :	C	32.0	H	2.8	N	21.7

Ω = 356 $Scm^2\ mol^{-1}$

μ_{eff} 293K 1.85Bm 93K 1.85Bm

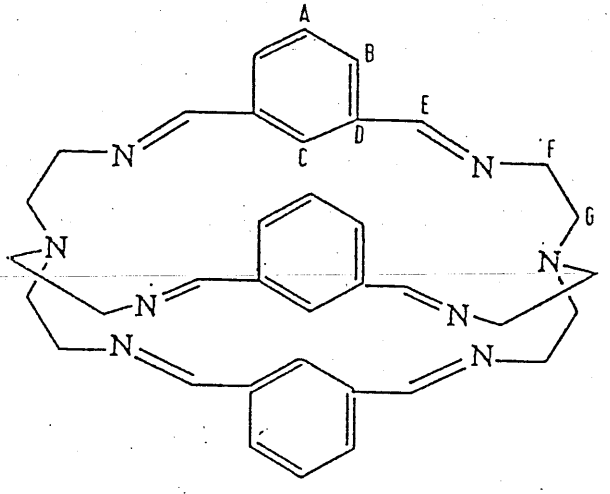

LIGAND 3Bm

THE LIGAND 3Bm AND ITS COMPOUNDS

ISOPHTHALALDEHYDE (benzene 2,6 dicarboxaldehyde). This was obtained from Aldrich Chemical Company Ltd. and used without further purification

3Bm

Isophthalaldehyde (.003 mole) was warmed to gentle reflux in MeOH (300ml) before tren (.002mole) was added in concentrated form. This solution was stirred at mild reflux for 2-3 hours. On cooling fine white crystals separated. After filtering, the filtrate was left to evaporate at room temperature in a beaker. This yielded white crystals of X-rayable dimensions. (Yield = 89%).

INFRARED SPECTRUM

Inter alia: 3281, 3042, 3024, C_{aro}-H, 2900-2800 C_{ali}-H, 1643 C=N
1432, 1354, 1336, 1290, 1065, 1034, 926, 799,693, (ligand)

ANALYSIS 3Bm: $C_{36}H_{42}N_8$

calc :	C	73.7	N	19.1	H	7.2
found :	C	73.9	N	19.2	H	7.3

NMR

^1H CD_2Cl_2 298k 360MHz

PROTON	δppm	multiplicity	integral	number of protons
A	7.52	t	16	3
B	8.19	d	29	6
C	5.33	s	15	3
E	7.58	s	30	6
F	3.72(br) 3.29(br)	d	59	12
G	2.89(br) 2.70(br)	d	61	12

^{13}C $CDCl_3$ 298k 90MHz

CARBON	δppm	off resonance
A/B/C	131.54 128.56 126.4 all 3 are doublets but are indistinguishable	
D	136.18	s
E	159.77	d
F	59.41	t
G	55.03	t

MASS SPEC $M^+ = 586$

NOTE : Despite many attempts no template species was obtained and in each case the metal free product was obtained.
Metals tried include :-
$Ba^{2+}(Ph_4B^-, ClO_4^-)$, Pb^{2+}, $Ag^+(ClO_4^-$, PF_6^-, $CF_3SO_3^-)Cu^{2+}$, Ca^{2+}, Cu^I
$Cs^+(I^-$, $NO_3^-)$ Sr^{2+} Mg^{2+}

Other variations eg. solvent mixtures, counterions, temperature and reaction time, were tried.

$Ag_2$3Bm$(CF_3SO_3)_2$.2EtOH (INSERTION)
3Bm (0.10g, 0.17mmol) was warmed to 40°C in an MeCN (50ml)/EtOH (50ml) solvent mixture before a solution of $AgCF_3SO_3$ (MeCN (50ml)/EtOH (50ml) was added over ½ hour. The resulting pale yellow solution was stirred at 40°C for 6 hours. On cooling the solution was reduced in volume until the first signs of solid. After filtering the flask was placed in a freezer at -20°C. This gave a white fine crystalline solid in 32% yield

NOTE: This reaction did not work at room temperature or when only MeCN was used.

INFRARED SPECTRUM.

Inter alia: 3490 (OH of EtOH) 3065 3030 (C_{aro}-H) 2917
2859 (C_{ali}-H) 1649 (C=N) 1598 (ligand)
1254, 1148, 1029 (CF_3SO_3)

ANALYSIS $Ag_2$3Bm$(CF_3SO_3)_2$.2EtOH

calc :	C	41.1	H	4.4	N	9.6
found :	C	40.9	H	3.9	N	9.3

Ω = 295 $Scm^2\ mol^{-1}$

NMR (labelling as 3Bm)

'H 294K CD_3CN 360MHz

PROTON	δppm	MULTIPLICITY	INTEGRAL	No. OF PROTONS
A	7.75	t	21	3
B	7.87	d	42	6
C	9.50br	s	42	6
E	8.59	s	44	6
F	3.46	s	87	12
G	2.90	s	85	12.

EtOH observed as triplet at 1.21 (integral 44 ie 6H)
quartet at 2.36 (integral 23 ie 4H)

F.A.B		% OF BASE PEAK
[$Ag_2$3Bm(CF_3SO_3)]$^+$	951	(68)
[$Ag_2$3Bm]$^{2+}$	801	(8)
[Ag3Bm]$^+$	693	(100)
[3Bm]$^+$	585	(7)

$Cu_2$3Bm$(ClO_4)_2.2H_2O$

3Bm (.2mmol, .11 g) was dissolved in deoxygenated CH_2Cl_2 before $Cu(MeCN)_4ClO_4$ (.4mmol .12g) in 20ml deoxygenated MeCN/EtOH (2:1) was added. After full development of the bright yellow colour the solution, being non oxygen - sensitive, was reduced in volume on a rotary evaporator to ≈20ml. On standing a yellow crystalline product formed in 58% yield.

INFRARED SPECTRUM

Inter alia 3060 3029 C_{arc}-H, 2869 C_{ali}-H 1646 C=N
1589 ligand 1086, 622 ClO_4^-

ANALYSIS $Cu_2$3Bm$(ClO_4)_2.2H_2O$

calc :	C	45.56	H	4.89	N	11.81
found :	C	44.51	H	5.21	N	11.35

Ω = 352 Scm^2mol^{-1} (10^{-4}M, MeCN)

NMR ^1H CD_3CN 294K 360MHz

PROTON	δppm	multiplicity	integral	No. of protons.
A	7.709	t	15	3
B	7.80	d	29	6
C	9.913	s	14	3
E	8.512	s	30	6
F	3.30	d	58	12
G	3.175, 2.7	d, m	30, 31	12

$[Cu_2$ 3Bm$]^{4+}$

3Bm (.3g, .54 mmol) was dissolved in CH_2Cl_2. A solution of $Cu(ClO_4)_2.6H_2O$ (.7g 1.89 mmol) was added in EtOH resulting in the instant precipitation of a bright green solid (.4g, 77%). Recrystallization of this powder gave a fine bright green microcrystalline product.

If the green powder is stirred over a period of ≈24hrs in CH_2Cl_2/MeCN/EtOH a bright blue crystalline powder is obtained (≈40%)

INFRARED SPECTRUM

Inter alia (Green product) - 3428, 3128, 2926, 2876, 1643, 1605, 1577, 1088, 624.

Inter alia (Blue product) - 3423, (OH) 3314 3273, (NH_2), 3107*, 2928, 2879, 1646, 1579*, 1556*, 1093, 623

* possibly deriveed from phenoxy - OPh.

ANALYSIS

Green product

$Cu_2$3Bm(OH)$(ClO_4)_3$	calc :	C	40.60	H	4.35	N	10.63
	found :	C	40.39	H	4.40	N	10.52

BLUE FORM $Cu_2$2Bm-O(OH)$(ClO_4)_3$

calc :	C	34.77	H	4.41	N	10.88
found :	C	35.22	H	4.58	N	11.59

Ω (Green) = 573 Scm^2mol^{-1} (10^{-4}M)

Ω (Blue) = 545 Scm^2mol^{-1} (10^{-4}M)

F.A.B Green form.

		% OF BASE PEAK (M/e = 110)
[$Cu_2$3Bm(OH)$(ClO_4)_2$]$^+$	929	(15)
[$Cu_2$3Bm(OH)ClO_4]$^+$	830	(50)
[$Cu_2$3BmOH]$^+$	729	(30)
[Cu3Bm]$^+$	649	(55)

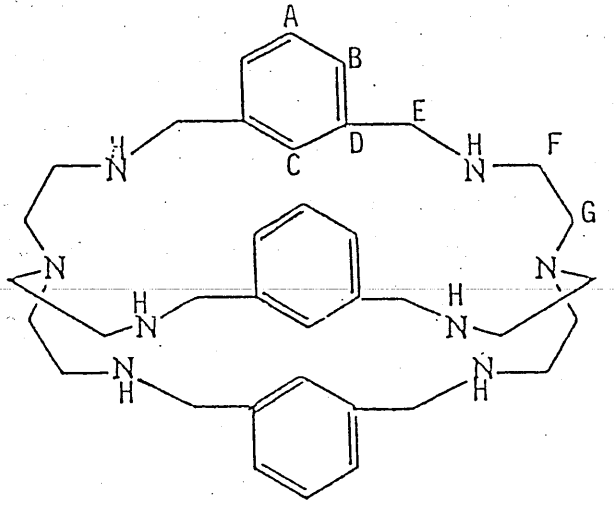

LIGAND R3Bm

R3Bm. H_2O (this was prepared in two ways)

METHOD A

3Bm (1.7627g) was suspended in EtOH (400ml) and brought to reflux. A large excess of $NaBH_4$ was added as a solid in small amounts until no further fizzing occurred upon addition. The solution was left to reflux for 3 hours before the heat was switched off - the solution was then left to stir at room temperature for 48 hours. After filtering, the solvent was removed and the resulting creamy white solid taken up in a strong NaOH solution (1g in 15ml H_2O). Chloroform (6x30ml) was used to extract the product, - the combined extracts then being washed with demineralized water (1x50ml). Na_2SO_4 was used as drying agent and a quantity added until the cloudiness of the washed extracts had disappeared. The chloroform solution was reduced to dryness leaving an oily material which was taken up in MeOH (250ml). This gave a small amount of white insoluble material which was filtered off. Again the solvent was removed leaving a waxy solid which was pumped for 48 hours to give a white solid (Yield = 66%)

NOTE Reaction needs 48 hour stir - mass spec. of product obtained after 3 hour reflux stage gave values of partially reduced species at 594, 595, 596, 597.

INFRARED SPECTRUM

Inter alia: 3298 N-H, 3105 3012 C_{aro} -H, 2878
2918 C_{ali} -H, 1455, 1438, 1127
1049, 780, 751, 694, cm^{-1} (ligand)

ANALYSIS R3Bm .H_2O

calc :	C	70.0	H	9.0	N	17.7
found :	C	70.0	H	8.6	N	18.1

MASS SPEC

m/e^+ 598 (100%)

NMR

^1H 298K 360MHz CD_3OD

PROTON	δppm	multiplicity	integral	no. of protons
A/B	7.20	M*	38	3+6
C	7.09	s	12	3
E	3.62	s	50	12
F	2.59	m	56	12
G	2.45	m	54	12

* undistinguishable multiplet

NH observed at 2.3ppm as broad hump - confirmed by D_2O shake

METHOD B

This involved an **in situ** reduction ie without isolation of the 3Bm ligand.

Isophthalaldehyde (.8181g .006mole) was brought to reflux in EtOH (≃300ml) before the concentrated amine (.004mole, .6ml) was added. This solution was left to stir at reflux for 3 hours before an excess of $NaBH_4$ was added until no further fizzing occurred upon addition. This solution was left refluxing for a further 3 hours before the heat was turned off. The solution was left to stir at room temperature for 48 hours before being worked up as before. This gave a yellow oily product in 54%yield.

MASS SPEC

M/e^+ 598 (-no partially reduced impurity observed)

NOTE - this method gives a lower yield and a poorer quality of product.

H_2R3Bm$(CF_3SO_3)_2$

This product was obtained whilst attempting to insert Ag^+ into the reduced ligand.

R3Bm (.1g 0.167 mmol) was dissolved in MeCN/EtOH (50ml/50ml) and warmed to 40°C. A solution of silver triflate (25ml MeCN/25ml EtOH) was added slowly over ½ hour. The resulting pale yellow solution was stirred for 3 hours at 40°C. On cooling the solution was concentrated and placed in the freezer over the weekend. Fine white platelet crystals were obtained in 19% yield.

INFRARED SPECTRUM

Inter alia 3289, N-H, 3070 C_{aro}-H 2824 C_{ali}-H
1256, 1159, 1029, $CF_3SO_3^-$

ANALYSIS H_2R3Bm$(CF_3SO_3)_2$

calc :	C	50.8	H	6.29	N	12.46
found :	C	50.6	H	6.4	N	12.3

F.A.B		% OF BASE PEAK
[H R3Bm]$^+$	600	(62)
[H_2 R3Bm CF_3SO_3]$^+$	749	(100)

Work on the transition metals with R3Bm is yet to be carried out

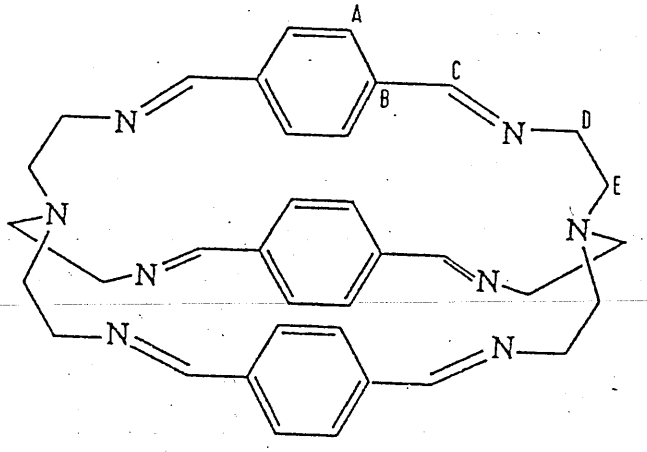

LIGAND 3Bp

THE LIGAND 3Bp AND ITS COMPLEXES

Benzene 1,4-dicarboxaldehyde (Terephthalaldehyde)

This was obtained from Aldrich Chemical Company Ltd. and used without further purification.

INFRARED SPECTRUM

Inter alia: 3363 C_{aro}-H, 2884 C_{ali}-H, 1694, C=O
1500, 1380, 1300, 1200, 805, 780, 480 cm^{-1}

$Ag_2$3Bp$(CF_3SO_3)_2$ (TEMPLATE)

$AgNO_3$ (.002 mole, .3398g) was dissolved in MeOH (100ml) at 50°C. Terephthalaldehyde (.003 mole, .4024g) in MeOH (50ml) and tren (.002mole, .30ml) in MeOH (50ml) were added simultaneously. This gave a brown murky solution which on stirring for 2 hours at 50°C became yellowy green. On cooling, the solution was filtered before being concentrated to ≈50ml. An excess of triflate in an equal volume of acetonitrile (ie ≈50ml) was added before the beaker was blacked out using perforated foil and placed in a fume cupboard to allow slow evaporation. This gave bright yellow crystals of X-rayable size (Yield = 89%).

INFRARED SPECTRUM

Inter alia: 3280 C_{aro}-H, 2842 C_{ali}-H, 1644 C=N
1266, 1162, 1028, CF_3 SO_3^-.

ANALYSIS $Ag_2$3Bp$(CF_3SO_3)_2$

calc	C 41.5	H 3.9	N 10.2
found	C 41.9	H 4.0	N 10.4

Ω = 262 $Scm^2\ mol^{-1}$

NMR

^1H 294K CD_3CN 400MHz

PROTON	δppm	multiplicity	integral	no. of protons
A	7.86	s	42	12
C	8.70	s	21	6
D	3.09	t	43	12
E	3.07	t	42	12

^{13}C

CARBON	δppm	off resonance multiplicity
A	116.9	d
B	162.227	s
C	127.46	d
D	56.2	t
E	50.7	t

F.A.B		% BASE PEAK
$[Ag_2 3BpCF_3SO_3]^+$	951	(22)
$[Ag3Bp]^+$	693	(100)
$[3Bp]^+$	587	(10)

NOTE: When using $AgClO_4$ the main reaction was the formation of an olive green silver-amine complex. This was confirmed by reacting silver perchlorate with tren in the absence of the dicarbonyl:- this also gave a green product. The ir of the 2 green products were identical showing NH_2 peaks at 3361 and 3342cm^{-1} as well as very weak or no signal at ca 1640cm^{-1} (C=N) in the case of the template attempted reaction.

$Pb_2$3Bp$(SCN)_4$

$Pb(SCN)_2$ (4 mmol, 1,358g) was suspended in MeCN (350ml) and heated to 50°C. Tren (.004mole, .60ml) in MeOH (75ml) and the dialdehyde (.006mole .8048g) in MeOH (75ml) were dripped in simultaneously. On stirring for 3 hours the solution gradually became a very pale yellow. Unreacted $Pb(SCN_2)$ was filtered off, and the filtrate reduced. The solution was left to evaporate. This gave a creamy yellow powder in 87% yield.

NOTE Despite efforts this product was never obtained in a pure form (ie unsatisfactory microanalysis). However it reduced successfully with sodium borohydride to give R3Bp. Presence of a black solid after reduction showed presence of the metal in the unreduced starting material.

Ba2Bp$(ClO_4)_2$ - When Ba^{2+} was used as templating agent the ir of the product indicated NH_2 but not C=O. Thus the product may be an open chain derivative - this will be followed up in the future as a means of obtaining assymmetric cryptands. NOTE:- in refluxing dry MeOH the open chain product, as indicated by ir was obtained, but at room temperature in MeOH an oily material showing both NH_2 and C=O signals in the ir was obtained

3Bp .$6H_2O$

Terephthalaldehyde (.4024g .003mole) was warmed to 50°C in MeOH (100ml). A solution of tren (.002mole .30ml) in MeOH (50ml) was dripped in over ½ hour and the solution was then stirred for 2½ hours at 50°C during which a bright yellow colour developed. On cooling, the solution was filtered and concentrated to ≈40mls. An equal volume of MeCN was added, and the beaker left in a well ventilated area to allow evaporation. Small cubed crystals of X-rayable size were collected and washed with ice cold MeCN (78%).

INFRARED SPECTRUM

Inter alia 3650-3000cm^{-1}, H_2O, 2841 C_{alk}-H, 1643, C=N,
1450. 1437, 1375, 1338, 1300, 1077, 1033,
907, 823, 742, 722, 514, ligand.

ANALYSIS 3Bp .$6H_2O$

calc :	C	62.1	H	7.8	N	16.1
found :	C	61.7	H	7.9	N	16.5

NMR

'H CD_3OD 298K 360MHz

PROTON	δppm	multiplicity	integral	no. of protons
A	7.32	s	40	12
C	8.29	s	20	6
D	3.84[c]	s[a]	41	12
E	2.83[c]	s[b]	40	12

(a) essentially singlet but really is a very poorly resolved quinted.

(b) essentially singlet but really is a very poorly resolved triplet.

(c) slightly broad.

NOTE: Water observed as singlet at 5.0ppm integral 41 (12H) ie $6H_2O$.

^{13}C CD_3Cl_3 RT 90MHz

CARBON	δppm	off resonance multiplicity
A	154.15	d
B	165.59	s
C	194.58	d
D	69.86	t
E	63.49	t.

MASS SPECTRUM

M^+ 587 (100%)

$Ag_2$3Bp$(CF_3SO_3)_2$ (INSERTION)

3Bp (.15g .256mmol) was dissolved in MeCN (50ml)/EtOH (50ml) at 50°C. A solution of $AgCF_3SO_3$ (.1645g .63mmol) in MeCN (25ml)/EtOH (25ml) was slowly dripped into the solution of the ligand heating at 50°C, and stirring was maintained for 2 hours before the solution was cooled, concentrated and placed at -20°C for 24 hours. This gave fine yellow needle crystals in 62% yield. (IR, analysis, mass spec, and nmr as for the templated form of the titled complex.)

$Cu_2$3Bp$(ClO_4)_2$

3Bp (.2mmol .1172g) was dissolved in deoxygenated CH_2Cl_2. $Cu(MeCN)_4ClO_4$ (.4mmol, .1308g) was added as a solution in MeCN(20ml). This gave a yellow colour. After ½ hour the solution was concentrated to ca 20ml on a rotary evaporator. This yielded bronzey crystals in 54% yield.

INFRARED SPECTRUM

Inter alia: 3038 C_{aro}-H, 2914, 2854 C_{ali}-H,
1627 C=N, 1088, 622, ClO_4^-

ANALYSIS $Cu_2$3Bp$(ClO_4)_2$

calc :	C	47.39	H	4.64	N	12.28
found :	C	47.23	H	4.63	N	12.24

Ω = 367 Scm^2mol^{-1} ($10^{-4}M$)

NMR

^{1}H nmr CD_3CN 400MHz 294K

PROTON	δppm	multiplicity	integral	no. of protons.
A	7.42	s	37	12
C	8.59	s	19	6
D	3.87	t	38	12
E	3.15	t	37	12

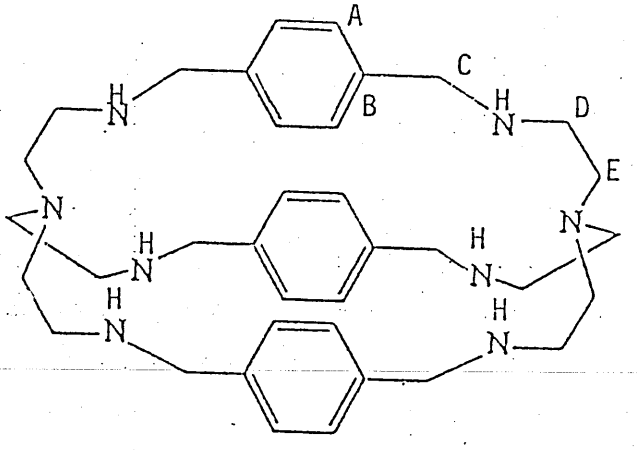

LIGAND R3Bp

R3Bp

The reduced form of the ligand 3Bp has been prepared in 4 ways - all use $NaBH_4$ as the reducing agent.

(A) reduction of $Pb_2$3Bp$(SCN)_4$ or $Ag_2$3Bp$(CF_3SO_3)_2$
(B) in-situ reduction of $Pb_2$3Bp$(SCN)_4$ or $Ag_2$3Bp$(CF_3SO_3)_2$
ie. forming $Pb_2$3Bp$(SCN)_4$ but not isolating it.
(C) reduction of 3Bp.$6H_2O$
(D) in-situ reduction of 3Bp .$6H_2O$

Yields and quality of reduced product were generally better where the unreduced product was isolated and then reduced rather than the in situ reduction.

The reduction of $Pb_2$3Bp$(SCN)_4$ required a shorter reaction time than the reduction of 3Bp.$6H_2O$. This seems to be a general trend in all the ligands of this series. The metal free ligands generally require a 48 hour stir at room temperature as well as the 3 hour reflux whereas for the metal derivatives the 3 hour reflux (in some cases with a 12 hour stir at room temperature) seems to suffice.

$Pb_2$3Bp$(SCN)_4$ (.74mmol .92g) was brought to reflux in EtOH (120ml). The $NaBH_4$ (3.9mmol .147g) was added in small portions (in solid form) over ½ hour. This produced a black colour and on adding a violent fizzing reaction occurred. Once all the $NaBH_4$ had been added the black suspension, in a now colourless liquid, (as opposed to the initial yellow colour) was heated at reflux for 3-4 hours. On cooling the black solid was filtered off and the filtrate worked up as in the case of 3Bm → R3Bm.

A white flaky solid - R3Bp - was obtained in 41% yield.

INFRARED SPECTRUM

Inter alia 3273, 3231 NH, 3041 C_{aro}-H, 2797 C_{ali}-H,
1513, 1458, 1362, 1326, 1296, 1127,
1053, 1017, 799, 772,

ANALYSIS R3Bp

calc :	C	70.7		H	9.3	N	17.5
found :	C	70.3		H	9.1	N	18.0

NMR

'H CD_3OD 298K 360MHz

PROTON	δppm	multiplicity	integral	no. of protons
A	6.8	s	48	12
C	3.67	s	23	6
D	2.8	t	48	12
E	2.65	t	48	12

BROAD NH at 2.01 ppm - confirmed by D_2O shake.

^{13}C CD_3OD 298k 360MHz

CARBON	δppm	multiplicity off resonance
A	127.51	d
B	138.4	s
C	54.1	t
D	53.6	t
E	47.95	t

MASS SPEC

M^+ 599

$Ag_2R3Bp(CF_3SO_3)_2.H_2O$

R3Bp (.167mmol .10g) was dissolved in MeCN (50ml)/EtOH (50ml) at 40°C. Ag CF_3SO_3 was dissolved in MeCN (25ml)/EtOH (25ml) and slowly dripped into the ligand solution. After 3 hours at 40°C the solution was cooled, filtered, concentrated and placed in the freezer for 48 hours. A white powder of the titled compound was collected in 48% yield.

INFRARED SPECTRUM

Inter alia: 3272, N-H, 3025 C_{aro}-H, 2851 C_{ali}-H, 1449 ligand, 1250, 1158, 1028, $CF_3SO_3^-$.

ANALYSIS $Ag_2R3Bp(CF_3SO_3)_2 . H_2O$

calc :	C	40.4	H	4.9	N	9.5
found :	C	40.4	H	4.2	N	9.9

Ω = 236 $Scm^2\ mol^{-1}$.

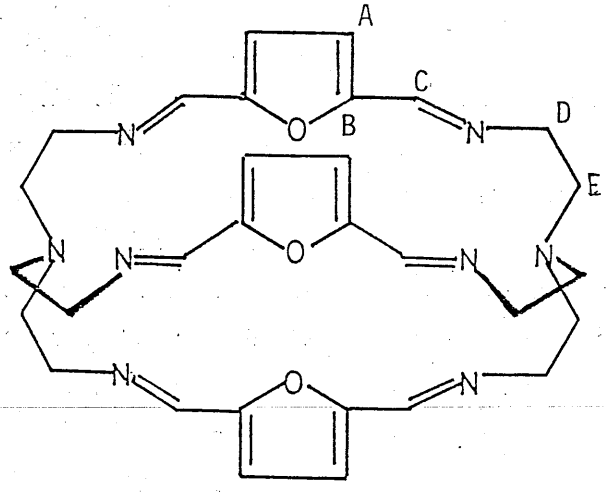

LIGAND 3F

THE LIGAND 3F AND ITS COMPLEXES.

Tris - (2-aminoethyl) amine '(TREN)' $(NH_2CH_2CH_2)_3N$

This reagent was obtained from Aldrich Chemical Company Ltd. and used without further purification.

2,5 - Diformylfuran (DFF)

2,5 - dimethanol furan (27.5g) was added to a suspension of freshly activated manganese dioxide (below) (290g) in dry toluene (1500ml). The mixture was stirred and refluxed for six hours during which the solution changed colour from deep orange/brown to yellow. On cooling, the solution was filtered to remove the manganese dioxide and the filtrate reduced to dryness on the rotary evaporator. The manganese dioxide was then heated and stirred in fresh toluene (200ml) to give another 2g of pale yellow crude product. The compound was recrystallized from chloroform/carbon tetrachloride and then sublimed at 60°C/0.45mmHg to give the pure 2-5 diformyl furan (Yield 82%). The product was characterized from CHN analysis, nmr, ir and mass spectrum

Infrared Spectrum

Inter alia 3140 C_{aro}-H, 2860 C_{ali}-H, 1680 C=O, 1510, 1410, 1260, 800

ANALYSIS $C_6 H_4 O_3$

calc :	C	58.0	H 3.2
found :	C	57.6	H 3.4

Mass Spectrum

p^+ m/e 124

'Hnmr Spectrum. 294K $CDCl_3$ 250MHz

PROTONS	ppm	
A	7.5	(s)
C	10.1	(s)

Preparation of Manganese dioxide

The compound was prepared by literature methods[2,3]. $MnSO_4.H_2O$ (150g) was dissolved in hot water (200 ml) and the pale pink solution was brought to the boil before a cold aqueous solution of $KMnO_4$ (120g in 4l) was added slowly (1l per ½ hour). Once all the $KMnO_4$ was added the resulting suspension was stirred and heated for a further 15min before being filtered using water suction. The brown/black solid was washed with boiling water (500ml). The MnO_2 was then placed in a large crystallization dish and heated in an oven at 120-125°C for 48 hours. Just before use the product was ground to a fine black powder in a well ventilated fume cubboard

My thanks go to Clarke Stevenson for his 'tips' and advice for carrying out these preparations

TEMPLATE FORMATION OF '3F'

Ba3F(ClO_4)(Ph_4B)

DFF (.004 mole, 0.4964g) and $Ba(ClO_4)_2$ (.0015 mole, 0.5043g) were stirred at 40°C in MeOH (300ml). The amine, tren, (0.3ml, .002mole) and Ph_4BNa (.0018mole, .6160g) were dissolved in MeOH (200ml) and dripped into the barium/DFF solution over 1½ hours. The resulting solution was stirred for a further 1½ hours during which a clear yellow solution developed. The product was obtained by rotatary evaporating the solution to dryness (62% yield)

INFRARED SPECTRUM

Inter alia: 3105,3055, C_{aro}-H, 2855 C_{ali}-H, 1648 C=N, 780, 720, Ph_4B^-, 1028, 622, ClO_4^-

ANALYSIS $Ba3F(ClO_4)(Ph_4B)$

calc:	C	58.29	H	5.07	N	10.07
found:	C	58.30	H	5.27	N	10.15

Ω = 244 Scm^2 mol^{-1} (402 for $10^{-4}M$)

F.A.B		% BASE ION PEAK = 122
$[Ba3FClO_4]^+$	793	(4.4)
$[Ba3FPh_4B]^+$	1013	(2.1)

$Ba3F(Ph_4B)_2$ BY TEMPLATE METHOD

- As for the $Ba3F(Ph_4B)(ClO_4)$ preparation but using over twice the amount of Ph_4BNa ie (.004mole, 1.3689g). This reduces the solubility of the product and makes it easier to obtain a cleaner product. It also increases the yield (72%).

$Ba3F(Ph_4B)_2$ BY INSERTION METHOD

$Ba(ClO_4)_2$ (0.65 mmol, .2187g) and 3F (0.65 mmol, 0.3682g) were dissolved in MeOH (200ml) at 40°C. A solution of Ph_4BNa (.0016mole, 0.5565g) in MeOH (50ml) was slowly added and the resulting yellow solution left to stir at 40°C for 3hrs. On cooling the volume was reduced until the first signs of solid appeared. After filtering the filtrate was placed in a freezer for 24 hours. A pale yellow microcrystalline product was obtained in 82% yield.

INFRARED SPECTRUM

Inter Alia 3348 3051, C_{aro}-H, 2854 C_{ali}-H, 1621 C=N, 747, 704, Ph_4B^-.

ANALYSIS $Ba3F(Ph_4B)_2$ by insertion

calc :	C	70.31	H	5.75	N	8.41
found :	C	70.10	H	5.60	N	8.53

Ω = 222 Scm^2 mol^{-1} (442 for $10^{-4}M$)

^{1}Hnmr CD_3CN RT 300MHz

PROTON	δppm	multiplicity	integral	no of protons
A	7.06	s	9	6
C	8.163	s	8	6
D	3.185 3.24 3.298	t	19	12
E	2.612 2.67 2.719	t	18	12

^{13}C CD_3CN RT 300MHz

CARBON ATOM	δppm	splitting (off resonance)
A	118.282	d
B	155.565	s
C	153.784	d
D	63.938	t
E	59.342	t

*Ph_4B^- at 168, 165, 163, 161, 136, 126, ppm

			% BASE ION PEAK = 298
F.A.B.	$[Ba3F(Ph_4B)]^+$	1013	(4.5)
	$[Ba3F]^+$	694	(13.2)

Sr3F(Ph$_4$B)$_2$.2H$_2$O INSERTION.

This was prepared in the same way as Ba3F(Ph$_4$B)$_2$, using Sr(ClO$_4$)$_2$.6H$_2$O. (.002 mole, .7892g) (Yield = 72%)

Infrared spectrum.

Inter alia 3120 furan, 3040 C$_{aro}$-H, 2945 C$_{ali}$-H, 1644 1621 C=N, 732 704 Ph$_4$B$^-$.

ANALYSIS Sr3F(Ph$_4$B)$_2$.2H$_2$O

calc :	C	73.03	H	5.97	N	8.74
found :	C	72.90	H	6.10	N	8.72

Ω = 250 Scm^2 mol^{-1} (460 for 10^{-4}M)

^{1}Hnmr CD$_3$CN RT 90MHz

PROTON	δppm	splitting	integral	no of protons
A	7.029	s	8	6
C	8.130	s	8	6
D	3.41(br)	m	16	12
E	2.6(br)	m	17	12

F.A.B. % BASE ION PEAK = 176

[Sr3F(Ph$_4$B)]$^+$	963	(4)
[Sr3F]$^+$	644	(10.8)

Ca3F(Ph$_4$B)$_2$.2H$_2$O (INSERTION).

This was prepared in the same way as the barium derivative using Ca(ClO$_4$)$_2$.6H$_2$O (.002mole .6941g) (Yield = 46%)

INFRARED SPECTRUM.

Inter alia 3060 furan, 3051 C$_{aro}$-H, 2849 C$_{ali}$-H, 1640 C=N, 734, 704 Ph$_4$B$^-$

ANALYSIS $Ca3F(Ph_4B)_2.2H_2O$

calc :	C	75.85	H	6.20	N	9.07
found :	C	75.22	H	6.43	N	9.54

Ω = 236 $Scm^2\ mol^{-1}$ (421 for 10^{-4}m)

NMR 'H CD_3CN RT 300MHz

PROTON	δppm	multiplicity	integral	no protons
A	6.98	s	12	6
C	8.089	s	12	6
D	3.49-3.57	m (sh)	25	12
E	2.67-2.78	m (sh)	27	12

CARBON	δppm
A	119.776*
B	153.44
C	154.531
D	59.457
E	59.112

* masked in solvent peak

BPh_4^- in evidence at 136, 126 and 122

F.A.B. % BASE ION PEAK = 307

$[Ca3F(BPh_4)]^+$	915	(10.4)
$[Ca3F]^{++}$	596	(41.9)
[3F]	557	(90)

NOTE - attempts to template on Sr^{2+} or Ca^{2+} gave products which were not fully closed ie. both NH_2 and C=O signals still apparent in ir. Only using insertion method could fully closed systems be obtained.

$Ag_2$3F$(CF_3SO_3)_2$. TEMPLATE METHOD.

$AgNO_3$ (.002mole, .3398g) was warmed to 40° in MeCN (300ml). A solution of tren (.002mole, .30ml in MeCN 100ml) and a solution of DFF (.003 mole, 3723g in 100ml MeCN) were added simultaneously over ½hr. The resulting solution was left to stir at 40°C for 3hrs. On cooling the volume was reduced to ≈40ml and $AgCF_3SO_3$ (large excess) in MeCN (10ml) added. The beaker was blacked out using foil. Holes were punched into the foil to allow slow evaporation of the solvent. This gave a mixture of products - the main product was a brown rubbery polymeric species but a small number of fine yellow crystals were also recovered (12%).

INFRARED SPECTRUM

Inter alia: 3583, 3510 water, 3103 C_{aro}-H, 2911 C_{ali}-H, 1647 C=N 1263, 1155, 1028 ($CF_3SO_3^-$)

ANALYSIS $Ag_2$3F$(CF_3SO_3)_2.H_2O.MeCN$

calc :	C	36.1	H	3.6	N	11.0
found :	C	36.0	H	3.2	N	10.6

Ω = 276 $Scm^{-1}mol^{-1}$

$Ag_2$3F$(CF_3SO_3)_2$ BY INSERTION METHOD.

The ligand 3F (0.26 mmol, .15g) was dissolved in methylene chloride (40ml) before a solution of $AgCF_3SO_3$ (0.89 mmol .23g in 80ml MeCN) was added. The resulting solution was stirred at 40°C for half an hour. On cooling EtOH (50ml) was added and the solution then concentrated until the first signs of solid appeared on the flask. The flask was left in a well ventilated area and after 24hrs fine yellow crystals were collected using EtOH (64%).

INFRARED SPECTRUM.

Inter alia 3130 furan, 2917, 2849, C_{ali}-H, 1643 C=N, 1268, 1155, 1028 (triflate)

ANALYSIS $Ag_2 3F(CF_3SO_3)_2$.

calc :	C	35.9	H	3.38	N 10.47
found :	C	35.49	H	3.34	N 10.70

Ω = 267 $Scm^2\ mol^{-1}$

F.A.B.

		% BASE ION PEAK
$[Ag_2 3F(CF_3SO_3)_2]^+$	1071	very weak
$[Ag_2 3F(CF_3SO_3)]^+$	921	80
$[Ag_2 3F]^+$	771	20
$[Ag 3F]^+$	666	100
$[3F]^+$	558	65

3F (NON-TEMPLATE SYNTHESIS)

A methanolic solution of tren (.002mole, 0.3mlin 100ml) was gently refluxed as a solution of DFF (.003 mole, .3723g) in MeOH (50ml) was slowly added. The solution was gently refluxed for 3hrs during which it became bright yellow. After cooling the solution was reduced to ca 20ml. An equal volume of MeCN was added and the beaker left to evaporate in the fume cupboard. Transparent cube crystals were isolated and washed in ice cold MeCN. (Yield 62%).

NOTE - This reaction requires the presence of water and will not proceed (in good yield) in dry solvents. In some cases addition of 20ml of water was required to bring about crystallization.

INFRARED SPECTRUM.

Inter alia 3375 (H_2O), 2895, 1634, 1580, 1439 1355, 1212, 1009 903 765, 743, 555

ANALYSIS $3F.\frac{1}{2}H_2O$ ($(3F)_2.H_2O$ $C_{60}\ H_{74}\ N_{16}\ O_7$)

calc :	C	63.6	H	6.5	N 19.8
found :	C	63.6	H	6.7	N 19.9

NMR ^1H $CDCl_3$ RT 250MHz.

PROTON	δppm	multiplicity	integral	no. of protons
A	7.09 (sh)	s	21	6
C	7.73 (sh)	s	20	6
D	3.538(sh)	s	40	12
E	2.735(sh)	s	41	12

^{13}C $CDCl_3$ RT 90MHz.

CARBON	δppm	multiplicity (off resonance)
A	111.012	d
B	153.410	s
C	152.115	d
D	59.821	t
E	54.75	t

mass spec m/e$^+$ 556

$Cu_2$3F$(ClO_4)_2.2H_2O$

3F (.0002mole, .1112g) was dissolved in deoxygenated methylene chloride - (30ml) and a solution of $Cu(MeCN)_4ClO_4$ (.0004mole, .1308g) in acetonitrile was added. After 5 minutes deoxygenated EtOH (10ml) was added. The yellow solution was stable in air and so the volume was reduced to ≃20ml using a rotary evaporator. A red microcrystalline product was obtained in 55% yield.

INFRARED SPECTRUM.

Inter alia : 3743, 3612, (H_2O) 3128 furan, 2922, 2863, C_{alk}-H 1629 C=N 1028, 621 ClO_4^-.

ANALYSIS $Cu_2 3F(ClO_4)_2$

anhydrous	calc	C	40.82	H	4.11	N	12.70
$.H_2O$	calc	C	40.04	H	4.26	N	12.45
$.2H_2O$	calc	C	39.22	H	4.4	N	12.2
	found	C	39.8	H	4.03	N	12.22

Ω = 280 Scm^2mol^{-1}

'Hnmr CD_3CN 294k 400MHz

PROTON	δppm	multiplicity	integral	no protons
A	7.1	s	30	6
C	8.22	s	30	6
D	3.42	m	30	
	3.25	d	15	12
	3.22	d	15	
E	3.14	d	15	
	3.10	d	15	12
	2.67	t	30	

$Cu_2 3F(OH)(ClO_4)_3(.H_2O?)$

3F (.5g, 0.89 mmol) was dissolved in methylene chloride and to it was added $Cu(ClO_4)_2.6H_2O$ (.1g 0.27 mmol) in EtOH. This resulted in a rapid precipitation of a yellow solid that slowly turned green on filtration in the air. Recrystallization in MeCN/EtOH gave emerald green small crystals.

INFRARED SPECTRUM

Inter alia 3742, H_2O 3435, OH, 3125 furan, 2933, 2876 C_{sat}-H, 1633 C=N, 1096, 622 ClO_4^-

ANALYSIS

Ω 389 Scm^2mol^{-1}

F.A.B.		% BASE ION PEAK
$[Cu_2 3F(OH)(ClO_4)_2]^+$	899	65
$[Cu_2 3F(OH)(ClO_4)]^+$	800	75
$[Cu_2 3FOH]^+$	699	50
$[Cu3F]^+$	619	100

PREPARATION OF $Cu^I(MeCN)_4ClO_4$.

This complex was prepared by the method of Hemmerich and Sigwart[4]. (7.0g, 0.05mol) of Cu_2O and 16ml (0.4 mol) of acetonitrile were refluxed in 60ml of deoxygenated 2N $HClO_4$ until all the Cu_2O had dissolved (2hours). The white crystalline product formed on cooling under nitrogen. It was filtered, washed with cold deoxygenated acetonitrile and dried under a stream of nitrogen. $[Cu(CH_3CN)_4]ClO_4$ was stored in a sealed flask under nitrogen. [Yield = 83%]

$Na3FClO_4.H_2O.2MeCN$.

3F (0.1g, 0.17 mmol) was dissolved in MeCN (40ml) by refluxing before $NaClO_4.6H_2O$ (0.1036g, 0.44 mmol) in MeCN (20ml) was added. The resulting solution was stirred at a gentle reflux for 1 hour. On cooling the solution was filtered and reduced in volume. After 72 hours at -20°C a yellow product was collected. (Yield 20%)

INFRARED SPECTRUM

Inter alia 3403 3347 H_2O, 3138 furan, 2892 C_{mii}-H, 2252 MeCN, 1640 C=N, 1040 621 ClO_4^-

ANALYSIS $Na3FClO_4.2H_2O.MeCN$

calc :	C	51.92	H	5.87	N	17.04	Na	3.09
found :	C	52.04	H	5.64	N	17.11	Na	3.25

Ω = 112 Scm^2mol^{-1}

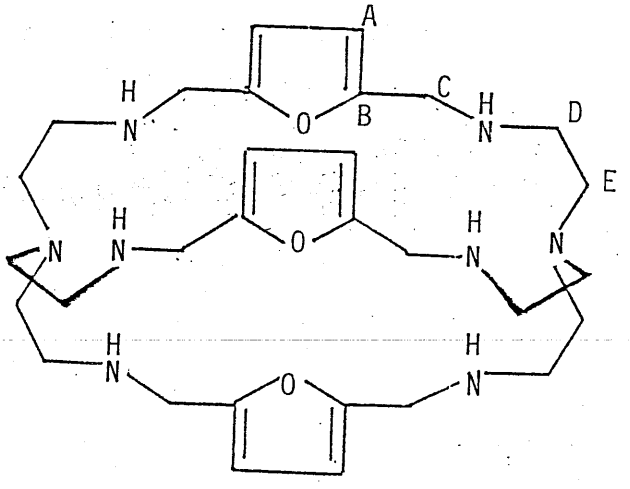

LIGAND R3F

F.A.B.		% BASE ION PEAK
$[Na3F]^+$	579	100
$[H3F]^+$	557	16

Note : Free ligand was recollected in the reaction with Li^+. Reaction with K^+ is yet to be carried out.

R3F.

DFF (.7446g, .006 mole) was dissolved in methanol (200ml) at room temperature. A methanolic solution of tren (.60ml .004 mole in 50ml) was added and the solution stirred at room temperature for 1 hour. $NaBH_4$ (.7566g .10mol) was added in solid form and the resulting solution left stirring at room temperature for 72 hours. The solution was worked up as in 3Bm -> R3Bm. (Yield 68%).

INFRARED SPECTRUM

Inter alia 3303 3249 N-H, 3124 furan,
2823 C_{sp3}-H, 1454 1204 792 ligand

ANALYSIS R3F (C_{30} H_{48} N_8 O_3)

calc :	C	63.3	H	8.5	N	19.7
found :	C	62.9	H	8.3	N	19.1

NMR

'Hnmr $CDCl_3$ RT 250MHz

PROTON	δppm	multiplicity	integral	no protons
A	6.0807	s	24	6
C	3.6991	s	47	12
D/E	2.5703	s	90	24

NH observed as small broad hump at 2.3ppm - confirmed by D_2O shake.

^{13}C $CDCl_3$ RT 90MHz.

CARBON	δppm	multiplicity
A	107.398	d
B	153.302	s
C	55.452	t
D	47.305	t
E	46.228	t

Mass spec. m/e^+ 568. (100%)

$Mn_2R3F(OH)_1(CF_3SO_3)_3.2H_2O$.

R3F (.100g .17 mmol) was suspended in MeCN (100ml) and gently refluxed. A solution of $Mn(CF_3SO_3)_2.6H_2O$ in MeCN (100ml) was added slowly and the resulting very pale yellow solution refluxed for ½ hour. On cooling EtOH (80ml) was added before the solution was reduced in volume and placed in a freezer overnight at -20°C. A product of fine, needle crystals was collected. (Yield = 57%)

INFRARED SPECTRUM

Inter alia 3564 OH, 3285 3241 NH, 3080 furan, 2866 C_{alk}-H, 1273 1160 1028 CF_3SO_3

ANALYSIS $Mn_2R3F(OH)_1(CF_3SO_3)_3.2H_2O$.

calc :	C	33.62	H	4.53	N 9.50
found :	C	33.79	H	4.14	N 9.42

Ω = 587 Scm^2mol^{-1} $(10^{-4}m)$

F.A.B

		% BASE ION PEAK
$[Mn_2R3F(OH)(CF_3SO_3)_2]^+$	993	(80)
$[Mn_2R3F(CF_3SO_3)_3]^+$	1126	(5)
$[MnR3F]^+$	623	(15)
$[MnR3F(CF_3SO_3)]^+$	773	(100)
$[H_2R3F]^+$	570	(23)

$Co_2R3F(OH)(ClO_4)_3.2H_2O$

R3F (.10g, 0.18 mmol) was suspended in MeCN (100ml) and while at a gentle reflux a solution of $Co(ClO_4)_2.6H_2O$ (.1740g, 0.44 mmol) was added. After reducing the volume to ca 30ml it was placed in a freezer at -20°C for 4 days. A green microcrystalline product was obtained (Yield=38%)

INFRARED SPECTRUM

Inter alia 3573 OH, 3264 NH, 3126 furan, 2881 C_{all}-H, 1097 622 ClO_4^-

ANALYSIS $Co_2R3F(OH)(ClO_4)_3.2H_2O$

calc :	C	34.9	H	5.1	N	10.8	Co	11.35
found :	C	34.7	H	4.7	N	11.0	Co	11.50

Ω = 316 Scm^2mol^{-1} (549 for $10^{-4}M$)

$Co_2R3F(OH)(CF_3SO_3)_3.2H_2O.$

As for the previous experiment except that $Co(CF_3SO_3)_2.6H_2O$ (.2044g, 0.44 mmol) was used. The product was much more soluble than the perchlorate derivative and ethanol was required to obtain the microcrystalline green crystals. (Yield = 57%)

INFRARED SPECTRUM

Inter alia 3558 OH, 3247 N-H, 3160 furan, 2884 C_{all}-H,
1262, 1163 1028 CF_3SO_3,

ANALYSIS $Co_2R3F(OH)(CF_3SO_3)_3.2H_2O$

calc :	C	33.4	H	4.5	N	9.5
found :	C	33.0	H	4.1	N	9.7

Ω 549 Scm^2mol^{-1} ($10^{-4}M$)

F.A.B.		% BASE ION PEAK
$[Co_2R3F(CF_3SO_3)_3]^+$	1133	very weak
$[Co3F]^+$	615	100
$[R3F]^+$	569	41

$Ni_2R3F(OH)_2(Ph_4B)_2.4H_2O$.

R3F (.1g, 0.18 mmol) was suspended in MeCN (100ml) at a gentle reflux and a solution of $Ni(ClO_4)_2.6H_2O$ (.1607g 0.44 mmol) was added. The resulting solution was stirred for ½ hour at mild reflux. An excess of Ph_4B^- in MeCN was added. On cooling the volume was reduced, ethanol added and then the solution was cooled to -20°C for 24hrs. A powdery product was obtained. (Yield = 37%). The nickel complex could not be isolated as the perchlorate or triflate derivative.

INFRARED SPECTRUM

Inter alia 3468 OH, 3265 NH, 3123 furan, 2982 C_{mli}-H, 734 707 Ph_4B^-

ANALYSIS $Ni_2R3F(OH)_2(Ph_4B)_2.4H_2O$

calc :	C	65.5	H	6.9	N	7.9
found :	C	65.5	H	6.6	N	8.6

$Cu_2^IR3F(ClO_4)_2$

The R3F (.10g, 0.18 mmol) was suspended in dry and deoxygenated MeCN (80ml) at 50°C. $Cu^I(MeCN)_4ClO_4$ (.1724g, 0.53 mmol) was added in its solid form. After ½ hour at 40-50°C nitrogen was bubbled through the solution to reduce the volume. At the first signs of solid the solution was filtered and the filtrate cooled in ice. A pale yellow green solid powder was obtained in 52% yield.

INFRARED SPECTRUM

Inter alia 3279 N-H, 2850 C_{mli}-H, 1089 622 ClO_4

ANALYSIS $Cu_2R3F(ClO_4)_2$

calc :	C	40.3	H	5.4	N	12.6
found :	C	40.6	H	5.4	N	13.0

Ω = 468 Scm^2mol^{-1} $(10^{-4}M)$

F.A.B. $[HR3F]^+$ 569

$[CuR3F]^+$ 632

No ions in M^+ region and no $[Cu_2L]^+$

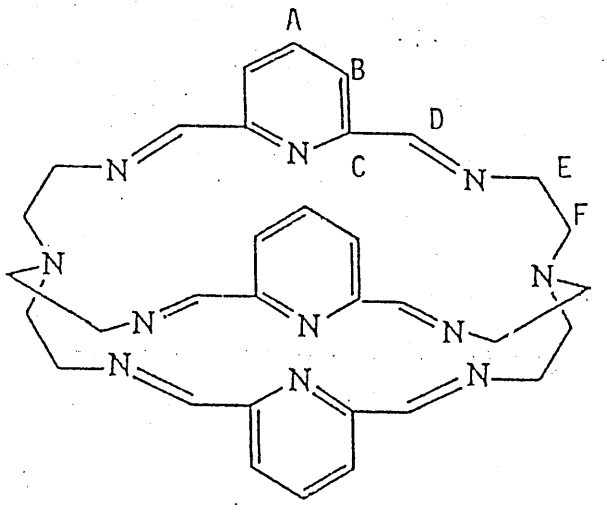

LIGAND 3P

THE LIGAND 3P AND ITS COMPLEXES.

The preparation of DFP (2,6 diformyl pyridine) has already been discussed in the section on ligand WT.

$Ba3P(ClO_4)_2$ (Template)

DFP (.004mole, .5404g) and $Ba(ClO_4)_2$ (.0015mole, .5043g) were brought to reflux in MeOH (200ml). Tren (.002.mole, .30ml). was dripped into the reaction vessel in concentrated form . A bright yellow colour developed within 5 mins. and on heating for ½ hour a solid began to form. This solid was removed by filtering and the filtrate cooled and concentrated to give a yellow microcrystalline product in 86% yield.

INFRARED SPECTRUM.

Inter alia 3076 C_{aro}-H, 2854 C_{ali}-H, 1650 C=N,
1587 (pyridine) 1460 1336 1265 870 820 770 ligand,
1090 622 (ClO_4^-)

Analysis $Ba3P(ClO_4)_2$

calc :	C	42.8	H	4.3	N	16.6
found :	C	42.8	H	4.1	N	16.8

Ω = 241 Scm^2mol^{-1} (512 for $10^{-4}M$)

NMR

^1H CD_3CN R.T. 250MHz

PROTON	ppm	multiplicity	integral	no. of protons.
A	8.262	t	4	3
B	7.855	d	8	6
D	8.5397	S	8	6
E	3.68, 3.15[a]	t, d	10,8	12
F	2.58, 3.15[a]	q, d	9,9	12

(a) These two doublets overlap to give a quartet

F.A.B		% BASE PEAK
$[Ba3P(ClO_4)]^+$	826	100
$[Ba3P]^{2+}$	727	37

$Sr3P(ClO_4)_2.2H_2O$ (Template)

As for $Ba3P(ClO_4)_2$ except using $Sr(ClO_4)_2.6H_2O$ (.0015mole, .5918g) (yield = 79%)

INFRARED SPECTRUM.

Inter alia. 3533 H_2O, 3075 C_{aro}-H 2852 C_{ali}-H).
1644 C=N 1584 (pyridine) 1457 ligand 1090 621 ClO_4.

Analysis Sr3P(ClO4)$_2$.2H2O.

calc:	C	43.5	H	4.7	N	16.9
found:	C	43.7	H	4.5	N	17.3

Ω = 307 $Scm^2\ mol^{-1}$ (471 for $10^{-4}M$)

NMR.

^1H RT CD_3CN 300MHz

PROTON	δppm	multiplicity	integral	no. of protons.
A	8.276	t	10	3
B	7.86	d	19	6
D	8.501	s	20	6
E	3.23, 3.13	t,d	41	12
F	2.497,2.905	t,d	42	12

^{13}C RT CD_3CN 300MHz

CARBON	δppm	Off Resonance Multiplicity
A/B	128.7 117.2	2 x d
C	166.032	s
D	141.087	d
E	63.909	t
F	58.587	t

F.A.B.		% BASE PEAK
$[Sr3P(ClO_4)]^+$	775	100
$[Sr3P]^+$	676	31

$Ca3P(ClO_4)_2.3H_2O$ (TEMPLATE)

Prepared as for $Ba3P(ClO_4)_2$ but using $Ca(ClO_4)_2.6H_2O$ (.0015mole .5205g), (Yield = 62%)

INFRARED SPECTRUM

Inter alia: 3528 H_2O, 3074 C_{aro}-H, 2854 C_{ali}-H, 1643 C=N, 1586 pyridine, 1087 1038 621 ClO_4^-

ANALYSIS $Ca3P(ClO_4)_23.H_2O$

calc :	C	44.8	H	5.1	N	17.4	
found :	C	44.4	H	4.3	N	18.2	
calc :	C	45.84	H	5.01	N	17.382	for $.2H_2O$
	C	46.81	H	4.28	N	18.20	for $.1H_2O$

Ω = 275 $Scm^2\ mol^{-1}$ (420 for $10^{-4}M$)

nmr 'H CD_3CN RT 300MHz

PROTON	δppm	multiplicity
A	8.3	t
B	7.84	d
D	8.5	s
E	3.1	m
F	2.48	t

F.A.B		% BASE ION PEAK
$[Ca3P(ClO_4)H_2O]^+$	746	15
$[Ca3P(ClO_4)]^+$	728	100
[Ca3P]	629	46

$Mn_2$3P(OH)$_2$(SCN)$_2$.2MeCN.

$Ba3P(ClO_4)_2$ (0.22 mmol .20g) was dissolved in MeOH (80ml)/MeCN (50ml) at room temperature. Solid $Mn(ClO_4)_2$. (0.45 mmol .1646g) was added and this was stirred at room temperature until it had dissolved. NaNCS (1.08 mmol .0876g) in MeCN (30ml) was slowly added and the resulting solution was left to stir at room temperature for 48 hours during which a very fine yellow precipitate formed in 16% yield.

INFRARED SPECTRUM

Inter alia 3379 (OH), 3066 (C_{arc}-H), 2846 (C_{ali}-H), 2073 (SCN), 1657 (C=N), 1591 (pyridine)

ANALYSIS $Mn_2$3P(OH)$_2$(SCN)$_2$.2MeCN

calc :	C	50.3	H	5.08	N	22.55
found :	C	50.30	H	4.95	N	22.55

$Fe_2$3P$(ClO_4)_2(Ph_4B)_2.3H_2O$

$Fe(ClO_4)_2.6H_2O$ (.1567g 0.43 mmol) and $Ba3P(ClO_4)_2$ (.2g .2mmol) were dissolved in deoxygenated MeCN at 40°C. A solution of Ph_4B^- (0.864 mmol .2957g) in deoxygenated MeCN (70ml) was added slowly. N_2 gas was bubbled through the solution until the first signs of solid were evident. After filtering ca 50ml deoxygenated EtOH was added and N_2 bubbling continued until substantial solid was present. This was filtered, washed with ice cold EtOH, and dried under nitrogen. The deep purple solid was collected in 41% yield.

INFRARED SPECTRUM

Inter alia 3441 H_2O, 3051 C_{aro}-H, 2849 C_{ali}-H, 1647 C=N, 1583 pyridine, 1087 624 ClO_4^-, 734 705 Ph_4B^-

ANALYSIS $Fe_2$3P$(ClO_4)_2(Ph_4B)_2.3H_2O$

calc :	C	61.1	H	5.3	N	9.6	
found:	C	61.3	H	4.6	N	9.3	
calc:	C	61.7	H	5.4	N	9.78	for $2H_2O$

F.A.B		% BASE ION PEAK
$[Fe_2P(Ph_4B)_2]^+$	1339	18
[3PPh_4B]	907	100

$Co3P(ClO_4)_2.2H_2O$ (Transmetallation)

$Ba3P(ClO_4)_2$ (.20g) was dissolved in MeOH (150ml) before $Co(ClO_4)_2.6H_2O$ (.2435g) in MeOH (50ml) was added. This gave a reddy brown solution which was stirred at 60°C for ½ hour before NaNCS (.0175g) in MeOH (150ml) was slowly dripped in over 1 hour. After a further ½ hour stirring at 60°C, during which the solution became cloudy, it was allowed to slowly cool to room temperature during which a reddy brown precipitate formed. The microcrystalline product was collected in 39% yield.

INFRARED SPECTRUM

Inter alia 3620 3550 H_2O, 3081 C_{arc}-H, 2938 2855 C_{ali}-H, 1654 C=N, 1595 pyridine, 1091 623 ClO_4^-

ANALYSIS $Co3P(ClO_4)_2.2H_2O$

calc :	C	44.8	H	4.9	N	17.4
found :	C	44.5	H	4.8	N	17.3

Ω = 274 $Scm^2\ mol^{-1}$

F.A.B		% BASE ION PEAK
$[Co3PClO_4]^+$	748	57
$[Co3P]^+$	649	100

$[Co3P(OH)_2][Co(NCS)_4].2H_2O$

$Ba3P(ClO_4)_2$ (.20g, 0.22 mmol) was dissolved in MeCN (160ml) at room temperature. Solid $Co(ClO_4)_2.6H_2O$ (0.45 mmol, .1705g) was added and stirred at room temperature until it had all dissolved. This gave a reddy brown solution. NaNCS (1.08 mmol, .0876g) in MeCN (40ml) was slowly dripped in with rapid stirring. The solution gradually became green and a green microcrystalline product was precipitated in 46% yield.

INFRARED SPECTRUM

Inter alia: 3445 OH 3063 C_{arc}-H, 2856 C_{ali}-H, 2048 SCN, 1652 C=N, 1585 pyridine

ANALYSIS $[Co3P(OH)_2][Co(NCS)_4]2H_2O$

calc :	C	41.5	H	3.6	N	19.4
found :	C	41.2	H	4.1	N	19.66

F.A.B		% BASE ION PEAK
[Ba3PClO$_4$]	826	22
[Ba3P]$^+$	727	50
[Co3P]$^+$	648	100
[Co3PNCS]$^+$ or [Co$_2$3P]$^+$	706	28

Insoluble in MeCN therefore no conductivity result.

Ni$_2$3P(NCS)$_3$(OH)2H$_2$O (TRANSMETALLATION)

Ba3P(ClO$_4$)$_2$(.40g, 0.43 mmol) was dissolved in MeOH (200ml) - this required warming. On cooling to room temperature a solution of Ni(ClO$_4$)$_2$ 6H$_2$O (.4200g 0.125 mmol) in MeOH (80ml) was added. This solution was stirred for 10 mins before NaSCN (.15g 3.8 mmol) in MeCN (50ml) was slowly dripped into the solution. After a 6 hour stir at room temperature, during which a yellow green microcrystalline precipitate was formed, the solution was filtered: Concentration of the filtrate and 36 hours at -20°C yielded a second batch of the yellow product. (Yield 57%)

INFRARED SPECTRUM

Inter alia 3430 OH, 3058 C$_{arc}$-H, 2849 C$_{ali}$-H,
2095 SCN, 1658 C=N, 1594 pyridine,

ANALYSIS Ni3P(NCS)$_3$(OH)2H$_2$O

calc:	C	46.3	H	4.7	N	21.0
found :	C	46.9	H	4.6	N	21.1

Insoluble in MeCN therefore no conductivity measurement.

$Ni_2$3P$(ClO_4)_2(OH)_2 2H_2O$

Ba3P$(ClO_4)_2$ (0.92 mmol .2g) was dissolved in MeOH (80ml) - this required heating. Once cooled to room temperature a methanolic solution (50ml) of $Ni(ClO_4)_2$ $6H_2O$ was slowly added to it. After a 3 hour stir at room temperature during which a feint cloudiness appeared the solution was filtered and then kept at -20°C for 48 hours. A yellowy green powder was collected in 47% yield.

INFRARED SPECTRA

Inter alia 3548 OH, 3600-3000 H_2O, 3082 C_{aro}-H, 2862 C_{ali}-H, 1656 C=N, 1596 pyridine, 1092 622 ClO_4^-

ANALYSIS $Ni_2$3P$(ClO_4)_2$ $(OH)_2$ $2H_2O$

calc :	C	40.6	H	4.6	N	15.8
found :	C	40.6	H	4.2	N	15.6

F.A.B		% BASE ION PEAK
[Ni3P]	647	100
$[Ni3PClO_4]^+$	746	70
$[Ba3PClO_4]^+$	826	13
$[Ba3P]^+$	727	9

3P

DFP (0.9 mmol 1.2159g) was dissolved in MeOH (150ml) at 60°C. A methanolic solution of tren (.006mole in 100ml) was added in a dropwise fashion and the resulting solution stirred for 1 hour at 50-60°C. On cooling the solution was filtered and MeCN (30ml) was added before taking the volume down to ca 50ml*. This was left in a beaker in a well ventilated area, to evaporate. This yielded a clean crystalline product (56% Yield). The cube-like crystals were of X-rayable size.

* On reduction of the volume a thick orangy brown gel may form. If so add more MeCN and ≈30ml H_2O : leave to evaporate or reduce in volume. This should give a crystalline product.

INFRARED SPECTRUM

Inter alia 3055 C_{aro}-H, 2884 2834 2887 C_{ali}-H, 1647 C=N, 1583 pyridine, 3286 1569 1453 1432 1329 1065 1035 919 803 740 626 555 ligand

ANALYSIS 3P (C_{33} H_{33} N_{11})

calc :	C	67.2	H	6.6	N	26.1
found :	C	67.4	H	6.6	N	25.9

NMR

'H CD_3Cl 250 MHz RT

PROTON	δppm	multiplicity	integral	no. of protons
A	7.81	t	12	3
B	8.12	d	23	6
D	7.59	s	23	6
E	3.56	s(br)	44	12
F	2.76	s(br)	43	12

^{13}C CD_3Cl 300MHz

CARBON	δppm	off resonance multiplicity
A/B	132.797, 117.677	2 x d
C	159	s
D	150.375	d
E	56.132	t
F	52.806	t

MASS SPEC M^+ 590 (100%)

$Fe_2$3P$(ClO_4)_3OH.4H_2O$ (INSERTION)

3P (.1g, 0.17 mmol) was suspended in deoxygenated MeCN (80ml) at 40°C. The $Fe(ClO_4)_2 6H_2O$ (.1848g 0.51 mmol) was added in solid form and the resulting deep purpley/black solution stirred for 20 minutes at 40°C. The volume of solvent was gradually decreased by bubbling N_2 gas through it. At approximately ½ volume the solution was filtered before deoxygenated EtOH (≈20ml) was added. The flask was placed in ice and the bubbling continued until signs of solid. The flask was kept under a N_2 atmosphere while the solid formed. This was collected and dried. (Yield = 74%).

INFRARED SPECTRUM

Inter alia 3419 OH, 3600-3000 H_2O, 2920 C_{alk}-H,
1632 C=N, 1607 pyridine, 1089 625 ClO_4^-

ANALYSIS $Fe_2$3P$(ClO_4)_3(OH).4H_2O$

calc :	C	36.4	H	4.5	N	14.1
found :	C	36.0	H	4.6	N	14.0

F.A.B

		% BASE ION PEAK = 309
[$Fe_2$3P$(ClO_4)_2OH$]	919	14
[Fe3P]	645	21

$Cu_2$3P$(ClO_4)_2.2H_2O$

3P (.2mmol .1178g) was dissolved in deoxygenated CH_2Cl_2 (30ml). A solution of $Cu^I(MeCN)_4ClO_4$ in deoxygenated MeCN (20ml) and deoxygenated EtOH (20ml) was added. After full development of the dark brown colour the volume was reduced on the rotary evaporator to ca 20ml. This gave black crystals of the titled compound in 53% yield.

INFRARED SPECTRUM

Inter alia 3435 H_2O, 3070 C_{arc}-H, 2921 2868 C_{alk}-H, 1635 C=N,
1587 pyridine, 1556 ligand, 1091 622 ClO_4^-

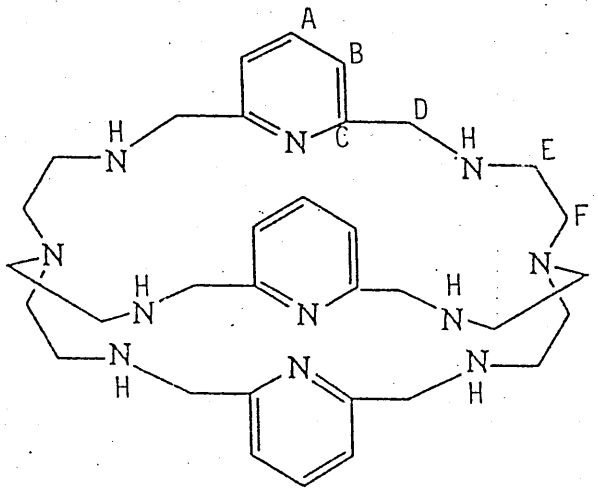

LIGAND R3P

ANALYSIS $Cu_2 3P(ClO_4)_2 2H_2O$

calc :	C	41.66	H	4.55	N	16.19
found :	C	42.21	H	4.46	N	16.09

Ω = 411 $Scm^2\ mol^{-1}$ $(10^{-4}M)$

NMR

PROTON	δppm	multiplicity	integral	no. of protons
A	8.148	s(br)	19	3
B	7.88	d(br)	36	6
D	8.549	s	36	6
E	3.189	s(br)	74	12
F	3.133, 2.6	d(br), t(br)	35, 36	12

R3P

As no metal-ligand species, suitable for reduction, could be formed in high enough yield, reduction of the isolated ligand or the in situ method was used.

IN SITU METHOD

DFP (.009 mole, 1.2159g) was dissolved in MeOH (200ml) at 50°C and the concentrated amine, tren, (.006mole .90ml) dripped in. This gave a pale yellow solution which was stirred at 50°C for 1 hour before the heat was increased to bring the solution to reflux. Then a large excess of $NaBH_4$ was added in its solid form in small amounts. The solution was left refluxing for 4 hours and then allowed to cool to room temperature. Some more $NaBH_4$ was added and the solution left to stir overnight at room temperature. It was then worked up in the standard way to give a creamy coloured solid in 47% yield.

INFRARED SPECTRUM.

Inter alia 3327 N-H, 3057 C_{aro}-H, 2957 2873 2834 C_{all}-H, 1590 pyridine, 1572, 1447, 1331, 1151, 1137, 1040, 1030, 781, 758, 735

ANALYSIS R3P.2H_2O $C_{33}H_{55}N_{11}O_2$

calc :	C	62.14	H	8.69	N	24.15
found :	C	62.49	H	8.9	N	23.4

NMR

^{1}H $CDCl_3$ RT 300MHz

PROTON	δppm	multiplicity	integral	no. of protons
A	7.08	s	5	3
B	7.52	s	9	6
D	3.89	s	22	12
E	3.19	s(vbr)	23	12
F	2.65	s	25	12

^{13}C $CDCl_3$ RT 300MHz

CARBON	δppm	off resonance multiplicity
A/B	116.897, 132.886	2 x d
C	155.424	s
D/E	51.085 51.726	2 x d
F	43.577	t

MASS SPEC

M^+ 602 (100%)

$Ag_2$2P$(CF_3SO_3)_2$.MeCN

This complex was formed completely by accident and unfortunately has not been synthesized again. Below is the prep. I 'think' I 'followed' - however being the first day back after Christmas it is quite likely I did something different! The aim had been to obtain the Ag^+ salt of this ligand (Lehn had achieved this with the same ligand[7]) - this has eluded me!

$AgNO_3$ (.002mole, .339g) was warmed in MeOH (200ml) and the DFP (.003 mole ,.4053g) and tren (.002 mole, .30ml) each in MeOH (50ml) were added simultaneously. The resulting bright yellow solution was stirred at 40°C for 3 hours. It was then reduced in volume and divided into 2 lots of 12ml. To one was added 12ml MeCN containing an excess of the $CF_3SO_3^-$ ion and to the second, an excess of the hexaflurophosphate (PF_6^-) ion again in MeCN (12ml). Both were left to slowly evaporate. The PF_6^- beaker gave an oily mess whereas a small number of yellow crystals of X-rayable size were obtained from the triflate beaker (Yield = 26%)

INFRARED SPECTRUM

Inter alia 3318 3275 NH_2, 3179 ligand, 3072 C_{aro}-H, 2894 2816 C_{ali}-H, 2396 2318 MeCN, 1655 1644* C=N, 1589 pyridine, 1272 1163 1029 $CF_3SO_3^-$.

* split amine.

ANALYSIS $Ag_2$2P$(CF_3SO_3)_2$MeCN

calc :	C	34.5	H	4.0	N	14.7
found :	C	34.7	H	4.1	N	14.4

F.A.B		%BASE ION PEAK
[$Ag_2$2P(CF_3SO_3)]$^+$	855	100
[Ag2P]$^+$	597	97

2,6,-Diacetyl pyridine (DFP)

This was obtained from the Aldrich Chemical Company Ltd and used without further purfication.

INFRARED SPECTRUM

Inter alia 3380, 3070, 2970 1705, 600 (cm^{-1})

Although I have been unsuccessful in re-obtaining the open chain derivative of 3P where DFP is the head unit dialdehyde, the open chain of 3P where DAP is the head unit dialdehyde would appear to be more accessible. Unfortunately I have only appreciated the significance of this whilst writing up the thesis and I hope the following preparations will be reinvestigated in the future.

$Ag_2 2P_{CH_3}(PF_6)_2.(MeCN)/Ag_2 2P_{CH_3}(CF_3SO_3)_2$

This reaction was a total mistake as well - I should have used DFP but instead used DAP. Again this was the first day back after Christmas!

$AgNO_3$ (.004 mole, .6795g) was heated to 50°C in MeOH (60ml). DAP (.006 mole,.8107g) in MeOH (20ml) and tren in MeOH (20ml) were added simultaneously over 20 minutes. The resulting yellow solution was stirred at 40°C for 3 hours. On cooling the volume was reduced and divided into 2 lots of 16ml. To one an equal volume of MeCN containing excess $CF_3SO_3^-$ ion was added while to the other an excess of PF_6^- ion was added again in an equal volume of MeCN. Both were left to evaporate slowly in the fume cubboard. Both gave crystalline products in 40-50% yield.

$Ag_2 2P_{CH_3}(PF_6)_2(.MeCN)$

INFRARED SPECTRUM

Inter alia 3390 3330 NH_2, 3105 C_{aro}-H, 2964 2885
2824 C_{ali}-H, 2230 MeCN 1641, 1606 C=N,
1583 pyridine, 1456 1301 979 ligand 840 PF_6^-

ANALYSIS $Ag_2 2P_{CH_3}(PF_6)_2(MeCN?)$

	found :	C 34.3	H 4.4	N 14.4
$Ag_2 2P_{CH_3}(PF_6)_2$	calc :	C 34.4	H 4.4	N 13.4
$Ag_2 2P_{CH_3}(PF_6)_2 MeCN$	calc :	C 35.1	H 4.5	N 14.1

F.A.B		% BASE ION PEAK
$[Ag_2 2P_{CH_3}PF_6]^+$	907	16
$[Ag_2 2P_{CH_3}]^+$	762	34
$[Ag 2P_{CH_3}]^+$	653	100

$Ag_2 2P_{CH_3}(CF_3SO_3)_2$

INFRARED SPECTRUM

Inter alia: 3365 3298 NH, 3111 C_{aro}-H, 2984 2856 C_{ali}-H, 1644 1610 C=N, 1592 pyridine, 1284 1172 1028 $CF_3SO_3^-$

ANALYSIS $Ag_2 2P_{CH_3}(CF_3SO_3)_2$

calc :	C	36.1	H	4.4	N	13.2
found :	C	35.6	H	4.5	N	13.4

F.A.B		% BASE ION PEAK
$[Ag_2 2P_{CH_3}CF_3SO_3]^+$	911	24
$[Ag_2 2P_{CH_3}]$	762	39
$[Ag 2P_{CH_3}]$	653	100

$Ba 2P_{CH_3}(ClO_4)_2$

$Ba(ClO_4)_2$ (.001 mole, .3362g) and DAP (.001 mole, .1632g) was dissolved in MeOH (100ml) and heated to reflux. The amine (.003 mole, 0.4387g) was added in undiluted form. The resulting solution was refluxed for 3 hours during which there was a colour change from colourless to yellow. On cooling the reaction vessel was placed in ice and left overnight. A white microcrystalline product was collected in the morning. The filtrate was concentrated and left in ice and this gave a 2nd batch (Total yield = 89%)

INFRARED SPECTRUM

Inter alia 3360 3236 NH_2, 3080 C_{aro}-H, 2924 2886
2852 Ca_{li}-H, 1625*, C=N, 1578 pyridine 1080 626 ClO_4^-

* shoulder/splitting

ANALYSIS $Ba2P_{CH3}(ClO_4)_2$

calc :	C	40.8	H	5.3	N	15.8
found :	C	40.8	H	5.3	N	15.6

F.A.B		% BASE ION PEAK
$[Ba2P_{CH3}(ClO_4)]^+$	782	100
$[Ba2P_{CH3}]^+$	681	681

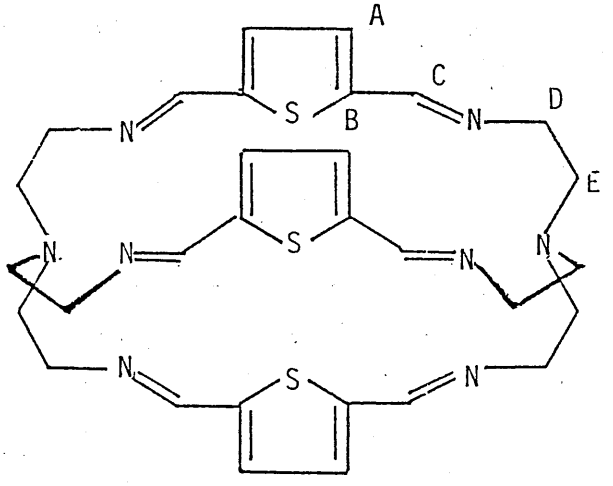

LIGAND 3S

THE LIGAND 3S AND ITS COMPLEXES

2,5 - Diformyl thiophene (DFT)

This preparation was carried out by a similar procedure to previous methods[5,6]. The preparation of a stock of this starting material by Clarke Stevenson is gratefully acknowledged.

A stream of dry hydrogen chloride gas was passed through a stirred solution of 37% formaldehyde (2mole) and hydrochloric acid 10M (36ml) allowing the temperature to rise to 50-60°C; after 2 hours the solution was saturated. The mixture was cooled to 30°C, and thiophene (0.6mole) was added dropwise with stirring. After 20 mins the oily layer was siphoned off and washed with cold water (5x35ml) and refrigerated overnight. The solid mass was allowed to warm to room temperature, filtered under vacuum, washed with toluene and dried in vacuo to yield the light brown solid, 2, 5-bis-(chloromethyl) thiophene in 75% yield. This was used in the next stage without further purification.

The 2,5-bis-(chloromethyl)thiophene (63g), pyridine (74ml) and absolute ethanol (70ml) were warmed gently on a water bath. After 20 mins a white solid precipitated. Heating was continued for 30 mins and then the precipitate was collected, washed with ether and recrystallized from ethanol to give the pyridine adduct in 96% yield.

The pyridine adduct (61g) was dissolved in ethanol (1l) together with p-nitroso-N,N dimethylliline (50g). A solution of sodium hydroxide (13g) in water (300ml) was added while the mixture was being ice cooled. After stirring for 1 hour, then warming to room temperature and stirring for 2 hours, the mixture was diluted with water (600ml) and allowed to stand overnight. The red precipitate was collected and recrystallized from ethanol to give the nitroso adduct in 70% yield.

The nitroso adduct (50g) was added to ice cold hydrochloric acid 2M (1l) and the brownish solution was stirred for 30 mins during which time a

yellow precipitate was formed. The mixture was allowed to stand for 2 hours at room temperature. The solid was collected, washed with cold water, dried and recrystallized from ether to yield pale yellow platelets of 2,5- diformylthiophene in 80% yield.

INFRARED SPECTRUM

Inter alia 3070 C_{aro}-H, 2880 C_{ali}-H, 1660 C=O
1520, 1380, 1185, 820, 720, 680, 480cm^{-1}

ANALYSIS $C_6 H_4 O_2 S$

calc :	C	51.4	H	2.9
found :	C	51.7	H	2.8

NMR

'H $CDCl_3$ RT 250 MHz

PROTON	δppm	multiplicity	integral
A	7.8	S	2
C	10.0	S	2

MASS SPECTRUM $M^+ = 140$

$Ag_2$3S$(CF_3SO_3)_2$

$AgNO_3$ (.002mole, .3398g) was dissolved in MeOH (100ml) and warmed to 40°C. DFT (.003mole, .4023g) and tren (.002 mole, .3ml) each in 50ml MeOH were added simultaneously, but with the DFT solution at a slightly faster rate to prevent formation of the silver-tren complex. This solution was stirred at 40-50°C for 2 hours during which the brown solution gradually turned yellowy green. On cooling, the solution was filtered and reduced in volume to ca 40ml. An equal volume of MeCN containing a large excess of lithium triflate (.01mol) was added. The solution was left to evaporate slowly in a fume cupboard.

NOTE 1: the container was surrounded in tin foil to prevent photo decomposition of the silver complex. Numerous pin-prick holes in the top of the foil allowed evaporation. Yellow crystals of X-rayable size were obtained in 81% yield.

NOTE 2: the temperature of this reaction is important - above 40°C a silver mirror is obtained .

INFRARED SPECTRUM

Inter alia. 3076 C_{aro}-H, 2854 C_{ali}-H, 1635 C=N, 1262, 1153, 1028 $CF_3SO_3^-$.

ANALYSIS $Ag_2 3S(CF_3SO_3)_2$

calc :	C	3.3	H	3.2	N	10.1
found :	C	3.2	H	3.3	N	10.4

Ω = 259 $Scm^2\ mol^{-1}$.

F.A.B		% BASE ION PEAK
$[Ag_2 3S(CF_3SO_3)]^+$	969	67
$[Ag\ 3S]^+$	711	100

NMR

'Hnmr 294K CD_3CN 360MHz

PROTON	**δppm**		**multiplicity**	**integral**	**no. of protons**
A	7.64		s	20	6
C	8.67		d	20	6
D	3.45	3.79(v,br)	d	41	12
E	2.90	2.89(sl,br)	d	40	12

^{13}C RT CD_3CN 90MHz

CARBON	δppm	off resonance multiplicity
A	135.2	d
B	141.8	s
C	159.1	d
D	59.2	t
E	54.5	t

$Ag_2$3S$(ClO_4)_2$

DFT (.0015mol .2102g) and $AgClO_4$ (.5 mmol .1037g) were warmed to 40°C in MeOH (200ml) giving a browny black solution Tren (.001 .15ml) in MeOH (100ml) was warmed to 30°C and added over 45 minutes. The solution became yellowy green. Once all the amine had been added the heat was switched off and the solution allowed to cool to room temperature. On cooling the solution went cloudy and a green fine precipitate formed. This was collected and the filtrate reduced in volume and placed in a freezer at -20°C for 24 hours. A yellow powdery precipitate was collected. Both the green and yellow product analyzed as the titled compound (Total yield = 6%)

NOTE:- The entire reaction should be carried out in a blacked out vessel. Perchlorate is not as effective a counter ion as triflate - pulling out the product too rapidly. The yield and quality of product is significantly poorer than the triflate reaction. The competing silver-tren (amine) complex forms very rapidly so it is important to have all the dicarbonyl in the reaction vessel before the amine is added, Therefore the procedure is different to that of the triflate reaction and a larger volume of MeOH is required.

INFRARED SPECTRUM

Inter alia: 3085 C_{aro}-H, 2912 C_{ali}-H, 1634 C=N,
1089, 622, ClO_4^-.

ANALYSIS $Ag_2 3S(ClO_4)_2$

calc :	C	35.2	H	3.6	N	11.0
found :	C	34.9	H	3.6	N	11.1

F.A.B

$[Ag_2 3S(ClO_4)]^+$ 919

$[Ag\ 3S]^+$ 717

Ω = 276 $Scm^2\ mol^{-1}$.

$Cu_2 3S(ClO_4)_2$)

METHOD A:- $Ag_2 3S(CF_3SO_3)_2$ (.0087 mole .1000g) was dissolved in MeCN (50ml) and warmed to 40°C. $Cu(ClO_4)_2\ .6H_2O$ was added as a solution (50ml MeCN) and the resulting green solution stirred for ½ hour at 40°C. On cooling, EtOH (30ml) was added and the solution concentrated before being left at -20°C for 12 hours. Alternatively after the EtOH had been added the solution was left to evaporate slowly. Both methods gave an orangy red microcrystalline product in 40-55% yield.

METHOD B:- $Ag_2 3S(CF_3SO_3)_2$ was dissolved in degassed acetonitrile and warmed to 40°C. $Cu(MeCN)_4ClO_4$ was added in its solid form. After ½ hour at 40°C EtOH was added and the solution concentrated by bubbling N_2 through it until the first signs of solid. The flask was then placed in an ice bath and a red orange microcrystalline product was collected (30% Yield)

The solution is stable in air and thus later attempts allowed use of the rotary evaporator as the means of concentrating the solution.

INFRARED SPECTRUM

Inter alia 3085 C_{aro}-H, 2918 2851 C_{ali}-H, 1627 1610 C=N, 1089 622 ClO_4^-,

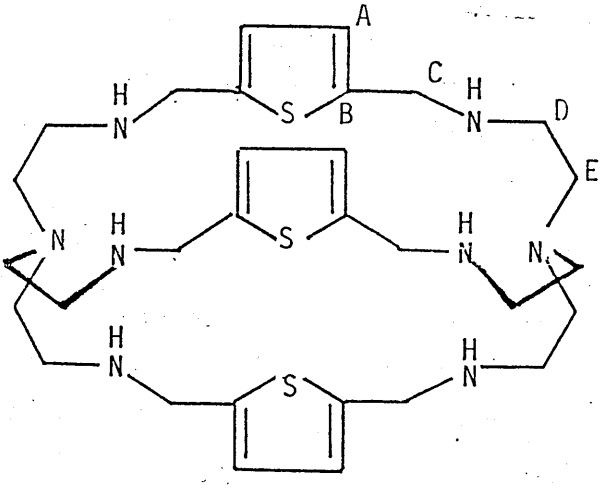

LIGAND R3S

ELEMENTAL ANALYSIS.

calc :	C	H	N
found :	C	H	N

Ω = 283 Scm^2mol^{-1}

NMR ^1H CD_3CN 294k 400MHz

PROTON	ppm	multiplicity
A	7.6	m
C	8.6	m
D	3.7-3.5	m
E	3.0,2.8	m

R3S

$Ag_2$3S$(ClO_4)_2$ (.80g .78mmol) was brought to reflux in EtOH (300ml). A large excess of solid $NaBH_4$ (.1g 2mmol) was added in small portions. The resulting suspension was refluxed for 3 hours. On cooling it was filtered to remove the Ag before being reduced to dryness. It was then worked up as in the case of R3Bm. This resulted in a cream white solid (≈55% yield)

INFRARED SPECTRUM

Inter alia 3336 NH, 3046 C_{aro}-H, 2784 C_{ali}-H, 1450, 1114, 1081 1053 803 708 ligand

ANALYSIS R3S

calc :	C	58.40	H	7.84	N	18.16
found :	C	58.15	H	7.36	N	18.47

MASS SPEC

M^+ 617 (100%)

CHAPTER 3

A MACROCYCLIC STUDY

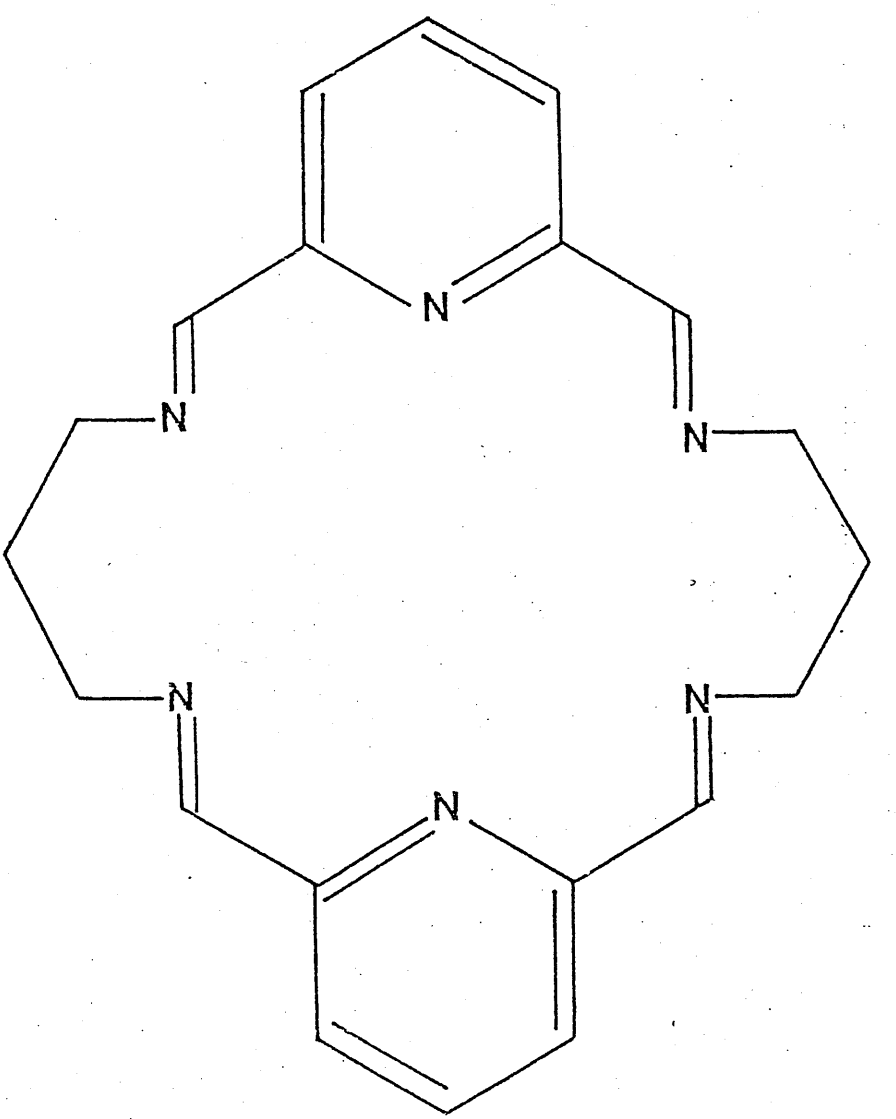

"WT"

20-[N6] Macrocycle.

igure 1

Binuclear Site	Enzyme	Function
Cu Cu	Haemocyanin	rev. O_2 carrier,
Cu Cu	Tyrosinase	monooxygenase,
Cu Cu	Laccase	oxidase,
Cu Cu	Ceruloplasmin	oxidase,
Cu Cu	Ascorbate oxidase	oxidase,
Cu Fe	Cytochrome-c-oxidase	electron transport,
Cu Zn	Superoxide dismutase	O_2^- disproportionation,
Fe Fe	Haemerythrin	rev. O_2 carrier,
Fe Fe	Rubredoxin	O_2 transfer in photosyn,
Ca Ca	Thermolysin	structural,
Mo Mo	Nitrogenase	6-e reduction of N_2 - $2NH_3$.

Figure 2

active site of Laccase

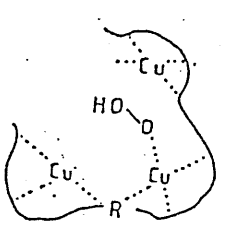

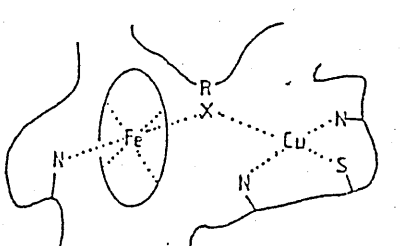

active site of
cyto-chrome-c-oxidase
Fe .... Cu 3.75Å

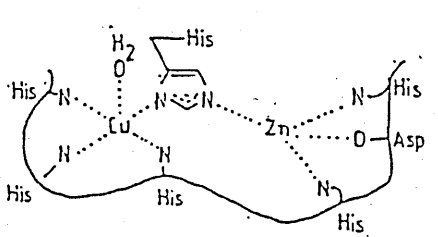

active site of
superoxide dismutase

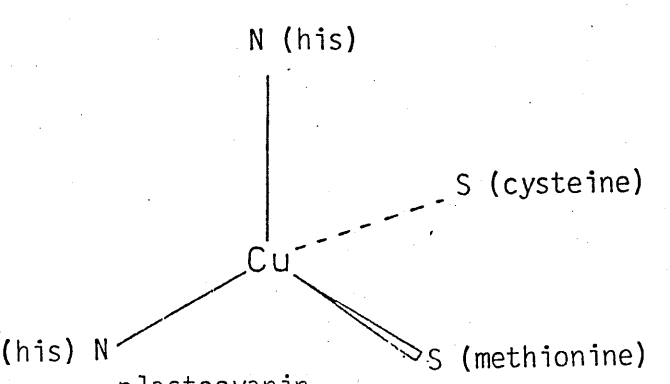

plastocyanin

INTRODUCTION

Over the last 25 years there has been a rapidly growing interest in binuclear metal complexes because of their potential as models for that group of metalloproteins for which the biological function is known or believed to be assocated with the occurance of the metal centres in pairs. From the table in FIG.1 it can be seen that prominent among the natural systems are copper containing proteins[1]. FIG.2 shows the active sites of some of these systems. It has been the aim of many research groups to mimic these systems by means of models incorporating the relevant functional groups held in suitable geometrical arrangements. Although these synthetic models cannot replicate all the physical and chemical properties of the natural systems much can be learned about the chemistry of the active sites from a study of model compounds. Molecular systems having two or more redox active metal centres in close proximity capable of co-operative interactions are also of interest in relation to their potential as catalysts for non-biological substrate oxidations particularly in reactions requiring multi electron transfer[2].

In recent years much work has been directed towards the design and synthesis of ligands capable of holding 2 metal cations at separations (≈2.5-6.0Å) which are subject to control by appropriate modification of the molecular topology. Alteration of the metal....metal separation and the number, nature and disposition of the donor atoms allows the study of those physical and chemical properties (spectroscopic, magnetic and electrochemical) which may depend on the binuclearity of the system[3]. In particular the possibility is offered of the binding and activation of small substrate molecules and ions between the metal centres and the investigation of the structural and physio-chemical host -guest, receptor-substrate relationships.

As has been observed already the copper ion is involved in a wide range of biological processes. The increasing sophistication of analytical techniques has played an important role in elucidating the nature of the active site of copper proteins. From these spectroscopic studies on copper

centres in various proteins the copper ions have been classified into 3 categories, types 1, 2 and 3, based on spectral properties of the metal.

TYPE 1 COPPER ("BLUE-COPPER CENTRES")

These intensely blue (for copper) species exist in an unusual non planar (tetrahedral) co-ordination geometry of two thioether (cysteine and methionine) and two unsaturated nitrogens (histidene). They can be characterized by [4,5]-

1) an intense absorption near 600nm ($\epsilon \simeq 4000 M^{-1} cm^{-1}$)
2) an esr spectrum with unusually small hyperfine coupling constants A_{11} (<100G)
3) a high positive redox potential for the Cu^{2+}/Cu^{+} couple, reflecting appreciable stability of the Cu(1) site.

N.M.R reveals the active site to be relatively inaccessible to solvent molecules[6].

TYPE 2 COPPER

This copper centre is present in all blue multicopper oxidases. They have spectroscopic properties similar to simple copper (11) complexes and exhibit normal esr spectra.

TYPE 3 COPPER (ESR non-detectable)

This site is also present in all multicopper oxidases. It is characterized by -

1) the occurrence of two copper ions in close proximity.
2) the absence of an esr signal due to strong antiferromagnetic coupling interactions.

It can thus act as a 2 electron donor/receptor and is essential to the reduction of dioxygen. The type 3 site also exhibits an intense 330nm absoption. (ϵ=3000-5000)

Structures of copper proteins containing only one of the different types of copper are known: Plastocyanin has a 'blue' type 1 copper, which is co-ordinated to 2 histidine residues and the sulphur atoms of cysteine and methionine in a distorted tetrahedral geometry[7] (FIG.2). The mixed zinc-copper enzyme superoxide dismutase contains a type - 2 copper(11) site which has 4 histidine ligands with slightly distorted square co-ordination[8] (FIG.2). This enzyme combats the potentially toxic effects of superoxide ions by catalysing the dismutation of the anion to dioxygen and hydrogen peroxide.

$$2O_2^- + 2H^+ \longrightarrow O_2 + H_2O_2$$

Haemocyanin (discussed in detail later) of Panulirus interruptus contains a type-3 pair of copper ions in an environment of 6 histidine ligands[9]. Tyrosinase is a mixed function oxidase which catalyses the 2-electron oxidation of o-diphenols to o-quinones and the monooxygenation of phenols to o-diphenols. It contains a binuclear type 3 copper active site[10] which is very similar to that found in haemocyanin.

THE BLUE COPPER OXIDASES.

The blue copper oxidases, which contain all three copper(11) types, are laccase, ceruloplasmin and ascorbate oxidase.

Laccase is the simplest of the blue oxidases, containing one each of type 1, 2 and 3 copper sites. The type 2 and 3 sites in laccase lie close together and there is a strong dependance of the geometric and electronic structure of the type 2 copper(11) on the oxidation state of the type 3 copper centre. Studies on the binding of small anions to laccase suggest that a type 2 - type 3 trinuclear copper active site may be active in the irreversible binding and multielectron reduction of dioxygen to water[11]. It is possible that the trinuclear copper cluster contributes to oxygen reduction by providing rapid three - electron transfer that would irreversibly break the O-O bond[11]. The structure and nature of the copper active sites in ceruplasmin have not yet been fully established

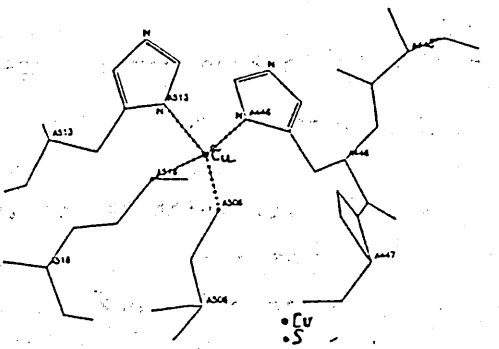

Fig. 3-1

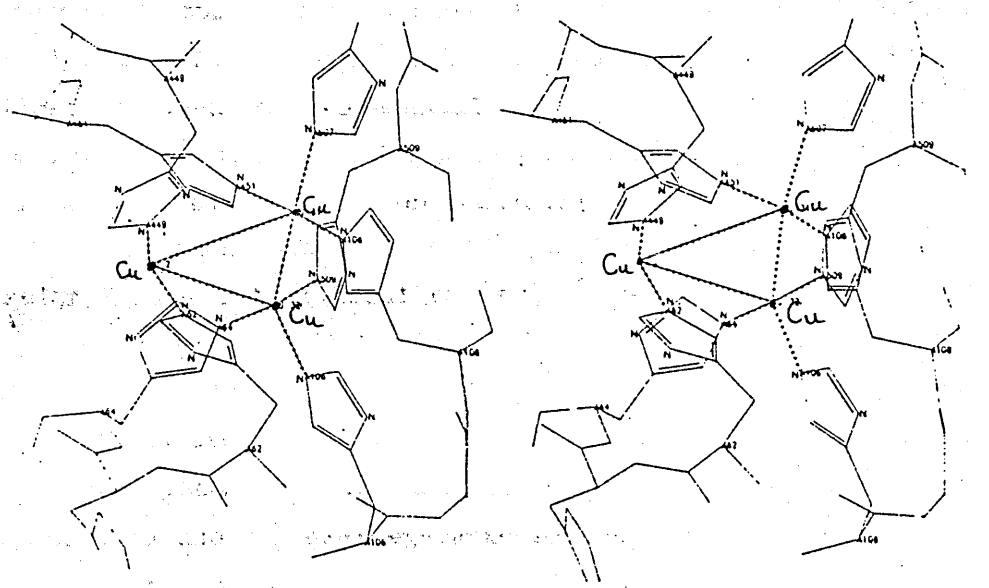

Fig. 3 - 2

Trinuclear copper site in ascorbate oxidase

although the enzyme is thought to have seven copper atoms per mole, with two type 1, one type 2, and 2 pairs of type-3 copper sites[12-14],

Sophisticated work by Huber[15], for which he received the Nobel Prize for Chemistry(1988), on the blue oxidase - ascorbate oxidase, has shown that type-2 and type-3 copper centres may work in unison to achieve the reduction of dioxygen. Ascorbate oxidase is a polypeptide of 553 amino acid residues folded into 3 tightly associated domains[16]. It is a dimer in solution although the functional unit is the monomer. In domain 3 of ascorbate oxidase a copper ion is found in a strongly distorted tetrahedral (approaching trigonal pyramidal geometry) co-ordination with the ligands His, Cys, His, Met (FIG.3-1). A trinuclear site is enclosed between domains 1 and 3 (FIG.3-2). Four (-His-X-His-) amino acid sequences provide the 8 histidine ligands. The trinuclear copper site contains a pair of coppers each with 3 histidyl ligands, forming a trigonal prism. It is a type-3 copper pair. The remaining copper has 2 histidyl ligands and is a type-2 copper. The trinuclear copper cluster is the site where dioxygen binds although the structure, including the presence of exogenic ligands, still requires full clarification. The close spatial association of the 3-Cu ions in the cluster, as in the laccase system, suggests facile electron exchange. The cluster serves as an electron storage site and may function as a co-operative three electron donor for the oxygen molecule to irreversibly cleave the O-O bond. The distribution of the redox centres as mono and trinuclear sites may also be found in the most complex oxidase - cytochrome oxidase[17]

Polynuclear copper(11) complexes are the best systems to establish magneto-structural correlations and to test the existing models for describing the nature and the intensity of the exchange interactions between paramagnetic centres.[18] The understanding of these interactions in dinuclear and/or oligonuclear species form provides background necessary to the design of syntheses of more complex systems with unusual magnetic properties. Anisotropic exchange has been widely studied in the last few years since it allows one to estimate exchange interactions between ground states and excited states[19]. The interactions in copper(11) couples determine, together with direct magnetic interactions, the zerofield splitting of the

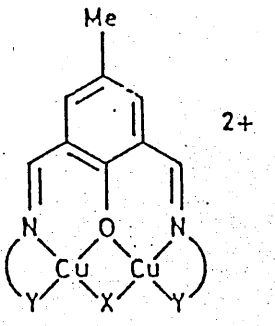

Fig. 4

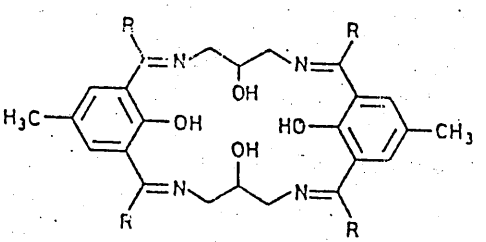

Fig. 5-1

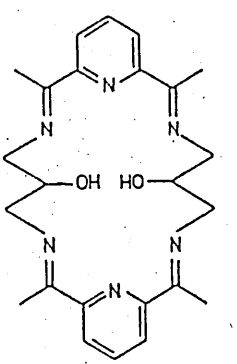

Fig. 5-2

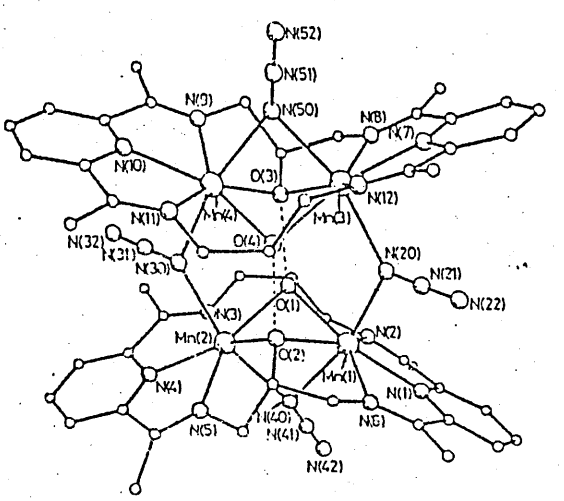

Fig. 5-3

triplet state arising from the isotropic exchange interaction and can in principle give measurable effects in the electron resonance spectrum (see Appendix 2)

The magnetic exchange interactions in binuclear copper(11) complexes occur very often via bridging ligands. A great amount of reported work in this area is available and concerns 2 kinds of bridged compounds: those with short intercationic distances which have one or two mono-atomic bridges and those complexes with long intercationic separations (>4A) corresponding to bimetallic compounds containing polyatomic bridges. The bridging group can be of an intramolecular source where it is referred to as an endogenous bridge. This can be monatomic or polyatomic in nature. Alternatively it can be a small molecule or ion which does not form part of the framework of the complex. This is an exogenous bridge which again can be monatomic or polyatomic.

Some natural systems exhibit both types of bridging and thus Kahn has used variations of the molecular structure shown in FIG.4 to study the magnetic properties of copper(11) binuclear compounds with 2 dissimilar bridges[20-23]. One of the bridges is an endogenous phenolato bridge and remains constant, the other is an exogenous bridge eg. hydroxo, cyanide or cyanato. Results showed that the μ-azido compound is less antiferromagnetically coupled than the μ-hydroxo (irrespectivce of structural detail) This is consistent with the fact that azido, N_3^-, tends to exert a ferromagnetic contribution when bridging in an end-on fashion owing to spin-polarization effects discussed later. Replacing NR_3 by SR_2 in the lateral bridging chain, N-Y, increases the magnitude of the antiferromagnetic interaction substantially, which shows that any kind of magneto structural correlation should exclusively concern series of related compounds in which the metal ions are surrounded by the same bridging as well as terminal atoms. Finally results seemed to indicate that as the bridging angle increases the value of -J increases, not only for X=OH[24] but also for N_3^- and OCN^-.

McKee has reported a potentially octadentate macrocyclic ligand[25] FIG.5-1 which is capable of providing endogenous alkoxy and phenoxy bridges and a

deoxy - Hc

Cu .... Cu = 3.8 Å

oxy - H_c

Cu .... Cu = 3.6 Å

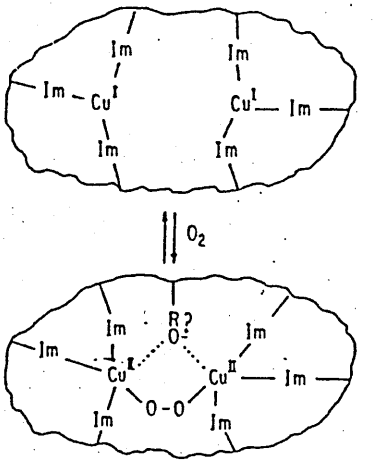

Fig. 6-1

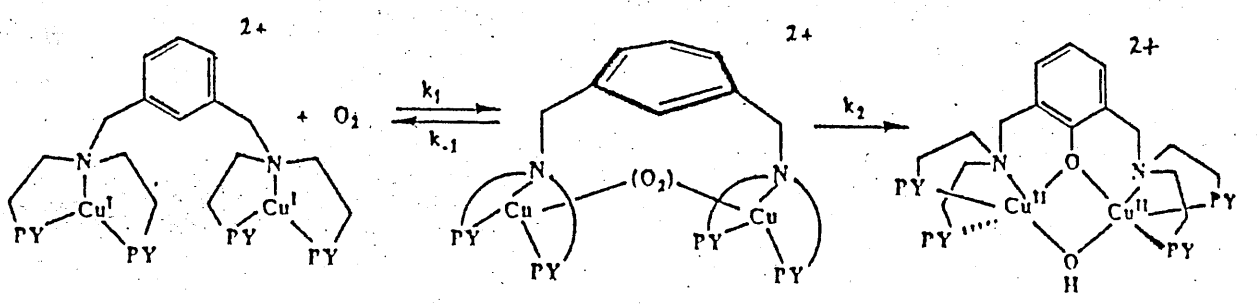

Fig. 6-2

potentially hexadentate ligand[26,27] offering alkoxy endogenous bridging facilities. FIG.5-2. The latter forms tetramanganese (11) complexes which in the presence of azide or chloride ions the 4 manganese (11) centres are bridged by both ligand alkoxides and chloride or azide groups FIG.5-3. This model is interesting since the biological active site of the photosynthetic oxygen-evolving complex[28] is now generally believed to contain four manganese ions bridged by oxygen donors[29,30]. If the central chloride or azide ligands could be replaced by hydroxide or water, the resulting complexes could constitute a model for the first step of dioxygen production. This reaction type has been found in the $Fe_4(OH)_2$ cores of models prepared by Lippard etal[31].

Karlin has been interested in the binding, interaction and subsequent reactivity of dioxygen (O_2) at copper ion centres in the enzymes haemocyanin (Hc) which transports O_2, the monooxygenases, tryrosinase and dopamine β- hydroxylase which incorporate oxygen (from O_2) into organic substrates. For many years it was believed that the copper(11) ions in oxyhaemocyanin resided in a ligand environment composed of 3 imidazole nitrogen atoms - derived from histidine residues, a bridging dioxygen ligand and an endogenous bridge[32]. This endogenous bridge was believed to mediate the very strong antiferomagnetic ($J < -500cm^{-1}$) spin exchange interaction between the metals which resulted in a pair of diamagnetic copper ions.[33]. The source of this endogenous bridge was attributed to an oxygen atom derived from hydroxide, phenoxide, carboxylate or a tyrosinase residue. Lack of enhanced tyrosinase in the resonance Raman experiment[34] indicated there was no tyrosine residue present in the immediate vicinity. X-ray structures on the haemocyanin of the spiny lobster, Panulirus interruptus shows that the two cuprous ions in this deoxy-Hc are each co-ordinated to 3 imidazole (histidine) nitrogen ligands in a hydrophobic environment, with Cu....Cu of 3.7 ± 0.4 Å [35] FIG.6-1, and no bridging ligand with the nearest tyrosine about 10.6A distant. The reaction with oxygen occurs via an inner sphere redox process to give oxy-Hc containing a dinuclear Cu(11) centre and a coordinated peroxo (O_2^{2-}) ligand. Karlin used a tyrosinase-like reaction to synthesize a phenoxo bridged tetra coordinated dicopper (I) complex which gave dicopper (II) complexes (Fig.6-2). This reacts at low temperatures in methylene chloride solution

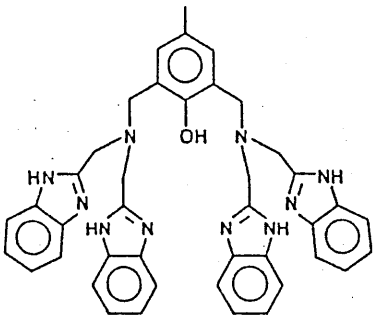

Fig. 7-1

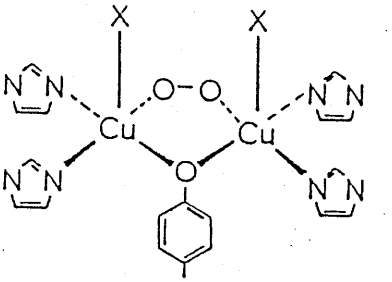

7-2

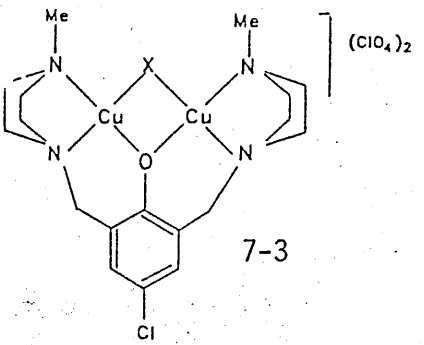

7-3

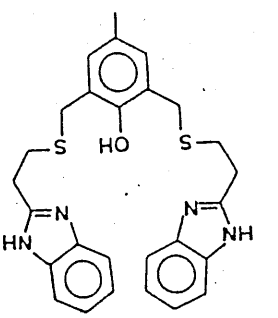

7-4

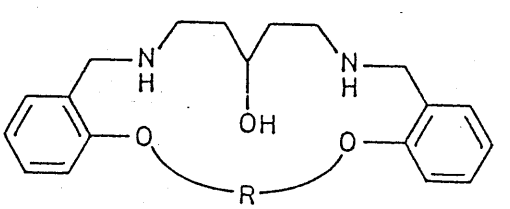

Fig. 8

R

$(CH_2)_2$

$(CH_2)_3$

$(CH_2)_4$

Fig. 9

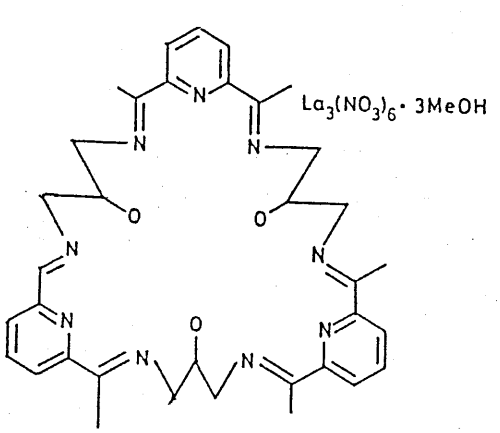

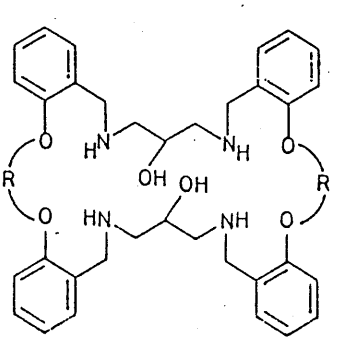

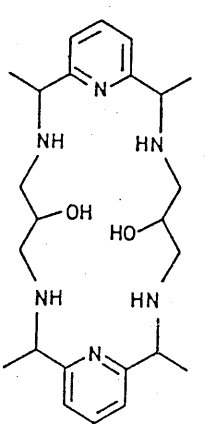

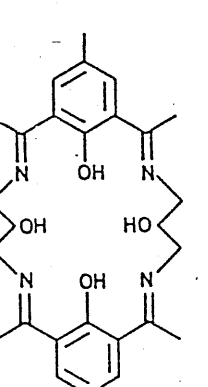

with 1 equivalent of dioxygen to give an intensely purple coloured dioxygen adduct. [36] The binding of oxygen is reversible and can be followed spectrophotometrically. The dicopper(1) complex also forms bis-adducts with the typical Cu(1) specific ligands CO and PPh_3. These complexes can also be formed by displacement of oxygen when the dioxygen complex is directly reacted with either CO or PPh_3 lending further support to the existence of the reversible equilibrium[37]. Kinetic and thermodynamic studies have subsequently been carried out[38] which again support the idea of reversible binding of oxygen. Comparing the rates of reaction to a system where the phenoxy bridge is absent indicates that forcing the two Cu(I) ions into close proximity by the presence of a bridging phenoxo ligand causes a dramatic enhancement of the reaction rate with dioxygen[39].

Other groups have, in recent years, reported biomimetic models for haemocyanin (and other enzyme systems) based on endogenous/exogenous bridging ligands. These include Stephan[39] FIG.7-1, Sorrell[40] FIG.7-2, Murray (type 3, Depleted Laccase Active site)[41] FIG.7-3 and Latour[42] FIG.7-4.

Fenton et al have published a series of papers on complexes of Schiff-base ligands providing endogenous bridges [43a-h] Most recently he has reported the synthesis of a series of [1+1][2+2] oxa-aza macrocycles[43h] derived from the non template condensation of 1,5-diamino-3-pentanol and acyclic dialdehydes followed by in situ reduction with tetrahydroborate FIG.8 Examples of some other ligands prepared by the Fenton group providing endogenous bridges are given in FIG.9. Many of these ligands, bearing endogenous bridges, have been used to prepare heterobinuclear complexes containing uranyl (VI)[44,45] and they have obtained interesting results with uranyl(VI) compounds containing U-SR_2 and UPR_2 bondings using potentially pentadentate Schiff bases of the type in FIG.10[46,47] and they also investigated the interaction of various acyclic and cyclic ligands FIG.11 with uranyl(VI), copper(II) and nickel(II)ions[48]

Catechol is a two electron reducing agent whose oxidation to quinone Fig.12 is catalysed by Cu(II)[49,50] and in particular by binuclear copper

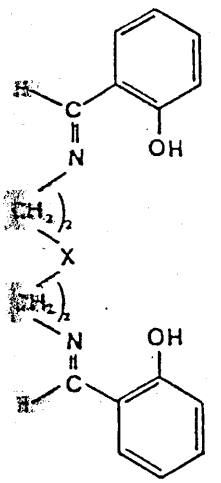

Fig. 10

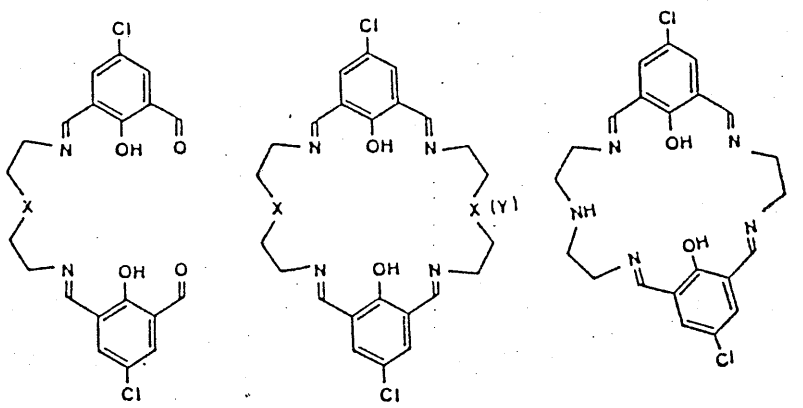

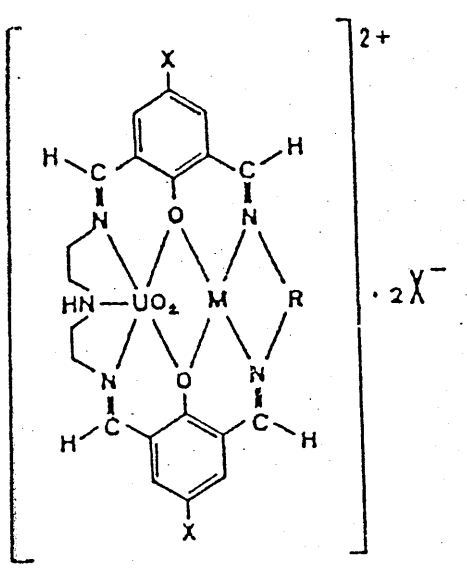

Fig. 11

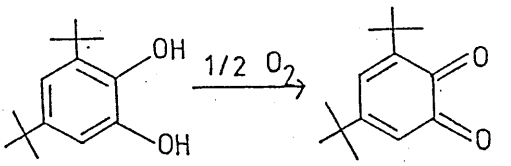

Fig. 12

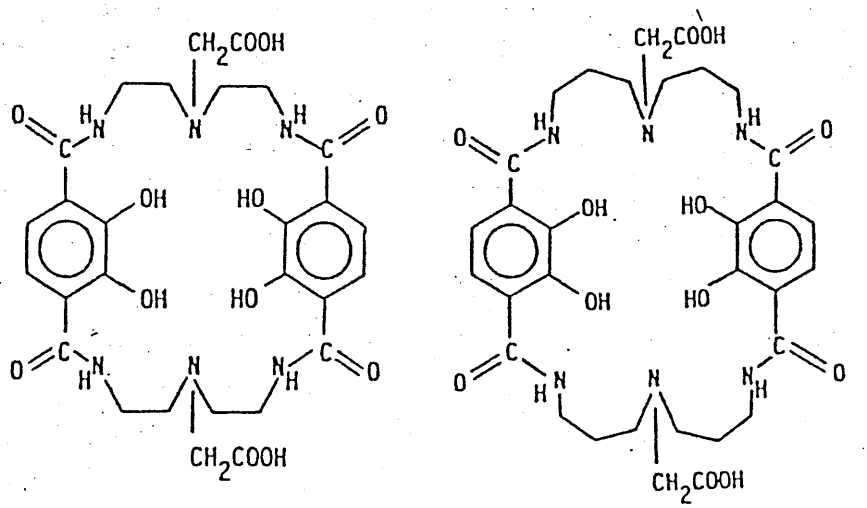

Fig. 13

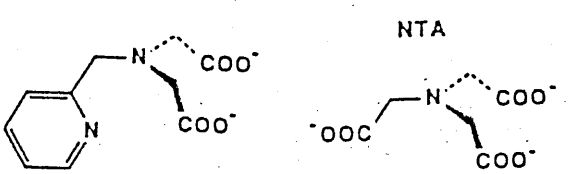

Fig. 14-1
TRIPODAL LIGANDS

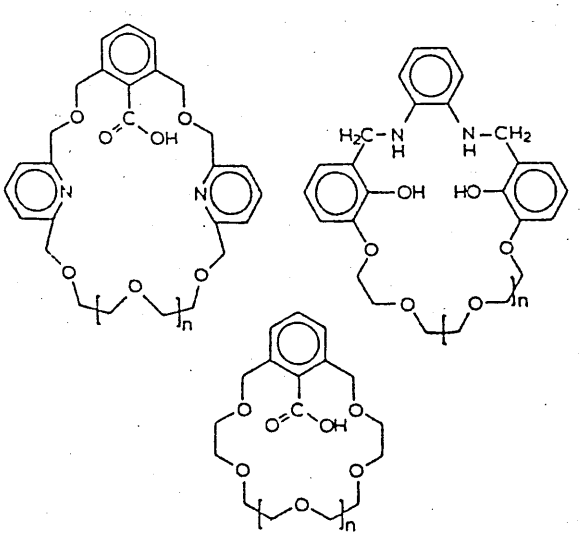

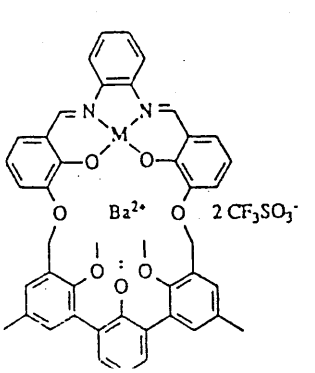

Fig. 14-5

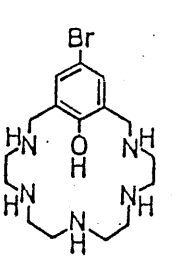

Fig. 15

systems[51]. There have been several reports on synthetic macrocyclic and cryptand catecholate siderophores with endocyclic donor groups[52,33]. Martell has synthesized 2 new macrocyclic ligands containing bidentate endocyclic catechol donor groups,[54]FIG.13, which differ in ring size. Both species are effective at binding Fe(III) at physiological pH although their stabilities are much lower than that of enterobactin. This is because the ligands cannot conform to the octahedral co-ordination sphere of the metal ion without considerable twisting of the connecting bridges between the bidentate donor groups. Que[55] has used trianion tripodal ligands FIG.14-1 as functional models for catechol-1,2-dioxygenase. Reinhoudt has introduced an intramolecular acidic group into the macrocyclic cavity for the complexation of urea[56] FIG.14-2, - 14-4 and has formed heterobinuclear complexes with some of the above ligands with both a cavity suitable for complexation of transition metal cations and a cavity for complexation of Group1 and II metal cations[57] FIG.14-5. Kimura[58] has synthesized intraanular phenol containing polyamines FIG.15 in an attempt to develop a selective sequestering agent for the harder metal ions. This is usually best achieved with polyether macrocycles while polyamine counterparts are generally used for heavy and transition metal ions. In non-basic conditions the degree of 1:1 association uniformily varies with the size of metal ions ie Mg>Ca>Sr>Ba whereas the monovalent alkaline metal salts do not dispel the phenolic proton of the ligands.

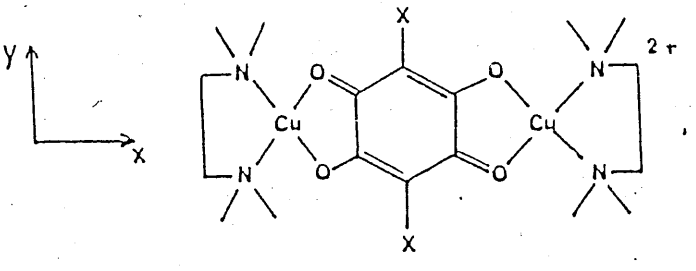

Fig. 16

EXOGENOUS BRIDGES.

As a result of studies [59-63] to investigate the various ways to maximize the interactions between 2Cu(II) ions separated by distances even as long as 5.4±0.3Å, Kahn proposed the following requirements:-

1) The 2 copper centres must show planar or square pyramidal coordination.. For the latter case, the apical bond length must be as large as possible.

2) The 2 basal planes around the copper (II) ions must be as co-planar as possible.

3) The HOMO'S of the bridges must be largely delocalized on the co-ordinating atoms and symmetry-adapted to interact with the singly occupied metal orbitals. The HOMO's must also be as high in energy as possible. (eg weakly electronegative groups present).

When these requirements are met the 2 magnetic orbitals ϕ_A and ϕ_B centred on the copper(II) ions are essentially located in the plane of the bridging network and are strongly delocalized (in an antibonding fashion) on the bridging atoms so that the overlap integral may be large, which favours an antiferromagnetic interaction. He has applied these rules to a series of copper(II) dinuclear compounds containing the halide derivative of the 2,5-dihydroxy-1,4.benzoquinone dianions as bridging ligands[64] FIG.16 to see what extent the interaction is reduced with a Cu...Cu separation of 7.5Å.

All compounds showed a maximum of χ_m in the 14-21K temperature range which is characteristic of a weak antiferromagnetic interaction as is the decrease in intensity of the esr signal with decreasing temperature. The largest interaction is observed in the μ-iodanilato compound ($J=-25.9cm^{-1}$). However from earlier studies the strongest interaction was $J=-730cm^{-1}$ for the dithioxoamide compound with a Cu...Cu distance of 5.67Å[63,64].

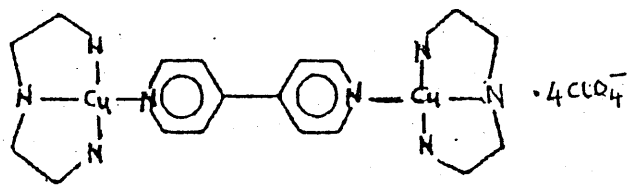

Fig. 17

Fig. 18

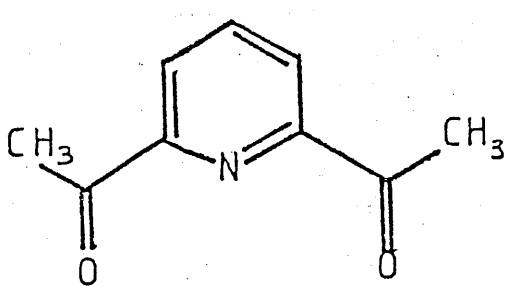

18-1 DAP

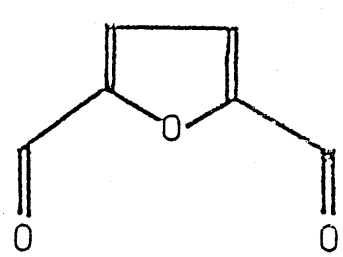

18-2 DFF

However 7.6Å is far from being the limit for the interaction between two copper(II) ions. Coffman and Buettners[65] have proposed the relation

$|J_{intm}| = 1.35x10^{7}\exp(-1.80R)$

for the limiting value of $J(cm^{-1})$ - the singlet-triplet gap in the binuclear complex versus R(Å) the distance between the metallic ions. Verdaguer therefore used 4,4'bipyridine as a suitable candidate to give R distances greater than 10Å[66] FIG.17. He used a mononuclear complex with a mondentate 4,4' bipyridine ligand to obtain an estimate of the intermolecular contribution to the magnetic interaction. From their results it was not possible to attribute the observed antiferromagnatic coupling to intramolecular interaction only.

In general more interest lies with the shorter Cu...Cu separations which are more applicable to many natural systems and thus smaller polyatomic bridging molecules are employed-azide, thiocyanate, hydroxide, methoxy and ethoxy - being common examples although pyrazole, halide, pyrrole and imidazole bridges are also of interest. An example of the latter is in bovine erythrocyte superoxide dismutase known to contain an imidazolate Cu(II).....Zn(II) active site[8]. Synthetic macrocycles having a cavity size large enough to encapsulate 2 metal ions, provide a means whereby the interactions and structural relationships between the metal centres may be studied in the laboratory. The macrocyclic ligands employed for such studies are commonly the binucleating Schiff-base macrocycles where particularly useful dicarbonyl precursors are 2,6 diacetylpyridine (D.A.P) FIG.18-1 and Diformyl furan (D.F.F) FIG.18-2. [2+2] condensations of these dicarbonyls with various amines give rise to many structures of various ring size. Although formed by template methods, transmetallation with copper(II) ions was easily achieved giving a range of binuclear Cu(II) (and other transition metal homobinuclear assemblies) complexes.

The occurence of bridging substrate molecules within such binuclear macrocyclic complexes may be recognized from the stoichiometry of the complexes and from a variety physico-chemical studies, particularly measurement of magnetic susceptibility as a function of temperature

Fig. 19

-1-

-2-

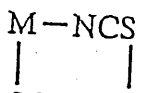

-3a-

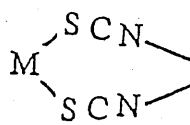

-3b-

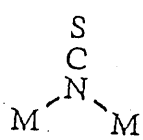

-4-

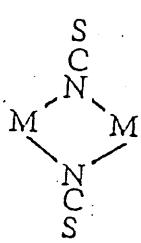

-5-

Fig. 20

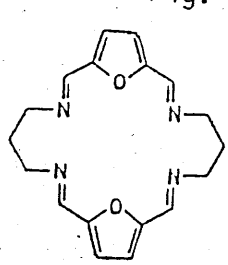

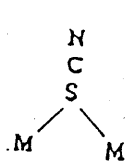

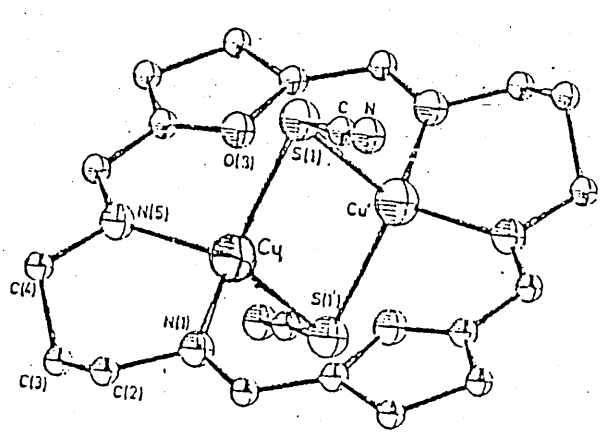

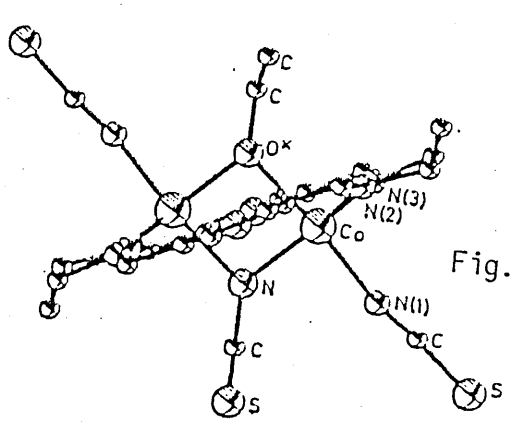

Fig. 21

(appendix 3) and esr (appendix 2). In addition the detailed structures of complexes solved by X-ray diffraction studies are invaluable in this area.

Nelson etal[67,68] have thoroughly investigated series of macrocycles in which the inner ring varies in size from 16 to 30 member atoms thus having appropriate cavity dimensions for the accomodation of bridging substrate molecules and ions of varying size. They have found many interesting results from such studies, in particular, with respect to the bridging mode of the thiocyanate ion.

THE THIOCYANATE ION

X-ray structural studies of crystalline KSCN derivatives[69] suggest that the free ion is linear and exists as a hybrid of $^{-}S-C=N$ and $S=C=N^{-}$. The charge can be located at either end (depending on chemical enviroment) of the ion producing ambidentate character[70] in the NCS^{-} ion which therefore has 5 binding modes FIG.19-1 - 19-5. The terminal nitrogen and sulphur bonding modes 19-1 and 19-2 together with the 3-atom bridging configuration 19-3a and 19-3b are used in almost all of the known thiocyanate complexes. In stark contrast, co-ordination in a single atom bridging fashion FIG.19-4, 19-5, has been rare and until 1979 unknown. To date the unique example of a structurally characterized "S" only bridge between transition metal ions remains that demonstrated by Nelson [71] Fig.20. However within the last couple of years an "S" only bridging thiocyanate group was diagnosed in a dilead assembly [72]. N' only bridging was first recognized by Cotton[73] in 1979 following the X-ray structural analysis of the mixed-valence metal bonded anion $[Re_2(NCS)_{10}]^{3-}$; however it was 2 years later before the first example of N-only bridging within a macrocyclic ligand was realized [74] by Nelson FIG.21. With the exception of Reedijks Cd (II) polymer[75] and Lindoys Ni(II) dimer[76] the occurrence of the single-atom bridging modes can be ascribed to an enforced close proximity of the metal centres which precludes formation of the 3 atom bridge. Thus the bridging mode of the thiocyanate ion, if bridging occurs at all, is indicative of the separation of the 2 metal centres.

For internuclear separation greater than 6.0Å, no form of bridging is possible and terminal -NCS or -SCN co-ordination applies, depending on the preferences of the metal ion, the N-donor end being selected by the relatively 'hard' class A transition series ions, and the S-donor by the softer class B main group ion Pb^{2+}. The internuclear separation typically[77] associated with the commonly observed centrosymmetric di μ-1,3,- NCS- arrangement 19-3a was estimated at 5.6Å and this was borne out by a survey of the Cambridge Crystallographic Database which showed distances between 5.3 and 5.8Å[78]. Where such an internuclear separation is not available, and particularly where the pair of metal ions are non identical an unsymmetrical arrangement such as 19-3b may be adopted, which can reduce the distance necessary for accomodation of the bridging unit[79] to ≃4.8Å. There is one example of a structurally determined single 1,1-μ-NCS bridge 19-4 which shows a metal-metal distance of 4.347(I)Å[80] and a Pb-N(CS)-Pb angle of 109.2°. With 2 such bridges 19-5, the metal-metal distance is much smaller and the one known structural example involving transition metals has a Ni...Ni distance of 3.28Å. The one example of bridging through S shows an internuclear separation of 2.87Å[72]. In this case however the mode of thiocyanate co-ordination is probably determined as much by the class B nature of the acceptor ion as by the available cavity space.

Several reports of N-only bridges have appeared in recent years including those described in 78, 80-82.

Despite the small number of structurally defined examples of N-only bridging, a simple physico-structural correlation based on infrared data is already emerging. (IR spectroscopy of co-ordinated thiocyonate has been extensively reviewed[83]). There are 3 normal vibrations for co-ordinated NCS^-, ν_{NC}, ν_{CS} and ν_{NCS}. Of these ν_{C-N} has been the most heavily studied because it is normally a strong absorption which falls around 2050cm^{-1} - a part of the spectrum which is normally free of potentially interfering ligand vibrations. This is not the case for the weaker, lower energy, ν_{NCS} and particularly ν_{C-S} vibrations which appear at ≃470 and 700-800cm^{-1} respectively.

Fig. 22

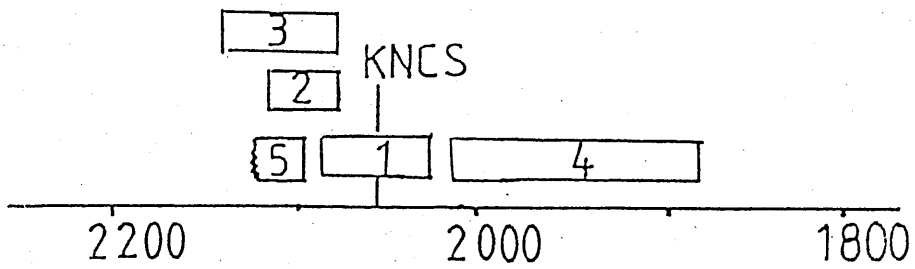

Fig. 23

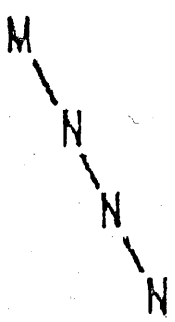

TERMINAL
FIG.23-1

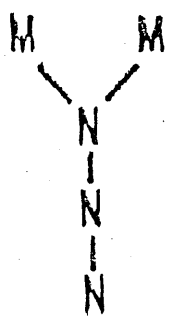

END ON
FIG.23-2

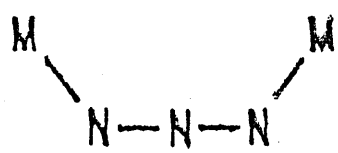

END TO END
FIG.23-3

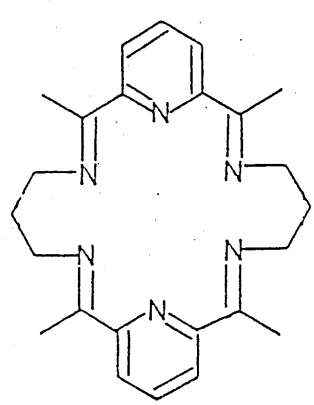

Fig. 24

The ν_{C-N} frequencies and their structural assignments for the first row transition metals are summarized in FIG.22. This shows that all types of co-ordination involving sulphur have overlapping regions (2,3,5). Terminal nitrogen bonding occurs at lower frequencies 2030-2080cm^{-1}. However the most striking feature is that (with the exception of [76] for which no ir data is reported) all the N-only bridging thiocyanates exhibit the ν_{CN} absorption at frequencies below 2030cm^{-1} and usually below 2000cm^{-1} (1885cm^{-1} [73] is the lowest recorded) well removed from the more familiar regions associated with NCS^-. So low, in fact, the ν_{CN} in these complexes that when first encountered by Cotton *etal* [84] in 1967 it was assigned as a $\nu_{C=O}$ frequency of a carbonyl group, only to be corrected 12 years subsequently on the basis of an X-ray crystal structure[73].

In similar manner the azide ligand can bind in one of three ways: terminal[85-87], end on μ-1-1 bridging [87-90] and end to end μ-1,3 bridging[85-87, 91-93] FIG.23. All modes are known in copper chemistry and modes 23-1 and 23-3 have been proposed to occur in methaemocyanin derivatives[92,94,95]. Because of the importance of azide co-ordination in protein studies Karlin *etal*[96-100] and others[91,92,101] have sought to examine its co-ordination properites in relevant model systems. Nelson *etal* have observed the long 3 atom bridge in several bi-Cu(II) complexes of binucleating ligands[102,103] such as the ligand (L) in Fig.24. Reaction of $Cu_2L(OMe)(ClO_4)_3 2H_2O$ with one equivalent of NaN_3 in methanol affords the complex $Cu_2LN_3(ClO_4)_3$ for which the assymmetric and symmetric stretching vibrations of the co-ordinated azide ion occurs at 2070 and 1347cm^{-1} respectively. The occurrance of the symmetric stretch as a moderately intense band is taken as evidence for a μ1-1, bridge since the vibration is expected to be inactive or of low intensity in symmetrically bridged μ1-3 azido complexes. A weak antiferromagnetic coupling interaction between the 2Cu(II) ions in this complex has been inferred from the esr spectra of frozen solutions[102].

It is the enormous variation of magnetic exchange interactions leading to diamagnetic, antiferromagnetic (weakly and very strongly coupled) and ferromagnetic azide bridged copper(II) dimers that makes these materials

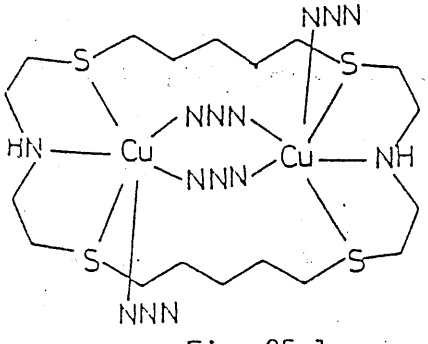

Fig. 25-1

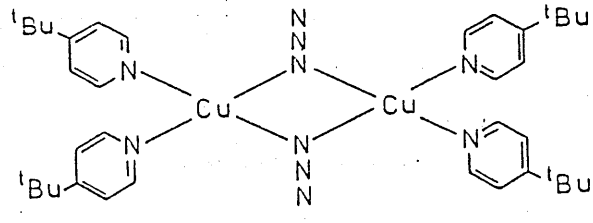

Fig. 25-2

ideal probes for the elucidation of magneto-structural correlations in these exchange coupled systems.

The magnetic properties of the two bridging type azido complexes differ markedly. When azide bridges in an end-to-end fashion the coupling between the magnetic centres can be strongly antiferronagnetic[95,104]. The complex in FIG.25-1 is diamagnetic and shows no esr signal over the temperature range 4-300K indicating that there is a very strong antiferromagnetic interaction between the two copper(II) ions despite the large Cu...Cu separation (5.15Å) [95]. When azide bridges in an end-on mode the ferromagnetic interaction between the metal ions is favoured [105-107,87]. For the complex in FIG.25-2 the Cu....Cu distance is 3.04Å and the coupling between the two coppers is ferromagnetic with $2J = +210cm^{-1}$ [107].

The design of ferromagnetically coupled dinuclear complexes [108,109] occurs at 2 levels of approximation for the theoretical approach.
1) only the metallic unpaired electrons are considered as active electrons [108,109]
2) spin polarization effects[108,109] from the highest occupied orbitals of the bridging ligands.

The active electron theory (not discussed here see ref 108,109)loses its validity when low energy molecular orbitals, doubly occupied by the so called passive electrons (non magnetic electrons) no longer differ much in energy from the magnetic orbitals (containing the unpaired metal electron). These doubly occupied molecular orbitals of the azide bridge can polarize the spin of the unpaired electron to favour either a singlet or triplet state.

The ab initio calculation [110] of the electronic structure of N_3^- has shown that the highest occupied level (πg^4) (of the ground state) is very separated in energy from the level located immediately below. (energy difference is 6.68eV). Thus the Πg molecular orbital in the plane of the bridging network can play a dominant role in the interaction between the Cu(II) ions through the azido bridge. At any given instance, in Πg, the

Fig. 26-1

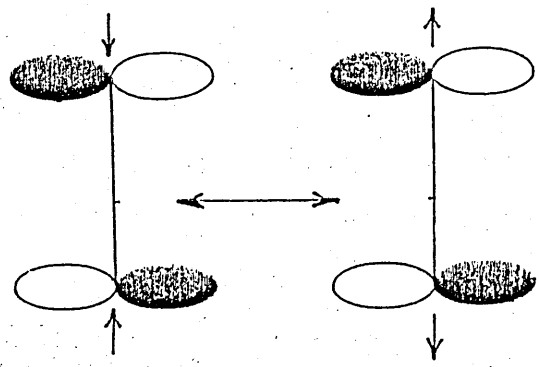

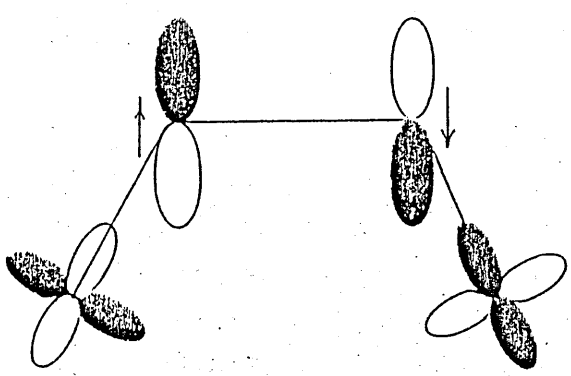

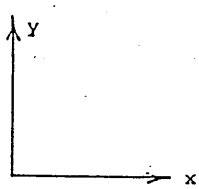

Fig. 26-2

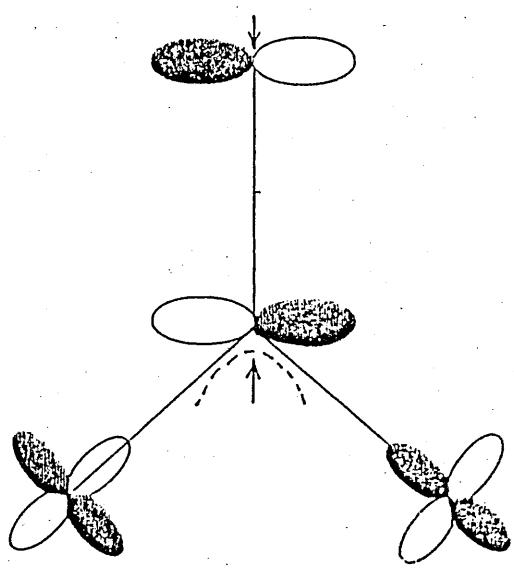

Fig. 26-3

electron with the α spin is localized around one of the terminal nitrogen atoms and the other electron, with β spin, in order to minimize repulsion effects, is localized around the other terminal nitrogen atom. FIG.26-1. Thus when N_3^- bridges in an end-to-end fashion FIG.23-1 $\pi g^{\vee}$ gives the bonding molecular orbital shown in FIG.26-2. If an α electron is partially delocalized towards a dxy metal orbital, a β electron is symmetrically delocalized towards the other metal orbital. Hence the unpaired electrons occupying the magnetic orbitals will tend to have spins β and α respectively. This favours the singlet state and thus an antiferromagnetic interaction.

When N_3^- bridges in an end-on fashion FIG.23 the electron on the bridging N (say with α spin) is partially delocalized towards the dxy metallic orbitals in the bonding molecular orbital (Fig.26-3). This delocalization is a function of the overlap < (dxy) Cu (px) N> and the energy gap between dxy and Πg. It gives an instantaneous density of α spin in each of the two dxy metal orbitals. Therefore each unpaired electron localized in its magnetic orbital with a mainly metallic character will have a probability of β spin larger than 0.5. This favours the triplet state. This theory has been tested[87,107] on di,-1-1 azido bridged dimers where indeed ferromagnetic interaction is observed. Weiss[90] has studied the interactions of μ-1-3 azido bridged copper(II) dimers of both unsubstituted and trimethyl substituted triazacyclononane and compared their results with monomeric species. Magnetic results show a strong intramolecular antiferromagnetic exchange coupling($J=-350cm^{-1}$) for the dimers whereas the monomeric species exhibits negligible coupling through intermolecular exchange. This large interaction is due to the symmetrical nature of the azide bridges. Kahn has thus proposed that with less symmetric ligands like NCO^- or NCS^- the spin polarization effect will be much less pronounced[108].

HYDROXO BRIDGES.

The best established magneto structural correlations concern bi-bridged copper(II) dimers, particularly the bis(μ-hydroxo) complexes. In this case

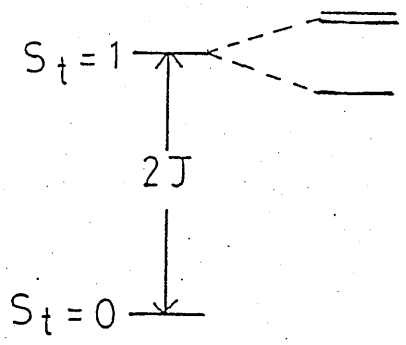

FIGURE 27

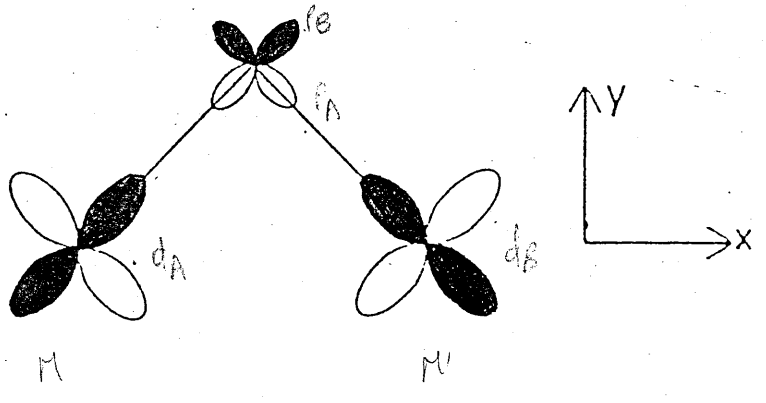

FIGURE 28

$d_A \perp p_A$ | $p_B \perp d_B$.

Hatfield and Hodgson[111] have shown that the singlet - triplet(S-T) energy gap(J) varied steadily versus the Cu-O-Cu (θ) bridging angle, with a singlet ground state for θ>97.5° and a triplet ground state for θ<97.5°. Too explain this, 2 semi-quantitative interpretations have been proposed;

1) One approach is that of Hay etal [112] J is expressed as a sum of an antiferromagnetic J_{AF} and a ferromagnetic J_F component. The latter is assumed to be weakly sensitive to small structural changes while J_{AF} is much influenced by the energy gap between the 2 singly occupied molecular orbitals in the low lying triplet states FIG.27.
2) A second interpretation, proposed by Kahn[113] is based on natural(non orthogonal) magnetic orbitals and on the overlap density between them. By defining 2 natural magnetic orbitals in a copper(II) dimer as ϕ_A^o and ϕ_B^o then the overlap density is expressed as -

$$\rho(i) = \phi_A^o(i)\,\phi_B^o(i)$$

The overlap integral (S) and the two electron exchange intergral 'j' are given by-

$$S = \int_{space} \rho(ii)\, dv(i)$$

$$j = \int_{space} \rho(i)\rho(j)\quad (dv(i)dv(j))/r(ij)$$

Again J appears as the sum of J_{AF} and J_F with J_{AF} varying as $-S^2$ and J_F as j.

For the magnetic orbitals in the bridging network in FIG.28, which are of d_{xy} type, the overlap density, noted as $\rho^{(xy,xy)}$ presents 2 positive lobes along the x axis and two negative lobes along the y axis around each bridge. For a θ value close to 90° around each bridge, positive and negative lobes compensate themselves so that the integral, S, of the overlap density is 0 as is J_{AF}. The magnetic orbitals are said to accidently orthogonal and J reduces itself to its ferromagnetic component. When θ increases, the magnitude of the positive lobes along the x axis increases and that of the negative lobes along the y axis decreases. The

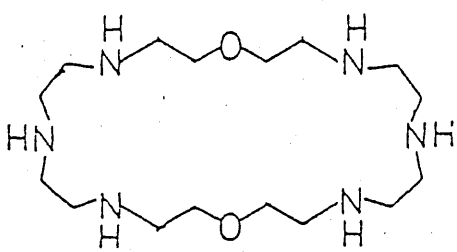

29-1

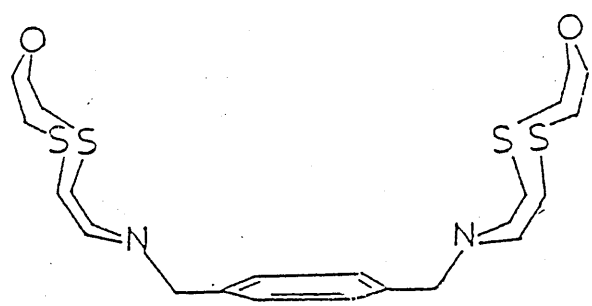

29-2

Fig. 29

result is that S^2 increases as well as $[J_{AF}]$. Thus when $\alpha > 97.5^\circ$ the J_{AF} component predominates and the observed coupling is antiferromagnetic ($J<0$). For $\alpha < 97.5^\circ$ J_F is dominant and a ferromagnetic interaction results ($J>0$). As the bridging angle α decreases below 90° the metal-metal direct interaction becomes important, leading to a singlet ground state and an antiferromagnetic interaction which is independant of α.

For di-μ-hydroxo dimers in which the 'Cu_2O_2' bridging chromophore is not planar, the 2J values are usually smaller than expected due to a decrease in the copper-oxygen antibonding overlap. A bridging angle $\alpha = 105^\circ$ with $d = 180^\circ$ (ie a planar Cu_2O_2 unit) gives a 2J value of $-600cm^{-1}$. However a characterized 'roof-shaped'[114] di-μ-hydroxo complex with a dihedral angle of 147.5° and $\alpha = 105^\circ$ has a singlet-triplet splitting of only $2J = -256cm^{-1}$.

Binuclear copper(II) complexes containing a single bridge are relatively rare, although there are a number of mono-μ-hydroxo complexes[78,115-118]. An approximately linear correlation has been observed between the hydroxo bridging angle and the coupling constant for a series of complexes all having a dx^2-y^2 ground state. For Cu-O-Cu angle between 101.3° and 126.2°, 2J values in the range $-191cm^{-1}$ to $-800cm^{-1}$ were observed[116]. The mono-μ-hydroxo bridged di-copper(II) complexes of the ligands in FIG.24 and FIG.29 have distorted square pyramidal geometries and dx^2-y^2 ground states[115,117,118]. Bridging angles of 110.3°, 132.2° and 143.7° give rise to 2J values of -64, -425 and $-500cm^{-1}$ for complexes 24, 29-1 and 29-2 respectively. These values correlate well with those ligands previously discussed. The values of the exchange constant for mono hydroxo bridged copper(II) dimers appear to be senstive to the nature of the associated non-bridging ligands and complexes having the trigonal bipyramidal geometry have a dz^2 ground state and do not fit the α-J correlation.

Thompson[119] has reported a series of binuclear copper(II) complexes of polyfunctional phthalazine and pyridazine ligands with predominantly hydroxide-bridged binuclear centres. These complexes showed larger exchange integrals ($-2J = 190-1304cm^{-1}$) than their analogous chloro-bridged complexes ($-2J = 55-131cm^{-1}$).

FIG. 30

30-1

LIGAND "BP"

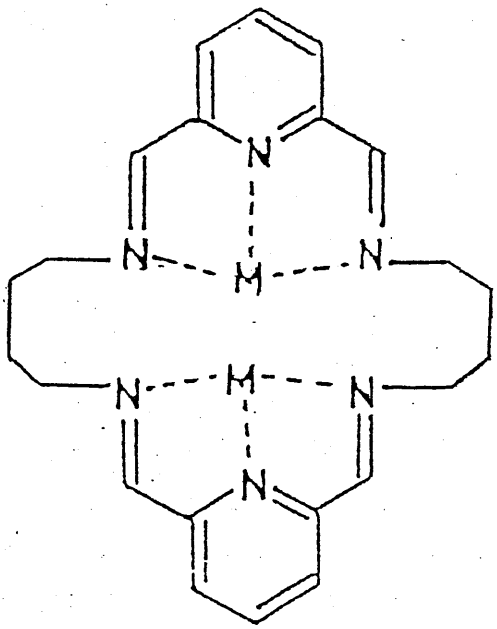

[22-N_6]

30-2

LIGAND 'WT'

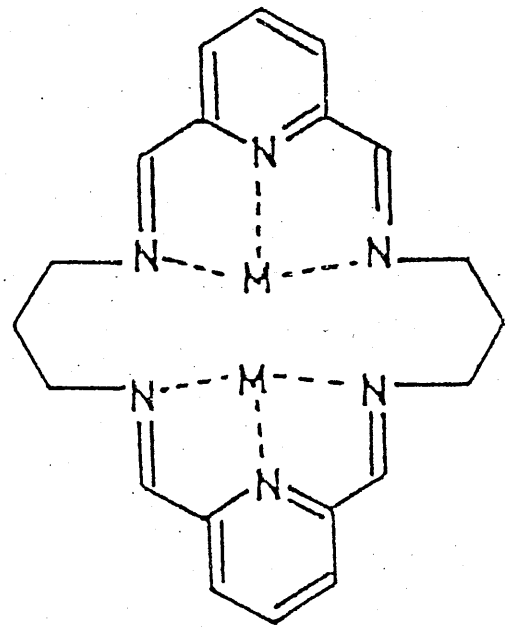

[20-N_6]

30-3

LIGAND E

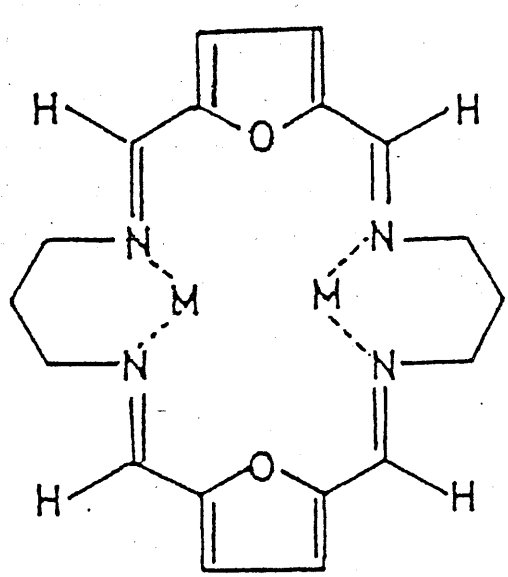

[20-N_4O_2]

30-4

LIGAND T

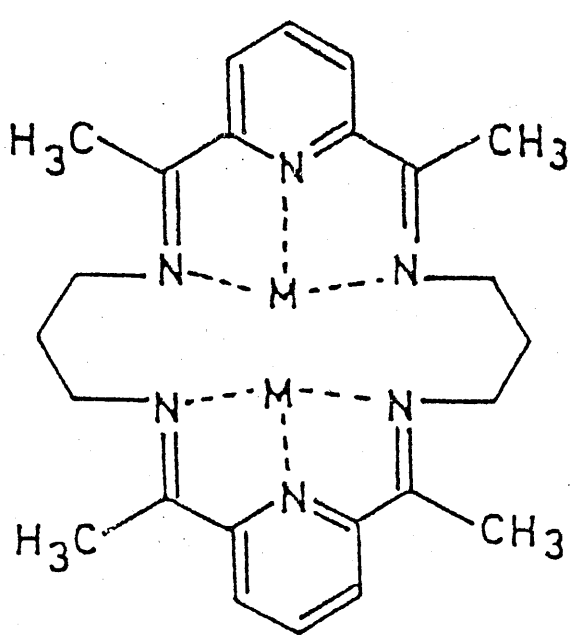

[20-N_6]

Several useful reviews on the interaction between bridged polynuclear metal complexes include. 24,120,121.

LIGAND 'WT'

The Nelson group has been interested in using various anions, mainly OH^-, N^-_3 and NCS^-, as probes of internuclear distance between various transition metal binuclear complexes. One aim of the work was to establish which of the above bridging ligands lent itself to mediating the strongest electronic exchange interaction. A second objective was to see if NCS^-, in its single N-atom bridging mode could induce the spin polarization effect, to give a ferromagnetic (S=1) interaction - and if so would it be, as proposed by Kahn[105], significantly less than the single atom azide bridge. Thus the group prepared three macrocyclic ligands each differing in potential internuclear distance. FIG.30 shows the 3 ligands, their ring sizes, modes of binding and their 'pet' names. I worked with only one of these systems ie. WT: the ligands *BP and *E were investigated by other members of the group - the work is hereby readily acknowledged.

Ligand E differs from WT and BP, not only in the nature of the donor set, N_4O_2 in E, compared to N_6 in WT and BP, but also because the oxygens of the furan rings are, with respect to transition metal ions at least, non co-ordinating. Thus the 3 systems represent a short series of macrocycles gradually increasing in size from E to BP and therefore potentially increasing in internuclear distance between the two metal centres. The ligands were synthesized using metal template methods, and by transmetallation, transition metal complexes were obtained, and their subsequent reaction and binding mode with the thiocyanate, azide and hydroxide ions investigated. A table of the analytical and infrared spectroscopic data for the complexes of the 3 ligands is shown in FIG.31 TABLE A.

* *C.Stevenson and S.Rahgunathan*

* *F.Esho, A.Lavery, K.McKillop and J.T.Grimshaw.*

FIG. 31 TABLE A

Analytical and Infrared Spectroscopic data for complexes of BP, (L') WT (L^2), E (L^3)

No.	Complex	Colour	Analytical data %N C F	%C C F	%H C F	Λ/Scm^{2}mol^{-1} [a]	$\nu_{as}(NCS^-)$ or (N_3^-)	$\nu_{C=N}$	Selected infrared data ν_{OMe^-}, ClO_4^- or BPh_4^-
[1]	$BaL^1(ClO_4)_2$	white	(11.8) 11.9	(37.2) 37.2	(3.7) 3.7	287		1648m,1635m	1130; 1100; 960br,s 635; 630; 622ms
[2]	$Mn_2L^1(NCS)_4$	yellow	(19.5) 19.9	(43.6) 43.8	(3.7) 3.9	b	2070s 1965 vs	1638m	
[3]	$Mn_2L^1(OMe)(NCS)_3$	orange-brown	(18.2) 18.0	(45.2) 45.0	(4.4) 4.1	b	2065vs 2005ms	1643m	2784mw
[4]	$Fe_2L^1(NCS)_4.H_2O$	red-brown	(19.0) 19.1	(42.4) 42.3	(3.8) 3.8	b	2080s 2045vs1960ms	1632m	
[5]	$Co_2L^1(NCS)_4$	bottle-green	(19.4) 19.4	(43.2) 43.2	(3.6) 3.6	b	2080sh2055vs1960ms	1633m	
[6]	$[Co_2L^1(NCS)(MeCN)_4](ClO_4)_3$	red-brown	(15.2) 14.8	(36.7) 36.2	(3.8) 3.6	b	1996s	1632m	1100br,s 630;625ms
[7]	$[Co_2L^1(N_3)_2(MeCN)_2](ClO_4)_2$	red-brown	(22.9) 23.2	(36.4) 36.3	(3.8) 3.7	349	2070vs 1355m[c]	1628m	1100br,s 632sh,628ms
[8]	$Ni_2L^1(NCS)_4.H_2O$	lime-green	(19.1) 19.1	(42.6) 42.3	(3.7) 3.7	b	2090s 2070vs 1965ms	1632m	
[9]	$Cu_2L^1(NCS)_4$	bright green	(19.0) 18.8	(42.3) 42.2	(3.6) 3.6	b	2105sh(ms) 2085s	1630m	
[10]	$Cu_2L^1(NCS)_2(ClO_4)_2$	green	(13.7) 13.9	(35.3) 35.3	(3.2) 3.2	279	2100s	1630m	1109;1055vs 630;625ms
[11]	$Cu_2L^1(N_3)_2(ClO_4)_2$	green	(21.4) 21.1	(33.7) 33.6	(3.3) 3.3	349	2090sh 2070vs 1348m[c]	1631mw	1100vs 628ms
[12]	$Cu_2L^1(OH)(ClO_4)_3$	blue-green	(10.3) 10.0	(32.3) 32.8	(3.3) 3.3	386		1635mw	1110; 1065vs 628;632ms
[13]	$Zn_2L^1(NCS)_4$	white	(19.0) 18.8	(42.3) 42.2	(3.5) 3.6	b	2070s 2060s	1640m	
[14]	$BaL^2(ClO_4)_2$	white	(12.3) 12.4	(35.2) 35.1	(3.2) 3.5	212		1635m	1130;1100;1050vs 627;625;618ms
[15]	$MnL^2(NCS)_2 2MeOH$	yellow	(19.1) 19.1	(49.6) 49.6	(5.2) 4.7	90	2085sh 2075s	1642m	
[16]	$Co_2L^2(NCS)_4$	light-brown	(19.6) 19.1	(40.3) 40.8	(3.1) 3.0	b	2090ms 1985vs	1628w	
[17]	$Ni_2L^2(NCS)_4$	green	(20.1) 20.3	(41.4) 41.4	(3.2) 3.4	b	2105ms 1985vs	1623m	
[18]	$[Ni_2L^2(NCS)_2(MeCN)_2](BPh_4)_2$	green	(10.8) 10.6	(68.2) 68.2	(5.3) 5.3	152	1975vs	1627mw	740;713ms
[19]	$Cu_2L^2(NCS)_2(ClO_4)_2$	green	(14.2) 14.0	(33.5) 33.5	(2.8) 3.0	b	2070s	1625mw	1090vs 629ms
[20]	$Cu_2L^2(NCS)_2(BPh_4)_2$	green	(9.1) 9.2	(68.4) 68.3	(5.1) 5.0	170	2029s	1623mw	740; 715ms
[21]	$Cu_2L^2(N_3)_2(ClO_4)_2$	green	(22.2) 21.7	(31.7) 32.0	(2.9) 2.8	356	2075s 1340ms[c]	1623mw	1090vs 628ms
[22]	$Cu_2L^2(OH)(ClO_4)_3$	pale-blue	(10.6) 10.5	(30.5) 30.5	(2.9) 3.1	409		1630m	1165;1091vs 623ms
[23]	$Cu_2L^3(OH)(NCS)_3.2H_2O$	green	(14.4) 14.2	(37.1) 37.3	(3.7) 3.3	b	2091s 1994ms	1632ms	
[24]	$Cu_2L^3(NCS)_4$	ox-blood	(16.4) 15.8	(38.6) 38.9	(3.0) 3.2	b	2086s 1952vs	1632ms	

a $\approx 10^{-3}$M MeCN soln. b insoluble c $\nu_s(N_3)^-$

The condensation of 1,3 diamino propane and 2,6 diformyl pyridine in the presence of Ba(II) in alcohol gives a mononuclear complex [14] of the 20 membered N_6 macrocycle called 'WT' FIG.30-2. Good yields and purity of product meant there was no need to use other template ions. The macrocyclic nature of the product was easily confirmed. Undoubtedly most convincing was an X-ray crystal structure, described below, but infrared (ir), mass spec, and conductivity also indicate that a [2+2] condensation resulting in a closed macrocyclic product had occurred.

The ir of the cream white solid showed a moderate to strong band at 1640cm^{-1} indicative of the formation of the imine (C=N) function. Absorbances at ≈1700cm^{-1} or 3400-3200cm^{-1} attributable to unreacted carbonyl or primary amine groups respectively, were absent. The two signals, due to perchlorate counter ion at 1170-1040cm^{-1} and 620cm^{-1} showed well defined splitting FIG.32 which strongly suggested these counter ions were co-ordinated rather than ionic. These observations indicate that Schiff base condensation has taken place but do not on their own distinguish between cyclic and polymeric condensations. However the crystalline nature of the product suggests low molecular weight and the conductivity suggests a 1:2 electrolyte which is again consistent with the formation of a cyclic rather than polymeric species.

The X-ray crystallographic structural determination, obtained by Dr.M.Drew at Reading, of the barium complex of WT is shown in FIG.33. The six Ba-N distances range from 2.834(16) to 3.03(18)Å and the ion is also chelated to two perchlorate ions at distances of 2.943(17) and 3.06(16)Å and to the oxygen atom of an ethanol solvent molecule at 2.855(20)Å. The metal ion therefore has a co-ordination number of 11. The macrocycle assumes a folded conformation so that all 6 'N' donors are within co-ordinating distance of the barium ion, and so the macrocycle is in a U-shaped form with the two pyridine rings tilted to each other at an angle of 73.4° resulting in a (pyN...Npy) distance of 5.28Å. This is shorter than the equivalent distance in the 9 co-ordinate barium complex of BP [1] FIG.34 [78] which is 5.59Å. However both distances suggest that several types of thiocyanate bridging modes are possible within these 2 structures including

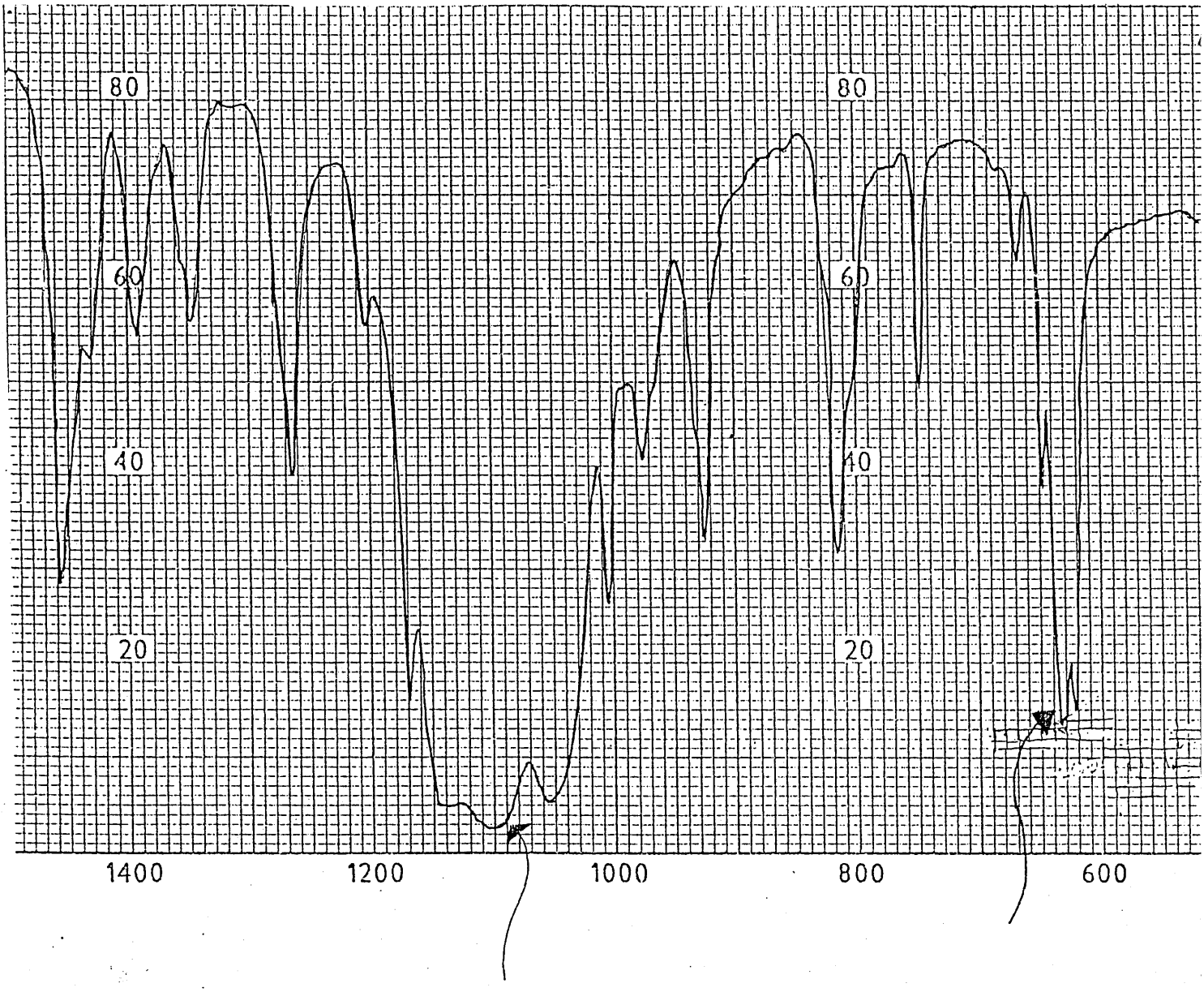

FIG. 32

IR. OF BaWT $(CLO_4)_2$ SHOWING

SPLIT PERCHLORATE PEAKS

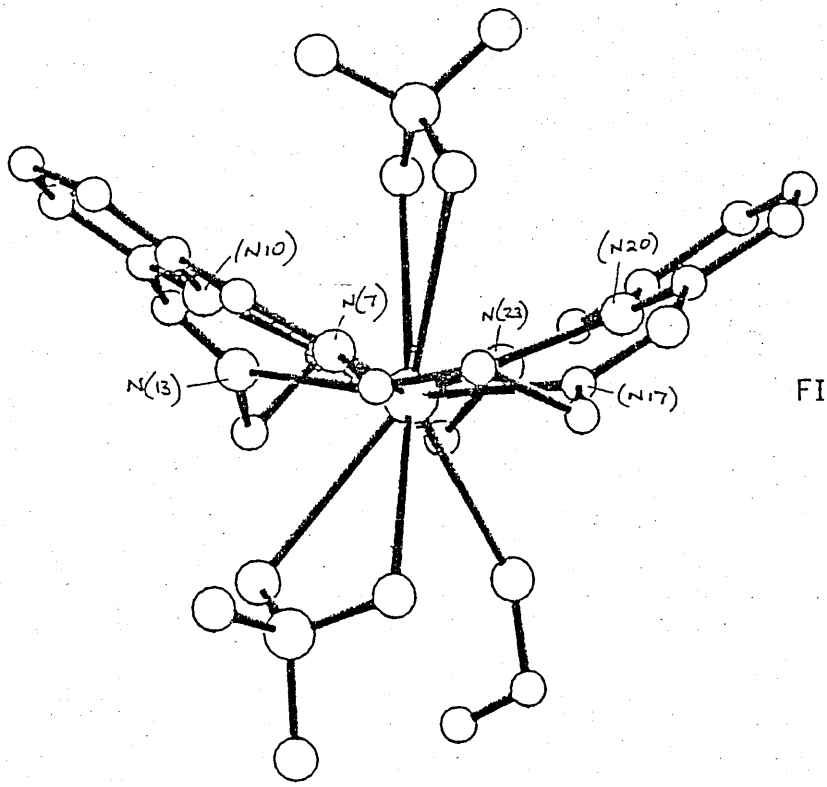

FIG. 33

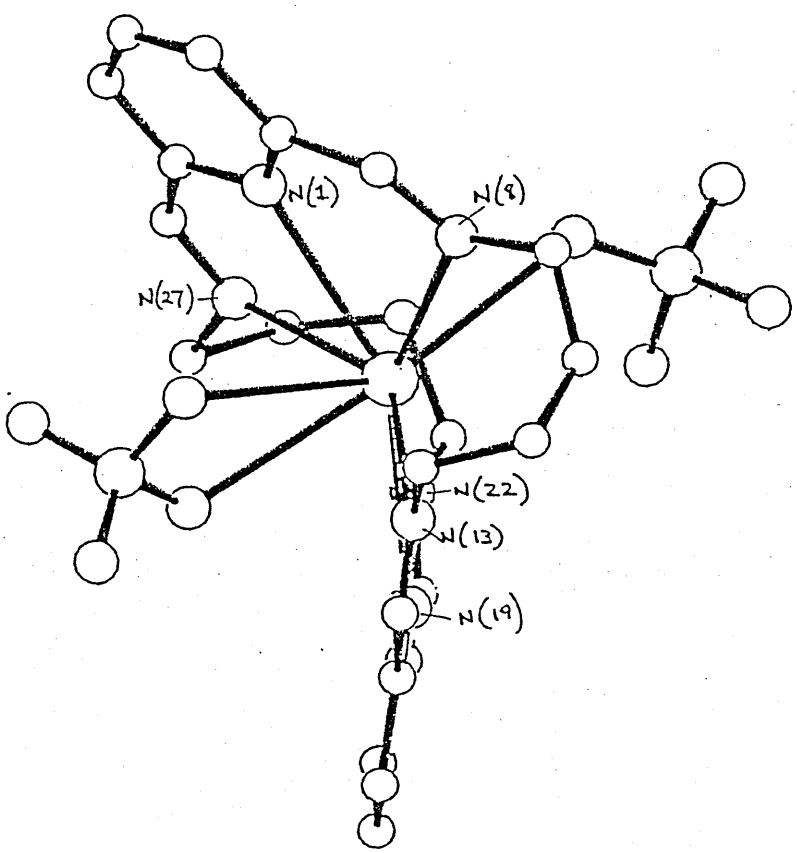

FIG. 34

19-3a, 19-4 and 19-5. Therefore Drew and Yates investigated the viability of the 3 binding modes within the 2 macrocycles using the method of molecular mechanics.

Six different structures were modelled to assess the suitability of the macrocycle to accomodate thiocyanate bridges of different types. These were -

1) $Co_2BP(NCS)_4$
2) $Co_2WT(NCS)_4$
} with 2 centrosymmetic μ-1-3, bridges (19-3a)

3) $Co_2BP(NCS)_4$ FIG.35-2
4) $Co_2WT(NCS)_4$ FIG.35-3
} with 2 μ-1-1 NCS bridges

5) $[Co_2BP(NCS)_3]^+$ FIG.35-1
6) $[Co_2WT(NCS)_3]^+$
} with a single μ-1,1 bridge (19-5)

Calculations were carried out using the M.M.2 program[122] in the manner described in ref 123. Results showed (FIG.35-4) that both macrocycles were too restricted to permit the 1,3 mode of attachment 19-3a. Both minimized $[Co_2L(NCS)_4]$ structures contain Co...Co distances of less than 4.0Å which is at least 1.0Å less than any known structure containing a 1,3, NCS bridge. Of the other four structures it is clear that the single 1,1 thiocyanate bridge is considerably more stable with the 22 membered macrocycle BP than with the smaller 20 membered macrocycle WT and results indicated that the single bridge structure 19-4, is unlikely in WT. On the other hand, both structures show similar energies and geometries for incorporating the bis 1-1, thiocyanate bridging arrangement.

Whilst a good general indication of possible binding modes this study is unable to accommodate a variation of metal ion size which will clearly play a significant role in determining the internuclear space and thus the mode of binding of the thiocyanate ion.

A series of transmetallation reactions on the barium template of WT were carried out giving a mononuclear complex (in the case of Mn(II)) and binuclear complexes (for Co(II), Ni(II), Cu(II)). These were then reacted in the presence of the thiocyanate anion and the products characterized.

FIGURE 35

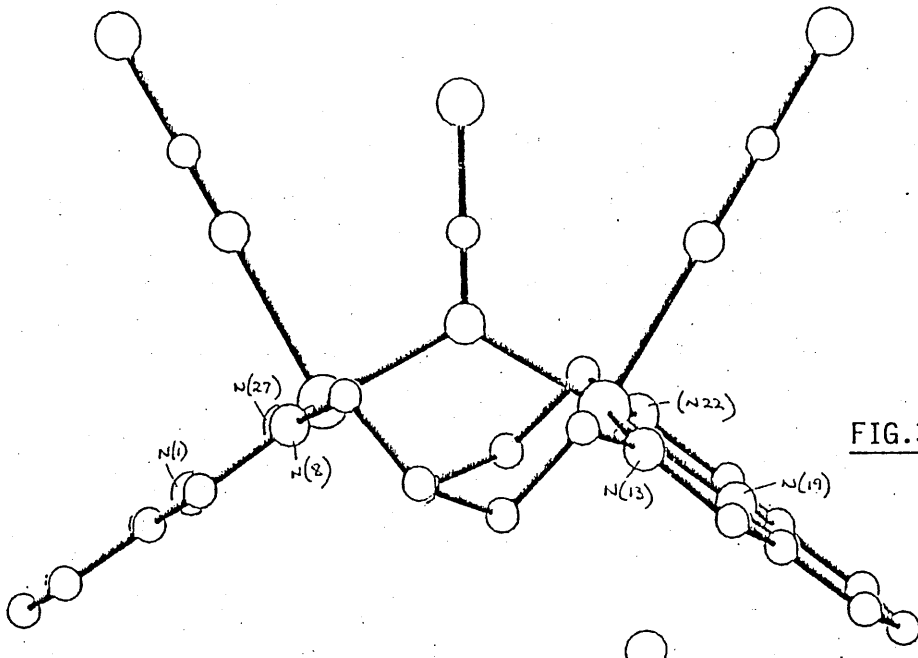

FIG.35-1

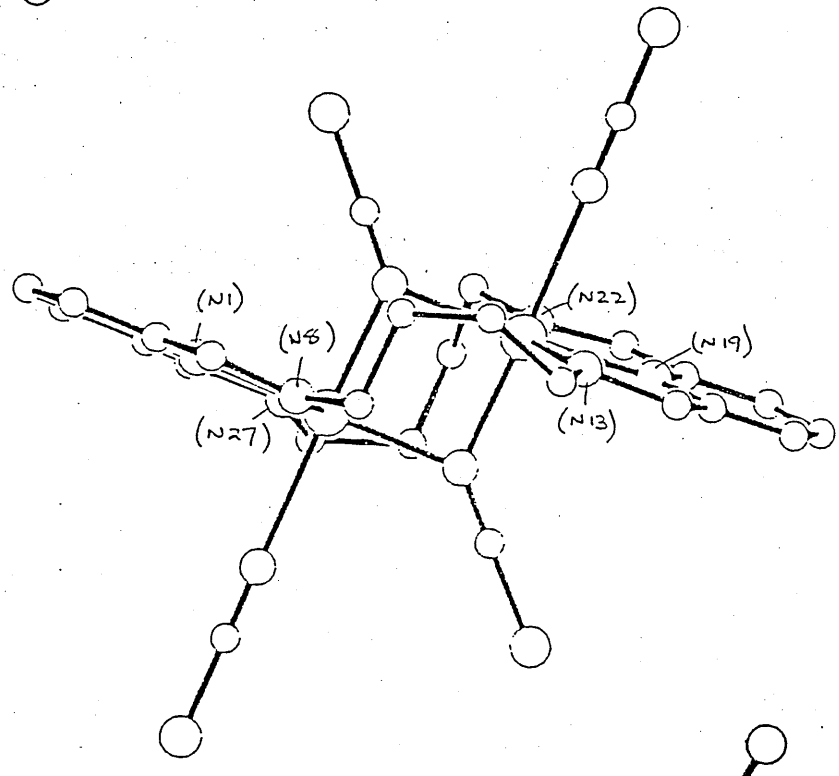

FIG.35-2

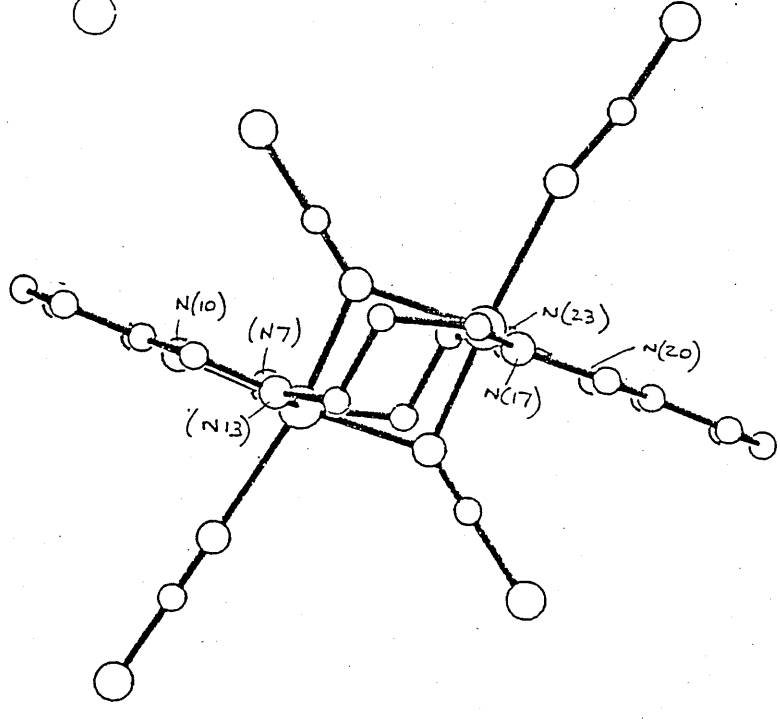

FIG.35-3

Results of Molecular Mechanics Calculations

Compound	Bridge type	Energy / kcal mol^{-1}	Metal-Metal Distance / Å
$M_2L^1(NCS)_4$	Two 1,1-NCS bridges	10.66	3.30
$M_2L^2(NCS)_4$	Two 1,1-NCS bridges	10.24	3.24
$M_2L^1(NCS)_3$	One 1,1-NCS bridge	7.48	3.66[a]
$M_2L^2(NCS)_3$	One 1,1-NCS bridge (i)	8.86	2.94[a]
	(ii)	13.83	3.29
$M_2L^1(NCS)_4$	Two 1,3-NCS bridges	38.52	3.59
$M_2L^2(NCS)_4$	Two 1,3-NCS bridges	32.62	3.47

[a] There are several possible conformations for these two compounds with for example the terminal and bridging thiocyanates on different sides of the molecules. However, we were unable to find any other conformations with an energy of less than 15 kcal mol^{-1}. All conformations led to values for the M...M distance that were similar to those in the Table.

Fig. 35-4

L^1 = BP

L^2 = WT

FIGURE 36

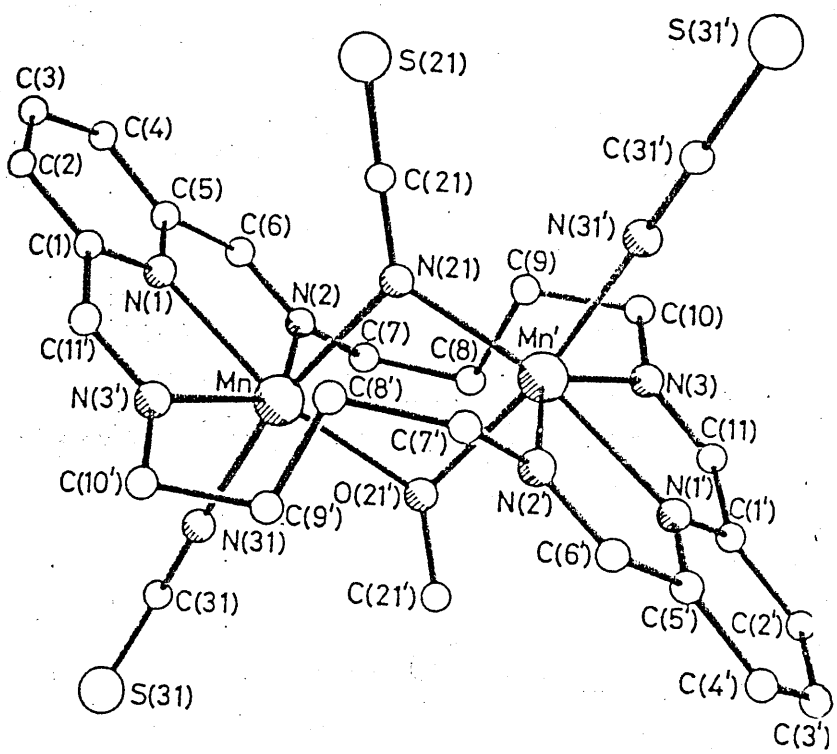
S(31')
S(21)
C(3)
C(4)
C(31')
C(2)
C(5)
C(21)
C(6)
N(31')
C(1)
N(21)
C(9)
N(1)
N(2)
C(10)
C(7)
C(8)
Mn'
C(11')
N(3')
Mn
C(8')
N(3)
C(11)
C(7')
C(10')
O(21')
N(2')
N(1')
C(1')
C(9')
N(31)
C(6')
C(21')
C(5')
C(2')
C(31)
C(4')
S(31)
C(3')

TRANSMETALLATED COMPLEXES

Most of the transmetallated complexes formed were binuclear. In the case of Mn(II) only a mononuclear complex was isolated and it was obtained no matter what excess of metal ion was used in transmetallation. The physical data for the mononuclear complex [15] is given in FIG.31 TABLE-A. From the ir data it can be seen that the thiocyanate group shows a terminal mode of co-ordination, most likely via the 'N' donor end due to the relatively 'hard' nature of Mn(II). This suggests that the Mn(II) has a co-ordination number of 6. Both the uv, which shows no evidence of d-d transitions and the magnetic moment are uniformative, with respect to geometry - the latter falling close to the spin only value of 5.92Bm as expected for the orbitally nondegenerate d^5 system. The conductivity lies in the lower range of 1:2 electrolytes due to its low solubility. Recently McKee[124] made an interesting tetranuclear bis-macrocyclic complex by the reaction of a closely related ligand-ligand T FIG.30-4 with $Mn(OAc)_3$. This ligand is the imine methylated form of WT. The X-ray structure of the tetranuclear complex shows a binuclear mixed valence Mn"/Mn" pair per macrocycle with an OH bridging group between the two macrocycles.

The largest ligand BP gave 2 manganese (II) complexes [2] and [3] both of which, in contrast to WT, were binuclear in nature. The crystal structure of $Mn_2BP(OMe)(NCS)_3$ has been determined[92] and shows μ-1,1, N only bridges confirming the ir criterion which indicates the presence of the M-N(SC)-M assembly where M=Mn(II). Using [3] as a calibrant, the relative intensity of the $< 2000cm^{-1}$ ir absorption in [2] indicates that two single atom 'N' bridges are present. This gives rise to the parallel planar macrocyclic conformation FIG.36 that is adopted by the system. No Mn(II) complexes of the smallest ligand E were isolated.

All other complexes formed by WT on transmetallation were binuclear in nature. However, in the attempted reactions of WT with Fe(II), no product of acceptable purity was obtained. The ir of crude $Fe_2WT(NCS)_4 . xH_2O$ was run and it showed a strong absorption below $2000cm^{-1}$ as well as terminal and ionic thiocyanate groups. Pure $Fe_2BP(NCS)_4 . H_2O$ [4] demonstrates, on the basis of ir, one N only bridge, 2 terminal and 1 ionic thiocyanate

FIG. 31 TABLE B

Electronic spectral and magnetic susceptibility data

No.	Compound	d-d bands[a] (Nujol Mull)	d-d bands[a] (MeCN soln.)[b]	μ/BM 293 K	μ/BM 93 K
[2]	$Mn_2L^1(NCS)_4$	-	-	6.05	6.09
[3]	$Mn_2L^1(OMe)(NCS)_3$	-	-	6.13	6.11
[4]	$Fe_2L^1(NCS)_4.H_2O$	21 000s[c], 16 900s[c]	d	5.12	5.04
[5]	$Co_2L^1(NCS)_4$	17 200wsh, 15 600ms, 8 980w, 7 400wsh	d	4.75	4.60
[6]	$Co_2L^1(NCS)(MeCN)_4(ClO_4)_3$	~22 000sh, 16 400mw, 9 500w	22 000sh, 17 200(10), 9 090(4.5)	5.08	4.98
[7]	$Co_2L^1(N_3)_2(MeCN)_2(ClO_4)_2$	~22 000sh, 17 000m, 9 500w,	21 500sh, 17 500(80), 9 600(16)	5.24	5.57
[8]	$Ni_2L^1(NCS)_4.H_2O$	~23 000sh, 14 900mw, 9 800mw	d	3.17	3.11
[9]	$Cu_2L^1(NCS)_4$	13 500ms	d	1.76	1.72
[10]	$Cu_2L^1(NCS)_2(ClO_4)_2$	14 000ms	13 700(450)	1.84	1.76
[11]	$Cu_2L^1(N_3)_2(MeCN)_2(ClO_4)_2$	15 900sh, 12 500ms	12 410(350)	1.89	1.89
[12]	$Cu_2L^1(OH)(ClO_4)_3$	13 300ms	13 300(200)	1.42	0.46
[16]	$Co_2L^2(NCS)_4$	~25 000sh, 17 000wsh, 15 000sh, 8 500w	d	4.63	4.30
[17]	$Ni_2L^2(NCS)_4$	~23 500sh, 16 300w, 10 100mw	d	3.11	3.10
[18]	$Ni_2L^2(NCS)_2(MeCN)_2(BPh_4)_2$	~26 000sh ~17 200w, 10 900mw	~24 000sh, 16 900(32), 10 530(90)	3.18	2.95
[19]	$Cu_2L^2(NCS)_2(ClO_4)_2$	14 700ms	14 420(420)	1.67	1.51
[20]	$Cu_2L^2(NCS)_2(BPh_4)_2$	15 100ms	14 050(400)	1.71	1.70
[21]	$Cu_2L^2(N_3)_2(ClO_4)_2$	14 800ms	14 200(300)	1.85	1.85
[22]	$Cu_2L^2(OH)(ClO_4)_3$	13 900ms	15 900sh, 13 300(152)	1.60	0.90
[23]	$Cu_2L^3(OH)(NCS)_3.2H_2O$	13 760; 9 800	d	1.84	1.84
[24]	$Cu_2L^3(NCS)_4$	~25 000brsh, 10 500brsh, 8 500brsh	d	1.89	1.85

[a] ν/cm^{-1} [b] Σ(in parenthesis)/$dm^3\ mol^{-1}\ cm^{-1}$ [c] C-T bands [d] insoluble

groups. This suggests a 5 co-ordinate metal centre in this complex. The ir pattern is identical to the crude WT complex so it is likely that the 2 iron complexes have the same thiocyanate binding modes and hence the same co-ordination and geometry. Ligand E gave no compounds with iron.

The ir of the $[Fe_2WT]^{4+}$ complex shows a significant weakening of the $\nu_{C=N}$ at 1640cm^{-1} and the pyridine signal at 1600cm^{-1} all but disappears. This possibly results from the delocalization of the chelate ring. The deep purply red colour of the crude product suggests a low spin state of the Fe(II).

A possible explanation for the impure nature of the product could be due to the presence of both mono and binuclear species. Mn(II) forms mononuclear species with WT whereas Co(II)(as we shall see) forms binuclear complexes only, and it may be that Fe(II) is behaving in an intermediate fashion giving a mixture of mono and binuclear products.

With Co(II) an interesting compound; the tetrakis - thiocyanato complex [16] was isolated and characterized. The ir shows an absorption at 1985cm^{-1} corresponding to ν_{as}(NCS) and the μ-1,1-NCS bridging mode. Terminal binding NCS is suggested for the second absorption at 2090cm^{-1}. The 1:1 intensity ratio of peaks suggests that there are two of each type of NCS present. This would give a 6 co-ordinate environment for each cobalt ion - 3 ligand nitrogen atoms, 2 from the thiocyanate bridges and 1 from the terminal NCS.

The nujol mull spectrum - electronic and magnetic susceptibility data are tabulated in FIG.31, Table B - consists of a series of ill defined shoulders which indicates that, rather than a regular octahedron, the Co(II) ions lie in a low symmetry 6 co-ordinate geometry. This idea is supported by the observed magnetic moment of 4.63Bm (spin only: high spin - 3.88 low spin- 1.73) which reduces slightly with temperature (80K: μ = 4.30Bm). In the absence of significant antiferromagnetic interaction the low moment (O_h field μeff = 4.5-5.2) may be the result of a reduced orbital interaction brought about by a low symmetry environment.

In the analogous complex of BP [5], the ir suggests not only μ1,1 bridging but also unco-ordinated (2050cm^{-1}) and terminal (2080cm^{-1}) co-ordination. From a comparison of intensities it appears likely that there are two terminal, one ionic and only one N-only bridge giving a 5 coordinate metal centre. The electronic spectrum supports this proposal with 3-4 d-d bands. The dominant feature is a strong band around 15600cm^{-1} with weak features around 8500 and 7000cm^{-1} poorly defined.(A similar spectrum has been observed[125] for a structurally characterized square pyramidal Co(11) complex). Magnetic data also favours a 5 co-ordinate geometry showing a low value for moment consistent with the no more than expected[126]small reduction of moment with temperature explained on the basis of depopulation of spin orbit coupled excited states and/or zero field effects. Another thiocyanate complex of BP ie [6] again has one μ1-1 thiocyanate bridge but in this case the complex has been assigned an octahedral geometry. This proposal is based on the electronic spectrum which shows a pair of absorptions of appropriate frequency and intensity to be assigned to 2 of the 3 absorptions expected for Co(11) in an approximate octahedral geometry. The sixth site is occupied by a coordinated acetonitrile solvent molecule[78].

The dicobalt complex of BP has also been bridged by two azide anions [7]. I.R indicates the end on 1,1 N_3^- bridging mode. UV indicates an octahedral geometry for the Co(II) ie 6 coordinate. [7] shows an appreciable increase in moment with temperature over the 293-93K range which continues in the 93-4K range, achieving the plateau characteristic of a molecular ferromagnet before falling off at lower temperatures presumably because of antiferromagnatic interdimer interactions. Thus the spin-polarization theory of Kahn[108,109] appears to hold quite satisfactorily for this μ1,1 azido compound. The recent[127] structural determination of [7] confirms the μ1,1 N_3^- bridge.

Ligand E also forms dicobalt complexes, showing both N-only thiocyanate bridging and 1,1-azide bridges[74]. The former shows only a small reduction of moment with temperature while the latter shows a small ferromagnetic interaction. The solid state electronic spectra are typical

Fig. 37

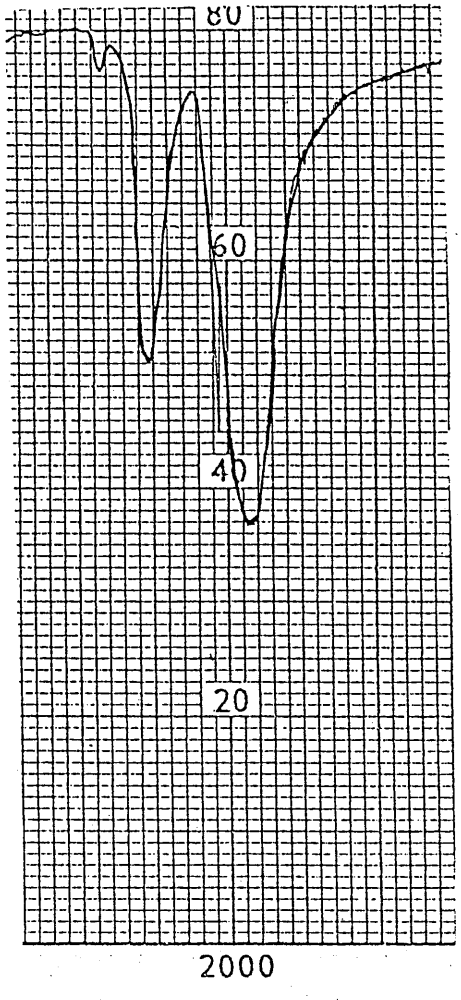

37-1

IR OF (17)

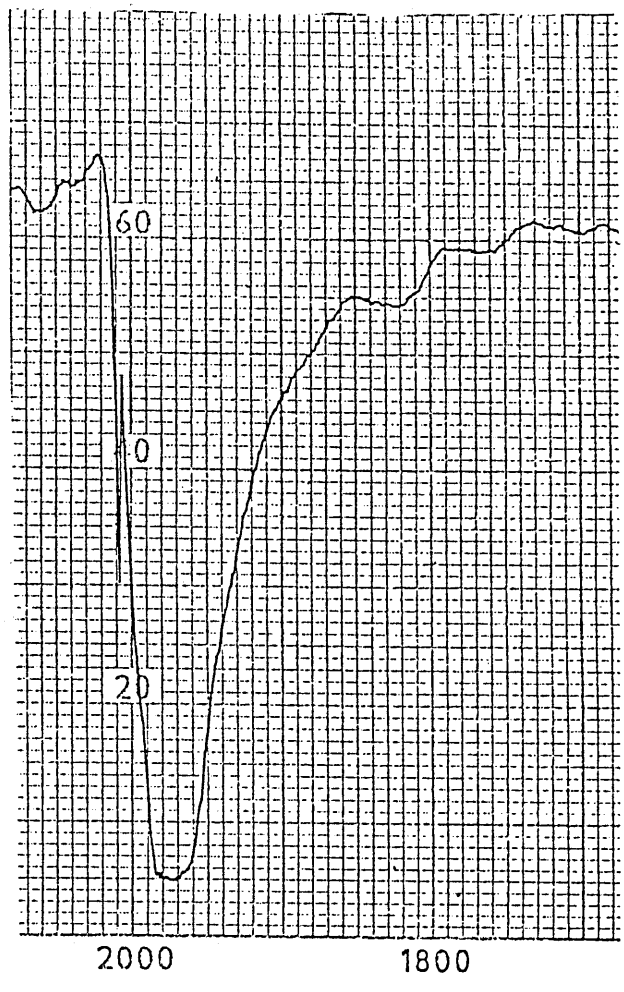

37-2

IR OF (18)

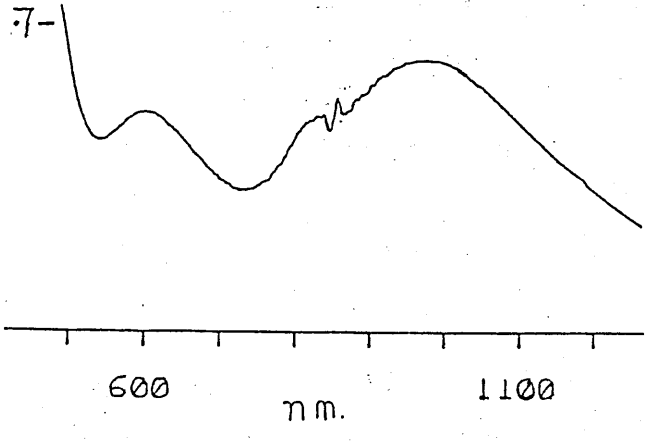

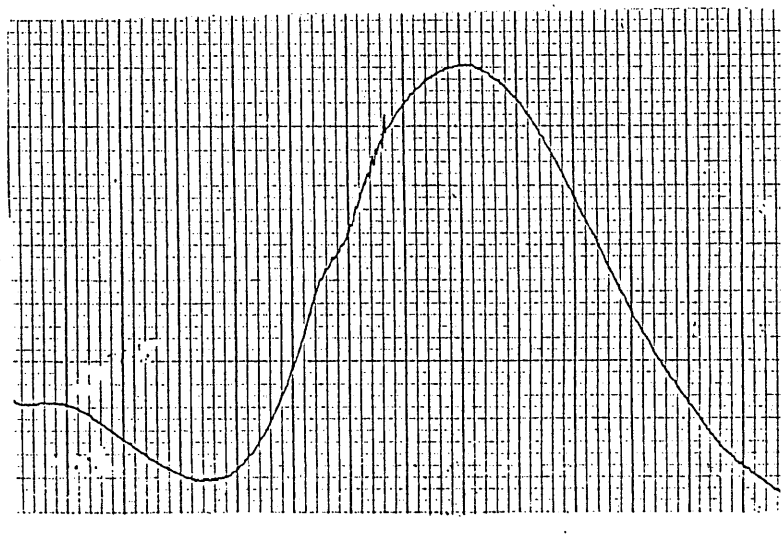

for high spin Co(11) in trigonal bipyramidal environments. The close similarity of spectra of the 2 complexes is strong evidence for a common structural framework comprising one nitrogen atom. This complex in fact forms bridges with a whole variety of bridging ligands - hydroxo, alkoxo, phenoxo, thiolate, halogens and pseudo halogeno bridges[128].

Two binuclear nickel complexes were formed on transmetallation of the barium complex ([17] and [18]). The ir of $Ni_2WT(NCS)_4$, [17], FIG 37-1 resembles that of $Co_2WT(NCS)_4$ in showing 2090cm^{-1} and 1985cm^{-1} absorptions in a 1:1 ratio, indicating 2 types of thiocyanate within the macrocyclic cavity; one set of 2 in a coordinated terminal mode and the other two in the form of μ1,1 NCS bridges. The formation of two thiocyanate single atom bridges suggests a short metal-metal distance and the one known structural example involving transition metals has a Ni...Ni distance of 3.28Å[81].

Compound [18] exhibits only a single very strong ν_{as} (NCS) absorption at 1975cm^{-1} FIG 37-2 which clearly originates from the di-μ-1,1NCS assembly. A weak absorption at 2250cm^{-1} was attributed to coordinated acetonitrile solvent molecules. The conductivity of this complex was typical of a 1:2 electrolyte suggesting that in solution the two bridging groups remain attached. For both compounds the electronic spectra show FIG.37-3 the 3 expected absorptions for a d^8 ion in an O_h environment. The 3 spin allowed transitions correspond to;

	[17]	[18]	$[Nien_3]^{2+}$	$[NiH_2O]^{2+}{}_6$
$^3A_{2g} \rightarrow {}^3T_{2g}$	10100	10900	11000	9000
$^3A_{2g} \rightarrow {}^3T_{1g}$ (F)	16300	17200	18500	14000
$^3A_{2g} \rightarrow {}^3T_{1g}$ (P)	23500	26000	30000	25000

In the tetra thiocyanate complex the electronic absorptions are shifted to slightly lower energies as a consequence of weaker axial ligands (Note: the highest energy absorption may be a strong ligand-metal (SCN^-) $\rightarrow$ Ni^{2+} charge transfer which effectively masks the d-d transition)

Thus we conclude and propose that in both complexes [17] and [18] the Ni(11) are in an ca octahedral environment with a coordination number of 6.

The magnetic data results for both complexes vary only slightly with temperature and lie close to the spin only value of 2.83Bm which indicates the absence of significant magnetic exchange interaction. As expected[126] for 6 coordinate octahedral nickel(11), there is no evidence of orbital contribution increasing μ significantly above the spin only value. The small reduction of moment with temperature could be explained in [18] on the basis of depopulation of the spin orbit coupled excited states of the ground state (ie mixing of the $^3A_{2g}$ and $^3T_{1g}$ states) although there could well be a contribution from weak antiferromagnetic exchange.

The tetrakis thiocyanato dinickel complex of BP [8], based on ir signal intensity, shows one N only bridge and terminally bound groups. Both the mull absorption spectra and magnetic data are similar to that of the WT analogue [17] indicative of 6 coordination. The water and fourth thiocyanate group must also be coordinating the metal centres.

All other complexes obtained were binuclear copper complexes which show a range of bridging groups. Analytical and ir spectroscopic data are shown in FIG.31 - Table A, whereas electronic spectral and magnetic susceptibility data for the BP, WT and E dimers are shown in FIG 31 - B. The esr data is tabulated in FIG 31 - C.

For bridged di-copper systems, which can potentially interact by means of a superexchange process, it is perhaps by esr that such an interaction can best be studied. (See Appendix 2). For non interacting copper ions in an isotropic environment eg. in fluid solution, the simple 4 line spectrum is observed derived from 2I+1 (I=nuclear spin quantum number - for Cu(11) I=3/2). In the solid state, of course, anisotropy means their $g_{\parallel}$ and $g_{\perp}$ signals are differential and hyperfine splitting is often large enough to be resolved only in $g_{\parallel}$, which therefore consists of 4 lines. For very strongly antiferromagnetic coupled systems ie where essentially there is a pairing of the magnetic electrons of the 2 copper ions via the bridging system, no esr spectrum will be obtained ie such a system is esr silent. However for bridged dicopper systems a pair of 7 line $g_{\parallel}$ signals (split by zero-field) is often observed showing that the 'magnetic' electron of each of the copper ions is no longer localized on the metal

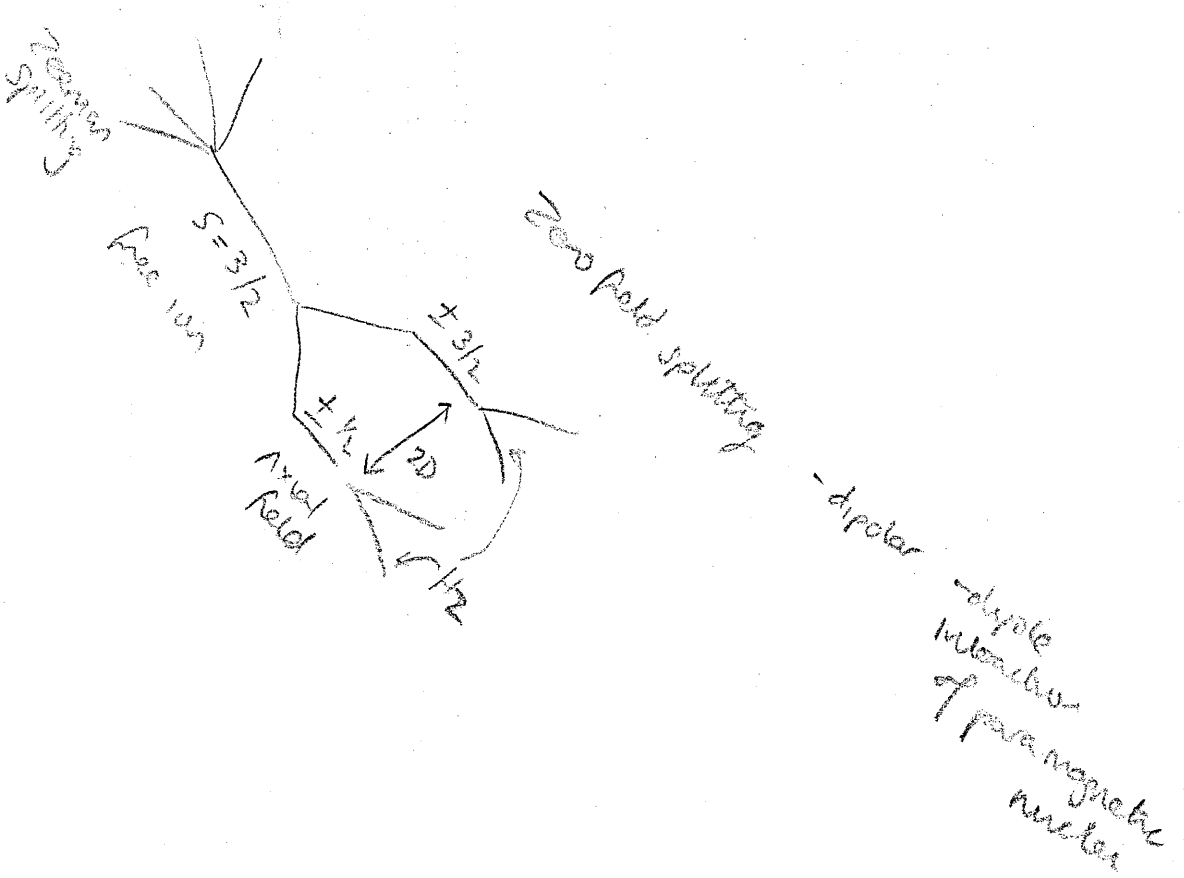
Zero field splitting
S = 3/2
Axial field
±3/2
±1/2
2D
±1/2
Zero field splitting
- dipolar
- dipole interaction
- paramagnetic nuclei

centre but delocalized over the binuclear assembly via orbitals of the bridging ion or group.

Whether this interaction is ferromagnetic or antiferromagnetically based can, in theory, be determined by reducing the temperature of the system. For antiferromagnetically coupled systems the intensity of the esr spectrum may show a decrease with decreasing temperature below to Neel point (appendix 3), whereas the intensity of the spectrum for a ferromagnetically coupled system should increase continuously. This is a result of a reduction of thermal randomization effects making it easier for the spins to pair (in antiferromagnetic, S=0, interaction) or align (in ferromagnetic, S=I, interaction) at the lower temperatures. For weakly interacting systems it is not always easy to observe these intensity effects.

Given the sensitivity of the esr technique to long range interaction between copper(11) ions it is not surprising that all the dicopper complexes in this study to some extent show triplet features arising from the ferromagnetic S=I state present either as ground or thermally accessible excited states. The triplet features expected [93,129-130] include

-1- a hyperfine coupling constant A_{11} (Cu) at ≈80G around half the normal value of 140-160G for a non interacting copper nucleus.

-2- anisotropy in the polycrystalline or glass spectrum arising from zero field splitting, generating for the normal axial symmetry site two $g_{\perp}$ and two $g_{x,y}$ signals separated by the zerofield splitting parameters 2Dz and Dxy respectively

-3- the appearence, with appreciable intensity of the normally forbidden half band, $\Delta m=2$, transition close to g=4.

Table C in FIG 31 shows that in all the dicopper(11) complexes where solubility allows the acquisition of glass spectra, A_{11}(Az) has a value close to 70G showing that the unpaired electron is delocalized over both

copper(11) sites. Where zero-field splittings are small, extensive overlapping of signals occurs making assignment of the high field hyperfine split gz' signal difficult although it is usually possible to identify the pair of relatively sharp g_{xy} signals. Thus the Dxy parameter is available and the magnitude of this offers some information on the degree of interaction between the paramagnetic centres. The experimental zerofield splitting arises from a combination of the dipole-dipole (D_{dd}) and pseudodipolar (D_{pseudo}) interactions. ie

$$D_{expt1} = D_{dd} + D_{pseudo}$$

Pseudodipolar zerofield interactions, which result from spin orbit mixing of excited states, depend on the exchange interactions in the excited states. Large D_{pseudo} effects indicate that exchange interactions in the excited states are greater than those observed for the ground state. This pseudodipolar zerofield splitting can make an appreciable contribution to interaction in esr spectra, and so an exact correlation between the purely ground-state parameter, 2J, obtained from magnetic susceptibility data and the zerofield parameters Dz or Dxy is not to be expected. However a large zero field feature can generally be assumed to be a result of significant interaction with the possibility of either a triplet or singlet level as ground state. Similarly where 2 binuclear assemblies show the same magnitude of D we can assume a similar bridging environment between the 2 paramagnetic centres.

<u>$Cu_2WT(Ph_4B)_2(SCN)_2$ [20] + $Cu_2WT(ClO_4)_2(SCN)_2$ [19]</u>

Bis-thiocyanato dicopper(11) WT complexes were prepared with the perchlorate [19] and tetraphenylborate [20] counterions and this difference appears to significantly alter the binding of the two NCS groups. For [19] a single strong ir absorption at 2070cm^{-1} points to terminal or long-bridge NCS coordination, but the single strong absorption at 2029cm^{-1} in [20] cannot be so easily explained. This is too low to be ionic or terminally bonded but not low enough to be unambiguously diagnostic of the single atom 'N' bridge. Conductivity data which points to a 1:2 electrolyte, rules out ionic thiocyanate and thus $Cu_2WT(NCS)_2(Ph_4B)_2$ may have weak >N only

bridges. Weak single atom bridging might be predicted due to the smaller size of the ion in comparison with Cu^{2+} with respect to Ni(11) and Co(11). Thus the internuclear distance might be just on the limits of forming the >μ1-1 NCS assembly as opposed to the long 1,3 intramolecular bridge. However conductivity could not be carried out on the insoluble [19] which points to long intermolecular bridging as opposed to terminal coordination.

The uv spectra of [19] & [20] show a single unresolved absorption band indicating a square based (tetragonal or square pyramidal geometry). From the ir and uv data we thus propose a 5 co-ordinate geometry for both the notionally di-N only bridged [20] and for the long intermolecularly bridged [19]. (the latter would be 4 coordinate if the NCS groups were terminally bonded).

There was no significant reduction in moment at 293 or 93K for [20]. Reasonably good fit with the Bleaney-Bowers equation (Appendix 3) was achieved over the temperature range of 4K-300K using a value of $-2J = +2$. Thus [20] is a possible candidate for weak ferromagnetic interaction of the kind postulated by Kahn[108,109]. On the other hand the perchlorate derivative [19] shows moderately weak antiferromagnetic interaction as judged by the small, but significant, reduction in moment going from 293K(1.67Bm) to 93K (1.51Bm). Using a Faraday balance susceptibility values were obtained over the 4-80K range - these were higher than anticipated on the basis of applying the Bleaney-Bowers to the 80-300K range: thus the Bleaney-Bowers equation is not obeyed. The esr spectrum of [19] FIG 38-1 indicates the features of a thermally accessible triplet state:

1) a half band,
2) a hyperfine coupling constant A_{11}(Cu) at 77G
3) anisotropy arising from zero field splitting.

No comparison of g_{11} and $g_{\perp}$ were possible due to overlapping of signals making an estimation of $g_{11}(g_{=})$ impossible. We assume, therefore, a small zerofield splitting and thus a small interaction between the two copper centres. The hyperfine coupling constant ($A_{=}$) of 77G is around half the

FIG. 31 TABLE C

Dicopper(II) complexes: esr spectral data and magnetic exchange parameters (DMA glass)

No	Compound	electron spin resonance parameters									Δm = 2 transition		magnetic exchange parameters		
		g_z	g_z'	g_z^{av}	$D_{z/G}$	$A_{z/G}$	$g_{x,y}$	$g_{x,y}'$	$g_{x,y}^{av}$	$D_{x,y/G}$	hfs/G	Rel intensity[a]	$2J/cm^{-1}$	g	$N_\alpha/10^{-6}$ cgsu
[10]	$Cu_2L^1(NCS)_2(ClO_4)_2$	2.45	2.20b	2.33b	150b	67	2.18	1.98	2.08	290	63	1/20	-34[h]	2.12	100
[11]	$Cu_2L^1(N_3)_2(ClO_4)_2$	2.66	b	b	b	c	2.26	1.91	2.08	530	52	1	+8[h]	2.10	100
[12]	$Cu_2L^1(OH)\ (ClO_4)_3$	2.46	b	b	b	70	2.18	1.97	2.07	320	67	1/20	-311	2.05	120
[19]	$Cu_2L^2(NCS)_2(ClO_4)_2$	2.61	b	b	b	77	2.24	1.92	2.08	490	80	1/2	d	d	d
[20]	$Cu_2L^2(NCS)_2(BPh_4)_2$	2.63	b	b	b	75	2.25	1.91	2.08	510	73	1	+2	2.02	100
[21]	$Cu_2L^2(N_3)_2(ClO_4)_2$	2.37	b	b	b	≈90[e]	2.27	1.92	2.09	520	70	b	+7[h]	2.08	120
													or -2	2.10	100
[22]	$Cu_2L^2(OH)(ClO_4)_3$	3.04	1.75	2.22	800	77	2.43	1.80	2.11	950	67	1	d	d	d
[23]	$Cu_2L^3(OH)(NCS)_3$[f]	b	b	b	b	c	2.4	2.1	2.2	550	c	b	or +10[h]	2.05	120
													-4	2.15	120
[24]	$Cu_2L^3(NCS)_4$[f]	g	g	2.27	g	≈160[e]	g	g	2.04	g	g	g	1	2.12	100

[a] peak height relative to g_z signal [b] estimation difficult because of overlapping [c] unresolved [d] poor fit to Eqn. 1

[e] broad, poorly resolved [f] insoluble; polycrystalline spectrum only

[g] no triplet features observed [h] in range 80-300 K

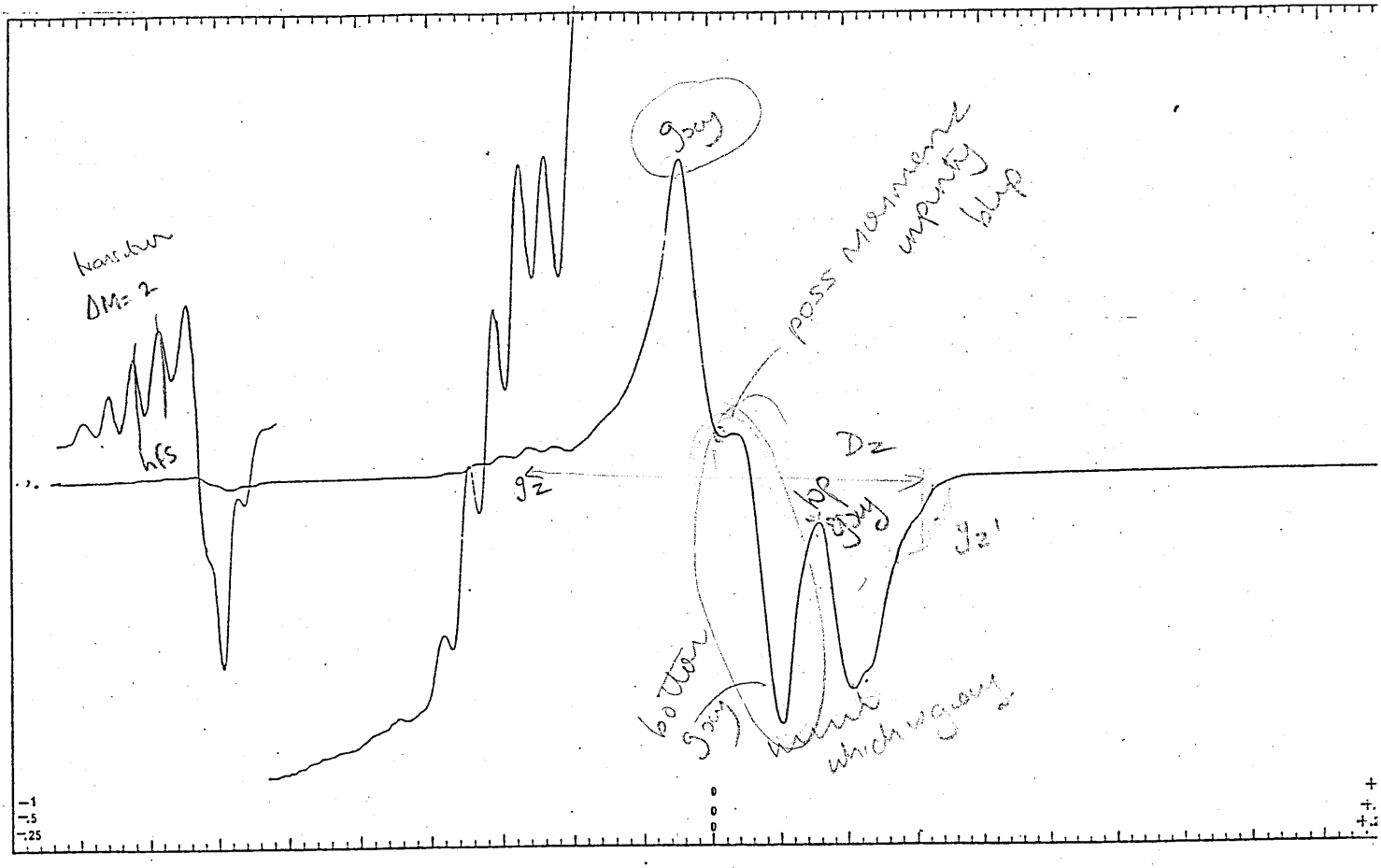

Fig. 38-1 FIELD SET = 3000G, SCAN RANGE = 4000G T = - 150°C

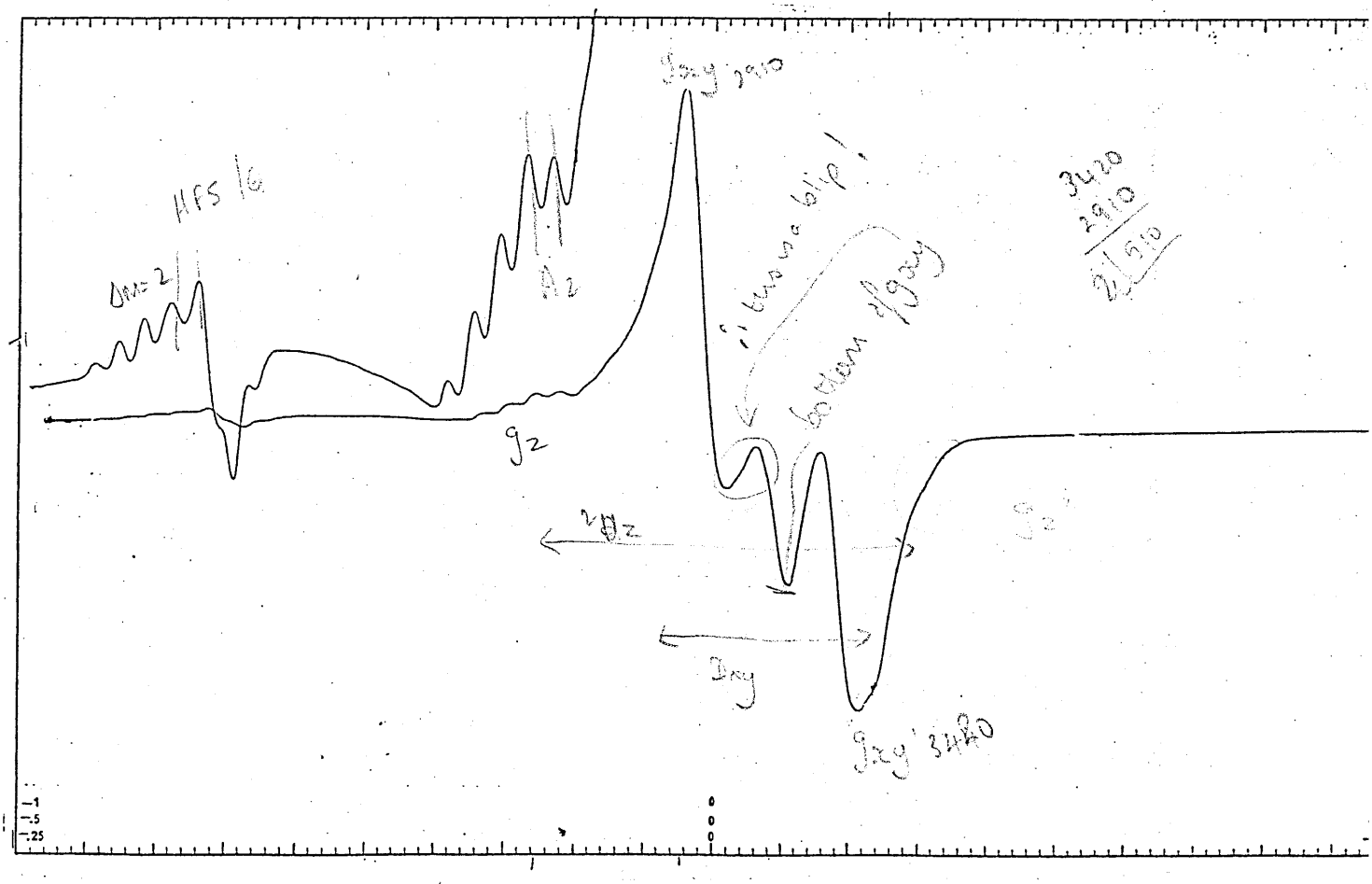

Fig. 38-2 F.S. = 3000G S.R. = 4 x 1k G T = - 130°C

normal value which again indicates that the unpaired electrons are delocalized over both copper(II) sites.

Compound [20] although having an moment of 1.71 BM gives a well defined triplet state in the esr spectrum FIG.38-2. It also shows a large zerofield splitting which suggests a large degree of interaction (Dxy = 510G). This result is incompatible with the observed Curie Law behaviour and thus a ferromagnetic (triplet) ground state is proposed for this compound which has a thermally accessible singlet state The discrepancy between the magnetic susceptibility results and the apparent large zerofield splitting may be caused by significant D_{pseudo} effects. Thus although showing a ferromagnetic ground state results suggest that the exchange interaction of the antiferromagnetic excited state is greater than that observed for the S=1 ground state.

The BP analogue of [19] behaves in a similar manner in terms of its ir, uv magnetic and esr results. The tetrakis thiocyanato compound [9] also shows similar magnetic and esr behaviour. Thus both [9] and [10] exhibit a weak antiferromagnetic interaction which is indicated by the small reduction of moment and by their esr features.

I.R indicates the presence of a pair of $\mu,1,1$ N(CS) bridges for the tetrakis derivative of ligand E [24]. It shows good Curie Law behaviour over the whole temperature range 4-300K although absence of interactions between the paramagnetic centres, ie no significant reduction in moment, is surprising given that the Cu...Cu distance must be in the order of 3.6-3.2Å. This may be a result of the cancellation of ferro and antiferromagnetic contributions. The esr spectrum of [24] is consistent with its magnetic (Curie Law: $\chi \alpha 1/T$) behaviour with poorly resolved hyperfine splitting (ca 160G) characteristic of non interacting Cu(11) ions.

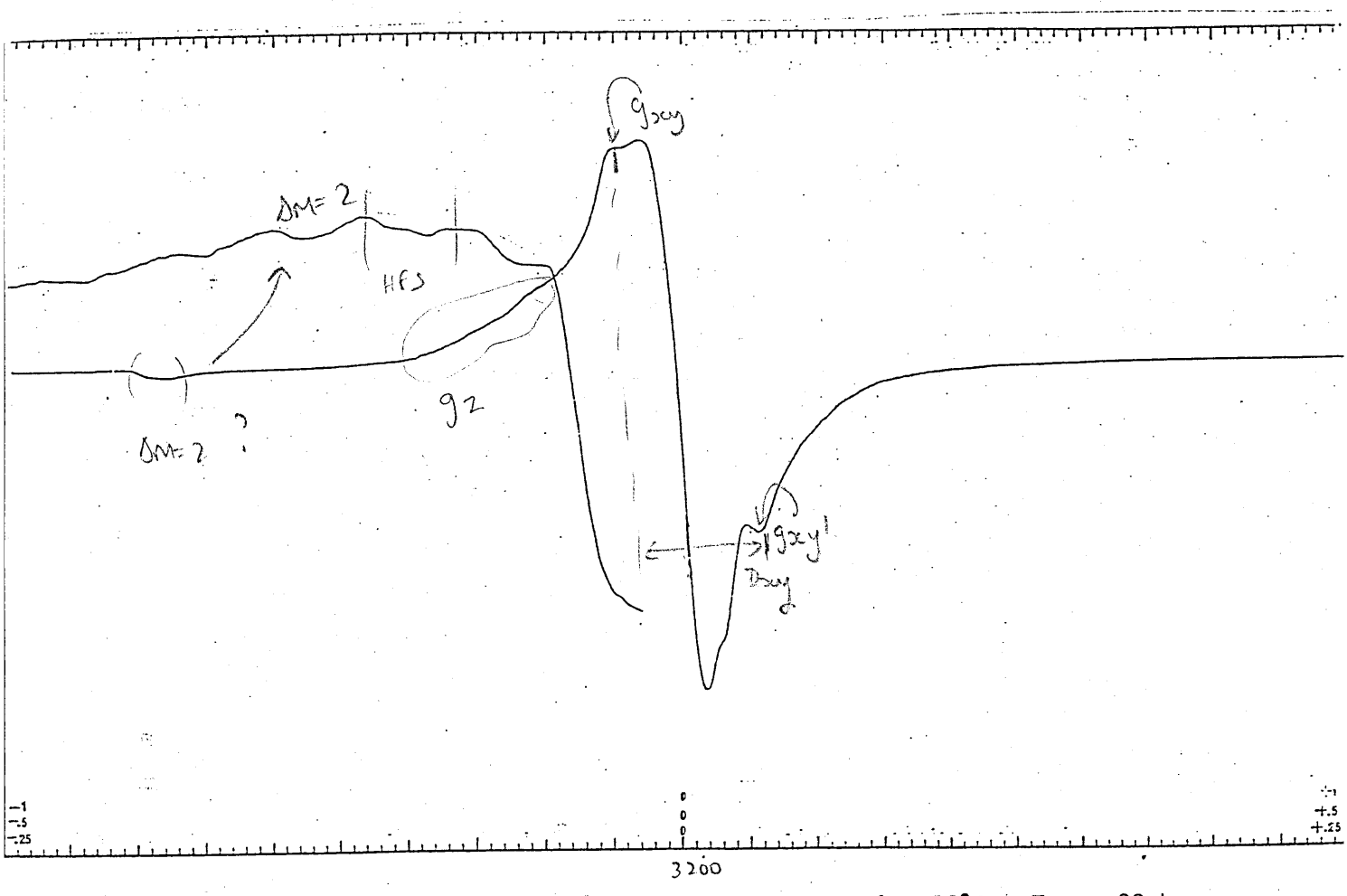

Fig. 38-3 F.S. = 3200G, S.R. 4 x 10^2G T = 20 k

Inset -	F.S	1600
Δ M = 2	S.R.	1 x 1k
	T	4.2 k

$Cu_2WT(N_3)_2(ClO_4)_2$ [21]

The ir of the bis azido di Cu(II) complex of WT exhibits $V_{(N=N=N)}$- as a medium weak absorption at 1340cm^{-1}. This together with the observation of $V_{as(N=N=N)}$- at the high frequency end of the normal range[102] constitutes a case for μ1,1 coordination of the azide ion in this complex. There are however two distinct peaks in the azide region - a high frequency absorption which has been interpreted as a >1,1(end on) bridge and a low frequency absorption attributable to ionic or long (μ-1,3) intermolecular bridged azide. Conductivity gave a value which was typical of a 1:3 electrolyte. This suggests that the single μ-1,1 azido bridge remains intact in solution and that the other azide group is a weakly bridging intermolecular bridge which dissociates in acetonitrile solution, or a terminal azide group. From these resuts we conclude a 5 coordinate geometry (3'N' donors of WT, 1'end-on' bridge and 1 terminal or long intermolecular bridge) for the Cu(II). This proposal is supported by the uv solution spectrum which again shows one broad unresolved peak corresponding to the d-d transitions. Also in evidence are 2 sharp absorptions at 390 ($\epsilon \simeq 10^3$) and 310($\epsilon \simeq 10^3$). Both are possibly azide to copper charge transfer bands[131] for the 2 types of azide bridge (although the higher energy absorption is may be an internal ligand absorption). From these observations it was not possible to distinguish between the various geometries available to the five coordinate copper(II)ions.

The esr spectrum of [21], FIG.38-3, is poorly resolved although the large zerofield splitting (Dxy = 520G) suggests that there is in fact significant interaction of the ions, with the possibility of either a triplet or singlet level ground state. A complex[127] that has been proven by X-ray analysis to have a $1,1N_3^-$ bridge has a similar value of Dxy and this helps to confirm that [21] contains a single end-on azide bridge.

On the basis of Kahn's models[108,109] a ferromagnetic interaction resulting from spin polarization had been predicted for [21]. Indeed this complex failed to show significantly reduced moments at 293 or 93K and this combined with the triplet state features in the esr spectrum supports the idea of weak ferromagnetic interactions. Reasonably good fit with the

Fig. 39

39-1

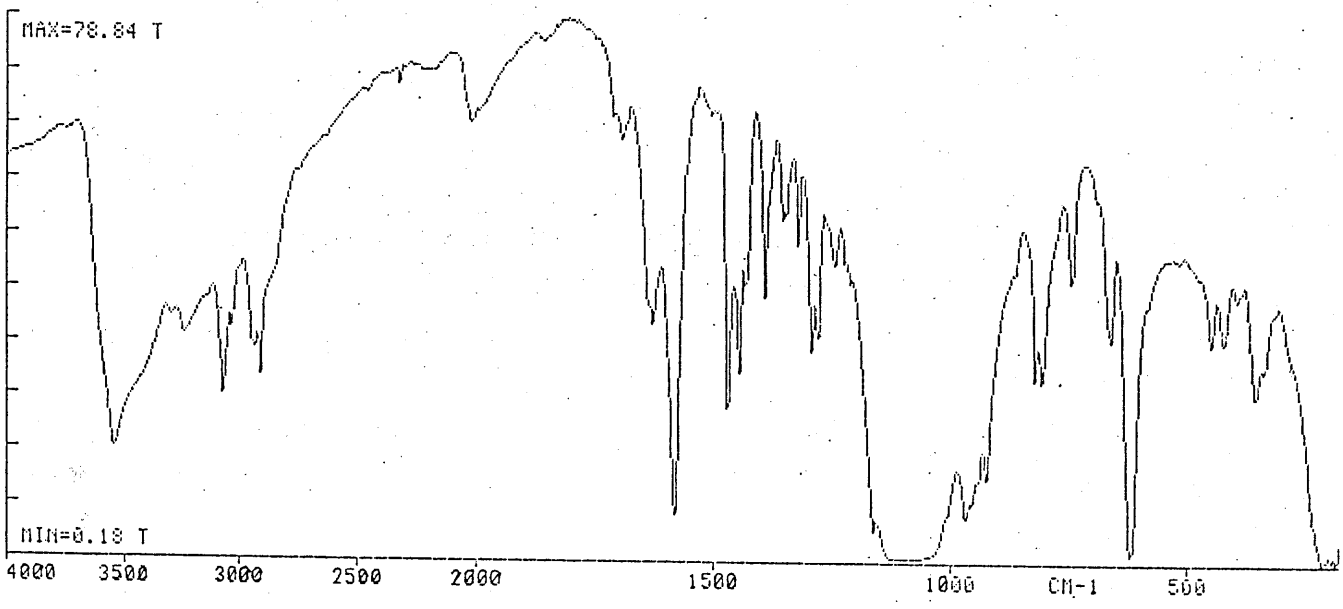

39-2

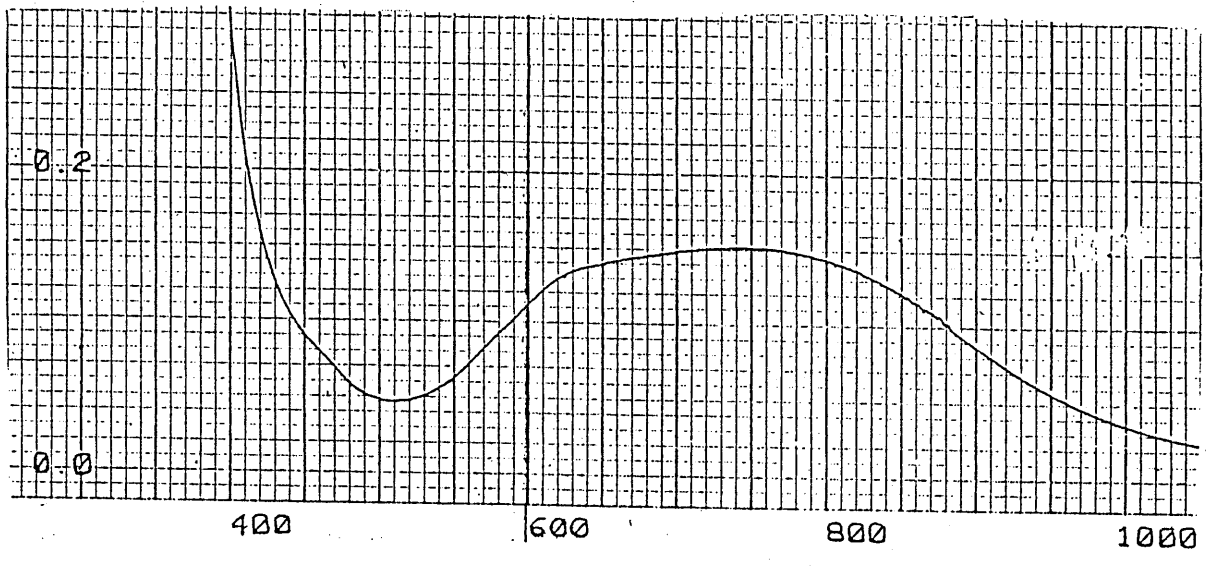

Bleaney-Bowers equation over the temperature range was achieved with -2J=+7. ie a ferromagnetic ground state: however over the full range 4-300K, the best fit is to a small negative value of J.

One possibility is that both ferromagnetic and antiferromagnetic interactions are involved ($J = J_{AF} + J_{F}$) so that we consider the magnetic behaviour of this complex as a combination of ferromagnetic intra (spin polarization of the end-on bridge) and antiferromagnetic inter dimer interactions (possibly via long μ1-3 intermolecular azide bridges). Best fit parameters over the range 4-300K and also over the higher temperature range, 80-300K, where inter dimer interactions are expected to be insignificant are given in Table C FIG.31. (of course paramagnetic impurities may be present which would significantly affect the low temperature values).

Ligand T FIG.30-4 the C - imino methyl substituted derivative of WT, also forms a dicopper mono azide complex $Cu_2T(N_3)(ClO_4)_3$[115]. IR data suggests that the azide is present in the $1,1,N_3^-$ bridging mode. The room temperature moment did not decrease appreciably on cooling providing no evidence of antiferromagnetic coupling between copper(11) ions. However proof of the occurrence of weak superexchange interaction came from the observation of a broad 'triplet' esr spectrum. A $\Delta M = 2$ transition was also seen and it displayed the expected 7 line hyperfine pattern characteristic of coupled copper(11) dimers.

The bis azido dicopper complex of BP,[11], shows a 1,1 μ-azido bridge. Despite the observation of a well defined triplet feature in the low temperature esr spectrum, and hence the indication of interaction of the 2 copper ions, there was no observable reduction in moment over the range 293-93K. Thus, once again there is the inclination to attribute this behaviour to the existance of a spin triplet (S=1) ground state as expected on Kahns spin polarization model.

$Cu_2WT(OH)(ClO_4)_3$ [22]

The ir of this complex has a strong sharp feature at 3547cm^{-1}, FIG 39-1, which indicates the presence of a bridging hydroxo group. It is a 3:1 electrolyte in MeCN indicating dissociation of the anions in solution and retention of the bridging hydroxide groups. Each copper centre would thus appear to have a coordination number of 4.

The C-imino methylated derivative of WT ie ligand T FIG.30-4, forms a hydroxo bridged dicopper assembly which has been characterized by X-ray analysis[115,132]. The occurence of the single bridging unit was traced to the presence of 2 rigid planar and powerfully coordinating trimethine moieties linked by 2 flexible chains. Each copper ion is thus strongly bound to one trimethine unit with the 3N donors occupying 3 corners of a square plane. The coordinatively unsaturated copper ions then complete the coordination square plane by the intramolecular binding of a single bridging substrate molecule or ion between the metal centres. The 2 complexes show similar magnetic, esr, and uv properties and thus it is likely the copper ions in the WT hydroxy-bridged species show the same coordination geometry, ie square planar, as in the analogous complex of ligand T.

The electronic absorption spectra of [22] was uninformative, the mull showing one unresolved peak at 13,900cm^{-1} whereas the solution spectra (39-2) shows a poorly resolved shoulder on the high energy side of the peak. This observation is suggestive of the 5 coordinate trigonal bipyramidal or low symmetry square pyrimidal geometry. This feature may be the result of weakly bound water molecules - although microanalysis favoured $Cu_2WT(OH)(ClO_4)_3$ rather than the dihydrate form.

[22] has a room temperature moment of 1.60Bm which is slightly lower than the spin only value of 1.73Bm. On reducing the temperature there is a significant reduction of the moment to 0,90Bm at 93K. This moderately strong antiferromagnetic exchange appears to operate through the single hydroxo bridge. This suggests a Cu-O-Cu bridging angle in the range 101.3° - 126.2° which gives antiferromagnetic interactions in the range -191cm^{-1}

38 - 4a
.S = 2800G
.R = 4x1kG
= 200 k

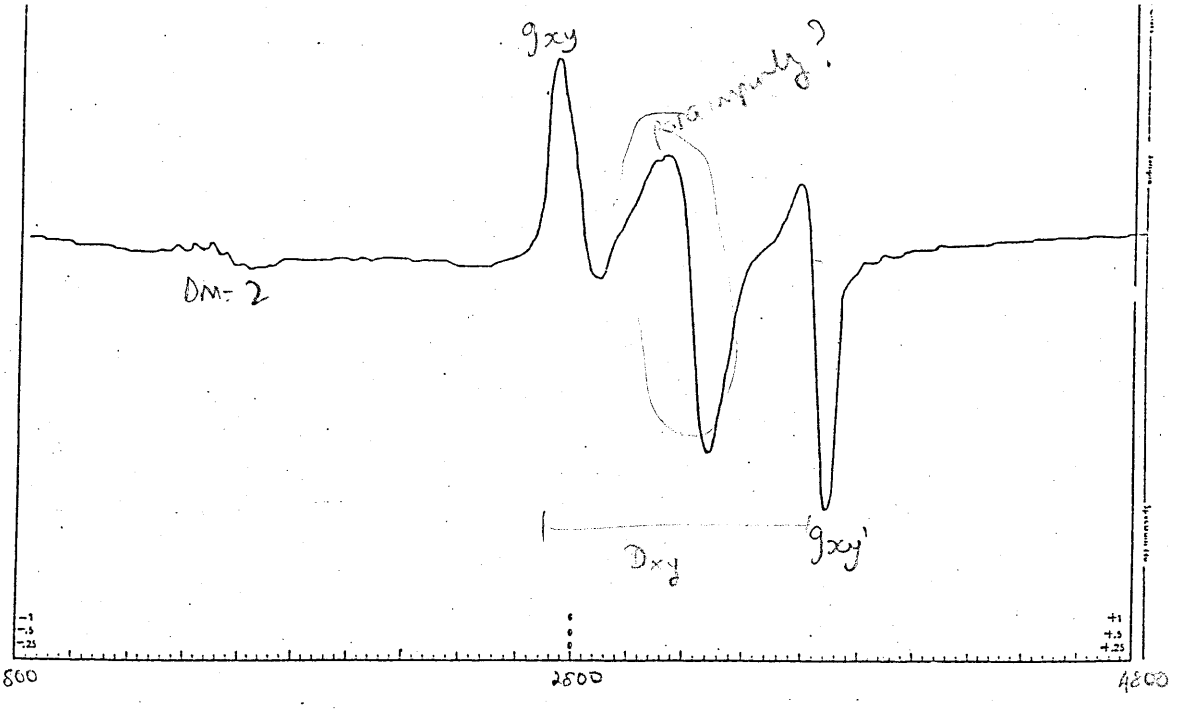

38 - 4b
F.S.= 3000
S.R. = 4x1k
T = 130 k

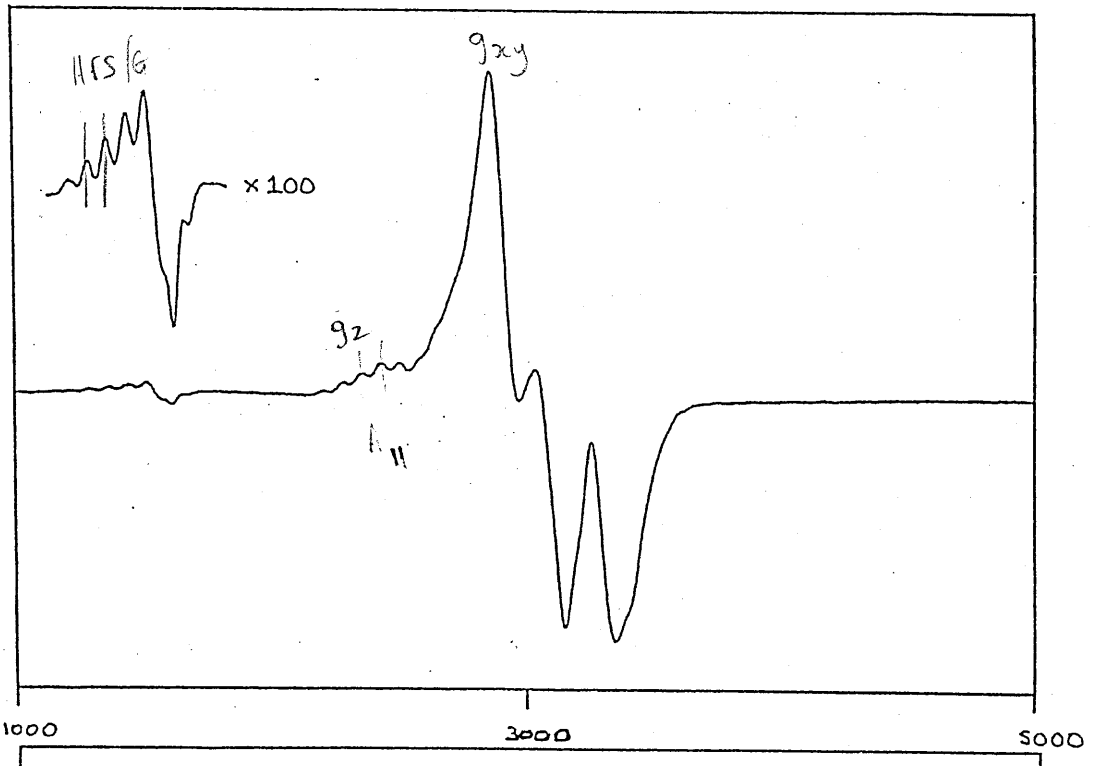

38-4c
F.S. = 2800
S.C. = 4x1k
T = 20 k

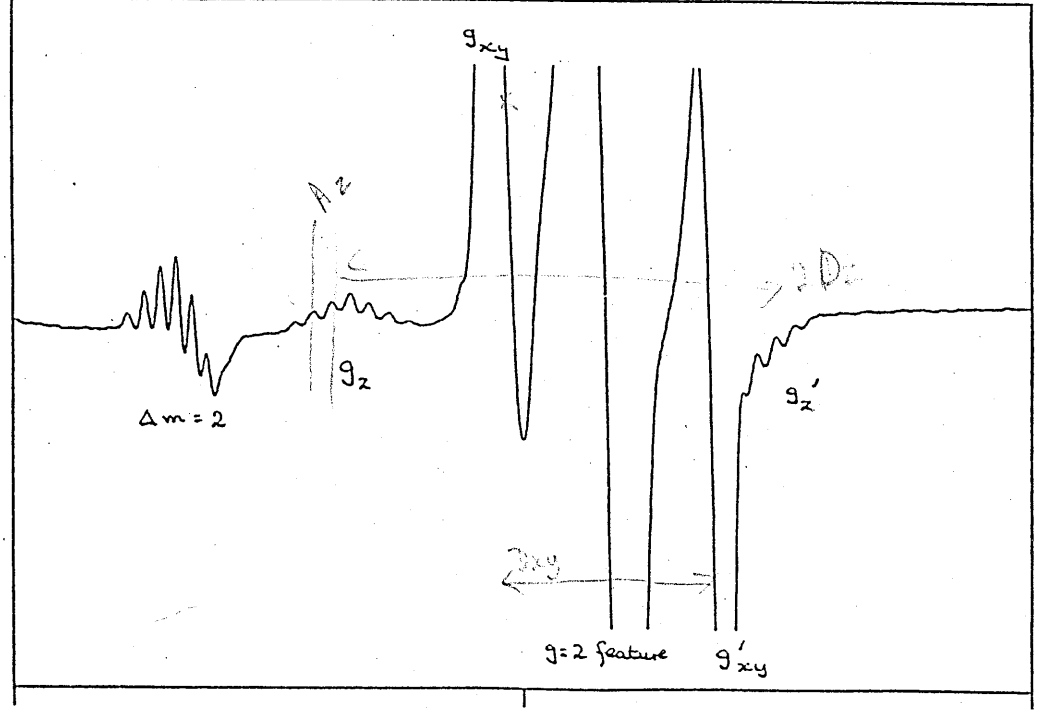

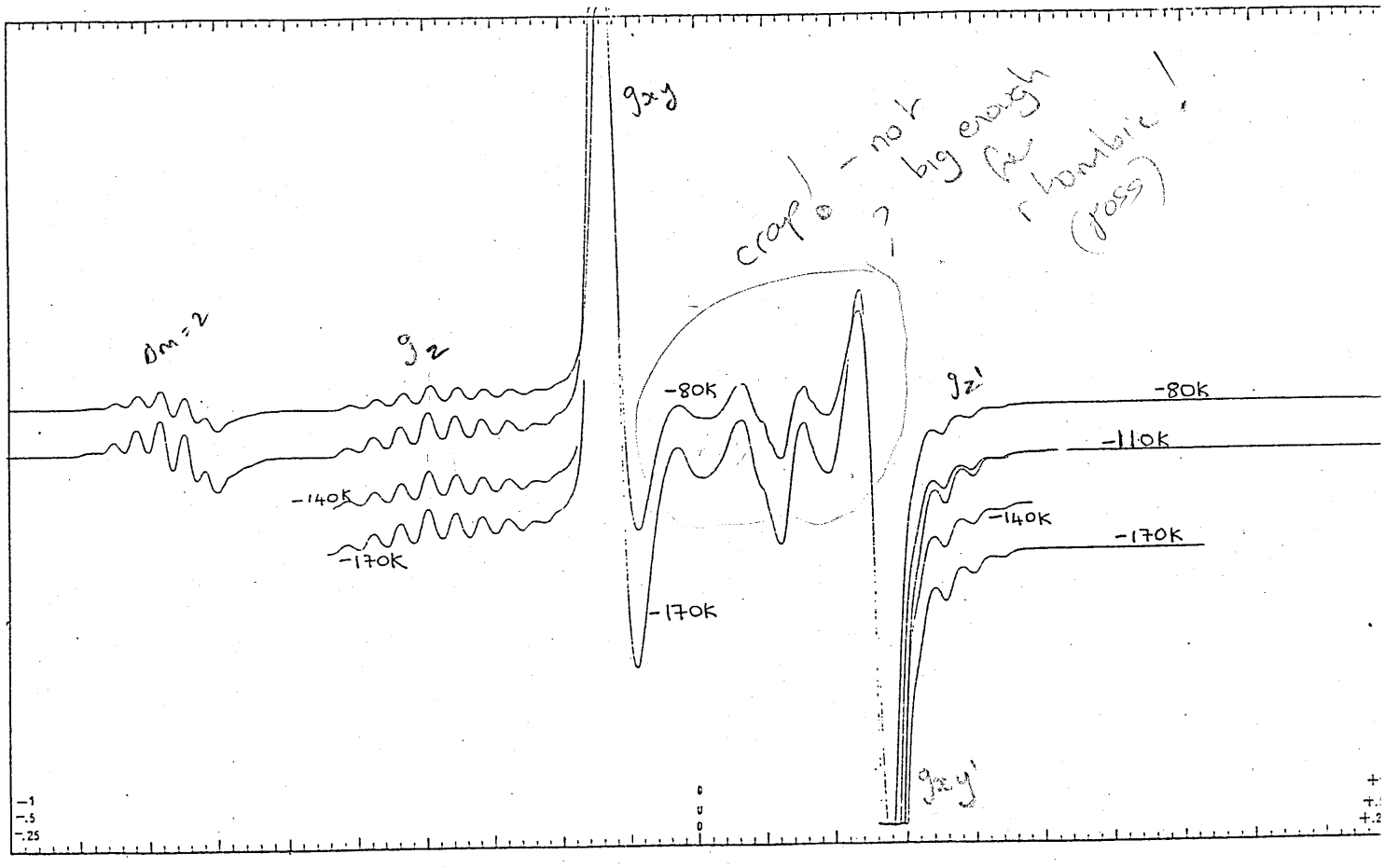

Fig. 38-5

F.S. = 3000G

S.R. = 4 x 1k

T = -80°C.

when g_z on LHS = ?

when g_z on RHS = ?

to -800cm^{-1} (116). The ligands showing these interactions had distorted square pyramidal geometries and a dx^2-y^2 ground state.

The temperature dependance of the susceptibility of [22] fails to conform to the Bleaney-Bowers equation and as a result no estimation of -2J could be made. Either a combination of intramolecular and intermolecular exchanges between metal ions in adjacent macrocyclic units or a sizeable fraction of paramagnetic impurity, may explain this failure. The higher than expected low temperature value of μ_{eff} = 0.90Bm (cf $Cu_2BP\mu OH(ClO_4)_3$ μ^{eff} 0.46) is consistent with the appearence of a moderately strong broad signal around g = 2.0 (FIG 38-4a-c show the esr spectra of [22] at 3 temperatures) in the esr spectrum which intensifies at low temperatures at the expense of the triplet spectrum. This suggests the presence of a paramagnetic impurity which at the lowest temperature dominates both the esr FIG.33-4c and magnetic measurements.

Despite the large antiferromagnetic interaction (singlet ground state) triplet features are still in evidence. Thus at room temperature the esr spectra, 38-4a, of [22] shows the triplet features arising from the S=1 state. As a result of the large splitting of the signals in the esr we conclude that the zerofield splittings are large ie there is a strong interaction between two copper centres. Thus Dxy (the zerofield parameter) = 950G which was the largest value of Dxy of all the copper dimers in this study. This suggests that, of the three bridging ligands investigated in this study, the hydroxo group is able to mediate the largest interaction between 2 copper ions. The large zerofield splitting leads to well resolved $g_{\perp}^{av}$ and $g_{\parallel}^{av}$ values. Cu(11) complexes having a square based geometry have a dx^2-Y^2 electronic ground state giving $g_{\parallel} > g_{\perp} > g_e$ = 2.003. For [22], $g_{\parallel}$ (2.22) > $g_{\perp}$ (2.11) > g_e = 2.0023, and thus a square based 4 or 5 coordinate geometry would seem to exist in this complex.

The magnetic results of $Cu_2T(OH)(CLO_4)_3$ $2H_2O$ gave a room temperature moment of 1.70Bm which fell to 1.43Bm at 93K. Thus the centres are antiferromagnetically coupled as in the analogous WT complex. This 'T' complex again showed poor fitting of data to the Bleaney-Bowers equation at low temperatures and this was attributed to a small amount of paramagnmetic

impurity. However an estimate of J was made at $-45cm^{-1}$. Again the esr showed a large zero-field splitting. The esr of this complx is shown in FIG.38-5.

The analogous hydroxy bridged BP complex also shows moderately strong antiferromagnetic interaction mediated by the single (OH) bridge. The temperature dependance of the magnetic susceptibility fits Bleaney-Bowers with $-2J = -311cm^{-1}$ (assuming a paramagnetic impurity of 4%). This compares with other 2J values in the range -60[102] to $-1000cm^{-1}$ [133] for other mono-μ-bridged di-copper(11) complexes of known structure. The best match[134] of exchange parameters J is at ($-161cm^{-1}$) for a bipyridyl di-copper dimer with a Cu-O(H)-Cu bridging angle of $\simeq 141.6^{\circ}$ and a Cu....Cu distance of 3.645Å.

The ir of compound [23] ie $Cu_2E(OH)(SCN)_3$ indicates both a single atom N bridge and a single atom O bridge - the other NCS groups being terminally coordinated. This implies a coordination number of 5 and indeed complex [23] showed the well defined splitting of the 2 electronic transitions, dx^2-y^2, $xy \rightarrow dz^2$ and $dxz, yz \rightarrow dz^2$, which is associated[135] with D_{3h}, trigonal bipyramidal, geometry. The magnetic behaviour is possibly a combination of ferro-intra and antiferromagnetic inter dimer interactions, requiring 2 sets of data to fit Bleaney-Bowers over the whole temperature as in [21].

FIG. 40

	BINUCLEAR SPECIES SHOWING SINGLE ATOM NCS^- BRIDGES.		
	BP	WT	E
Mn	✓	MONONUCLEAR	
Fe	✓		
Co	✓	✓	✓
Ni	✓	✓	
Cu	LONG	SINGLE ATOM 'O'	Cu^{I} S-BONDED Cu^{II} N-BONDED

CONCLUSIONS

(1) Molecular mechanics predicted that the single bridged structure 19-5 was unlikely for the 20 membered WT; this arrangement being considerably more stable in the 22 membered macrocycle BP. It was also predicted that the doubly bridged μ1,1 structure 19-4 is equally likely in both ligands. With respect to the thiocyanate ion, these predictions were upheld by experimental results, BP forming both singly and doubly bridged structures whereas WT complexes contain only the former bridging assembly. However with the azide group WT will form a singly bridged structure [22].

(2) A summary of binuclear 1,1μ NCS bridged species of the 3 ligands is shown in FIG.40 TABLE A.

Using this set of macrocyclic ligands, BP, WT, E, the group were successful in preparing >1,1 NCS binuclear complexes of five members of the first transition series from Mn(11) to Cu(11). The best fit for the M M assembly is achieved for M=Mn(11) within the 22-membered macrocycle BP, and for M=Co(11) and Ni(11) for the 20 membered macrocycle WT. (also possibly Cu(11) although evidence not conclusive). The mono bridged M-N(CS)-M assembly occurs within BP for M=Fe(11) Co(11) and Ni(11) but is not observed with WT due to its smaller size. In order to ensure good fit for either di or mono > NCS bridges with dicopper(11) the ligand E had to be employed which, because of the disposition of donor atoms, has a smaller effective cavity than WT. When the copper centres are in their monovalent form this favours the softer sulphur end giving rise to the 'S' single atom bridged structure.

3/ One of the main aims of this work was to establish whether the thiocyanate bridge was an effective mediator of magnetic interaction. If so, could the nature of the interaction (ie. ferro- or antiferromagnetic) be attributed to the mode of bridging (- long μ1-3 or single atom -) and thus be explained in terms of spin polarization effects. Results clearly indicate that while a ferromagnetic interaction may result from a μ1-1 thiocyanate bridge, [20] and [24], any interaction was significantly weaker

than the relatively strong antiferromagnetic interaction transmitted via the hydroxo group or the ferromagnetic interaction via an 'end-on' azide bridge. Kahn's proposal[108,109] that the unsymmetrical nature of the NCS bridging ligand would result in a reduced ability to induce a spin polarization effect, was upheld.

Thus, although not a good mediator of magnetic interactions, the thiocyanate ion is a useful probe for monatomic bridging distances giving a rough estimate of metal .....metal separation.

APPENDICIES.

Due to the majority of copper complexes in this study, the following 3 appendices will be discussed in reference to this metal. (The other relevant first row transition metals will be discussed briefly at the end of each section).

Copper(II) has a d^9 configuration and is subject to Jahn Teller distortions if placed in a field of cubic symmetry. This leads to a large range of coordination geometries distorted from normal transition metal geometries. Copper(II) also shows a wide range of coordination numbers from 2-8 of which 4,5 and 6 are by far the most common.

APPENDIX 1. ELECTRONIC SPECTRA.

Two main types of electronic transitions in copper(II) complexes give rise to their electronic spectra, viz, pure d-d transitions and charge transfer transitions.

The d-d transitions are Laporte forbidden ($\Delta L=0$). However, various mechanisms which exist for the breakdown of this selection rule enhance the intensity of d-d absorptions [136]. These include:-

1) d-p mixing in non-centrosymmetric systems.
2) vibronic coupling in which strong metal ligand coupling allows coupling of a vibrational mode of the molecules with the electronic excited state and;
3) intensity borrowing from an energetically near allowed transition (usally a charge transfer transition) These give rise to extinction coefficents for a Cu(II) d-d transtions, in the range 50-200$M^{-1}cm^{-1}$.

Often only a single, broad, poorly resolved band is found in the visible region. However it is possible to make some general correlations between electronic spectra and the copper(II) co-ordination geometry. Jahn Teller

41-1

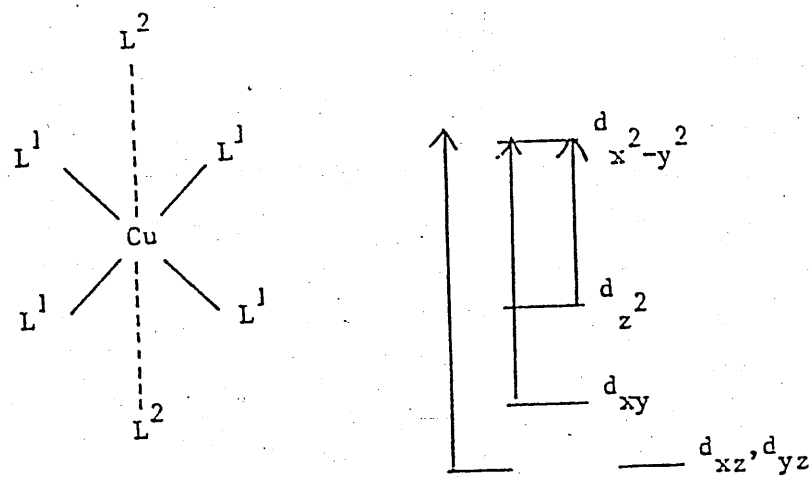

—— Normal Cu-ligand bond

- - - - Lengthened Cu-ligand bond

Splitting of d orbitals at a tetragonal copper(II) centre

→ square planar square based geometry

41-2

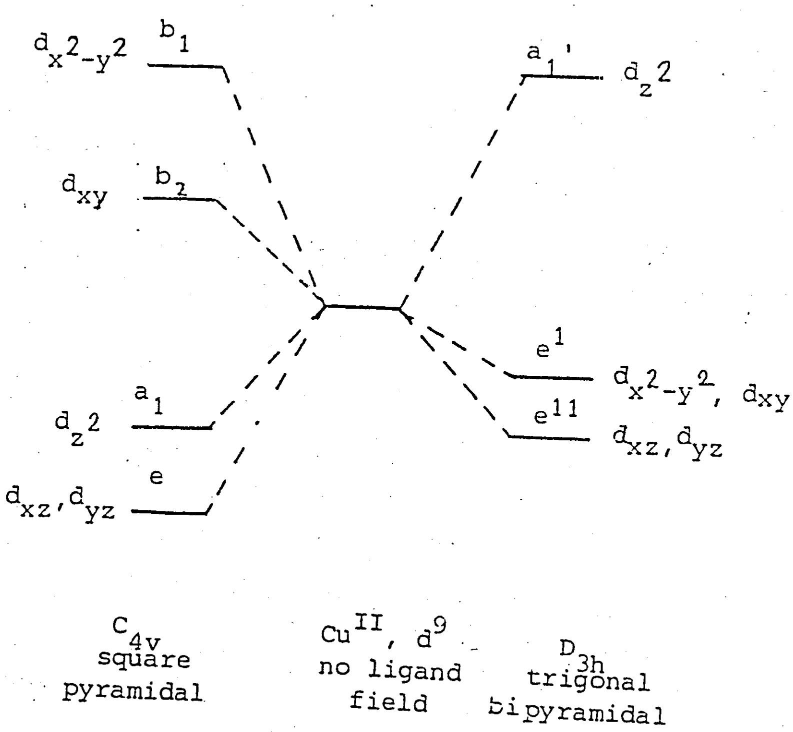

probably = to tetragonal but ~½ as there are e⁻ in 2 axes

distortions lead to a tetragonal splitting of the e_g level such that dz^2 lies below $d_{x^2-y^2}$. Thus for tetragonally distorted six co-ordinate Cu(II) complexes, 3 bands are expected from the energy level diagram FIG.41-1 ie $dz^2 \rightarrow dx^2-y^2$, $dxy \rightarrow dx^2-y^2$ and $dxy,yz \rightarrow dx^2-y^2$. These 3 bands generally overlap giving one broad band.

In a trigonal bipyramidal geometry the d orbital splitting is calculated for D_{3h} symmetry giving rise to 3 levels: $A_1=z^2$; $E''=xz,yz$; and $E'=xy,x^2-y^2$. FIG.41-2. Therefore only 2 d-d transitions are predicted, dx^2-y^2, $xy \rightarrow dz^2$ and $dxz,yz \rightarrow dz^2$.

For a 5 co-ordinate copper (II) ion in a square pyramidal geometry, the C_{4v} point group yields a dx^2-y^2 ground state FIG.41-2. Thus 3 transitions are expected in the electronic spectrum, $dxy \rightarrow dx^2-y^2$, $dz^2 \rightarrow dx^2y^2$ and $dxy,yz \rightarrow dx^2-y^2$. Again, often a broad unresolved band is observed but the presence of a poorly resolved shoulder on the low frequency side [137] which is often seen is evidence for square pyramidal copper complexes and contrasts with trigonal bipyramidal complexes which show a shoulder on the high energy side of the band maximum [138].

Square planar copper (II) complexes are assigned to the D_{4h} point group. This gives rise to a dx^2-y^2 ground state and the possibility of 3 transitions to dx^2-y^2 from dz^2, dxz,yz and dxy FIG.41-3. This geometry occurs widely in the 'CuN_4' chromophore.

The deep colour in some copper complexes is often due to the transfer of an electron from an orbital localized primarily on the ligand to one primarily on the metal, or vice versa. Such charge or electron transfer processes are termed ligand-to-metal-charge transfer (LMCT) (metal-to-ligand-charge transfer (MLCT) transitions are also known).

The charge transfer processes are closely related to the oxidation process. Thus many copper (II) complexes give rise to LMCT transitions because of the relatively easy reduction of copper (II) to copper (I). Charge transfer bands are spin allowed and Laporte allowed and consequently are

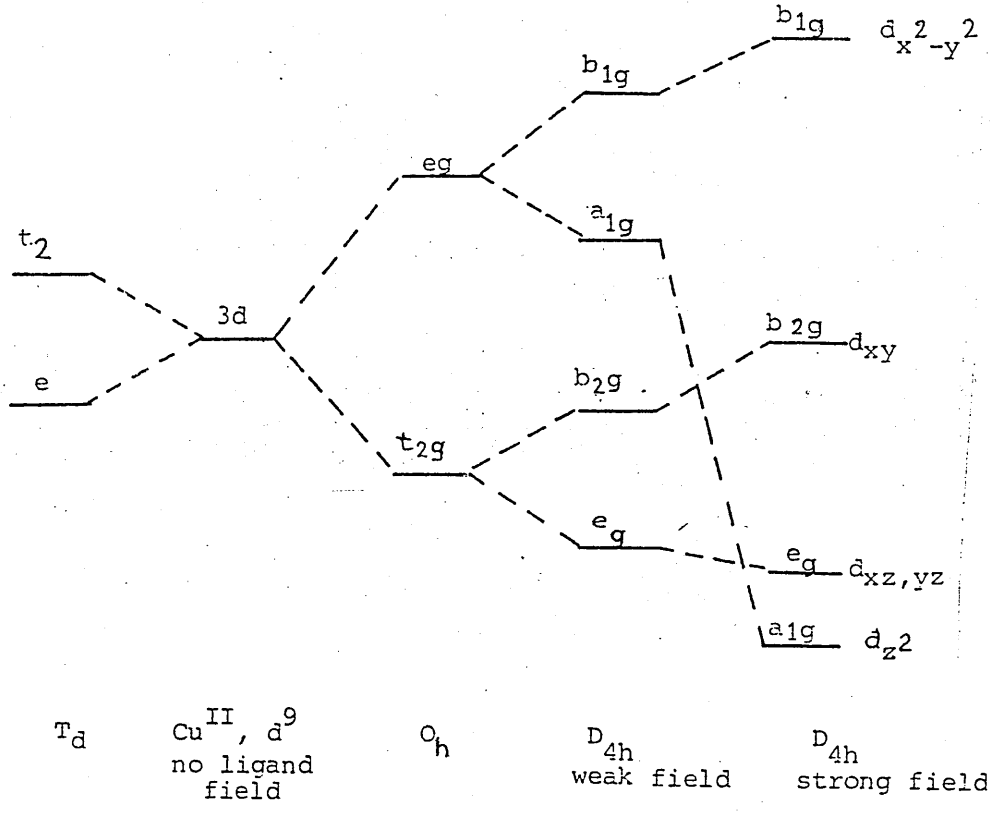

FIGURE 42

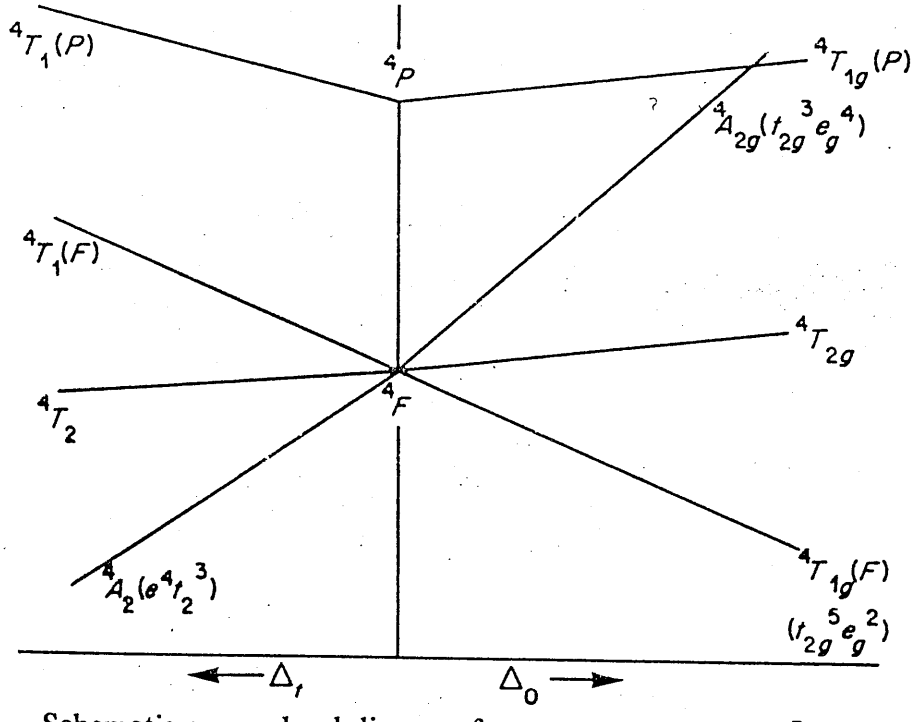

Schematic energy level diagram for quartet states of a d^7 ion in tetrahedral and octahedral ligand fields.

more intense ($\epsilon \approx 10^3 M^{-1} cm^{-1}$) than d-d transitions;-they also usually occur at higher energies.

FIG.42 gives the splitting pattern for $d^8(Ni^{2+})$ and $d^7(Co^{2+})$ in octahedral and tetrahedral fields and the transitions resulting from them.

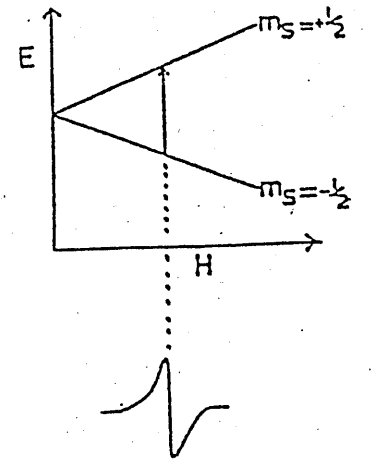

Isotropic

No hyperfine splitting

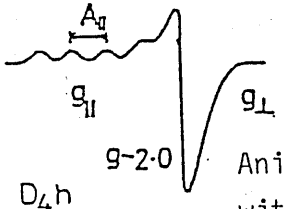

Anisotropic with h.f.s.

$nI + 1 = 4$

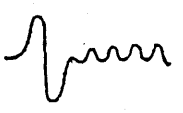

FIG.43-1

FIG.43-2

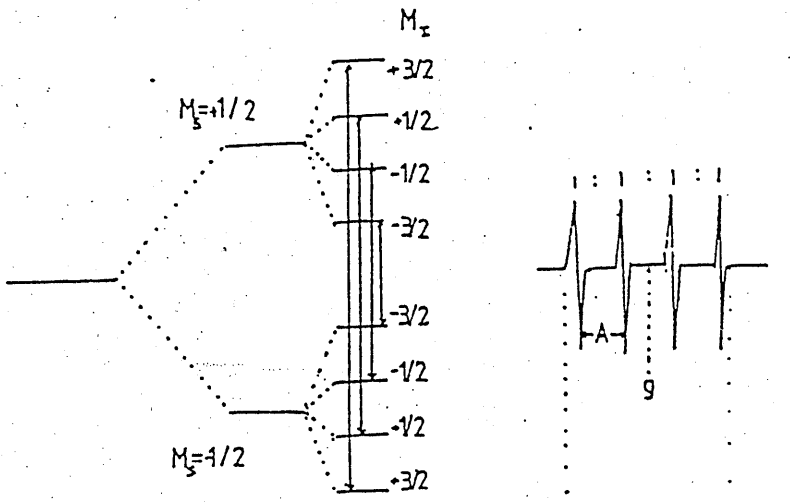

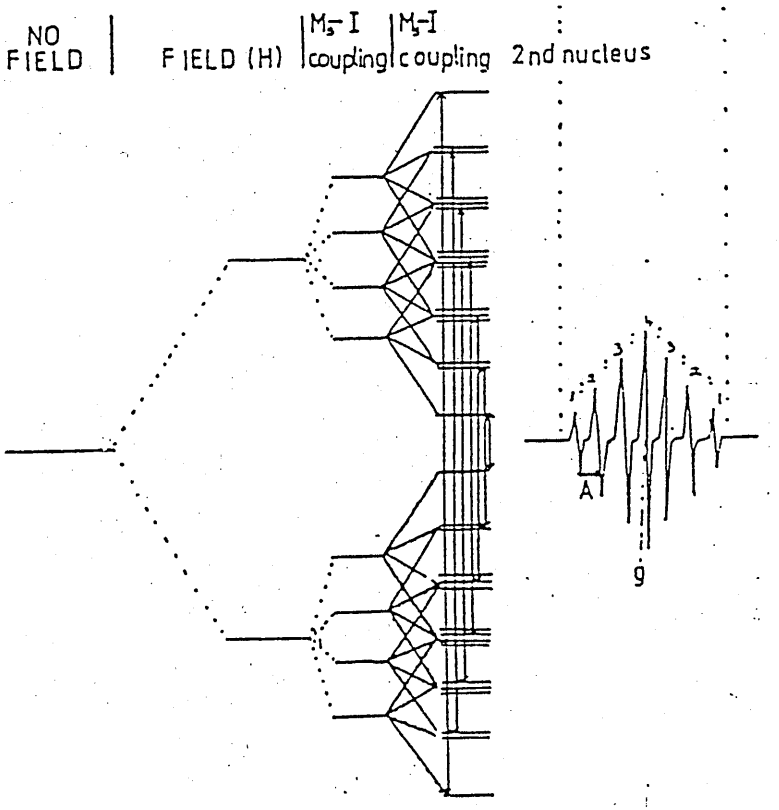

FIG.43-3

APPENDIX 2 ESR SPECTRA.

The relative low symmetry of copper(II) co-ordination environments often makes interpretation of electronic spectra difficult. In such cases, electron spin resonance (esr) spectroscopy can be used to provide information about the electronic ground state and the co-ordination geometry.

In electron spin resonance the magnetic dipoles of unpaired electrons are normally aligned with the applied field causing the degeneracy of the ± ½ spin states of the electron to be removed (Zeeman effect). The energy difference between the two states is $g\beta H$, where g is the gyromagnetic ratio, β is the Bohr magneton and H the applied field strength. For a free electron the value of g is 2.0023.

If the electron is associated with a nucleus possessing spin then the energy of the electron will depend on which of the possible nuclear spin states it is coupled to (Nuclear Zeeman Effect). This gives rise to hyperfine structure consisting of 2I + 1 (I = nuclear spin quantum number) lines of equal intensity.

The d^9 configuration of the copper(II) cation means that one of the d orbitals contains an unpaired electron. When radiation of frequency ν is applied to a copper(II) complex in a magnetic field a net absorption occurs when $h\nu = g\beta H$. This results in an absorption peak and it is the first derivative of this peak that the esr records.

Figure 43-1 shows how the esr signal arises for magnetically dilute copper(II). Only one transition is possible which obeys the selection rule $\Delta m_s = \pm 1$ and the signal is shown for the axially symmetric case FIG.43-1. The $g_{\parallel}$ signal is obtained when the magnetic field is oriented along the axial direction (z - axis) and the $g_{\perp}$ signal is obtained when the field is in the equatorial (x,y) plane. Since in the situation of axial symmetry, the $\perp$ axes are doubly degenerate, the probability of transition is twice that in the parallel axis and hence the $g_{\perp}$ signal has a greater intensity (x2) than the $g_{\parallel}$ signal. When the unpaired electron couples to the

copper nucleus, which has a spin I = 3/2, a hyperfine pattern of four equally intense lines is produced (FIG.43-2). The hyperfine is usually seen in the g_{11} region (A_{11} > 120G-200G where A is the hyperfine coupling constant) but often unresolved in the $g_{\perp}$ region.[129]. For rhombically symmetric copper(II) the x and y axes are not equivalent and therefore three signals g_x, g_y and g_z are observed.

The type of esr spectrum of copper(II) complexes will be determined by a number of factors including the nature of the electronic ground state and the co-ordination geometry of the copper(II) ion.[139] Copper(II) complexes with a square based geometry have a dx^2-y^2 electronic ground state. For these complexes, when the applied magnetic field is along the z-axis, the dx^2-y^2 orbital can commute into d_{xy}. Thus there will be spin orbit coupling and

$$g_{11} = g_e + \frac{8\lambda}{dx^2-y^2-dxy}$$

where λ is the spin orbit coupling constant.[140] Rotation of d_x2-y2 about the x or y axis when the applied field is in an equatorial direction can lead to rotation of dx^2-y^2 into dxy or dyz and

$$g_{\perp} = g_e + \frac{2\lambda}{dx^2-y^2-dxy,yz}$$

Thus for copper(II) complexes with square based geometry $g_{11} > g_{\perp} > g_e$ = 2.0023 [140] as the spin orbit coupling constant is positive. The g values are smaller for square planar complexes than for other square based geometries.[141]. The hyperfine splittings. A_{11}, are large for complexes with square based geometries and $A_{\perp}$ is often unresolved.

For trigonal bipyramidal[142,143] copper(II) geometries, the dz^2 orbital contains the unpaired electron. An axial field (z direction) cannot commute dz^2 into any other orbital geometry and so g_{11} will equal the free electron value of 2.0023.

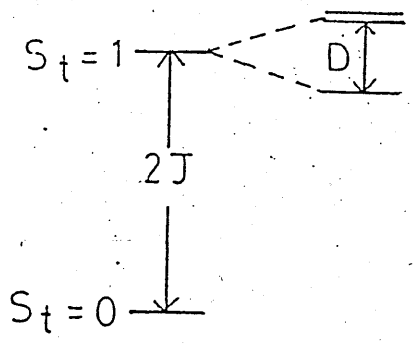

FIG.43-4

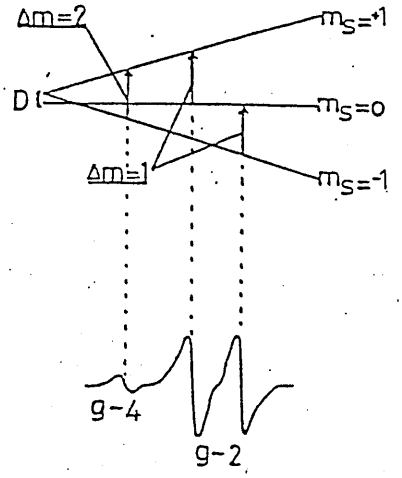

FIG.43-5

Isotropic
No hyperfine splitting

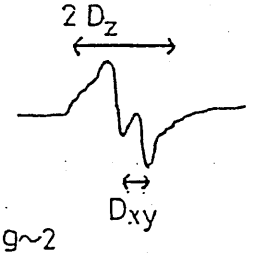

g~2

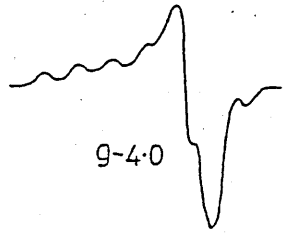

anisotropic
with h.f.s.
nI + 1 = 7

When the applied magnetic field is in the equatorial (x,y) direction, d_{xz} can rotate into d_{xy} or d_{yz} with

$$g_{\perp} = 2.0023 + \frac{6\lambda}{dx^2 - y^2\text{-}dxy,yz}$$

and therefore $g_{\perp} > g_{\parallel} = 2.0023$ [129]. The $A_{\parallel}$ hyperfine splittings are usually lower than observed for complexes with a $dx^2\text{-}y^2$ electronic ground state.[139,144].

For binuclear copper(II) complexes in which the copper centres are magnetically coupled through a bridging ligand, a zero-field splitting (D) of the triplet states occurs (FIG.43-4).

The magnitude of D is determined by both dipolar and exchange effects.[18,145]. The exchange contribution to D is not proportional to the isotropic coupling constant J (which is evaluated by magnetic susceptibility measurements: see Appendix 3) but depends on exchange interactions between one ion in its ground state and the other in its excited state.[18]. Thus binuclear copper systems with large J and small D, or small J and large D, are possible.

As a result of the triplet state splitting, in addition to the $\Delta M = 1$ transition there will also be a $\Delta M = 2$ transition which is forbidden by the selection rules, and this gives rise to the 'half-band' esr signal shown in Figure 43-5. The half-band signal can usually be resolved into a relatively isotropic seven line pattern ($2nI + 1 = 7$) due to a hyperfine interaction (FIG.43-3), the intensity ratios of the lines often as simple as the expected 1:2:3:4:3:2:1. The hyperfine spacing of about 75G is approximately one-half that found in mononuclear copper(II) spectra.[102,146]. The 'triplet-type' spectrum in the $\Delta M = 1$ region is often complicated by distortions from regular geometries and by hyperfine splitting patterns on components of the $\Delta M = 1$ transitions.[93].

FIGURE 44

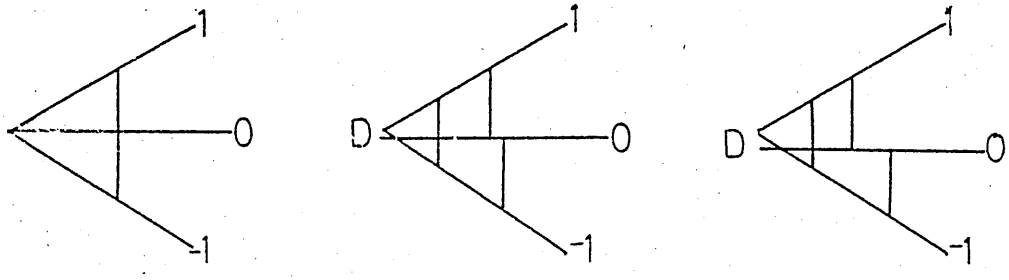

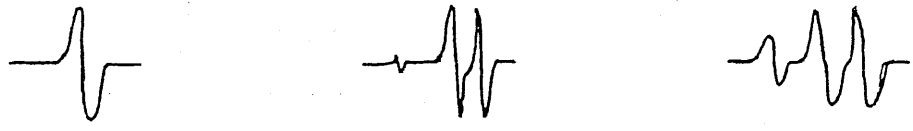

r>7 Å r=4Å r=3Å

|D| 0.01cm^{-1} |D| = 0.05cm^{-1} D| = 0.13cm^{-1}

The intensity of the esr signals depends on the number of unpaired electrons which decreases as the extent of interaction between the copper centres is increased. Thus, for strongly antiferromagnetically coupled copper(II) centres (see Appendix 3) the signal is considerably weakened and may eventually be lost (esr silence).

If two copper(II) ions are not directly bonded and there is no bridging ligand present then the copper(II) ions can only interact by dipolar coupling. In this case the zero-field splitting (D) has no exchange contribution and is inversely proportional to r^3 (r is the distance between the copper centres), and so the esr spectrum reflects the Cu(II)...Cu(II) separation (Fig.44). Thus for r > 7Å , D is of the order of 0.01 cm^{-1} and a single transition is observed. As the two centres come close the zero-field splitting can dominate producing a split and broadened $\Delta M=1$ signal and a narrower $\Delta M=2$ half-band transition. The $\Delta M=1$ signal can extend over a wide magnetic field range.

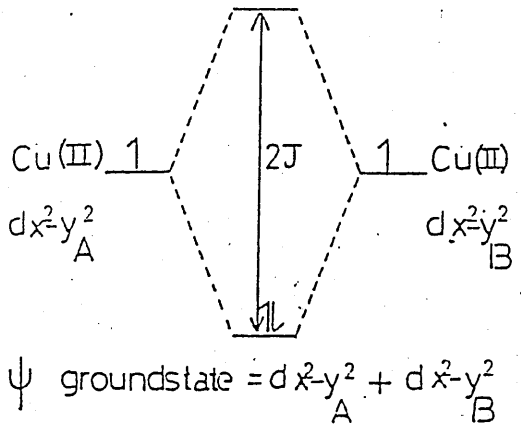

FIG.45-1

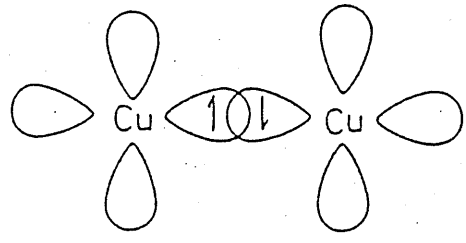

Direct interaction
(Cu-Cu bond)
$2J \sim 20{,}000\ cm^{-1}$

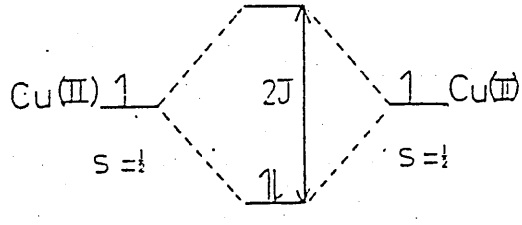

FIG.45-2

$-J \sim 0\text{-}550\ cm^{-1}$

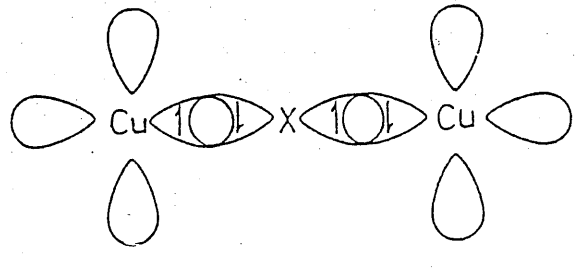

Superexchange interaction
(Cu-X-Cu)
$-2J\ 0 - > 600\ cm^{-1}$

APPENDIX 3

MAGNETIC PROPERTIES OF di-Cu(II) COMPLEXES.

For binuclear copper(II) complexes there is the possibility of magnetic interaction between the 2 paramagnetic copper centres and the complexes can be categorized into 3 groups depending on the extent of interaction.

-1- In non-interacting binuclear complexes the magnetic properties of the dimer are essentially unchanged from the paramagnetic monomer and thus lie close to the spin only value of ≃ 1.73Bm (observed range 1.75Bm-2.20Bm as a result of orbital contribution). The moments are independant of stereochemistry and temperature (except at extremely low T [<5k]) [147]

-2- In the limit of 2 very close copper(II)'s, direct overlap between d-orbitals on the 2 metal atoms can occur. FIG.45-1. This results in a strong interaction, the new molecular orbitals of the binuclear complex formed having an interaction energy of the order of $10,000cm^{-1}$. This produces a completely diamagnetic ground state and is therefore esr silent.

-3- For binuclear copper(II) complexes in which the 2 coppers are far enough apart to eliminate direct overlap, a weak interaction can result, if a bridging ligand is present. This bridge provides a superexchange pathway between the two d^9 metal centres and allows magnetic coupling FIG.45-2. which can be of a ferromagnetic (S=1, unpaired electrons) or an antiferromagnetic (S=0 spins paired) nature. For copper (II) binuclear systems the interaction between the single-ion spin doublet states leads to a pair of spin singlet and spin triplet states. Antiferromagnetic interaction can cause the singlet state to be hundreds of wavenumbers below the triplet state leading to a diamagnetic ground state at room temperature in the case of a ferromagnetic interaction the ground state is triplet.

The singlet-triplet separation is given by the exchange coupling parameter 2J which is defined by the Hamiltonian operator $H= -2JS_1.S_2$ where S_1 and S_2

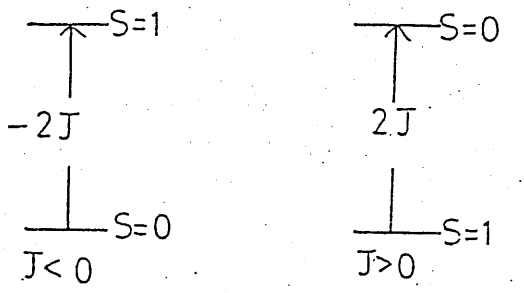

antiferromagnetic ferromagnetic

FIG.45-3

FIGURE 46

The Bleaney Bowers Equation

$$\chi_A = \frac{N g^2 \beta^2}{3kT}\left[1 + {}^1/_3 \exp\frac{-2J}{kT}\right]^{-1} + N\alpha$$

$$\mu_{eff} = 2.84\,(\chi_A . T)^{\frac{1}{2}}$$

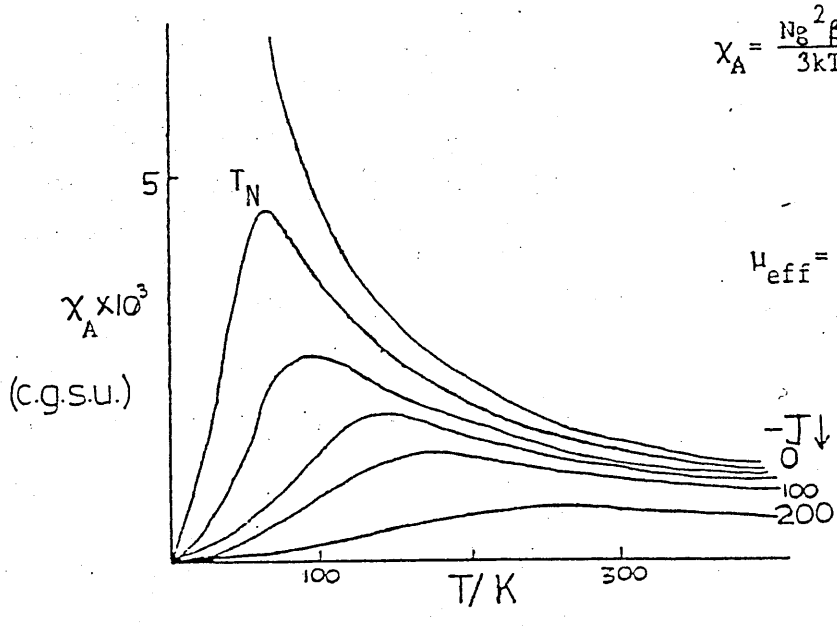

are the spins of the two coupling nuclei ($S_1=S_2=½$ for di copper(II) complexes.) J is negative for antiferromagnetic coupling and positive for ferromagnetic coupling, FIG.45-3.

The extent of the superexchange interaction in binuclear copper(II) complexes depends largely on the overlap of the 2 magnetic orbitals[24] via the orbitals of the bridging ligand. The coupling constant J can be expressed as the sum of a positive ferromagnetic component, J_F, and a negative antiferromagnetic component, J_{AF},

$$J=J_F+J_{AF}.$$

both of which will vary with the magnetic orbital overlap density, ρ [105].

The symmetry of the bridging ligand orbitals and the electron density on the bridging ligand are the most important factors affecting superoxide exchange although non bridging ligands have 2 important effects: they effect the electron density at the metal atom and secondly they affect the geometry of the bridging unit through steric hindrance.

To understand these factors which influence exchange there has been extensive research into the magnetic properties of coupled copper centres and correlations in the structural - property relationships of such complexes. The magnitude and sign of the coupling constant J for these complexes is calculated from the Bleaney-Bowers equation [148] according to the variation of magnetic susceptibility (X_A) with temperature as a function of J. for an antiferromagnetic interaction FIG.46.

A successful correlation, established between the Cu-O-Cu bridging angle and/or Cu...Cu distance with J for the di-μ-hydroxo-bridged copper(II) dimers is discussed in the text.

A table of the spin-only values and observed moments for the relevant transition metal ions is shown in FIG.47

FIGURE 47

Ion	Ground state quantum numbers		Spectroscopic symbol	u_s	u_{s+L}	Observed moments
	S	L				
Cu^{2+}	1/2	2	^2D	1.73	3.00	1.7-1.8
Ni^{2+}	1	3	^3F	2.83	4.47	2.8-4.0
Co^{2+}	3/2	3	^4F	3.87	5.20	4.1-5.2
Fe^{2+}	2	2	^5D	4.90	5.48	5.1-5.5
Mn^{2+}	5/2	0	^6S	5.92	5.92	5.9

For Mn^{2+} the ground state is an ^6S state ie. (L=0) and there is no orbital angular momentum even in the free ion. Hence there cannot be any orbital contribution to the magnetic moment and the spin only formula $\mu_S=g(S(S+1))^{1/2}$ applies.

In general the transition metal ions are F or D ground states and possess orbital angular momentum. If the orbital motion makes its full contribution to the magnetic moments they will be given by

$$\mu_{S+L} = (4S(S+1) + L(L+1))^{1/2}$$

μ frequently exceeds μ_s, but is seldom as high as μ_{s+L} because electric fields of other atoms, ions and molecules surrounding M^+ restrict orbital motion of the e^- so that the orbital angular momentum and hence the orbital moments are wholly or partially "quenched"

In some cases (eg. d^8 (Ni^{2+}) in octahedral and d^7 (Co^{2+}) in tetrahedral) one expects total quenching of L but these systems often deviate from the spin only behaviour, and when the effect of spin-orbit coupling is considered, it is found that orbital angular momentum is mixed into the ground state (ie $T_{1g}(P)$ and $A_{2g}(F)$) from the first excited state of the system - this leads to an increase from the spin only value.

CHAPTER 4
A MACROBICYCLIC STUDY

Introduction to Cyclophane Chemistry

Cyclophanes are simply macrocyclic compounds which incorporate aromatic rings into the macrocyclic skeleton. If the aromatic ring is a heterocycle eg. pyridine, pyrrole, furan, thiophene etc then the system is referred to as a heterophane. In some cyclophanes the aromatic rings are auxillary binding sites or rigid structural units ie. crown ethers or cryptands having aromatic rings, cyclophane porphyrins etc. In others, the aromatic rings are the major binding sites. Thus, cyclophanes are characterized by their aromatic rings which may in principle act as rigid structural units, as hydrophobic and/or van der Waals binding sites and as π donor or acceptors. These aromatic rings confer on the inclusion cavities well defined structure and depth. However the larger ring structures tend to make their conformations less rigid than those of their smaller analogues. Therefore it is important to determine which of the possible conformations is preferred in solution and for this purpose various spectroscopic studies have been carried out, mainly in nonaqueous media.

Cyclophane chemistry has undergone a virtual explosion since the widespread introduction of nmr spectroscopy as a common organic characterization technique. Indeed today, the word cyclophane is almost synonymous with an unusual ^{1}H nmr spectrum. Although the assignment of the structure of cyclophanes was relatively straightforward throughout the 70's, current easy access to high field nmr instrumentation suggests that a rapid expansion of our knowledge of cyclophane properties will again occur. This is because very detailed stereochemical assignments which were often impossible with other low-field instruments can now be made, Thus nmr techniques have been used to assign stereochemistry in the fixed (smaller) cyclophanes.These are phanes in which steric constraints prevent interconversion between possible conformers and thus the structure exists in a simple conformation. The signals in the nmr spectra are sharp and essentially temperature independent. On the other hand many larger cyclophanes are mobile and restricted conformationally at room temperature and can exist in a number of differnt conformations; their ^{1}Hnmr give an average of the spectra of all conformers. Usually the signals are never

FIG.1-1

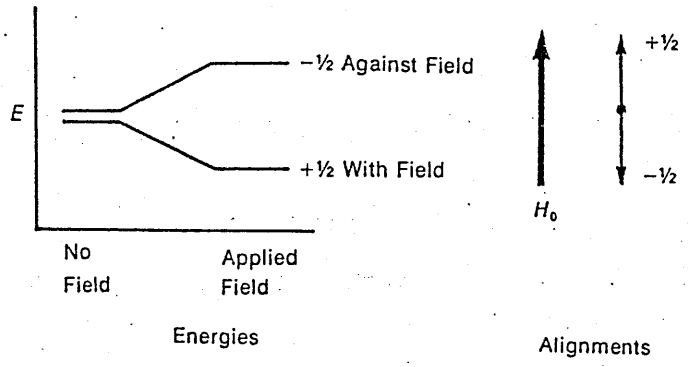

FIG.1-2

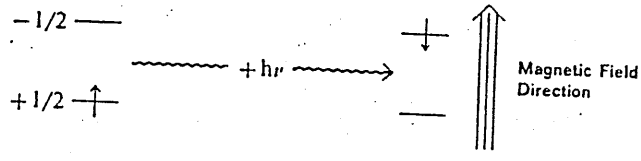

FIG.1-3

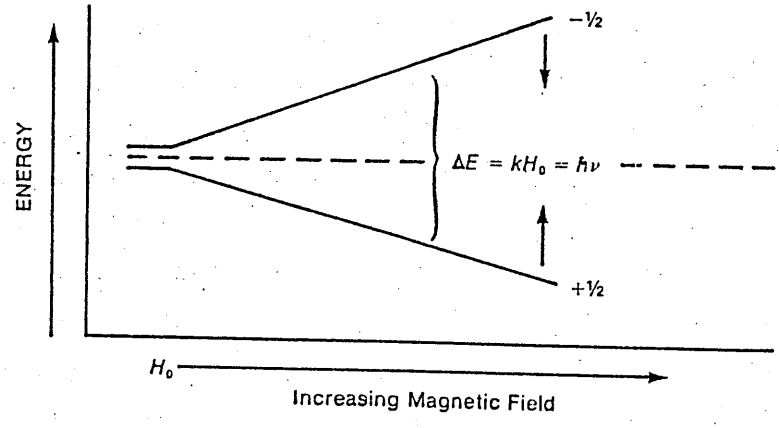

FIGURE 2

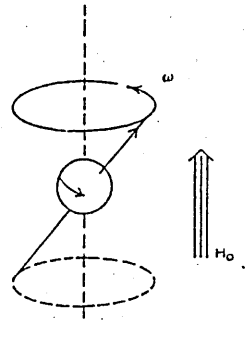

completely frozen out into the discrete conformers indicating that conformational exchange is rapid on the nmr time scale. However broadening and incipient separation of the signals are sometimes observed at lower temperatures indicating restricted conformational mobility.

NUCLEAR MAGNETIC RESONANCE SPECTROSCOPY (NMR)

This technique gives information about the number of each type of hydrogen and the nature of the immediate environment of each of these types of hydrogen atoms.

BASIC THEORY

Any atomic nucleus possessing either odd mass number or odd atomic number or both has a quantized spin angular momentum and a magnetic moment. For each of the nuclei with spin, the number of allowed spin states which it may adopt is quantized and is determined by its nuclear spin quantum number I. For a given value of I there are 2I+1 allowed spin states which range from +I to -I. For the hydrogen nucleus (ie the proton) I=½ and thus it has 2 allowed spin states; ±½. In the absence of an applied (external) magnetic field, Ho, all the spin states are degenerate and equally populated, with equal numbers of atoms having each of the allowed spins. However in an applied magnetic field these spin states are not degenerate because the nucleus is a charged particle and any moving charge generates a magnetic field of its own. Thus in an applied magnetic field all protons will have their own magnetic moments either aligned with the field (+½ - lower energy) or aligned against the field (-½ - higher energy) FIG.1-1. The nuclear magnetic resonance phenomenon occurs when nuclei aligned with an applied field are induced to absorb energy and change their spin orientations with respect to the applied field FIG 1-2. The energy absorption is a quantized process and the energy absorbed must equal the energy difference between the 2 states involved.

$E_{abs} = (E_{-½}\text{state} - E_{+½}\text{ state}) = h\nu$

This energy difference is a function of the strength of the applied magnetic field, Ho. FIG 1-3. The stronger the applied magnetic field the greater the energy difference between the possible spin states:

$\Delta E = f(Ho)$

When Ho is applied, the nucleus will precess about its own spin axis with an angular frequency w FIG 2; the frequency of precession is directly proportional to the strength of the applied magnetic field. Since the nucleus has a charge, the precession generates an oscillating electric field of the same frequency. When the frequency of the oscillating electric field of the incoming radiation just matches the frequency of the electric field generated by the precessing nucleus, the two fields can couple, and energy can be transferred from the incoming radiation to the nucleus, thus causing a spin change. This condition is called resonance.

Not every proton has resonance at exactly the same frequency because each proton is influenced by the field of the electrons from neighbouring nuclei, which serves to differing extents to shield them from the environment. In Ho, the circulating valence electrons of the protons generate counter magnetic fields which oppose Ho. Each proton is therefore shielded from Ho to an extent that depends on the electron density in its neighbourhood - thus each proton, which has a slightly different electronic environment from its neighbours, will have a slightly different resonance frequency. These differences are very small (1ppm) and no attempt is made to measure the exact resonance frequency of any proton. Rather, by means of an internal standard, the frequency difference of the signals are measured. This reference is tetramethylsilane (TMS) in which the protons of its methyl groups are more shielded than those of most commonly encountered compounds. Thus when a compound is examined, the resonance of its protons are reported in terms of how far, in Hz, they are shifted from TMS. The chemical shift, δ, where

$$\delta = \frac{\text{(shift from TMS in Hz)}}{\text{(spectrometer frequency in MHz)}}$$

is a parameter which is independent of field strength, and it expresses the amount by which a proton resonance is shifted from TMS in ppm of the spectrometers basic operating frequency. Typical spectrometers use a constant frequency and vary Ho to bring each proton in turn into resonance. Since highly shielded protons precess at a slower rate than relatively unshielded protons it is necessary to increase the field to induce them to precess at the frequency of the instrument. Hence highly shielded protons appear close to TMS at the right of the spectrum (high/up field) and less shielded protons appear down/low field.

Protons in a chemically identical environment often exhibit the same chemical shift thus giving rise to only one signal. The protons are said to be chemically equivalent. The area under each signal is proportional to the number of hydrogens generating that peak. The spectrometer electronically "integrates" the area under each peak by tracing over each peak a vertically rising line the height of which is directly proportional to the area under the peak. The integral line does not give the absolute number of each hydrogen, rather the relative number in the simplest ratio of each type of proton.

CHEMICAL ENVIRONMENT & FACTORS AFFECTING THE CHEMICAL SHIFT

Not only do different types of proton have different chemical shifts δ, they also have a value of δ which is characteristic of the type of proton they represent. Each type of proton usually exhibits a limited range of δ values over which they give resonance FIG.3. Hence the numerical value (in δ units) of the chemical shift gives a clue to the type of proton originating the signal eg. aromatic protons have resonance near 7-8δ due to ring current deshielding effects (discussed below). These values are not invariant and several factors strongly influence the chemical shift values.

-1- **ELECTRONEGATIVITY EFFECTS** - Electronegative substituents reduce the electron density around the protons and thus reduces the shielding of that proton. The greater the electronegativity of the substituent, the more it "deshields" protons and the greater is the δ value of those protons.

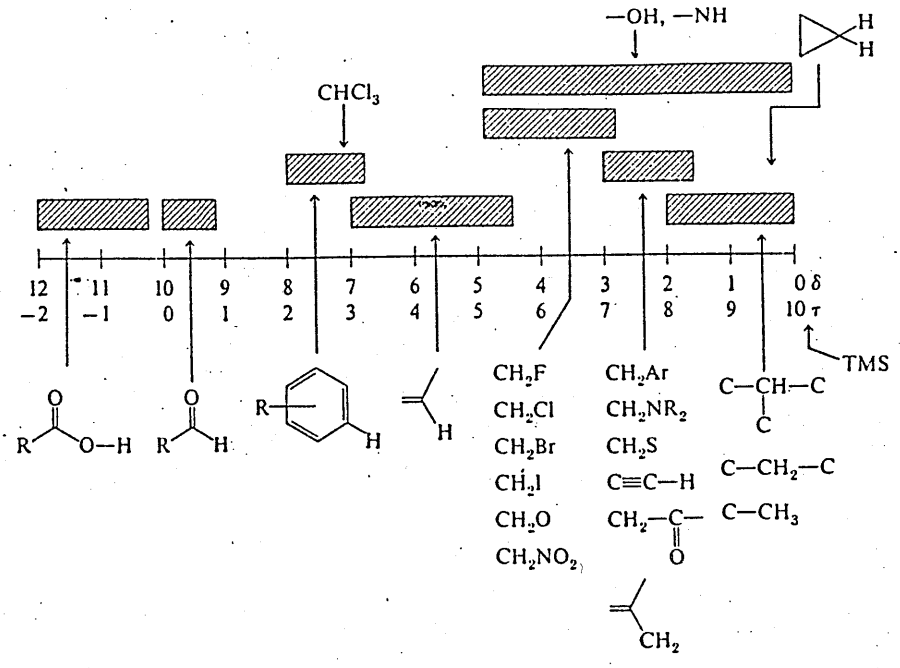

FIGURE 3

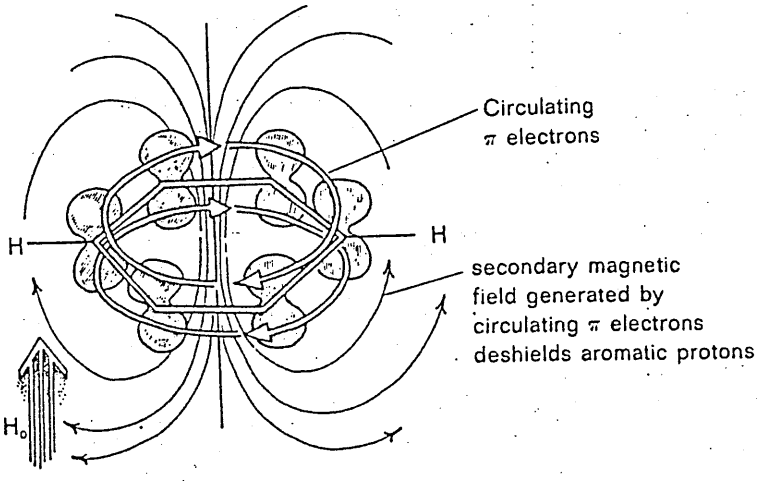

FIG.4-1

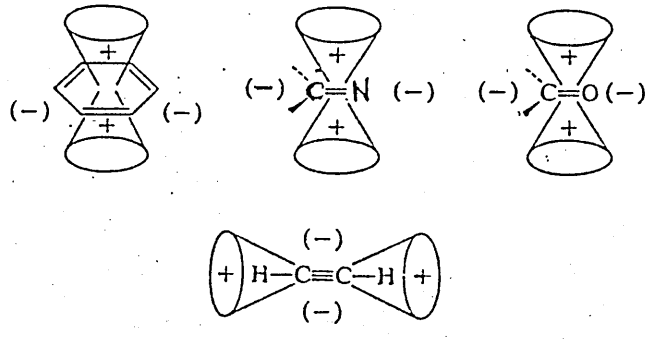

FIG.4-2

-2- HYDROGEN BONDING; EXCHANGEABLE HYDROGENS.- Protons which can exhibit hydrogen bonding (OH, NH, NH_2) exhibit extremely variable absorption positions due to the time averaged picture of bound and free protons as "seen" by the spectrometer. The more strongly hydrogen bonded a proton, the more deshielded it becomes. The bound:unbound equilibrium is usually affected by concentration and temperature.

-3- HYBRIDIZATION AND MAGNETIC ANISOTROPY EFFECTS.- On the basis of hybridization alone one would expect a greater chemical shift for acetylenic protons ("sp") than the vinyl proton (sp^2) which in turn should be greater than hydrogens attached to purely sp^3 carbon atoms. This is a result of the decrease in 's' character of the C-H bond. S orbitals hold their electrons more tightly and by increasing the s character of the bond it behaves as if it were more electronegative. For sp^3 carbon-hydrogen protons, the resonance range is 0-2δ (except when the carbon is attached to an electronegative heteroatom, a greater value of δ is observed) sp^2 or vinyl carbons, have resonance in the range from 4.5 to 7δ because of the increased s character. Aldehyde protons (also attached to an sp^2 carbon) appear even further downfield (9-10δ) since the inductive effect of the electronegative oxygen further decreases the electron density on the attached proton. However acetylenic protons, which we would expect to lie at δ values greater than those observed for the vinyl protons appear at 2-3δ. This is due to the presence of an unsaturated system (ie Π electrons) in the vicinity of the proton in question.

When a π system, eg benzene, is placed in a magnetic field the π electrons in the aromatic ring systems are induced to circulate about the ring (ring current). This generates a magnetic field which covers a spatial volume large enough that it influences the shielding of the benzene hydrogens. FIG.4-1. The benzene hydrogens are said to be deshielded by the diamagnetic anisotropy of the ring (anisotropy:non uniform) If a proton is placed over the centre of the ring rather than on its periphery it is shielded since the field lines there have the opposite direction. The magnitude of the anisotropic field diminishes with distance and beyond a certain distance there will be essentially no effect due to anisotropy. All groups in a molecule which have π electrons generate these secondary anisotropic fields

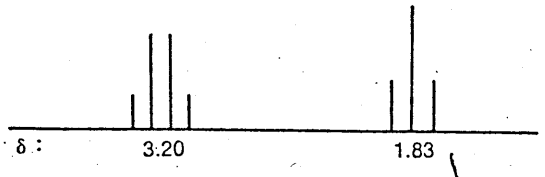

FIG.5-1 THE ETHYL SPLITTING PATTERN.

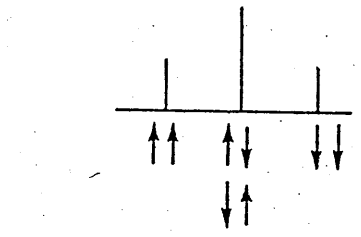

NET SPIN: +1 0 −1

Possible Spin Arrangements of the Methylene Protons

FIG.5-3

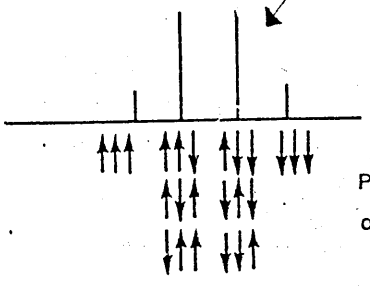

ET SPIN: +3/2 +1/2 −1/2 −3/2

Possible Spin Arrangements of the Methyl Protons

↑ = spin +½

↓ = spin −½

FIG.5-2

FIG.5-4

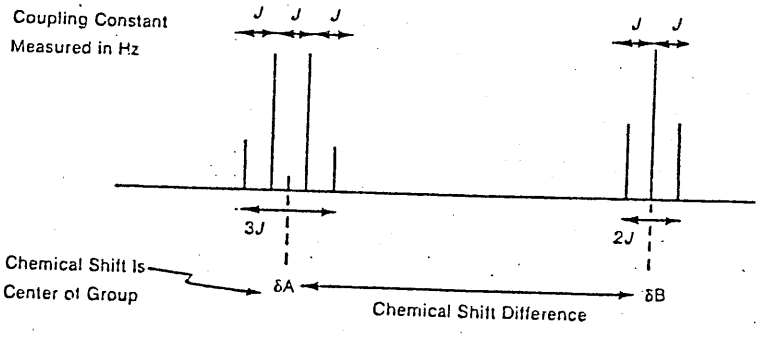

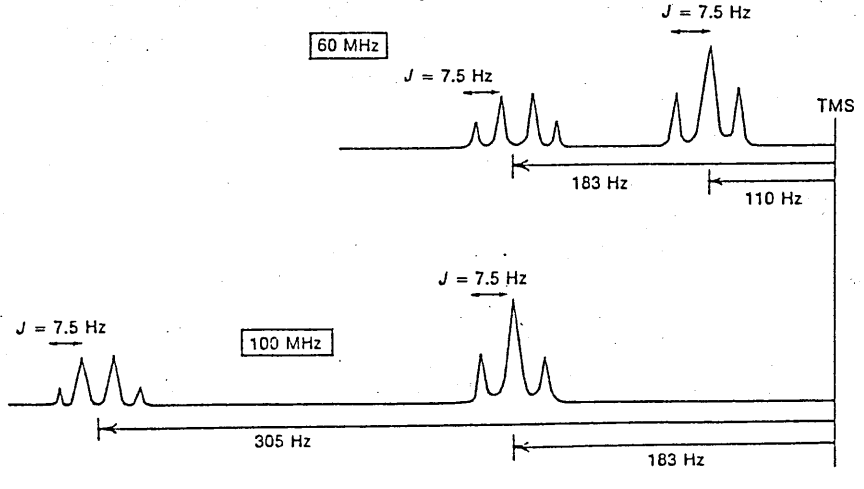

FIG.5-5

FIG.4-2. Protons falling within the cones (+ areas) will be shielded while those falling outside the conical areas will be deshielded - thus the acetylenic 'sp' protons are shielded.

SPIN-SPIN SPLITTING AND THE COUPLING CONSTANT J.

The phenomenon of "spin-spin" splitting reveals how many adjacent hydrogens there are to each type of hydrogen giving an absorption peak. Each type of proton 'senses' the number of equivalent protons (n) on the carbon atom(s) next to the one to which it is bonded. These protons are said to be coupled and the magnetic environment of the proton is affected by whether the adjacent protons have a net +½ or net -½ spin state. Except in unsusal cases spin-spin splitting ie coupling, occurs only between hydrogens on adjacent carbon atoms.

Thus the ethyl group ,(CH_3-CH_2) gives a triplet and a quartet in the spectrum. This is explained by considering FIG.5. The intensity ratio of the multiplets derived from the n+1 rule (where n=no.of adjacent equivalent protons) follow the values obtained from Pascals triangle. The magnitude of the "spin-spin" splitting arising from coupling is field independent, and thus the same irrespective of the frequency of spectrometer used, ie the amount of coupling is constant. The parameter, J, which is the coupling constant, gives the distance (in H_z) between the peaks. FIG.5-4.

The relationship between δ and J for the ethyl group in ethyl iodide is given in FIG.5-5. While δHz will be much larger in the 100MHz spectrum (NOTE δ(ppm) will be the same in both spectra) the coupling constant remains at $7.5H_z$ in both spectra. The magnitude of J can often provide structural and conformational clues and this is considered in later discussion.

THE MECHANISM OF COUPLING: COUPLING CONSTANTS.

The Dirac vector model[1] gives the best theory of how the spin of one proton influences that of another. The model proposes that the lowest energy interaction of the nuclear and electronic spins occurs when the spin

FIG.6-1

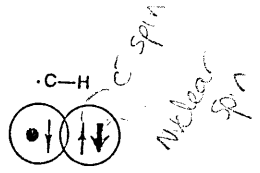

FIG.6-2

FIG.6-3

AN ILLUSTRATION OF THE METHOD OF TRANSFERRING SPIN INFORMATION BETWEEN TWO ADJACENT CH BONDS.

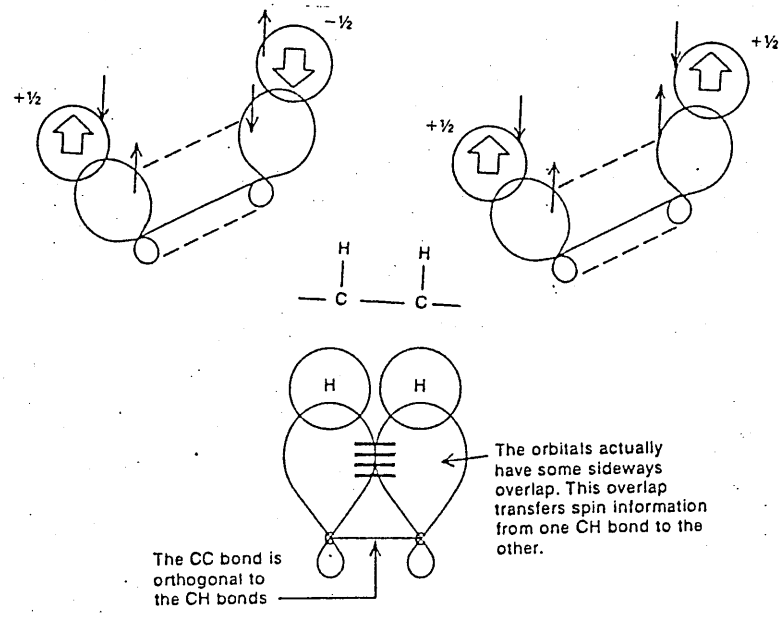

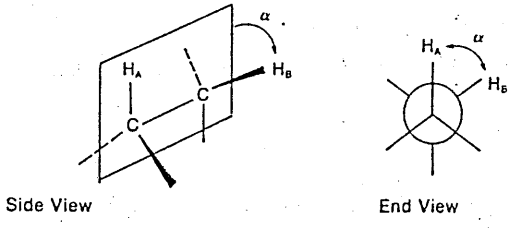

FIG.7-1

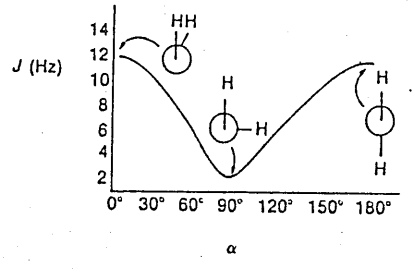

FIG.7-2

Vicinal protons Geminal protons

FIGURE 8.

of the nucleus is paired with that of the electron FIG.6-1. However ^{12}C exhibits no spin and thus the spin coupling is as shown in 6-2. In a typical hydrocarbon this spin coupling situation in one C-H is coupled to that in adjacent C-H bonds. Since the σC-C bond is orthogonal (perpendicular) to the σC-H bonds, the electrons cannot interact through the σ bond systems, rather interaction occurs via the small amount of parallel orbital overlap that exists between adjacent C-H bond orbitals FIG.6-3. This allows spin interaction between the electrons near the 2 carbon nuclei. That this picture is essentially correct has been shown in that J, a measure of the interaction, depends directly on the dihedral angle α between these two bonds FIG.7-1,7-2. The magnitude of the "spin-spin" splitting between H_A and H_B is largest when $\alpha=0^\circ$ or 180° and is smallest when $\alpha=90^\circ$ This agrees with the Dirac model since when the 2 C-H bonds are orthogonal ($\alpha=90$) there is little or no orbital overlap and thus little or no splitting of the absorption peaks. The coupling between protons on adjacent carbon atoms is called vicinal coupling whereas geminal coupling refers to protons on the same carbon atom.FIG,8. This coupling often does not lead to any spin-spin splitting, as the protons are in identical magnetic environments and have the same chemical shift. Thus the 3 protons in methyl iodide give one signal - they are said to be magnetically equivalent protons. Evidence that geminal coupling exists comes from the nmr studies of conformationally rigid cyclic compounds (later discussion)

The mechanistic picture for geminal coupling also invokes nuclear-electronic spin coupling as a means of transmitting information from one nucleus to the other. FIG.9-1,9-2. The amount of splitting ie. geminal interaction, has been shown to be dependent on the HCH angle α FIG.9-2. When the protons on the same carbon are magnetically nonequivalent (ie different δ), spin-spin splitting is observed and thus the n+1 rule no longer applies. One must then examine each proton individually taking into account its coupling with every other proton (remembering that each coupling is independent of each other). A spin-spin splitting diagram FIG.10 also called a tree diagram is a convenient technique for the analysis of splitting patterns.

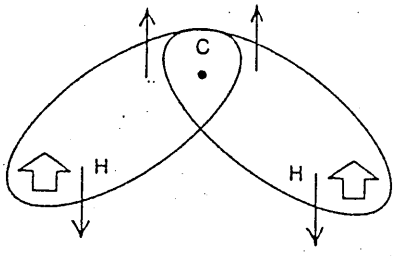

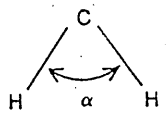

FIG.9-1

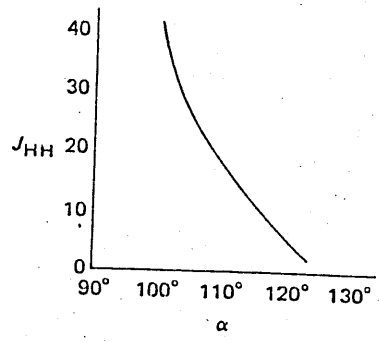

FIG.9-2

FIGURE 10

THE TREE DIAGRAM

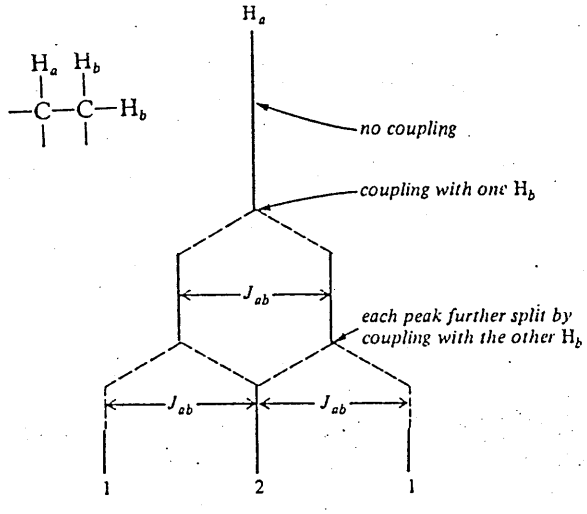

FIGURE 11

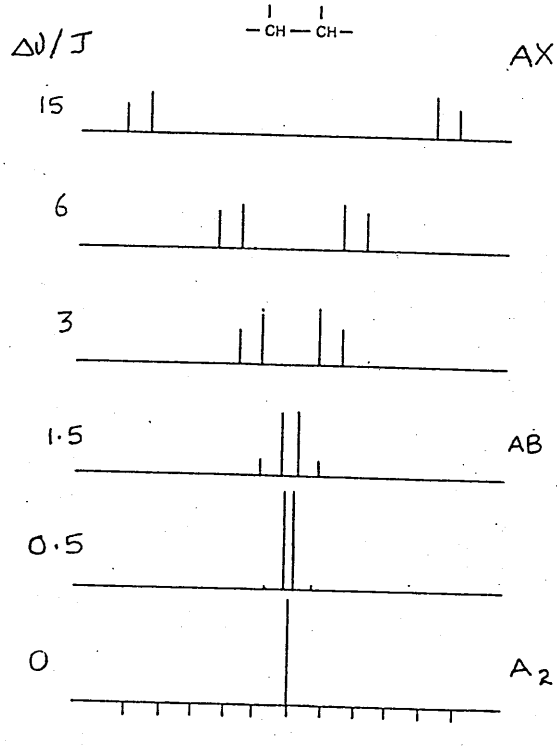

THE SPLITTING PATTERN OF A TWO-PROTON SYSTEM H_AH_B FOR VARIOUS RATIOS ν/J

THE SPLITTING PATERNS OF A TWO-PROTON SYSTEM H_AH_B

FIG. 12

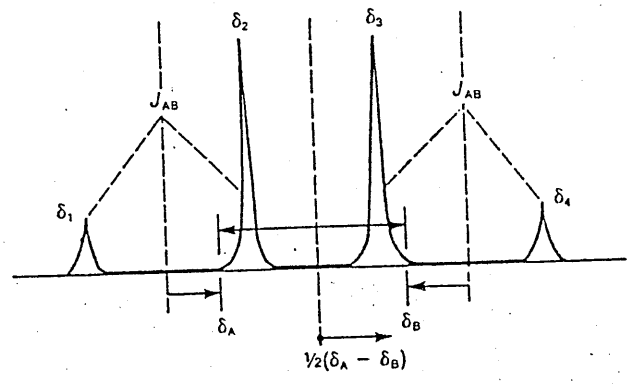
δ2
δ3
JAB
JAB
δ1
δ4
δA
δB
½(δA − δB)

FIG. 13

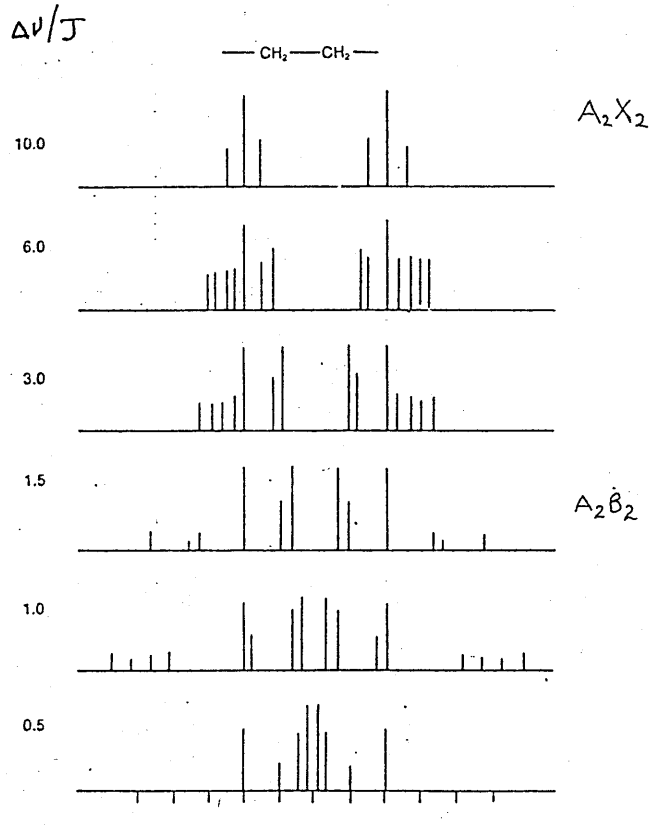
Δν/J
— CH2 — CH2 —
A2X2
10.0
6.0
3.0
1.5
A2B2
1.0
0.5

SECOND ORDER SPECTRA

Spectra which can be interpreted using the n+1 rule are said to be first order spectra - to observe such a spectrum the ratio of the chemical shift difference ($\Delta\nu$) to the coupling constant (J) (both in Hz) must be large - ie $\Delta\nu/J>10$. Spectra requiring more advanced analysis are said to be second order spectra. These occur where the difference in δ betweem the two groups of protons is similar in magnitude (in Hz) to the coupling constant J (in Hz) which links them ie $\Delta\nu/J\simeq1$. Thus second order spectra are observed for coupling between nuclei which are nearly equivalent but not identical. FIG.11 shows how the splitting pattern for a two proton system H_A, H_B changes as the δ of H_A and H_B come closer together and the ratio $\Delta V/J$ becomes smaller. When $\delta H_A=\delta H_B$ $\Delta V/J=0$ and no splitting is observed - both protons give rise to a single absorption peak.

While the central point of a doublet gives the δ of the proton in a simple first order spectrum, the situation is more complex in second order spectra. The shift of a particular proton is found closer to the inner peaks and is calculated from

$$(\delta_A-\delta_B) = (\delta_1-\delta_4)\ (\delta_2-\delta_3)$$ of FIG.12

δ of H_A and H_B are then displaced $\frac{1}{2}(\delta_A-\delta_B)$ to either side of the centre of the group.

Each chemically different type of proton is given a letter - protons of similar δ are assigned letters that are close together in the alphabet (A,B,C etc) whereas protons of widely different δ are assigned letters far apart (XYZ v's ABC). Thus a 2 proton system giving rise to a simple first order spectra ($\Delta\nu/J>10$) is termed an AX system while an AB system is the usual term where a second order spectra (protons having similar δ) is observed. Where 2 protons have identical δ giving only one signal the system is designated A_2. The subscript indicates that there is more than 1 proton of that type. FIG.13 - the splitting pattern for a four proton system ($-CH_2-CH_2-$) for various ratios of $\Delta\nu/J$ summarises this.

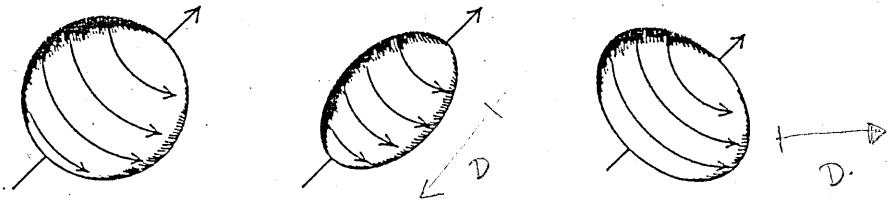

Spherical Spinning Nucleus
(I = 0 or I = ½)

PROLATE

OBLATE

Ellipsoidal Spinning Nuclei

(I > ½)

Have Quadrupole Moments

FIGURE 14.

PROTONS ON NITROGENS.

In simple amines, as in alcohols, intermolecular proton exchange is usually fast enough to decouple spin-spin interactions between N-H and adjacent C-H protons. This results in a single sharp unsplit singlet for the amino protons - the α carbon protons are also unsplit. However ^{14}N has a nuclear spin. I=1, and thus can adopt spin states, +1, 0 and -1. When I=½ there is a small electric quadrupole moment and a spherical distribution of charge. When I>½ there is an ellipsoidal distribution of charge, FIG.14, which gives the nucleus an "internal dipole moment" - the electric quadrupole moment. This makes the ^{14}N nucleus more sensitive both to interaction with H_o and the perturbations of the valence electrons and/or their enviroments. Thus they undergo relaxations at a faster rate than spherically symmetric nuclei and have very short lifetimes in the nuclear excited states. In many cases the transition rate of the nitrogen is very close to the rate at which 'Hnmr absorption is taking place. In these cases hydrogen is only partially decoupled from nitrogen ie the proton is 'less sure of what it sees' and thus the absorption peak of the N-H proton broadens. This phenomenon is called nuclear quadrupole broadening of the nmr absorption peak.

^{13}C NMR SPECTROSCOPY.

Although ^{12}C has I=0 and is thus nmr silent, ^{13}C has I=½. However due to its low natural abundance (1.1% of all carbon atoms) and its low magnetic moment, the ^{13}C resonances are ≃ 6000 times weaker than 'H. ^{13}C gives δ (in ppm) and the shifts cover an extremely wide range of up to 200ppm (cf'H ≃20ppm). Thus even adjacent $-CH_2-$ carbon atoms in a long chain hydrocarbon have their own distinct resonance peaks. C atoms usually only have the same δ when they are equivalent by symmetry. Integrals are unreliable because they are obtained by Fourier Transformation of the decay signal and relaxation effects dominate the decay pattern. Also integrals are not necessarily related to the relative number of ^{13}C atoms.

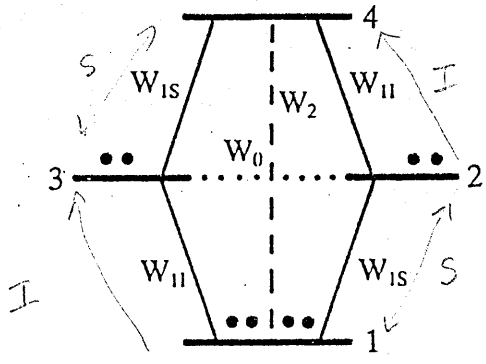

Energy levels and equilibrium population distribution for dipole-dipole relaxation in a homonuclear two-spin system.

FIG. 15-1

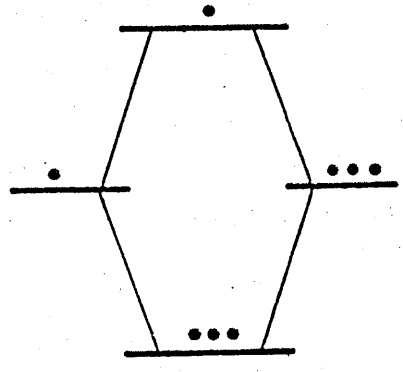

Population distribution in the homonuclear two-spin system immediately after saturation of the S spin.

FIG. 15-2

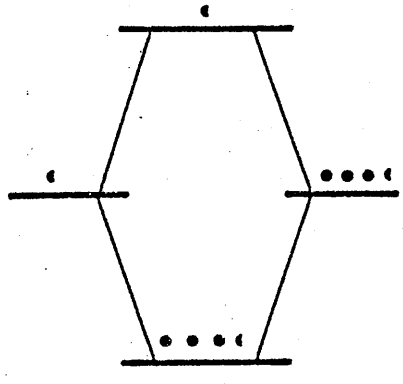

Steady-state population distribution in a rapidly tumbling homonuclear two-spin system with S being saturated.

FIG. 15-3

Spin-spin splitting resulting from 2 adjacent ^{13}C is rare due to the very low probability of finding two ^{13}C next to each other. ^{1}H-^{13}C splitting may lead to very complicated spectra and it is customary to decouple all the protons in the molecule by irradiating them all simultaneously with a broad spectrum of frequencies in the proper range. In such a decoupled spectrum each peak represents a different C atom.

One of the most powerful features of the ^{13}C technique is that it allows a determination of the number of different C atoms in a molecule and thus allows for recognition of equivalence or a symmetry element.

NUCLEAR OVERHAUSER ENHANCEMENT (NOE) EXPERIMENTS

The preceding discussion has centered on through-bond J-coupling phenomena that take place in the xy plane. In contrast spin lattice relaxation (see Appendix 1) is a through space effect which contains information about the distances between spins - it is concerned with the return of magnetization to the equilibrium position along the z axis following some perturbation. FIG.15 shows (1) the energy level diagram for two protons I and S which are relaxing each other but are not J coupled, and (2) the equilibrium population distribution. The spectrum of I consists of 1 line corresponding to transitions 1,3 and 2,4. The transition probability for relaxation by this process is W_{1I}. The single peak for S, arises from the transitions 1,2 and 3,4: W_{1S} is the transition probability. W_2 is a double-quantum process corresponding to the simultaneous relaxation of both spins, while Wo is a zero-quantum process corresponding to a mutual spin flip. This process gives no net relaxation but leads to the excess energy being moved from one spin to another. As the intermolecular separation between I and S increases, the efficiency of relaxation decreases as does the intensity of the field produced by their interaction. Quantitatively, there is an r^{-6} dependance of relaxation rate: thus doubling the internuclear separation decreases the relaxation rate by a factor of 64.

If the spin of S is saturated by irradiation, there is , initially, no change in either of the populations linked by W_{1S} and W_{1I} (Fig15-1) with

levels 1 and 3 having lost equal amounts of population to levels 2 and 4 respectively (FIG.15-2) so if the state of the spin system is read by a pulse immediately after such a short pre-irradiation is turned off there will be no S signal and a normal intensity singlet for the I signal. If irradiation of S is continued for a longer time, then a new population distribution gradually develops as relaxation occurs through W_2 and W_0. W_2 increases the intensity of the I transitions by attempting to establish a Boltzmann distribution between levels 1 and 4 while Wo decreases the intensity of I by equilibration of levels 2 and 3. The resulting net change in the intensity of I as a result of the competition of W_2 and Wo is the Nuclear Overhauser enhancement. An increase in intensity is a positive NOE FIG.15-3 which is normally found in relatively small molecules where the rapid tumbling of spins means that $W_2 > W_0$.

DYNAMIC NMR STUDIES.

Conformation changes in molecules are now quite commonly studied by variable temperature nmr (V.T. nmr). Useful references on this aspect of nmr include 2-6.

Many conformational changes are brought about by rotation of a bond. In such a rotation there are energetically favoured positions of the substituents eg a planar arrangement is most favourable for the substituents on 2 carbon atoms joined by a (p-p) π band. The dependance of the energy on the angle of rotation about the double bond is shown in FIG.16. To convert isomer A into isomer B, $\Delta G^{\#}_{AB}$, the free energy of activation must be supplied. The reverse isomerization $\Delta G^{\#}_{BA}$, differs from $\Delta G^{\#}_{AB}$ by ΔG^{o}. The magnitude of the free enthalpy of activation determines the rate of the thermal isomerization. If $\Delta G^{\#} > 23$ Kcal/mol the isomers are stable at room temperature; smaller $\Delta G^{\#}$ values lead to more or less thermal isomerization, the rate constant, kr, of which is related to $\Delta G^{\#}$ in accordance with the Eyring equation[6]:

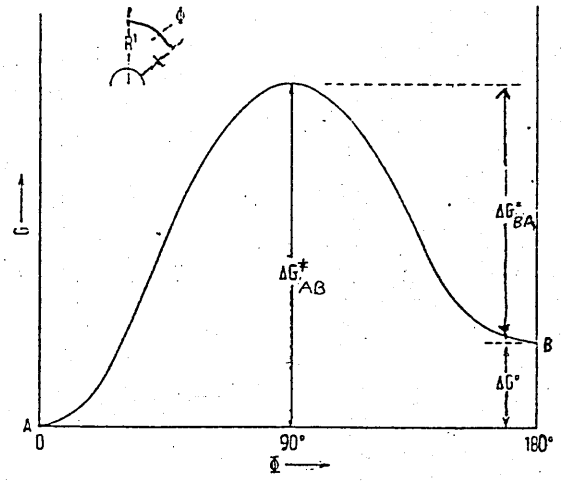

FIGURE 16

Energy profile for rotation about a double bond. For A and B.

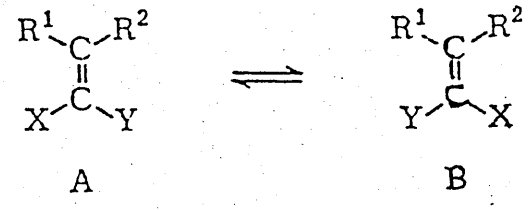

FIGURE 17

FIGURE 18

Temperature dependence of the NMR spectra chemical exchange (uncoupled AB case)

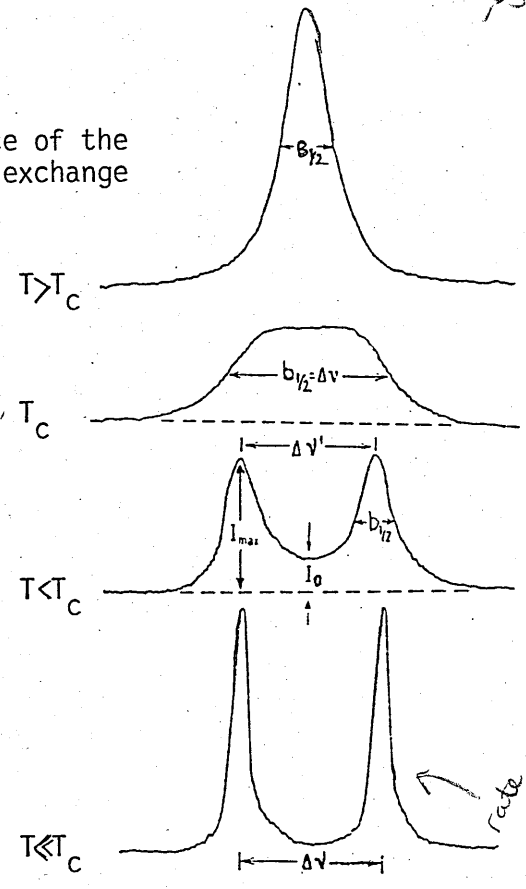

FIG. 18-1

FIG. 18-2

FIG. 18-3

FIG. 18-4

$$k_r = \frac{k_B T}{h} e^{-(\Delta G/RT)} \qquad \text{EQN 1.}$$

(K_B=Boltzmann constant; h=Plancks constant; R = gas constant; T = absolute temperature)

$$\Delta G^{\#} = 4.57T(10.32+\log T/Kr)$$

Separation of isomers is possible if the mean lifetime is of the order of a few hours or more ie Kr < 10^{-4} sec^{-1} or $\Delta G^{\#}$ >23Kcal mol^{-1} (25°C)

The conditions for nmr spectroscopy studies are particularly favourable when $R^1=R^2$ in FIG.17. A and B are then chemically identical (degenerate isomers) However if X and Y are different, R^1 and R^2 are no longer equivalent and rotation leads to exchange of R^1 and R^2 'Slow' isomerization ($K_c<\Pi\Delta V/2^{1/2}$) where ΔV = signal splitting without exchange) leads to 2 separate signals for R^1 and R^2 FIG.18-4 while fast rotation gives only one signal with an intermediate chemical shift FIG.18-1. For thermally induced rotations the shape of the signal in the transition region 18-2,18-3 can be used to determine the rate constants. The theory of line broadening is well developed[7] with respect to conformational changes, and several methods of evaluation are available (a) approximation equations (b) by graphical evaluation of certain spectral features/parameters (c) computer matching of measured and calculated spectra, (The work in this thesis was concerned with method (a) only).

FIG.18 shows the situation when 2 atoms (or groups) with initially sharp signals of equal intensity (18-4) undergo chemical exchange (uncoupled AB case). For evaluation by approximation equations, parameters such as line separation, $\Delta\nu$[8], and the coalescence temperature[9], are found from the spectrum. The coalescence temperature (Tc) is the temperature at which the 2 signals just coincide FIG.18-2. Kc - the rate of chemical exchange at Tc is given by

$$Kc = \pi\Delta\nu/2^{1/2} = \tau^{-1} \qquad \text{EQN 2}$$

($\Delta\nu$ - line separation (H_2) without exchange), τ = relaxation time) for the uncoupled AB case.

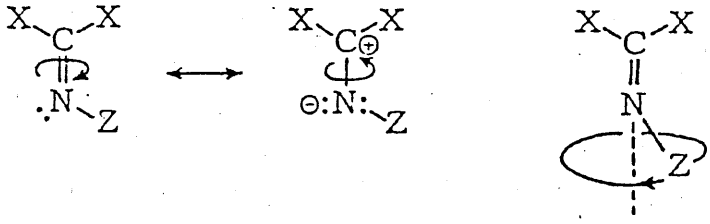

FIG.19
"OUT OF PLANE" ISOMERIZATION.

CARBON-NITROGEN DOUBLE BOND ROTATION
AND INVERSION.

FIG.20
"IN PLANE" ISOMERIZATION

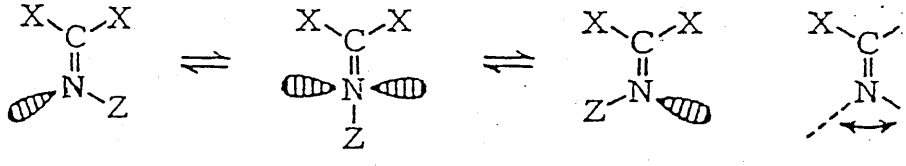

For the coalescence of an AB type spectrum to A_2 there is[9]

$$K_c = \Pi(\Delta\nu^2 + 6J^2)^{1/2}/2^{1/2} \qquad \text{EQN 3}$$

(J - coupling constant for the nuclei A and B)

The free enthalpy of activation $\Delta G^{\#}_T$ can be calculated from the rate constant Kr by means of the Eyring eqn (EQN.1).
By letting

$$\frac{k_B T_c}{h} = A \quad (A = \text{frequency factor})$$

then $K_c = Ae^{-(\Delta G_c/RT_c)}$ EQN.4

The rate of intramolecular rotations and inversions, like that of other reactions, also depends on the solvent and on the concentration of the solute. Free rotation about a bond in a molecule may be sterically and electronically hindered - the latter due to resonance effects which give the single bond partial double bond character.

The systems of interest in the current study have imine (C=N), functions as well as bridgehead nitrogens, which may contribute to rotation and inversion - and thus these 2 possibilities for the syn and anti isomerization of imines - are briefly considered at this point.

ROTATION (FIG.19). During a rotation the substituent, Z, describes a circle about the axis of the C=N bond ("out of plane" isomerization). The process is favoured by polarization of the CN double bond. The sp^2 hybridization of N and hence the bond angle C-N-Z is retained.

INVERSION (FIG.20) The N-Z bond swings in the bond plane of the imine system from the syn into the (identical) anti position ("in-plane" isomerization). The bond angle C-N-Z increases to 180° in the transition

FIGURE 21

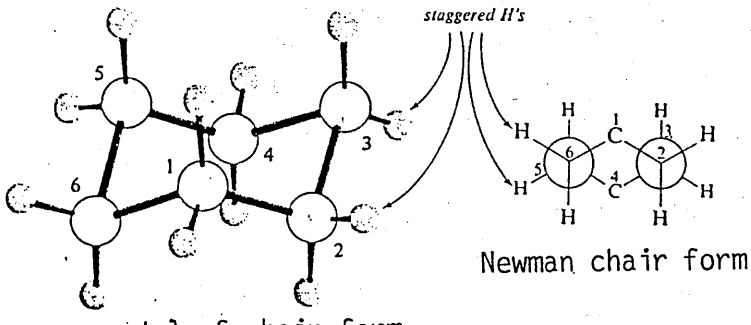

FIG.22

Molecular models and Newman projections of the chair and boat forms of cyclohexane

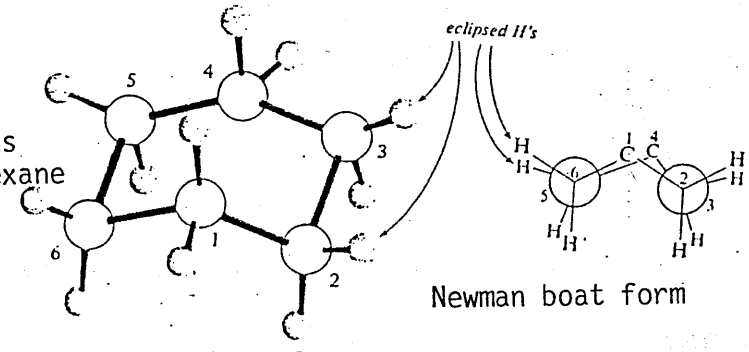

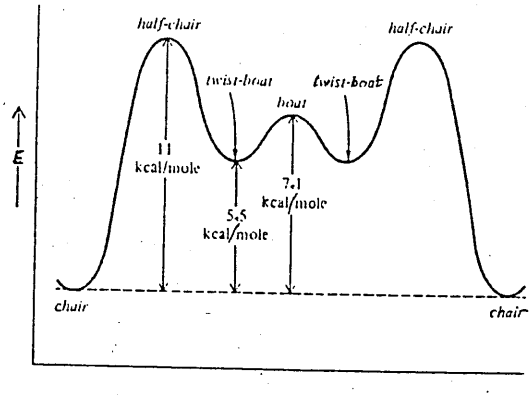

FIGURE 23

Relative potential energies of the conformations of cyclohexane.

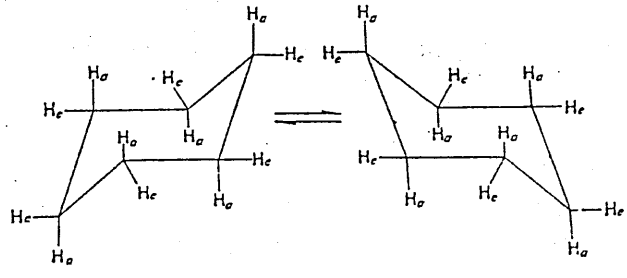

FIGURE 24

state. Therefore the C=N double bond is, to a first approximation, unaffected.

The inversion of the nitrogen pyramid in amines is known to proceed via a planar state by a change in the hybridization of the N atom from sp^3 to sp^2. The barrier in ammonia and in amines is so low (<6Kcal/mol) that it is difficult to detect by nmr. In ring compounds this barrier is usually higher (especially in small membered rings). This is because in the planar transition state the N is sp^2 hybridized so that the bond angle must increase to 120° during the inversion. When the nitrogen is incorporated into a small ring however, the necessary spreading is hindered ie the activation energy increases.

CONFORMATION OF SATURATED RING COMPOUNDS.

Early nmr investigations of the conformation of ring compounds were mainly centered on cyclohexane and its derivatives. The cyclohexane ring can adopt various shapes FIG.21 and any single cyclohexane molecule is in a continuous state of flexing into different shapes. However only the chair form has the favourable staggered - hydrogen structure in which repulsions between the bonding electrons to the hydrogen atoms are minimized FIG.22. The eclipsing of the hydrogens, as in the boat form increses the energy of the molecule. The energy requirements for the interconversion of the different conformations are shown in FIG.23. At any given time about 99.9% of cyclohexane molecules are in the chair form. Thus the single proton resonance absorption band observed at room temperature is attributed to the rapid chair-to-chair interconversion FIG.24. The rapid equilibrium averages the chemical shift difference between the axial and equatorial protons since the process of interconversion (brought about by partial rotation of each C-C bond) puts an equatorial (eq) H into an axial position and vice versa FIG.25. As the temperature is decreased the signal shows a progressive broadening of the absorption band until at -70°C 2 distinct bands appear[10]: the signal at lower fields being assumed to be that of the equatonal hydrogen nuclei[11]. The chemical shift difference between ax and eq protons probably has its origin in a long range shielding effect

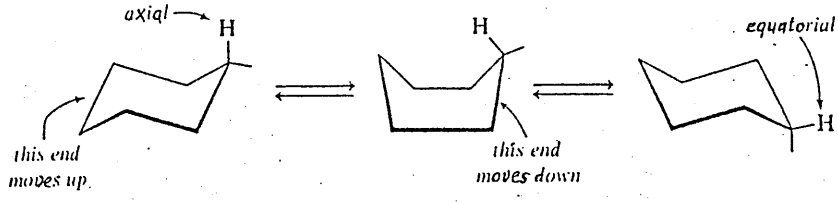

FIGURE 25

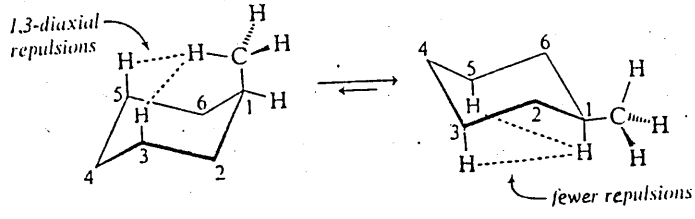

FIGURE 26

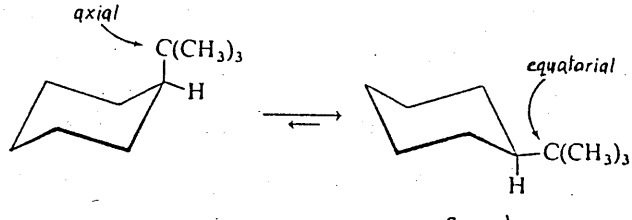

FIGURE 27

favored

connected with the diamagnetic anisotropy of the C-C bond. For the above equilibrium., T_c=-66.5°C and $\Delta G^{\ddagger}$ = 10.1 Kcalmol^{-1}. It is, however, only when the cyclohexane ring is 'locked' and made conformationally rigid by substitution on the ring, that information about the coupling constants for the axial and equatorial protons in the various vicinal and geminal relationships may be obtained.

When a substituent is in an axial position - there are repulsive interactions between the substituent (eg a CH_3 group) and the axial hydrogens on the same side of the ring (FIG.26) Thus at room temperature about 95% of methyl cyclohexane molecules are in the conformation in which the methyl group is equatorial. The bulkier the group, the greater is the energy difference between the axial and equatorial conformers. When the substituent is the tertiary butyl group the energy difference is quite large (5.6Kcal/mol) and t-butyl-cyclohexane is essentially "frozen" in the conformation in which the t-butyl group is equatorial. This allows investigation of the coupling constants. (FIG.27). The observed magnitude of the coupling constants show a close correlation between dihedral angles in vicinal relationships and the HCH angle α, in the geminal coupling situation (cf FIG.7-2 and 9-2 respectively). Thus when α=180°, in vicinal coupling there is a large coupling (Jaxax' J=10-14H_z) resulting from effective overlap of the orbitals. However the other vicinal couplings- Jax,eq' α=60° & J=4-5 Hz) shows a smaller coupling due to less effective orbital overlap.

For geminal coupling, where α=109° there is a large orbital interaction and this is reflected in the magnitude of the coupling constant Jgem ≃ 12-18Hz

Early work on the mono, di and higher halogen substituted cyclohexanes sufferred from lack of resolution and thus overlapping signals, due to the low frequency spectrometers available. However in the chloro[12,13], bromo[12,13], and fluoro[14] derivatives the broader band of the 2 methylene signals was attributed to the axial proton signal resulting from the larger coupling between axial protons.

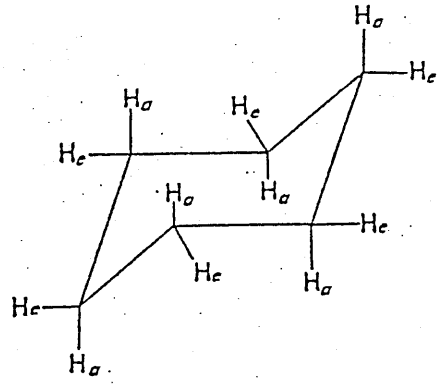

FIG. 28 NN'-DIMETHYL PIPERAZINE.

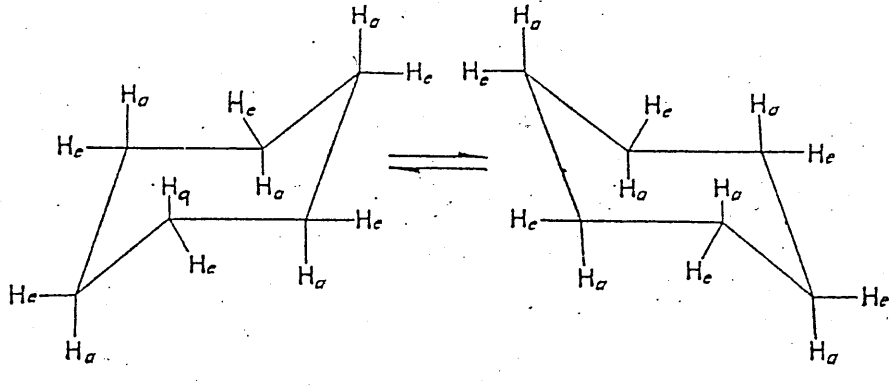

FIG.29 THE EQUILIBRIUM OF THE TWO IDENTICAL CHAIR FORMS OF NN' - DIMETHYL PIPERAZINE

A particularly useful reference compound for the systems under discussion in this thesis is the heterocyclic 6-membered ring compound NN'-dimethylpiperazine[15] FIG.28. At room temperature the ^1H spectrum of the compound in CH_2Cl_2 shows a fairly sharp low field band from the ring methylene protons. From T_c = -27.5°C and the exchange broadened single peak near the fast exchange limit, ($\Delta\nu$), the energy conversion between the 2 identical chair forms FIG.29 was estimated at 13.3 Kcal/mol. At -40°C the low field band resolves itself into an AA'BB' type spectrum. (ie. 4 magnetically non equivalent nuclei forming 2 sets of symmetrically equivalent nuclei separated from each other by a chemical shift which is = to the coupling constants involved). The AA'BB' analysis yielded the following constants-$J_{axax'}$=7.43H_z J_{axeq}(J_{gem}) =13.2H_z, $J_{eqax'}$=2.4H_z. The chemical shift difference between the axial and equatorial hydrogen nuclei is 0.27ppm

The inversion frequency about the nitrogen atom in a 6 membered ring is similar to that for ammonia and therefore the methyl resonance remains sharp at all the temperatures used. Reeves and Stromme noted[15] that increasing the bulk of the substituents may be responsible for the significant increase in energy barrier (per mole) in the series: cyclohexane 29.7 Kcal; chloro and bromocyclohexane ,10.9 Kcal; trans-1,2-dichloro and trans-1,2,dibromo cyclohexane, 1.8 Kcal and NN' dimethylpiperazine 13.3 Kcal.

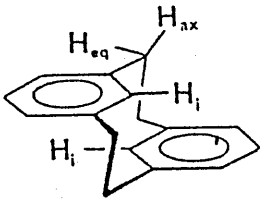

FIG.30-1

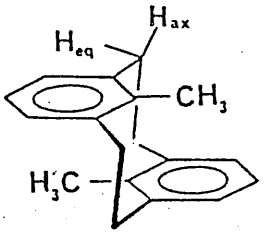

FIG.30-2

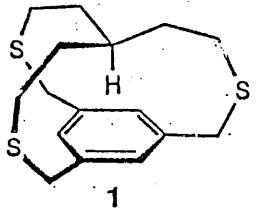

1

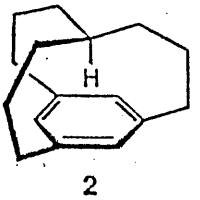

2

FIGURE 31
SMALL STRAINED
CYCLOPHANES.

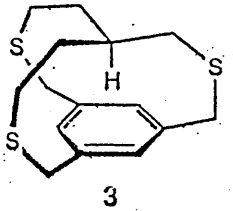

3

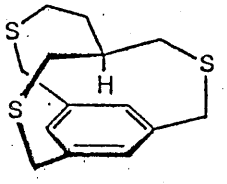

4

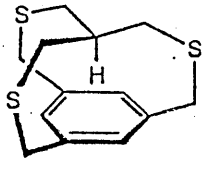

5

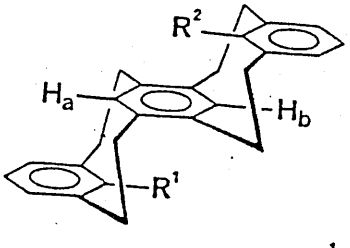

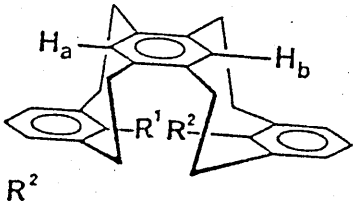

	R^1	R^2	
32-1	H_c	H_c	32-2
32-3	CH_3	CH_3	32-4
32-5	H_c	CH_3	32-6

FIGURE 32
STEPPED CYCLOPHANES.

SELECTED EXAMPLES OF CYCLOPHANES AND THEIR NMR STUDIES

Only one example of a small fixed cyclophane, [2:2] metacyclophane, will be discussed in this section to show what factors affect the nmr spectra of cyclophanes. Firstly though, a brief look at the naming of these compounds. The word 'phane' is the root for all bridged aromatic molecules. To this is prefixed the class name of the aromatic ring(s) that is (are) bridged (eg meta, para, pyridino, furano,...). Preceeding the full name is, at least, 1 set of numbers. The size of the bridge(s) is shown in square brackets. If the position of substitution of the aromatic nucleus is not indicated by the prefix (meta (2,6), para(1,4)) then these are given in parenthesis after the square brackets.

For [2.2] metacyclophane, FIG.30-1, the upfield shift of the internal protons Hi to δ4.20[16], from their normal position of$\simeq$ δ7.0 in meta-xylene is a result of shielding by the opposite benzene ring. This is well investigated[17] and substantiated in terms of ring current theory[18]. Indeed a recent publication [19] shows an extreme case of shielding in a series of small strained cyclophanes FIG.31-1 to 31-5. The methine proton is directed towards the center of the nearby aromatic ring and as a result of their extreme proximity, the signals of the methine proton appears upfield from TMS. FIG.31-2, shows the greatest shielding with the methine proton signal appearing at -4.03ppm (ie.4.03ppm up field from TMS)
The non equivalent AA'BB' bridge protons in [2.2] metacyclophane have a fixed staggered arrangement between -80 and +90°C with H_{ax} at δ2.04 and H_{eq} at δ3.05[20]. The analogous 8-16 dimethyl derivative, FIG.30-2, behaves similarly[21] with the internal methyl protons appearing at δ0.56, considerably shielded from those in 1,2,3-trimethyl benzene (δ2.15). The difference in shielding of Hi in Fig.30-1 ($\Delta\delta$=2.75ppm), and of CH_3 in Fig.30-2 ($\Delta\delta$=1.6ppm) may reflect different conformational geometries in the 2 structures in which the C_8-C_{16} distance is somewhat greater (0.13Å) in the methyl substituted case. This is rationalized by the fact that the methyl protons will be further out of the plane along the Z axis and hence will be less shielded[22]. Both 30-1[20] and 31-2[23] have been shown by X- ray to have the stepped anti structure as shown.

FIG.33-1

FACE CONFORMATION

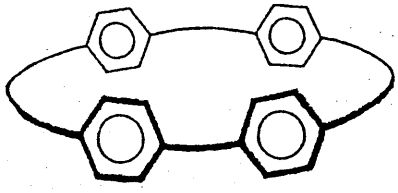

FIG.33-2

LATERAL CONFORMATION

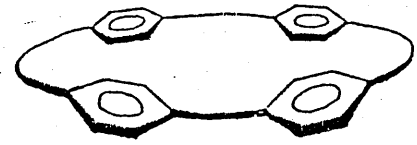

FIGURE 33 TWO EXTREME CONFORMATIONS OF PARACYCLOPHANES.

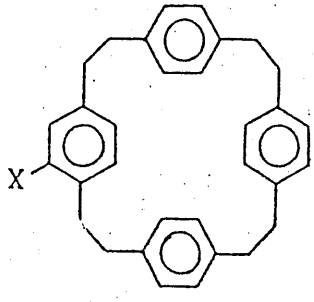

FIGURE 34

34-1 X=H

34-2 $X=NO_2$

34-3 X=CN

34-4 $X=COCH_3$

34-5 X=Br

34-6 X=OH

34-7 $X=OCOCH_3$

34-8 $X=NEt_2$

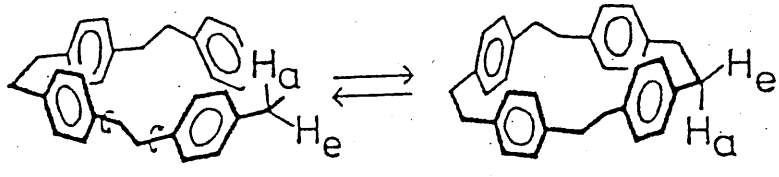

FIGURE 35 TWISTING OF THE ETHYLENE CHAINS.

The introduction of a double bond into one or both of the bridges of 30-1 and 30-2 still leaves the molecules conformationally rigid but it has a rather dramatic effect on Hi[24,25] which in the case of 30-1,ene increases to δ5.62 and for 30-1,1,9 diene, to δ7.90. This deshielding effect, which is greater for Hi than Me_i, has been explained [25 26] as an anisotropic effect of the double bond.

Two compounds [27] exist for the double metacyclophanes 32-1,32-2 $R^1=R^2=H$, 32-3, 32-4 $R^1=R^2=CH_3$ and 34-5, 34-6 $R^1=H$, $R^2=CH_3$ which have been assigned the up-up (uu) and up down (ud) stereochemistry in each case. All internal protons are shielded and thus the structures have been assigned the anti conformation. The ud conformer 32-6 was assigned its structure on the basis of an NOE enhancement of H_c when the CH_3 was irradiated, whereas 32-5 showed no such effect.

For the larger phanes there is a degree of conformational mobility and it is important to determine the preferred conformation of the aromatic rings. In paracyclophanes there are 2 extreme conformations[28,29]: face. FIG.33-1 and lateral (edge). 33-2. The face conformation allows inclusion cavities with a sufficient depth whereas the lateral conformation fills up the cavities so that inclusion of guest molecules is not favoured. This conformation problem can be examined by observing 'Hnmr chemical shift(s) of the aromatic protons. If the face conformation is preferred the protons of each aromatic ring will be in the shielding region of the other aromatic ring(s). As a result the signals of the aromatic protons of the cyclic compound will appear at higher field than those of the acyclic reference compound having aromatic rings that are presumed to rotate freely ie. there is a negative cyclization shift in the aromatic protons-:

$\Delta\delta$(cyc) = δ cyclophane - δ acyclic reference ppm.

This is the case for a number of the larger cyclophanes and moderate $\Delta\delta$cyc values of -0.1 to -0.5ppm have been observed[28-30]. In addition this shielding effect should be stronger with decreasing size of the macroring. Detailed studies were carried out by Tabushi and co-workers[28,31] for [2⁴] paracyclophane FIG.34-1 and its derivatives 34-2 to 34-8. The signal for the ethylene protons of 34-1, a singlet at room temperature, splits into

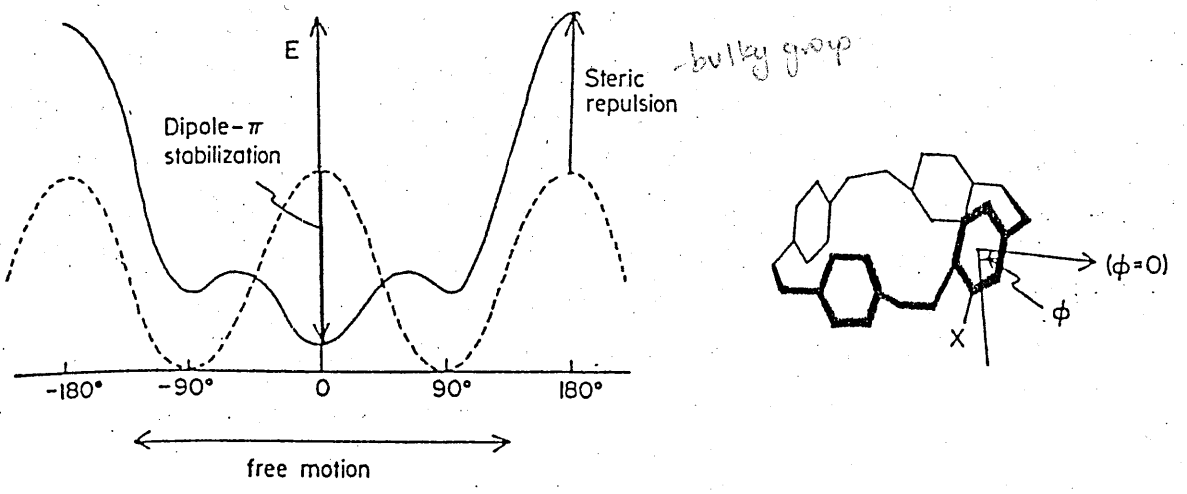

FIGURE 36 ASSUMED POTENTIAL CURVE OF SUBSTITUTED (2.2.2.2) PARACYCLOPHANE (dotted line: unsubstituted paracyclophane).

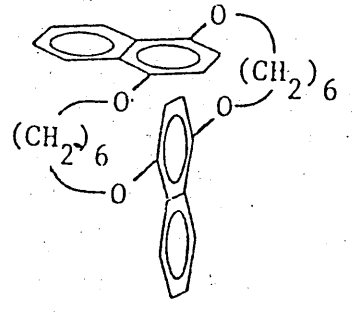

FIG.37-1

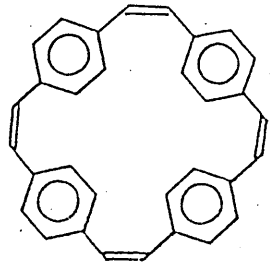

FIG.37-2

FIGURE 37

two doublets at temperatures below -85°C. This splitting is attributed to a restricted twisting of the ethylene chains, and the two signals are assigned to the protons frozen in axial and equatorial sites FIG.35. In contrast the signal of the aromatic protons show only little line broadening indicating that the motions of the benzene rings are not greatly restricted. In such circumstances the δ of the 2 ethylene protons would reflect the average orientation of the benzene rings. The observed chemical shift difference of Hax and Heq ($\Delta\delta$obs=0.51ppm) was compared with the theoretically calculated values for the 3 extreme states of the benzene ring orientation-

all face conformation, $\Delta\delta$calc = 1.0ppm

all lateral conformation $\Delta\delta$calc = 0ppm

non restricted rotation with freely
rotating benzene rings $\Delta\delta$calc = 0,12pmm.

Comparison of the observed value with the calculated value may suggest that the benzene rings still vibrate or rotate to produce a statistically averaged shielding effect but that the face conformation is favoured in a statistical sense.[28] - consistent with aromatics H's showing only small ring shielding.

When the aromatic ring has a bulky or an electron withdrawing substituent (eg.34-2 to 34-5 and 34-8) the lateral conformation tends to be favoured, possibly by steric repulsion and by dipole-π interaction respectively.[31] FIG.36 Although many cyclophanes in solution adopt the face conformation this is not alway the case as exemplified by 34-2, to 34-5 and 34-8 but also by 37-1 and 37-2. In 37-2 and related compounds a planar conformation tends to be favoured because of the conjugated structure[32].

Triple layered cyclophanes have been synthesized[33] FIG.38. For the case of 38-1 it seemed that if each pyridine ring were essentially perpendicular to the central benzene ring direct interaction between the 2 pyridine nitrogens might be possible. In 38-2 this interaction may result in the expulsion of Cl^- to give the ion 38-3. The low temperature (-70 °C)

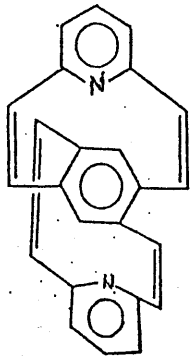

FIG.38-1

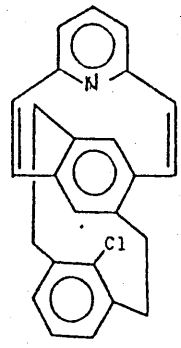

FIG.38-2

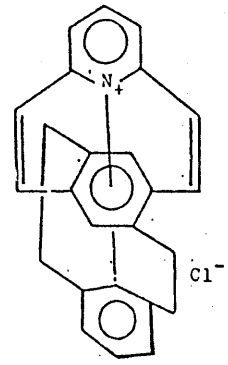

FIG.38-3

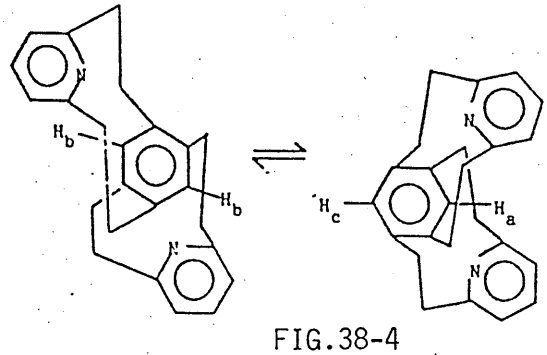

FIG.38-4

FIGURE 38 "TRIPLE-LAYERED 2-6,PYRIDINOCYCLOPHANES

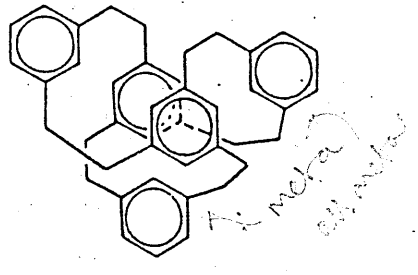

FIG.39-1

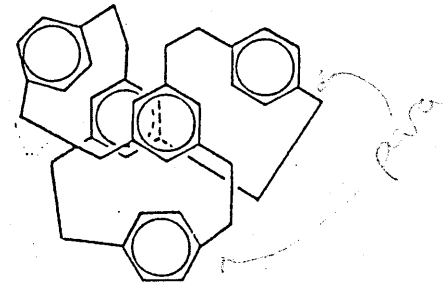

FIG.39-2

FIGURE 39 "CAGE" CYCLOPHANES.

spectrum of 38-4 showed 3 aromatic signals at δ7.5(H_c), δ5.82(H_b) and δ4.41(H_a) (1:2:1 intensity) At room temperature only 1 signal at δ5.9 is observed. This can be explained if the system exists as a mixture of interchanging conformers 38-4 ⇌ 38-5. The Tc = -39°C giving $\Delta G^{\#}$ = 11Kcal/mol for the conformational flipping process. Its behaviour is similar to that of the simple [2.2] (2,6) pyridino-paracyclophanes[34].

The two six-bridged cyclophanes[35] 39-1,39-2 show barriers of $\Delta G^{\#}_c$=36 and 27kJ/mol respectively, and it has been proposed [5] that the meta or para substituted rings might rotate about the methylene bridges. The 'Hnmr of 39-1 at room temperature is simple and the methylene protons appear as an AA'BB' multiplet (δ2.86) Below -88°C these protons appear as 3 peaks and this observation along with the strongly shielded meta ring protons (δ5.73ø and trisubstituted ring protons (δ6.18) is best explained by assuming a compact conformation eg the D_3 symmetry as shown. For 39-2 a high symmetry conformer also seems likely at low temperatures.

Few nmr studies on ^{13}C nuclei have appeared in the cyclophane field, possibly in part because ring current effects for carbon signals are often swamped by other effects caused by geometry changes, steric effects etc. However data for a number of cyclophanes have been published. This includes studies on the tetramethyl substituted metacyclophane[36] shown in FIG 40-1. Although at room temperature it exists in a fixed conformation at higher temperatures the 'Hnmr spectrum shows fluxional behaviour (Tc 50°C, $\Delta\nu$=108Hz, giving $\Delta G^{\#}$ =15.4Kcal mol^{-1}). Molecular models had shown several conformers were possible. Various structures were ruled out by considering the 'Hnmr but the AA'BB' spectrum of the bridge -CH2-CH2 - was not clearly enough resolved to positively distinuish between 40-2 and 40-3. However the ^{13}C spectrum, at -30°C, shows 12 types of aromatic proton, 2 different (CH_2CH_2) carbons, a single type of $-CH_2-$ bridge carbon and two $-CH_3$ carbons. This is consistent with the more symmetrical 40-3.

The triaza [2.2.2] metacyclophane[37] derivative shown in 41-1 adopts a Crown conformation 41-2 in the solid state. Dynamic nmr spectroscopy indicated that in solution it exists as interconverting mixtures of Crown and Saddle, 41-3, conformations - the former predominates at equilibrium.

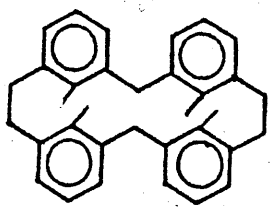

FIG.40-1

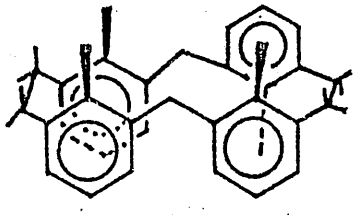

FIG.40-2

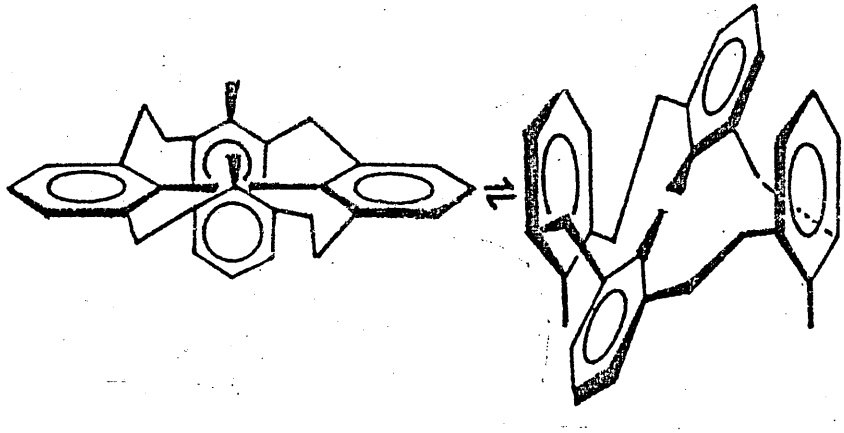

FIG.40-3

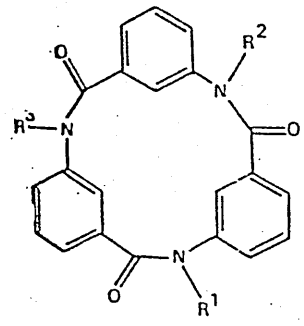

FIG.41-1

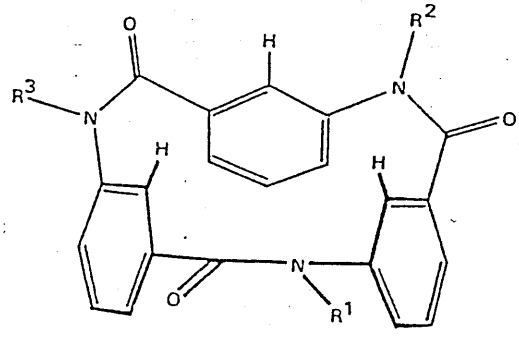

FIG.41-2

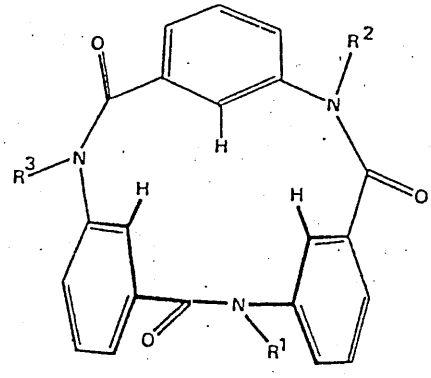

FIG.41-3

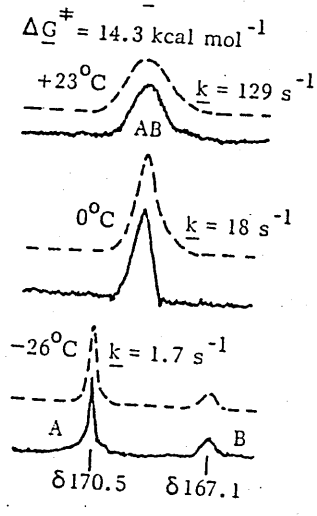

FIG.41-4

It was the temperature dependance of the ^1H decoupled ^{13}C spectrum 41-4 - for the resonances of carbonyl carbons, one of the quaternary aromatic carbons and the N-methyl carbons - that gave the activation parameters for the interconversion of the conformations. At -65°C, two signals with relative intensities 4:1 were observed for each of the above carbons thus enhancing the evidence for the presence of two unequally populated conformations in solution. Line shape analysis gave $\Delta G^{\ddagger}$ of 14.4kcal mol^{-1} for the interconversion of the major into the minor (saddle) isomer.

FIG.42: REACTION SCHEME FOR THE SYNTHESIS OF THE LIGANDS 3Bp AND 3Bm.

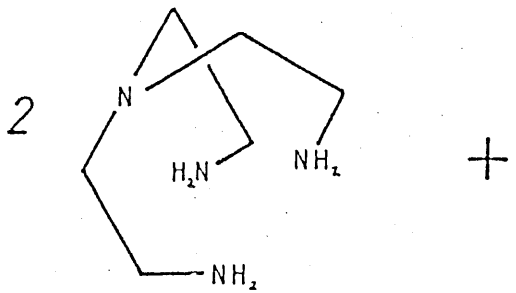

TREN

+

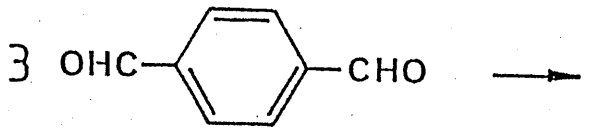

TEREPHTHALALDEHYDE

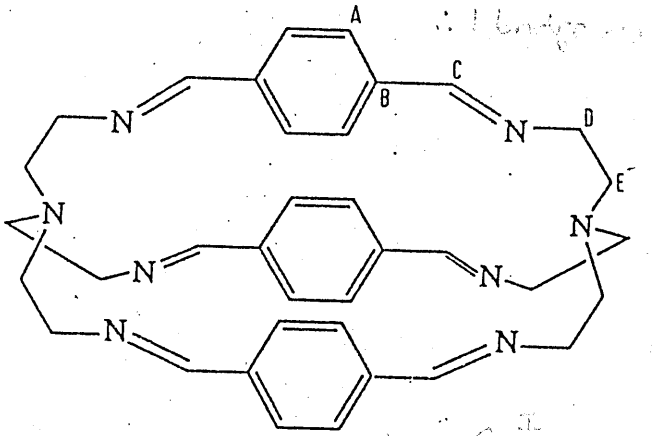

FIG.42-1 3Bp.

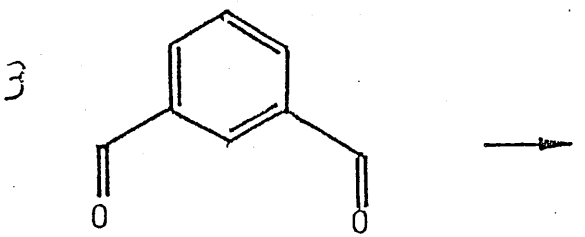

ISOPHTHALALDEHYDE

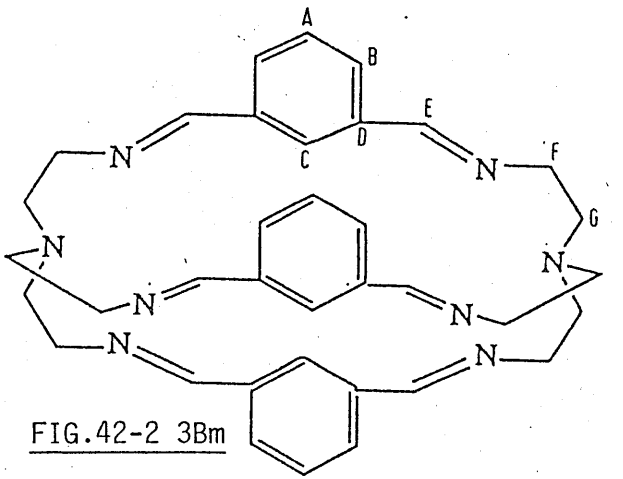

FIG.42-2 3Bm

THE CYCLOPHANES 3Bm AND 3Bp

The two macrobicyclic cyclophanes, 3Bm and 3Bp, were prepared by a (3+2) dicarbonyl/tren Schiff base condensation in methanol. Both are polyaza ligands offering a N_6 donor set. 3Bp can be isolated metal free (78%) by reaction of terephthalaldehyde with tren giving 42-1 whereas 42-2 can be isolated at up to 89% when isophthalaldehyde is condensed with tren. These yields are remarkable considering that the synthesis requires the formation of 6 bonds in a single condensation step. This approach was used by Newkome[38] in the condensation of tris (ethanol) amine with 2,6 dichloro pyridine to give the resulting diazahexaoxo cryptand in only 2% yield, presumably reflecting the low probability of simultaneous formation of 6 bonds. It is not clear why our condensations are so much more efficient: it may perhaps be related to an internal hydrogen-bonding template effect keeping the amine in its appropriate conformation. 3Bp was also obtained as a binuclear cryptate when templated on Ag^{+} and Pb^{2+}. In comparison with 3Bp the meta substituted cage 3Bm would not template with any of the many metals that were tried. Although this is the exception rather than the rule, other macrocyclic Schiff base ligands have been synthesized in the absence of metal ions. Fenton[39] has used a non template synthesis of dinucleating macrocyclic Schiff bases derived from thiophene. The yield depended on the reaction conditions but was maximized at 55%. He explained this metal free ligand synthesis in terms of the predominating cis, cis conformer of the dialdehyde FIG.43-1. This, he proposed, is the conformer that leads most readily to macrocyclization - therefore no metal template is required. Tasker's group[40] have also prepared a series of di-imine tetraaza macrocycles without using a "metal-ion template' or 'high dilution' techniques. The success of this synthesis is attributed to the formation of intramolecular hydrogen bonds in the product which reduces unfavourable lone-pair - lone-pair interactions between the nitrogen atoms. Other references to metal free macrocycles include ref. 41 to 43.

The table in FIG.44 lists appropriate spectral data for both ligands and also for their reduced octaamine derivatives (R3Bm and R3Bp.) Mass spec.

FIGURE 43

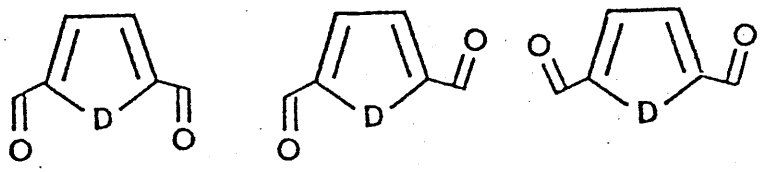

cis,cis cis,trans trans,trans

DIALDEHYDE CONFORMERS.

FIGURE 44. SOME SPECTROSCOPIC DATA FOR THE LIGANDS 3Bm, R3Bm, 3Bp and R3Bp

LIGAND	M^+	EXPERIMENTAL ANALYSIS[a]	IR		ELECTRONIC SPECTRA		
			$\nu_{C=N}$	ν_{N-H}	SOLVENT AND CONCENTRATION	λ[b] (nm)	$\epsilon/M^{-1}\ cm^{-1}$
3Bm	586	C 73.69 (73.9) H 7.2 (7.3) N 19.1 (19.2)	1643		MeOH 10^{-5} M	315 295 256 215[b,c]	6000 8000 21000 197000[c]
3Bp	586	C 62.1 (61.7) H 7.8 (7.9) N 16.5 (16.1)	1643		MeOH 10^{-5} M	263[b] 205[c]	248000 183000[c]
R3Bm.H_2O	598	C 70.7 (70.0) H 9.0 (8.6) N 17.7 (18.1)		3298	MeOH 10^{-5} M	286 250 205[b,c]	4000 7000 67100[c]
R3Bp	598	C 70.7 (70.3) H 9.9 (9.1) N 17.5 (18.0)		3231	MeOH 10^{-5} M	260 204[b,c]	1000 34000[c]

(a) Experimentally found result in parenthesis.

(b) λ_{max}.

(c) Unreliable result.

FIGURE 45 THE IR SPECTRUM OF THE LIGANDS 3Bm, R3Bm, 3Bp, and R3Bp. (KBr disc)

FIG 45-1

3Bm

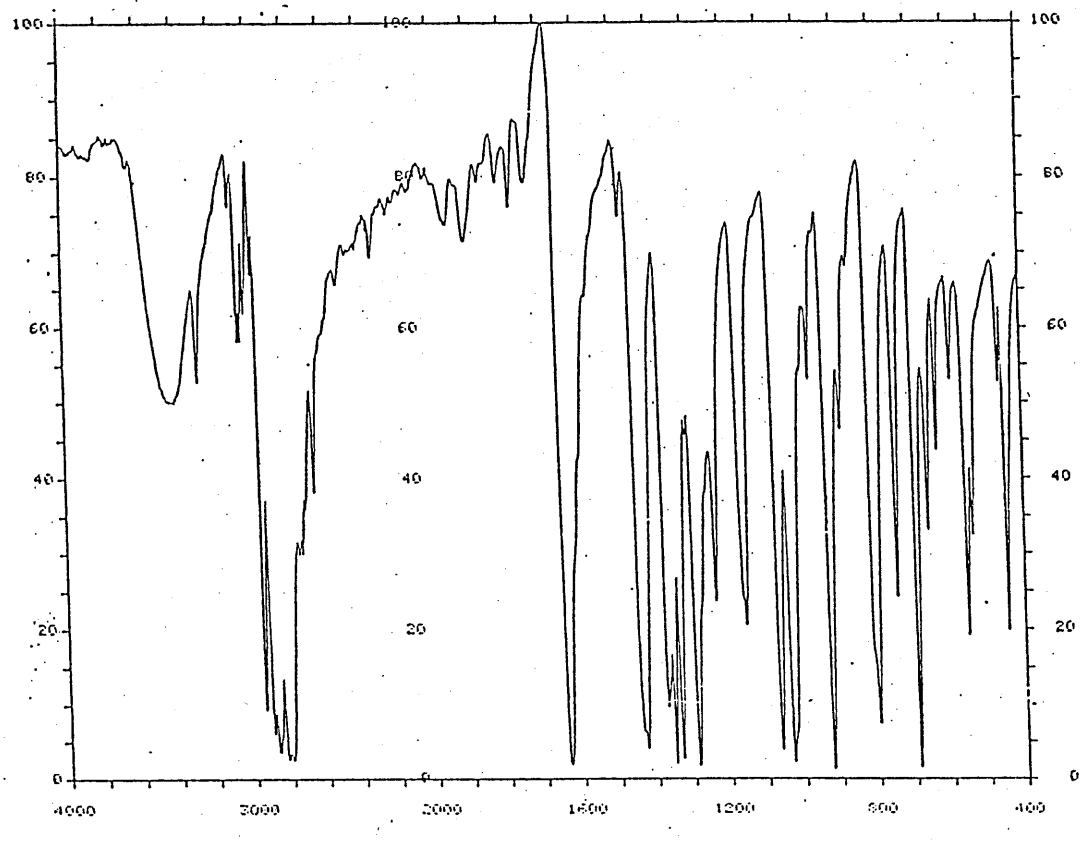

FIG.45-2

R3Bm

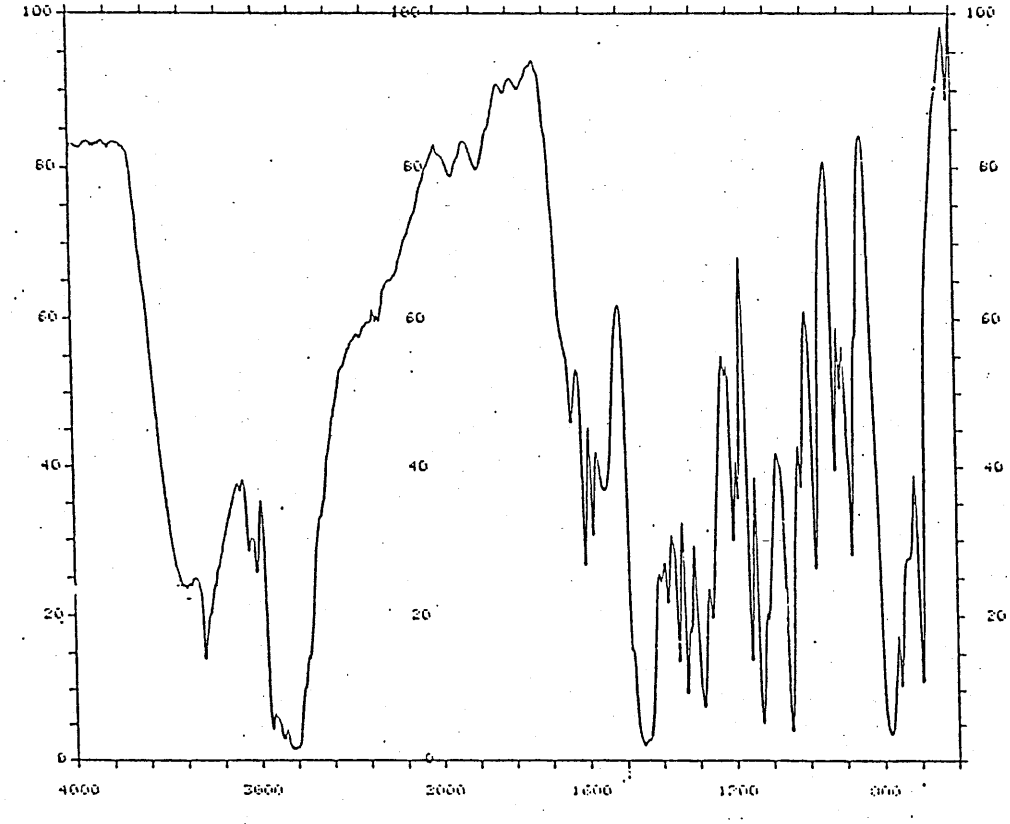

FIG.45-3
3Bp

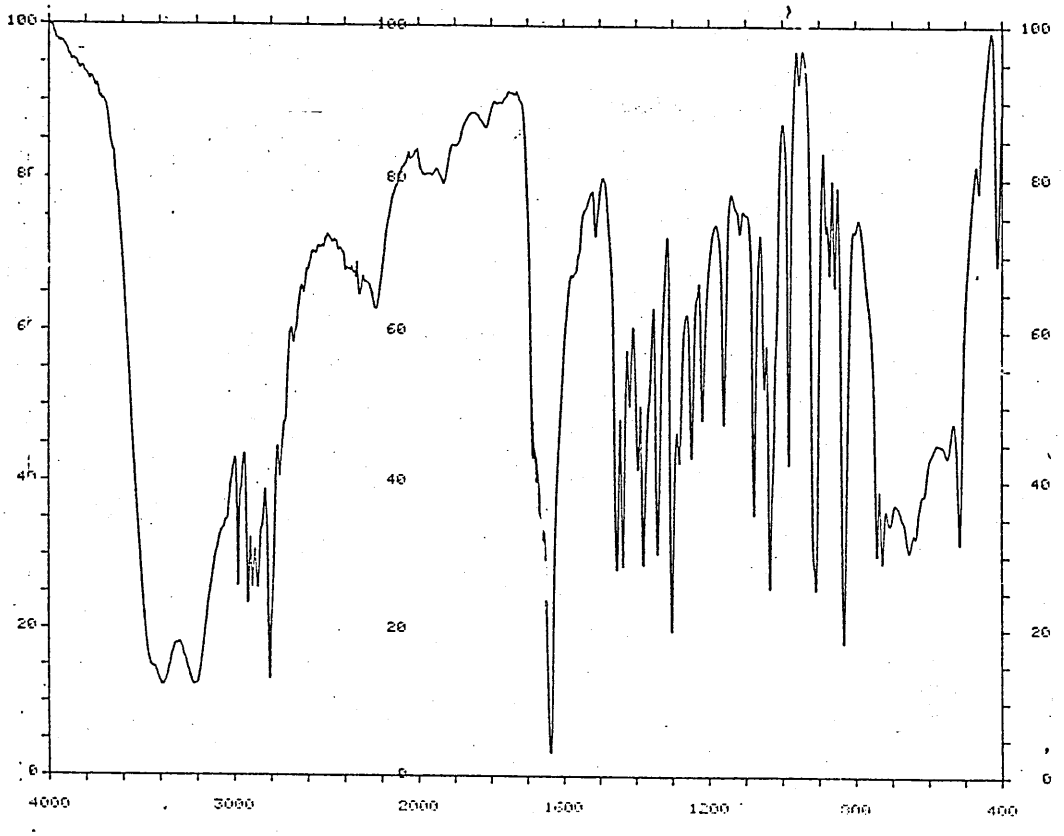

FIG.45-4
R3Bp

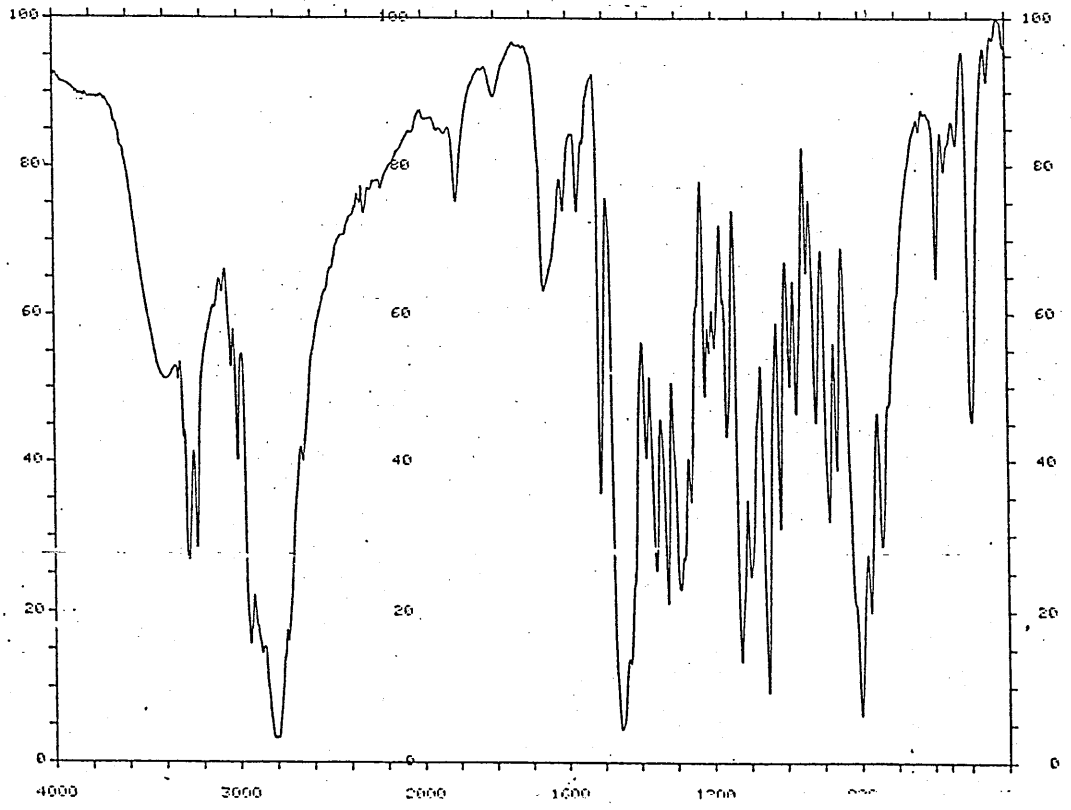

FIG.46-1
ENERGY STATES FOR BENZENE.

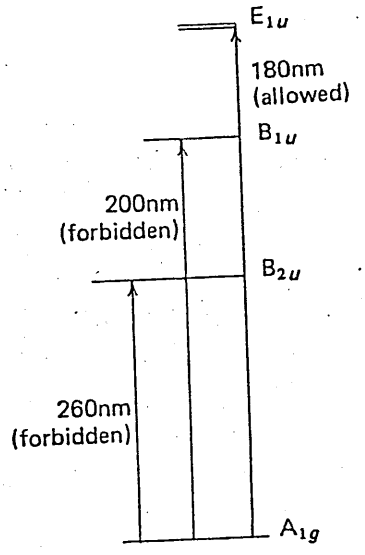

FIG.46-2

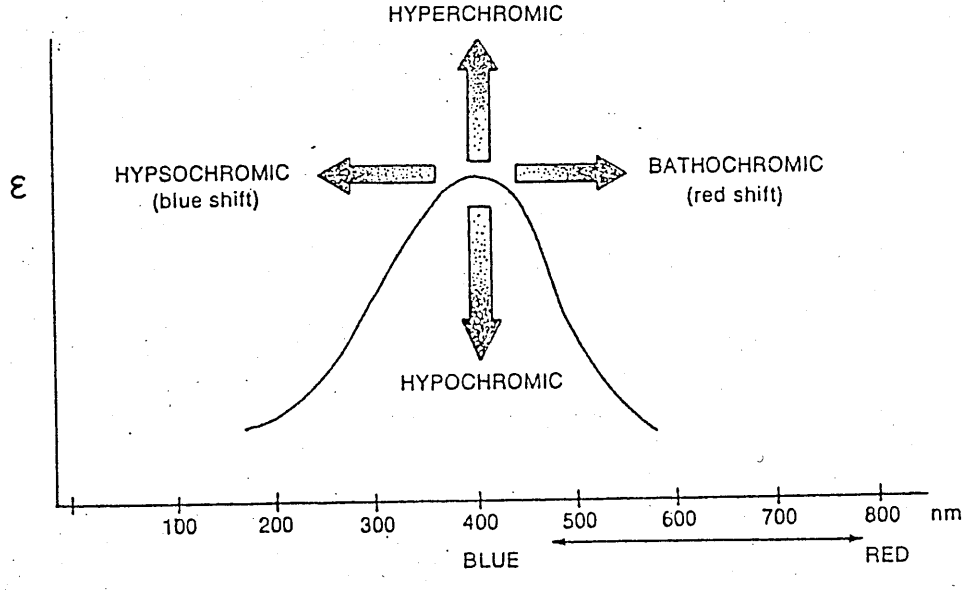

was used to confirm the cyclic as opposed to polymeric nature of the products. The absence of absorptions due to ν_{NH_2} (3500-3300cm^{-1}) or C=O (~1700cm^{-1}) in the ir spectrum of 3Bm and 3Bp (Fig.45-1, 45-3 respectively) together with a medium-strong absorption at 1643cm^{-1}, for both ligands, due to $\nu_{C=N}$, showed Schiff base condensation to be complete. A satisfactory elemental analysis confirmed formation of the desired cryptands in the reaction scheme shown in FIG.42.

The uv spectra of the two ligands are significantly different, FIG.47, and both can be compared with that of benzene[1]. FIG.47-5 Benzene normally shows three π-π^* electronic transitions FIG.46-1. The allowed primary band at 180nm (ϵ = 47,000) is not observed under usual experimental conditions. However in polycyclic aromatic compounds or when another π system is present this band is often shifted to longer wavelengths (ie. a bathochromic shift[1] FIG.46-2. The 202nm absorption is much less intense (ϵ =7,400) and it corresponds to a forbidden transition. The secondary band, which is also forbidden and the least intense of the benzene bands at 260nm, (ϵ = 230), is caused by interaction of the electronic energy levels with vibrational modes and so appears with a great deal of fine structure. This fine structure is lost if the spectrum of benzene is determined in a polar solvent or if a single functional group is substituted onto the benzene ring. In such cases the secondary peak appears as a broad low intensity peak, lacking in any interesting detail. Substitution on the benzene ring is able to cause bathochromic and hyperchromic shifts. Fig.46-2 and thus it is not possible to formulate empirical formula for predicting the spectra of aromatic substances.

Substituents which are themselves chromophores (ie. a group capable of absorbing in the visible and uv regions of the spectrum) usually contain π electrons, eg C=N, C=O. Interaction of the benzene ring electrons and the π electrons of the substituent can also produce a new electron transfer band. This band may be so intense that it obscures the secondary band of the benzene. The position of these high energy transitions are sensitive to the presence of substituents. Unsaturated molecules which contain atoms such as O, or N may also undergo n-π^* transitions which again are sensitive

FIGURE 47. THE UV SPECTRA OF 3Bm, R3Bm, 3Bp, R3Bp and BENZENE.

3Bm

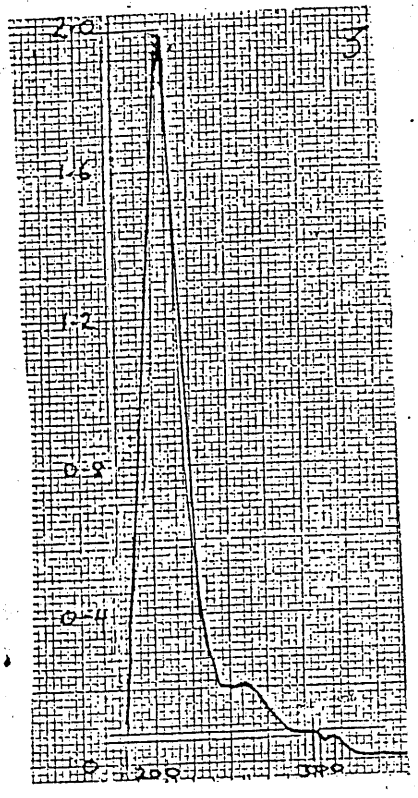

FIG.47-1

R3Bm

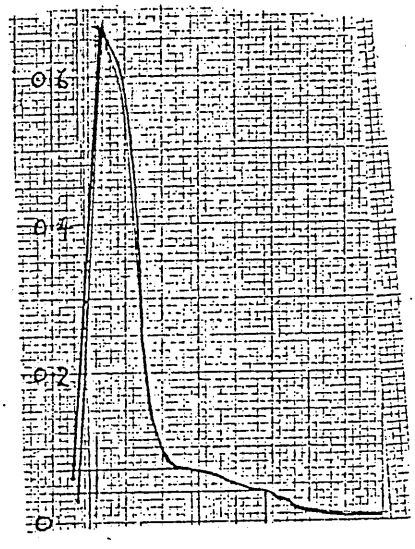

FIG.47-2

BENZENE

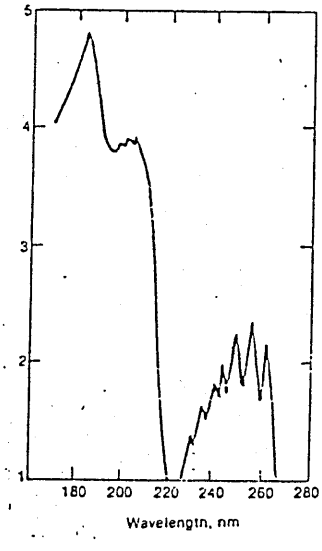

FIG.47-5

3Bp

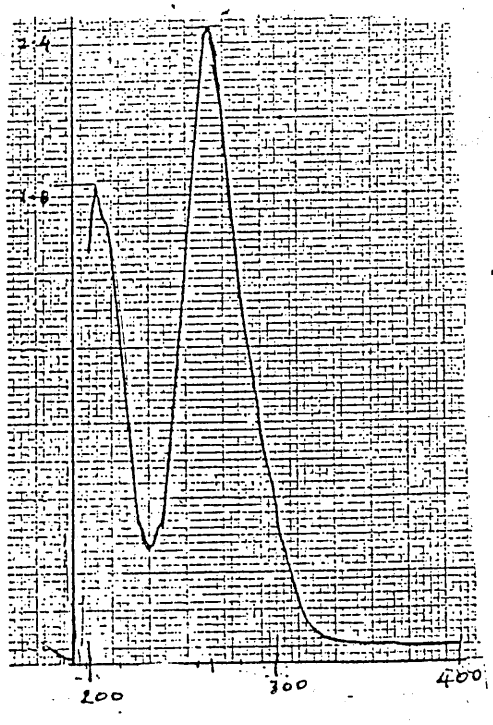

FIG.47-3

R3Bp

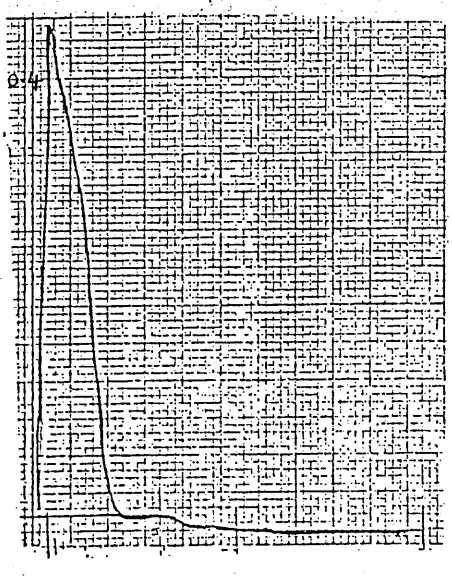

FIG.47-4

to substitution on the chromophoric structure. Most n-Π* transitions are forbidden and of low intensity.

One of the best ways to bring about a bathochromic shift is to increase the extent of conjugation. In the presence of conjugated double bonds the electronic energy levels of the chromophore move closer together resulting in a decrease in the energy required to produce a transition from an occupied energy level to an unoccupied level. Thus the wavelength of light becomes longer and a bathochromic shift is observed. Conjugation of two chromophores not only results in bathochromic shifts but it can also significantly increase the intensity of the absorption.

The ligands 3Bm and 3Bp each contain 2 sets of chromophores - the aromatic benzene units and the imine (C=N) functions. The main difference between the ligands is that in 3Bm the benzene rings are meta substituted whereas in 3Bp the benzene units are para substituted. Thus, because of the shorter length of the imine-ring-imine unit in 3Bm, we would expect this system to show greater steric constraints and indeed greater interaction of the 2 sets of chromophores. This may well be the cause of differences in the electronic absorption spectrum of 3Bm(47-1) and 3Bp(47-3). Indeed it may also be the cause of differences between the reduced and unreduced forms of the ligands (discused later) 3Bm shows only one intense peak (λmax 215nm ϵ=197000) whereas 3Bp shows 2 intense peaks (λ205m ϵ=183,000 λmax 263nm ϵ=248,000). All 3 peaks show substantial hyperchromic behaviour with the extinction coefficients well above those observed for the 2 primary absorption bands of benzene. The range given in many textbooks[1] for a $\pi\pi^*$ transition is one in the order of $\epsilon \simeq 10^4$, thus some of the observed extinction coefficients of these macrobicyclic ligands are quite high (10^5). Certainly many of the very intense absorptions observed in the ligand series lie close to the cut-off points of the solvents used (acetonitrile 190nm; methanol 205nm) and to the cell cut off points and thus their extinction coefficients are unreliable. However the 3Bp absorption at 263nm (ϵ = 248,000) cannot thus be explained. There are two possible explanations for this high (10^5) value. Firstly, absorptions may be additive - in 3Bp there are 3 aromatic units and this would correspond to $\epsilon \simeq 82,000$ ($\epsilon \simeq 10^4$) per aromatic unit. This additive effect does not appear

to be effective in Tabushi's 4°,5° paracyclophanes [44] where λ_{max}=274nm and ϵ≃1300, ϵ=1700 respectively. The explanation for the observed extinction coefficients may thus lie in the second reason - that is conjugation. Indeed many anthracene or naphthalene based compounds show $\epsilon \simeq 10^5$ and extinction coefficients of the order of 10^6 have been observed. Unlike Tabushi's paracyclophanes, in which the aromatic rings are the only chromophores, 3Bp has 2 sets of chromophoric units - the aromatic rings and the imine functions. A high degree of conjugation, ie. delocalization, can lead to significant interactions of the chromophores and thus to a significant hyperchromic effects and/or bathochromic shifts. However it is interesting to note that the solid state conformation of 3Bp (X-ray structure-discussed later) indicates that these imine functions are in fact quite localized. The 3Bp spectrum may also be showing a significant bathochromic shift of the two benzene primary bands (180 -> 205nm and 202nm -> 263nm). Alternatively we may be observing the benzene Π-Π^* at 205nm and that of the imine at 263nm. There was no evidence of any other absorptions in 3Bp. 3Bm on the other hand showed various other absorptions with the intense aromatic Π-Π^* at 215nm. A broad absorption (λ=256nm ϵ = 21000) may be the secondary absorption band of the benzene unit although it may also be the Π-Π^* absorption of the C=N function. Two less intense absorptions may be n-Π^* imine absorptions.

I.R and nmr gave no indication of any intermolecular interactions of eg. hydrogen-bonded water in the case of 3Bm but both ir and 'Hnmr spectra indicated that 3Bp retains solvate water. This was confirmed in its X-ray crystallographic structural determination; 3Bm and 3Bp have both been structurally characterized.

THE CRYSTAL STRUCTURE AND NMR OF 3Bm

The structure of the macrobicycle 3Bm (determined by Vickie McKee and Ward.T.Robinson, University of Canterbury, Christchurch, New Zealand) is shown in FIG.48-1. The end-on view, FIG.48-2, has a "Manx" emblem profile, with a 3 fold non crystallographic axis running through the 2 bridgehead nitrogens, N(1) and N(2) which are 10.677Å apart. It also has a mirror

FIGURE 48 - X-RAY STRUCTURE OF 3Bm.

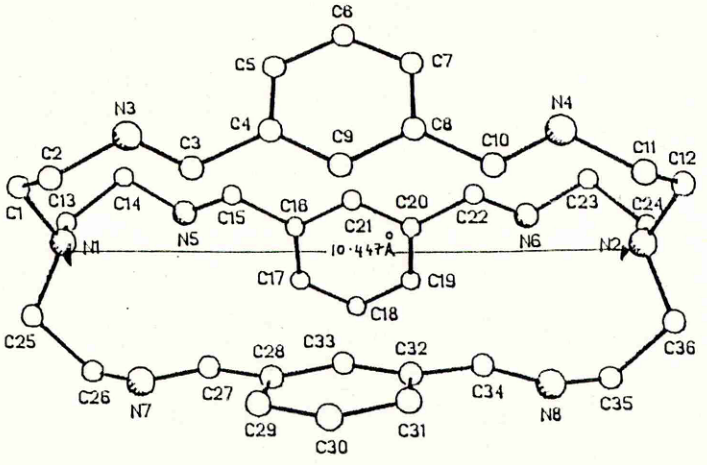

FIG.48-1

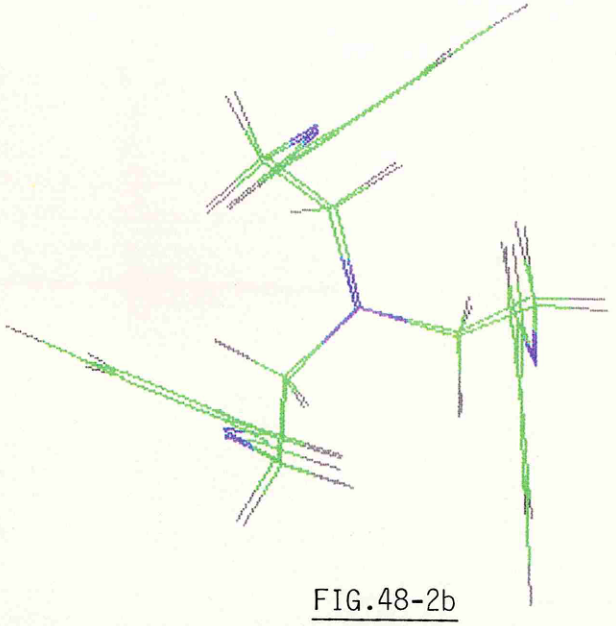

FIG.48-2b

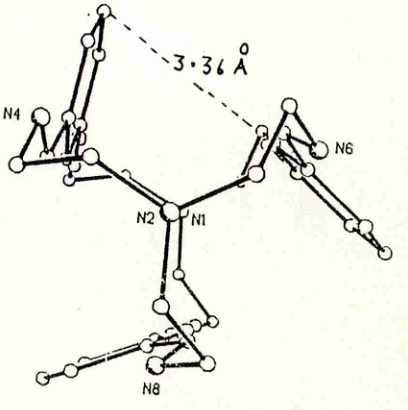

FIG.48-2a

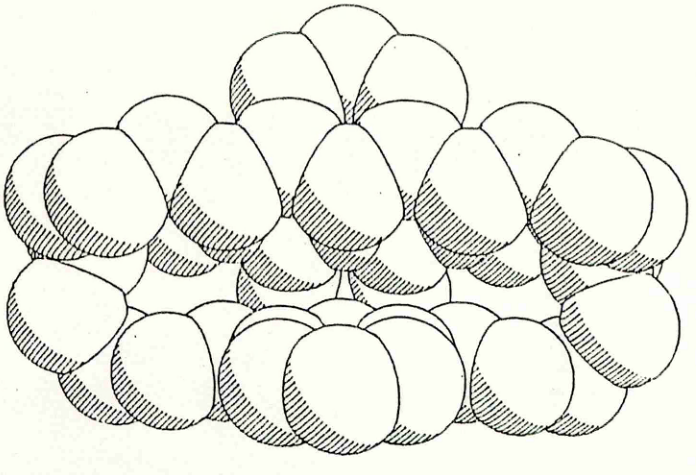

FIG.48-3

plane (non-crystallographic) running through C_{31}, C_{21} and C_{33} (ie C_c of each aromatic ring). From 48-2 it can also be seen that the methylene carbon atoms are eclipsed. FIG.48-3 shows how little free space there is inside the molecule in this conformation. In each case Cc is 3.6Å from the mean plane of the adjacent ring. Both X-ray and modelling studies (the latter by M.Drew of Reading University) indicate close approach of the Hc proton to the adjacent aromatic ring. The 'Hnmr of 3Bm (later discussion) strongly suggests that the Hc proton lies within the shielding area of ring current provided by the adjacent ring. Thus although this ligand would appear to offer good steric protection to an encapsulated guest atom or molecule the small size of the cavity, shown in Fig.48-3, makes it seem unlikely that 3Bm, in this conformation with the CH_2 groups eclipsed, could act as a host to many guests. Indeed M^{c}Kee has calculated that a sphere of no more than 1.46Å radius could be accomodated within this triangular array of the aromatic rings.

Coordination of one or more metal ions by the ligand in its X-rayed conformation would effectively mean that any small atom inside the cavity would have to bond to the Cc atoms of the aromatic ring because of the unsuitable arrangement of the N-donor atoms which are directed away from the cavity, FIG.48-2, ie they are divergent. This may, partly, help to explain the reluctance of this ligand to form by means of a template reaction using main group ions such as Pb^{2+} or Ag^{+} or GroupII metal ions, so often employed in this capacity. Within the last couple of months we have succeeded to 'insert' rather than'template' a pair of silver ions and a pair of Cu^{I} and Cu^{II} ions into 3Bm. (These are discussed in the next section). This implies that FIG.48-2, where the N donors are divergent, does not represent the only possible conformation. Fluxionality in the 'Hnmr spectrum of 3Bm FIG.49 suggests that the convergent conformation might also be accessible, at least in the presence of suitable metal ions. A table of nmr data for 3Bm is given in FIG.50.

Initially it was thought that the fluxionality might be explained by rotation of the aromatic ring about the imine-aromatic bond (H_D—C—H_E). This would generate a conformation very different from that seen in the solid state. However even at room temperture FIG.49-1 the signal of the

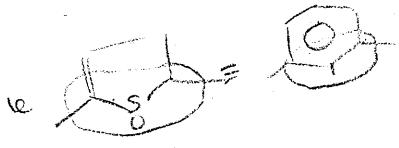

See P 21 2nd para

FIGURE 49 Hnmr of 3Bm.

FIG.49-1

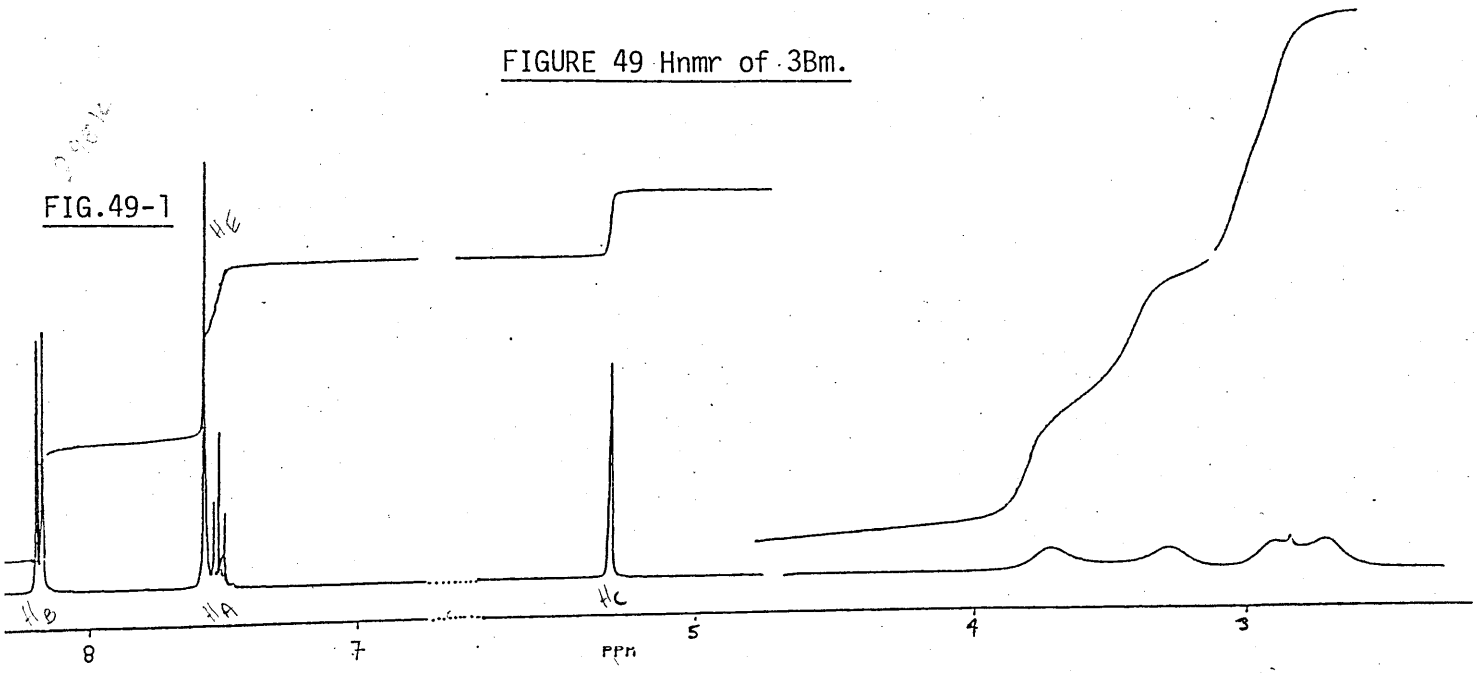

FIG.49-2

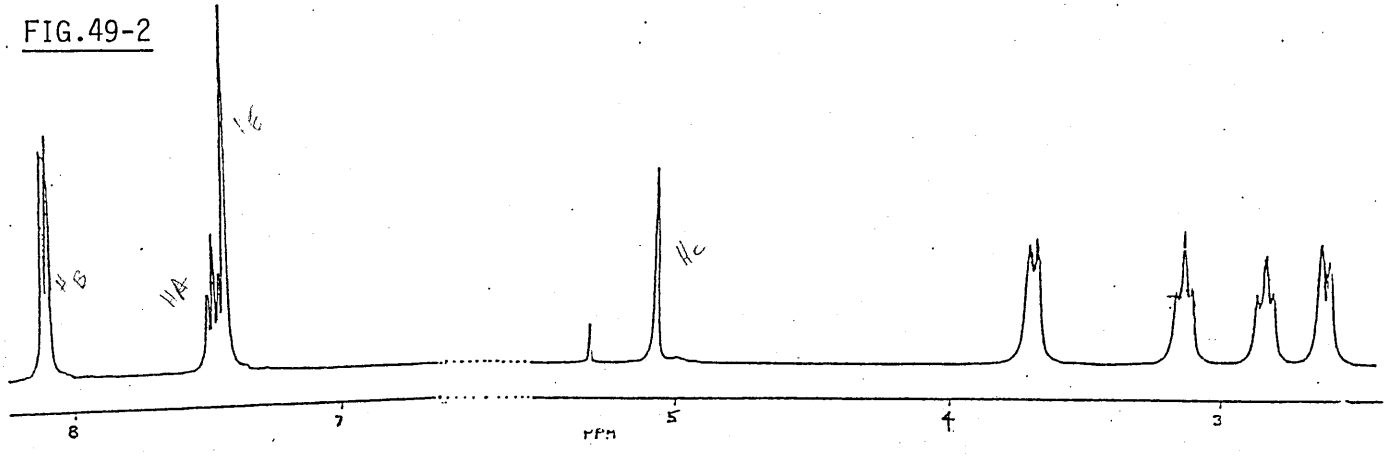

FIG.49-3

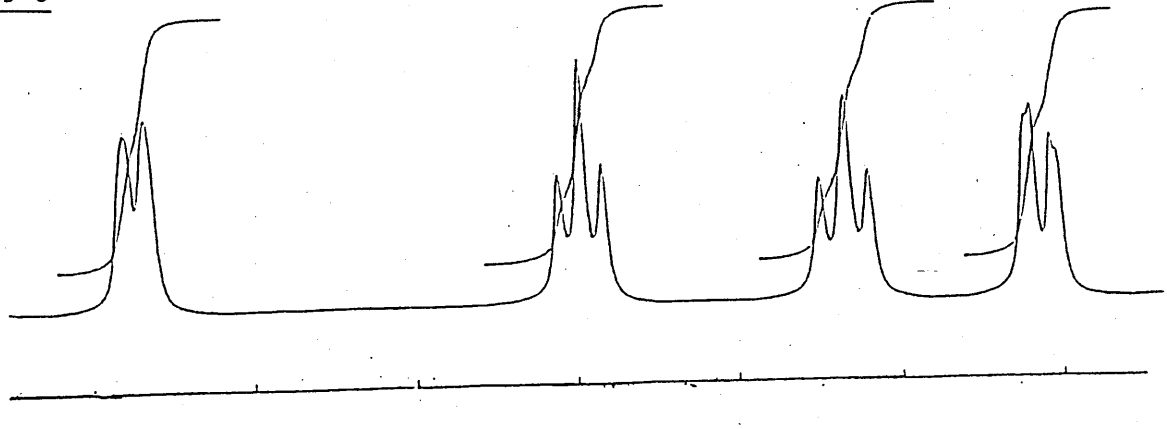

FIGURE 50. A TABLE OF $^{1}H^{a}$ AND ^{13}C N.M.R. DATA FOR THE LIGAND 3Bm

TEMPERATURE (K)	SOLVENT	SPECTRUM	HYDROGEN/CARBON SITE						
			A	B	C	D	E	F	G
298	CD_2Cl_2	^{1}H, 360 MHz	7.52 (tr)	8.19 (d)	5.33 (s)		7.58 (s)	3.72 3.29 (br,s)	2.89 2.70 (br,s)
203	CD_2Cl_2	^{1}H, 400 MHz	7.52 (tr)	8.14 (d)	5.14 (s)		7.49 (s)	3.75 (d)[b] 3.19 (tr)	2.87 (tr) 2.62 (d)
203	CD_2Cl_2	^{1}H, NOE 400 MHz	c	2.8[d,e]	14.28[d]		c	3.6 (ax)[d] 1.47 (eq)[d]	
203	CD_2Cl_2	^{1}H, NOE 400 MHz		2.1[d]	c		7.4[d]		
298 203	$CDCl_3$	^{13}C[f] 90 MHz	131.54, 128.58, 126.0 all doublets			136.18(s)	159.77 (d)	59.41 (t)	55.03 (t)

(a) ppm from TMS = (s) singlet, (d) doublet, (tr) triplet, (br) (broad), (ax) axial, (eq) equatorial

(b) Poorly resolved

(c) Irradiation into this signal.

(d) % NOE enhancement.

(e) Partly due to accidental irradiation of H_A.

(f) Symbol in brackets represents multiplicity in off resonance spectrum.

aromatic protons appear as a sharply defined doublet (H_B) and a triplet (H_A).. H_B, which has an integration value corresponding to six protons (ie $2H_B$ protons per each of the 3 aromatic rings) appears as a doublet as a result of coupling ($J_{AB}=7.6H_z$) with the single H_A proton. H_A appears as a triplet because of coupling with the 2 adjacent H_B protons and thus the n+1 splitting rule applies here, where n is the number of neighbouring equivalent protons. The J coupling constant is of course equal to that seen in the H_B signal, because each set of protons, H_A and H_B, couple with each other equally. The doublet feature (which is really a pair of unresolved doublets) also shows a small coupling of J=1.6 H_z with the Hc proton, with which it has a 'meta' relationship. No coupling of H_A and H_c is evident in the spectrum. The aromatic signal thus being 'frozen' into sharp triplet and doublet features implies that the aryl rings are rigidly held in their triangular disposition even in solution. Therefore there is no evidence of involvement of the aromatic protons in the fluxional process.

The aromatic Hc proton appears essentially as a sharp singlet at δ.5.33 (although there are signs of its coupling with H_B($J=1.6H_z$)) which is significantly at the highfield range of the spectrum for an aromatic proton. Although significantly shielded it is not experiencing as large a shielding force as the equivalent proton in [2.2] metacyclophane FIG.30-1 which appears at δ4.25. Indeed it is closer in value to that of the more flexible monoene form of [2.2] metacyclophane where Hc appears at δ5.62. It is clear therefore that although Hc in 3Bm is experiencing a shielding effect from the adjacent ring, it is not pointing as far into the ring current as in [2.2] metacyclophane (where Hc is 2.689Å from the mean plane of the adjacent aromatic ring)[45] and thus as is indicated by the X-ray structure of 3Bm FIG.48-2, the Hc proton is not lying over the centre of the adjacent ring (where it would experience the maximum shielding effect) but off centre. At 3.36Å it also lies further away from the adjacent ring which also serves to decrease the effective shielding.

Just as the Hc protons are at unusally high fields for aromatic protons, the H_B signal (the doublet) lies downfield, at δ8.19 about 1ppm from the

normal position of 7.2-7.0ppm. This may result from a deshielding effect of the ring current of an adjacent aromatic ring and the imine function.

The imine proton, H_E, which was unassignable in amongst the aromatic signals in the initial 250MHz spectra, was assigned on the basis of coupling patterns in the high resolution 400MHz nmr spectrum in which the ~~the~~ coupling patterns are quite distinguishable. It is therefore possible to assign the singlet at 7.58H_z to the imine protons H_E and the triplet feature centred at δ7.52 to the aromatic H_A protons.

Although at room temperature the methylene proton signals appear as broad unresolved doublets near their coalescence temperature , at -70° (203K) each methylene group is frozen out into a sharp triplet and doublet. ie an AA'BB' spectrum. In these systems the more shielded (upfield) methylene group is assigned to the CH_2 group α to the bridgehead nitrogen while that of the CH_2 group α to the imine nitrogen is assigned to the downfield signal. This is at least partly a result of local anisotropic fields from the imine groups deshielding the H_F protons relative to the H_G protons. (Fig.4-2 shows how any proton on the imine C or lying close to the imine function ie H_F relative to H_G, will be deshielded.) Although the resolution is not good enough to carry out a rigorous analysis, the coupling constants can be estimated approximately as Jaxax' = Jaxeq = 11Hz >> Jaxeq' = Jeq,eq'=2-3Hz. These coupling constants correspond well with NN' dimethyl piperazine, except there Jaxeq (ie Jgem) =13.2Hz was greater than Jaxax' = 7.43H_z. Also in [2.2] metacyclophane Jgem = 12.0Hz[45], Jaxax' = 8-10Hz[46] (ie trans coupling) and Jaxeq' ≃ Jeqeq' ≃ 2-3Hz[46]. From these values cited in literature it is clear that the large splitting is due to :-

1. geminal splitting of the axial and equatorial protons (ie protons on the same C atom) where the value of J will be determined by the HCH angle α (FIG.9-2)

2. The vicinal coupling of trans protons (ie those in the 2 axial positions which leads to a good overlap of the bonding orbitals (FIG.51-1)

FIGURE 51

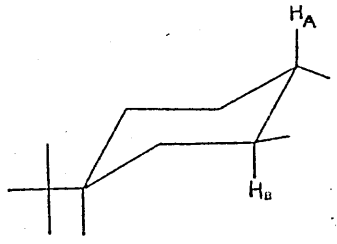

J = 10-14 Hz
α = 180°

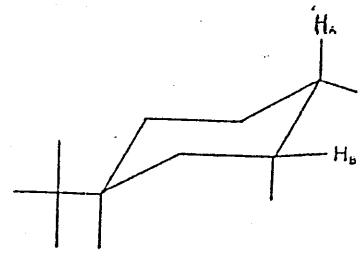

J = 4-5 Hz
α = 60°

FIG.52-1 THE ORIGIN OF THE AXIAL TRIPLET SIGNAL.

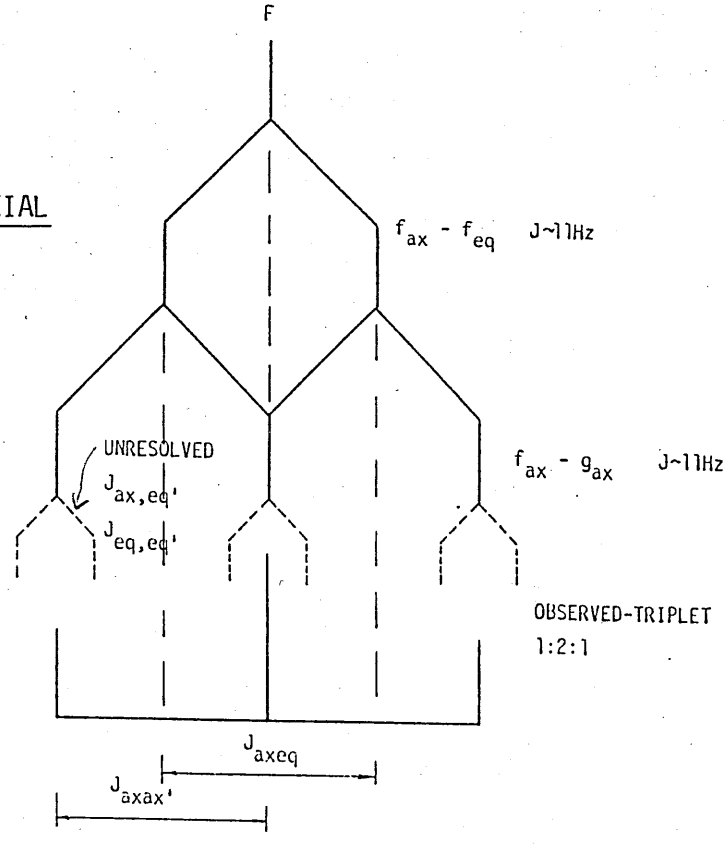

6 Jgem = Jaxax'

FIG.52-2 THE ORIGIN OF THE EQUATORIAL DOUBLET.

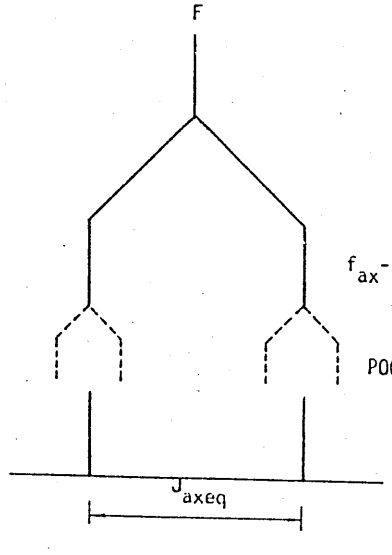

fgFeq.
Geq.

The other two vicinal couplings, Jeqeq' and Jaxeq' (Fig.51-2) are small ie not exceeding 4-5H_z. It is thus possible to assign the triplet signal (FIG.52-1) to the axial protons and the poorly resolved quartet(FIG.52-2) to the equatorial protons.

From 49-3, the methylene signal of 3Bm at the lowest temperature studied, it is seen that the signal F_{eq} is a doublet showing no clear signs of F_{eq} - G_{ax} vicinal coupling or indeed F_{eq} - G_{eq}, whereas the signal for G_{eq} does show signs of such vicinal coupling. However the spectrum is not completely resolved and the anticipated splitting could easily be contained within the relatively broad band envelope. The unequal nature of the inner and outer lines of the doublets (FIG.49-3) result because of the second order nature of the spectrum ie.$\Delta V/J < 10$ where ΔV is the difference in chemical shift (in Hz) of the two signals. There is distortion such that the innermost line (ie that which is nearest the other signal) increases in intensity at the expense of the outermost lines (those furthest from the other signal). This can have a qualitative usefulness in indicating on which side of the multiplet signal the related multiplet must be.

From the variable temperature nmr study of 3Bm it appears that steric constraints exist within the molecule which prevent interconversion of the axial and equatorial sites at temperatures below ambient. The room temperature spectrum at 90,250,and 360MHz indicates that the system is below its coalescence point. In order to calculate $\Delta G^{\#}_c$ at any of these fields it would be necessary to increase the temperature to find Tc.

The ^{13}Cnmr spectrum was temperature independant (FIG.50) over the experimental temperature range.(298K-203K) All signals were sharp singlets at both temperatures giving no evidence for fluxionality of the carbon atoms.

In order to look at the possible solution conformations Nuclear Overhauser Effect (NOE) experiments were carried out with the assistance of Dr. O. Howarth (S.E.R.C Highfield nmr service) FIG.50. On irradiation of the imine proton signal (H_E at δ7.58) there was an exceptionally large enhancement of 14.28% of Hc which indicated the close proximity of the

imine H_E protons and the aromatic Hc protons (FIG.53) Irradiation of H_E also generates preferential enhancement of the F_{ax} triplet (Fig.53-3) Both results suggest that the solid state conformation of 3Bm, with divergent imine functions, is also the dominant, (if not exclusive) conformation in solution. The imine signal remains unsplit in the 'Hnmr spectrum throughout the temperature range and this also provides evidence that only one conformer is present in solution over the temperature range 298-203K. Thus there is no indication of the presence of the coordinating (convergent) conformation which must exist in $[Ag_2\ 3Bm]^{2+}$.

The soft(broad) nature of the spectrum at the lowest temperature (203K) is presumably due to solvent viscosity which increases the relaxation time and slows down the exchange process on the nmr time scale.

FIGURE 54 NOE EXPERIMENT - IRRADIATION INTO H_E GIVES ENHANCEMENT OF H_B, H_C, F_{ax} and F_{eq}.

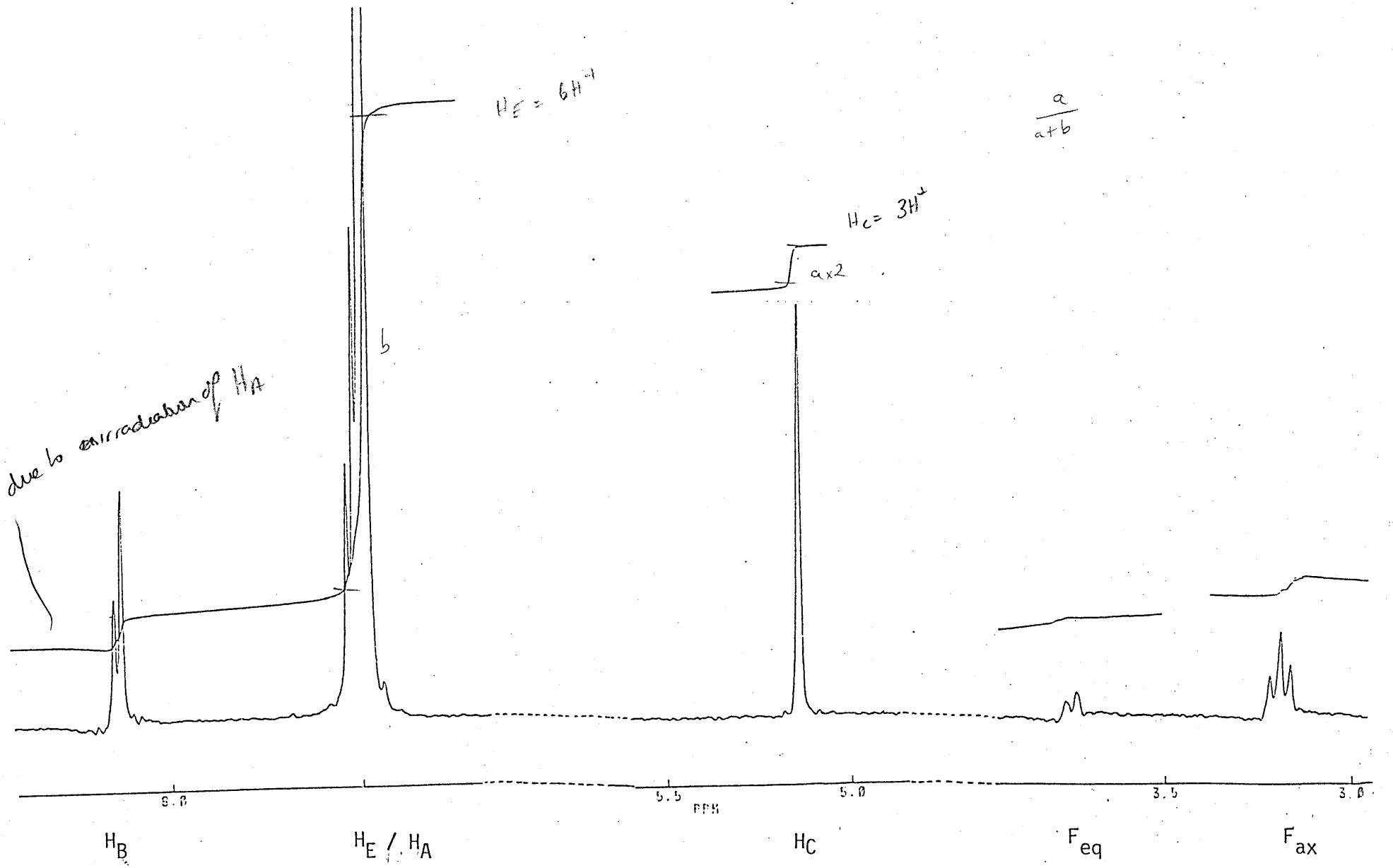

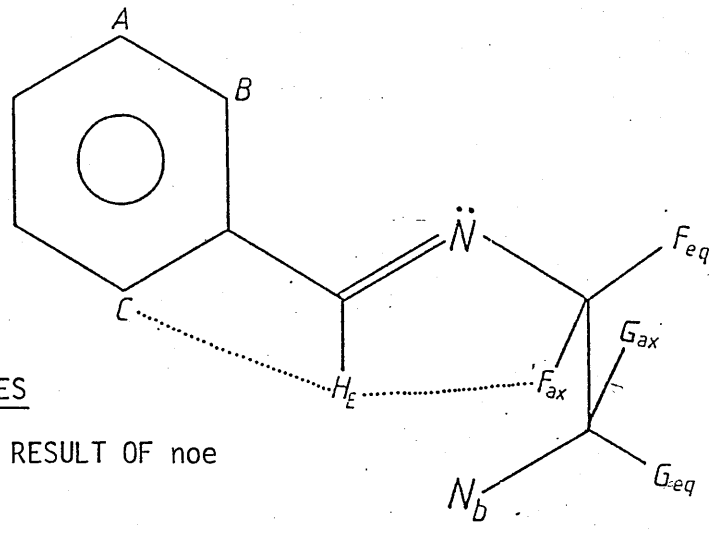

DIVERGENT IMINES

- SUPPORTED BY RESULT OF noe

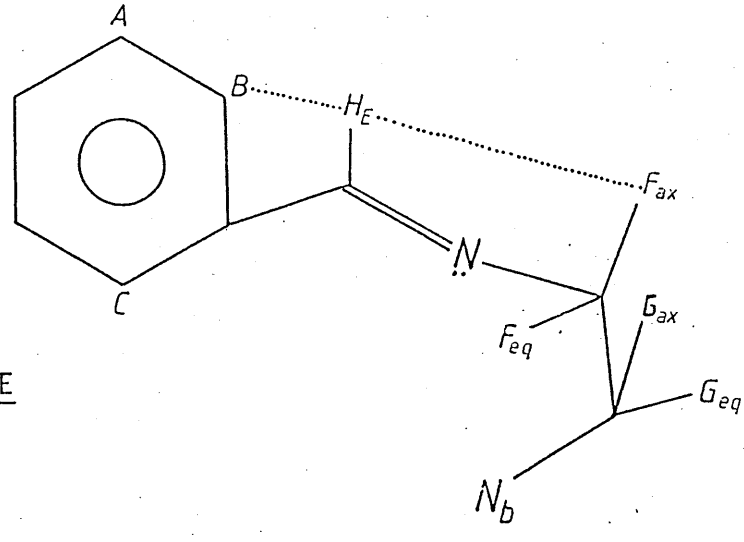

CONVERGENT IMINE

FIG.53 NOE EXPERIMENT OF 3Bm

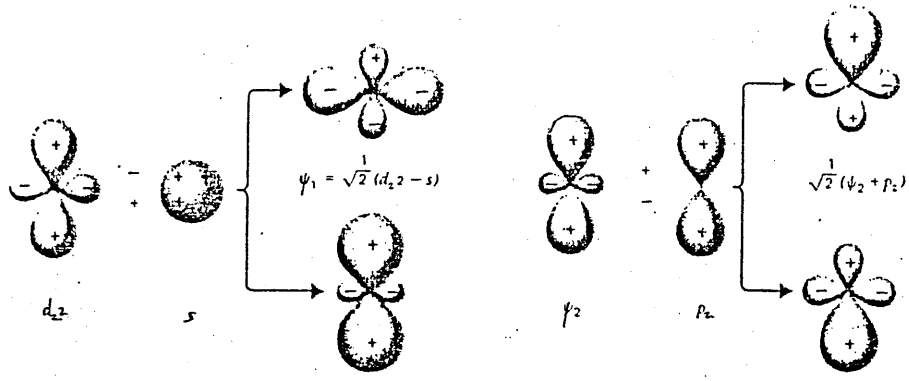

FIGURE 55.

THE INSERTION REACTIONS OF 3Bm WITH Ag^{+}, Cu^{+} AND Cu^{2+}

Silver ions will insert into 3Bm under mild conditions to give the dinuclear silver cryptate. The ir of the white crystalline product showed no sign of carbonyl or amine frequencies indicating that the insertion had occurred without significant ligand modification ie without opening of the macrocylic ring. Physical data for this complex is tabulated in FIG.54. The ability to insert metal ions into 3Bm suggests that the convergent (coordinating) conformation is thermally accessible but not favoured in the absence of a suitable guest. This may result from steric hindrance by the Hc protons which can perhaps be compensated for by the Π donor-acceptor interaction in the disilver cryptate. This results from the relatively small energy difference between the filled d orbitals and the unfilled valence shell s orbital which permits extensive hybridization of the dz^2 and s orbitals Fig.55[47]. The electron pair initially in the dz^2 orbitals occupies ψ_1, giving a circular region of relatively high electron density from which ligands are somewhat repelled and regions above and below this ring in which the electron density is relatively low. Ligands are attracted to the latter regions.

The 'Hnmr of the complex is interesting in several respects and NOE experiments have been used to investigate the conformation of the ligand in the complexed form. The 'Hnmr spectra of $Ag_2$3Bm$(CF_3SO_3)_2$ (FIG.56-1,56-2) differs from the uncomplexed ligand in several respects.

-1- in the free ligand the imine, H_E, signal remains insplit over the temperature range investigated whilst the silver complex sometimes shows splitting of this signal at low temperatures.

-2- the Hc protons, which appeared upfield in 3Bm are now significantly deshielded and the signal appears at δ9.0.

-3- the reversal of δFax (triplet) and δFeq (doublet) from 3Bm.

FIGURE 54. PHYSICAL DATA FOR THE Ag^{+}, Cu and Cu^{2+} INSERTION PRODUCTS WITH 3Bm

COMPLEX (Colour)	M^{+} OR F.A.B.[a]	Ω[b] S cm^2 mol^{-1}	ELEMENTAL ANALYSIS[c]	INFRARED SPECTRUM (cm^{-1})				ELECTRONIC SPECTRUM		
				C=N	CF_3SO_3	ClO_4	OH	SOLVENT CONC.	WAVELENGTH[d] (nm)	ε (M^{-1} cm^{-1})
$Ag_2$3Bm$(CF_3SO_3)_2$ .2EtOH (pale yellow)	951 (68) 801 (8) 693 (100)	295	C 41.4 (40.9) H 4.4 (3.9) N 9.6 (9.3)	1649	1254 1148 1029		3490 (EtOH)	MeCN 10^{-3} 10^{-4} 10^{-5}	420 310 298 255 220[e,d]	67 4651 5922 43689 178640[e]
$Cu_2$3Bm$(ClO_4)_2$ .2H_2O (yellow)		352[b]	C 45.6 (44.6) H 4.9 (5.2) N 11.8 (11.4)	1646		1086 622		MeCN 10^{-4} 10^{-5}	354 250 206[e,d]	5100 40000 232000[e]
$[Cu_2$3Bm$]^{4+}$ .2H_2O (green)	929 (15) 830 (50) 729 (30) 649 (55)	573[b]	C 40.60 (40.39) H 4.35 (4.40) N 10.63 (10.52)	1643		1088 622	3428	MeCN 10^{-4} 10^{-5}	630 270 250 225 202[d,e]	350 31000 93800 142000 156000[e]

contd.....

DO NOT
FILM THE
2 PAGES
DUP.

FIGURE 54. (contd.)

COMPLEX (Colour)	M^+ OR F.A.B.[a]	Ω^b S cm^2 mol^{-1}	ELEMENTAL ANALYSIS[c]	INFRARED SPECTRUM (cm^{-1})				ELECTRONIC SPECTRUM		
				C=N	CF_3SO_3	ClO_4	OH	SOLVENT CONC.	WAVELENGTH[d] (nm)	$\varepsilon(M^{-1}\ cm^{-1})$
$[Cu_2 3Bm]^{4+}$.$2H_2O$ (blue)		545^b	C 34.77 (35.22) H 4.41 (4.58) N 10.98 (11.59)	1646		1093 623	3423	MeOH 10^{-4}	615 374 232 $201^{d,e}$	540 2800 73000 124000^e

(a) % of base peak in parenthesis

(b) 10^{-4} M.

(c) Experimentally determined result in parenthesis.

(d) λ_{max}.

(e) Unreliable result.

FIGURE 56 THE 'Hnmr SPECTRA OF $(Ag_2 3Bm)^{2+}$ and $(Cu_2 3Bm)^{2+}$ at 294k and 233k.

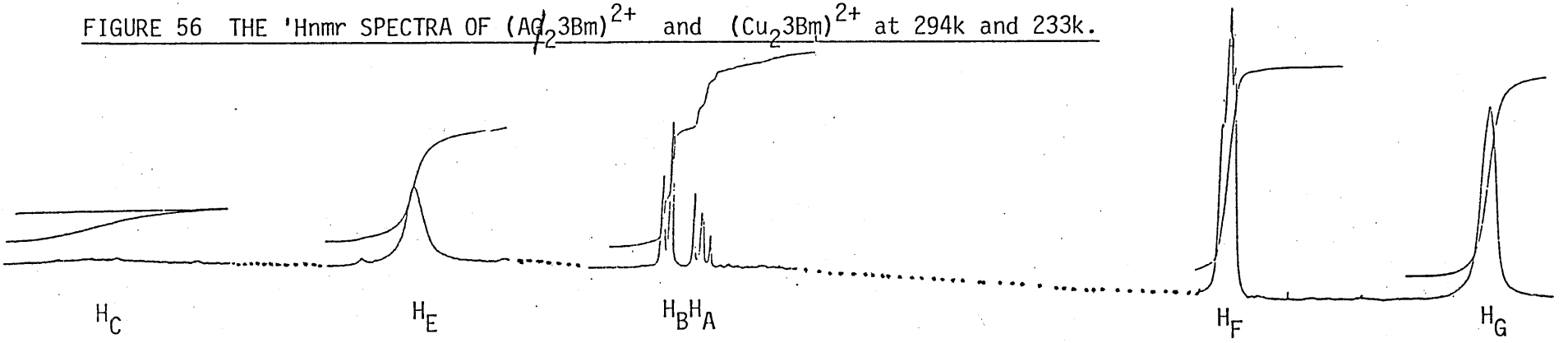

FIG.56-1 $(Ag_2 3Bm)^{2+}$ 294k

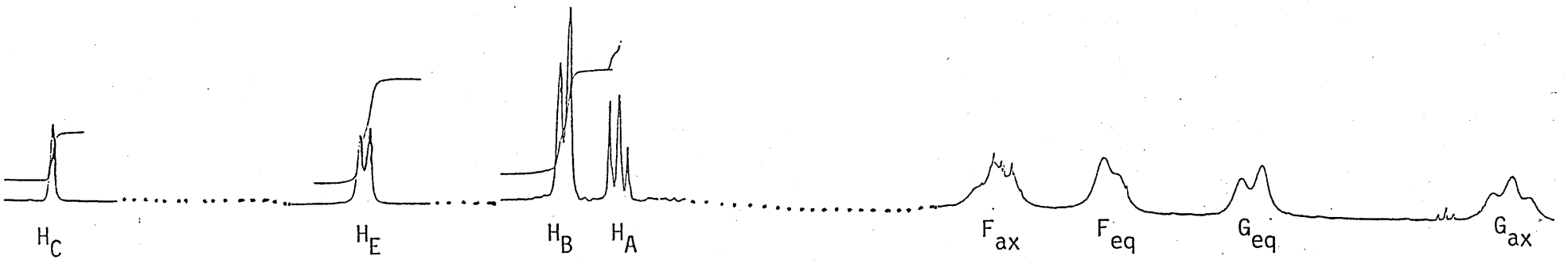

FIG.56-2 $(Ag_2 3Bm)^{2+}$ 233k

FIGURE 56(-3) THE N.M.R.[a] DATA FOR $[Cu_2 3BM]^{2+}$ AND $[Ag_2 3Bm]^{2+}$

COMPLEX	TEMPERATURE (K)	SOLVENT	SPECTRUM	HYDROGEN SITE					
				A	B	C	E	F	G
Ag^+	294	CD_3CN	^1H 360 MHz	7.75 (t)	7.87 (d)	9.50 (br,s)	8.59 (s)	3.46 (s)[b]	2.90 (s)
Ag^+	233	CD_3CN	^1H 360 MHz	7.75 (t)	7.87 (d)	9.85 (s)	8.62 (d)	3.51 (m) 3.52 (s)[c]	3.75 (br,t) 3.07 (br,d)
Ag^+	294	CD_3CN	^1H, NOE, 400 MHz		8.7[e]		d	8.0[e]	
Cu^+	294	CD_3CN	^1H 360 MHz	7.70 (t)	7.80 (d)	9.91 (s)	8.51 (s)	3.30 (d)	3.17 (d) 2.69 (br,m)
Cu^+	233	CD_3CN	^1H 360 MHz	7.69 (t)[f]	7.78 (d)[f]	9.89 (s)	8.49 (s)	3.30 (d)	3.21 (d) 2.68 (q)

(a) ppm from T.M.S.: (s) singlet, (d) doublet, (t) triplet, (m) multiplet, (q) quintet, (br) broad.

(b) Poorly resolved triplet.

(c) Poorly resolved doublet.

(d) Irradiation into this signal.

(e) % noe enhancement.

(f) Show signs of splitting.

The idea of steric constraints within this silver cryptate is substantiated by the 'Hnmr spectrum,. Fig.56-1 shows the room temperature spectrum (294K) while FIG.56-2 shows the spectrum at 233K. Relevant data is tabulated in FIG.56-3.

The sharp aromatic signals (a doublet and a triplet-assigned as in the free ligand) give no hint of fluxional behaviour even at 294K whereas the methylene signals show broadening at room temperature and indeed when the temperature is decreased the axial and equatorial protons become distinguishable and hence give the doublet and triplet components. For the same reasoning used in 3Bm (FIG.52) these are assigned to the equatorial and axial protons respectively. The arrangement of these signals is triplet(F_{ax}), doublet (F_{eq}), doublet (G_{eq}) triplet (G_{ax}), FIG.56-2 whereas in 3Bm FIG.49-3 the signals appear as doublet, (F_{eq}), triplet (F_{ax}), triplet(G_{ax}), doublet (G_{eq}). Thus in the complexed form F_{ax} is deshielded relative to F_{eq} - this situation being reversed in the uncomplexed 3Bm resulting, presumably, from the change in comformation. This can perhaps be rationalized by considering the structures in FIG.57. FIG.57-2 is the crystal structure of uncomplexed 3Bm with the C-H bonds shown in black, whereas FIG.57-1 is a result of a molecular mechanics study (M.Drew) of the free ligand. This shows that Fax points downwards - thus it lies in the shielding area of the imine and is shielded relative to F_{eq}, which may even lie in the deshielding area of the imines diamagnetic anisotropic current. Unfortunately no such model is available of the silver structure. However using the furan system, discussed later, M. Drew modelled the meta-benzene derivative (by replacing O of furan with C-H). Results show that the equivalent F_{eq} is now relatively closer to the shielding region of the imine current and thus appears at higher fields to F_{ax}. (see furan discussion and cf Fig.73-4a and 73-4b). This is schematically represented in 57-3. We have also used NOE experiments to investigate this conformational aspect. When H_E, the imine proton of $[Ag_2 3Bm]^{2+}$was irradiated at 294K there was an 8.7% enhancement of the H_B doublet and an 8% enhancement of the H_F signal. In order to confirm our proposal that Fax will be deshielded in the complexed form (ie H_{Fax} now lies in the deshielding range of the imines current and is therefore deshielded with respect to the F_{eq} proton) we attempted an NOE at 233K to see if

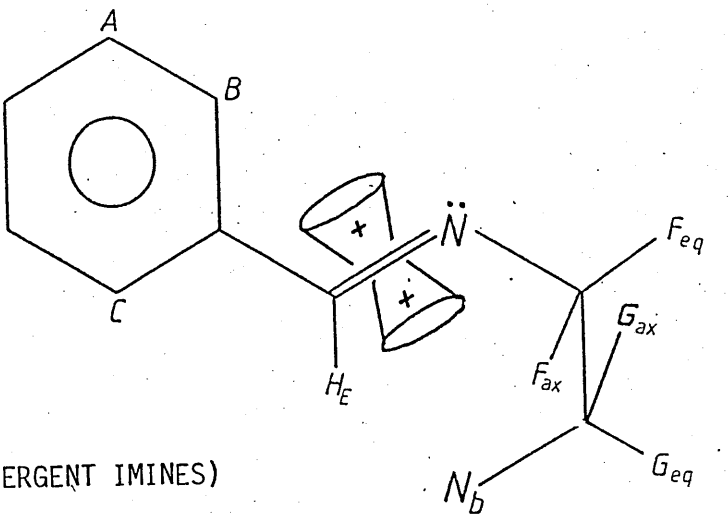

CRYPTAND

(METAL FREE DIVERGENT IMINES)

FIG.57-3i

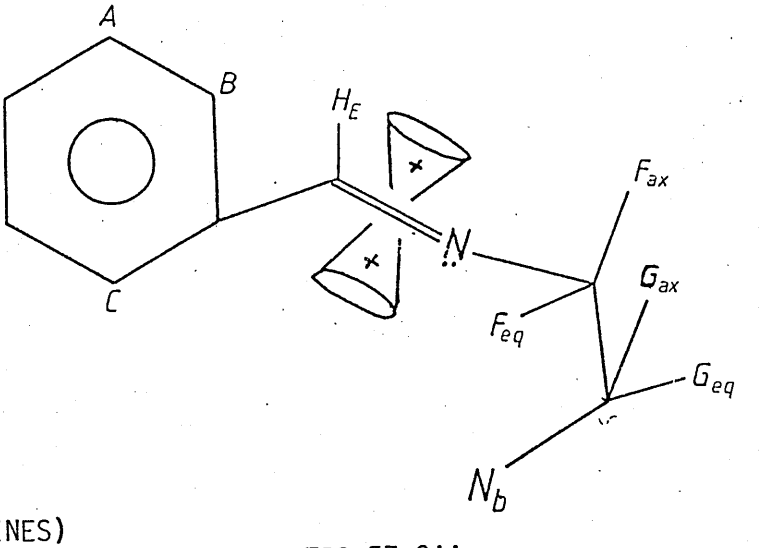

CRYPTATE

(CONVERGENT IMINES)

FIG.57-3ii

FIG.57-1

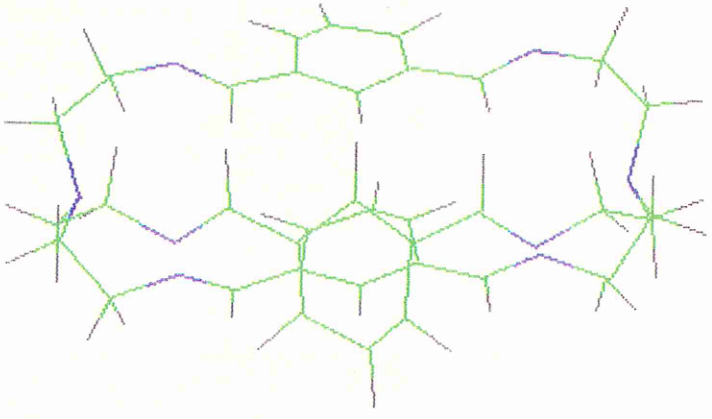

FIG.57-2

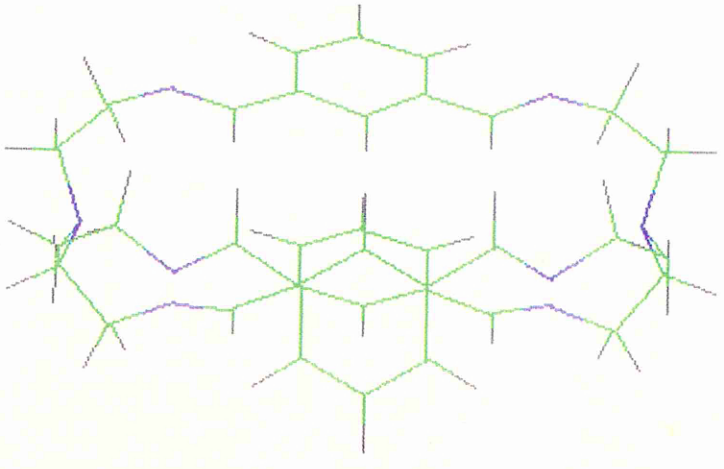

irradiation into H_E would enhance the doublet or triplet component of the F signal. Unfortunately the sample decomposed before being run suggesting a low stability of this silver complex. It is hoped to repeat this experiment in the near future.

An interesting feature of the ^{1}Hnmr spectra of this system is the low temperature splitting of the signal at δ8.62 (FIG.56-1,56-2) J=8Hz, a phenomenon which is not observed in the low temperature spectrum of 3Bm in which, even at 203K, the imine remains a sharp singlet. There are several possible explanations for this -

-1- the imine has been split because of the presence of 2 main conformers - however none of the other signals show such significant splitting attributable to the presence of additional conformers -

-2- at low temperatures the molecule is frozen into an unsymmetrical molecular conformation with respect to the imine functions. However this makes it difficult to explain the 1:1 intensity ratio. A low temperature NOE, irradiating into H_B, would show if one of the imine components was closer to the H_B protons than the others. This was attempted for $[Ag_2 3Bp]^{2+}$ (see later) but there was no enhancement of one peak of the doublet relative to the other.

-3- it is possible that at low temperatures we are observing a coupling interaction between the Ag^+ metal centre (I=+½ for both ^{107}Ag and ^{109}Ag) and the imine hydrogen H_E. This splitting is not observed at room temperature because the silver ions are undergoing fast exchange between free and complexed environments. Exchange occurs so rapidly with respect to the nmr time scale that coupling cannot be observed. However as the temperature is decreased the exchange process slows down to the extent that the imine proton can see the Ag^+ ion in the cavity for long enough to couple to it. Because Ag^+ has a nuclear spin number I=½ a doublet is obtained. It is difficult to investigate this idea by nmr because silver presents a 2 fold problem with respect to nmr studies. It is an insensitive nucleus with receptivities of 0.195 (^{107}Ag) and 0.276(^{109}Ag) and the silver nucleus shows long relaxation values leading to difficulties in observing a silver nucleus.

One way in which we have attempted to investigate that the splitting of the imine signal is a coupling rather than a chemical shift effect is by recording the ^{1}Hnmr at 2 different frequencies. Although the chemical shifts of the two components of the doublet will be affected (in units of Hertz, not in ppm from TMS) J the coupling constant should remain constant (FIG.5-5) therefore the value of J=8Hz should be observed at both 360MH$_z$ and 500MH$_z$ (500MH$_z$ spectra run at Q.U.B by Dr.Paul Stevenson). Although this experiment confirmed ^{107,109}Ag coupling in the other disilver cryptates neither the room temperature or the 223K spectrum of $[Ag_2 3Bm]^{2+}$ show splitting of the imine signal observed in the 400MHz low temperature spectrum. However the same sample was not used for both spectra because the complex decomposes after ≈4 weeks. For the 500MHz spectra the sample used had not been fully analysed. Although ir. indicated the presence of the triflate counter ion it may be that this second sample is in fact protonated.

However evidence for the silver - H$_E$ coupling in the initial experiment lies in the observation that there is no doublet splitting of the imine signal at low temperatures in the presence of the Cu^I nucleus. For ^{64}Cu I=3/2 which leads to quadrupole broadening so that the resolution of 4 lines is not expected. Although the imine signal is broadened in $[Cu_2 3Bm]^{2+}$ it is not clearly resolved even at the lowest temperature studied. FIG.56-5.

This splitting of the imine signal by silver may be a useful indication of how stable a complex is and thus may give some information about the conformation involved. It is interesting to note at this point that the silver complex of the thiophene derivative shows splitting of the imine signal even at room temperature and thus the complex may show a greater degree of stabilty compared to the ligands where fast exchange of the silver ions can occur at room temperature.

Another very significant feature of the spectrum of $[Ag_2 3Bm]^{2+}$ is the position of the Hc signal. In 3Bm this signal appears high field at δ5.33 (294K). Initial room temperature spectra run on the silver cryptate from 9ppm to TMS gave no signs of a signal for the 3Hc protons. Thus a spectrum

was run looking highfield from TMS in case Hc had formed a "hydride" type proton. This might occur because the Hc protons in this convergent conformation would, of necessity, be held between the pair of silver ions in the cavity. This could lead to very effective shielding of the Hc protons, or even, at the extreme, lead to incipient Ag-H bonding. However, when we looked from 0 to -8 ppm no signal was found. Thus we looked further downfield ie down to 12ppm. Although no definite signal is seen a broad baseline hump ≈9.50ppm is observed - this has an integral value of 3 protons. That this was not the OH signal of the ethanol but due to the 3 Hc protons was confirmed by a D_2O shake. The broadened base line hump was also apparent in the 500MHz spectrum. On cooling the sample to 233k, two things happen to this signal in both the 360MHz and 500MHz spectra -

-1- The signal is shifted to δ9.85Å indicating a greater degree of deshielding. This deshielding of the Hc protons was also observed in the nmr spectrum of the Cu^I complex, and may originate from the anisotropic circulation of electrons of the encapsulated metal ions. However, it is also likely that the complexation of metal ions leads to a geometrical rearrangement of the 3 aromatic ring such that Hc no longer points towards the adjacent ring (and so towards the shielding area of the ring current). Rather the rings are angled/tilted with respect to each other so that Hc now lies in the deshielding region of the ring current.

-2- The signal sharpens up significantly. The broadened room temperature spectrum probably is a result of fast exchange of silver ions. The Hc protons point directly into the cavity and thus they are not "sure" whether the Ag^+ are in or out of the cavity - the signal therefore appears broad. In the 360MHz spectrum with the silver ions held inside the cavity, as evidenced by the splitting of the H_E signal, the Hc proton is in a more stable magnetic environment and thus the signal sharpens up to the singlet. The sharpening up of the Hc signal in the 500MHz spectra despite the absence of splitting of H_E, which implies that silver is not held in the cavity, suggests that the deshielding of the Hc proton is not the result of a deshielding effect of the valence electrons of the metal cation but rather is the result of a geometrical rearrangement of the metal free ligand upon complexation which is frozen out at the lower temperature.

The room temperature 'Hnmr spectrum of $[Ag_2 3Bm]^{2+}$ showed a triplet (δ=1.7), and a quartet (δ=4.13) attributed to the ethanol that had been indicated by both ir and microanalysis. Integral values of the signals supported the proposed 2 ethanol solvent molecules per macrobicycle. The position of the broad OH signal which was a function of temperature, was confirmed by a D_2O shake. The 500MHz low temperature spectrum also shows the ethanol features with the quartet superimposed on the low field axial signal.

The work with 3Bm and copper is in its early stages and is unavoidably incomplete.

The reaction of 3Bm with $Cu^{I}(MeCN)_4ClO_4$, in the appropriate degassed solvent mixture gave a yellow microcystalline product which analysed for $Cu_2 3Bm(ClO_4)_2\ 2H_2O$. The product was stable in air in its solid state. The ir not only indicated the solvate water as a broad band at 3356cm^{-1} (3600-3000cm^{-1}) but it also showed significant splitting of the perchlorate signals at 1080cm^{-1} and 623cm^{-1}. This could indicate either a coordinated mode of binding for this counterion or hydrogen bonding to solvent. The physical data of the copper complexes of 3Bm is given in FIG.54. The absence of signals at 3400-3200cm^{-1} (NH) or 1700-1670cm^{-1} (C=O), and the presence of the medium strong imine feature at 1633cm^{-1} suggest that insertion of the Cu^{I} ions have not caused significant structural ligand modification. Conductivity measurements, made at 10^{-4}M *. lie within the 1:2 electrolyte range for this concentration.

The electronic absorption spectrum shows a strong absorption at 206nm (ϵ-10^5 unreliable) which is assigned to an aromatic Π-Π^* ligand transition. A second absorption at 250nm (ϵ=40,000) may be the secondary band absorption

** A range of 420 to 520 was established for this concentration using known 1:2 template macrobicyclic species - these had also been run at 10^{-3}M , giving typical values for this concentration.*

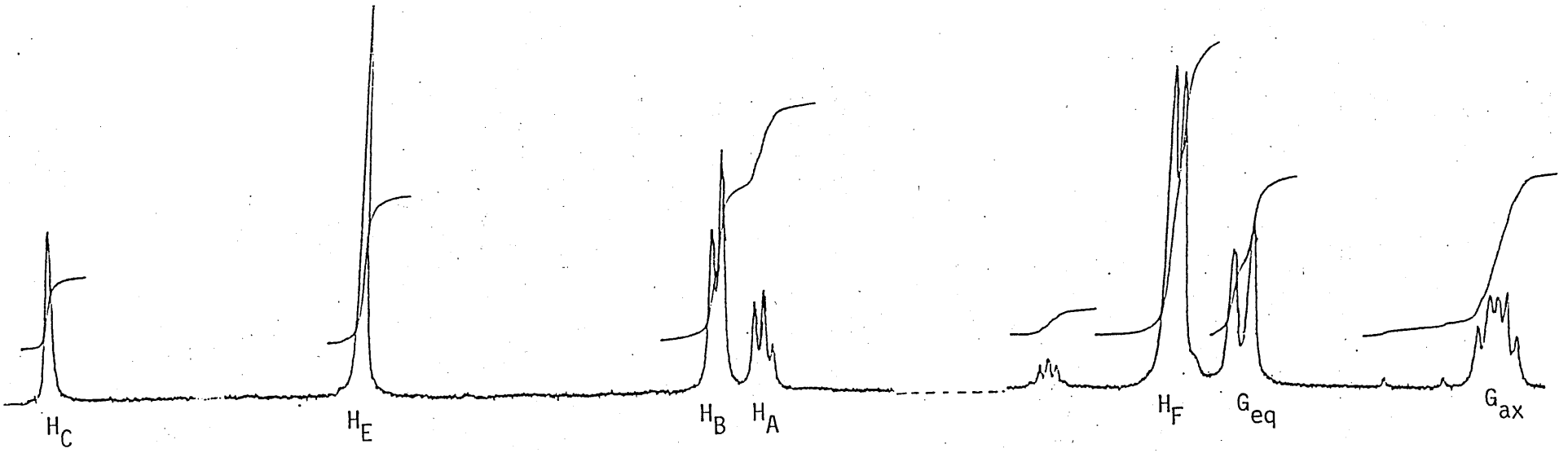

FIG.56-4 $(Cu_2 3Bm)^{2+}$ 294k

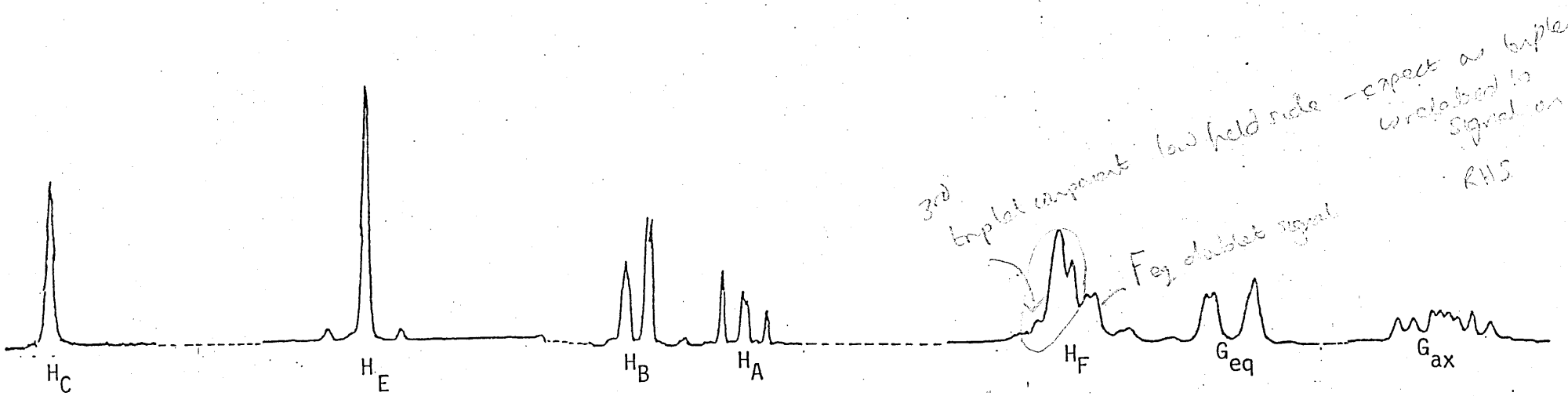

FIG.56-5 $(Cu_2 3Bm)^{2+}$ 233k

of the benzene unit or it may be the Π-Π^* transition associated with the imine function. A moderate absorption at 352nm (ϵ=5100) is likely to be a metal to ligand charge transfer band.

The room temperature 'Hnmr of $[Cu_2 3Bm]^{2+}$, FIG.56-4 is similar to that of the silver complex showing the Hc protons deshielded at δ9.91. * The aromatic signal is resolved into the doublet and triplet features indicating a fixed conformation for the aromatic residue even at room temperature.

The room temperature signal for the two methylene groups are complicated. The signal for H_F appears as a doublet (integral $12H^+$), the 2 components of which are separated by $7Hz$ which is an average of the larger couplings (Jgem, Jax-ax) and the smaller couplings (Jax-eq', Jeq-eq' $\simeq$ $1\text{-}2Hz$), H_G, on the other hand, is split into its axial and equatorial components (each signal having an integral = $6H^+$). The higher field component appears as a quintet whereas the lower field signal is a broadened doublet. This would suggest a potential ax,eq,eq,ax, arrangement of resolved methylene signals that is observed in the silver complex of 3Bm., Thus the higher field multiplet is assigned to the H_G axial proton and the lower field doublet to the H_G equatorial proton. That this assignment is essentially correct is confirmed by the low temperature spectrum (223K) Fig.56-5. This shows that the axial quintet at room temperature is not the result of a triplet structure (discussed previously for uncomplexed 3Bm where Jgem = Jax,ax'), being further split by other vicinal couplings but rather it is a result of Jgem$\neq$Jax-ax'. At room temperature the small vicinal couplings are not fully resolved whereas at 223K, each line of the quartet resulting from Jgem$\neq$Jax-ax' gives rise to a doublet - resulting in the 8 line spectrum. A tree diagram FIG.58-1 shows the splitting of G_{ax}- this gave the following coupling constants Jgem = 13.9Hz, Jax-ax'=10.64Hz and Jax-eq' = 6.0Hz.

** The signal is a well defined singlet suggesting that at room temperature there is no fast exchange process.*

FIG.58-1 at 294k

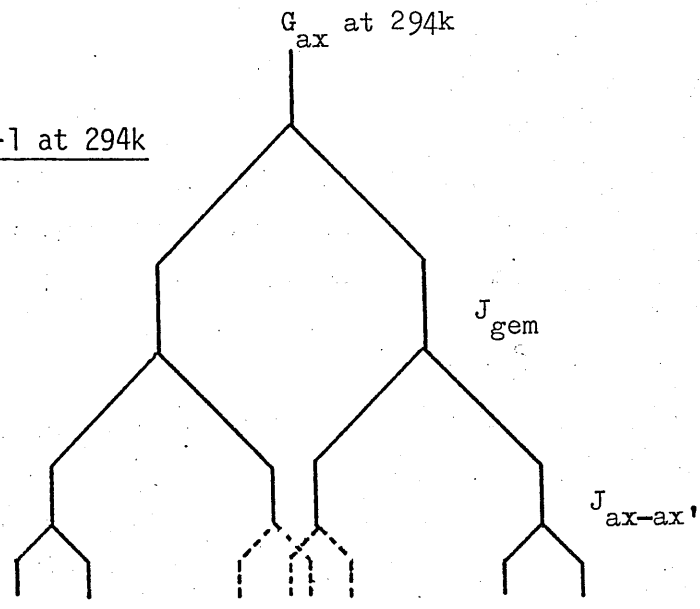

FIGURE 58.

TREE SPLITTING DIAGRAM FOR $Cu_2 3Bm(ClO_4)_2 \cdot H_2O$

FIG.58-2 at 233k

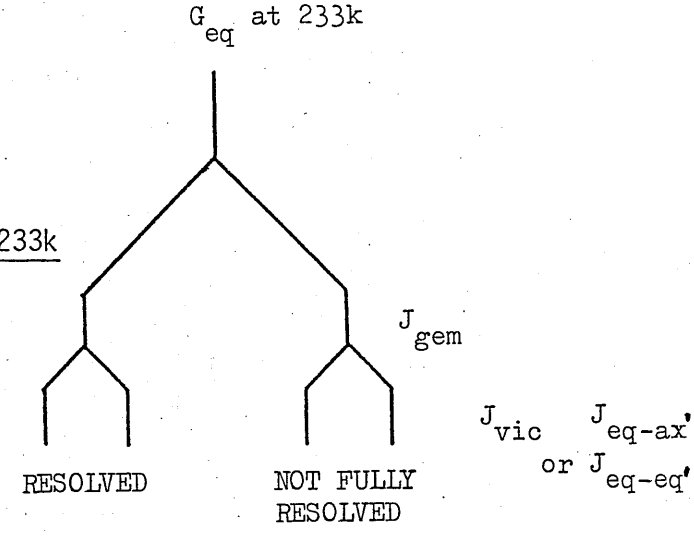

J_{gem} = 13.9Hz.

J_{vic} = 2.3Hz.

Thus Jgem≠Jax-ax' which results in the complicated multiplet. FIG.58-2 gives the tree diagram for G_{eq} - this yielded the following constants: Jgem = 13.9Hz, Jeq-eq' = 2.3Hz. The Jax-eq' is not observed - presumably being incorporated in the broad Jgem band.

The signal from the H_F protons even at this temperature is not resolved into its axial and equatorial components. The difference in behavior of H_F and H_G might be attributed to different Tc values rather than different $\Delta G^{\ddagger}_c$ values. This is shown to be the situation for some of the other ligands eg 3Bp and 3F and is discussed more fully later. However it means that for the H_G protons, which show splitting into the axial and equatorial protons at room temperature, the Tc value is higher than that for the H_F protons.

At 233K the imine signal remains unsplit and shows no broadening - thus there is no visible evidence of its coupling with the copper nucleus (I=3/2). The aromatic H_A, H_B, protons give rise to the triplet and doublet signals. However there is evidence of further coupling - this might be long range coupling with Hc. (J_{BC}=1.4Hz). Although the coupling is not fully resolved in Hc, the signal does appear broadened and thus the small couplings may be contained within it.

When a solution of $Cu(ClO_4)_2.6H_2O$ is added in alcohol to a solution of 3Bm in CH_2Cl_2 there is an instant precipitation of a green solid which on recrystallization from MeCN/EtOH gives a bright green microcrystalline product. When this green powder is stirred in air in the presence of CH_2Cl_2 at room temperature, over a 12-16 hour period the solution turns blue and a bright blue crystalline product is obtained on concentration of the solvent. The ir of the green and blue products show significant differences as do their electronic absorption spectra.

The i.r of the green product shows a medium intensity sharp feature at 3428cm^{-1}. This is often observed when a bridging OH group is present. On the basis of the signal intensity and microanalysis, it would seem that a structure $Cu_2$3Bm(OH)$(ClO_4)_3$ is likely for the green product. Both F.A.B. and the electronic absorption spectra would support this. F.A.B. gives

FIGURE 59.

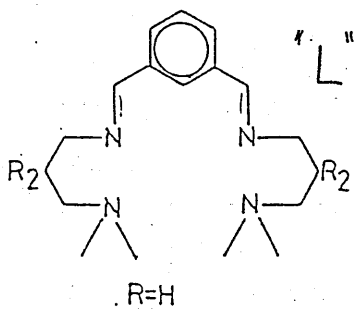

R=H

FIG.59-1

	Selected IR Bands/cm^{-1}
$[Cu_2^{I}L\ (MeCN)_2][ClO_4]_2.MeCN$	3030, 2980, 2925, 2870, 2835, 2310, 2300, 2280, 2260, 1628, ca. 1090(br), 627
$[Cu_2^{II}(L\ -O)(OH)][ClO_4]_2$	3560(sh), 3420, 3040, 2905, 2880, 1630, 1560, ca. 1090(br), 620
$[Cu_2^{II}L\ (OH)_2][ClO_4]_2$	3505(br), 3040, 2910, 2840, ca. 1090(br), 620
$[Cu_2^{I}(L\ -O)(N_3)_3]$	3000, 2950, 2920, 2840, 2042, 2020, 1640, 1560
$[Cu_2^{II}(L\ -O)(OH)(NCS)_2]$	3440(br), 3040, 2920, 2870, 2035, 1635, 1570

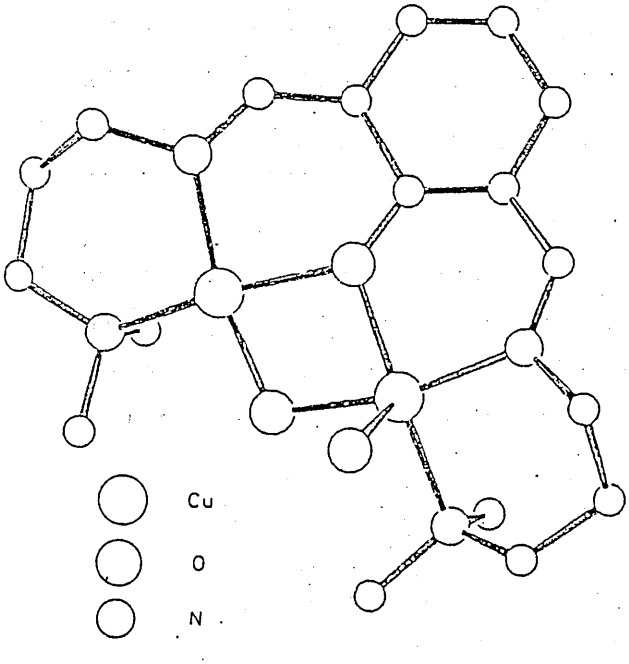

FIG.59-2

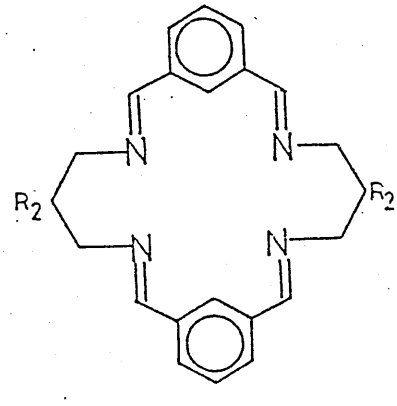

R=H

FIG.59-3

peaks at 929(15%), 830(50%), 729(30%), and 649(55%), which correspond to $[Cu_2 3Bm(OH)(ClO_4)_2]^+$, $[Cu_2 3Bm(OH)(ClO_4)]^+$, $[Cu_2 3Bm(OH)]^+$, and $[Cu3Bm)^+$, respectively. The uv. spectrum shows absorptions at 202nm (ϵ=156,000)* 225(ϵ=142,000)* and 270nm(31,000). This may correspond to a red shifted absorption spectrum of benzene (46-5) each band experiencing a bathochromic shift of about 20nm. The band at 250nm (ϵ=938,00) may be the Π-Π* transition associated with the imine function. No charge transfer band (ligand to metal) was observed although a single low intensity d-d transition at 15,800cm^{-1} (ϵ=350) was seen.

The blue product also shows a moderately broad strong ν_{OH} in the ir spectrum. This may be due to bridging OH or water, but strikingly, there are ν_{NH2} absorptions on the side of this main band. Additional splittings and intensity changes around 1550-1580cm^{-1} may suggest the existence of a phenoxy group[48-52].

Using the acyclic ligand shown in FIG.59-1 it was shown[53] that when only a bridging OH group was present in the diCu(11) complex, signals at 3505 and 3040 cm^{-1}were observed but when the phenoxy group was also present signals at 3560,3420,3040 and 1560cm^{-1} were observed. When only the phenoxy bridge was present the signals appeared at 3000 and 1560cm^{-1}. An X-ray structure of the phenoxy-hydroxy form of this acyclic ligand has been obtained,[53] FIG.59-2 showing that the complex contains two Cu(11) ions within the ligand cavity bridged by an oxygen atom of the phenoxide and an oxygen atom from hydroxide. Similar behaviour was also observed in the macrocyclic ligand in FIG 59-3.

* *Unreliable values and absorptions.*

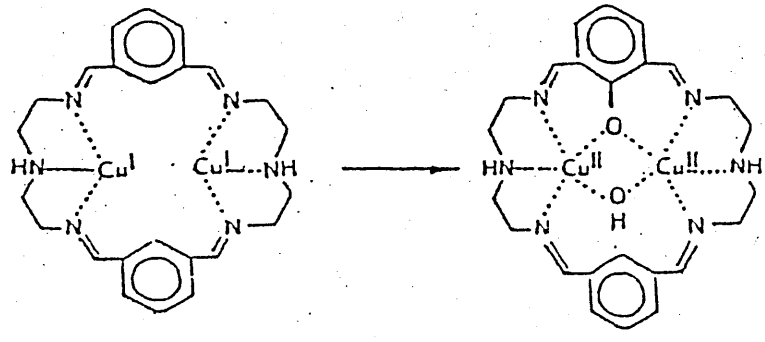

FIGURE 60.

For the blue form of $[Cu_2 3Bm]^{4+}$ the electronic absorption spectrum, is very different to that of the green product suggesting that a benzene nucleus may have undergone modification. Indeed this spectrum shows peaks at 232 and 280mm (the latter appears as a shoulder) which is very similar to the absorptions of a phenoxy group (235nm and 287nm).

The ir and uv features of this blue $[Cu_2 3Bm]^{4+}$ product are characteristic of the 2-hydroxyphenyl imino chromophore (46,54-56). The infrared band at $\approx 1570 cm^{-1}$ is typical for the V(C-O) vibration of the phenol of such a chromophore. It assumes partial double bond character in a chelate ring that contains C=N linkages. The uv absorption at 374nm (ϵ=2800 is characteristic of the Π-Π^* transition of the C=N chromophore although it could also be a metal to ligand charge transfer transition.

It would thus seem at these early stages that one aromatic ring of the binucleating ligand 3Bm may have been hydroxylated - formally an insertion of an oxygen atom into an aromatic C-H bond. The source of the oxygen ie O_2 v's H_2O, is not clear - isotopic ^{18}O, studies would be required to clarify this. However if the yellow Cu^I product is stirred in air dissolved in acetonitrile, the solution gradually becomes green and then blue - from which the blue form of $[Cu_2 3Bm]^{4+}$ can be isolated. Although this points to molecular oxygen as the oxygen source, the change may simply be a result of the copper complex picking up moisture from the solvent or air.
A recent publication(57) proposes formation of a phenoxy-hydroxy bridged dicopper assembly in a similar macrocyclic ligand to 3Bm. FIG.60. Martell is currently using labelled $^{18}O_2$ to assess the origin of the inserted oxygen atom.

We can predict a strong antiferromagnetic interaction for this blue $[Cu_2 3Bm]^{4+}$ as this is often observed for such a bridging arrangement (53,58). For 59-1 a strong antiferromagnetic exchange between the two Cu(II) ions (293K μ=0.61Bm ; 203K μ<0.1Bm) was observed. This coupling between the 2 copper centres is a result of the good overlap of the copper magnetic orbitals (dx^2-y^2) with oxygen p-orbitals. The observed Cu-O(H)-Cu angle of

108° [59] is well above the 97.5° angle where the switch from ferromagnetic to antiferromagnetic interaction occurs.

Attempts to obtain a crystal of suitable size for X- ray structural analysis of both the green and blue product of the $[Cu_2 3Bm]^{4+}$ are high priority.

THE CRYSTAL STRUCTURE AND NMR OF 3Bp AND $Ag_2$3Bp$(CF_3SO_3)_2$.

The appearence of strong OH absorptions in the ir(FIG.45-3) and in the 'Hnmr spectrum of (63-1) of 3Bp originally led us to believe that water or some other hydroxylic guest (eg.MeOH, EtOH) might be coordinated within the cavity. It was, therefore, not altogether surprising that the X-ray structure showed water solvate FIG.61-1. Indeed there were 6 water solvate molecules lying outside the cavity. Mike Drew shows, using molecular modelling, that in both the convergent and divergent arrangement of imine bonds, it is possible to encapsulate a water molecule at the centre of the cavity. However, placing 2 water molecules within the cavity created considerable strain within the macrobicyclic structure. Moreover unfavourable geometry prevents the formation of imine-water hydrogen bonds within the cavity. This difficulty may account for the divergent conformation of 3Bp.$6H_2O$ where hydrogen bonds can be formed to water molecules outside the macrocycle. The X-ray structure shows 6 water molecules each forming a fairly strong hydrogen bond to an outwardly directed imine nitrogen (O...N < 2.90A). These water molecules are also hydrogen bonded to each other and thus they link individual macrocyclic units. This may be the source of stability in the metal free form of the ligand. The molecule has a crystallographically imposed C_2 symmetry.
In 3Bm the methylene groups were eclipsed FIG.48-2 and the imine functions divergent but in 3Bp although the imine functions are still directed away from the cavity, now when we look down the N_b-N_b vector (9.32Å) FIG.61-2, 61-3 we observe that the methylene carbon atoms lie in the more open staggered arrangement with the aromatic-imine groupings virtually all planar (torsion angles,ie N=C-C_{aryl}, all within 3° of 0° or 180°). The staggered, planar, arrangement of atoms together with increased cavity length (≃ 1.3Å, brought about by the para as opposed to meta aromatic length) increases the flexibility of this system, making it, potentially, a better candidate for the coordination of metal ions.

The X-ray structure of 3Bp shows that the free cryptand prefers a conformation involving divergent sites as in 3Bm. However the

FIGURE 61 - X-RAY STRUCTURE OF $3Bp.6H_2O$

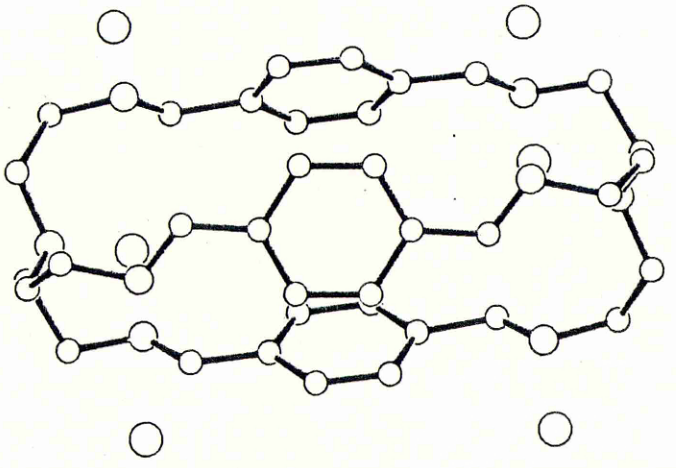

FIG.61-1

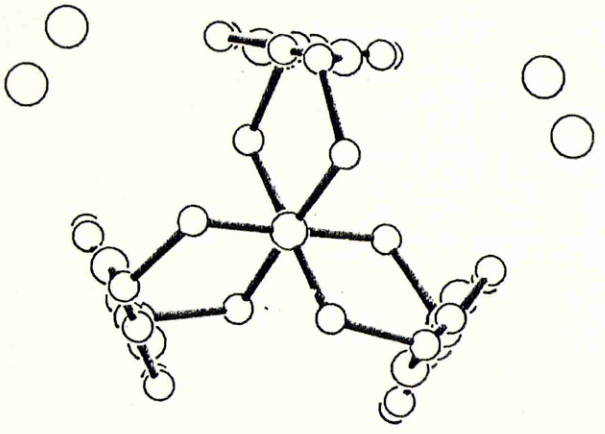

FIG.61-2

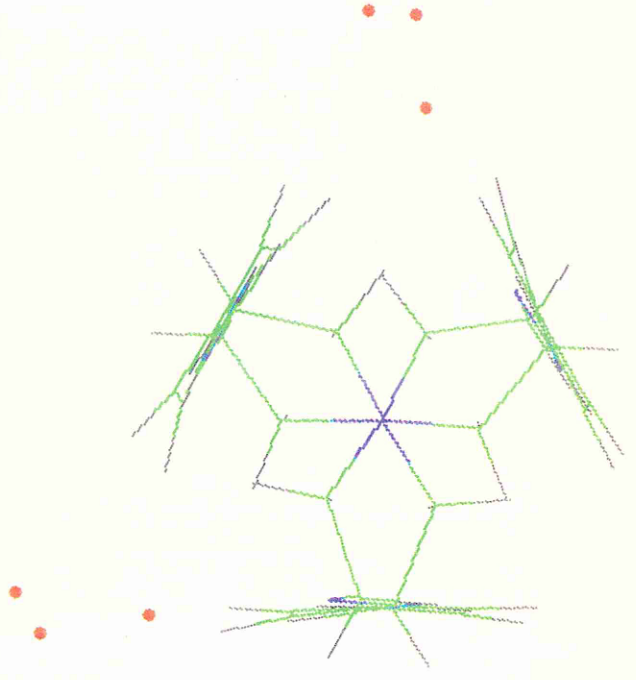

FIG.61-3

transformation to a convergent binding conformation is easily achieved by insertion or with the template reaction of silver triflate, tren and terephthalaldehyde giving crystals of $Ag_2$3Bp$(CF_3SO_3)_2$ suitable for X-ray structural analysis.

A general view of the disilver salt is shown in FIG .62-1. The structure consists of discrete $[Ag_2$3Bp$]^{2+}$ cations and anions. In the cation, two silver atoms are encapsulated at a distance of 6.06Å apart. We might have expected the silver ions to show a 4 coordinate based geometry achieved using the ligand nitrogen donors and indeed each silver atom is bonded to a bridgehead nitrogen [Ag(1) - N(1),2.42Å: Ag(2) - N(2), 2.37Å] and to 3 methylene nitrogen donors [Ag - N, 2.27 - 2.38Å]. However the geometry of the silver environment is equivalent to that of a seven coordinate capped octahedron with the uncapped face removed. The bridgehead nitrogen atoms (N_b), which are separated by 10.83Å and thus further apart than in the metal free ligand (9.32Å), cap a triangular face of N atoms with N_b-Ag-N angles of 75.4 - 78.8° and N-Ag-N angles of 110.3-119.1°. However it appears that both silver atoms also have contacts with 3 hydrogens from the bridging benzene rings (62-1). These Ag-H distances (using calculated hydrogen atom positions) are from -

Ag(1)	- H(40)	2.72Å	Ag(2)	- H(39)	2.37Å
	- H(60)	2.65Å		- H(59)	2.32Å
	- H(80)	2.52Å		- H(79)	2.26Å

The Ag - H distances imply Ag - C distances in the $[Ag_2$3Bp$]^{2+}$ complex in excess of 3.0Å. This distance would seem to be too long to allow any significant Ag^+ - C_{aryl} interactions. In a series of silver ion - aromatic complexes[59] formed by the reaction of Ag^+ with cyclohexyl benzene, and o-, m- and p-xylene, it was found that (m-xylene)$_2$ $AgClO_4$ was composed of silver ions bound to 2 aromatic entities such that each silver has 2 close Ag-C distances at 2.47 + 0.02Å. The distance allows interaction of the π systems. The next nearest Ag-C distance varied over wide limits - up to 2.96Å. Using p-xylene, the crystals showed severe disordering yielding no useful information.

FIG.62-1 A GENERAL VIEW OF $Ag_2 3Bp(CF_3SO_3)_2$

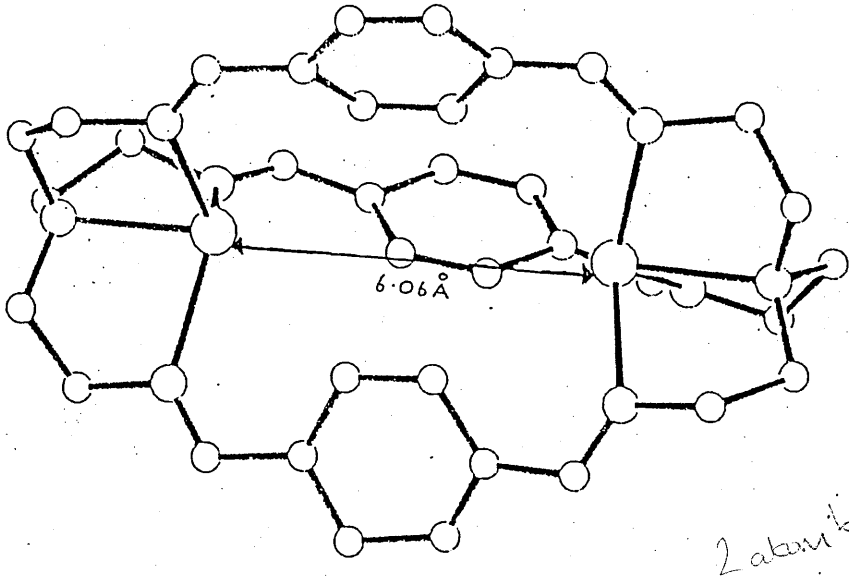

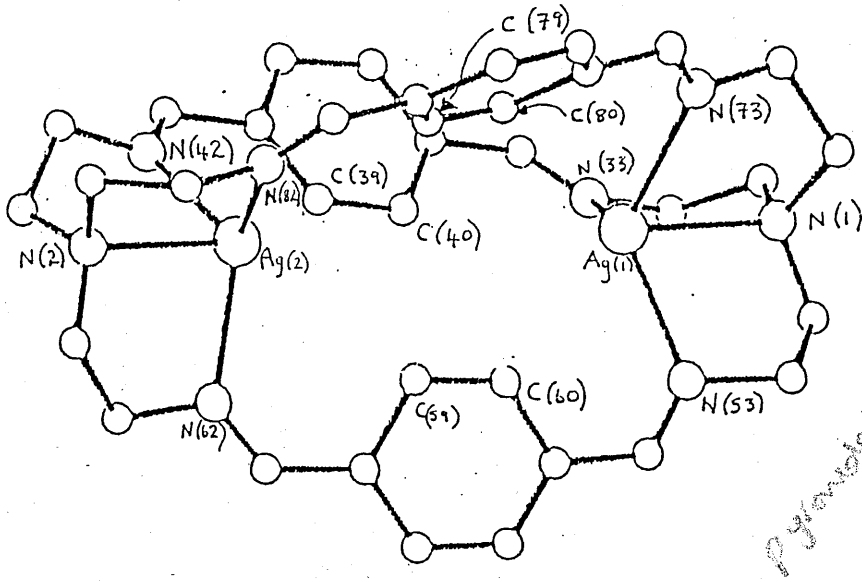

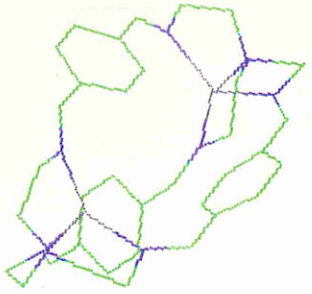

(a)

Ag....Ag 6.06A

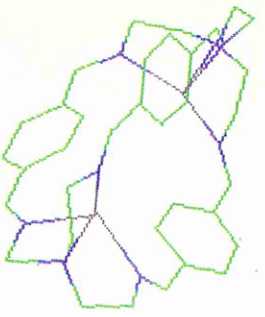

(b)

Ag....Ag 7.27A

FIG.62-2

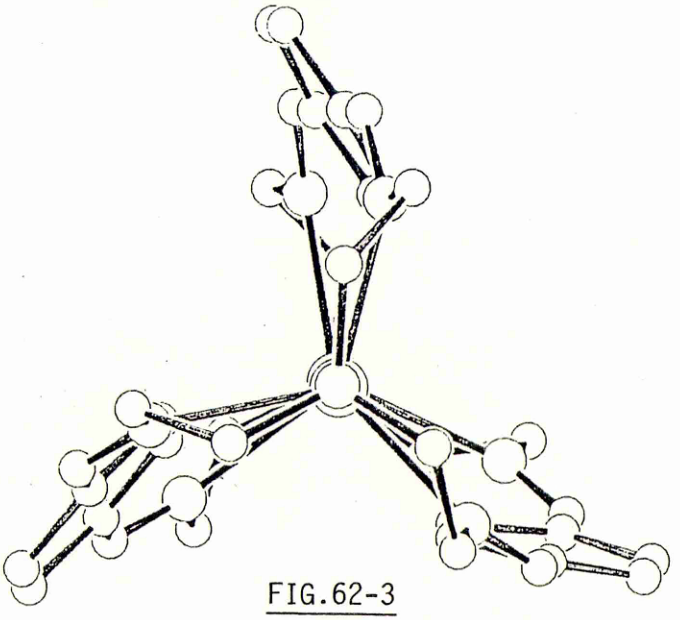

FIG.62-3

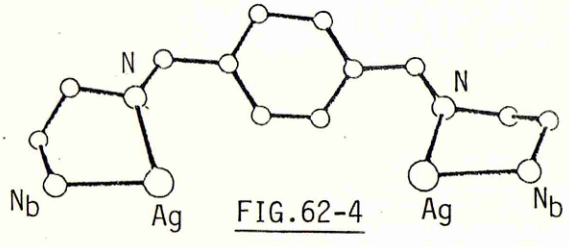

FIG.62-4

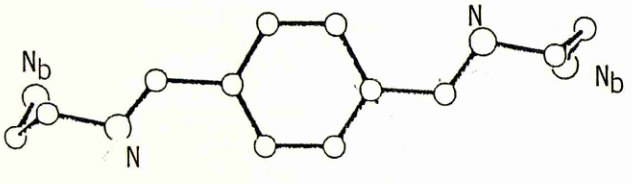

FIG.62-5

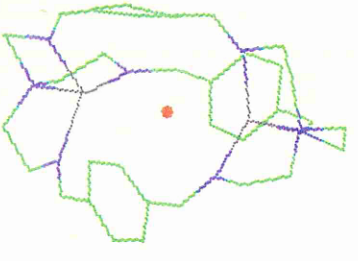

FIG.62-6

MODELLED WITH O_2

Ag....Ag 7.02A

Thus although the Ag-H distances in[$Ag_2$3Bp]$^{2+}$ may be on the 'short' side, the Ag-C_{aryl} distances do not appear to be so.

When the structure was minimized by molecular mechanics (this work by Mike Drew is gratefully acknowledged) and the Ag-H distances increased to normal van der Waals contact distances, a modification which the macrobicyclic structure can accomodate without a significant increase in the strain of the system, the Ag-Ag distance increases to 7.27Å (from 6.06Å in the X-rayed structure) FIG.62-2a&b. However the 'Hnmr spectrum of [$Ag_2$3Bp]$^{2+}$ (FIG.63-5) shows no sign of splitting of the aromatic signal indicating free rotation of the p-phenylene unit - this would seem incompatible with strong Ag-H_{aryl} interactions. Thus, both the short Ag-H contacts and the unusual coordination of Ag^+ may result from steric necessity rather than any weak binding interaction. FIG.62-3 shows a view of the cation down the N_b--Ag....Ag--N_b vector,. As observed in the dicopper (1) cryptate of Lehn's macrobicyclic hexamine[60] the two sets of bridgehead N-C bonds are eclipsed giving an approximate D_3 symmetry with the N-M...M-N vector axial. Although the mean torsion angle in 3Bp was essentially 0°, in [$Ag_2$3Bp]$^{2+}$ the N=C-C-C mean is 21.3°. Thus the conformation adopted in [$Ag_2$3Bp]$^{2+}$ results in a closing up of the potential cavity even at the cost of considerable loss of planarity in the conjugated phenylene bis imino link.

It is apparent from the crystal structures of complexed and uncomplexed 3Bp that the two show very different conformations. This essentially results from the arrangement of the imine groups relative to each other: this is cis in the disilver cryptate FIG. 62-4 and trans in the free ligand 62-5.

The possibility of guest inclusion in the disilver cryptate was modelled. Taking the crystal structure of [$Ag_2$3Bp]$^{2+}$ (Ag...Ag 6.06Å) 62-2a as a starting point, an atom X, at a point intermediate between the two silver atoms would be only 2.62Å away from the phenyl C atom and indeed only 3.03Å from the two silver atoms. This implies there is little room within the cavity of this conformation for guest inclusion. However on energy minimization (previously discussed: giving Ag...Ag 7.27Å 62-2b), X, given parameters appropriate to oxygen, fitted into the cavity with no contacts to the macrocycle (less than 3.0Å.) - This refined structure showed a

Ag....Ag distance of 7.02Å Fig.62-6. Presumably the macrobicycle has to expand outwards to make more room in the middle (to accomodate and hold the oxygen) - as a consequence the Ag...Ag distance is less. It was not possible to fit a diatomic molecule into this cavity without causing severe distortions.

The different conformations of 3Bp in the free and complexed forms give rise to significant differences in the 'Hnmr spectrum. FIG.63-1 to 63-5 show the variable temperature nmr spectra recorded for 3Bp while 63-6,63-7 show the spectra for $Ag_2$3Bp$(CF_3SO_3)_2$. The nmr data are tabulated in FIG.64 whilst other physical data for 3Bp and its related complexes is given in FIG.65.

An immediate observation is that neither set of spectra show unusual chemical shifts for the aromatic protons (eg. H_c of 3Bm at δ5.33, H_b of 3Bm at δ8.13). However in $[Ag_2 3Bp]^{2+}$ there is a downfield shift of the aromatic proton signal (H_A) by - 0.6ppm and of the imino proton signal by ≃0.4ppm as against the uncomplexed cryptand. These shifts may be caused in part by co-ordination of the imine function in the cryptate which result in decreased electron density, and hence deshielding, at the imine proton.

The 'Hnmr of 3Bp was taken over the range 330-183K. The higher temperature spectra of 3Bp are quite simple in comparison with 3Bm (FIG.49-1). At 330K(63-1) all signals appear as sharp singlets except for a very slight fluxional broadening of the methylene signals. Thus it appears that at this temperature there is no distinction between Hax and Heq and therefore only minimal steric constraint within the molecule. At the lowest temperature studied, ie 183K (63-4), only the imine peak remains unsplit and relatively sharp. This shows that the observed broadening of the other signals, which in part is due to increasing solvent viscosity due to the low temperatures involved, is a result of fluxional behaviour of 3Bp. The sharp singlet (at room temperature), assigned to the aromatic protons, is now observed as a series of unresolved broad signals. This indicates that some fluxional process involving the aryl protons is operational, and that this process is very slow on the nmr time scale at the low temperatures. There thus appear to be two separate sources of fluxionality in 3Bp - one

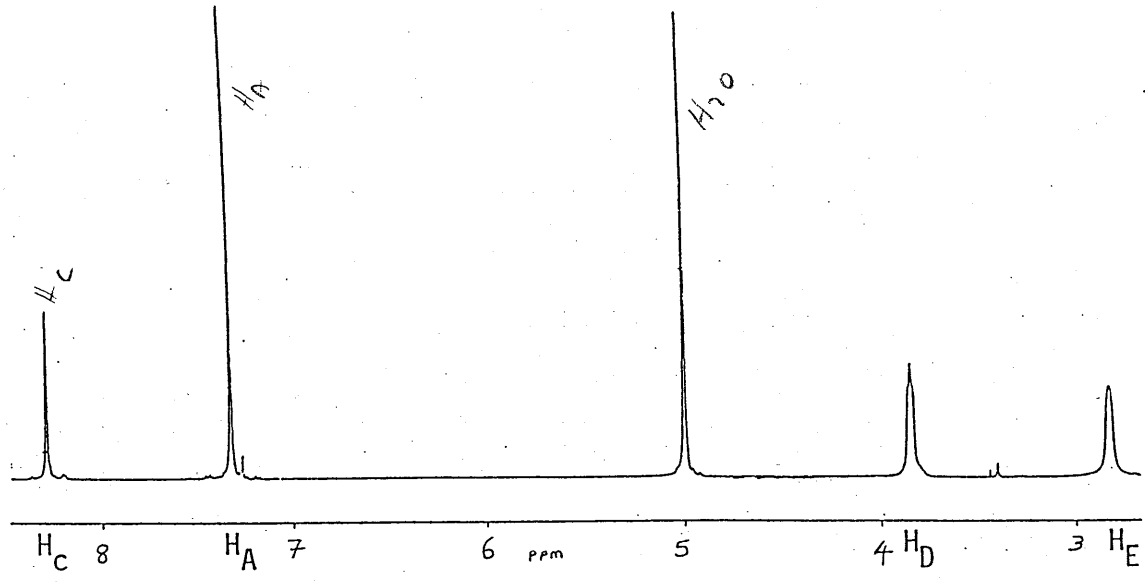

FIG.63-1 FULL SPECTRUM 330k.

FIG.63-2
METHYLENE SIGNAL 258k

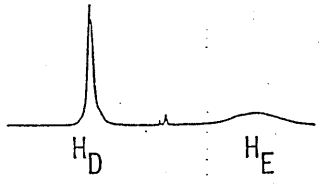

FIG.63-3
223k

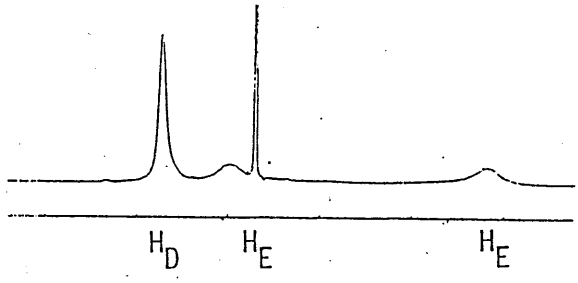

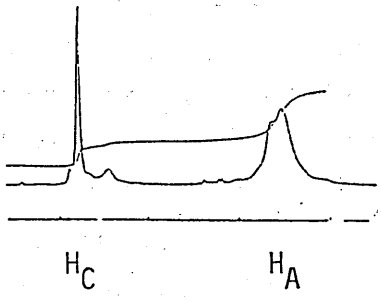

FIG.64-4
FULL SPECTRUM
203k

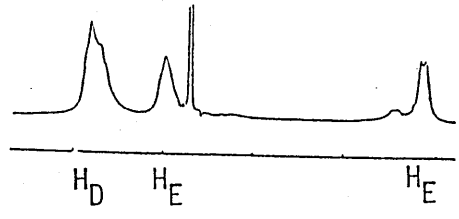

FIG.63-5 193k

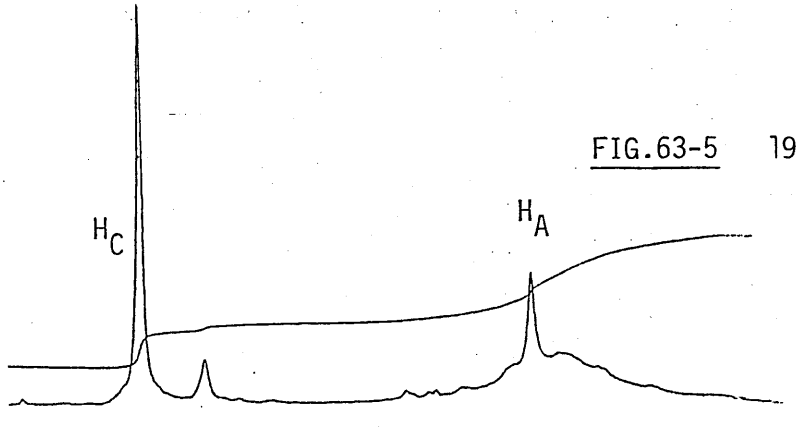

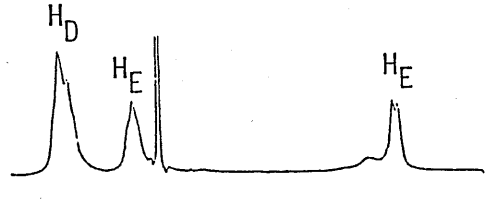

associated with the methylene protons and another associated with the aromatic units in the macrobicycle.

Firstly, the methylene groups which exhibit very different behaviour over the temperature range studied. The methylene protons α to the imine function ie H_D do not appear to reach their Tc until ≃223K 65-4 whereas H_E passes through its Tc at a relatively higher temperature, T_c -15°C, 258K, and thus shows greater resolution of its axial and equatorial components. In order to see if this difference in coalescence temperature was a result of different $\Delta G^{\ddagger}_c$ for H_D and H_E, Eqn 2. and Eqn 4. (see introduction to this section) were applied. Results allowing for experimental error suggest that $\Delta G^{\ddagger}_c$ = 47 KJ applies for both H_D and H_E protons. The main values used in determining this are tabulated below -

PROTON SITE	$\Delta\nu$ (obtained from 203K spectrum)	τ^{-1} from $\tau^{-1}=\pi\Delta\nu/2^{1/2}$	T_c	FREQUENCY FACTOR $A=K_B.T_c/h$	$\Delta G_c^{\ddagger}$ $kJmol^{-1}$
H_D	≃20Hz*	44.43	223*	4.646×10^{12}	47.1
H_E	572Hz	1271	258*	5.38×10^{12}	47.54

*(These values could only be estimated)

Despite having to use estimates of Tc and $\Delta\nu$ the results seem to correlate quite well. Thus it would appear that the large difference in the splitting of the axial and equatiorial signals for H_D and H_E is not a result of a significant difference in $\Delta G^{\ddagger}_c$ values. They also show that the more widely split signal ie H_E shows the higher T_c value. Thus at lower temperatures a doublet (equatorial) and an unresolved axial signal result. From the doublet an estimate of $J_{gem}=10.33H_z$ was possible. If it had been possible to take the temperature down further we might well have observed a similar arrangement of the signals as in uncomplexed 3Bm ie eq,ax,ax,eq. However the coalescence temperatures for 3Bp are significantly lower than in 3Bm. This presumably reflects a lower activation energy for the fluxional process of the methylene groups in 3Bp, which result from its

FIG.63-6
294k 500MHz

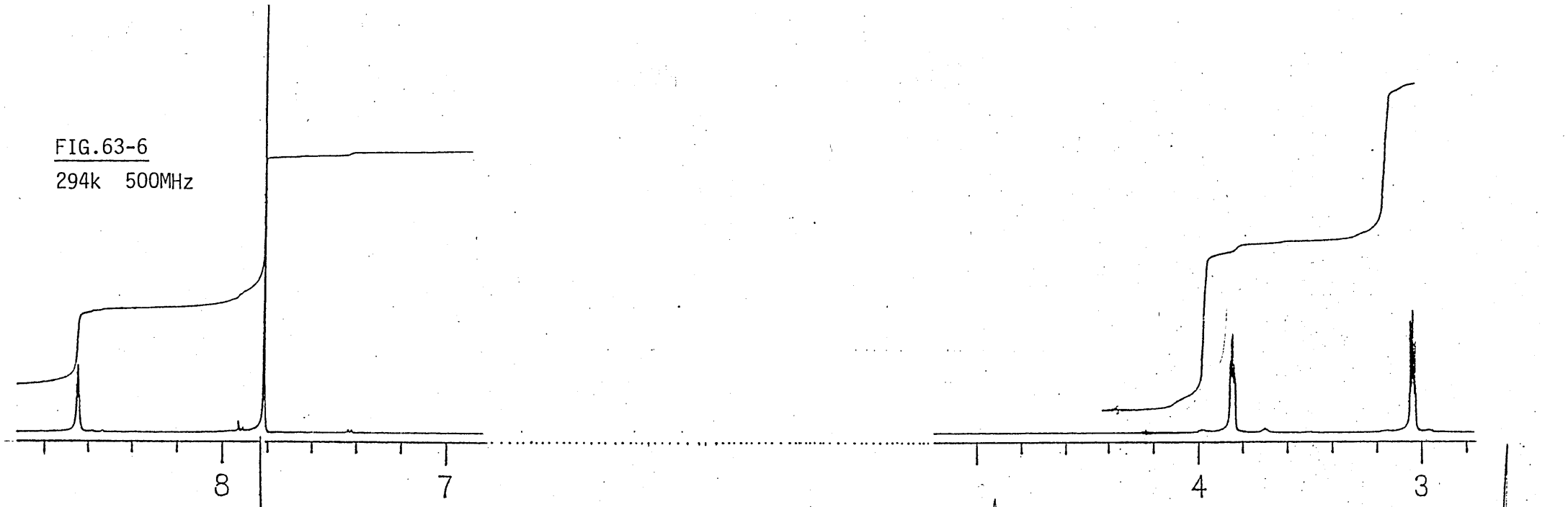

FIG.63-7
233k

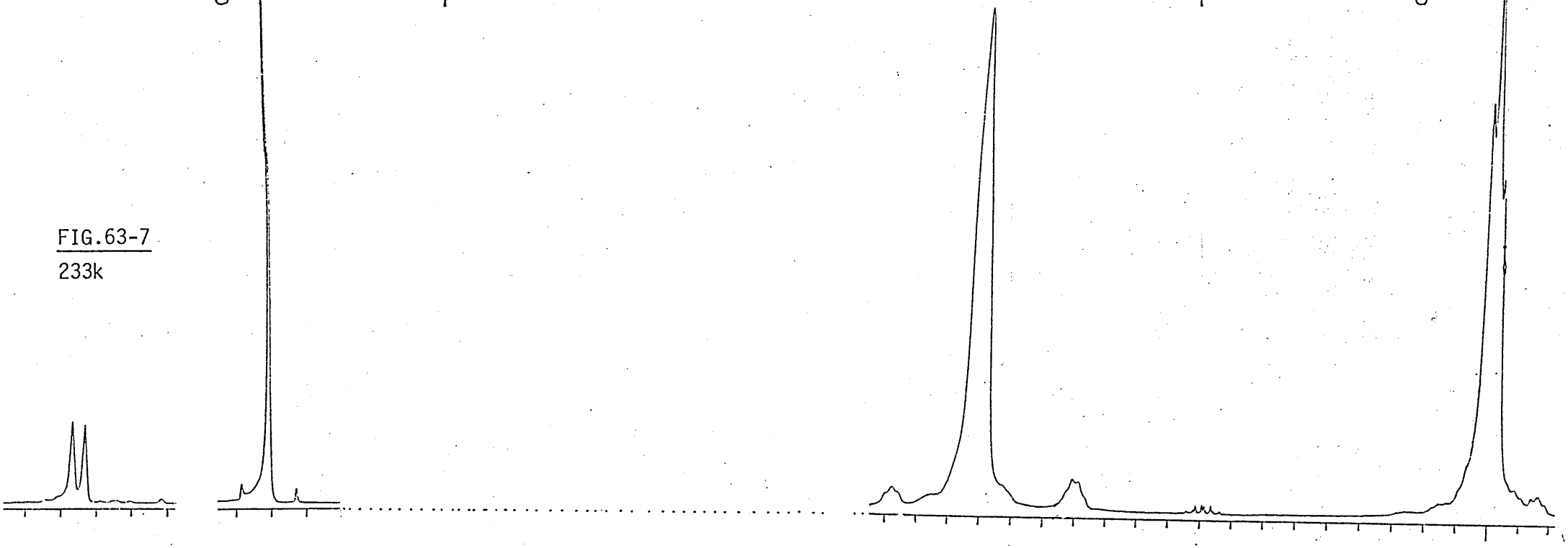

FIGURE 64. NMR[a] DATA FOR 3Bp AND ITS INSERTION PRODUCTS

LIGAND/COMPLEX	TEMPERATURE (K)	SOLVENT	SPECTRUM	HYDROGEN/CARBON SITE				
				A	B	C	D	E
$3Bp^{c}.6H_2O$	298	CD_3OD	^1H 360 MHz	7.32 (s)		8.29 (s)	3.84 (t)	2.83 (br,s)
$3Bp.6H_2O$	183	CD_3OD	^1H 360 MHz	7.0-7.5 (br,m)		8.4 (s)	3.84 (br,s)	3.4 (br) 2.1 (br)
$3Bp.6H_2O$	298	$CDCl_3$	$^{13}C^{b}$ 90 MHz	153.15 (d)	165.59 (s)	194.58 (d)	69.86 (t)	63.49 (t)
$[Ag_2\ 3Bp]^{2+}$	293	CD_3CN	^1H 400 MHz	7.86 (s)		8.70 (s)	3.90 (t)	3.07 (t)
$[Ag_2\ 3Bp]^{2+}$	233	CD_3CN	^1H 400 MHz	7.86 (s)		8.68 (d)	3.85 (s)	3.05 (t)[d]
$[Cu_2\ 3Bp]^{2+}$	293	CD_3CN	^1H 400 MHz	7.42 (s)		8.59 (s)	3.87 (t)	3.15 (t)
$[Cu_2\ 3Bp]^{2+}$	233	CD_3CN	^1H 400 MHz	7.22 (s)		8.58 (s)	3.83 (br,t)	3.11 (t)
$[Ag_2\ 3Bp]^{2+}$	294	CD_3CN	$^{13}C^{b}$ 90 MHz	116.9 (d)	163.227 (s)	127.46 (d)	56.2 (t)	50.7 (t)

(a) ppm from T.M.S.: (s) singlet, (d) doublet, (t) triplet, (br) broad.

(b) Off resonance multiplicity shown in brackets.

(c) Water at 5.5 ppm (integral = 12 H).

(d) Poorly resolved.

increased cavity size and flexibility, so reducing the steric constraints seen in 3Bm.

The second source of fluxional behaviour in 3Bp is associated with the aromatic component of the molecule. The spectra show that the aromatic rings are mobile down to temperatures of about 220K. However below this temperature the aromatic moieties are restricted in their motion-this may reflect a slow rotation about the C_B - C_C bond.

The peak at 5.5ppm in the spectrum is assigned to 6 hydrogen bonded waters. (integral values support this assignment) and it is temperature independent. This suggests that these waters are associating strongly with the macrocyclic unit, because water signals would "wander" with temperature if a significant fraction were uncomplexed at the higher temperatures. When uncomplexed in solution the water will at one instance be free and at another time it will for example be bound to the N_b. The spectrum would record the average position of the water which would change with time and temperature.

In the case of $[Ag_2 3Bp]^{2+}$ the temperature range was governed by solvent choice. At room temperature 63-6 all signals are sharp and well defined with no splitting of the aromatic or imine signal. This suggests free rotation of the aromatic rings about the C_B-C_C bond because from the crystal structure (62-1) it would be difficult to explain how the aromatic protons could be equivalent with respect to distance and their relationship to the encapsulated Ag^+. The methylene resonances appear as sharp triplets [(n+1) rule obeyed, 1st order signal, $\Delta v/J > 10$] giving no evidence for any dynamic process taking place on the nmr time scale. As in Lehn's structure[60] FIG.66, large downfield shifts of 0.41ppm and 0.54ppm of the imino and aromatic protons respectively are evident on complexation. At 233K(63-7) the aromatic signal remains sharp and unsplit which again points to free rotation. However at this temperature the imine signal is now split into a doublet (J=8Hz). This large coupling, for the 3 bond interaction, is too large not to be observed at room temperature if the Ag^+ was permanently fixed inside the cavity. Thus at room temperature, there may be a fast exchange process between free and complexed Ag^+ ions, as we

FIGURE 65. PHYSICAL DATA FOR 3Bp AND ITS RELATED COMPLEXES

COMPLEX	M^+ OR F.A.B.[a]	Ω^b S cm^2 mol^{-1}	ELEMENTAL ANALYSIS[c]	INFRARED SPECTRUM (cm^{-1}) C=N	NH	OTHER	ELECTRONIC SPECTRUM SOLVENT CONC.	λ (nm)[d]	ε (M^{-1} cm^{-1})
$3Bp.6H_2O$	587 (100)		C 62.1 (61.7) H 7.8 (7.9) N 16.1 (16.5)	1643		H_2O 3600- 3000 H_2O	MeOH 10^{-5}	263[d]	248000 183000[e]
$Ag_2 3Bp(CF_3SO_3)_2$	951 (22) 693 (100) 587 (10)	262	C 41.5 (41.9) H 3.9 (4.0) N 10.2 (10.4)	1644		$CF_3SO_3^-$ at 1266 1162 1028	MeCN 10^{-4} 10^{-5}	333 263[d] 215[e]	1630 80600 42800[e]
$Cu_2 3Bp(ClO_4)_2$	599 (100)	367[b]	C 47.39 (47.23) H 4.64 (4.63) N 12.28 (12.24)		3273		MeCN 10^{-4} 10^{-5}	362 260 208[d,e]	8000 75000
$Ag_2 R3Bp(CF_3SO_3)_2 .H_2O$		236	C 40.4 (40.4) H 4.9 (4.2) N 9.5 (9.9)		3272		MeCN 10^{-3} 10^{-5}	448 257 210[d,e]	100 5700 30400[e]

(a) % of base peak. (b) 10^{-4} M. (c) Experimentally found result in brackets.

(d) λ_{max}. (e) Unreliable result.

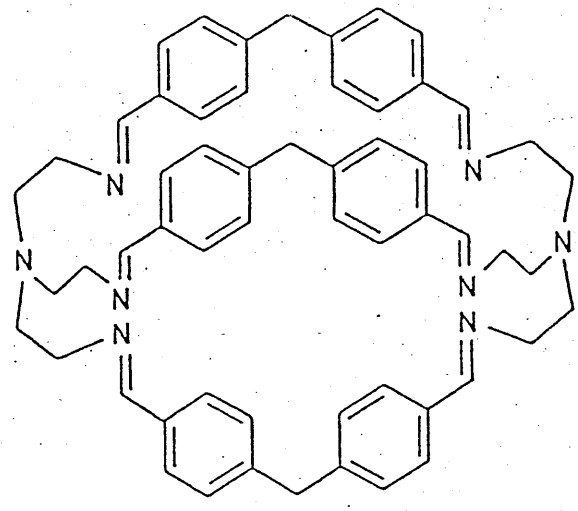

FIGURE 66

suggested for the $[Ag_2 3Bm]^{2+}$ situation. Again in the analogous $diCu^{I}$ cryptate of 3Bp there is no splitting, only broadening of the imine signal. The methylene signals at this lowest temperature show broadening due to a slowing down of the ax-eq fluxional process.

A 500MHz spectrum of $[Ag_2 3Bp]^{2+}$ has recently been run (Dr.P.Stevenson, Q.U.B) and the low temperature (233K) spectra is shown in Fig.63-7. As in the 400MHz spectrum the H_D signal has lost much of its triplet structure and is well on its way to coalescence. H_E still retains it triplet structure to some extent (J_{ED} = ≈5Hz ie first order coupling). However the interesting features seen in this spectrum are -

-1- the 2 small bands on either side of H_D and to a lesser extent H_E

-2- the presence of small baseline features on either side of the imine function.

By offsetting the H_D signal by 0.3ppm it was shown that these were not ^{13}C satellite peaks which would have reflected this offset and remained equally spaced on either side of the main peak - rather these features remained unaffected by the offset and thus they indicate the presence of at least one other conformation. Indeed by looking closely at these features it is possible to make out a triplet (lowfield) and a doublet(highfield) feature associating with H_D, and a triplet on the highfield side of H_E. Collaborative work with M.Drew is in progress in which the various conformations and their relative energies (and hence the equilibrium concentration) is in progress.

The splitting of the imine signal into a doublet with J=8Hz is the same value seen in the 400MHz spectrum giving support for the idea of Ag-H_E coupling.

The ^{13}C spectrum of 3Bp was simple with one signal per each carbon type. The data is given in FIG.64. A weak ^{13}C spectrum of the disilver cryptate allowed us to note the existence of upfield shifts of 30-40ppm in the aromatic signals and ≈13ppm in the methylene signals. These shifts are

FIGURE 67 THE ^{1}Hnmr SPECTRA OF $(Cu_2 3Bp)^{2+}$

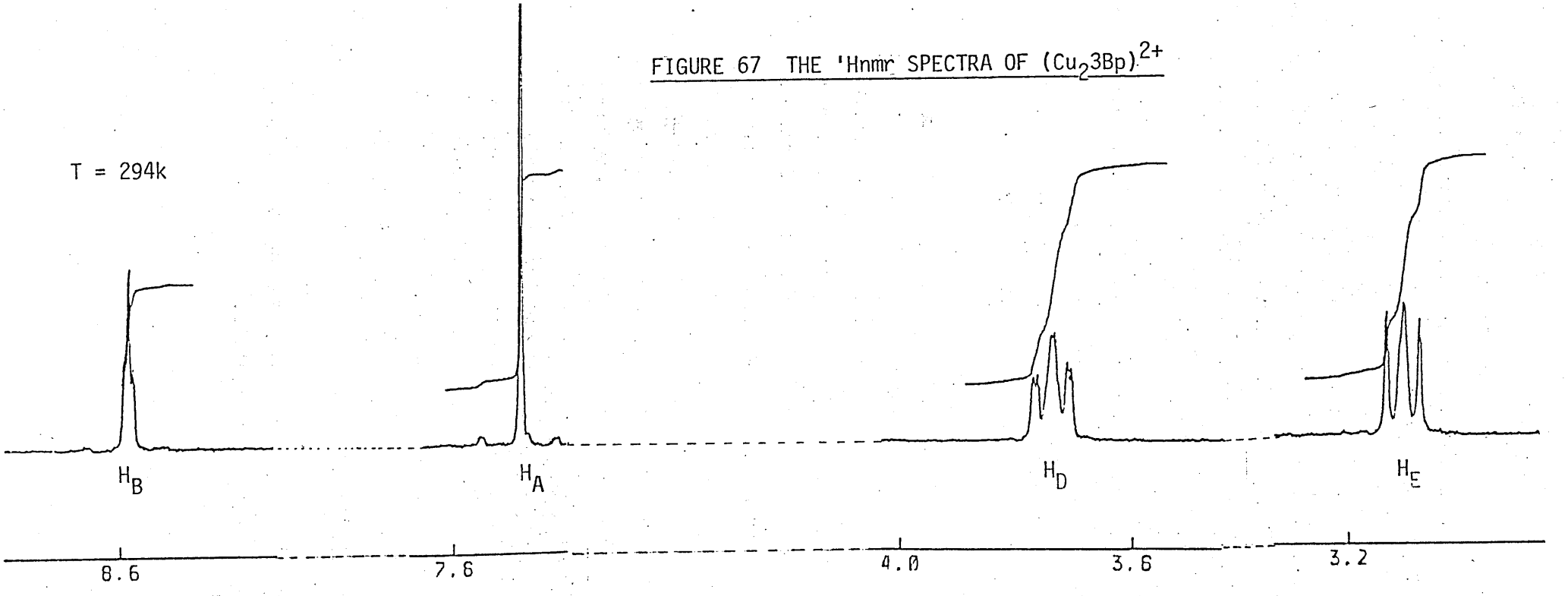

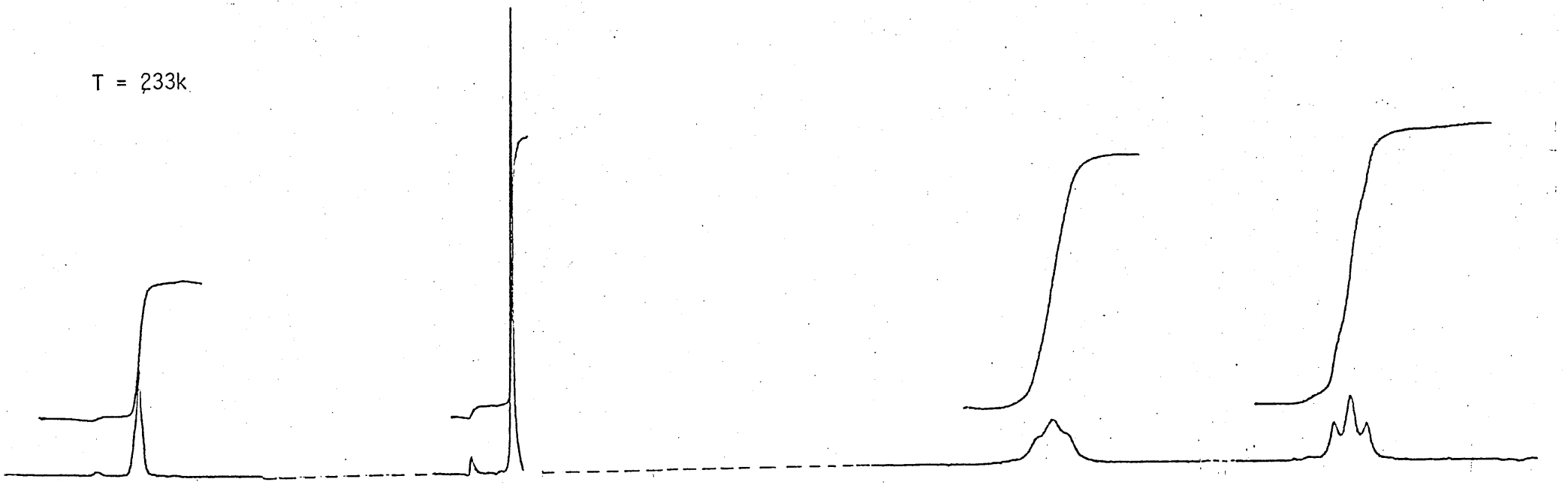

likely to result from the different conformations of the free and complexed ligand. Fluxional behaviour was not observed in either of the ^{13}C spectra.

Cu^{I} will insert into 3Bp in inert conditions to give an orange crystalline product that is stable in air and microanalysis confirms that the complex $Cu_{2}3Bp(ClO_{4})_{2}$ has been formed. The physical data for the compound are tabulated in FIG.65 while the nmr data are given in FIG.64 and the spectra shown in FIG.67.

The electronic absorption spectra shows the 2 ligand absorptions at 208 and 260nm seen in the uncomplexed form of the ligand. However an absorption at 362nm(ϵ=8000) is likely to a MLCT transition although the $\Pi\Pi^{*}$ or $n\Pi^{*}$ transition of the imine function might also account for this absorption.

The room temperature proton nmr of $[Cu_{2}3Bp]^{2+}$ is quite simple. The methylene protons H_{D} and H_{E} are triplets ie a first order spectrum with $\Delta V/J>10$. Each triplet component of H_{D} shows slight splitting (J=1.46Hz). The imine signal at δ8.59 also shows slight splitting into a triplet and again J=1.46Hz. Thus there appears to be a long range coupling of the Hc and H_{D} protons. The triplet fine structure in the imine signal results from coupling to 2 H_{D} protons. The aromatic signal appears as a sharp singlet at 7.7ppm thus indicating that the aromatic rings are not sterically constrained and thus able to undergo free rotation about the C_{B}-Cc bond. At 233K the methylene signals are significantly broadened. Indeed H_{D} is very close to its Tc appearing as a broad singlet showing shoulders rather than the definite triplet structure still observable for the H_{E} protons. The imine signal has lost the fine structure and appears as a slightly broadened structure. This may result from coupling with the copper nucleus which, as discussed previously, is unlikely to be resolved. The aromatic signal remains sharp and unsplit. Thus even at the lowest temperature the aromatic rings are freely mobile.

Unlike 3Bm, the reaction of 3Bp with Cu^{2+} gave only a very crude, poor quality product which was too insoluble to be recrystallized.

FIGURE 68 - THE OCTAAMINO DERIVATIVES OF 3Bm and 3Bp

FIG.68-1
R3Bm

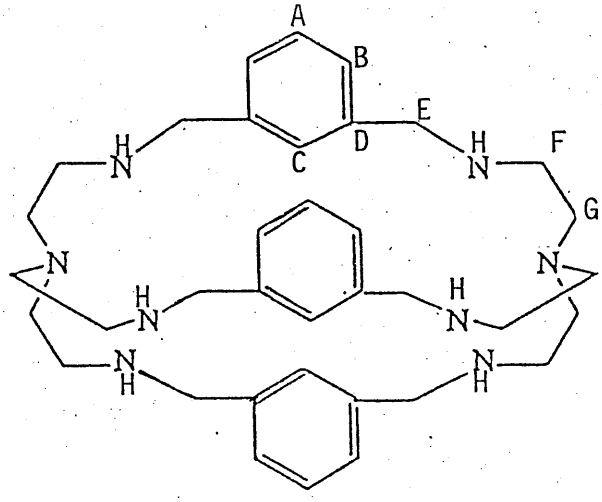

LIGAND R3Bm

FIG.68-2
R3Bp

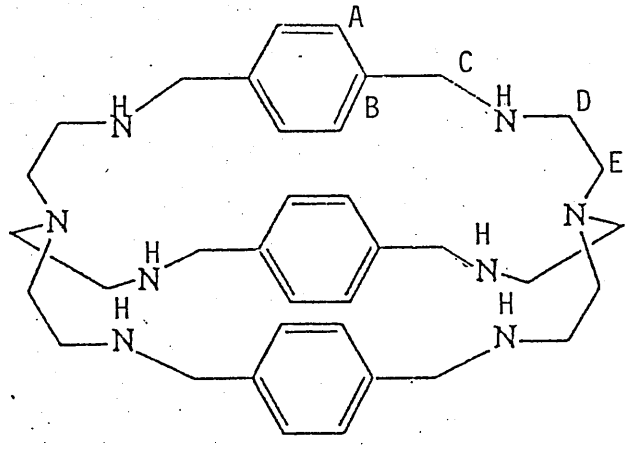

LIGAND R3Bp

R3Bm and R3Bp - The Octaamino Derivatives of 3Bm and 3Bp.

The imine functions in the macrobicyclic cyclophanes may be readily hydrogenated yielding the octaamine derivatives, R3Bm FIG.68-1 and R3Bp, FIG.68-2, which are superior in chemical robustness and flexibility to their Schiff-base parent derivatives. Reduced ligands of this type may be capable of acting as "hosts" for small guest molecules as they have polarity appropriate to the encapsulation of inorganic ions or small polar organic guests. Indeed, their more flexible nature should make it easier for them to accept a wider range of substrates than their unreduced hexaimine form.

It was possible to reduce ligand 3Bp in a variety of ways:

a - on the isolated disilver or dilead cryptate

b - via in situ reduction of the silver or lead systems.

c - from the free ligand 3Bp.

d - via in situ reaction between terephthaladehyde, tren and BH_4^-.

In each of the 4 cases sodium borohydride ($NaBH_4$) was used as the reducing agent although conditions varied according to the method used. Yields also varied but were optimized when the metal templated species was isolated before being reduced. Hence method a gave a 41% yield, b, 22%, c, 34%, d, 19%. In each case the product was a waxy solid which gave a strong mass spectral parent ion peak at 598.[3Bp + $12H^+$], 3Bm was similarly reduced using $NaBH_4$ but only methods c and d could be employed resulting in yields of 66% and 54% respectively. Again the parent ion peak in the mass spec was 598 corresponding to [3Bm + $12H^+$] ,ie. the octaamino derivative.

Both octaamine ligands are soluble in dilute aqueous acids, presumably as a result of protonation at the amine nitrogens. Attempts to obtain a crystal suitable for X-ray structural analysis are in progress, using HBr, HCl and HI.

Physical data for R3Bm and R3Bp are tabulated in FIG.44 while their ir and uv spectra are shown in FIG.45-2, 45-4 and 46-2,46-4 respectively. The

ir's of the products of the reduction reaction are very different to those of the hexaimine parent macrobicycles. Gone is the strong signal at $\simeq$1640cm^{-1} associated with the imine function. The appearence of a medium intensity peak at 3298cm^{-1} for R3Bm and 3231cm^{-1} for R3Bp indicates that NH groups are now present and that the hexaimine ligand has been successfully reduced to the octaamine macrobicycle.

The uv spectra of the 2 reduced ligands (FIG.47-3, 47-4) show significant differences when compared to their Schiff base derivatives, however the spectra of the 2 reduced ligands when compared to each other are really quite similar. Both show a decrease in the intensity of their absorption bands (hypochromic effect) resulting from the loss of the imine chromophore. R3Bp also shows a blue shifted spectrum (hypsochromic shift) from that in 3Bp. Alternatively the signal lost is the Π-Π^* transition associated with the C=N function in 3Bp. Thus it appears that R3Bm having lost some of its steric constraints in losing the C=N is more like R3Bp than 3Bm is to 3Bp where steric constraints and close approach of the benzene rings create significant differences in the hexaimine ligands. Both reduced ligands now show λmax at 205nm(ϵ=67,100) for R3Bm and at 204nm(ϵ=34,000) for R3Bp although the extinction coefficients are again ~~are~~ unreliable.

The proton nmr spectrum of R3Bm is shown in 69-1, 69-2 and that of R3Bp in 69-3, 69-4. The relevant data is tabulated in 69-5. Neither of the room temperature spectra show any evidence of fluxional behaviour, or separation of the methylene group protons into the axial and equatorial components. Reduction results in the loss of the imine function, which eliminates the signal at 7.58 and 8.29ppm for 3Bm and 3Bp respectively, and the formation of a new methylene group. This comes ito resonance at 3.62ppm for R3Bm and 3.67ppm for R3Bp.

The reduction process also creates six amino groups (NH), the signal of which is observed as a broad singlet at $\simeq$2.2ppm at room temperature. However on cooling the system down to low temperatures the signal moves to higher fields ($\simeq$1.7ppm). In each case the NH resonance was identified by a D_2O shake. These room temperature spectra, which show no fluxional

FIG.69-1 R3Bm 294k

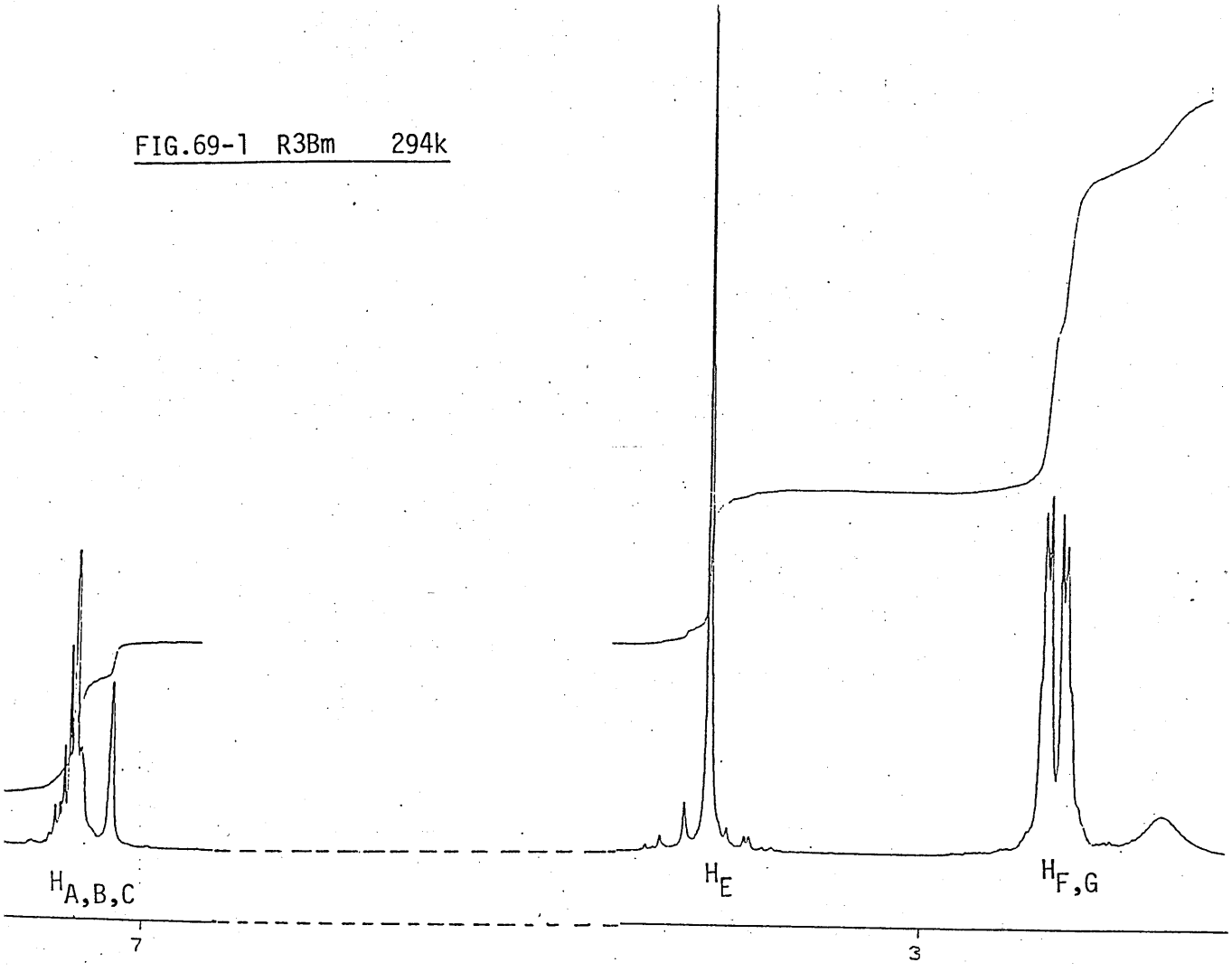

FIG.69-2 R3Bm 233k

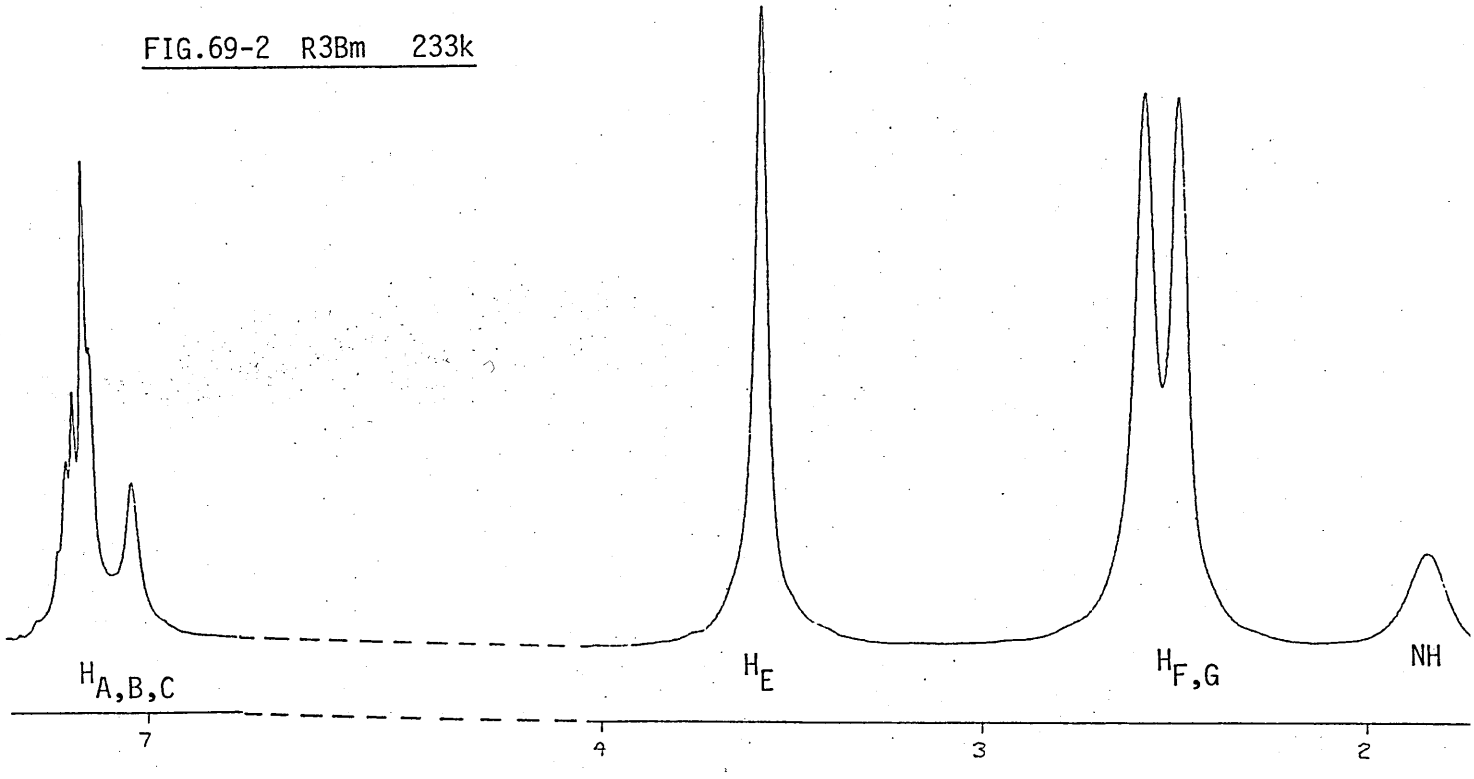

FIG.69-3 R3Bp 294k

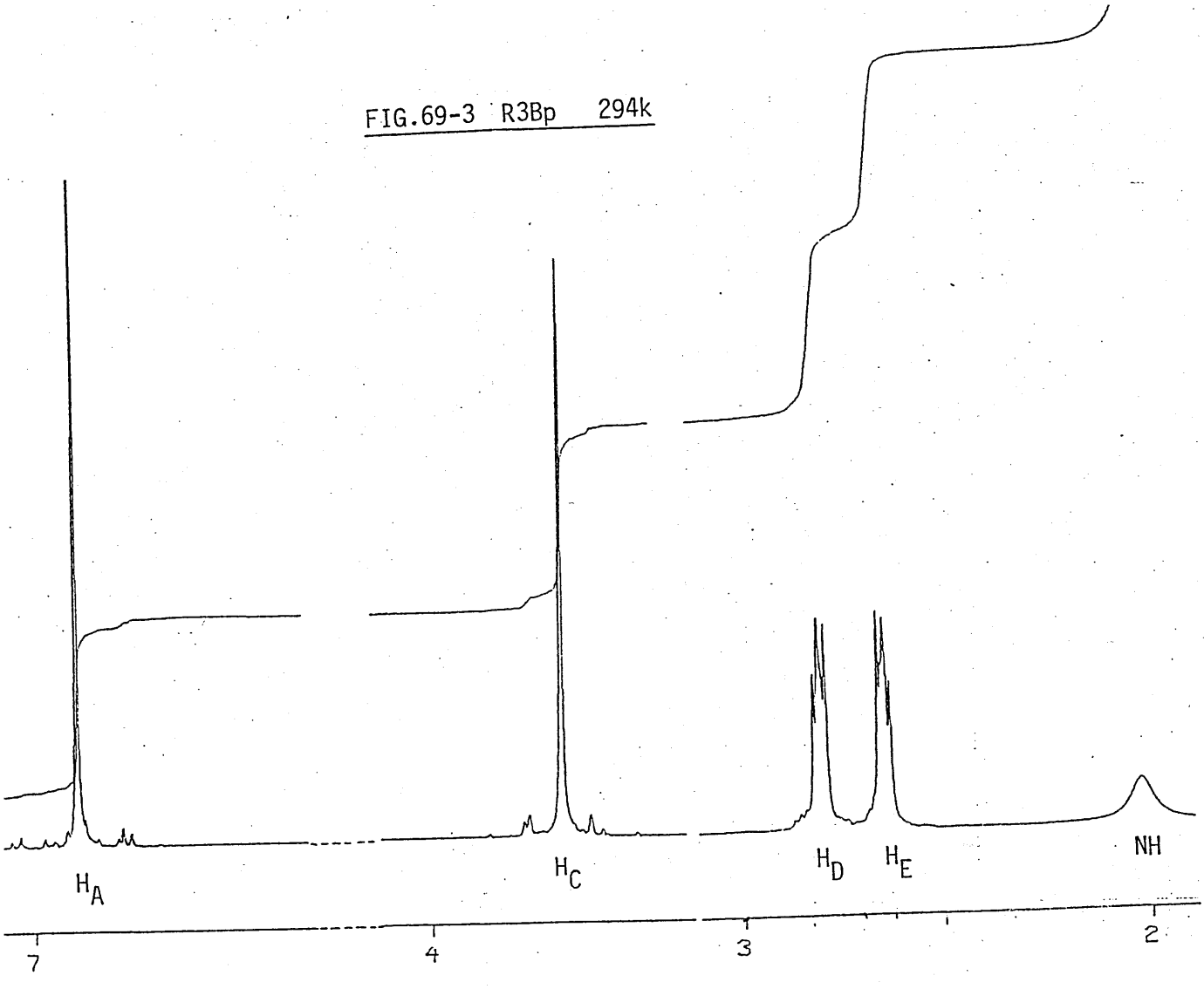

FIG.69-4 183k

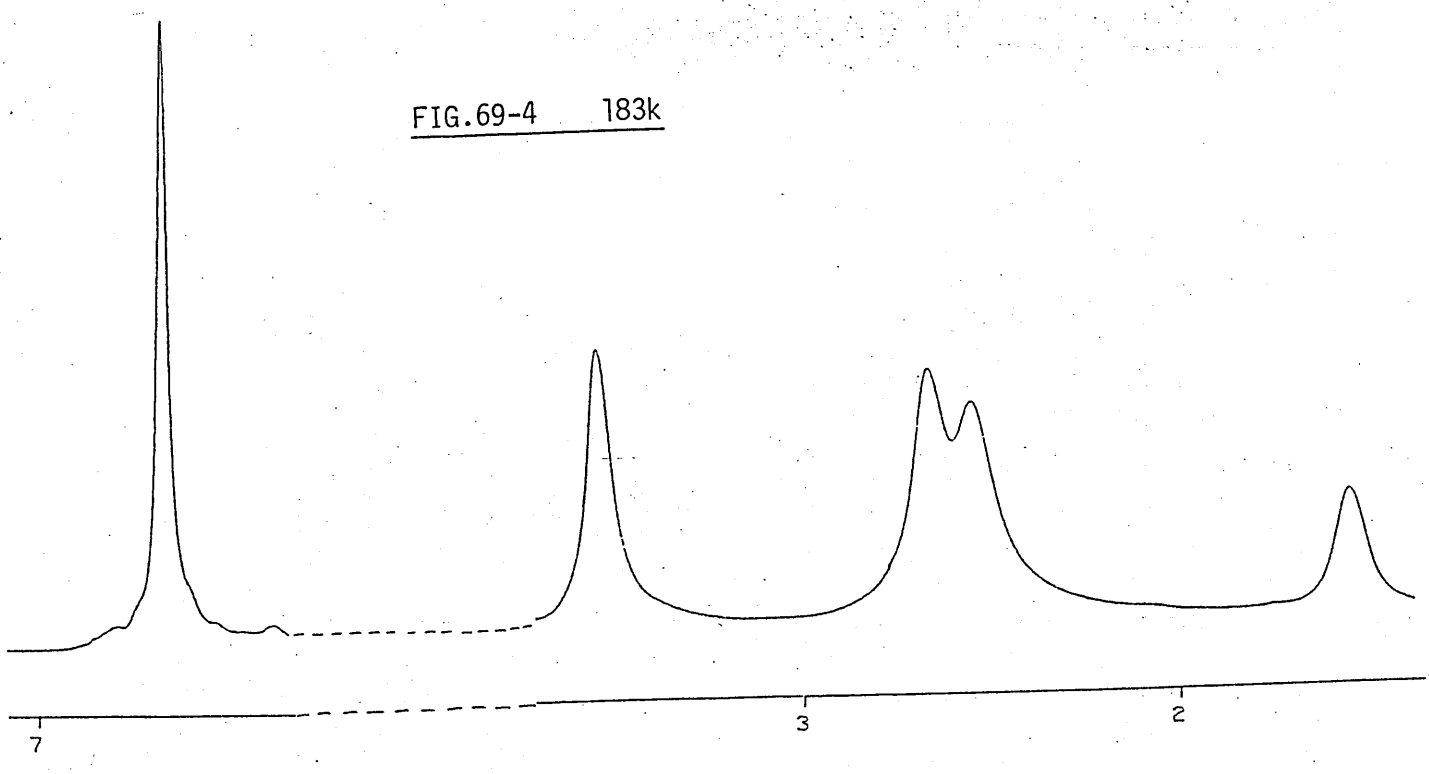

broadening support the idea that there is a greater degree of flexibility in these reduced systems which may indicate a greater amount of free space in the cavity. In the case of R3Bm there are no longer the abnormal shifts of the Hc protons caused by the close approach of adjacent aromatic rings. The Hc signal which had been at 5.33ppm in 3Bm now lies at 7,039ppm which is a typical chemical shift for an aromatic proton. The appearance of the aromatic signal suggests that even in the reduced ligand a degree of steric constraint is still in operation.

At room temperature the H_F and H_G methylene groups of R3Bm 69-1 give a pair of sharp well resolved doublets. These are a result of 2nd order spectral complications (ie.$\Delta v/J < 10$) leading to distortion of the H_F and H_G signals. A simple 1st order spectra ($\Delta v/J>10$) would have given 2 triplets each showing a 1:2:1 intensity ratio resulting from the time averaged picture of 2 equivalent neighbouring protons (equivalence resulting from the rapid interconversion of the axial and equatorial protons). As the temperature is decreased, the rate at which the axial and equatorial protons are exchanging is slowed down and at 203K the rate of exchange is very similar to the nmr time scale. Solvent viscosity may also play a significant role at these very low temperatures. Thus the signals have lost their fine structure and become broad featureless signals. If it had been possible to reduce the temperature further we might have observed the resolved triplet and doublet structures for the axial and equatorial protons frozen out into their unique sites.

An noe experiment was carried out to see if any information about the conformation in solution for the reduced ligand, R3Bm, could be obtained. Irradiation into the new methylene group, H_E, at 3.62ppm gave enhancement of the proton signals Hc (10.9%), H_B(5%), H_F(2.6%) and H_G(0.08%). However H_E now comprises 2 protons, each of which in free rotation will enhance different protons, and so it becomes difficult to make any conclusions on the conformation of the system.

So the room temperature spectrum of R3Bm is an AA'BB' type spectrum which is complicated because of its 2nd order nature. This is a result of the easy interconversion of the axial and equatorial protons on the nmr time

FIGURE 69-5 N.M.R.[a] DATA FOR R3Bm AND R3Bp

LIGAND/ COMPLEX	TEMP.	SOLVENT	SPECTRUM	PROTON/CARBON SITE							
				A	B	C	D	E	F	G	NH[f]
R3Bm	298 K	$CDCl_3$	^1H 360 MHz	7.20[c] (m)		7.09 (s)		3.62 (s)	2.59 (m)	2.45 (m)	2.45
R3Bm	203 K	$CDCl_3$	^1H 360 MHz	7.20[c] (m)		7.03 (s)		3.57 (s)	2.58 (s)	2.49 (s)	1.84
R3Bm	294 K	$CDCl_3$	^1H NOE 360 MHz		5[e]	10.9[e]		d	2.6[e]		
R3Bp	298 K	CD_2Cl_2	^1H 360 MHz	6.88 (s)		3.67 (s)	2.8 (t)	2.65 (t)			2.01
R3Bp	183 K	CD_2Cl_2	^1H 360 MHz	6.66 (s)		3.53 (br,s)	2.64 (br,s)	2.53 (br,s)			1.54
R3Bp	294 K	$CDCl_3$	^{13}C[b] 90 MHz	127.51 (d)	138.4 (s)	54.1 (t)	53.6 (t)	47.95 (t)			

(a) ppm from T.M.S. (s) singlet, (d) doublet, (t) triplet, (m) multiplet, (br) broad.

(b) Symbol in bracket represents the multiplicity in off resonance spectra.

(c) Unassignable multiplet.

(d) Irradiated into this signal.

(e) % NOE enhancement.

(f) Confirmed by D_2O shake.

scale. Increased flexibility of this reduced species is implicit in these results and we therefore plan to investigate the ability of R3Bm to encapsulate metal cations and small non-polar guests.

R3Bp also shows a second order spectra with 2 triplets observed for H_D and H_E (resulting from the time averaged signals.)FIG.69-3. The intensity ratio of 1:2:1 is not observed due to minimal 2nd order distortions. Thus $\Delta\nu/J$ for R3Bm < $\Delta\nu/J$ R3Bp≃10. (and only slight distortion of the triplets in R3Bp). As the temperature decreases the rate of exchange of the axial and equatorial protons also decreases giving, at 183K, broad overlapping singlets FIG. 69-4. Again increased viscosity at these low temperatures (suggested by the soft/broadened nature of all the signals at this temperature) may be playing a role in the broadening of the signals.

In 3Bp the aromatic signal showed signs of splitting and fluxionality at 203K but for its reduced derivative, R3Bp, even at 183K the signal remains unsplit. Again this result implies a greater flexibility in R3Bp over the hexaimine 3Bp.

Attempted insertions of Ag^+ into R3Bm and R3Bp have given very different results for the two ligands. Early attempts to insert Ag^+ into R3Bm indicate that this ligand does not show the tendancy to form complexes. The product of this reaction however was not simply R3Bm but the protonated species H_2 R3Bm $(CF_3SO_3)_2$. IR shows strong signals for the triflate anion and microanalysis, FAB and Ω results all support this structure. The double protonation may occur at the bridgehead nitrogens - obviously the ligand must show weak basic properties. Basicity studies might be worth investigation. It is not clear why this double protonation should occur ie whether it is a conformational/geometrical consideration or whether it is simply that the ligand offers a particularly favourable site for the proton.

On the other hand Ag^+ inserted in R3Bp successfully giving a microcrystalline product - ir, microanalysis and FAB all confirming the nature of the product (FIG.65). The uv spectra of $[Ag_2 3Bp]^{2+}$ shows a hypochromic effect when compared to $[Ag_2 3Bp]^{2+}$ (λmax 263 ϵ=80,612 and λmax

FIGURE 70.

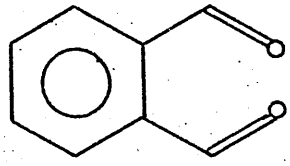

FIG.70-1 ORTHOPHTHALALDEHYDE.

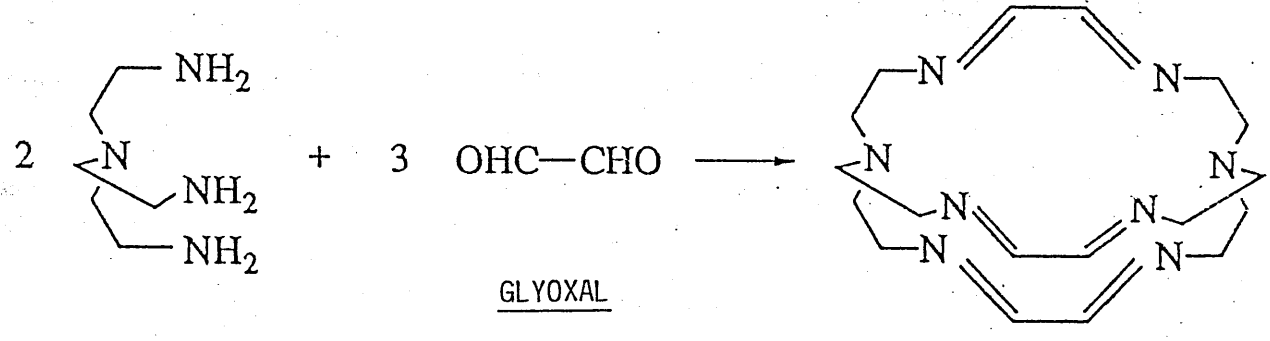

261 ϵ=5,960 respectively) Again this probably is a result of the loss of the chromophoric imine group.

My friend and colleague Josie Hunter has successfully developed the complexation chemistry of R3Bp with the 1st row transition metals. Initial experiments show that the triatomic M-O(H)-M assembly is readily accomodated within this macrobicyclic host.

Despite two months concentrated effort the condensation reaction of tren with orthophthalaldehyde FIG.70-1 was not achieved GrpI, II, 1st row transition metals, Ag^{+} and Pb^{2+} were all used as potential templating agents but none of them succeeded in giving anything more than a rubbery polymeric product. However when the aliphatic dialdehyde - glyoxal was reacted with tren in the presence of a Grp.II metal ion and the Ph_4B^{-} counter ion mononuclear cryptates were formed FIG.70. These template cryptates transmetallated successfully with the transition metals and some lanthanides. In all cases, except copper where a binuclear cryptate was obtained, the mononuclear cryptate was formed. This work was carried out by Josie Hunter. A possible explanation for the lack of success with this aromatic unit may be that it is on the "losing" side of a competing reaction, a monomer v's polymer competetion or alternatively a phthalamide type reaction may be taking place.

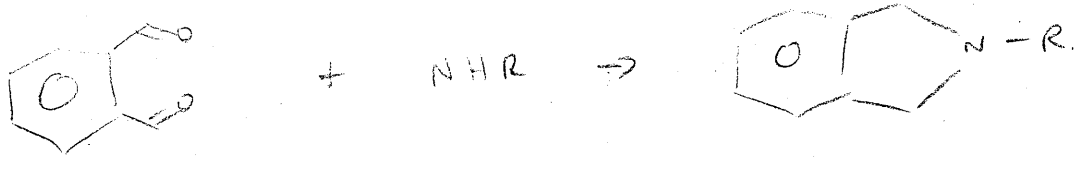

FIGURE 71

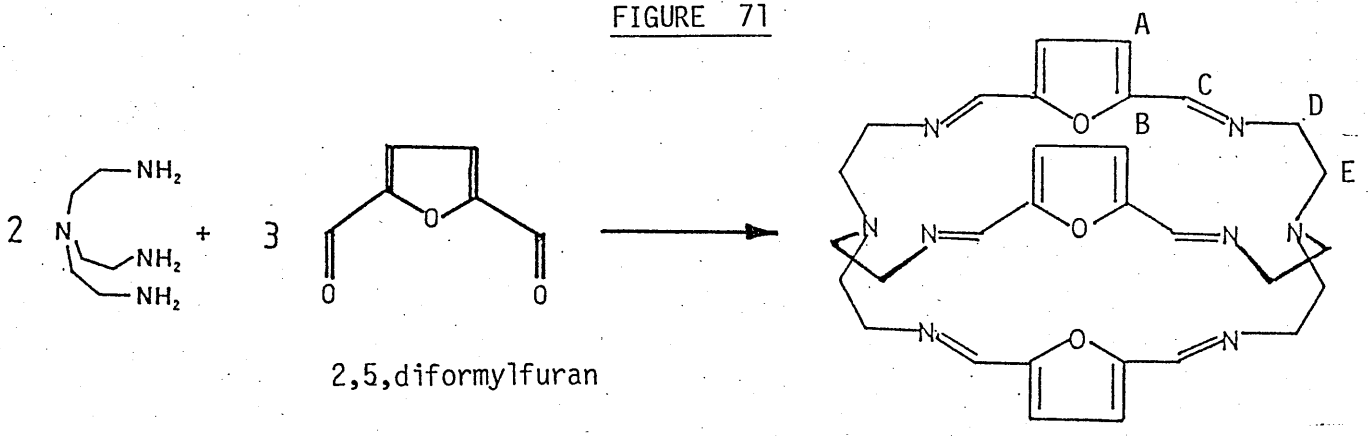

2,5,diformylfuran

FIG.71-2

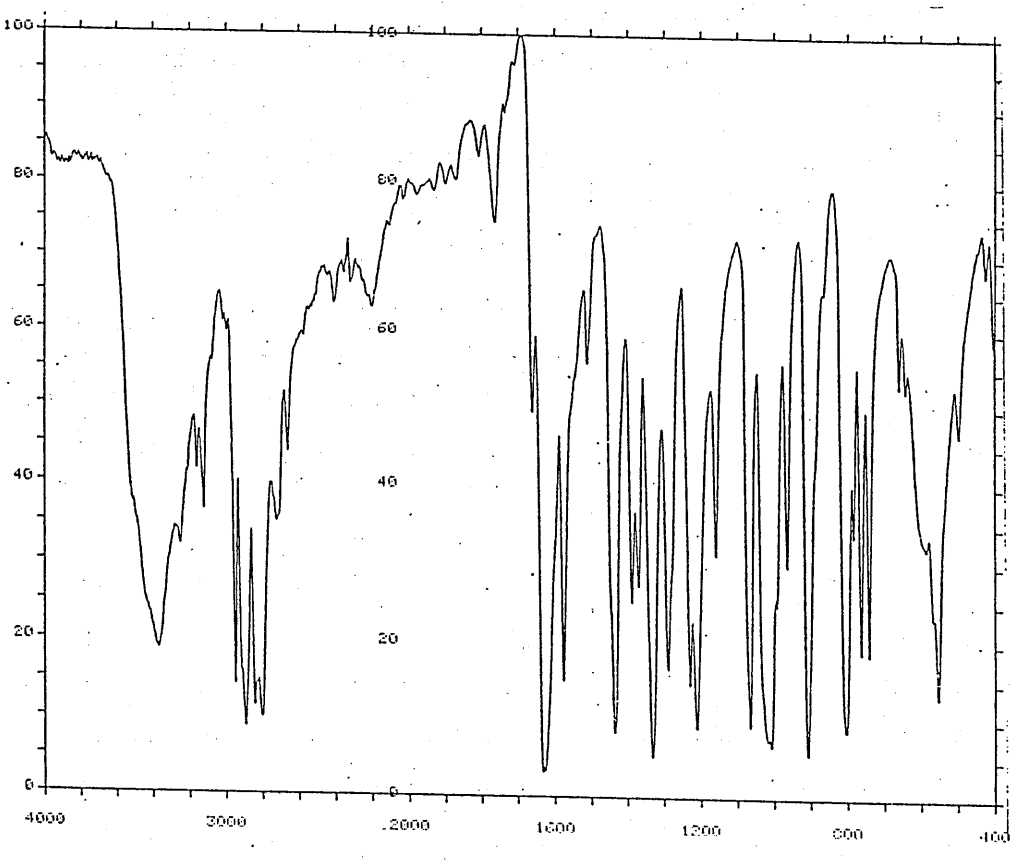

FIG.71-3

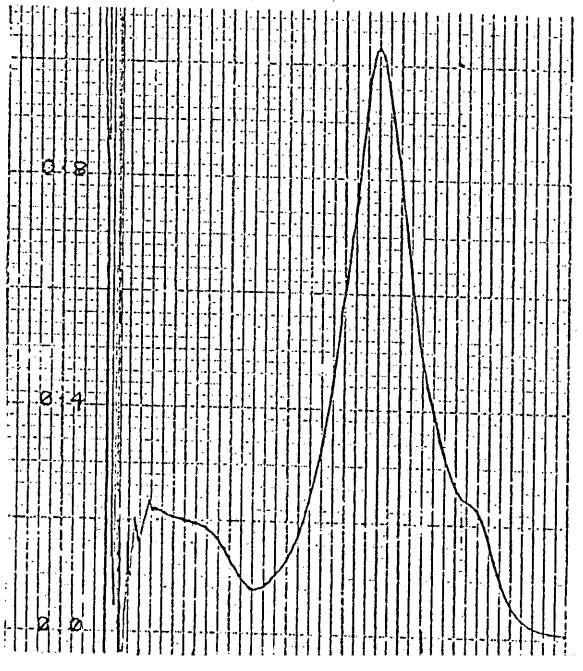

FIGURE 72. (contd.)

COMPLEX	MASS SPEC. F.A.B.[a]	Ω[b] S cm^2 mol^{-1}	ELEMENTAL ANALYSIS[c]	INFRARED SPECTRUM (cm^{-1})			ELECTRONIC SPECTRUM		
				C=N	X^-	OTHERS	SOLVENT	λ(nm)	ϵ(M^{-1} cm^{-1})
$Na(3F)ClO_4$	579 (100)	112	C 51.92 (52.04)	1640	1040,	2252	MeCN	315	28000
$.H_2O.2MeCN$	557 (26)		H 5.87 (5.64)		621	(MeCN)		276[d]	99000
			N 17.04 (17.11)			3403			
			Na 3.09 (3.25)			(H_2O)			

(a) % of base peak ion in brackets.

(b) 10^{-4} M

(c) Experimentally determined results.

(d) λ_{max}.

(e) Unreliable result.

The preparations involving DFF and 3F, are very sensitive to the temperature at which the reactions are carried out. Above 40°C two products are usually obtained - a rubbery polymeric product and a white powdery product which in the ir shows carbonyl (1690cm^{-1}), NH_2 (3240cm^{-1}) and imine (1630cm^{-1}) signals. This suggests incomplete ring closure. Contamination of the monomeric macrobicyclic product, by yellow polymeric material often occurs even at ambient. Such temperature sensitivity of DFF is common in furan based macrocyclic synthesis.

The electronic absorption spectrum of 3F, FIG.71-3, is dominated by a strong Π-Π^* absorption at 280nm ($\epsilon \simeq 10^5$). Two other absorptions at 218nm ($\epsilon=10^4$) and 314nm (25,000) are also probably Π-Π^* ligand transitions. The very intense absorption may result from significant interaction of the furan and imine chromophores brought about by the increased electron density of the furan ring. This is a result of the presence of the oxygen heteratom in the furan heterocycle and is discussed more fully later in this section.

The general structure of the macrobicyclic 3F is shown in FIG.73-1. It shows a 3 fold non-crystallographic axis running through N(1) and N(2) which are 10.40Å apart. Other N-N distances are given in FIG.73-1. From FIG 73-2 we see that as in 3Bm the methylene carbons are eclipsed. The triangular array of aromatic rings is very similar to that in 3Bm with the 3 furan oxygens 3.4, 3.4 and 3.6Å from the adjacent ring. (cf 3Bm Hc was 3.6Å from the mean plane of the adjacent benzene ring). The imine functions diverge from the cavity and thus lie in an uncoordinating arrangement. Only the bridgehead nitogens lone pairs are directed into the cavity. Thus the dicarbimine functions are in a trans, trans geometry relative to the furan C-O bonds - a conformation which has not been previously observed in a furan-derived macrocycle.[61]. The imine bond lengths of 1.26Å indicate that this is a fairly well localized -C=N-. This lack of conjugation should assist rotation about the furan-carbimine bond ie C_B - C_C.

Unlike 3Bp in which each of the 6 outward pointing imine functions are coordinated to a water molecule, there is only one solvent per 3F

FIG.73-1

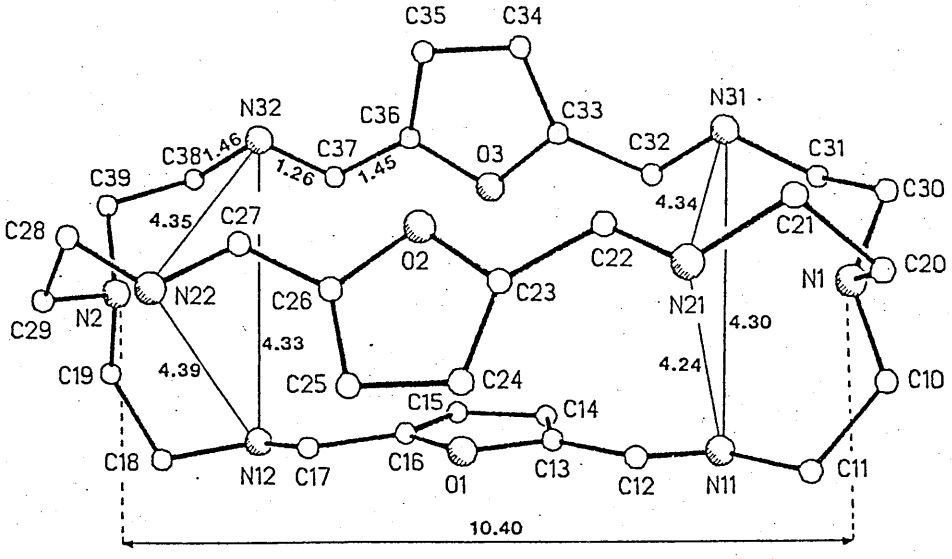

N(11) - N(21)	4.24	N(1) - N(2)	10.40
N(11) - N(31)	4.30	O(1) - O(2)	3.60
N(21) - N(31)	4.34	O(1) - O(3)	3.91
N(12) - N(22)	4.39	O(2) - O(3)	3.69
N(12) - N(32)	4.33		
N(22) - N(32)	4.35		

4 or 5 coordinate depending on O's and N's

FIG.73-2

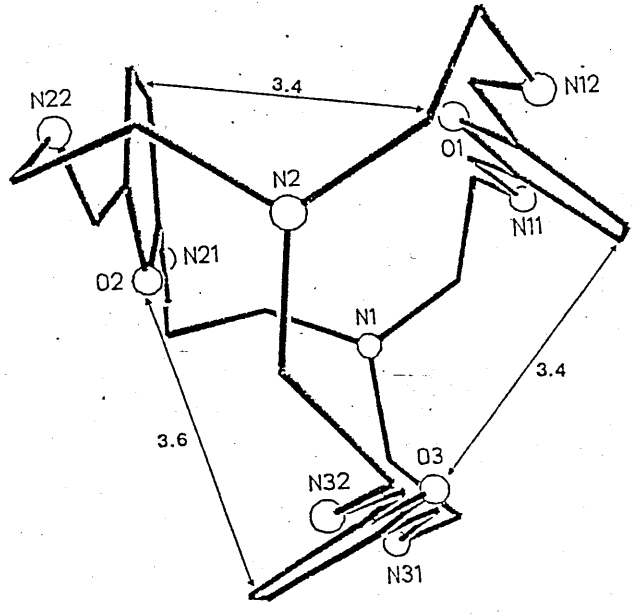

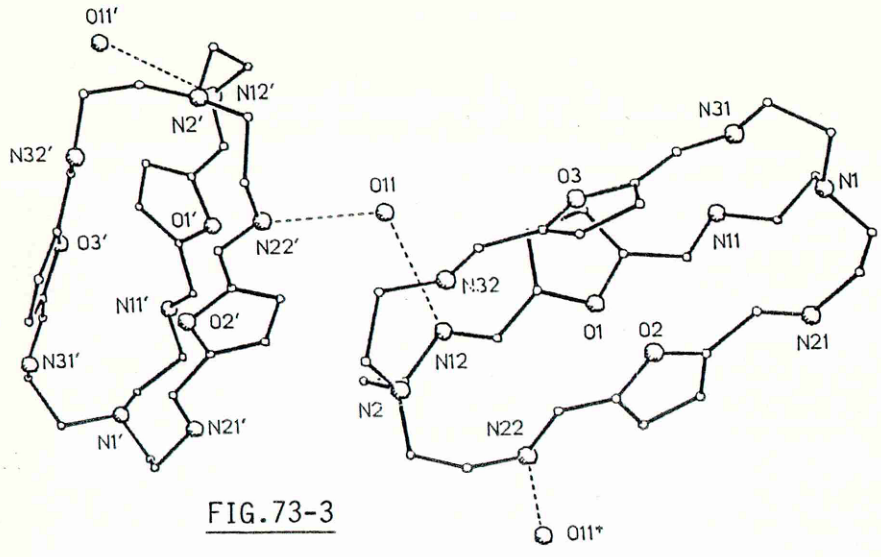

FIG.73-3

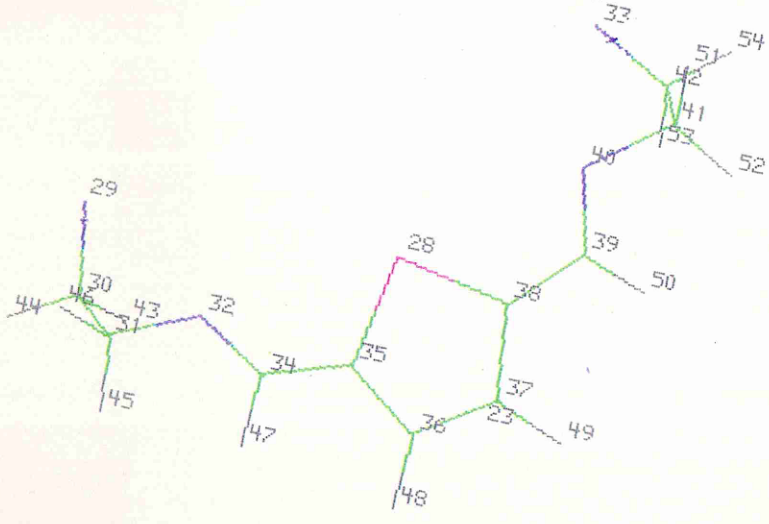

FIG.73-4 COMPLEXED

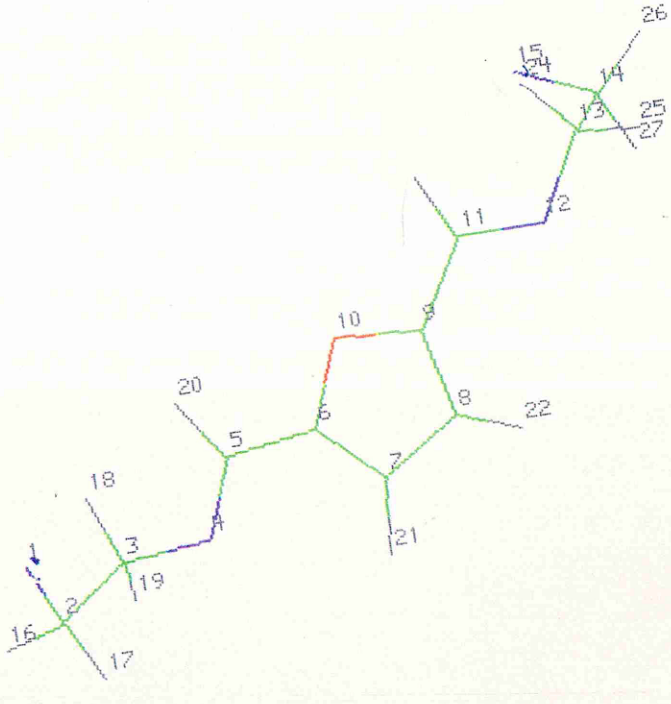

FIG.73-5 UNCOMPLEXED

macrocycle FIG.73-3. The water is in fact hydrogen bonded to imine nitrogens on 2 adjacent macrocycles; O(11)-N(12), 3.00(1)Å, O(11)-N(22'), 2.95(1)Å. Hence the macrocycles are linked in one dimensional chains through the structure.

Thus 3F is a macrobicyclic ligand that offers a "cavity" about 10Å long and 4Å in diameter, which in its X-rayed conformation with the trans arrangement of imine functions makes complexation unlikely. Michael Drew has however shown using molecular mechanics that it is possible to go from the furan structure-trans-trans, to the cis cis structure where the ligand can bond to two metals. By assuming that the binuclear furan complex has the same structure as the disilver thiophene complex (dicussed later) he showed that this conformational change could occur by rotation about the C_B-C_C bond. However this necessarily involves rotation of the methylene bond close to the bridgehead sp^3 nitrogen. Thus the trans trans to cis cis conformational change involved in the complexation process is not a simple rotation of the C_B-C_C bond and would seem to be quite complicated. FIG.73-4 shows one linkage from Nsp^3 to Nsp^3 in both the complexed Fig.73-4a, and uncomplexed Fig.73-4b form.

The nmr data for 3F is tabulated in FIG 74. while the spectra are shown in FIG.75. These were run at Q.U.B on a 250MHz instrument by Dr.R. Hamilton, although the low temperature study was run on a 90MHz spectrophotometer. The room temperature spectrum on the 250MHz instrument is shown in FIG 75-1. The sharp singlet nature of the imine and aromatic signals at 7.73 and 7.09ppm respectively imply non-restricted motion and this is in contrast to the 2 methylene signals which appear as 2 broad featureless humps lying close to Tc. FIG.75-2 to 75-8 shows the change in the appearence of the spectra as the temperature is altered in small increments. Unlike 3Bp where H_D and H_E had very different Tc values (223 and 258K respectively) the methylene groups of 3F have very similar coalescence temperature values of 0° for H_D and -5°C for H_E. Thus as the temperature is decreased a difference in splitting of the equatorial and axial signals is not nearly so evident. As in 3Bp it was possible to determine if the fluxional process for the two sets of methylene protons showed the same $\Delta G^{\#}$. The relevant figures are shown in the table below:-

FIGURE 74. N.M.R.[a] DATA FOR 3F AND ITS RELATED COMPLEXES

LIGAND/ COMPLEX	TEMP. (K)	SOLVENT	SPECTRUM	PROTON/CARBON SITES				
				A	B	C	D	E
3F	293	$CDCl_3$	^1H 250 MHz	7.09 (s)		7.73 (s)	3.54 (br,s)	2.74 (br,s)
3F	233	$CDCl_3$	^1H 90 MHz	7.07 (s)		7.64 (s)	3.76 (d) 3.26 (t)	2.93 (t) 2.56 (d)
3F	293	$CDCl_3$	^{13}C[b] 90 MHz	111.3 (d)	153.6 (s)	152.4 (d)	60.1 (t)	55.6 (t)
$Ba3F(Ph_4B)_2$	293	CD_3CN	^1H 90 MHz	7.06 (s)		8.16 (s)	3.24 (t)	2.67 (t)
$Sr3F(Ph_4B)_2 .2H_2O$	293	CD_3CN	^1H 90 MHz	7.03 (s)		8.13 (s)	3.41 (br,m)	2.60 (br,m)
$Ca3F(Ph_4B)_2 .2H_2O$	293	CD_3CN	^1H 90 MHz	6.99 (s)		8.10 (s)	3.49-3.57 (m)	2.67-2.78 (m)
$Ba3F(Ph_4B)_2$	293	CD_3CN	^{13}C[b] 90 MHz	118[c]	153.7 (s)	155.6 (d)	65.9 (t)	59.3 (t)
$Ca3F(Ph_4B)_2 .2H_2O$	293	CD_3CN	^{13}C[b] 90 MHz	120[c]	153.4 (s)	154.5 (d)	59.4 (t)	59.1 (t)
$Ag_23F(CF_3SO_3)_2$	293	CD_3CN	^1H 500 MHz	7.17 (s)		8.24 (d)	3.55 (br,s) 3.22 (br,s)	2.98 (br,s) 2.60 (br,s)
$Ag_23F(CF_3SO_3)_2$	233	CD_3CN	^1H 500 MHz	7.17 (s)		8.24 (d)	3.54 (t) 3.19 (d)	2.96 (d) 2.55 (t)
$Cu_23F(ClO_4)_2$	293	CD_3CN	^1H 400 MHz	7.1 (s)		8.22 (d)	3.42 (m) 3.25 (d) 3.22 (d)	3.14 (d) 3.10 (d) 2.67 (t)
$Cu_23F(ClO_4)_2$	233	CD_3N	^1H 400 MHz	7.10 (s)		8.16 (s)	3.36 (t) 3.2 (d) 3.1 (d)	3.07 (d) 3.0 (d) 2.64 (t)

FIGURE 74. (contd.)

LIGAND/ COMPLEX	TEMP. (K)	SOLVENT	SPECTRUM	PROTON/CARBON SITES				
				A	B	C	D	E
R3F[d]	293	$CDCl_3$	^1H 250 MHz	6.08 (s)		3.7 (s)	2.57 (s)	
R3F	293	$CDCl_3$	^{13}C[b]	107.3 (d)	153.3 (s)	55.45 (t)	47.3 (t)	46.2 (t)

(a) ppm from T.M.S. (s) singlet, (d) doublet, (t) triplet, (m) multiplet, (br) broad.

(b) Off resonance multiplicity (s) singlet, (d) doublet, (t) triplet.

(c) Masked by solvent.

(d) NH at 2.25 - confirmed by D_2O shake.

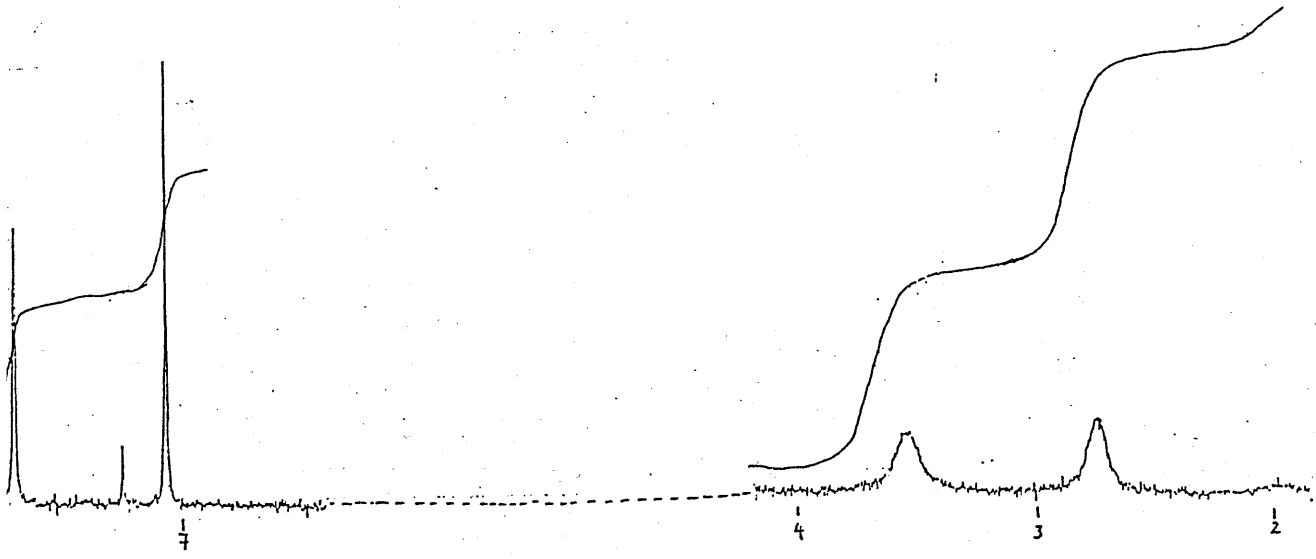

FIG.75-1 250MHz 294k

FIG.75-2 to 75-8 90MHz v.t.nmr study.

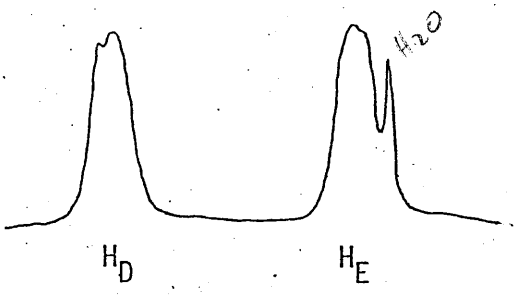

FIG.75-2 294k

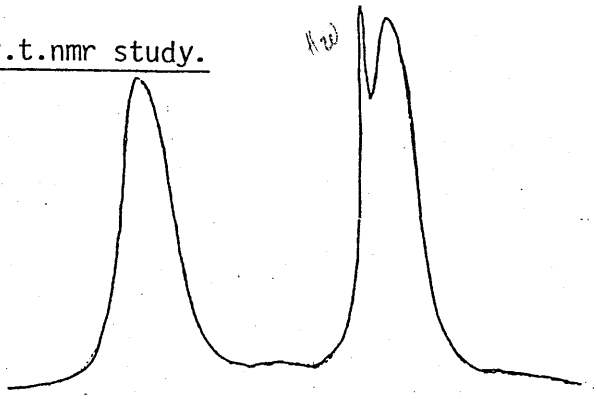

FIG.75-3 283k

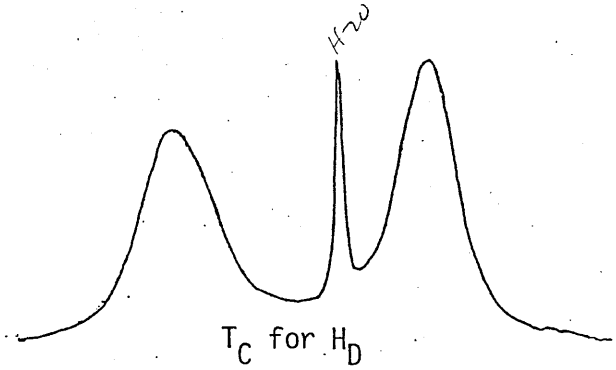

T_C for H_D

FIG.75-4 273k

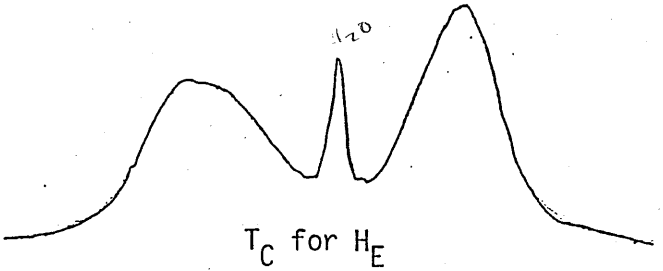

T_C for H_E

FIG.75-5 268k

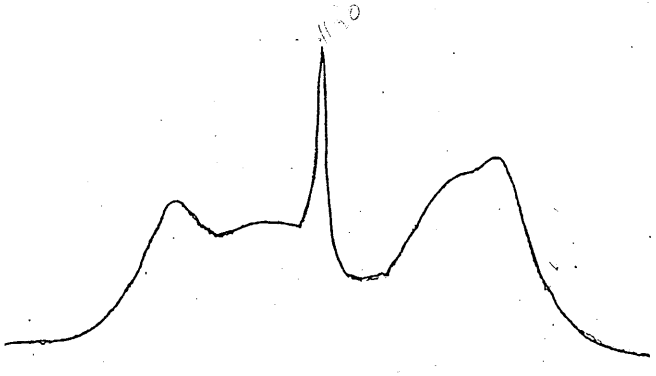

FIG.75-6 263k

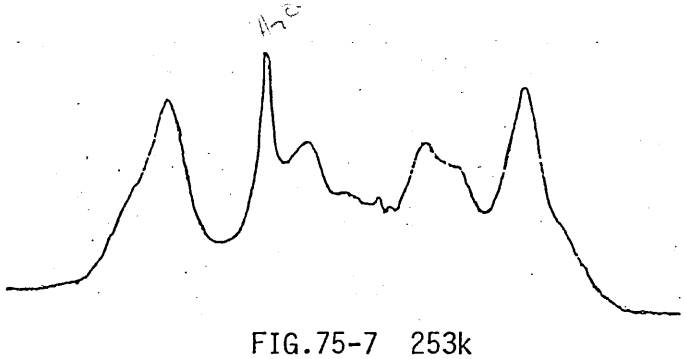

FIG.75-7 253k

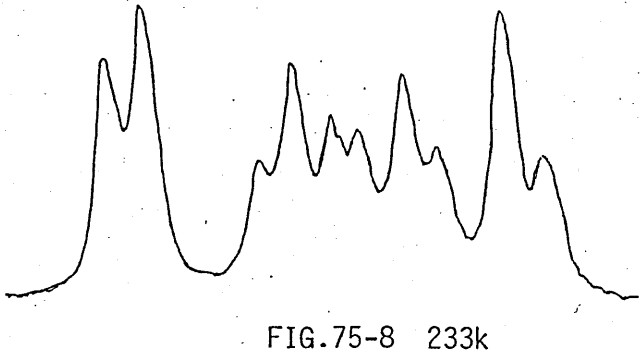

FIG.75-8 233k

PROTON SITE	Δν in Hz (from 233k spectra)	τ^{-1} $(\pi\Delta\nu/2)^{1/2}$	T_c	A $=(K_B T_c/h)$	$\Delta G^{\#}_c$ $KJmol^{-1}$
H_D	40.9	90.86	273	$5.688x10^{12}$	56.43kJ
H_E	27.81	61.78	268	$5.584x10^{12}$	56.21kJ

The activation energy for the fluxional process of the methylene protons is 56KJ which is ≈9KJ higher than in 3Bp. This can be rationalized by the fact that the cavity length in 3F is shorter than in 3Bp and thus there is probably a greater degree of steric constraint within the 3F molecule.

As in uncomplexed 3Bm and 3Bp the arrangement of the frozen out axial and equatorial signals are d(eq), t(ax), t(ax), d(eq), and the multiplicities of these signals have previously been discussed. Coupling constants from the 233K spectra were estimated at Jgem = Jaxax' = 11.5Hz.

At the low temperatures the aromatic signal remains sharp and unsplit and so shows no sign of restricted rotation about the C_B-C_C bond.

The ^{13}Cnmr spectrum is simple consisting of one signal for each of the carbon atoms A-E -each shows the expected off-resonance multiplicity.

GROUP II METAL IONS AND 3F

The template reactions of 3F with the GroupII metal ions were disappointing both in terms of the yield and/or the quality of product obtained when compared with the product obtained when the metal ion was inserted into the pre-isolated free ligand (yields=82%). The product of the [2+3] template condensation of tren and DFF on Ba^{2+}, in the presence of BPh_4^-, as characterized by ir, microanalysis, F.A.B, FIG 72 and 'Hnmr FIG 74 is identical with that obtained by treatment of the free ligand, 3F, with Ba^{2+} and Ph_4B^- under mild conditions (Similarly the template reaction on Ag^+ was less efficient than the insertion of Ag^+ into 3F; see next section). That these insertion reactions take place supports the idea that, as in 3Bp, the interconversion of one conformer into the other (ie divergent when uncomplexed to the cis cis, convergent form when complexed) can be readily achieved.

Strontium and calcium were inserted into 3F; their template reactions gave products which from their ir appeared to be not completely closed. (ie NH_2 and C=O signals). Thus a small series of Group II mononuclear complexes, resulting from insertion reactions, have been isolated and characterized. The physical data for the three complexes is given in FIG. 72 and the nmr data is tabulated in FIG.74.

While the ir of the barium complex shows no obvious signs of water being present, both the strontium and calcium complexes have a broad feature from 3600-2800cm^{-1}, suggesting the presence of water. This was borne out by the microanalysis where 2 waters helped fit the results. The ir of the strontium complex is very interesting with the imine peak being split into 2 equal intensity peaks FIG.76-2a. This suggests that only 3 of the 6 imine functions are coordinating the metal centres. That this feature is not observed in the ir of the calcium complex is interesting as is a comparison of the ir $\nu_{C=N}$ frequencies for the 3 complexes:-

	C=N (cm^{-1}) ir	δH_c (ppm) nmr
$Ba3F(Ph_4B)_2$	1621	8.16
$Sr3F(Ph_4B)_2.2H_2O$	1621,1644	8.13
$Ca3F(Ph_4B)_2.2H_2O$	1640	8.10
3F	1634	7.73

It is perhaps possible to interpret these results in terms of coordinating (barium complex) and uncoordinating (calcium complex) imine nitrogens (with the strontium complex having 3 coordinated and 3 uncoordinated imines as suggested by the 1:1 ratio of imine peaks in the ir. By assuming that for the 3 complexes the furan oxygens and 2 bridgehead nitrogen atoms are all coordinating this implies a coordination number of 11, 8 and 5 for the barium, strontium, and calcium complexes respectively. It may be that the 2 water molecules, as indicated by ir and analytical data for the latter 2 complexes, are coordinating the metal centre although the broad nature of the water signal makes this seem unlikely.

Unfortunately the low field nmr data does not support this explanation with only a minimal difference in the imine resonance frequency between the 3 complexes. Indeed comparison with 3F indicates that in each case a coordination shift of $\simeq$0.4ppm has taken place on complexation thus suggesting at least time-averaging of coordinated and uncoordinated imine shifts.

Further investigation and higher field nmr studies are planned.

The essential features of the electronic absorption spectra of the 3 complexes are tabulated below for comparative purpose - the extinction coefficients ($M^{-1}cm^{-1}$) are given in parenthesis.

	λmax	
3F	280 (130,000)	320 (25,000)
$[Ba3F]^{2+}$	210 (311,000)	283 (77,000)
$[Sr3F]^{2+}$	210 (135,000)	289 (43,000)
$[Ca3F]^{2+}$	210 (131,000)	289 (46,500)

The 3 complexes when compared to 3F, would appear to show a hypsochromic shift (blue shift). This may result from steric necessity resulting in loss of co-planarity, or alternatively from a decrease in conjugation of the imine and furan chromophores on complexation. The second absorption, $\epsilon=10^4$, is likely to be a second ligand $\Pi-\Pi^*$ transition.

In each case the FAB spectrum was very weak. For both the strontium and barium complexes the 2 main observable signals could be assigned to $[M3F(Ph_4B)]^+$ and $[M3F]^{2+}$. Neither spectra gave a peak at 557 corresponding to 3F. The calcium complex on the otherhand gave a strong signal at 557 (90% of maximum peak). It is not known if this effect reflects the smaller size of the calcium cation and the above suggestion that it is not as strongly coordinated.

All 3 complexes gave conductivity values typical of a 1:2 electrolyte (10^{-3}M). These 3 complexes were used to help determine a range of 1:2 electrolytes for 10^{-4}M solutions. The results are given below, (conductivites measured in and corrected for - acetonitrile).

COMPLEX	Ω 10^{-3}M	Ω 10^{-4}M
$Ba3F(Ph_4B)_2$	222	442
$Sr3F(Ph_4B)_2$	250	460
$Ca3F(Ph_4B)_2$	236	421
$Ba3P(ClO_4)_2$	241	512
$Sr3P(ClO_4)_2$	307	471
$Ca3P(ClO_4)_2$	275	420

FIG.76-1b

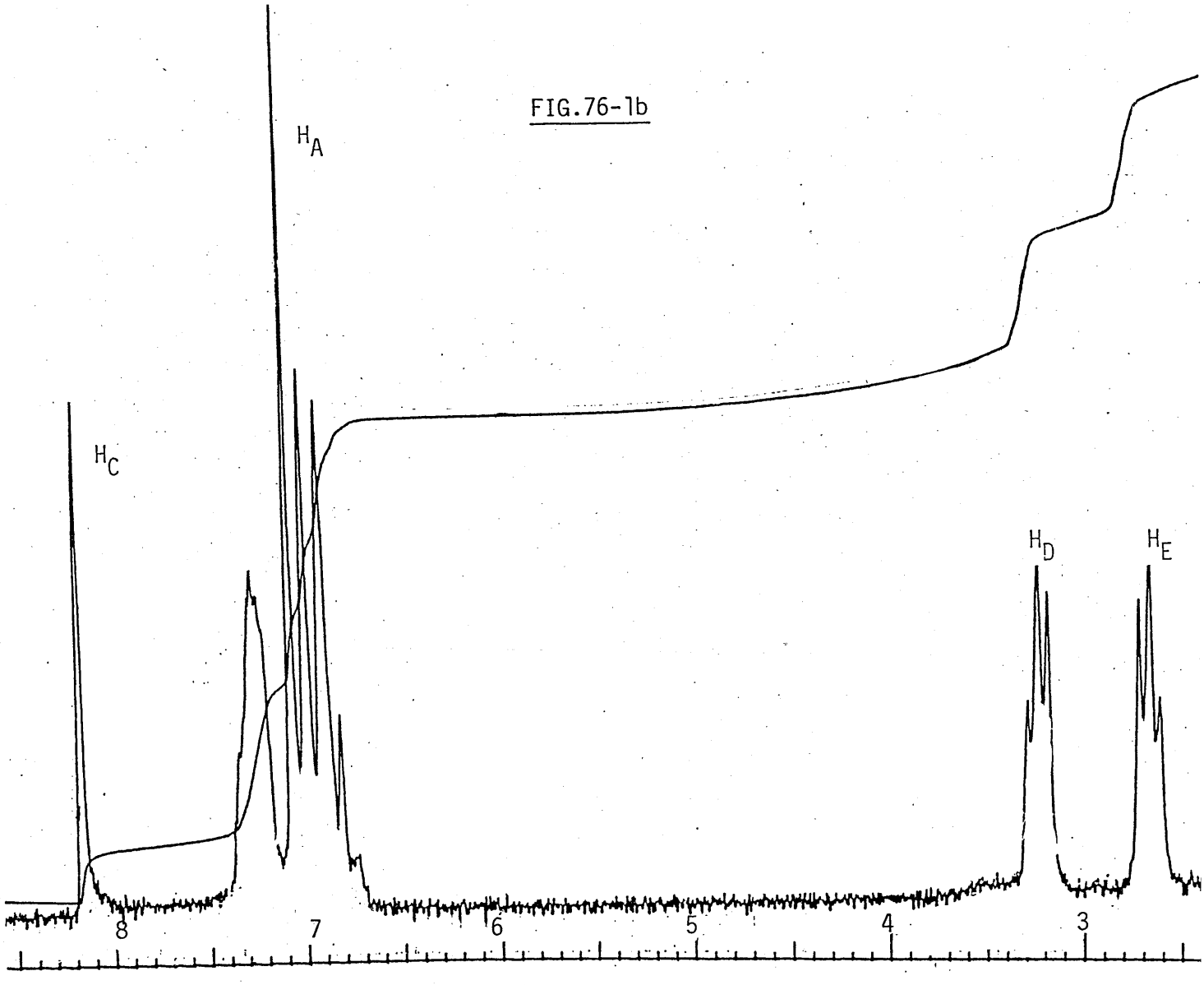

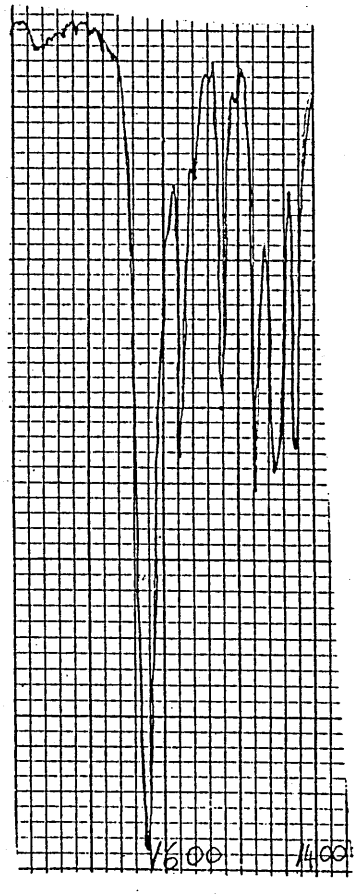

FIG.76-1a

The room temperature 90MHz spectra for the 3 complexes are shown in FIG 76 while the data is tabulated in FIG.74.

All 3 spectra show;

a) varying degrees of fluxional behaviour
b) complexation shifts
c) singlets for the aromatic and imine signals.
d) Ph_4B^- aromatic signals and
e) a water signal at different δ

The spectrum of $Ba3F(Ph_4B)_2$ is shown in FIG.76-1b. A water peak at δ2.1 is assumed to come from the CD_3CN solvent. The aromatic signal is sharp and unsplit and shows no complexation shift relative to the free ligand. I had felt initially that this implied the furan oxygen atoms were uncoordinated. However on comparison with 2 complexes of Ligand E (Chapter3:FIG.30) it would appear that this is unjustified. Both the barium and di-copper(1) complexes of ligand E have been characterized by X-ray structural analysis: the former complex shows coordinated furan oxygens and δH_A=6.97 whereas in the copper complex the furan oxygen atoms are not coordinating the metal centre and appear at δ7.19. This suggests that the furan protons are not very sensitive to coordination effects and thus we can only assume on the basis of the large cation size and the ir data that the oxygen atoms are coordinating the barium cation.

On the other hand the imine signal, H_C, shows a shift of 0.52ppm downfield as a result of the imine nitrogen donors coordinating the metal centre. The methylene signals, H_D and H_E, appear as unsymmetrical triplets as a result of small second order distortions. However the simple n+1 rule is essentially obeyed and from the splitting of the triplet J_{DE} = 4.7Hz. This value probably reflects an average of the various axial, equatorial proton interactions. This implies a fluxional process rapid on the nmr time scale.

The spectrum of the strontium complex of 3F is shown in FIG.76-2b. The imine signal shows a coordination shift of 0.49ppm which is slightly smaller than that observed for the barium complex. This may be a

FIG.76-2

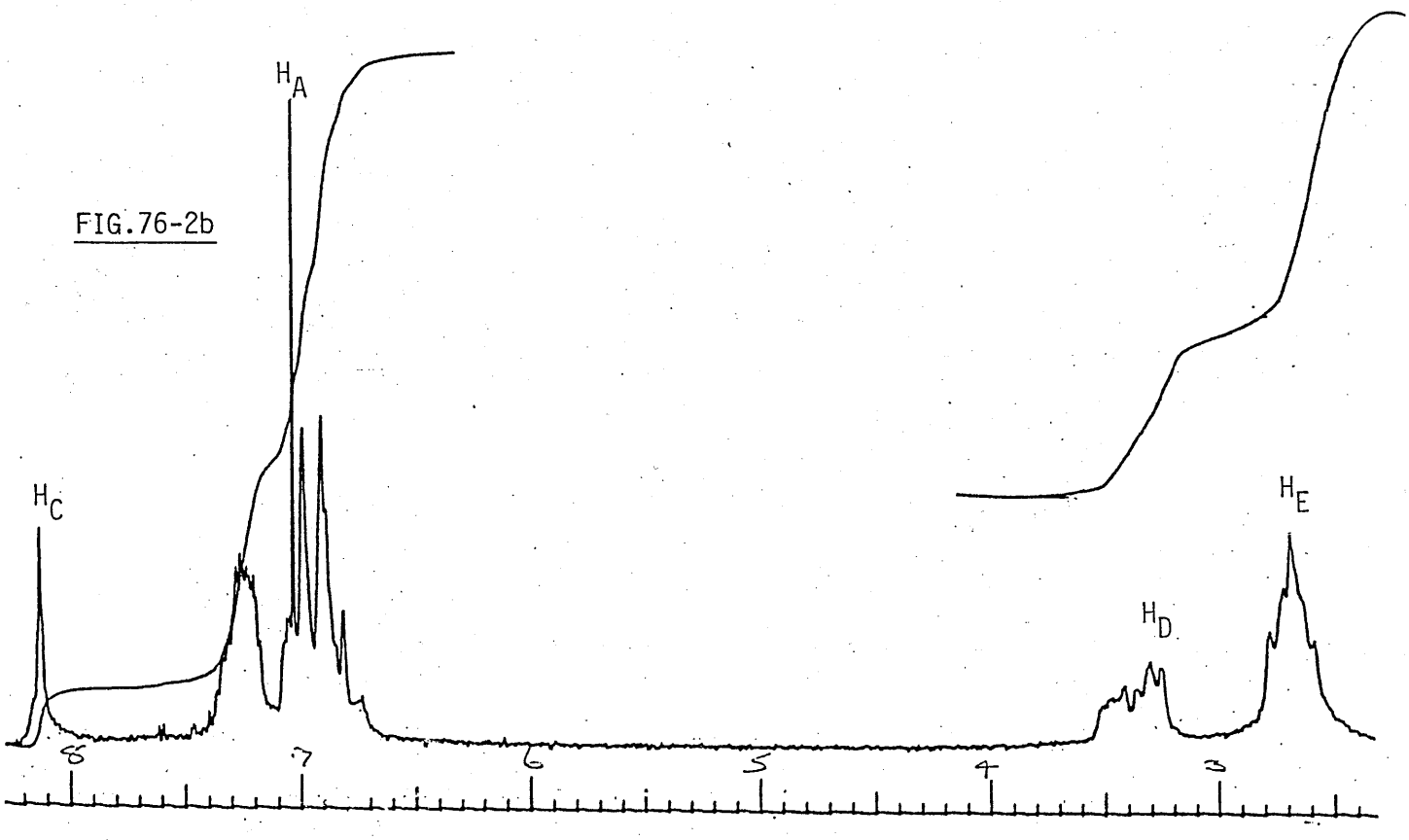

FIG.76-2b

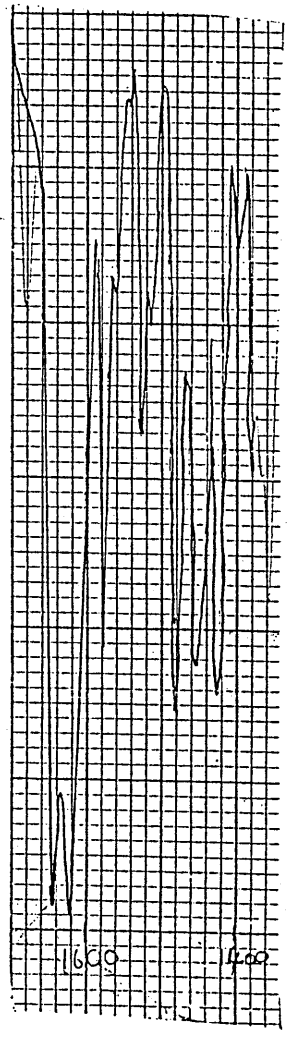

FIG.76-2a

reflection of the smaller size of the strontium cation resulting in slightly weaker coordination of the imine and metal centre. However the unsplit nature of this signal does not support a 1:1 ratio of coordinated and uncoordinated imine functions unless there is rapid exchange of cation between coordinated and uncoordinated environments.

The most obvious difference between the barium and strontium complexes is the appearence of the methylene signals. The higher H_E resonance has the water signal superimposed on it resulting in the obvserved unequal integral. However, more importantly, gone are the well resolved triplets of the barium complex and instead we observe, at 90MHz, broad unresolved multiplets. This implies that rotation of the CH_2 - CH_2 groups is more difficult in the strontium complex than the barium complex. One way of interpreting these results is by considering that the smaller cation will pull the cryptand in around itself thus making the rotation of the methylene groups more difficult ie increasing $\Delta G^{\ddagger}$ for the fluxional process. It may be that this contraction of the ligand leads to assymmetry with respect to the imine functions which is detectable by ir but which at room temperature is averaged out by a rapid fluxional process on the nmr time scale. Low temperature, high field studies should be most useful in this case.

The 'Hnmr spectrum of the calcium complex of 3F is shown in FIG 76-3b. As with the other 2 complexes the aromatic signal at δ6.99 is sharp and unsplit. The imine signal at δ8.10 shows the smallest of the coordination shifts observed in the 3 complexes having a value of 0.46ppm. The water signal is observed as a broad singlet at 2.9ppm and it does not interfere with either of the methylene signals. The methylene signals are, as in strontium spectrum complicated multiplets, but appear to have sharpened up significantly. This sharpening up may result from a 'freezing out' of the axial and equatorial protons -these signals being uncompletely resolved in the 90MHz spectrum. Certainly the blown up signal, shown in 76-3b, of H_E signal suggests overlapped triplet and doublet components. This implies that the CH_2-CH_2 fluxional process has essentially been prevented which is in line with the proposal put forward in the strontium case of the pulling in of the cryptand making the methylene rotation move difficult. This

FIG.76-3

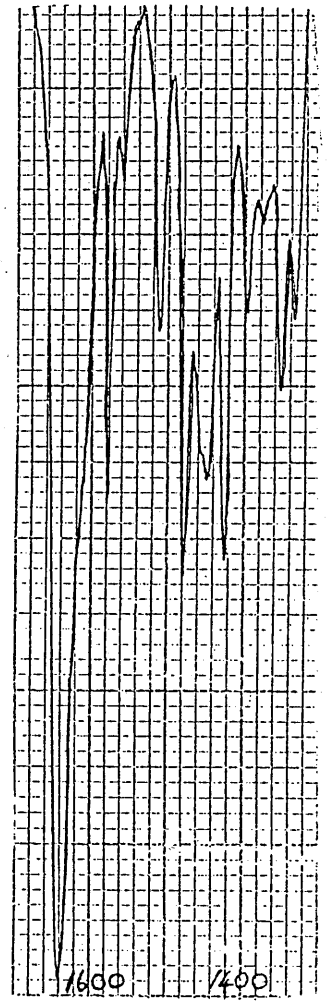

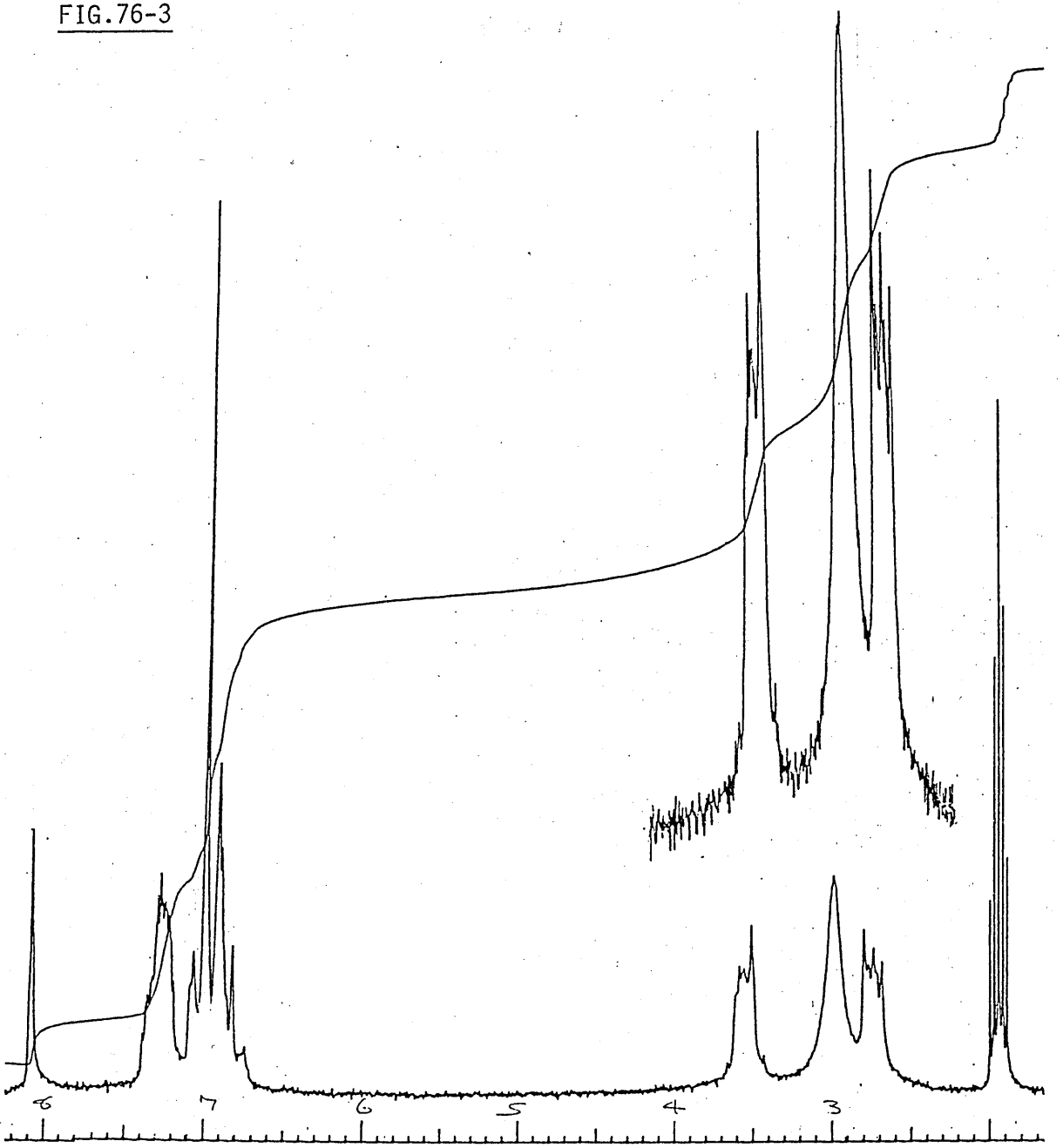

FIG.76-4 ^{13}C spectrum of $(Ba3F)^{2+}$

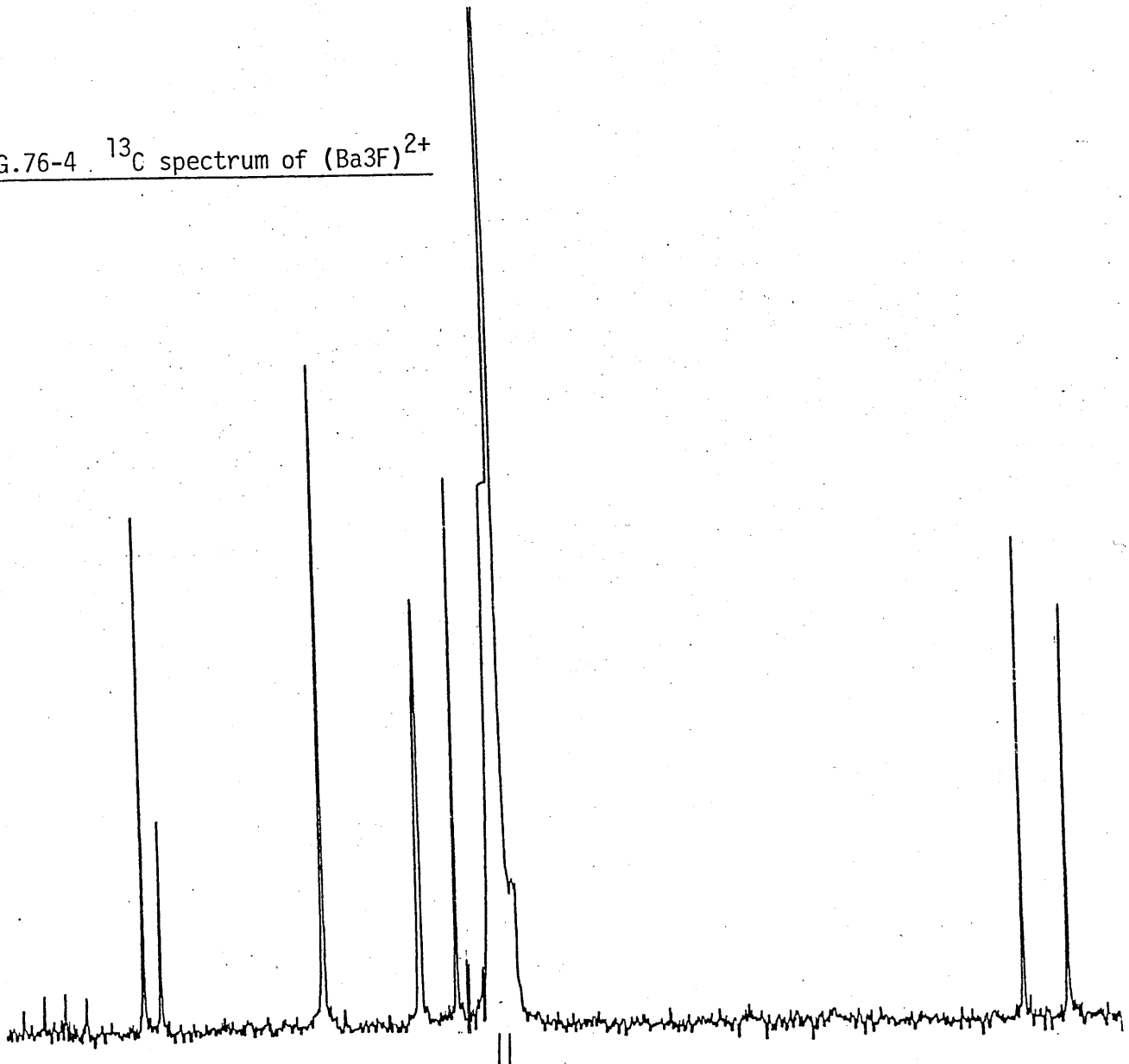

FIG.76-5

^{13}C spectrum of

$(Ca3F)^{2+}$

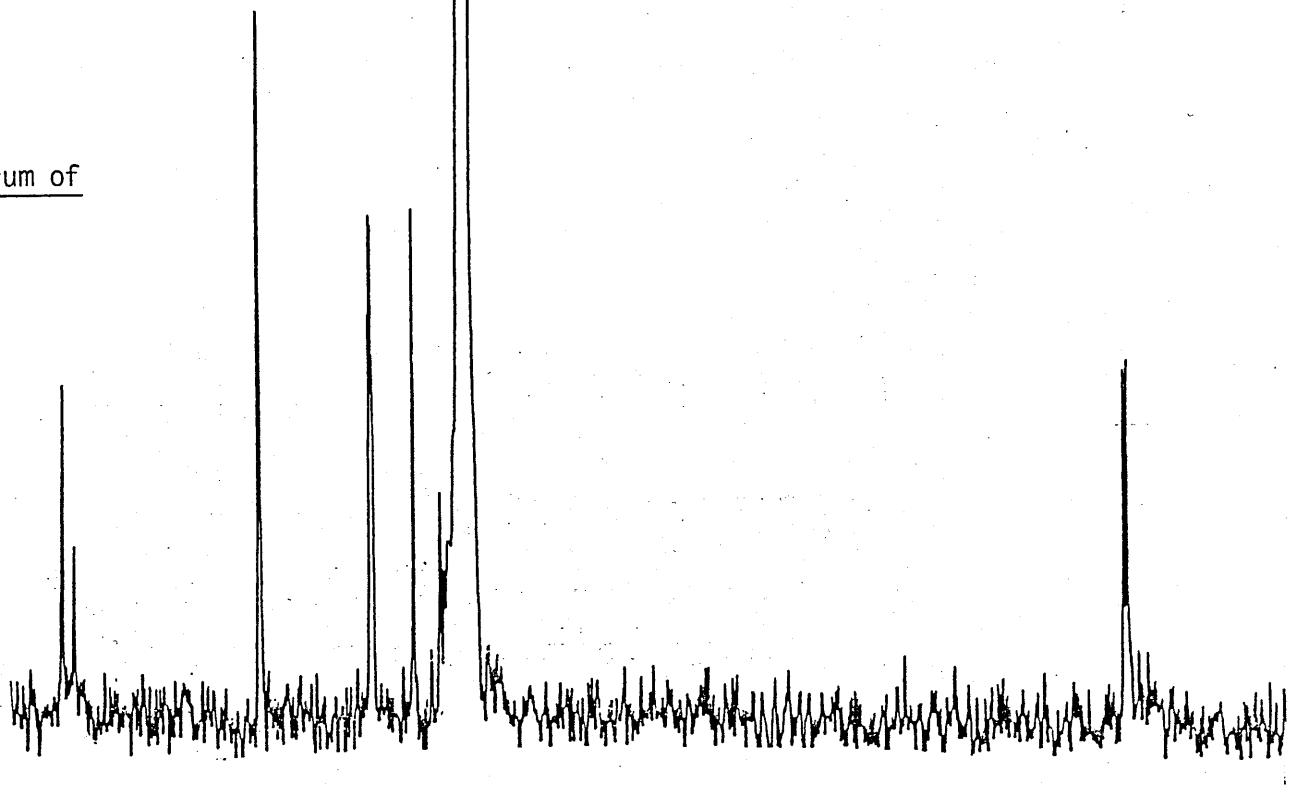

contraction may be limited to the furan rings and bridgehead nitrogen atoms only thus leaving the imine functions uncoordinated.

It is interesting to note that in the ^{13}C spectra of the calcium and barium complexes (again 90MHz) the methylene carbons show very different behaviour. FIG.76-4 and 76-5, for the barium and calcium complexes respectively show how in $[Ca3F]^{2+}$ spectrum the 2 methylene carbons lie close together (Δv=7.7Hz) whereas in the $Ba3F^{2+}$ these carbon signals are well split - Δv=103.6Hz. Whether or not this effect can be rationalized in terms of the steric argument where a tightening up of the cavity affects the chemical shift of these carbons is not clear although it does suggest a significant difference in conformation.

The ready interconversion between the trans trans and cis cis, conformers of 3F means that despite the unfavourable disposition of donor pairs in the solid state this cryptand can, as above , function as a mononucleating ligand for metal cations. Comparison with ligand E (Chapter 3, FIG 30) the furan based macrocycle[62], suggests that ligand 3F may be useful for forming mononuclear group I metal complexes.

Work with lithium has as yet only given the free ligand back while work with potassium is yet to get underway. Early attempts with sodium are more promising. The first reactions gave ring opened products as evidenced by the carbonyl and amine frequencies in the ir. More recently we obtained a sample which analysed as $Na3F(ClO_4)\cdot MeCN\ 2H_2O$. That sodium is present was shown by elemental analysis: for the above molecular formula % Na calc=3.09, %found=3.25. A conductivity value of 112 Scm^2mol^{-1} was recorded for this complex. F.A.B results suggest that the sodium cation has been incorporated into the cavity with peaks at 579 (100%) and 557 (16%) corresponding to $[Na3F]^+$ and $[H3F]^+$ respectively. A ^{23}Na nmr study is planned.

That the ligand 3F is also capable of forming binuclear complexes was shown by its reaction with silver. Although only a small amount of product (12%) was isolated from the template reaction of DFF and tren on silver triflate (a rubbery polymeric substance was the main product of such a reaction)

FIGURE 77 'Hnmr of $(Ag_2 3F)^{2+}$

FIG.77-1

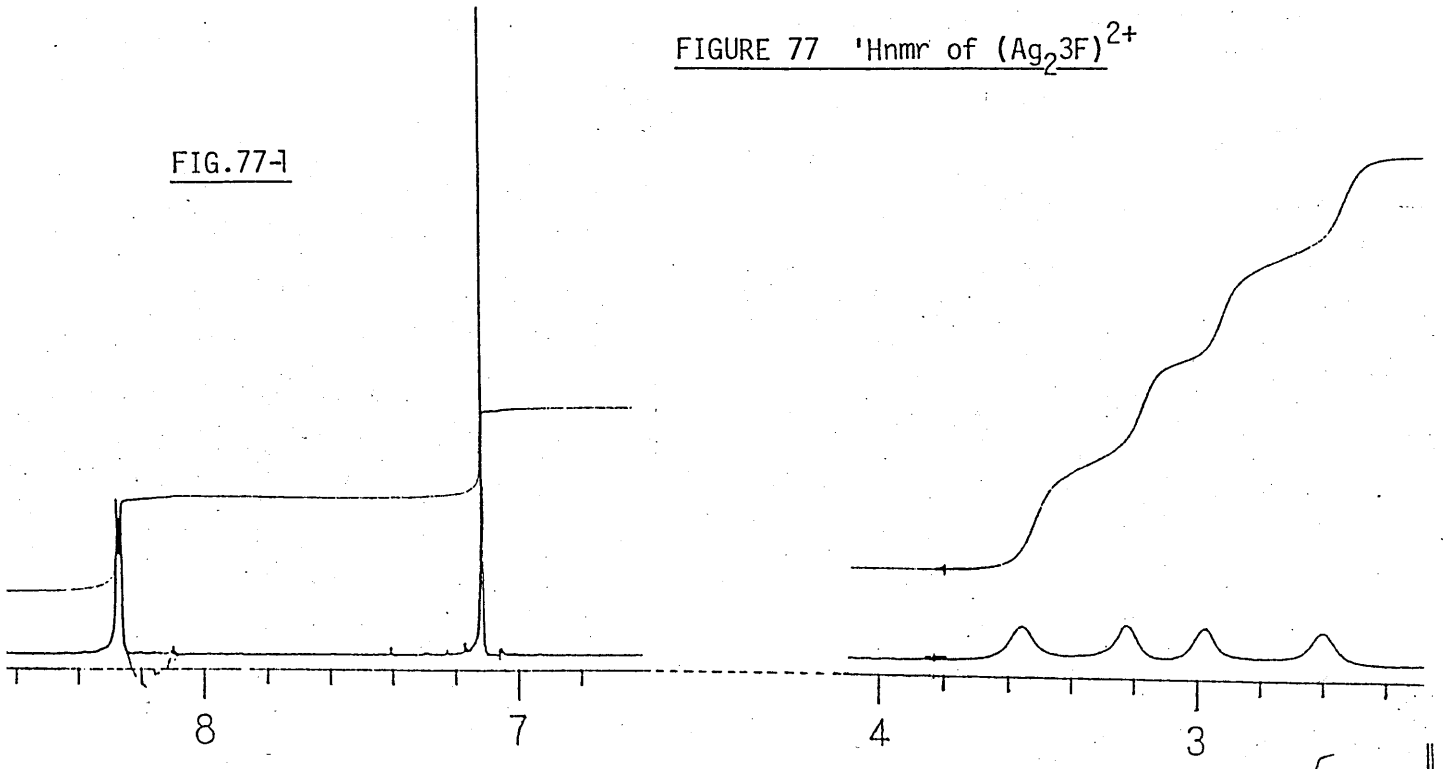

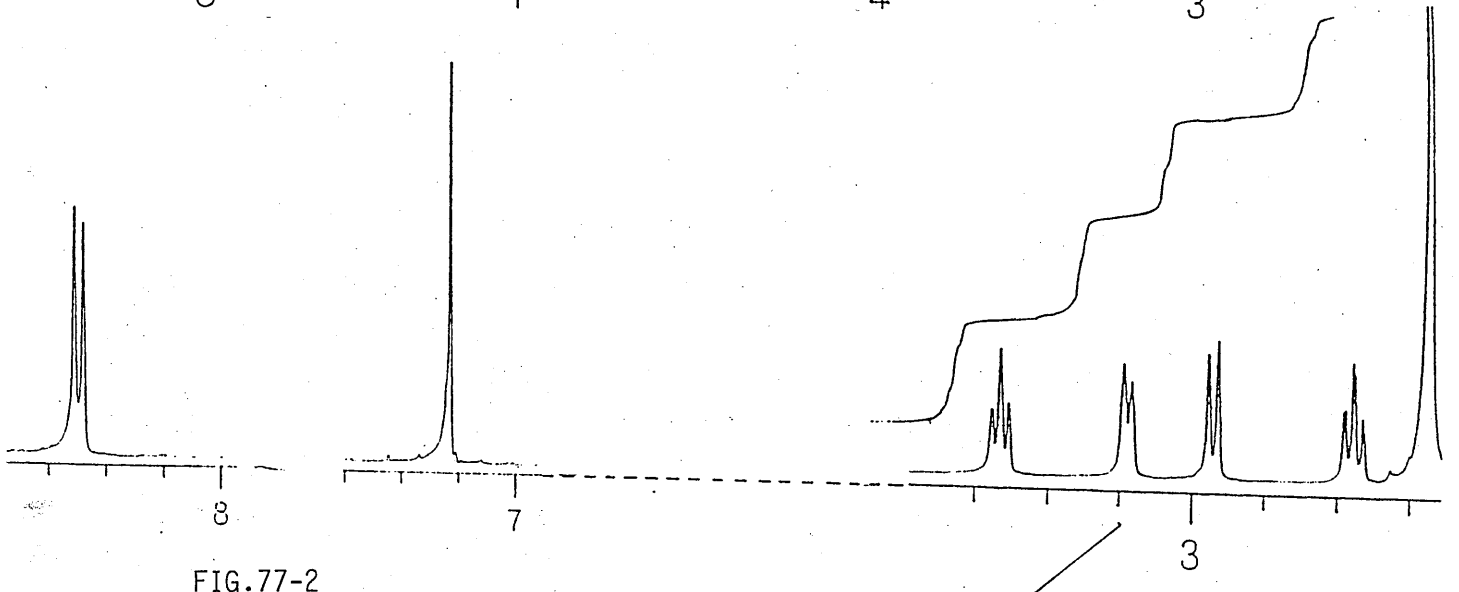

FIG.77-2
500MHz 233k

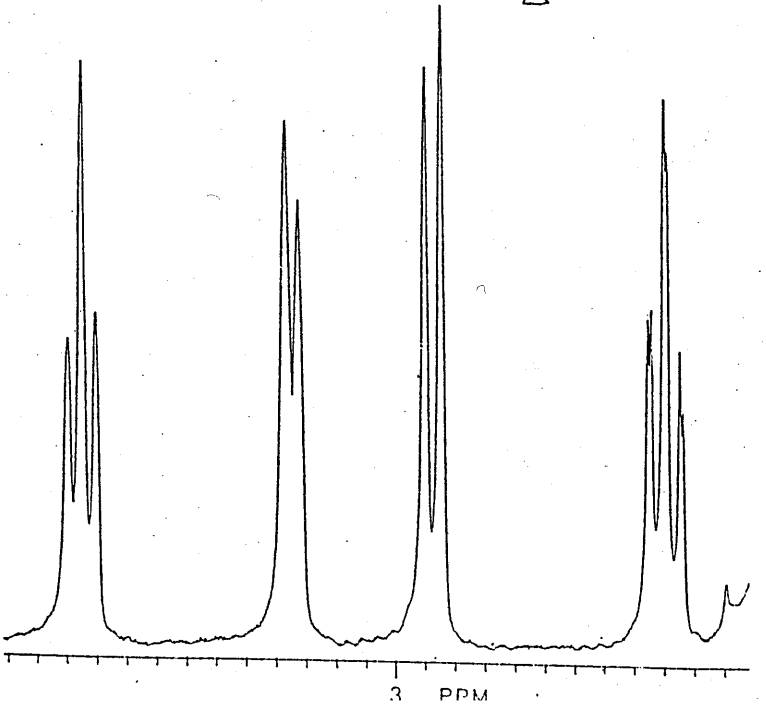

insertion of silver ions into 3F gave a clean pale yellow microcrystalline product in 68% yield. The ir suggests the presence of water or ethanol solvent molecules although analytical data is not yet available on this complex. FAB results certainly suggest a molecular formula based on $Ag_2 3F(CF_3SO_3)_2$ giving peaks at 921(80%), 771(20%), 666(100%) and 558(65%). These correspond to $[Ag_2 3FCF_3SO_3]^+$, $[Ag_2 3F]^+$, $[Ag3F]^+$, $[H3F]^+$ respectively. The conductivity value of 267 Scm^2mol^{-1} is typical for a 1:2 electrolyte (10^{-3}M). The 3 observed signals in the electronic absorption spectrum all show $\epsilon=10^4$ and are therefore attributed to $\Pi\Pi^*$ ligand transitions.

The 500MHz ^{1}Hnmr spectrum of this disilver complex has been run at room temperature FIG.77-1 and at 233k FIG.77-2. In both spectra the aromatic signal at ≈7 ppm is sharp and unsplit. A significant feature of this spectrum is the splitting of the imine signal even at room temperature (recall that in the cases of the disilver complexes of 3Bm and 3Bp this signal only split at the lower temperature). Thus the imine proton and the silver nucleus can couple at room temperature which necessarily implies that the Ag^+ is held within the cavity and not undergoing a rapid exchange process in solution as is believed to be the case of the analogous 3Bm and 3Bp systems. This further implies that the silver complex of 3F is more stable than either that of 3Bm of 3Bp. Indeed $[Ag_2 3Bm]^{2+}$ has a bench lifetime of only a couple of weeks -after 2-3 weeks the complex becomes brown/black indicating a degree of decomposition has occurred; whereas the silver complex of 3F appears to be quite stable showing no signs of blackening even after several months. ($[Ag3S]^{2+}$ has remained yellow and crystalline and the sample is 2 years old!) The splitting of the imine signal gives a J_{HcAg} = 7.95Hz. The methylene signals at room temperature appear as 4 broadened featureless humps corresponding to the axial and equatorial protons beginning to resolve into their individual components.

The low temperature spectrum shows that while the aromatic and imine resonances have remained unchanged the methylene groups are now "frozen" out into their axial (triplet) equatorial (doublet) equatorial (doublet) axial (triplet) signals. The high field axial triplet is further split by the smaller vicinal $J_{Eax-Deq}$ coupling. This coupling is not resolved in the Deq doublet although this signal does appear slightly broadened.

The basic triplet appearance of the H_E axial signal suggests that Jgem = Jax-ax' and indeed this was found to be the case with J = 13.2Hz. The small $J_{Eax-Deq}$ = 3.2Hz. No couplings from the Dax, Deq, Eeq signals were available at the time of writing.

FIGURE 78. PHYSICAL DATA FOR Cu^{+}, Cu^{2+} COMPLEXES OF 3F

COMPLEX (Colour)	F.A.B.[a]	Ω[b] S cm^2 mol^{-1}	EXPERIMENTAL ANALYSIS[c]	INFRARED SPECTRUM			ELECTRONIC SPECTRUM		
				C=N	ClO_4^-	OTHER	SOLVENT	λ(nm)	ϵ(mol^{-1} dm^3 cm^{-1})
$Cu_2$3F$(ClO_4)_2.2H_2O$ (red)		280	C 39.22 (39.84) H 4.39 (4.03) N 12.20 (12.22)	1629	1028, 621	3743	MeCN	410 285 210[d,e]	4900 70000 125000[e]
$Cu_2$3F$(OH)(ClO_4)_3$ (green)	899 (65) 800 (75) 699 (50) 619 (100)	389		1633	1023, 622	3742 3453	MeCN	728 (13,700 cm^{-1}) 291[d] 212[e]	380 73700 39000[e]

(a) % of base ion peak in brackets.

(b) 10^{-4} M.

(c) Experimentally determined results in brackets.

(d) λ_{max}.

(e) Unreliable result.

TRANSITION METALS AND 3F (INSERTION REACTIONS)

Early attempts to prepare the transition metal complexes of 3F were centered on the transmetallation reaction. These were not very successful giving low yields and unreproducable results. Indeed many attempts simply resulted in an anion exchange reaction. However recent work with insertion type reactions are proving much more hopeful. First attempts with manganese and cobalt seem to give, from their ir, a hydroxo bridged binuclear assembly. However we are waiting for microanalysis and FAB analysis. Products of the reactions of Cu(I) and Cu(II) with the free ligand have though been analysed.

The red microcrystalline product of the reaction of $Cu^{I}(MeCN)_4(ClO)_4$ and 3F has been analyzed by ir, microanalysis, uv, (data tabulated in FIG.78) and ^{1}Hnmr (data in FIG.74 and spectra shown in FIG 79)

On the basis of the ir and microanalysis the di-hydrate form of this complex is strongly favoured. The ir shows two distinct absorptions at 3743 and 3612cm^{-1} which might suggest the presence of 2 strongly hydrogen bonded water molecules. The strong sharp imine signal at 1629cm^{-1} and the lack of C=O or NH2 absorptions suggest that insertion has occurred without ring opening.

The electronic absorption spectrum shows a very strong feature at λmax = 210nm (ϵ=125,000) although the extinction coefficient is again unreliable being so near the solvent and/or cell cut-off. A second strong absorption at 285nm (ϵ=70,000) is likely to be a ligand Π-Π^* transition while the medium intensity signal at 410nm (ϵ=4900) is assigned to the MLCT band ie Cu^{I} $d\Pi$ --> Π^* of the imine or the furan unit.

From FIG 79 it is seen that the room temperature and low temperature (233K) nmr spectra are essentially similar so that even at room temperature the methylene protons are frozen out into their axial and equatorial sites. So well resolved are these signals that it is possible to obtain estimates for

FIGURE 79 400MHz SPECTRA OF $(Cu_2 3F)^{2+}$

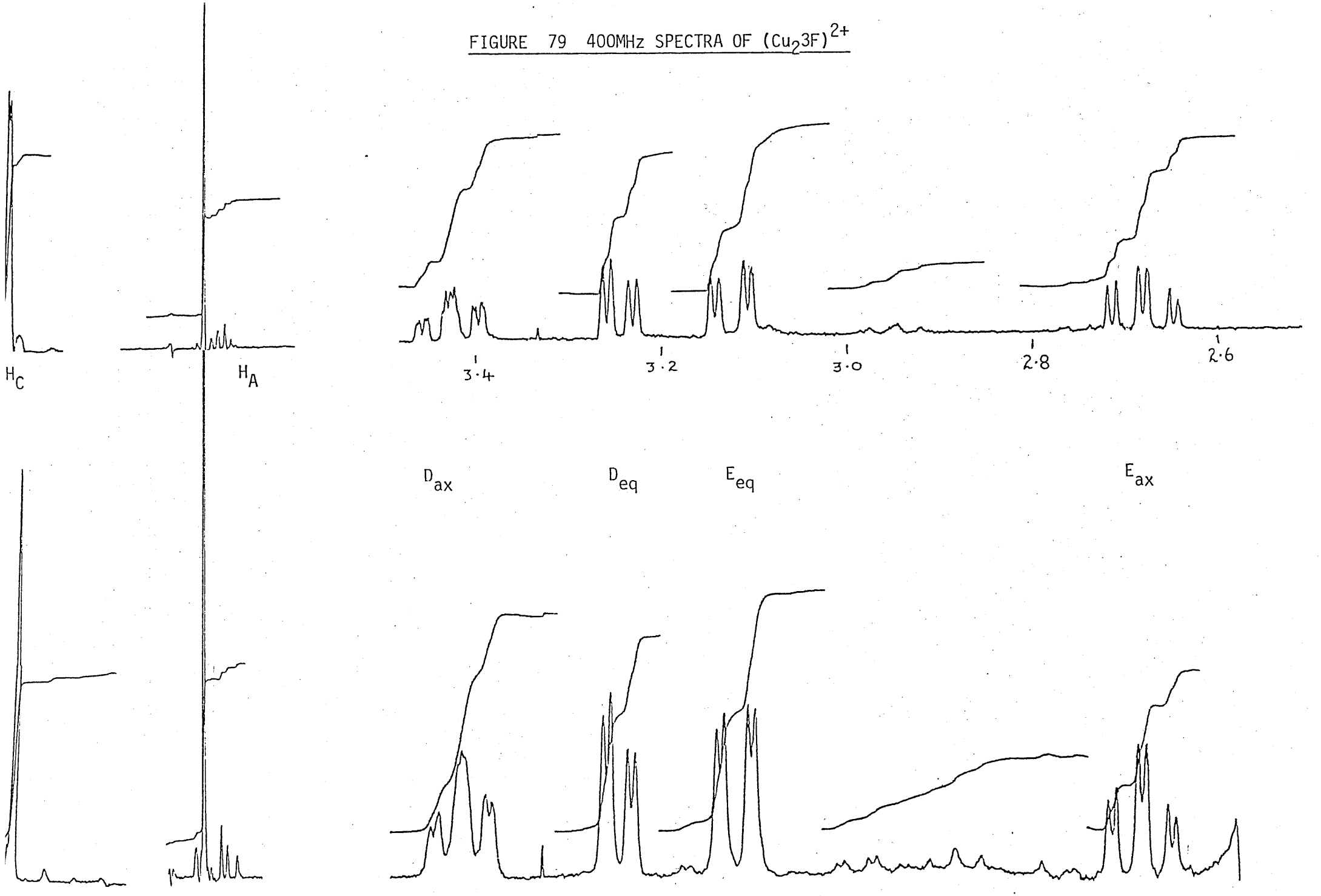

all the couplings. FIG.80-1 shows the tree diagram rationalzing the pair of doublets obtained for each of the equatorial protons ie $H_{D_{eq}}$ and $H_{E_{eq}}$. From the analysis of coupling constants Jgem for H_E = 13.8 Hz while Jgem for H_D is smaller at 11.2Hz. This implies that the Hax C Heq angle, which determines Jgem, is different for H_D and H_E. The further splitting of the equatorial signal is the result of the smaller vicinal Jeq-eq' or Jeq-ax' couplings. For the equatorial signals these 2 small couplings are not resolved and J_{vic} for H_D = 3.6Hz and for H_E = 3.5Hz. However from an analysis of the axial signals from which only the Jax-eq' small vicinal coupling is possible (see below) Jax-eq' for H_E = 3.9Hz and for H_D = 3.1Hz and thus it would appear that it is this Jeq-ax' coupling that is mainly responsible for the further splitting of the equatorial signal.

FIG.80-2 shows the tree diagram rationalzing the appearence of the E_{ax} signal. The basic triplet structure of the resonance suggests that Jgem = Jaxax' and indeed it was found that Jgem = Jaxax' = 13.8Hz (The value of Jgem from E_{ax} correlated well (.14Hz) with Jgem from the E_{eq} value). The smaller Jax-eq' coupling was determined to be 3.9Hz.

The shape of the Dax signal differs from that of Eax, showing fine structure on each of the main component signals. The Dax signal is rationalized by the tree diagram shown in FIG.80-3. The complexity of the signal made it difficult to establish the mid/centre points of the various components of the signal and thus Jgem was determined from the axial signal as Jgem Dax = 11.6Hz (compared to 11.2Hz from Deq signal). The complexity of the middle component of the signal compared to that of Eax results in part from Jaxax' (12.6Hz) ≠ Jgem. The smaller Jax-eq' coupling further splits the signals. Again there is a discrepancy between the 2 values derived from the axial and equatorial signals. For H_D Jax-eq' (3.1Hz) ≠ Jeq-ax' (3.6Hz) - this is a consequence of the 2 differing Hax C Heq angles implicit in the different Jgem values for H_D and H_E.

There is evidence of long range coupling of the Dax protons with the imine proton. This would account for the fine structure of the H_D signals and also for the splitting observed in the imine signal at 8.2ppm. It was possible to determine a value for this long range coupling J_{CD} = 1Hz. By

80-1

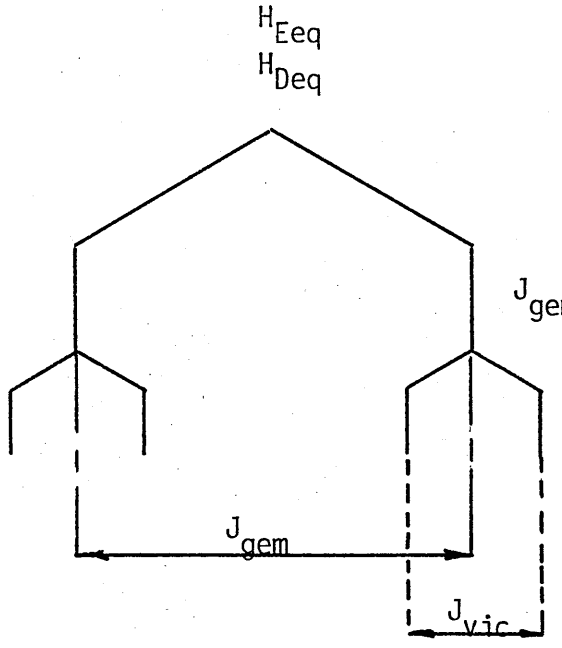

J_{gem} ie. D_{eq}-D_{ax}

E_{eq}-E_{ax}

J_{vic} ie. D_{eq}-E_{eq} or D_{eq}-E_{ax}

E_{eq}-D_{eq} or E_{eq}-D_{ax}

80-2

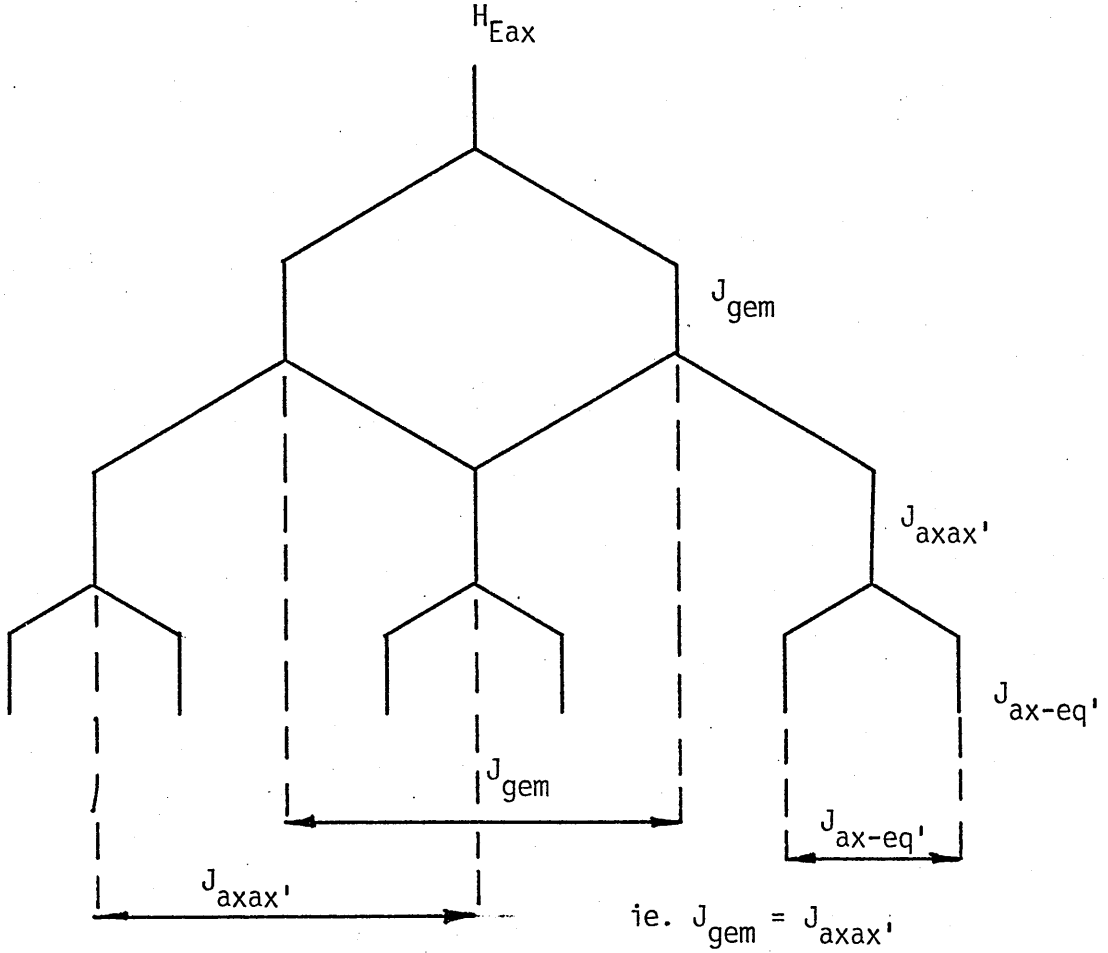

ie. $J_{gem} = J_{axax'}$

Fig. 80-3

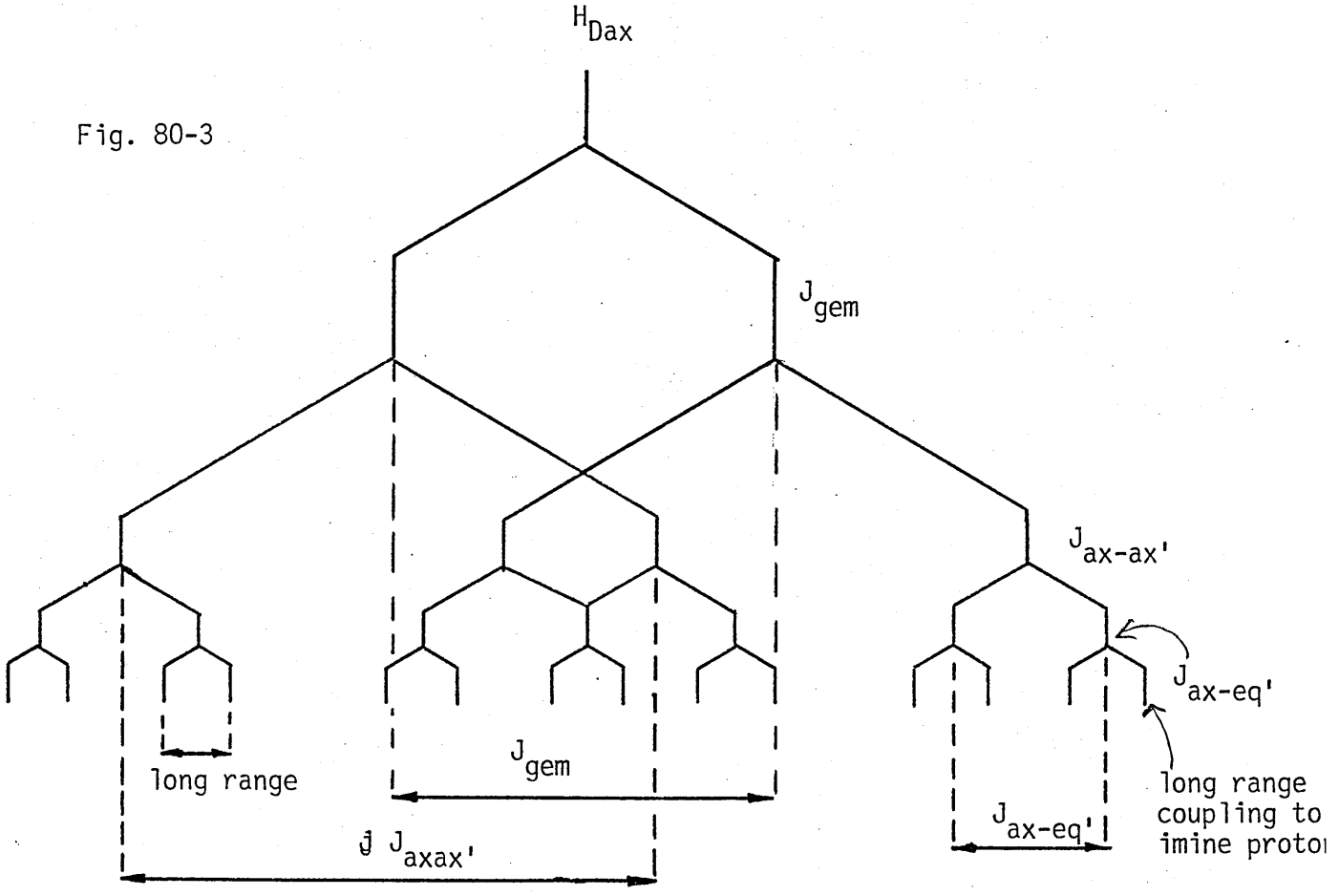

ie. $J_{axax'} > J_{gem}$

FIG.81-1

COMPLEXED 3F

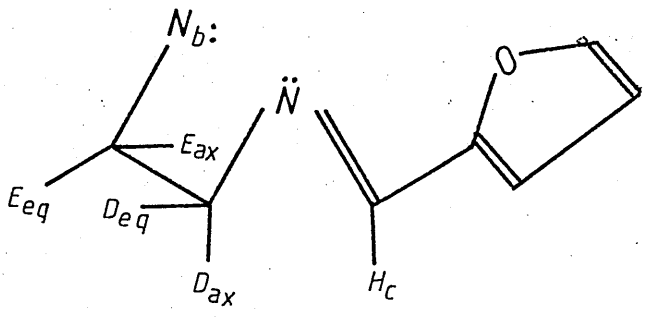

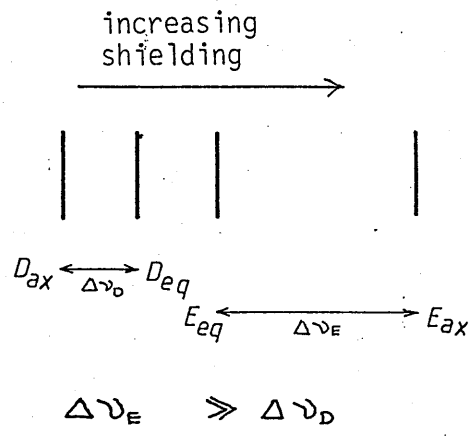

$\Delta\nu_E \gg \Delta\nu_D$

FIG.81-2

UNCOMPLEXED 3F

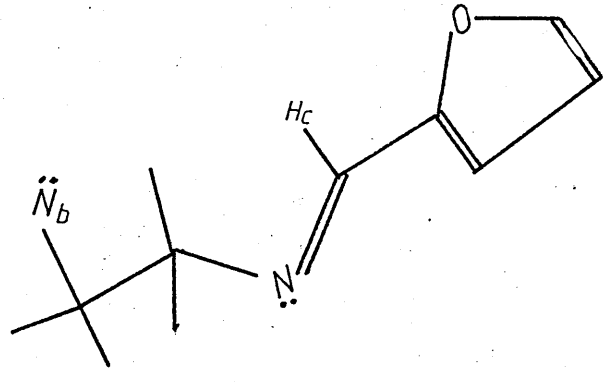

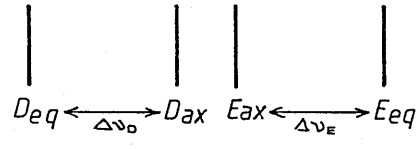

$\Delta\nu_D \geq \Delta\nu_E$

considering FIG.73-4, ie the proposed complexed form of 3F, it is possible to see how the imine and Dax proton can couple eg: take H_{47} and H_{45} - these protons lie in a suitable arrangement for allowing a small degree of orbital overlap and thus coupling. No such overlap is posible with Deq, ie H_{46} and no splitting from long range coupling is observed for Deq.

The aromatic signal is a sharp singlet (δ7.1Hz) at both temperatures and thus the aromatic rings appear to be freely mobile over the temperature range investigated. It is possible that a strong sharp singlet at 2.2ppm might incorporate the water that is suggested by both I.R and analytical data.

Evident from the 'Hnmr of this complex is the large difference in splitting of the axial and equatorial components of H_D and H_E. In this case ΔV Hax - Heq = 74Hz while ΔV Eax - Eeq = 179Hz. This large difference in splitting has been observed, in some of the other systems but as yet has not been commented on. The reason for this splitting difference is not clear and work, in collaboration with M.G.B.Drew is in progress. However an initial explanation (purely hypothetical) - involves the effect of the lone pair of the bridgehead nitrogen on the adjacent methylene protons. Consider FIG.81-1 and 81-2 which are drawn out representations of FIG.73-4 and 73-5 respectively.

In the complexed form of the ligand 3F, 81-1, we see that the axial proton on E will experience the shielding effect of the lone pair on N_b (effect brought about by increased electron density) more than Eeq and thus the difference in chemical shift between these 2 protons will be significant. This results in the pattern schematically shown in the diagram.

In the uncomplexed form, where only a 90MHz spectrum is available, neither Eax or Eeq will experience a significant shielding effect from the lone pair and thus, in the 90MHz spectrum at least, there is not a significant difference in the splitting of the components of H_D and H_E signals.

If the lone pair on the bridgehead nitrogen does prove to be the source of such splitting effects then it could prove very useful in determining the conformation of a particular complex or ligand.

Copper (II) will insert into 3F giving a bright emerald green product. The physical data are given in the table in FIG.78. The ir spectrum shows a strong feature at 3423cm^{-1}, which is commonly associated with the bridging hydroxide function. As in the green form of $(Cu_2 3Bm)^{4+}$ there are no signs of NH_2 signals on the side of the 3423cm^{-1} band and thus it appears that the indicated hydroxo bridge has formed without ligand modification. Thus from the ir the molecular formula for this complex would seem to be $Cu_2 3F(OH)(CLO_4)_3$.

Indeed, the results of FAB analysis would support this with peaks at 899(65%), 800(75%), 699(50%) and 619(100%) corresponding to $[Cu_2 3F(OH)(CLO_4)_2]^+$, $[Cu_2 3F(OH)CLO_4]^+$, $[Cu_2 3FOH]^+$ and $[Cu3F]^+$ respectively. The conductivity value of 390 lies in a 1:3 electrolyte range[63] and thus it would seem that the OH bridge remains in place even in solution.

The electronic absorption spectrum of the complex shows a broad absorption over 650-900nm (15300-11000cm^{-1}) showing λmax at 730nm (ϵ = 380). A poorly resolved shoulder on the low energy side of this band suggests a square pyramidal 5 coordinate geometry for this complex. However without further evidence all we can really say is that the copper does not have a regular octahedral geometry. Other electronic absorptions were at 291nm (72700) and 212nm (39,000). A shoulder on the main absorption peak at ≃340nm (ϵ-16,000) may be a LMCT band.

Magnetic and e.s.r studies are in progress and a RT moment of $[Cu_2 3FOH](ClO_4)_3$ at only ≃0.6BM testifies to an unusually strong antiferro magnetic interaction via the single OH bridge. Ligand E, the furan based macrocycle discussed in Chapter 3 forms the complex $Cu_2 E(OH)_2(ClO_4)_2$, H_2O, the ir of which shows a signal at 3490cm^{-1} [53]. This complex showed antiferromagnetic interaction with μ_{293} = 1.37 Bm falling to μ_{93K} = 0.72BM.

FIGURE 82

FIG.82-1

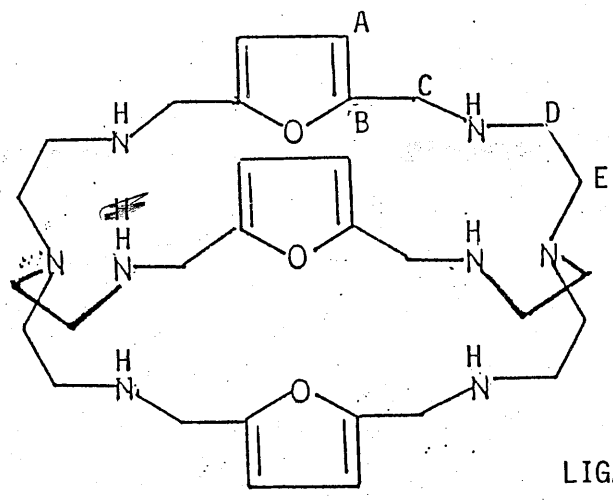

LIGAND R3F

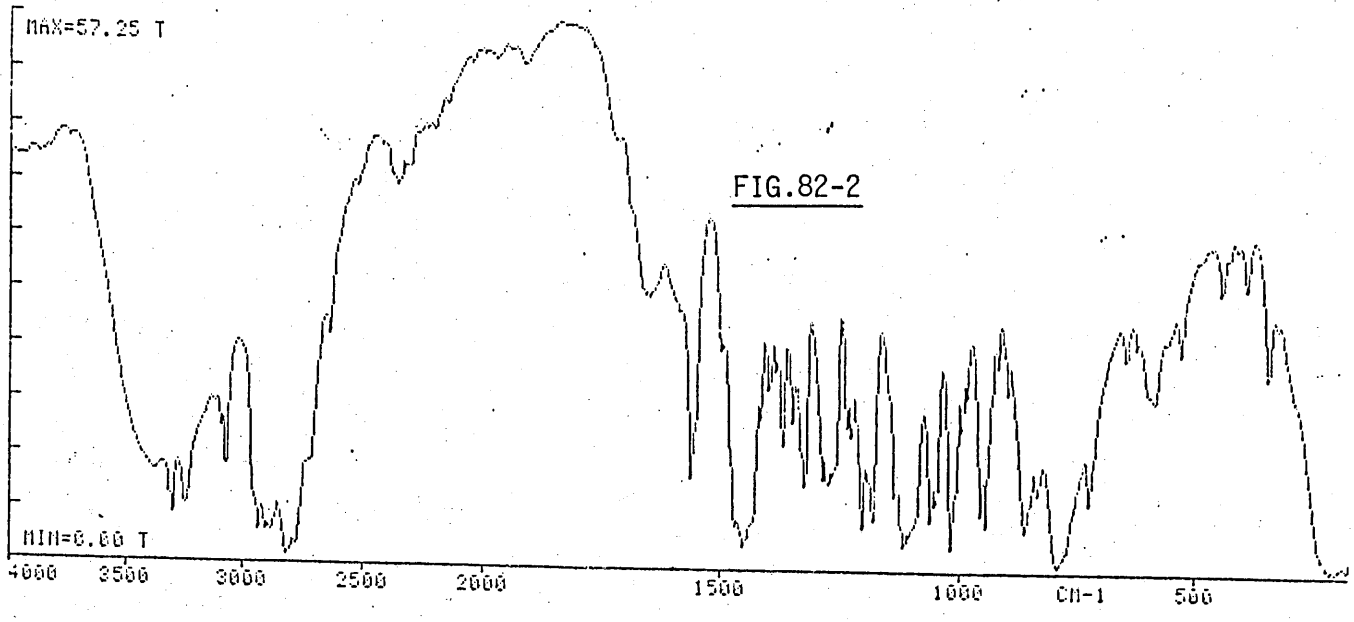

FIG.82-2

FIG.82-3

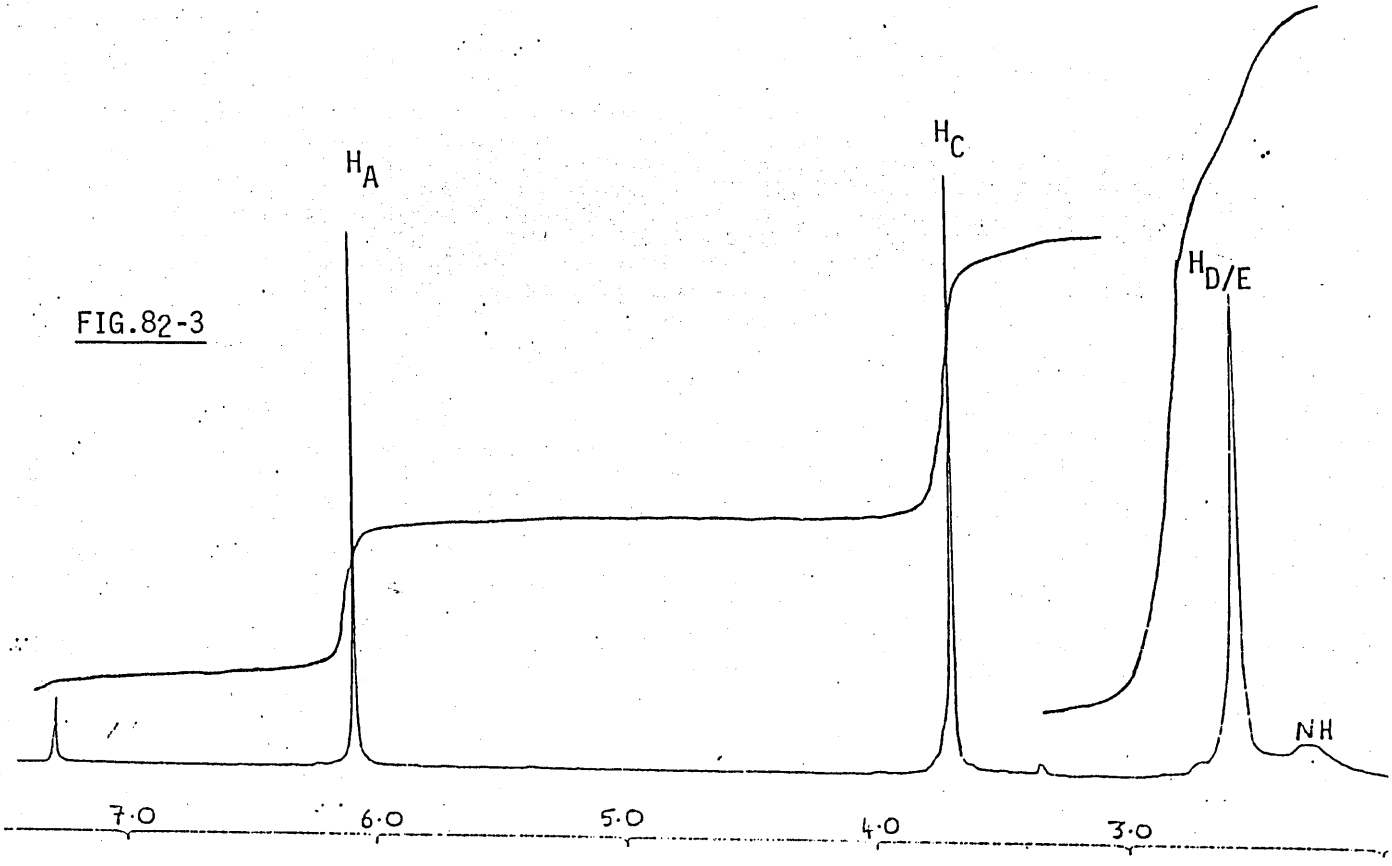

THE OCTAAMINE DERIVATIVE OF 3F ie LIGAND R3F

An in situ room temperature reduction of 3F gave optimum yields for the preparation of the reduced form of this ligand FIG 82-1 which was isolated as a creamy white solid. The physical data for this reduced ligand and its complexes is given in FIG.83 while its nmr data is tabulated in FIG 74. As expected the ir of the solid FIG.82-2 gave no peak at $\simeq 1640cm^{-1}$ showing that the imine function had been successfully hydrogenated. The appearence of a NH signal at $3249cm^{-1}$ confirmed this, as did the mass spec (m/e^{+} = 568 ie 3F + $12H^{+}$)

The 250MHz 'Hnmr of R3F FIG 82-3 is interesting in that it shows only 3 sharp singlets and a low intensity broad signal at δ2.25. The latter was attributed to the 6NH functions and a D_2O shake confirmed this assignment. Although the aromatic signal is a sharp unsplit singlet it appears relatively highfield at 6.08ppm. This is a direct result of the aromatic ring being a 5 membered heterocycle. For such a ring to be aromatic the heteroatom must have two electrons to donate to the aromatic pi cloud. Furan, thiophane and pyrrole all meet this criterion. Because the heteroatom ie 0,S or N for the above 3 examples, donate 2 electrons to the aromatic pi cloud the heteroatoms are electron deficient. However the rings have 6π electrons for only 5 ring members. Thus the ring is electron rich and partially negative (ie. the ring carbons are the negative part of the 5-membered ring). It follows that the protons attached to these ring carbons will experience a shielding effect (relative to the ring carbons of a benzene ring) and thus come into resonance at higher fields. This effect is not observed in the unreduced ligand where conjugation of the aromatic ring and imine function pi clouds will serve to reduce the excess negative charge in the aromatic ring.

The new methylene group derived from the reduced imine function is presumed to be the relatively low field (for aliphatic sp^3 protons) signal at 3.7ppm on comparison with the R3Bm and R3Bp spectra. The intergral value corresponds to $12H^{+}$. The remaining singlet, which shows some broadening, has an integral equivalent to 23.5 ie 24 protons. On comparison with the equivalent H_D and H_E protons of R3Bp (H_f and H_G protons of R3Bm) this

signal is then assumed to be that of the H_D and H_E methylene protons superimposed on one another, rather than the imine derived methylene group with either H_E or H_D. A higher field spectrum (ie 400MH_2) spectrum should resolve these two signals. It is not easy to say why H_D and H_E are chemically and magnetically equivalent, which is implicit in their having the same chemical shift, when joined to 2 different types of N atom (H_D to a secondary amine and H_E to a tertiary amine (bridgehead). From the ^{13}C spectrum it is interesting to note that we observe 3 different methylene carbons signals. This may suggest that the carbons and thus the protons associated with them are not equivalent by symmetry. The C_A carbon shows a significant shift of ≃11ppm from the equivalent carbons in the unreduced form. Again this can be attributed to the electron density in the ring. This shielding effect is not observed for the C_B carbon atoms probably as a result of resonance forms of the ring cycle. (This aspect is considered in the pyridine based cryptand 3P).

R3F and the Tranisition Metals - Early Results

The reactions of R3F and the transition metals are currently underway but early results are encouraging that this ligand will be a useful transition metal host.

Mn_2R3F(OH)$(CF_3SO_3)_3$ $2H_2O$

Physical data for this compound is tabulated in FIG.83. The ir shows a strong sharp feature at 3564cm^{-1} which was assigned to a bridging hydroxide group. This feature was well resolved out of a broad absorption band that is often indicative of water being present. Indeed, microanalysis gave the best fit when 2 water molecules are included in the proposed formula Mn_2R3F(OH)$(CF_3SO_3)_3 2H_2O$. FAB analysis also supported this molecular formula giving signals at 1126, 994(82%), 773(100%), 623(12%) and 570(18%) corresponding to [Mn_2R3F$(CF_3SO_3)_3$]$^+$, [Mn_2R3F(OH)$(CF_3SO_3)_2$]$^+$, [Mn_2R3F(CF_3SO_3)]$^+$, [MnR3F]$^+$ and [HR3F]$^+$ respectively. No peak corresponding to [Mn_2R3FOH] was found and this may suggest that the OH is not strongly held.

FIGURE 83. PHYSICAL DATA FOR R3F AND ITS COMPLEXES

COMPLEX	MASS SPEC[a] OR F.A.B.	Ω^b S cm^2 mol^{-1}	ELEMENTAL ANALYSIS[c]	INFRARED SPECTRUM (cm^{-1}) NH	X^-	OTHER	ELECTRONIC SPECTRUM SOLVENT	λ (nm)[d]	ε (M^{-1} cm^{-1})
R3F	568 (100)		C 63.3 (62.9) H 8.5 (8.3) N 19.7 (19.1)	3303 3249					
Mn_2R3F(OH)$(CF_3SO_3)_3$.$2H_2O$	1126 (5) 994 (80) 773 (100) 623 (15) 570 (23)	587[b]	C 33.62 (33.79) H 4.53 (4.14) N 9.50 (9.42)	3285 3241	1173 1160 1028	3564	MeCN	360 280 219[d,e]	290 2800 18600[e]
Co_2R3F(OH)$(CF_3SO_3)_3$.$2H_2O$	615 (100) 569 (40)	316 549[b]	C 33.4 (33.0) N 4.5 (4.1)	3274	1162 1163	3558	MeCN	600 480 335 252 220[e] 210[d,e]	190 180 24000 45000 105000[e] 298000[e]
Ni_2R3F(OH)$_2(Ph_4B)_2$.$2H_2O$			C 65.5 (65.5) H 6.9 (6.9) N 7.9 (8.6)	3265	734 707	3468			

contd.....

FIGURE 83 contd.

COMPLEX	MASS SPEC[a] OR F.A.B.	Ω[b] S cm^2 mol^{-1}	ELEMENTAL ANALYSIS[c]	INFRARED SPECTRUM (cm^{-1})			ELECTRONIC SPECTRUM		
				NH	X^-	OTHER	SOLVENT	λ(nm)[d]	ϵ(M^{-1} cm^{-1})
$Cu_2R3F(ClO_4)_2$	569 (12) 632 (64)	468[b]	C 40.3 (40.6) H 5.4 (5.4) N 12.6 (13.1)	3279	1089 622				

(a) % of base peak in parenthesis.

(b) 10^{-4} M

(c) Experimentally determined result in parenthesis.

(d) λ_{max}.

(e) Unreliable result.

The conductivity value is above the range for the 1:2 electrolyte (10^{-4}M) however it has not yet been possible to establish a range for 1:3 electrolytes at 10^{-4}M concentrations.

As yet only 10^{-4} and 10^{-5}M solutions of this complex have been analysed by its electronic absorption spectra and thus we cannot report the d-d transition absorption spectra (Yields did not permit a 10^{-3}M solution). The absorption at 219nm (ϵ=18600) is assigned to a ligand $\pi\pi^*$ transition while those at 280nm (ϵ = 2800) and 360nm (ϵ = 290) are tentatively assigned to a furan $n\pi^*$ and a MLCT band respectively.
Preliminary magnetic susceptibility studies indicate a room temperature moment of 5.89Bm, suggesting interaction between the manganese(11) centres is not strong.

$Co_2R3F(OH)(CF_3SO_3)_3\ 2H_2O$

The ir of the product of the reaction between cobalt triflate and R3F in an MeCN/EtOH solvent mixture shows, as in the case of the manganese a strong sharp feature at 3558cm^{-1}. Again this signal appears out of a broad water band and microanalysis results gave best fit for $Co_2R3F(OH)(CF_3SO_3)_3\ 2H_2O$. The results of the FAB analysis are not easily interpreted. A signal at 569(41%) is assignable to R3F. However the base ion peak at 615 is assignable to $[Co3F]^{2+}$ ie the mononuclear form of the unreduced ligand. Although the mass spec of the starting R3F gave m/e^+ at 568 (corresponding to R3F) with no signal at 556, 564 - 567 (indicating the presence of 3F or partially reduced ligand). The ir of R3F shows feint traces of an imine signal at 1650cm^{-1}. Thus the binuclear dicobalt of R3F may be contaminated with mononuclear $[Co3F]^{2+}$ impurities although FAB did not indicate the presence of 3F as there was no signal at 556. There were also many signals in the range 1100-1650 of the FAB spectrum which suggest ion association, however I was unable to assign them.

The uv showed 2 low energy d-d bands at 600nm/16,600cm^{-1} (ϵ =190) and 480nm/20,800cm^{-1} (ϵ = 180), the former peak showing a shoulder on its high energy side. A broad baseline feature at 750-900nm (13300-11000cm^{-1}) may be the third d-d transition. This appearence of the d-d absorption spectrum

FIGURE 84. MAGNETIC DATA FOR $Co_2R3F(OH)(CF_3SO_3)_3 \cdot 2H_2O$

T	χ_w	χ_m Observed	μ	χ_m Calculated
5.0*	10.73	6640	0.52	
10.0	10.31	6400	0.72	
20.0	13.06	8010	1.14	
30.0	14.66	8947	1.47	8137
40.0	15.38	9368	1.74	9120
50.0	15.78	9603	1.97	9660
60.0	16.07	9772	2.17	9975
80.0	16.40	9960	2.54	1019
100.0	15.30	9315	2.74	1004
180	13.46	8244	3.48	8303
210	11.73	7225	3.50	7652
293	10.63	6587	3.96	6210
320	8.75	5487	3.76	5843

*This value was not used in calculation of J using Bleaney-Bowers equation (see Appendix 3). Best fit to this equation was obtained using:

$$-2J = 36$$
$$g = 2.17$$
$$N\alpha = 3.5 \times 10^{-4}$$

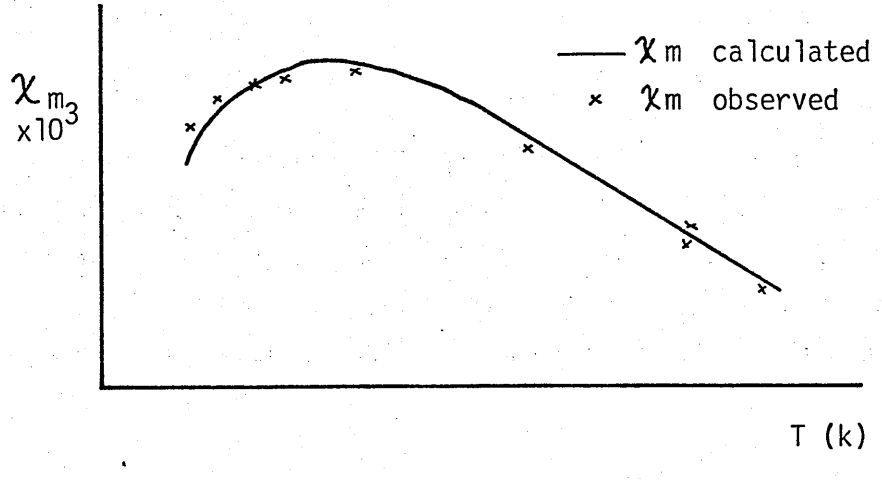

suggests a low symmetry octahedral environment of the Co^{2+} ions, and the 3 electronic transitions correspond, in order of decreasing energy, to the $^4T_{1g}$ (F) --> $^4T_{1g}$(P), $^4T_{1g}$(F) -->$^4A_{2g}$, and $^4T_{1g}$(F) -->$^4T_{2g}$ transitions expected for octahedral symmetries. Other absorptions were observed at 335nm (24000), 251nm (45000), 220nm (105000) and 210nm (198000). The band at 335nm may be a charge transfer band although at $\epsilon=10^4$, it is perhaps too strong, and thus may, like the other bands be a result of $\pi-\pi^*$ ligand absorptions.

A low temperature magnetic study has been carried out on this complex. Antiferromagnetic interaction is observed as expected for a complex containing paramagnetic centres bridged by a hydroxo group. The results are shown both graphically and in table form in FIG 84. From the graph the Neel temperature (T_N) is estimated to be ≃75K. Above this temperature normal Curie-Weiss behaviour is observed ie

$$\chi = C/(T-\theta)$$

$$\text{ie.} \quad \chi \propto 1/T$$

where C = Curie Constant
θ = Weiss Constant.

and the magnetic susceptibility increases with decreasing temperature. However below T_N the complex shows decreasing susceptibility with decreasing temperature. In a spin coupled system this is the result of the'spin' influence of the intervening hydroxo group which results in half of the ions having their magnetic moments lined up in the opposite direction to those of the other half of the ions within the binuclear assembly[47]. ie. antiferromagnetic interactions.

The lowest temperature (ie 5K) susceptibility was discarded when estimating -2J from the Bleaney -Bowers equation. Its lack of fit with the rest of the data may result from paramagnetic impurity (possibly the mononuclear $[Co3F]^{2+}$ indicated in the F.A.B) and also intermolecular interactions which generally only become significant at such low

temperatures. On applying the Bleaney-Bowers equation (see Appendix 3 of Chapter 3) and by using a 'best-fit' program the following values were obtained:

$-2J = 36cm^{-1}$

$g = 2.17$

$N\alpha = 3.5 \times 10^{-4}$ cgsu.

where $N\alpha$ is the temperature indepentant paramagnetism. A plot of χm observed against χm calculated is shown in Fig.84-3.

As yet no really satisfactory product has been obtained in the reaction between R3F and Ni(II). Preparations involving the perchlorate or triflate counterion gave only tacky oils. However when tetraphenyl borate ions were present a dull green powder was isolated. This analyzed as $Ni_2R3F(OH)_2(Ph_4B)_2\ 4H_2O$. As yet no further analysis has been carried out on the complex.

The Cu^I ion has also been inserted into R3F giving a yellow/green product which on standing in air gradually, over weeks, becomes a darker green colour. The initial product of the reaction analysed as $Cu_2R3F(ClO_4)_2$ and indeed the ir of this product gave no evidence of water or other solvent molecules being present. Results of FAB analysis also support this molecular formula with peaks at 797(4%), 669(30%), 631(22%), and 569(100%) corresponding to $[Cu_2R3FClO_4]^+$, $[H_2R3FClO_4]^+$, [CuR3F], and $[HR3F]^+$ respectively. Again no further study has been made on this complex.

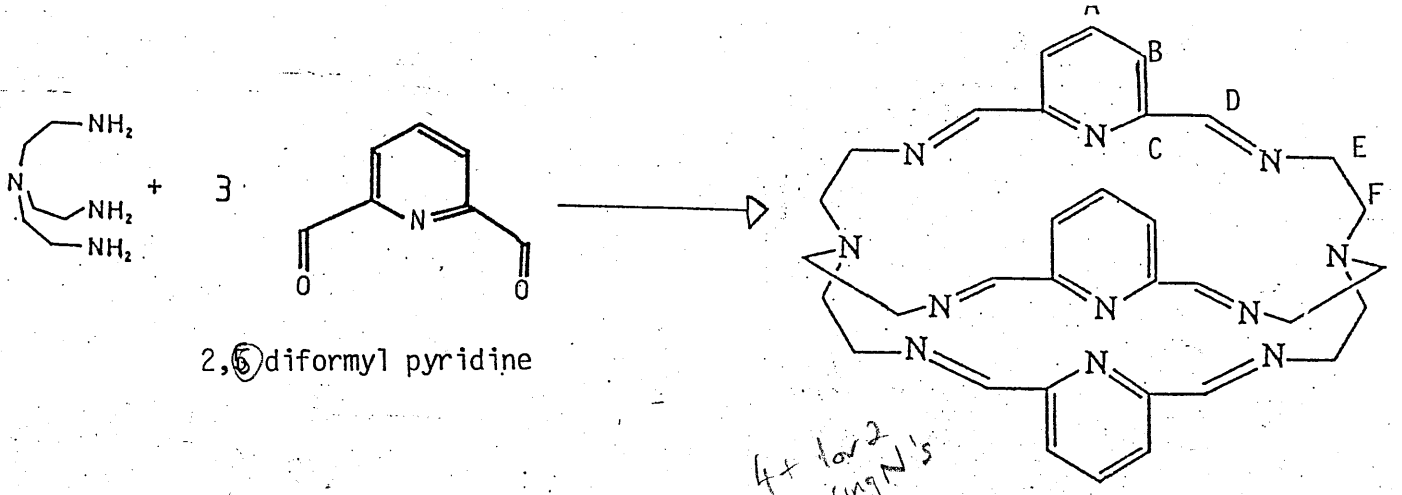

2,6 diformyl pyridine

4+ for 2 ring N's each geometry?

LIGAND 3P

FIG. 85-2

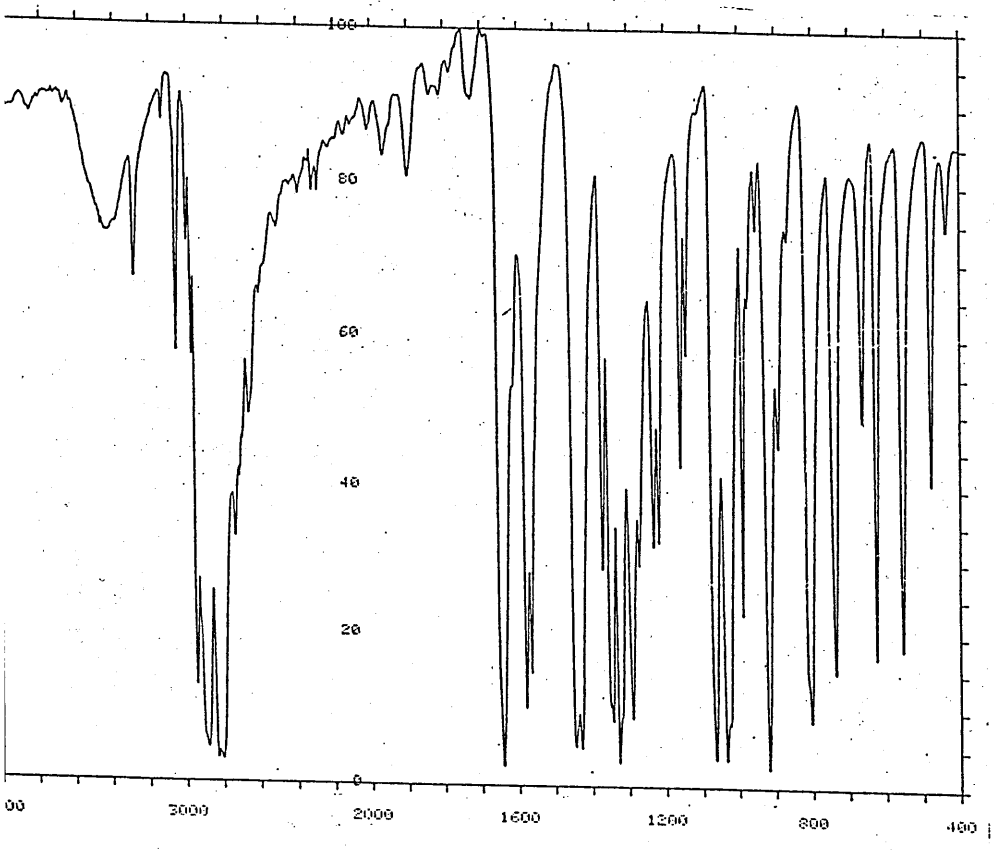

FIG 85-3

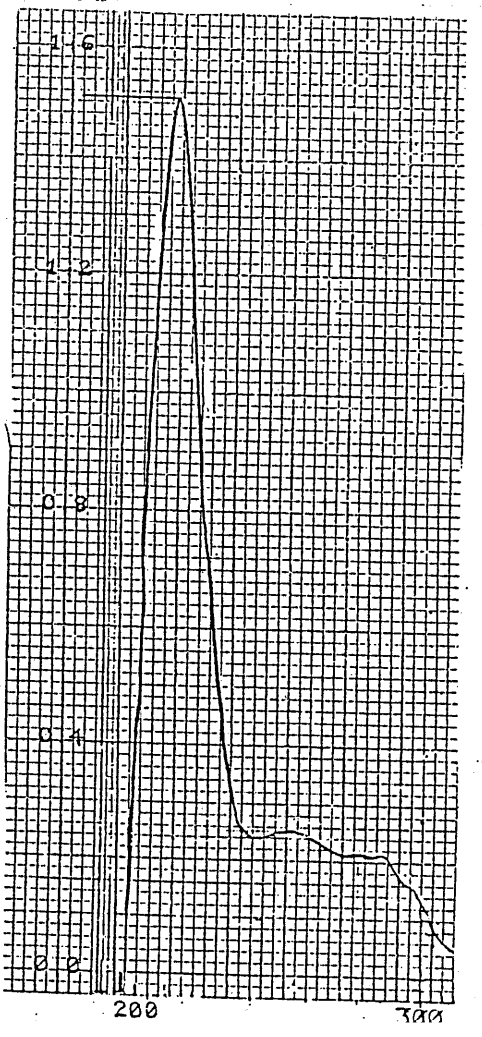

LIGAND 3P

This ligand has been reported both by Lehn[60] and ourselves[64]. It is the product of a Schiff-base condensation reaction between diformyl-pyridine (DFP) and the amine tren in methanol. FIG 85-1. The ligand is a macrobicyclic heterophane which offers an N_{11} donor set and thus should be a useful transition metal molecular host.

As in 3F and 3Bp the ligand has been synthesized in both its metal free and templated form - the Group II metal ions were very successful giving ≈86% yield. For the non template synthesis yields of up to ≈56% have been obtained. For pyridine 2,6-dicarboxaldehyde the only important conformer is trans trans[61], thus the Group II metal ion in the template synthesis is redirecting conformer distribution to predominantly cis,cis through complexation prior to macrocyclization. The yield of the metal free ligand suggests that as in the case of 3F it is the trans trans conformer that leads to the formation of the uncomplexed 3P. It is however interesting to note that this reaction does not take place when dried solvents are used - indeed water (20-30ml) has to be added to the reaction vessel in order that a solid 3P product can be obtained. Until a crystal structure is obtained it is not possible to know if, as in the case of 3Bp, there are water molecules associating with the molecular framework of the macrobicycle.

3P AND THE TEMPLATED FORMS OF 3P

The physical data for 3P and its templated forms is tabulated in FIG.86 while the nmr data is given in FIG.87.

The ligand 3P is usually isolated as a white microcrystalline solid, however a set a cubic transparent crystals, suitable for X-ray structural analysis, have been obtained and the structure is currently being solved. Newkome has reported the ether derivatives of 3P[38,65] FIG 88-1 and 88-2. The X-ray of 88-1 (Shown in FIG 88-1b) showed that the bridgehead nitrogen

FIGURE 86. PHYSICAL DATA FOR 3P,R3P AND ITS TEMPLATED FORMS

LIGAND/ COMPLEX	MASS SPEC[a] OR F.A.B.	Ω[b] S cm^2 mol^{-1}	ELEMENTAL ANALYSIS[c]	I.R. cm^{-1}				ELECTRONIC ABSORPTION SPECTRUM		
				C=N	py	NH	ClO_4	SOLVENT	λ(nm)[d]	ε(M^{-1} cm^{-1})
3P	590		C 67.2 (67.4) H 6.6 (6.6) N 26.1 (25.9)	1647	1583			MeOH	211[d,e] 254 277 296	151,000[e] 25,600 21,800 16,000
$Ba3P(ClO_4)_2$	826 (100) 727 (37)	241 512[b]	C 42.8 (42.8) H 4.3 (4.1) N 16.6 (16.8)	1650	1587		1090 622	CD_3CN	210[d,e] 280 305	304,000[e] 22,600 15,000
$Sr3P(ClO_4)_2$ $.2H_2O$	775 (100) 676 (31)	307 471[b]	C 43.5 (43.7) H 4.7 (4.5)	1644	1584		1090 621	CD_3CN	210[d,e] 280 306 340	310,000[e] 24,000 20,000 2,400
$Ca3P(ClO_4)_2$ $.2H_2O$	728 (100) 629 (46)	275 420[b]	C 44.8 (44.4) H 4.4 (5.0) N 18.2 (18.6)	1643	1586		1087 621	CD_3CN	210[d,e] 230 306 340	56,000 38,000 15,000 2,000

contd.....

FIGURE 54. (contd.)

COMPLEX (Colour)	M^+ OR F.A.B.[a]	Ω^b S cm^2 mol^{-1}	ELEMENTAL ANALYSIS[c]	INFRARED SPECTRUM (cm^{-1})				ELECTRONIC SPECTRUM		
				C=N	CF_3SO_3	ClO_4	OH	SOLVENT CONC.	WAVELENGTH[d] (nm)	$\varepsilon(M^{-1}\ cm^{-1})$
$[Cu_2 3Bm]^{4+}$.$2H_2O$ (blue)		545[b]	C 34.77 (35.22)	1646		1093	3423	MeOH 10^{-4}	615	540
			H 4.41 (4.58)			623			374	2800
			N 10.98 (11.59)						232	73000
									201[d,e]	124000[e]

(a) % of base peak in parenthesis

(b) 10^{-4} M.

(c) Experimentally determined result in parenthesis.

(d) λ_{max}.

(e) Unreliable result.

FIGURE 54. PHYSICAL DATA FOR THE Ag^{+}, Cu and Cu^{2+} INSERTION PRODUCTS WITH 3Bm

COMPLEX (Colour)	M^{+} OR F.A.B.[a]	Ω[b] S cm^2 mol^{-1}	ELEMENTAL ANALYSIS[c]	INFRARED SPECTRUM (cm^{-1})				ELECTRONIC SPECTRUM		
				C=N	CF_3SO_3	ClO_4	OH	SOLVENT CONC.	WAVELENGTH[d] (nm)	ϵ (M^{-1} cm^{-1})
$Ag_2$3Bm$(CF_3SO_3)_2$ .2EtOH (pale yellow)	951 (68) 801 (8) 693 (100)	295	C 41.4 (40.9) H 4.4 (3.9) N 9.6 (9.3)	1649	1254 1148 1029		3490 (EtOH)	MeCN 10^{-3} 10^{-4} 10^{-5}	420 310 298 255 220[e,d]	67 4651 5922 43689 178640[e]
$Cu_2$3Bm$(ClO_4)_2$ .2H_2O (yellow)		352[b]	C 45.6 (44.6) H 4.9 (5.2) N 11.8 (11.4)	1646		1086 622		MeCN 10^{-4} 10^{-5}	354 250 206[e,d]	5100 40000 232000[e]
$[Cu_2$3Bm$]^{4+}$ .2H_2O (green)	929 (15) 830 (50) 729 (30) 649 (55)	573[b]	C 40.60 (40.39) H 4.35 (4.40) N 10.63 (10.52)	1643		1088 622	3428	MeCN 10^{-4} 10^{-5}	630 270 250 225 202[d,e]	350 31000 93800 142000 156000[e]

contd.....

FIGURE 86 (contd.)

LIGAND/ COMPLEX	MASS SPEC[a] OR F.A.B.	Ω[b] S cm^2 mol^{-1}	ELEMENTAL ANALYSIS[c]	I.R. cm^{-1}				ELECTRONIC ABSORPTION SPECTRUM		
				C=N	py	NH	ClO_4	SOLVENT	λ(nm)[d]	ε(M^{-1} cm^{-1})
R3P.$2H_2O$	602 (100)		C 62.14 (62.49) H 8.69 (8.9) N 24.15 (23.4)		1590	3327		MeOH	210[d,e] 264	46,200[e] 16,000

(a) % of base peak in parenthesis.

(b) 10^{-4} M.

(c) Experimentally determined results in brackets.

(d) λ_{max}.

(e) Unreliable result.

FIGURE 87. N.M.R.[a] DATA FOR LIGAND 3P AND ITS TEMPLATE FORMS

LIGAND/ COMPLEX	SOLVENT	TEMP.	EXPERIMENT	PROTON/CARBON SITE						
				A	B	C	D (Imine)	E	F	NH
3P	$CDCl_3$	294 K	^1H 250 MHz	7.8 (t)	8.10 (d)		7.7 (s)	3.45 (br,s)	2.87 (s)	
3P	$CDCl_3$	223 K	^1H 90 MHz	7.73 (t)	8.0 (d)		7.4 (s)	3.24 (t) 3.77 (d)	2.73 (br,s)	
3P	$CDCl_3$	294 K	^{13}C[b] 300 MHz	117 132 150 159				56.132	52.806	
Ba3P $(ClO_4)_2$	CD_3CN	294 K	^1H 250 MHz	8.23 (t)	7.8 (d)		8.53 (s)	3.45 (t) 3.0 (m)[c]	2.48 (t) 3.0 (m)[c]	
Sr3P$(ClO_4)_2$. $2H_2O$	CD_3CN	294 K	^1H 300 MHz	8.27 (t)	7.86 (d)		8.5 (s)	3.2 (t) d	2.4 (t) d	
Sr3P$(ClO_4)_2$. $2H_2O$	CD_3CN	294 K	^{13}C[b] 300 MHz	117 128 141 161				63.909	58.587	
Ca3P$(ClO_4)_2$. $2H_2O$	CD_3CN	294 K	^1H 300 MHz	8.30 (t)	7.84 (d)		8.5 (s)	3.1 (m) e	2.48 (t) e	
R3P	$CDCl_3$	294 K	^1H 300 MHz	7.08 (s)	7.52 (s)		3.89 (s)	3.19 (s)	2.65 (s)	
R3P	$CDCl_3$	294 K	^{13}C[b] 300 MHz	116 132		155	51.0	51.7	43.5	

(a) ppm from T.M.S. : (s) singlet, (d) doublet, (t) triplet, (m) multiplet, (br) broad.
(b) Off resonance spectra not yet run. (c) Overlapping signals.
(d) 2 Doublets but unable to assign to partner triplet. (e) Second component of signal indistinguishable.

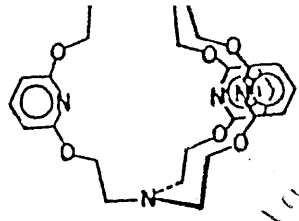

FIG. 88-1

Skeletal rigidity & intramolecular bridges

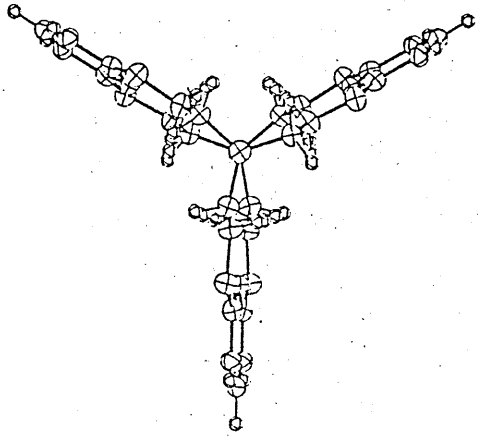

88-1b

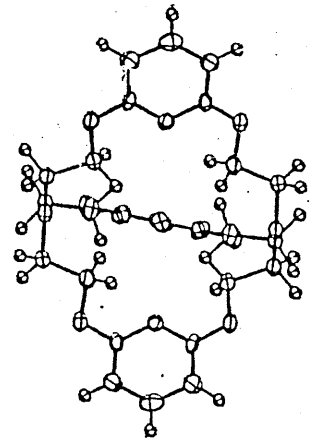

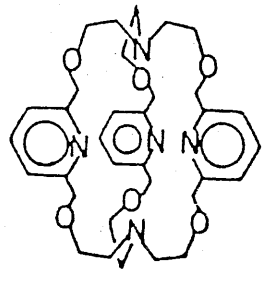

Fig. 88-2

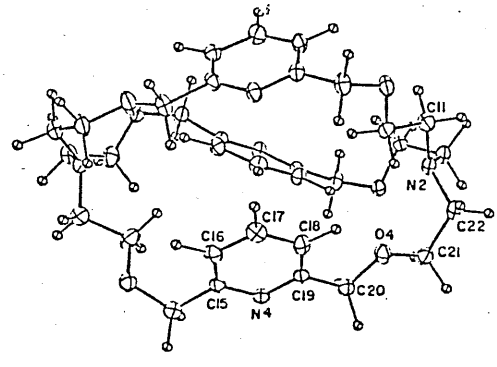

Fig. 88-2b

FIG. 88 - NEWKOME'S POLYETHER DERIVATIVES OF 3P

atoms have a planar configuration with crystallographically equivalent 120°(sp^2) bond angles. This was one of the first X-ray structures of a molecule having nitrogen bridgeheads to contradict the up to then accepted in-in, in-out or out-out configuration arrangement of the sp^3 bridgehead nitrogen lone pairs[66]. Newkome attributed the deviation from the anticipated sp^3 configuration to the observed planar sp^2 arrangement to skeletal rigidity of the bridges or intramolecular hindrance imposed by substituents on the bridges - these being two of the known effects that can determine the configuration of the bridgehead nitrogen. Thus Newkome synthesized 88-2[38] in which a methylene group is inserted between the O atom and the aromatic pyridine ring in order to decrease steric constraints. The X-ray of this product, 88-2b, showed that the bridgehead nitrogen has an sp^3 non-planar configuration - thus the nitrogen lone pair could be available for internal coordination.

The V.T.nmr. of 88-2 showed that the 3 pyridine rings are equivalent and freely rotating and that on average, one of the pyridine rings is included in the cavity. Coalescence of the pyridine rings occurred at -78°C although no estimate of ΔG_c was reported. This is in contrast to 88-1 where a greater degree of steric constraint within the molecule is evidenced in the nmr spectrum (100MHz). The following features were observed -

δ3.08 (t, NCH_2, J = 6Hz, 12H)

δ4.32 (t, OCH_2, J = 6Hz, 12H)

δ6.13 (d, 3,5 PyrH, J = 8Hz, 6H)

δ7.30 (t, 4, PyrH, J = 8Hz, 3H)

Thus the pyridine rings are no longer free to rotate but instead are frozen out into the doublet, triplet features.

As with the other ligands, ir, microanalysis uv, mass spec, and 'Hnmr have all been used to confirm the cyclic nature of the macrobicycle 3P.

Fig. 89-1 300 MHz SPECTRUM OF 3P

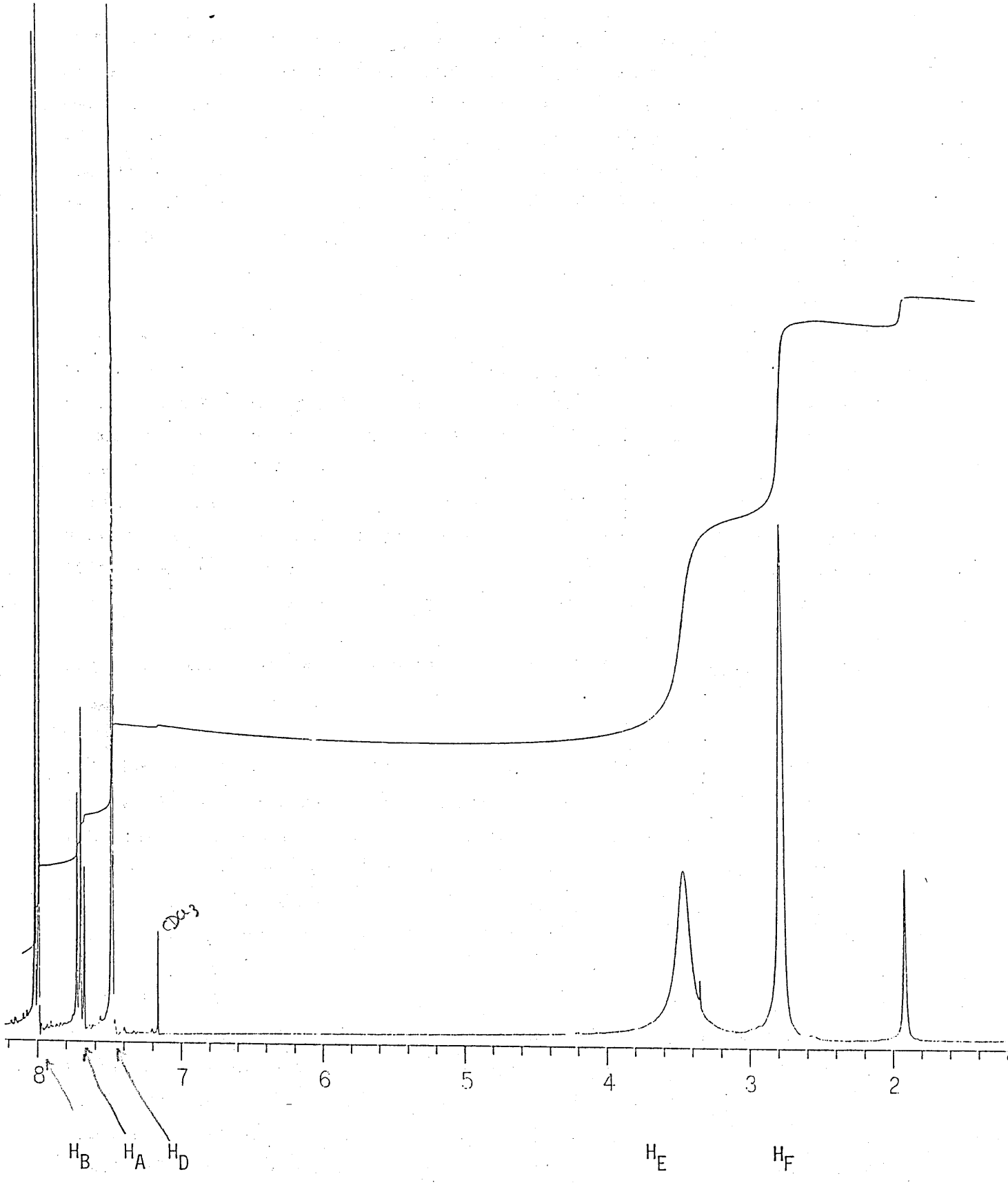

The ir of a crystalline sample of ligand 3P is shown in FIG 85-2. Despite the apparent need for the presence of water in the preparation, there is no indication that water is present in the isolated crystalline product obtained on slow evaporation of solvent. However if the product is isolated very quickly using a rotary evaporator both ir and microanalysis show water with the latter giving best fit when 1 water solvate is included. The imine signal appears at $1647cm^{-1}$ with the pyridine signal at $1583cm^{-1}$.

The uv spectrum of 3P is quite complicated and is shown in 85-3. Pyridine itself shows a broad band absorption at ≈240-260nm, and this band often shows fine detail (this may be lost in conjugated systems). As a heterocyclic molecule the electron transitions can include $n\pi^*$ ($\epsilon \simeq 10^1$ in 250-360nm range) and the π-π^* transitions for both the pyridine and the imine functions. Both features can also give rise to charge transfer bands. The main feature observed in the uv spectrum of 3P is the very intense absorption at 210nm ($\epsilon \simeq 10^5$). The other signals all have $\epsilon \simeq 10^4$ which suggest they are also derived from π-π^* transitions.

Mass spec confirmed the monomeric cyclic nature of 3P giving the $m/e^+ = 589$ (100%).

As yet only a 250MHz 'Hnmr spectrum and a 90MHz V.T.nmr study is available for ligand 3P. From the room temperature 250MHz spectrum FIG 89-1 we can see that the pyridine rings are, as in 88-1, frozen so that we observe a triplet for H_A and a doublet for H_B. The difference between 3P and 88-2, for which a sharp singlet for the pyridine rings is observed, may in part be due to the steric constraint that the imine double bond places on the system thus preventing the free rotation that is observed in 88-2. This idea is given support from the 'Hnmr of the octaamine (reduced) derivative of 3P which shows only a sharp singlet for the aromatic protons indicating free rotation is possible when the imine functions are replaced by a single bond. The imine signal also appears as a sharp singlet. However it is interesting to note the chemical shifts of the aromatic H_A and H_B protons. The H_A triplet appears at 7.80ppm while the H_B doublet is at 8.1ppm ($J_{AB} = J_{BA} = 7.8Hz$). These signals appear significantly downfield from the

expected aromatic resonance of ≃7.1ppm. On the other hand the imine singlet appears at 7.6ppm which is comparable with that observed in the other ligands in the study.

The deshielding effect observed for the aromatic protons may result from the close approach of the pyridine rings (recall in 88-2 one pyridine rings lies within the cavity). However a more likely explanation is probably that in which the effect of the heterocyclic ring is taken into account. Unlike the furan or thiophene heterocyclic rings which creates a π-excessive system, the heterocyclic pyridine gives rise to a π-deficient aromatic system[67]. This is reflected in the dipole moment of pyridine (2.26D) with the N heteroatom bearing the negative end of the dipole. (cf pyrrole 1.81D) and other 5 membered heterocycles such as furan and thiophene where the heteroatom bears the positive end of the dipole). Thus for pyridine, the aromatic protons will be less well shielded as a result of the reduced π electron density and thus appear downfield. The extent of deshielding may be reduced if there is significant conjugation with the imine function.

In the 3F system the shielding of the aromatic protons is only observed in the reduced form of the ligand when H_A appears at 6.08ppm. That it is not observed in the unreduced form suggests that in 3F there is effective conjugation of the 2 chromophores. This implies that in 3P therefore, conjugation may be less effective as such a significant deshielding effect of H_B is observed. Alternatively in 3F, where the aromatic rings are free to rotate the signal given is the time averaged value of adjacent ring currents. In 3P where rotation is prevented, no such averaging is possible.

At room temperature in the 250MHz spectrum the methylene signals appear as broadened singlets (with H_E significantly broader than H_F) The V.T.nmr spectra (90MHz) for the methylene protons are shown in 89-2 to 89-7. Although at room temperature some second order splitting of the signals is observed, by 283K resolution is being lost so that by 273K and 263K the coalescence temperatures for H_E and H_F respectively are achieved. By 243K we observe that H_E is beginning to resolve into the equatorial doublet and

Fig. 89 v.t. nmr (90 MH_z) of 3P

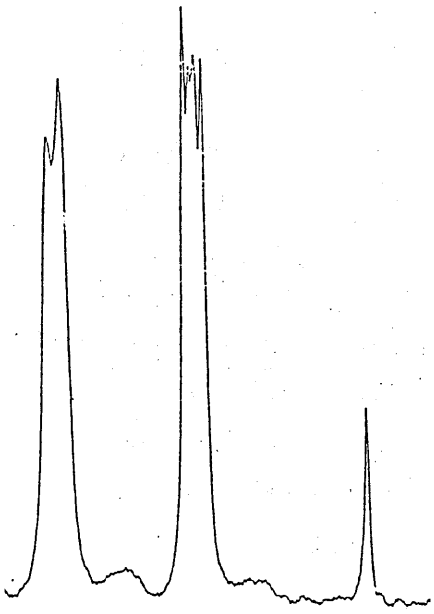

H_E H_F H_2O

293k

89-2

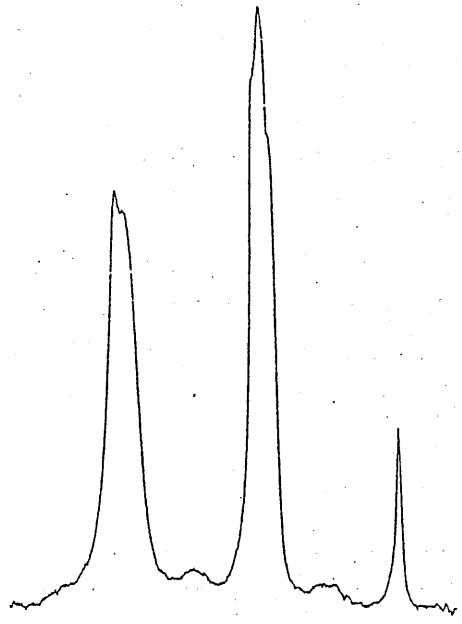

283k

89-3

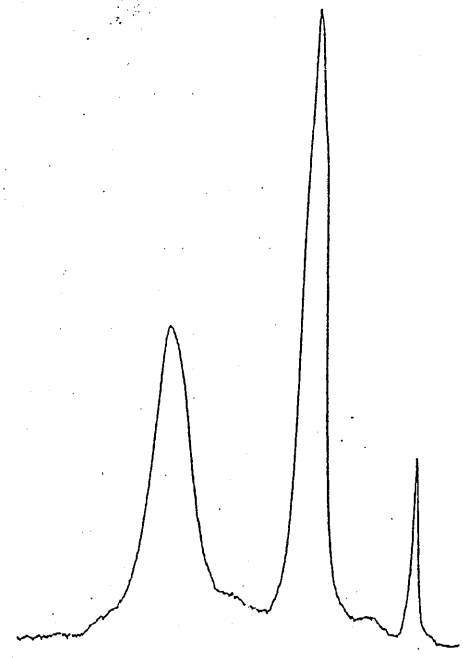

273k

Tc for H_E

89-4

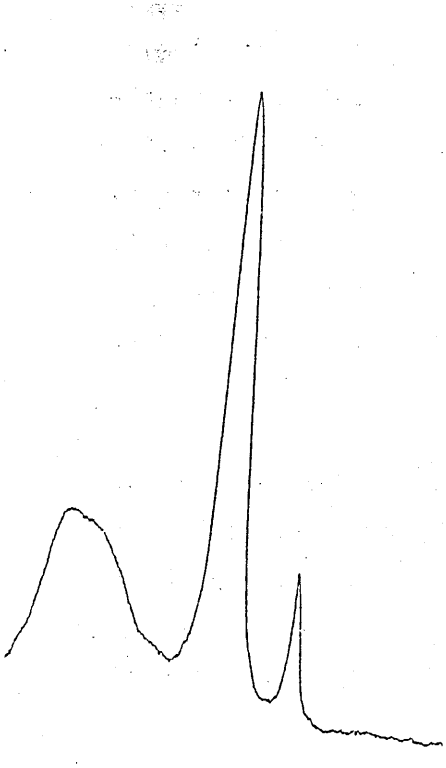

263k

Tc for H_F

89-5

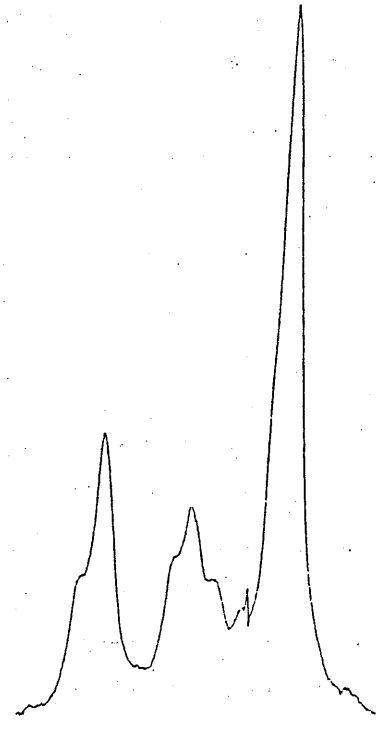

243k

89-6

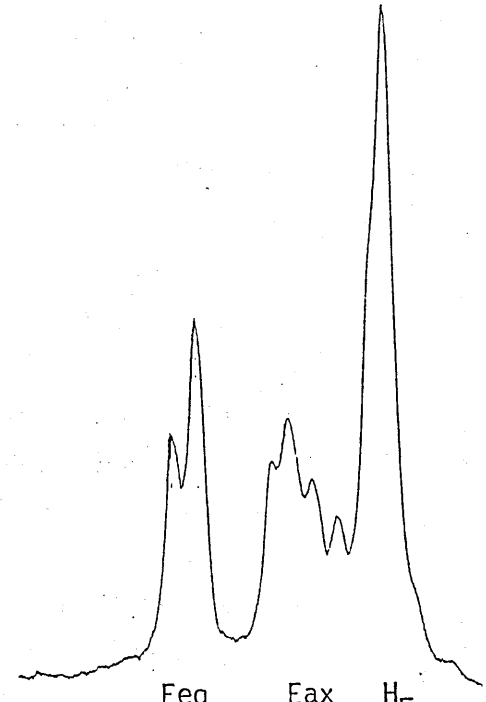

Eeq Eax H_F

223L

89-7

higher field axial triplet (as in 3F, 3Bm and 3Bp) and by 223K these signals are well resolved. H_F however shows no tendency to split into its axial and equatorial components. Thus $\Delta G^{\#}_c$ can be calculated for H_E only and ΔG = 56KJ. This is the same value calculated for 3F and therefore is again larger than that obtained for 3Bp which has the larger cavity length. Thus it would appear that increased cavity length in 3Bp plays a significant role in reducing the steric constraints within the macrobicycle. The ^{13}C spectrum gave a six line spectrum as expected. However this was returned without the off resonance spectrum and thus accurate assignment of the carbon signals cannot be made.

Ba3P$(ClO_4)_2$

The physical data for the Ba, Sr and Ca complexes of 3P is given in FIG 86 while the nmr data is shown in FIG 87.

The barium complex analysed as the anhydrous molecule although the ir had shown a broad band at 3500-3000cm^{-1} usually indicative of the presence of water. Neither the imine or pyridine peaks show significant shifts from the uncomplexed 3P, although the intensity of the signals is reversed compared to 3P ie in 3P the imine signal was more intense than the pyridine whereas in the complexed ligand the pyridine signal becomes more intense than the imine. The FAB spectrum gave signals at 826 (100%) and 727 (3.7%) corresponding to $(Ba3PClO_4)^+$ and $(Ba3P)^+$ respectively. There was no signal at 590 corresponding to $(H3P)^+$. Again, it is not known whether this indicates that the cation is tightly bound within the macrocyclic cavity - however results - or lack of results! - in the transmetallation attempts (discussed later) might suggest that this is indeed the case.

The electronic absorption spectrum of the barium complex is very similar to that observed in 3P. Again it is a very intense absorption at 210nm (ϵ-10^5) that dominates the spectrum. A broad shoulder on this peak at 260-280nm ($\epsilon=10^4$)may be the $\pi\pi^*$ transition associated with the pyridine ring. However this is the region where $n\pi^*$ absorptions are expected to be seen and thus the band may be an intense $n\pi^*$ absorption.

FIG.90-1

250MHz 'Hnmr SPECTRUM OF $(Ba3P)^{2+}$

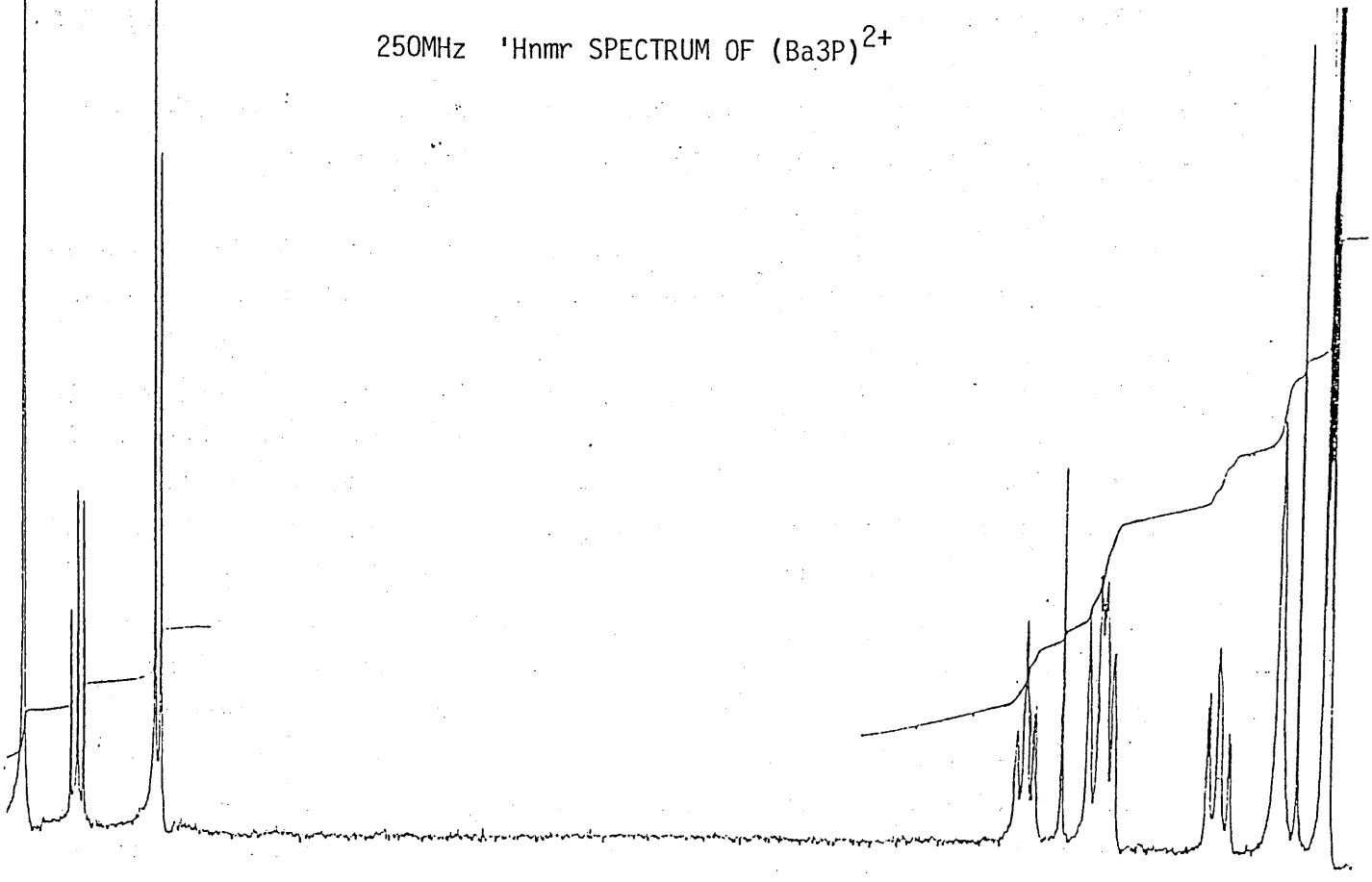

FIG.91-1

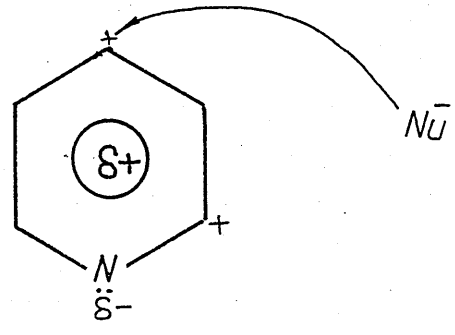

FIG.91-2

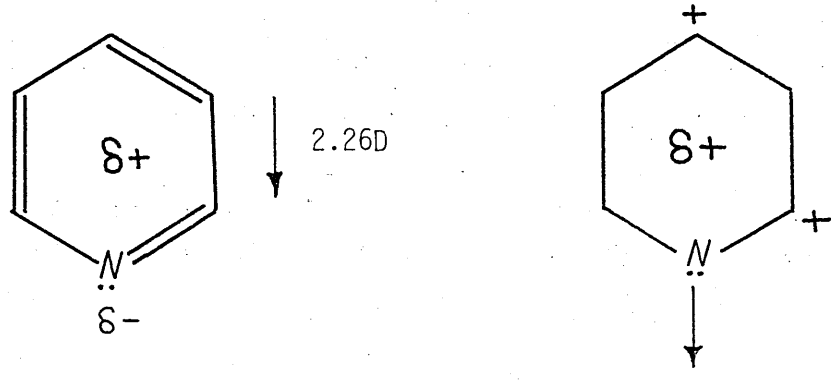

The conductivity value of 241Scm^2mol^{-1} for a 10^{-3}M solution falls in the range expected for 1:2 electrolyte (for 10^{-4}M Ω = 510 Scm^2 mol^{-1})

The '250MHz Hnmr spectrum of Ba3P$(ClO_4)_2$ is shown in FIG 90-1 and some interesting features are observed when compared to the uncomplexed ligand.

The imine singlet has undergone a 0.83ppm downfield shift on complexation (a 0.37ppm downfield shift was observed for the coordination shift in 3F and Ba3F$(Ph_4B)_2$). This suggests a strong interaction between the imine nitrogen donors and the metal centres resulting in a significant loss of electron density from the imine double bond and thus the observed deshielding of the imine proton. The H_A triplet is also deshielded on complexation (0.43ppm) whereas the H_B doublet appears to become more shielded (0.3ppm) as a result of complexation. Thus the arrangement of the signals in Ba3P$(ClO_4)_2$ ie (H$_D$ singlet, H_A triplet, H_B doublet) is reversed compared to 3P (H_B doublet, H_A triplet, H$_D$ singlet). The reason for this may be rationalized on the basis that compared to benzene, coordinated pyridine is further activated at the para and ortho (to the N heteroatom) ring positions which essentially assume a net positive charge FIG.91-1 and 91-2. This results in the protons at position A being deshielded relative to those protons in position B.

These results suggest that the 6 imine N's and the 3 N's of the pyridine rings are all coordinating the barium centre.

From 90-1 it is observed that not only are the aromatic signals frozen out at room temperature but that the methylene signals are also frozen. The axial triplets are well resolved and analysis of F_{ax} suggests that J_{gem} = J_{axax} = 13.06Hz and thus the fine structure is a result of the small vicinal coupling $J_{Fax-Eeq}$ = 2.75Hz. Analysis of E_{ax} gives J_{gem} = $J_{ax-ax'}$ = 10.9Hz. Thus J_{gem} for E $\neq$ J_{gem} for D which implies that the Hax C Heq angles are different for the 2 methylene groups.

The 2 equatorial signals are not fully resolved and it is not possible to determine any of the coupling constants from them. The integral confirms that this multiplet is derived from the 2 equatorial protons. High field

FIG. 90-2

300 MHz SPECTRUM

OF Sr 3p $(ClO_4)_2$

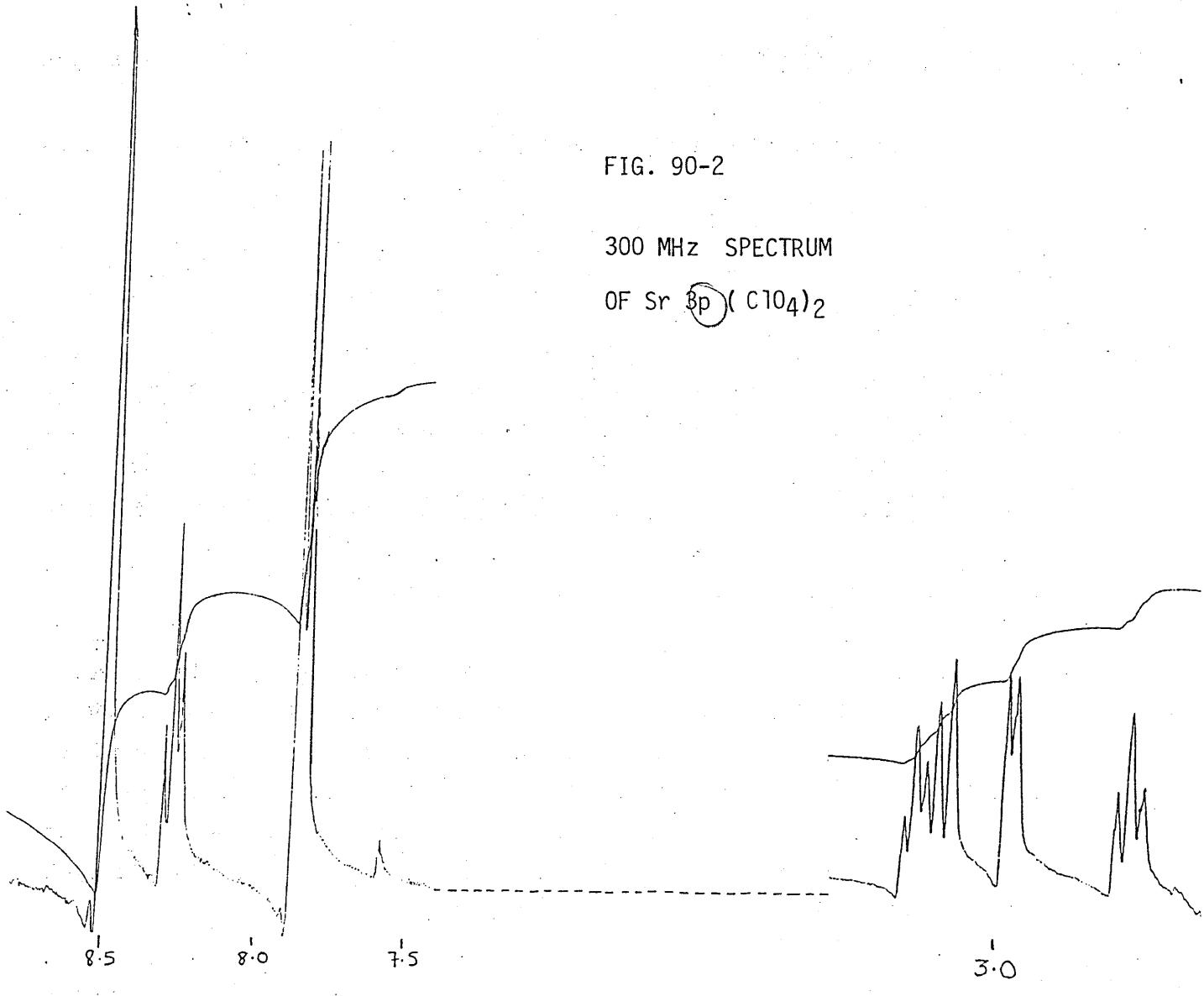

Fig. 90-3

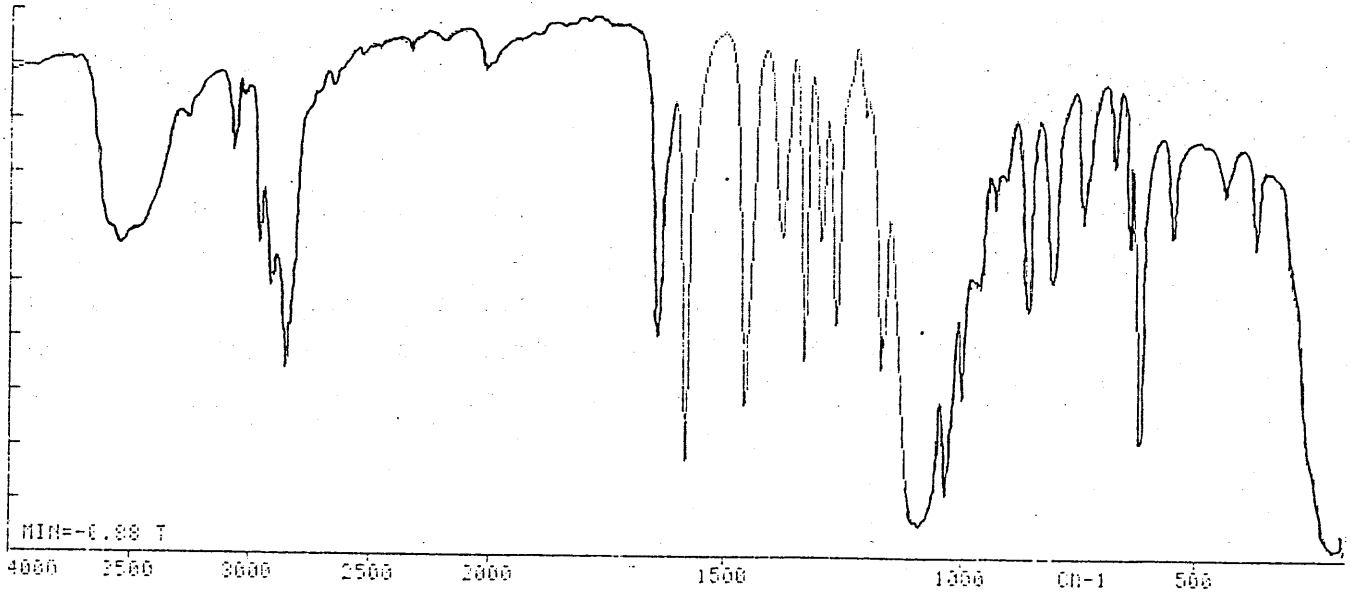

spectra will greatly assist the analysis of the 'Hnmr spectrum of this complex,

Sr3P$(ClO_4)_2$ $2H_2O$

Both the ir Fig.90-3 and microanalysis of this complex indicated that water was present- in the former as a sharp feature at 3533cm^{-1}. As in the barium complex the pyridine signal at 1584cm^{-1} is more intense than the imine signal at 1644cm^{-1}. F.A.B results again show no signal for the free 3P ligand with only 2 observable peaks showing at 776 (100%) and 667 (31%) corresponding to $[Sr3P\ ClO_4]^+$ and $[Sr3P]^+$ respectively.

The electronic absorption spectrum showed a very intense ligand absorption at 210nm ($\epsilon=10^5$) and two other $\pi\pi^*$ transitions at 280nm ($\epsilon-10^4$) and 305nm ($\epsilon-10^40$ with the former likely to be the $\pi\pi^*$ transition associated with the pyridine ring. A weaker band at 340nm ($\epsilon=10^3$) is less easy to assign being too intense for the $n\pi^*$ transition associated with either the pyridine or imine function. The conductivity value of 307 Scm^2mol^{-1} ($10^{-3}M$) is high for a 1:2 electrolyte[63] (471 for $10^{-4}M$).

The 300MHz nmr spectra of Sr3P$(ClO_4)_2$ $2H_2O$ is shown in FIG 90-2 - the relevant data is tabulated in FIG.87.The arrangement of the H_A, H_B and H_D signals is the same as that in the barium complex ie H_D singlet. H_A triplet, H_B doublet and can therefore be rationalzed in the same way. Indeed the chemical shift value of these signals in the two complexes are very similar indicating that in both cases there is strong coordination of the metal centre. For the smaller metal this implies that the ligand will have been pulled in around the cation to get the same good fit achieved with the larger barium cation.

The methylene signals are now better resolved than in the barium complex although it is not obvious which doublet goes with which triplet. However signs of fine structure of the highfield doublet and triplet make it likely that these 2 signals are related by coupling ie $J_{Fax-Eeq}$ and $J_{Eeq-Fax}$ are observed. Thus it may be that the two doublets have exchanged places.

However if this is the case then the spectrum should be well enough resolved so that the coupling constant J_{gem} for F should be the same from both the F axial and equatorial signals and Jgem for E should be the same from both its component signals. Analysis of the signals gives:-

From the low field triplet, Jgem = Jaxax' = 10.61Hz

From the high field triplet, Jgem = Jaxax' = 12.5Hz

Jax-eq' = 3.41Hz.

From the highfield doublet, Jgem = 9.58Hz.

From the lowfield doublet, Jgem = 14.15Hz.

Certainly the 2 smaller values for Jgem come from the low field triplet and the highfield doublet which suggests that it is these 2 signals that are related by coupling. However the 2 larger values are quite different and are probably complicated by the smaller couplings. High temperature nmr experiments which are planned should clarify the situation if coalescence can be achieved.

Ca3P(ClO$_4$)$_2$.2H$_2$O.

The calcium complex of 3P gave an identical ir spectrum to that of the strontium complex showing a sharp feature at 3528cm^{-1} attributable to the waters that both ir and microanalysis indicated. However in the case of this complex 3 rather than 2 waters gave best fit to the data. Unlike [Ca3F]$^{2+}$, [Ca3P]$^{2+}$ shows no sign of the free ligand in the FAB spectrum. Peaks at 728 (100%) and 629 (46%) corresponding to [Ca3PClO$_4$]$^+$ and [Ca3P]$^+$ respectively showed that the complex was mononuclear. A small peak at 746 (15%) could be attributed to [Ca3PClO$_4$.H$_2$O] which may thus indicate a small degree of ring opening. However 647 does not appear. ~ Ca3P·H$_2$O
The uv shows several $\pi\pi^*$ transition absorptions at 210, 230 and 306nm (all show $\epsilon \simeq 10^4$). A less intense absorption at 344nm (ϵ = 2000) may be the $n\pi^*$ of either the imine or pyridine functions.

A poor 300MHz 'Hnmr of the calcium complex shows the same arrangement of aromatic and imine signals. Although a sharp high field triplet and doublet can be made out as in the strontium case it is not possible to determine if the doublet is related to the high field or low field triplet signal. Again a high temperature and high field study is planned.

It is interesting to note that this series of complexes represents the first case (except perhaps for $[Ca3F]^{2+}$ where the evidence is not conclusive) in which all the signals are frozen out in the complexed form of the ligand at room temperature suggesting a tight fit of the metal ion within the macrobicyclic cavity.

ATTEMPTED TRANSMETALLATIONS OF $Ba3P(ClO_4)_2$

The results of the transmetallation reactions of $Ba3P(ClO_4)_2$ have been very disappointing and have been irreproducible. Any reasonably "hopeful" products were analyzed by ir, microanalysis, FAB, μ, and uv. FAB results often showed peaks at 826 $[Ba3P(ClO_4)]^+$ and 727 $(Ba3P)^+$ showing that the product was (often severly) contaminated with the starting material. On the basis that this was a result of the barium fitting too tightly in the cavity the smaller cations, strontium and calcium were used. However there was no improvement with the starting template species clearly in evidence in the FAB spectrum. On the 'Hnmr results of the 3 template species I feel that the failure of the transmetallation reaction for the three complexes is a reflection of an "over efficient" template reaction in which the template ion fits so snugly in the cavity that it is difficult to remove. Despite this, some products have been isolated and characterized and the data is tabulated in FIG.92

MANGANESE AND $Ba3P(ClO_4)_2$

Only one product has been obtained in the reaction of manganese and $[Ba3P]^{2+}$. When $Mn(ClO_4)_2.6H_2O$ and $Ba3P(ClO_4)_2$ were stirred together in the presence of NCS^- (stirred 48hrs at room temperature) a small amount of a fine yellow precipitate formed.

The ir of this solid showed a relatively sharp feature at 3379cm^{-1} attributed to OH and a signal at 2073cm^{-1} which can be attributed to terminal coordinating thiocyanate. On the basis of ir and microanalysis the molecular formula is $Mn_23P(OH)_2(SCN)_2.2MeCN$.

A room temperature magnetic susceptibility measurement using this formula gives μ = 5.25Bm, implying that the dinuclear formulation is correct.

Spin only = 5.92 observed 5.9 can be lowered only by superexchange antiferro interactions as Mn²⁺ is A state ∴ no orbital contribution

FIGURE 92. PHYSICAL DATA FOR THE TRANSMETALLATED AND INSERTION COMPLEXES OF $Ba3P(ClO_4)_2$

COMPLEX	F.A.B.[a]	Ω[b] S cm^2 mol^{-1}	ELEMENTAL ANALYSIS[c]	INFRARED SPECTRUM			ELECTRONIC SPECTRUM		
				C=N	SCN^- ClO_4 Ph_4B	OTHER	SOLVENT	WAVELENGTH[d] (nm)	$\epsilon(M^{-1}\ cm^{-1})$
$Mn_2 3P(OH)_2(SCN)_2$ .2MeCN			C 50.3 (50.3) H 5.08 (4.95) N 50.3 (22.55)	1657	2073	3379	MeCN	300 275 242 210[d,e]	12000 25000 36000 48000[e]
$Fe_2 3P(Ph_4B)_2$ $(ClO_4)_2.3H_2O$	1339 (18) 907 (100)	f	C 61.1 (61.3) H 5.3 (4.6) N 9.6 (9.3)	1647	1087, 624 734 705	3441 (broad)		f	f
$Co3P(ClO_4)_2$ $.2H_2O$	747 (57) 648 (100)	274	C 44.8 (44.5) H 4.9 (4.8) N 17.4 (17.3)	1654	1091,	3620 3550	MeCN	495 1030	500 100
$[Co_2 3P(OH)_2]$ $[Co(NCS)_4]$	706 (28) 648 (100) (826 & 727)	f	C 41.5 (41.2) H 3.6 (4.1) N 19.4 (19.66)	1652	2048	3445		f	f

contd.....

FIGURE 92. (contd.)

COMPLEX	F.A.B.[a]	Ω^{b} S cm^2 mol^{-1}	ELEMENTAL ANALYSIS[c]	INFRARED SPECTRUM			ELECTRONIC SPECTRUM		
				C=N	SCN^- ClO_4^- Ph_4B^-	OTHER	SOLVENT	WAVELENGTH[d] (nm)	$\epsilon(M^{-1}\ cm^{-1})$
$Ni_2 3P(OH)_2(ClO_4)_2 .2H_2O$	746 (100) 647 (70) (727,826)	f	C 40.6 (40.6) H 4.6 (4.2) N 15.8 (15.6)	1656	1092, 622	3548	MULL	920 580 420	
$Ni_2 3P(SCN)_3(OH)$	919 (14)	f	C 46.3 (46.9) H 4.7 (4.6) N 21.0 (21.1)	1658	2095	3430	MULL	970 610 440	
$Fe_2 3P(OH)(ClO_4)_3 .4H_2O$	919 (14) 645 (21)	f	C 36.4 (36.0) H 4.5 (4.6) N 14.1 (14.0)	1632	1089, 625	3419		f	f
$Cu_2 3P(ClO_4)_2 .2H_2O$		411[b]	C 41.66 (42.21) H 4.55 (4.46) N 16.19 (16.09)	1635	1091, 622	3453	MeCN	455 280 212[d,e]	5300 14400 52000[e]

(a) % of base peak ion in brackets.

(b) 10^{-4} M.

(c) Experimentally determined results.

(d) λ_{max}.

(e) Unreliable result.

(f) Insoluble in MeCN.

The (10^{-5}M)uv of this complex showed several ligand $\pi\pi^*$ transitions at 275nm, 242nm, and 210nm ($\epsilon \simeq 10^4$). A broad absorption at 300nm ($\epsilon \simeq 10^4$) may be another $\pi\pi^*$ transition or alternatively a charge transfer band. Not surprisingly given the low solubility no d-d transitions were observed.

From the data available it is not possible to reach any conclusions on the coordination geometry. (Also the FAB spectrum in this case was not strong enough to be useful).

Recent attempts failed completely with the FAB base ion peaks at either 826($Ba3PClO_4$)$^+$ or 727(Ba3P)$^+$. A small peak at 645 (12%) corresponds to $(Mn3P)^{2+}$ which suggested a small amount of cation exchange had occurred. Thus we increased the reaction time, and/or the reaction temperature but these steps did not improve the degree of transmetallation.

IRON(11) AND $Ba3P(ClO_4)_2$

Again many of these attempts failed with poor microanalysis, FAB which indicated starting template species, and in general poor quality products. However one preparation did yield a deep purple powder product.

The ir showed a strong broad water peak as well as perchlorate and tetraphenylborate features. The 1:1 intensity ratio of the anion peaks suggested a molecular formula $Fe3P(ClO_4)_2(Ph_4B)_2\ xH_2O$. Data from the microanalysis suggests X = 2 or 3, but the result is not conclusive. The complex was insoluble in MeCN and so no Ω or uv data are available.

A FAB analysis gives no evidence of the reactant barium complex but shows only one relevant peak at 1339(18%), which corresponds to [$Fe_2$3P$(Ph_4B)_2$]. The base ion peak, 907, corresponds to [3P Ph_4B]$^+$.

Although further transmetallation attempts failed, insertion attempts seem more hopeful and are discussed in the next section.

COBALT AND $Ba3P(ClO_4)_2$

The reactions of cobalt and $Ba3P(ClO_4)_2$ have had some limited success with a mononuclear complex $[Co3P(ClO_4)_2\ 2H_2O]$ and a "suspect" binuclear complex $[Co_2\ 3P(OH)_2]\ [Co(NCS)_4]\ 2H_2O$

Despite adding NaNCS to the reaction a reddy brown microcrystalline product was obtained which analysed as $Co3P(CLO_4)_2\ 2H_2O$. The ir of the product showed a very sharp feature at $3551cm^{-1}$ which may indicate that 1 or both of the waters are strongly coordinating the metal centre. Although the pyridine signal is unsplit at $1595cm^{-1}$ the imine signal has a definite shoulder on it which may indicate that only some of the imine functions are coordinating. Indeed the mononuclear nature of the complex necessarily implies that the 3 pyridine 'N',6 imine 'N' and 2 bridgehead 'N' atoms cannot all be coordinating. The uv spectrum of the complex looks 5 coordinate in profile with 2 observable d-d bands at 495nm ($20,200cm^{-1}$:ϵ=500) and a broader band at 1030nm ($9700cm^{-1}$: ϵ = 100). Indeed it is known that Me_6tren ie $N(CH_2N(CH_3)_2)_3$ forms 5 coordinate complexes of Co(11) and gives rise to the high spin derivative showing a magnetic moment of $\simeq 4.8Bm^{(66)}$. 3.7 spin only 5.2 — orbital M S+L

For the complex $Co3P(ClO_4)_2\ 2H_2O$ the room temperature moment is 4.9Bm which is above the spin only value of 3.89 suggesting orbital contribution. As expected the value reduces slightly on reducing the temperature (μ_{80} = 4.58Bm.)

The mononuclear nature of the product is surprising since both manganese and iron can form binuclear complexes. However FAB analysis supported the mononuclear nature of the product with peaks at 747(57%) and 648(100%) corresponding to the mononuclear $[Co3PClO_4]^+$ and $[Co3P]^{2+}$ fragments. There was no evidence for binuclear species or of the starting barium complex.

Conductivity also supported the mononuclear formula showing a value of $274Scm^2mol^{-1}$ which is typical for a 1:2 electrolyte.

Fig. 93 IR OF A NICKEL COMPLEX OF 3P

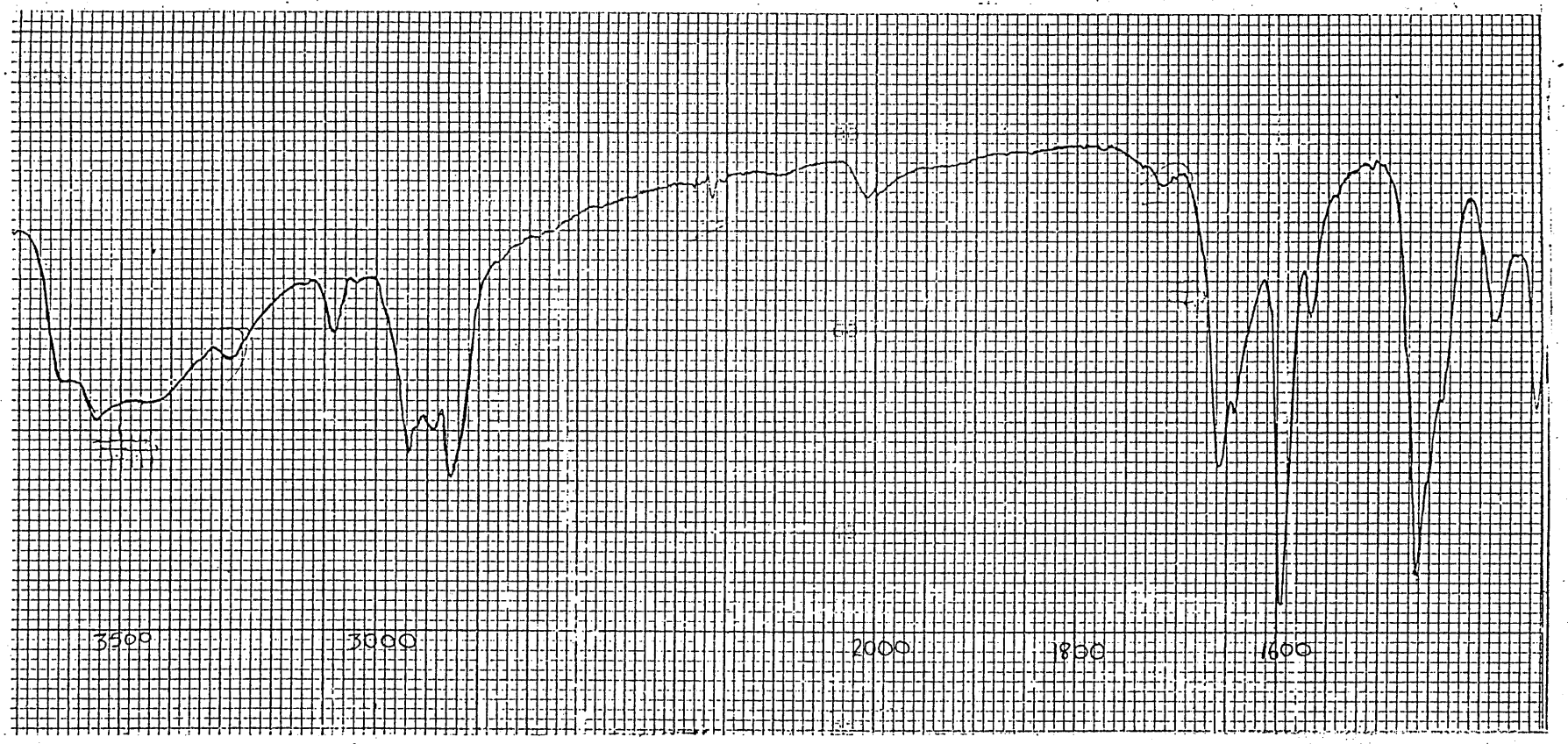

A green microcystalline product was obtained when $(Ba3P)^{2+}$, $Co(ClO_4)_2 6H_2O$ and NaNCS were stirred at room temperature. Although both ir and microanalysis supports the molecular formula $(Co_2 3P(OH)_2)$ $(Co(NCS)_4)$ $2H_2O$ there are several conflicting results.

Firstly from the ir the thiocyanate frequency for the cobalt tetrathiocyanate anion comes at $2048cm^{-1}$. However using $HgCo(NCS)_4$ as a reference compound for this counter ion, the thiocyanate signal was observed at $2095cm^{-1}$. Unfortunately no uv comparison could be made as both were insoluble in MeCN. This also prevented conductivity measurements being made.

Secondly although good fit is observed for the proposed molecular formula and the results of microanalysis, the F.A.B spectrum shows that there is reactant barium complex present with signals observed at 826(22%) and 727(50%). The base ion peak at 648 does however correspond to $[Co3P]^+$ and a peak at 706 (28%) could either be due to $[Co3PNCS]^+$ or $[Co_2 3P]^{2+}$.

Further attempts to prepare this compound have not been successful.

Nickel and $Ba3P(ClO_4)_2$

Two complexes were isolated in the various attempts at transmetallation using Ni(11) ions.

In the absence of the thiocyanate ion a yellowy green microcrystalline product was isolated from a room temperature stir of $Ni(ClO_4)_2$ $6H_2O$ and $Ba3P(ClO_4)_2$ in methanol.

The ir is interesting in several respects. Firstly the broad water region has a sharp feature superimposed on it at $3543cm^{-1}$ which was attributed to the presence of bridging hydroxide. Secondly the imine signal is split into two signals in a 1:2 intensity ratio FIG.93. This suggests that not all the imine functions are coordinating the metal centres. From a comparison of frequencies with the other 3P complexes the signal at $1655cm^{-1}$ is likely

80K

298K

ScN

10222 +DC

χ

80K RT

298

$2\chi_m$

χ

ClO4

13125

3837

to be that of the coordinating imines while the signal at 1640cm^{-1} is likely to be from the uncoordinating imines. The molecular formula $Ni_2$3P$(OH)_2(ClO_4)_2$ $2H_2O$ provided best fit for the microanalysis data. As in the previous complex FAB shows the presence of the reactant barium complex with 826 (13.6%) and 727 (9.1%) signals evident. Also present were signals at 746 (70%) and 647 (100%) which correspond to $[Ni3PClO_4]^+$ and $[Ni3P]^{++}$ respectively. Thus the FAB result gives no evidence for the binuclear bridged assembly suggested above. The magnetic moment of the complex also shows no evidence for a binuclear system showing μ_{293} = 3.1 reducing slightly to μ_{80} = 2.8. This result then also points to a mononuclear nickel complex.

Lack of solubility prevented solution uv (or conductivity) measurements but a mull spectrum shows 3 broad features centered at 920nm (10,800cm^{-1}) 580nm (17,200), 420nm (23,800cm^{-1}). This suggests an octahedral coordination geometry for the nickel.

A second nickel complex of 3P was also isolated and ir and microanalysis suggest the molecular formula $Ni_2$3P$(OH)(SCN)_3$ $2H_2O$. (The imine signal appears split as in the previous complex). Unfortunately solubility - or lack of it - meant that FAB solution uv or conductivity measurements were not possible. A uv mull spectrum again showed the 3 broad features at 970nm(10,300cm^{-1}), 610nm (16,400cm^{-1}) and 440nm (22,700cm^{-1}) which suggests an 'octahedral' geometry for the nickel centre.

Although the magnetic data suggests a binuclear complex, a room temperature moment of 3.1Bm per Ni(11) (reducing slightly with temperature μ_{80}=2.8Bm) suggests that interaction between the metal centres is small.

No transmetallation attempts with Cu(11) or Cu(1) ions were successful.

All in all the ligand 3P did not live up to our 'expectations' that this N_{11} donor would be a suitable transition metal host. Certainly from the results it would appear to be 'too successful' a Group II metal host. Indeed for the 'binuclear' complexes that appear to be mononuclear on a magnetic basis it may be that a heterobinuclear assembly of the Group II

template cation and a transition metal cation is being formed at least as an impurity. Further work is currently in progress.

THE INSERTION REACTIONS OF 3P

The startling lack of success with the transmetallation reactions prompted us to try insertion reactions. This approach appears to be more hopeful and so far two complexes have been isolated and characterized.

$Fe_2$3P(OH)$(ClO_4)_3$ $4H_2O$

The quality of product obtained from the insertion reaction of iron (11) is much superior to that from the transmetallation reaction. The yield was also significantly improved. However the 2 products are very different with the product of insertion appearing, on the basis of ir, microanalysis and F.A.B results, to form a single hydroxo bridged binuclear assembly.

The ir of the deep purple complex showed a sharp feature at 3419cm^{-1} emerging out of a broad peak and indeed best fit for the microanalysis data was achieved when 4 waters were included in the molecular formula $Fe_2$3P(OH)$(ClO_4)_3$$4H_2O$. The product was very insoluble and thus recrystallization was not posible. It also prevented solution uv or conductivity analysis. A weak FAB spectrum however gives some evidence for the proposed molecular formula giving peaks at 919 (14%) and 645 (21%) which correspond to [$Fe_2$3P$(ClO_4)_2$OH]$^+$ and [Fe3P]$^+$ respectively.

A magnetic study is currently in progress to establish the magnetic properties of the complex, but initial room temperature susceptibilty results (μ = 1.6Bm / Fe^{2+})suggest a singlet ground state for Fe^{2+}, with iron using 10 of the available 11 ligand donors together with μOH.

FIGURE 94 400MHz Hnmr SPECTRA OF $(Cu_2 3P)^{2+}$

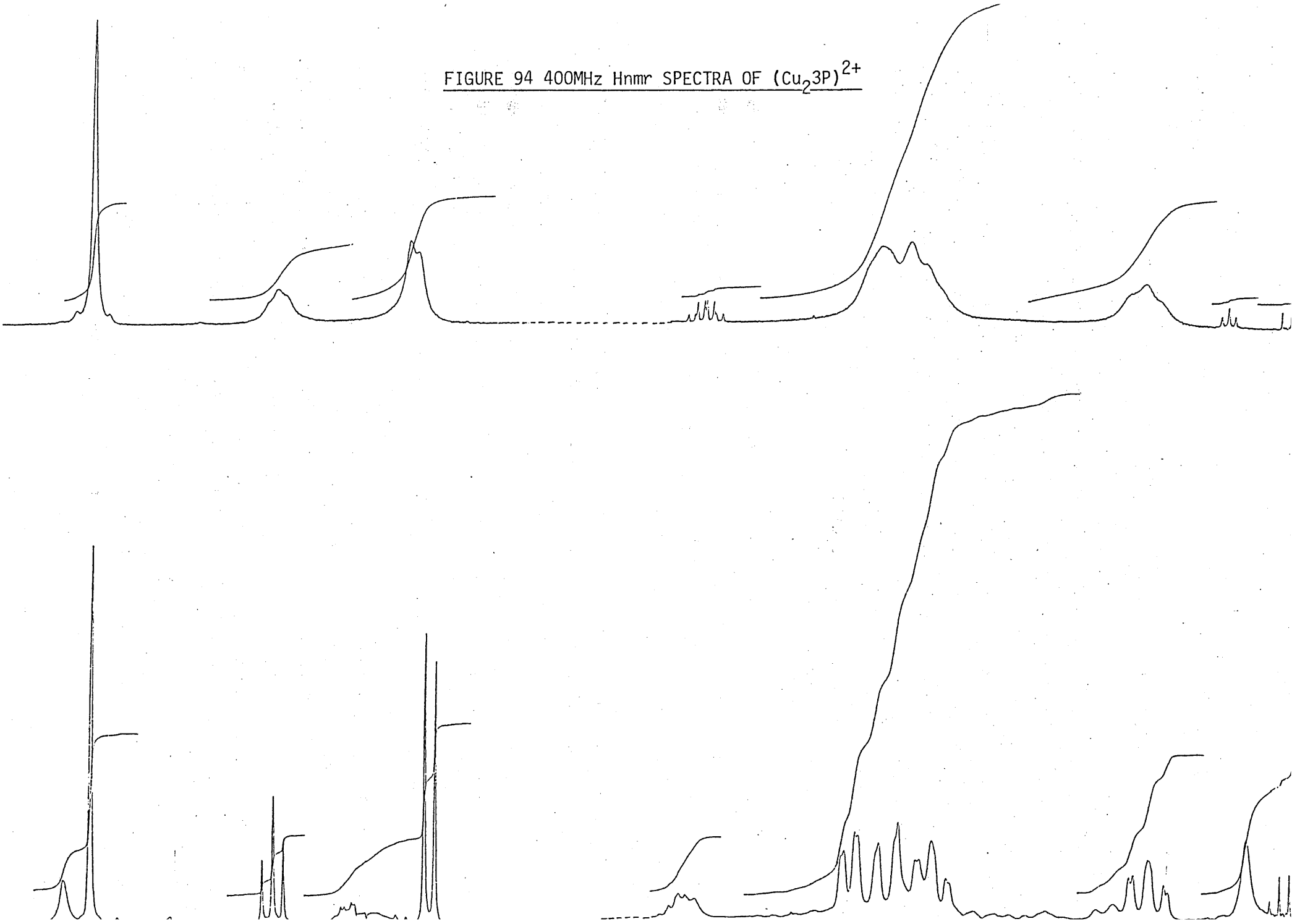

$Cu_2 3P(ClO_4)_2 \cdot 2H_2O$

Although attempts to insert copper(11) ions into 3P have been unsuccessful a black crystalline product has been obtained with Cu^I.

The ir of this product shows that the imine signal is unsplit suggesting that all the imine functions are coordinating the metal centres. The broad appearence of the water signal and the unsplit nature of the perchlorate signal makes it seem unlikely that these groups are coordinating the copper. A conductivity reading of $411 Scm^2 mol^{-1}$ for a $10^{-4}M$ solution lies at the low end of the range established for 1:2 electrolytes at this concentration.

The black colour of the product suggests a Cu^I to pyridine charge transfer absorption[53] and an absorption at 455nm ($\epsilon \simeq 5300$) is attributed to this. Two other absorptions at 280nm ($\epsilon \simeq 14400$) and 212 ($\epsilon \simeq 52000$ "unreliable") are both attributed to $\pi\pi^*$ transitions.

The data for the 'Hnmr is tabulated in FIG.87 while the room temperature and 233K spectra are shown in FIG.94-1 and FIG.94-2 respectively.

The room temperature spectrum shows only one relatively sharp signal ie the imine signal, H_D, at 8.52ppm. The H_A and H_B signals appear as broad features but on the basis of the 1:2 integral ratio the higher field signal at 7.8ppm can be assigned to H_B while the lower field signal at 8.14ppm can be assigned to the H_A proton. The broad nature of these 2 signals indicates a fluxional process very similar in rate to that of the nmr time scale. The methylene signals are broad and from the integral it is clear that the H_F signal has split into its axial and equatorial signal with the lower field component having been incorporated into the unresolved H_E signal. Thus once again the higher field signal (ie the protons α to the bridgehead nitrogen) are significantly more split and thus have a higher Tc than the protons α to the imine nitrogen.

The low temperature spectrum shows well resolved aromatic triplet and doublet features with $J_{AB} = J_{BA} = 7.8Hz$. As in 3P and its templated

complexes H_A appears downfield from the expected aromatic resonance position and again is attributed to the further activation of the para position on complexation as has already been discussed.

The methylene signals although better resolved are quite complicated. The high field triplet is assigned to F_{ax} and from this we obtain J_{gem} = 12.97Hz and $J_{ax-eq'}$ = 2.05Hz. The small difference in J_{gem} and J_{ax-ax} accounts for the broad nature of the middle component of the triplet.

The integral of the low field multiplet shows that the H_F equatorial doublet is incorporated in the multiplet. The multiplet appears to be composed of 2 doublets and a relatively high field axial triplet which suggests, the previously unseen arrangement d(eq), d(eq), t(ax), t(ax). From the various components we obtain:-

Lowfield doublet: Jgem = 9.176, Jeq-ax' = 2.27Hz

Highfield doublet: Jgem = 14.16Hz

Lowfield triplet: Jgem = 10.58Hz, Jaxax = 10.54Hz, Jax-eq' = 2.51Hz

Highfield triplet: Jgem = 12.97Hz, Jaxax = 13.37Hz, Jax-eq' = 2.05Hz

Thus it appears that the arrangement of signals is Eeq, Feq, Eax, Fax. The Hax C Heq angles are different for the 2 methylene groups because:-

$J_{Eeq-Fax} \neq J_{Fax-Eeq}$

The arrangement of the signals implies that both equatorial protons are deshielded relative to the 2 axial protons and that Feq is significantly deshielded relative to its axial counterpart.

The low temperature spectrum provides strong evidence for the presence of additional conformers. The lowfield feature at the imine signal suggests the presence of a conformer (in reasonable proportions) and it may be that the multiplet at 3.5ppm is also due to additional conformers. Certainly

FIGURE 95 - LIGAND R3P

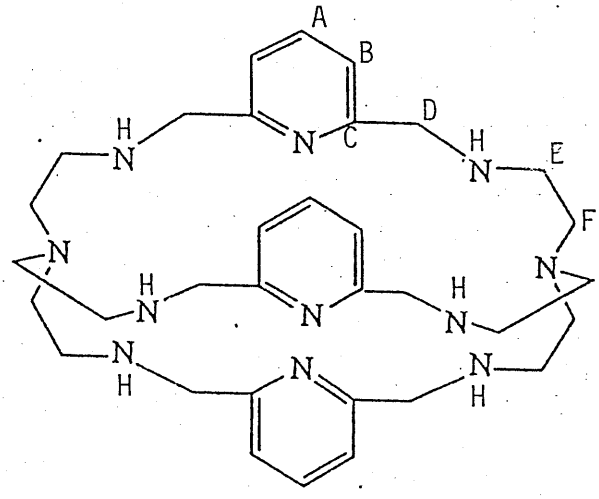

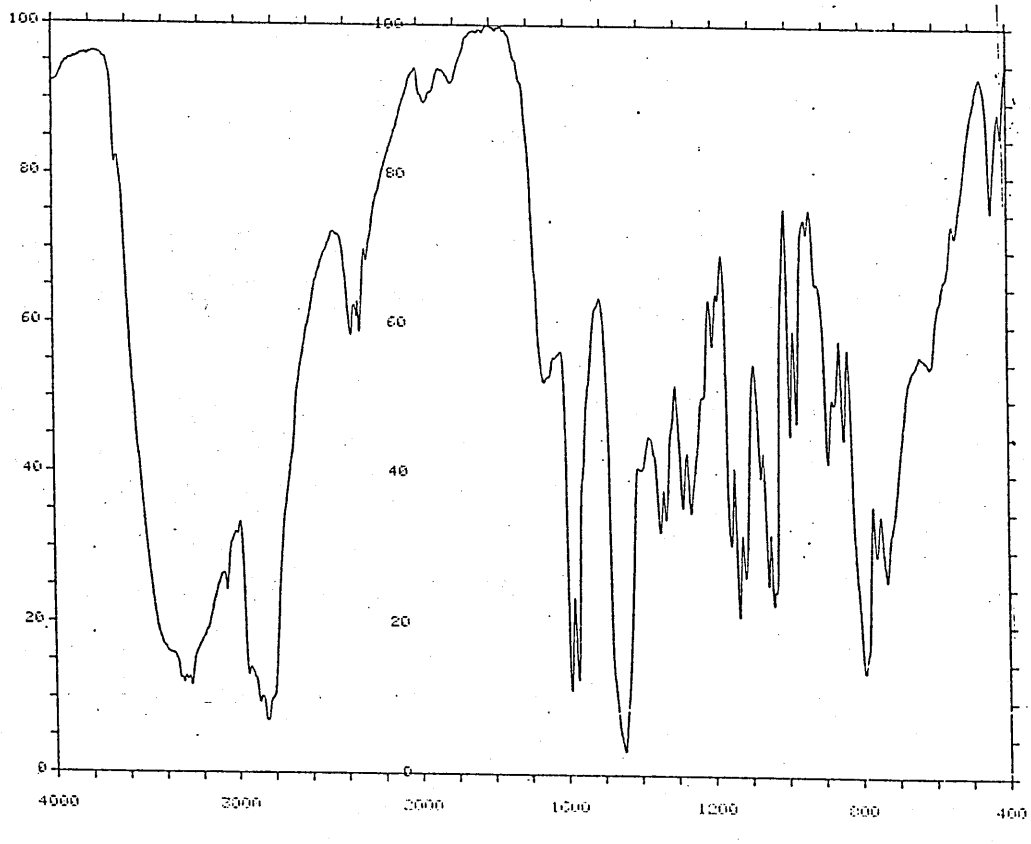

the high field triplet has two relatively strong features associating with it that suggests additional conformer.

R3P

As with the other ligands in this series 3P was successfully reduced. Physical data for the octaamine derivative is given in FIG 87.

I.R, microanalysis and mass spec were used to determine that reduction had been successful. The ir FIG.95 showed the normal features for such a reduced ligand ie signals at 3327, 3280cm^{-1} (NH) and the absence of signals at ≈1640cm^{-1} indicated that the imine functions had been hydrogenated. Mass spec gave a strong signal at 601 (69%) which corresponds to 3P + $12H^{+}$- ie the octaamine derivative of 3P. The uv spectrum of R3P is very similar to 3P except that there is a significant decrease in intensity of the absorption peaks resulting from loss of conjugation ie

	λ	ε	λ	ε
3P	311	(151,000)	254	(25,600)
R3P	210	(46,200)	264	(16,000)

Although the high energy signals are lying close to solvent/cell cut off points the relative magnitude of the extinction coefficients are probably real enough.

The room temperature 'Hnmr spectrum of R3P is as expected showing the new CH_2 signal (ie derived from the reduced imine function) at 3.9ppm and a broad NH signal at 1.4ppm. It is interesting to note that H_A is now at relatively normal aromatic resonance ie at 7.52ppm with H_B at 7.08ppm. This is the reverse situation to 3F -> R3F where it was only in the reduced form of the ligand that the effect of the oxygen heteroatom was effective in shielding the aromatic protons.

FIG. 96

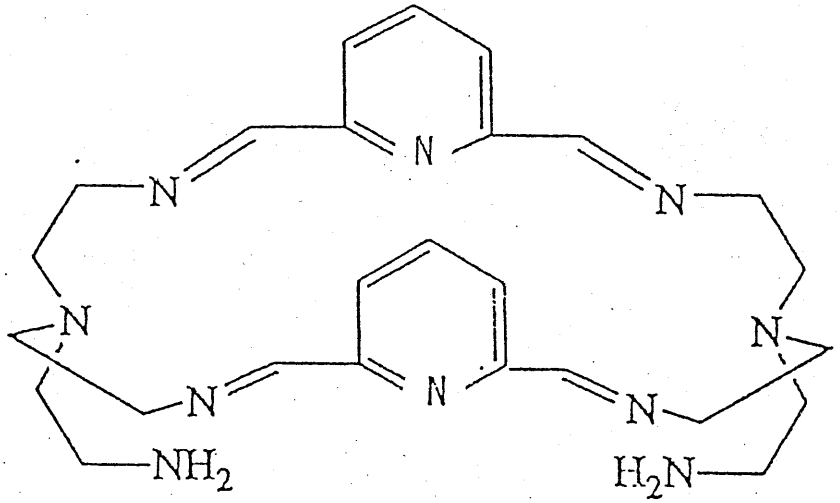

LIGAND 2P.

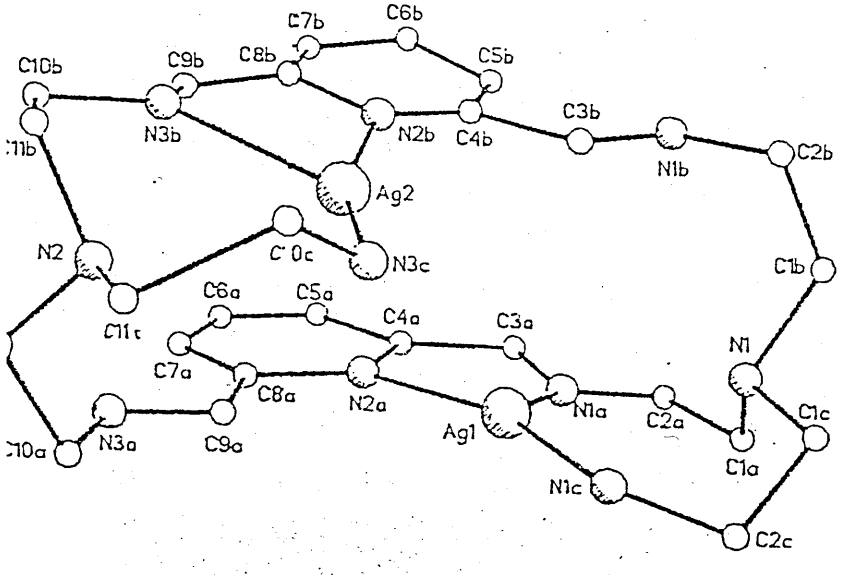

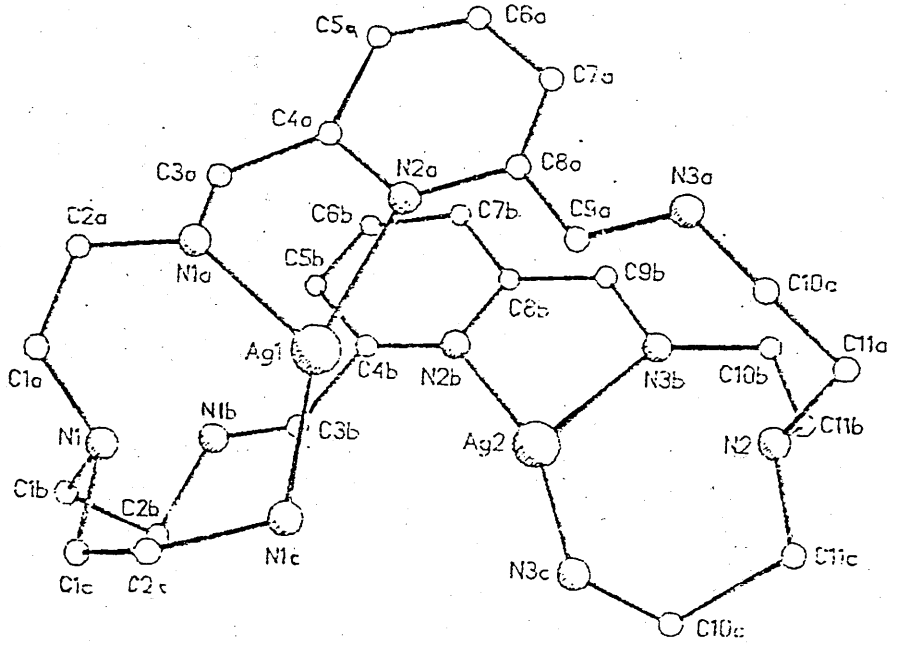

As yet this ligand has not been investigated with respect to its complexation properties.

2P AND $2P_{CH_3}$

The ligand 2P FIG 96-1 was obtained whilst trying to prepare $Ag_2 3P (CF_3SO_3)_2$ by template methods (the hexafluro phosphate derivative has been reported by Lehn[60]). On slow evaporation of a beaker containing $AgNO_3$, tren, DFP and excess triflate ions in MeOH/MeCN yellow crystals of X-rayable size were obtained (no solid product was obtained when excess hexaflurophosphate ions were used!). Physical data for this complex is given in FIG.97. The ir of these crystals - shown in FIG.98 - is interesting in several respects. Firstly the appearence of 2 bands at 3318 and 3275cm^{-1} and no signal in the carbonyl region suggested that a pendant arm product with free amine groups had been isolated. Secondly the ir shows a significant splitting of the imine peak (1655, 1644cm^{-1}) although there is no splitting ofthe pyridine signal at 1589cm^{-1}.

The crystals were sent to V. McKee for X-ray structural analysis. The slightly cloudy nature of the crystals resulted in a poor data set (not communicated) which could not be refined past R = 0.15. However Dr.McKee did manage to obtain two different views of the cations which are shown in FIG 96. These show that each silver is tricoordinate taking one pyridine nitrogen, 1 imine nitrogen and one of the pendant arm NH_2 groups ie $N3_c$ or $N1_c$. This structure explains both the splitting of the imine signal and the appearance of the NH_2 signal in the ir. It also explains why the pyridine signal is unsplit with both pyridine nitrogens being coordinated. We can also observe that the two free amine groups are well disposed to undergo a Schiff base condensation with a dicarbonyl of suitable dimensions. This may offer the chance of introducing a different aromatic moiety into the system eg DFT, DFF etc which may lead to a ligand suitable for the synthesis of heterobinuclear assemblies.

Despite concentrated effort, once I purposely set out to prepare 2P, I found I could not. Our hopes for 2P were left in the air - well that was

FIGURE 97. PHYSICAL DATA FOR THE PENDANT ARMED SPECIES

Complex	F.A.B.[a]	Elemental Analysis[b]	INFRARED SPECTRUM		
			NH_2	C=N	Counter Ion
$Ag_2 2P(CF_3SO_3)_2.MeCN$	855 (100) $[Ag_2 2PCF_3SO_3]^+$	C 34.5 (34.7)	3318	1655	1271
	597 (97) $[Ag2P]^+$	C 4.0 (4.1)	3275	1644	1163
		N 14.7 (14.4)			1029
$Ag_2 2P_{CH_3}(PF_6)_2.MeCN$	907 (16) $[Ag_2 2P_{CH_3} PF_6]^+$	C 34.3 (34.4)	3390	1641	840
	762 (34) $[Ag_2 2P_{CH_3}]^+$	H 4.4 (4.4)	3330	1606	
	653 (100) $[Ag2P_{CH_3}]^+$	N 14.4 (13.4)			
$Ag_2 2P_{CH_3}(CF_3SO_3)_2$	911 (24) $[Ag2P_{CH_3} CF_3SO_3]^+$	C 36.1 (35.6)	3365	1644	1284
	762 (39) $[Ag_2 2P_{CH_3}]^+$	H 4.4 (4.5)	3298	1610	1172
	653 (100) $[Ag2P_{CH_3}]^+$	N 13.2 (13.4			1028
$Ba2P_{CH_3}(ClO_4)_2$	782 (100) $[Ba2P_{CH_3} ClO_4]^+$	C 40.8 (40.8)	3360	1625[c]	1080
	681 (54) $[Ba2P_{CH_3}]^+$	H 5.3 (5.3)	3236		626

(a) % base ion peak in brackets.

(b) Experimentally determined result in brackets.

(c) Not 2 distinct peaks but signal is shouldered.

FIG. 98

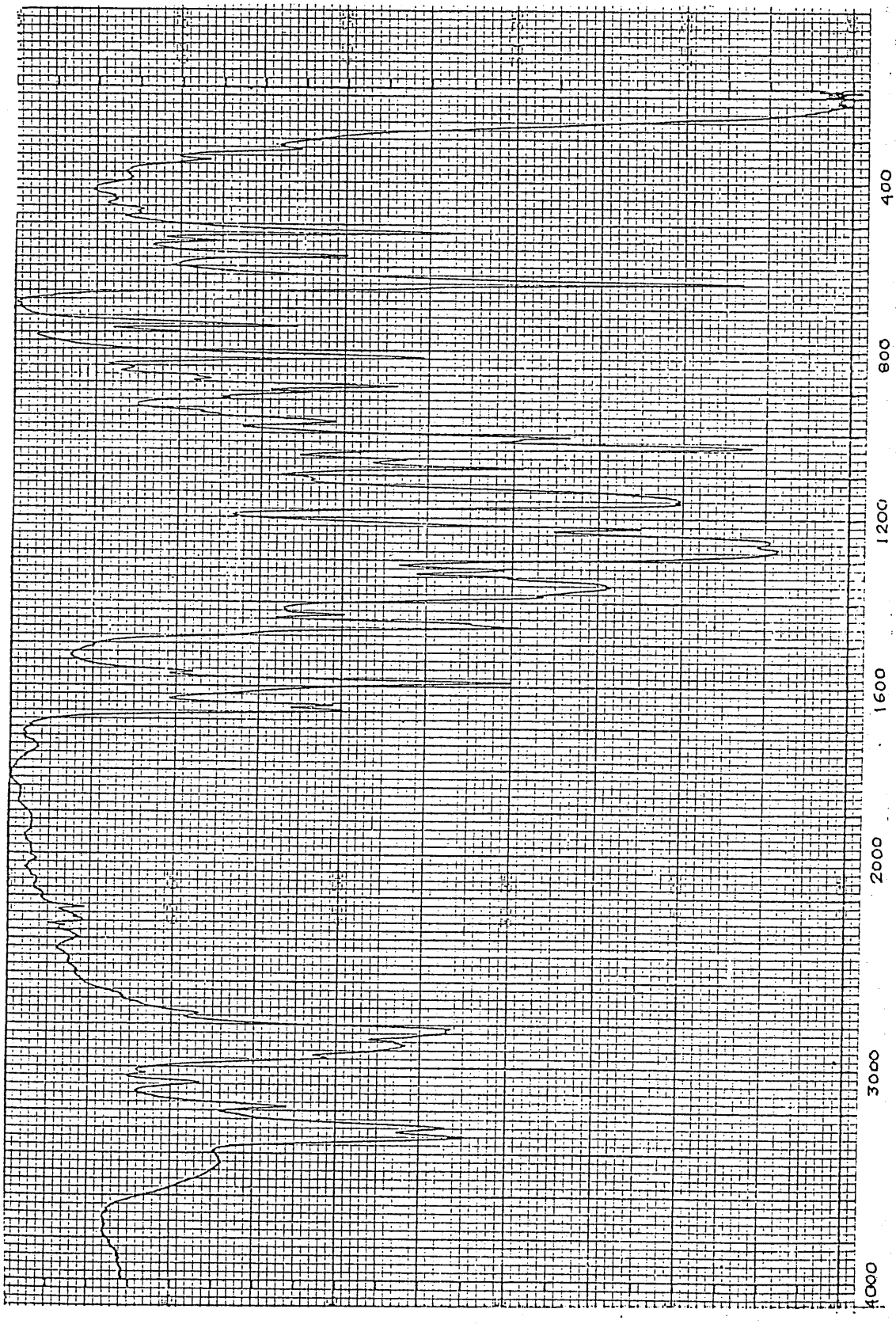

until I started writing up the work. So desperate was I to find something positive to write about this ligand I battled with microanalysis forms. Hey presto! - another experiment that was essentially a mistake has given the pendant arm species. The mistake - I had used diacetyl pyridine (DAP) instead of DFP, and in each of the 3 cases where I had done this, a pendant armed species was obtained. The physical data (as it stands ie ir, microanalysis and FAB) is given in FIG 97.

Thus it would appear that the condensation reaction of tren and DAP is going to, in a reproducible manner, provide pendant armed species, potentially suitable for further condensation.

FIGURE 99. PHYSICAL DATA FOR THE LIGAND 3S

COMPLEX	MASS SPEC[a] OR F.A.B.	Ω^{b} S cm^2 mol^{-1}	ELEMENTAL ANALYSIS[c]	INFRARED SPECTRUM			ELECTRONIC SPECTRUM		
				NH_2	C=N	COUNTER ION	SOLVENT	λ(nm)	ε(M^{-1} cm^{-1})
$Ag_2$3S$(CF_3SO_3)_2$	969 (67) 711 (100)	259	C 34.3 (34.2) H 3.2 (3.3) N 10.1 (10.4)		1635	1262 1153 1028	MeCN	302[d] 270 215[e]	41400 25000 36500[e]
$Cu_2$3S$(ClO_4)_2$	668 (39) 731 (39) 743 (90) 701 (100)	283			1627 1610	1030 622	MeCN	383 280[d]	2600 34100
R3S	617 (100)		C 58.40 (58.15) H 7.84 (7.36) N 18.16 (18.47)	3336					
Cu_2R3S$(OH)_2(ClO_4)_2$.$2H_2O$	968 (42) 869 (64) 768 (100)		C 35.28 (35.57) H 4.2 (5.3) N 11.69 (11.10)	3282		OH at 3574, 1115, 622			

(a) % of base ion peaks in brackets.

(b) 10^{-4} M.

(c) Experimentally determined results in brackets.

(d) λ_{max}.

(e) Unreliable result.

Ligand 3S.

An investigation into the complexing and conformational properties of this ligand are only just underway. Already some interesting results have been observed.

Despite 6 weeks effort the ligand 3S could not be formed in the absence of the silver template ion . The reactant dialdehyde shows an 80:20 ratio of cis cis, cis trans, isomers with little or no trans trans conformer present. Thus it appears that for this particular series of macrobicycles (ie 3Bm,3Bp,3F,3P and 3S) it is the trans trans conformer that is required for cyclization. Certainly for 3F and 3P where the trans trans form of the starting dialdehyde is available we can achieve metal free synthesis, and the X-rayed structure of 3F shows this trans,trans arrangement in the solid phase. This arrangement is also seen in the X-rayed structures of uncomplexed 3Bp and 3Bm (however no data on the initial conformer ratio's was found and thus it is not known if the trans trans conformer is important in these reactant dialdehydes- although from the preceeding discussion it is presumed that this is the case.)

For the templated complexes the cis cis arrangement of carbimine functions relative to the aromatic ring is observed (eg. $Ag_2$3Bp$(CF_3SO_3)_2$ and $Ag_2$3S$(CF_3SO_3)_2$ to be discussed). It would therefore appear that due to the absence of the trans,trans conformer, a metal free synthesis of ligand 3S is not possible.

$Ag_2$3S$(CF_3SO_3)_2$

The disilver complex of 3S has been isolated both as the perchlorate and the triflate. The preparation of the perchlorate derivative is very sensitive to temperature and light - early reactions suffered from photo- and/or thermal decomposition, giving a silver mirror on the side of the reaction flask. However by carrying the reaction out at temperatures below 30°C and in a blacked out reaction vessel and evaporation vessel a yellow crystalline sample of $Ag_2$3S$(ClO_4)_2$ was isolated. The triflate form of the disilver complex, although sensitive to temperature (reaction temperature

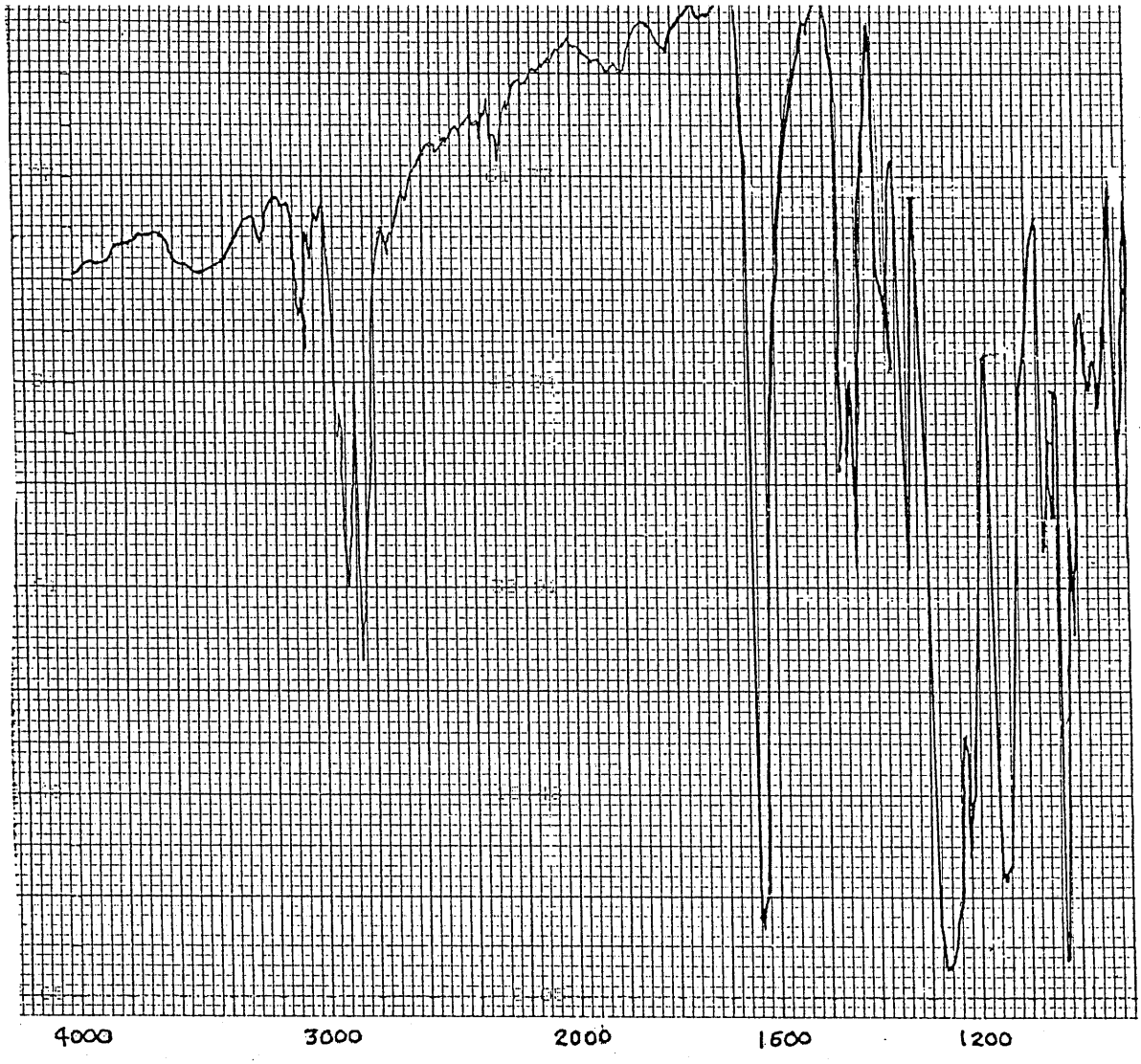

FIG. 100-1

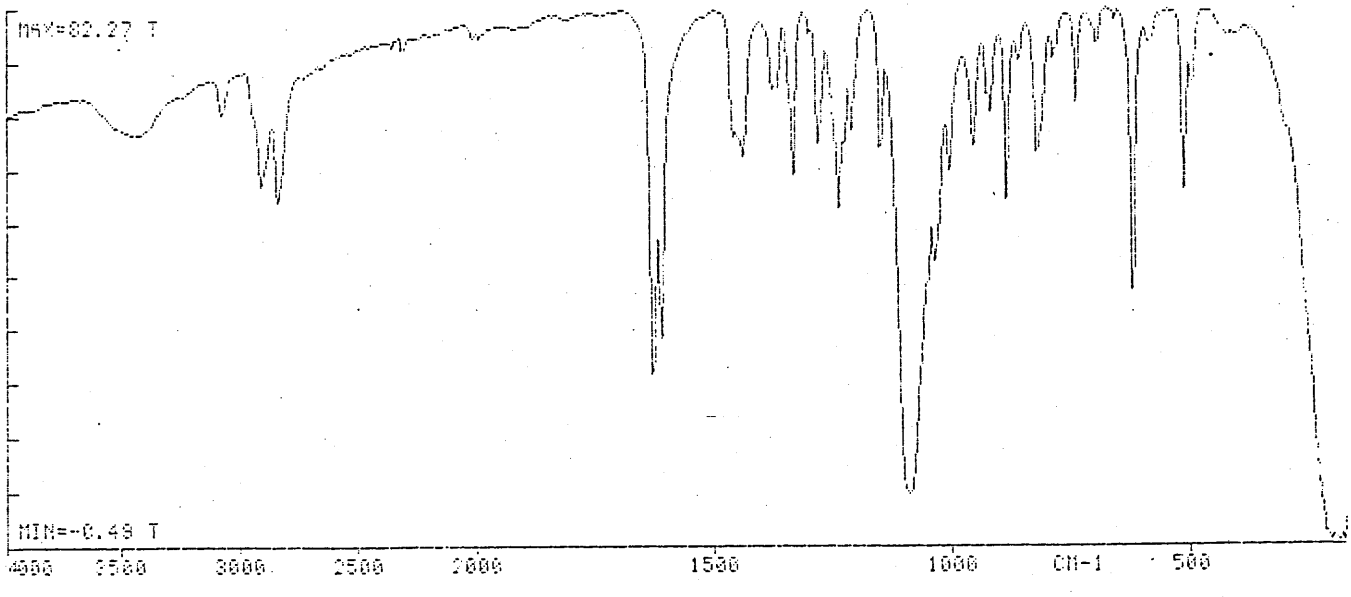

FIG. 100-2

(40°C) was not as sensitive to light and so it was only at the slow solvent evaporation stage was the precautionary measure of blacking out the beaker taken. The crystals of $Ag_2 3S(CF_3SO_3)_2$ so obtained in 81% yield were of X-rayable size.

The physical data for the complexes of 3S so far obtained are tabulated in Fig.99. (this is unavoidably incomplete.) The ir of the disilver complex is shown in Fig 100-1 and it is seen that there is no evidence for water or solvent being present-this was confirmed by microanalysis which supports the molecular formula $Ag_2 3S(CF_3SO_3)_2$. FAB results also strongly support this with signals at 969 (67%) and 711 (100%) corresponding to $[Ag_2 3S(CF_3SO_3]^+$ and $[Ag3F]^{2+}$ respectively. Conductivity measurements gave a value corresponding to a 2:1 electrolyte.
The uv spectrum of this complex shows 3 strong absorptions at 302 (42,000) 270 (25,000) and 215 (36,000) and all are attributed to $\pi\ \pi^*$ transitions.

The 500 MHz spectrum at 294k Fig 101-1 and 233k Fig 101-2 show interesting differences. The data is tabulated in Fig 101-3. As in the disilver cryptate of 3F, but unlike the silver complexes of 3Bm and 3Bp the imine signal is split into a doublet at room temperature. This splitting is resolved even in the 250MHz spectra. As in the other complexes we attribute this splitting to a coupling of the imine hydrogen with the silver ion, with J_{H_C-Ag}=8.1Hz. As in $[Ag_2 3F]^{2+}$ the aromatic signal appears as a sharp singlet at δ7.64

The methylene signals show very different behaviour with H_D. just resolved into its axial and equatorial components-these appear as 2 broad humps at 3.45ppm and 3.80ppm. H_E on the other hand, appears as a slightly broadened singlet, on its way to coalescence at 2.89ppm. By comparing this spectrum to the room temperature spectrum of $[Ag_2 3F]^{2+}$ or $[Ag_2 3Bm]^{2+}$ we see that it is usually the higher field methylene signal that shows the higher Tc value, and thus the greater splitting. Indeed if we look at the spectra of uncomplexed 3Bp and 3F we see that this situation is reversed with the lower field signal showing greater splitting. Thus the conformation of this complexed 3S may be quite different from the complexed forms of the other ligands in the series.

FIG. 101

500 MH_Z SPECTRUM

OF $(Ag_2\ 35)^{2+}$

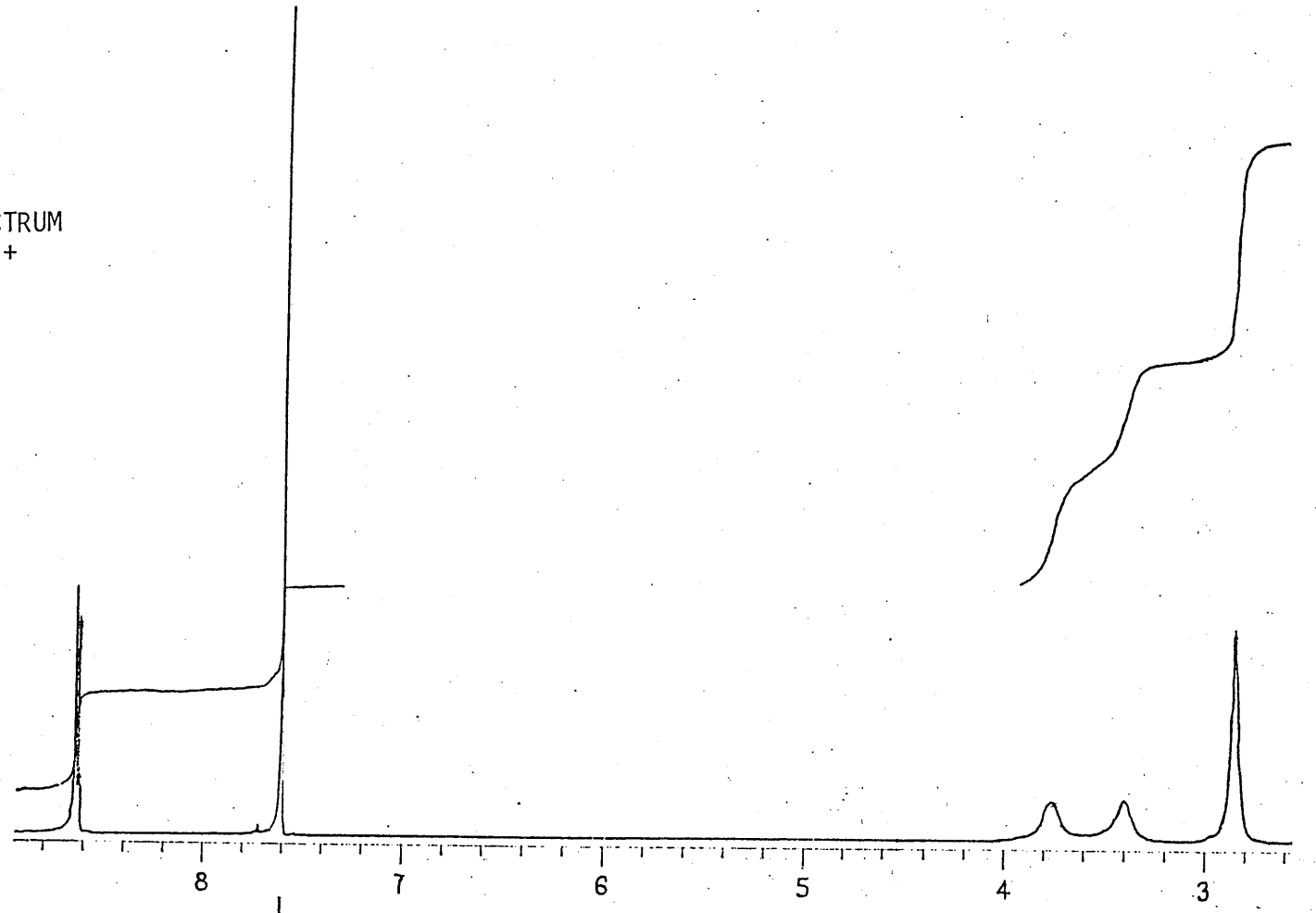

FIG. 101-1

294k

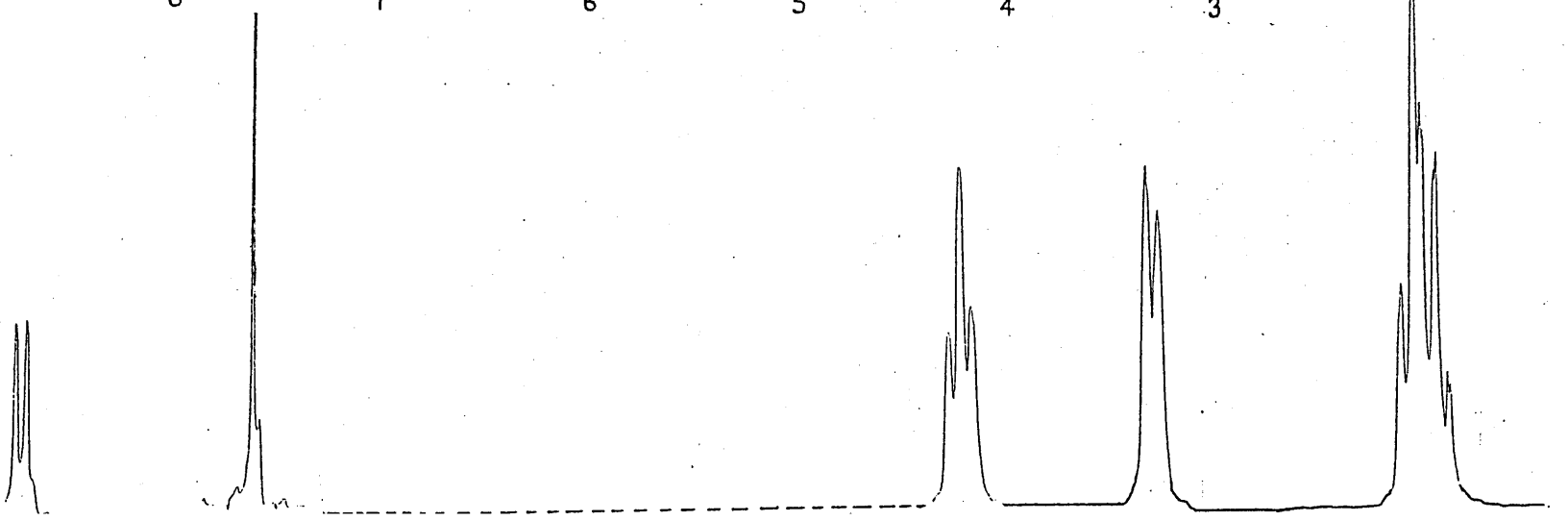

101-2

233k

FIGURE 101-3. NMR[a] DATA FOR THE COMPLEXES OF 3S

COMPLEX	SOLVENT	TEMPERATURE	SPECTRUM	PROTON SITE			
				A	C	D	E
$Ag_2$3S$(CF_3SO_3)_2$	CD_3CN	294 K	^1H 400 MHz	7.6 (s)	8.6 (d)	3.79 (br,s) 3.45 (br,s)	2.9 (d)
$Ag_2$3S$(CF_3SO_3)_2$	CD_3CN	233 K	^1H 400 MHz	7.6 (s)	8.6 (d)	3.7 (t) 3.3 (d)	2.8 (m)
$Ag_2$3S$(CF_3SO_3)_2$	CD_3CN	233 K	^1H NOE 400 MHz	10.5[c]	b	Deq. 10.5[c]	
$Cu_2$3S$(ClO_4)_2$	CD_3CN	294 K	^1H 400 MHz	7.6 (m)	8.6 (m)	3.7-3.5 (m)	3.0 (m) 2.8 (m)
$Cu_2$3S$(ClO_4)_2$	CD_3CN	233 K	^1H 400 MHz	7.6 (m)	8.6 (m)	3.7-3.5 (m)	3.0 (m) 2.8 (m)
$Cu_2$3S$(ClO_4)_2$	CD_3CN	233 K	^1H NOE 400 MHz	6[c]	b	Deq 6[c]	

(a) ppm from T.M.S. (s) singlet, (d) doublet, (t) triplet, (m) multiplet, (br) broad.

(b) Irradiation into this signal.

(c) % NOE enhancement.

The 233k spectrum sees no change in the imine or aromatic signals, however there has been a significant change in the appearence of the methylene signals. Again the feint traces of baseline shoulders implies the presence of other conformations of this complex in solution and this is under investigation. H_D is now resolved into triplet and doublet features, however complete analysis at this temperature was not achieved because the apparent values of J_{gem} coupling constants from the doublet (J_{gem} = 10.49) and the triplet (J_{gem} = 11.55) are not consistent.

H_E although better resolved than at room temperature has not split into distinct axial and equatorial signals. This implies that the H_E protons are chemically and magnetically very similar.

The behaviour of the signals may be explained by considering Fig 102. The protons numbered 44 and 43 represent the H_E. protons. The axial and equatorial protons are symmetrically placed with respect to the bridgehead nitrogen and will therefore both experience an equal shielding effect of the lone pair of the bridgehead nitrogen atom. They should therefore have very similar chemical and magnetic environments resulting in the observed, very similar chemical shift. Protons H_{45} and H_{46} are the 2 H_D protons. Proton 45 is much more likely to experience a shielding effect from the imine's magnetic anisotropic field than H_{44} and thus the 2 will have different magnetic environments and so different chemical shift values (as observed). H_{45} is assumed to be the equatorial proton as the doublet signal appears at higher fields than the relatively deshielded axial triplet.
That this is the case was confirmed by a low temperature noe experiment. By irradiating into H_E the imine signal, enhancements at H_A(10.5%) and D_{eq} (10.5%) were observed.This is a very large enhancement of the methylene proton compared to the other systems where enhancements of 1-4% have been noted for these protons. This suggests a closer approach of H_E and D_{eq} in this complex.

That the imine is split even at room temperature as in $[Ag_2 3F]^{2+}$ implies that the silver ions are held within the cavity rather than undergoing fast exchange as in the disilver cryptates of 3Bm and 3Bp. This necessarily implies a greater stability for $[Ag_2 3S]^{2+}$ than $[Ag_2 3Bm]^{2+}$ or $[Ag_2 3Bp]^{2+}$

FIGURE 102

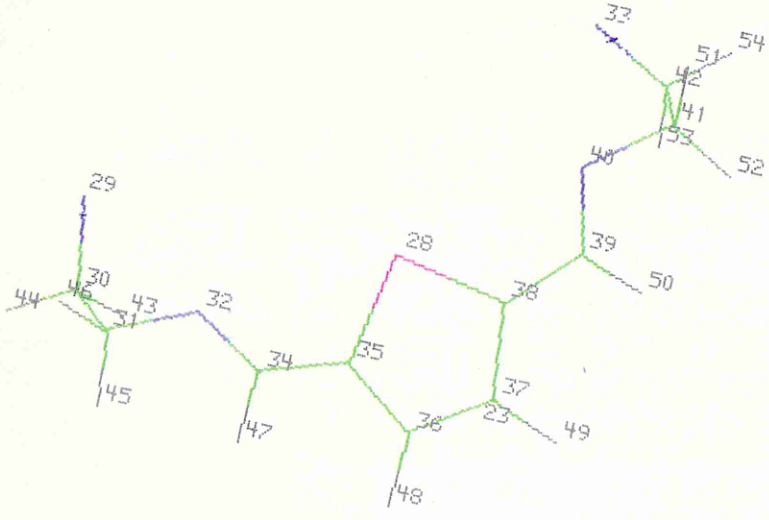

COMPLEXED

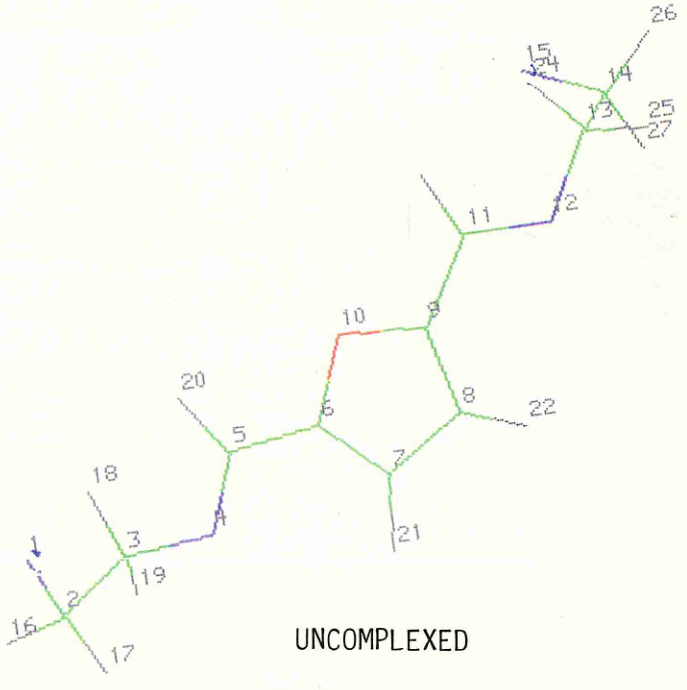

UNCOMPLEXED

This is not surprising given the enthalpic donor atom preference of silver for S > NH > O >C [69]

Parker [69] in studies towards a kinetically inert silver (1) complex for use in vivo (ie. stable with respect to acid or metal-catalysed dissociation) has been looking at the [18]-N_4S_2 system shown in Fig 103.
The mononuclear complex shows a crystallographically imposed symmetry with the silver cation lying on the symmetry axis. The silver ion is hexacoordinate, with the N_4S_2 donor atoms in a distorted octahedral geometry. He found that donors in the ring give rise to favourable enthalpies of complexation which is offset by unfavourable entropy changes associated with the tendacy of the sulphur lone pairs in the ligand to adopt exodentate conformations which therefore require unfavourable conformational reordering prior to metal ion complexation. The protonated silver complexes have good stabilities compared to the parent complex because loss of one nitrogen binding site does not greatly impare silver complexation. Such a situation may be contrasted with the more dramatic loss of binding that occurs on protonation of silver complexes of polyaza cryptands[70].

THE X-RAY STRUCTURE OF $Ag_2(CF_3SO_3)_2$ 3S

The structure of the disilver complex of 3S (determined by M.Drew) is shown in FIG 104.

The silver....silver distance is 4.65Å. The structure shows there to be 4 strong Ag-N bonds and 3 weak Ag-S bonds. Unfortunately the bond distances were unavailable at the time of writing. However it will be interesting to compare them with the 2 short (2.665Å) and 4 longer (2.781Å) silver-sulphur bonds of the silver complex in FIG 103.

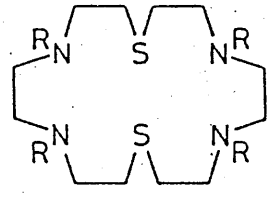

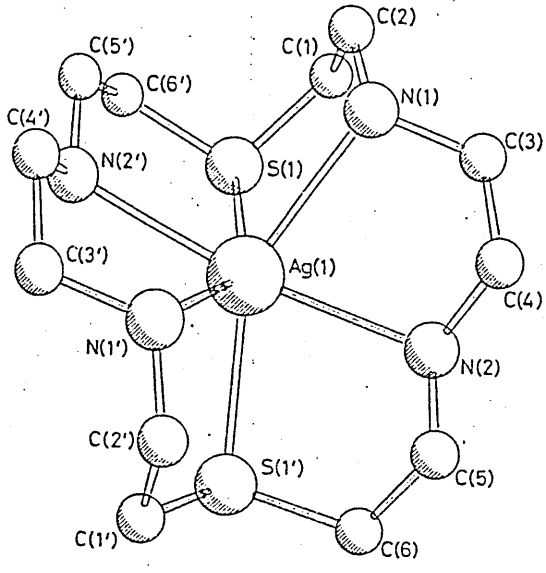

FIG. 103

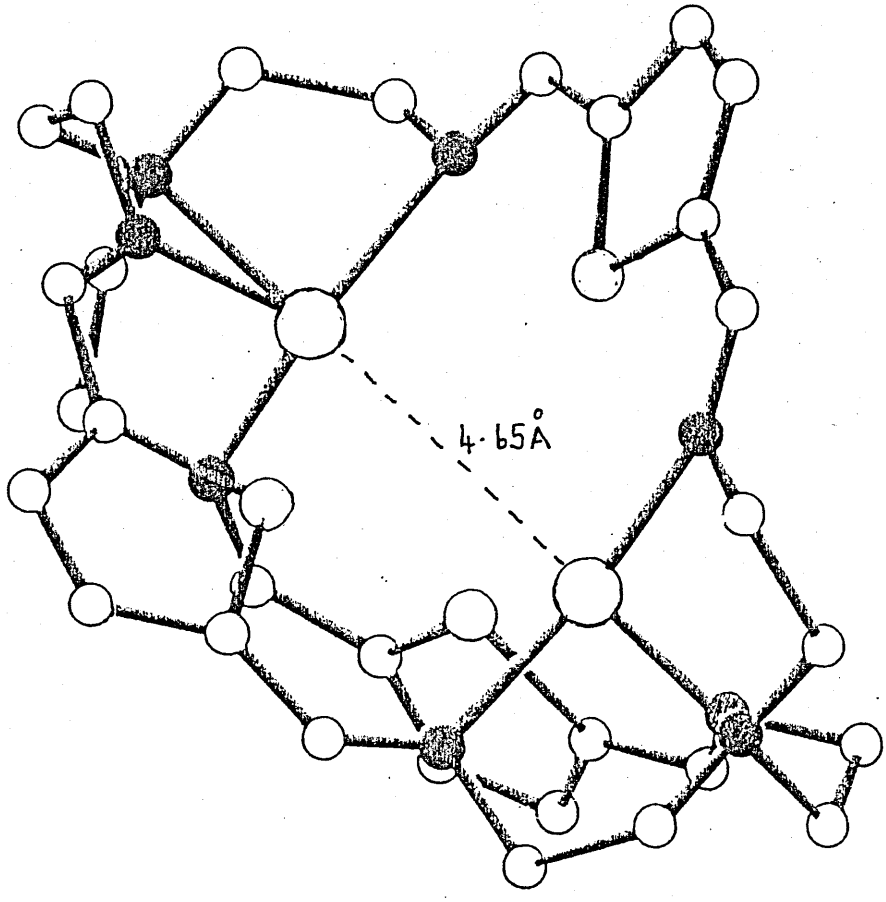

FIGURE 104

● N

○ Ag

$Ag - N$ ~ 2·34Å

$Ag - N_b$ ~ 2·52Å

$Ag - S$ ~ 3·25Å

$Ag \ldots Ag$ 4·65Å

Porter.
2·665Å Ag–S
2·781 Ag–S

TRANSMETALLATION OF $Ag_2$3S$(CF_3SO_3)_2$

As yet only transmetallations involving Cu(1) and Cu(11) have been attempted. However both reactions give the same product- a bright orange microcrystalline product. Thus when copper (11) perchlorate is warmed with $Ag_2$3S$(CF_3SO_3)_2$ in MeCN it is the orange product that crystallizes out of a green solution.

The ir of the complex is shown in Fig.100-2 and it shows a significant difference to that of the silver complex of 3S. The imine signal is clearly split (1627, 1610cm)$^{-1}$ which suggests that not all the imine functions are coordinated. The perchlorate signals at 1030 and 622cm^{-1} are unsplit and thus the anions are not coordinated. Results of microanalysis are not yet available but a possible molecular formula on the basis of the ir is $Cu_2$3S$(ClO_4)_2$ with perhaps 1 or 2 waters) The electronic absorption spectrum shows only one $\pi\pi^*$ transition at 280nm. However there is also evidence of a MLCT band at 383nm(2600). FAB analysis certainly gives evidence for the binuclear copper complex giving peaks at 668 and 731 (both 39% of base ion peak) corresponding to [Cu3S] and [$Cu_2$3S] respectively. However a strong peak at 743 (90%) corresponds to [Cu3S +12$^+$ ie Cu_2R3S]. I was unable to assign other main peaks at 614(95%), 701 (100%) and 915(40%). (They cannot be attributed to starting [$Ag_2$3S] Conductivity results are in the range of a 1.2 electrolyte.

A 400MHz 'Hnmr of the orange [$Cu_2$3S]$^{2+}$, complex has been run at room temperature and at 233k Fig 105. Both are very similar and very complicated!. Data is tabulated in Fig. 101-3.

Both the imine and aromatic signals are very complicated. The imine appears to have 2 major components- a lower field quartet and a higher field singlet. This may well represent two conformers being present- one in which the ligand is uncomplexed (the singlet) and one which the ligand is complexed. Indeed the quartet component of the multiplet may be the ^{64}Cu(I=3/2))-H_c coupling being resolved.

The ir shows that the imine signal is split and it may be that the signal in the nmr is merely reflecting the presence of coordinated and uncoordinated imine functions within the individual molecules rather than

FIG. 105. 233k SPECTRUM OF $(Cu_2\ 3S)^{2+}$

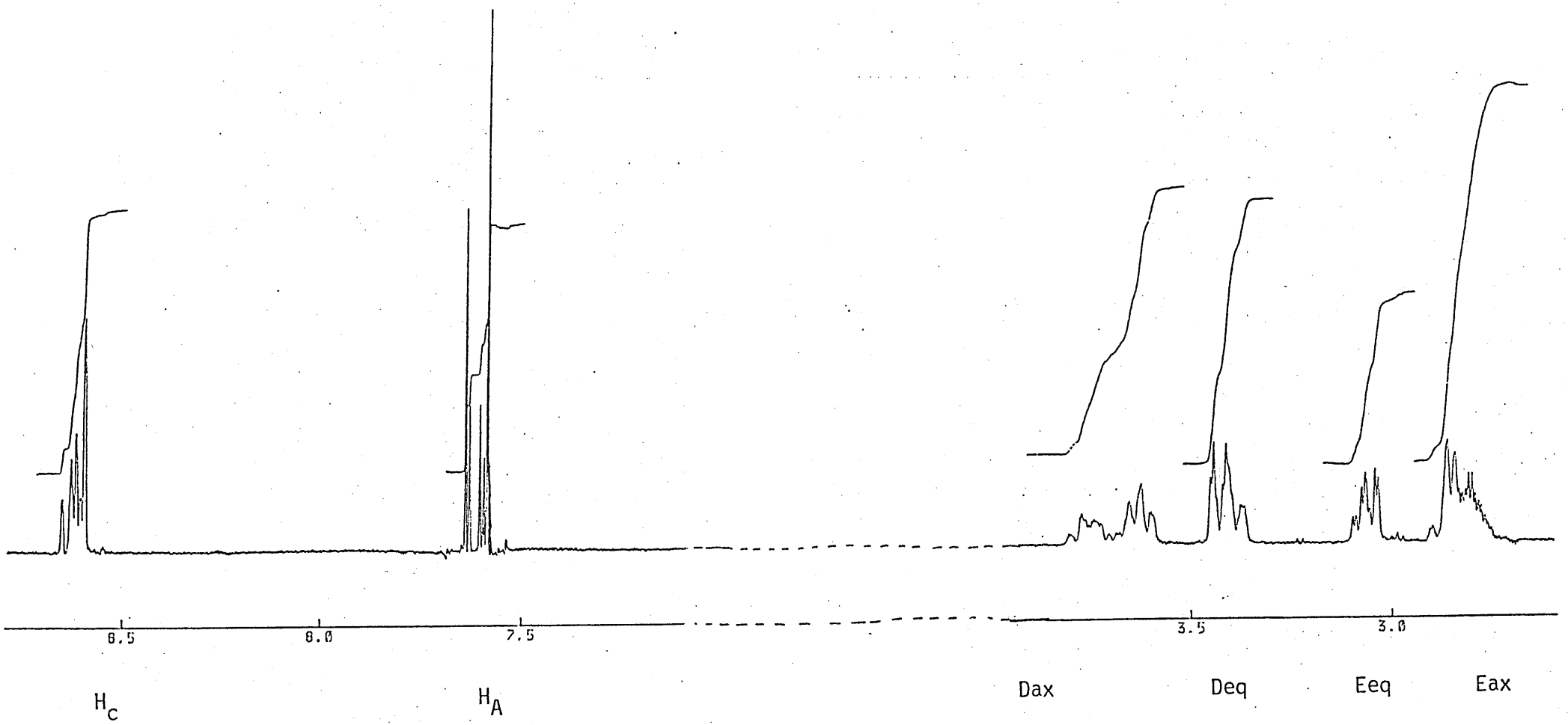

the presence of complexed and uncomplexed macrocycles. Of course the signal may be reflecting both of the above situations.

The aromatic signal at a ≈7.6ppmm is again a multiplet that would appear to be composed of a dominant highfield singlet and a pair of doublets. The pair of doublets suggests that the two H_A protons are not equivalent The coupling value for each doublet is 3.8H_z and this would support a coupling of the aromatic protons. We would only expect to observe coupling when the two H_A protons are not equivalent and this would be the case if the Cu^1 ions were not symmetrically held in the cavity. The presence of the singlet would again suggest that there is another conformer present in the solution phase in which the aromatic protons are equivalent (and thus no coupling is observed).

This idea of 2 major conformers being present is given strength by the results of a low temperature noe experiment. (Fig. 106).On irradiation of the singlet component of the H_c signal it is only the singlet component of the H_A signal is enhanced (6.0%). The result favours the convergent form of the imine functions .

The methylene signals are also very complicated. If, as we now expect in a complexed form of the ligand, that we get the axial(triplet), eq(d),eq(d), ax(t) arrangement of signals then the lowfield signals would certainly suggest the presence of 2 conformers (in an ≈ 1:1 ratio) with two H_D axial triplets and 2 H_D equatorial doublets observed. H_E is very complicated and the integral suggests that it is not fully resolved into its axial and equatorial signals. From the noe experiment discussed above, there was also enhancement of only one of the Deq. signals (6.0%). This noe result is very similar to that in $Ag_23S(CF_3SO_3)_2$. where Deq. and the aromatic signal were enhanced to exactly the same extent- thus one of the conformers at least is in the cis cis arrangement, as in $Ag_23S(CF_3SO_3)_2$. This cis cis arrangement would correspond to the singlets of the H_c, H_A signals. (this is deduced by comparison with the spectra of the silver comlex).

FIG. 106

NOE EXPERIMENT

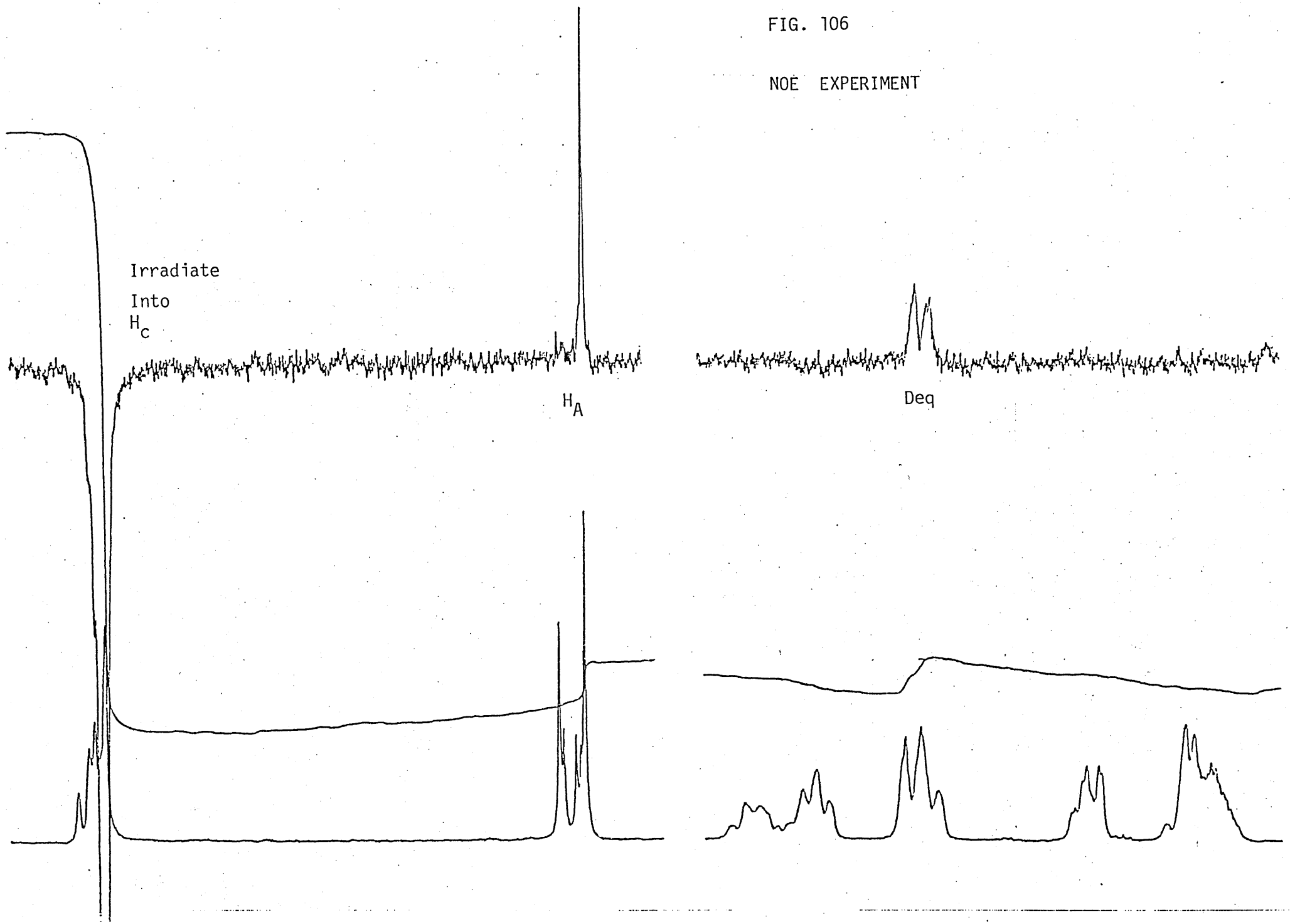

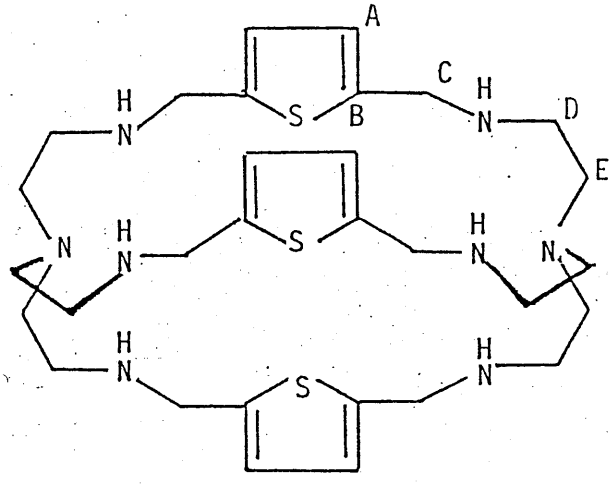

LIGAND R3S

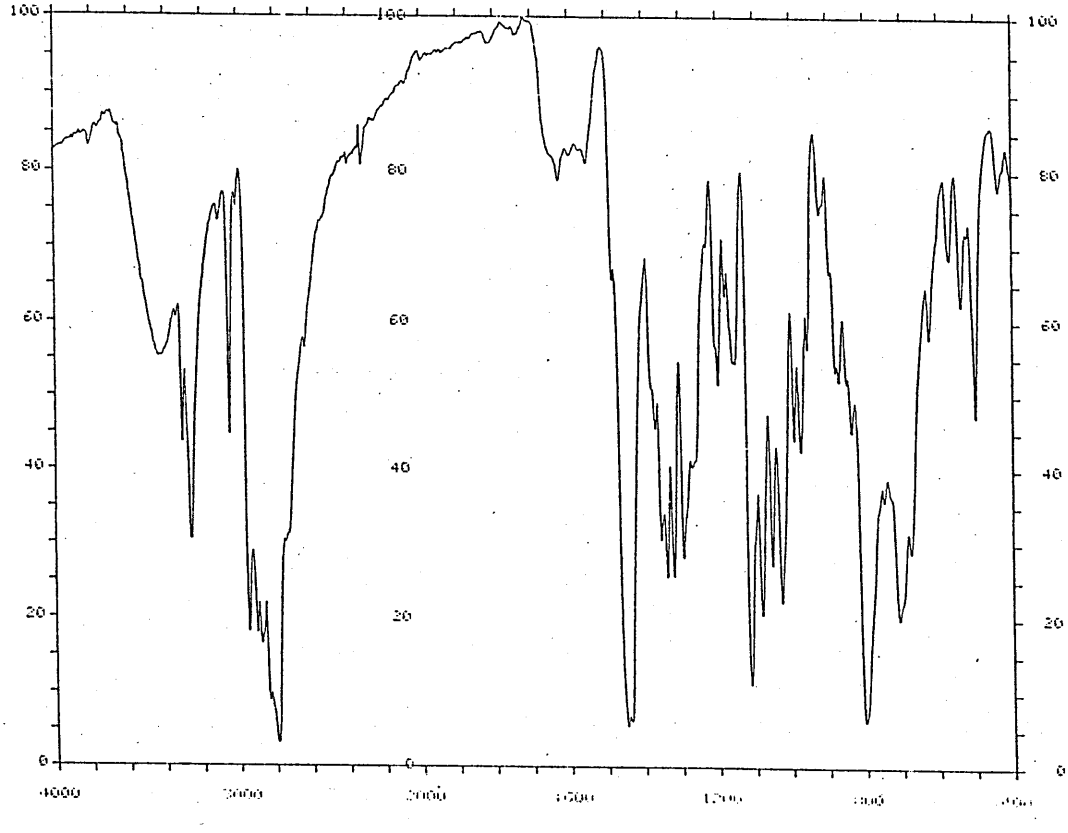

FIG. 107 - THE LIGAND R3S.

R3S.

The reduced form of 3S Fig107-1 has only just been obtained. Again reduction was achieved using sodium borohydride. The ir of the product of reduction Fig 107-2 shows the expected NH signal at 3336cm^{-1} and the absence of an imine signal at 1640cm^{-1}. Both ir and microanalysis suggest that no water or solvent is present in the product. Mass spec also confirmed the cyclic nature of the product giving the mass ion peak at 617 which corresponds to R3S.

First attempts at inserting Cu(1) and Cu(11) ions into R3S suggest that in contrast to the hexaimine derivative, the Cu(11) ion is favoured. As yet any attempt to insert Cu(1) has yielded a green Cu(11) product. The ir suggests that a hydroxo bridged assembly is being formed and although a satisfactory microanalysis has not yet been obtained a doubly hydroxo bridged dicopper complex is favoured by the results. Although FAB shows peaks that suggest successive loss of ClO_4^-, 968, 869, 768, these correspond respectively to

$[Cu_2R3S(OH)(ClO_4)]+9H^+$

$[Cu_2R3S(OH)(ClO_4)]+9H^+$

$[Cu_2R3S(OH)] +7H^+$

No further results were available at the time of writing.

CONCLUSIONS AND RECOMMENDATIONS FOR FURTHER WORK.

GENERAL.

The work described in this thesis is far from complete and there are many areas of work that are worthy of development.

The nmr study of the ligand series still requires a great deal of work, especially on the 3 heterophane systems where highfield V.T.nmr spectra and noe experiments are still to be carried out. The recent availability of a 500MHz nmr spectrometer will be "well exploited" in this respect. Indeed it is hoped that this together with molecular modelling studies will greatly assist in our understanding of the fluxional processes in these molecules.

Both nmr and X-ray crystallographic analysis results suggest that the uncomplexed ligands show a trans trans arrangement of carbimine functions (ie divergent) in contrast to the complexed form of the ligands where a cis cis arrangement of these functions is observed. The trans trans arrangement in the metal free derivatives suggest that it is the trans trans conformer of the reactant dialdehyde that leads to macrocyclization. This is supported by the fact that the ligand 3S, which cannot be isolated in its uncomplexed form, is derived from a dicarbonyl precursor which has no trans trans conformer present in the initial equilibrium ratio of conformers.

One of the main incentives for moving from the macrocyclic study to the macrobicyclic study was to try and find a system that offered better steric protection for bridged binuclear assemblies and thus offered a more truely isolated environment for magnetic interaction. This aspect of the study is not yet fully underway due to lack of success of the transmetallation reactions. Insertion reactions are in progress for the reduced and unreduced ligands; initial results suggest that the cavities provided by these ligands are suitable for hosting a M-O(H)-M assembly.

The silver complexes of the hexaimine ligands are worthy of a stability study, with respect to aqueous or acid catalysed decomposition. The Hnmr spectrum of $Ag_2$3S$(CF_3SO_3)_2$ suggests that ligand 3S may be a useful silver ion molecular host.

A11 5 hexaimine ligands form $[Cu_2L]^{2+}$ complexes and an electrochemical study on this series is planned.

LIGANDS 3Bm/R3Bm.

1. A high temperature nmr study is required to establish the coalescence temperature of the fluxional process of the methylene groups.

2. A full investigation of the reaction of copper(11) with 3Bm is required, with magnetic, esr, and electrochemical studies, of both the green and blue complexes, being high priority.

3. The complexation properties of R3Bm are currently being investigated by Josie Hunter. However the isolation of the protonated form of this ligand suggests that a study of the basic properties of R3Bm could be made

LIGANDS 3Bp/R3Bp.

From the low temperature nmr spectrum of the silver complex of 3Bp (Fig. 63-7) it is clear that other conformations are present in solution;a full investigation in collaboration with M. Drew is underway.

LIGANDS 3F/R3F.

1. The behaviour of ligand 3F with Group I metal ions is certainly worthy of development. The stability of the mononuclear sodium cryptate in aqueous solution and ^{23}Na nmr studies are obvious first steps in this investigation.

2. The hexaimine ligand 3F formed a hydroxo bridged di-copper(11) complex and early magnetic results suggest a strong antiferromagnetic interaction

can be mediated via this single bridging group. For the more flexible R3F this bridging group is formed with both manganese and cobalt. In the case of nickel it is the bis-hydroxo bridged unit that is formed. No copper complex has been isolated with R3F suggesting that the unreduced ligand is required to provide good fit for the smaller copper(11) ion.

LIGANDS 3P/R3P.

1 A study of 3P with the Group II metals should be made to see if it is possible to account for the lack of success of the transmetallation reaction. It is hoped that the "insertion" approach to complex synthesis will be more successful.

2. The octaamino derivative of 3P requires a full investigation both in terms of nmr and its complexation properties.

3 The pendant armed species, 2P and $2P_{CH3}$ might be useful precursors of asymmetric cryptands. The complexation properties of such ligands might prove interesting.

LIGANDS 3S/R3S.

A full investigation of these ligands is required. However the stability of the silver complex of 3S is especially worthy of investigation.

HEXAAZA LIGANDS.

A move to the analogous carbon bridgehead cryptand series is planned in order to ensure coordinative unsaturation of encapsulated metal ions and in particular copper.

Appendix 4 Spin Relaxation Effects.

The equilibrium magnetization, of a sample is aligned along the z axis. This magnetization is M_o. and is a direct result of the difference in energy between the states. To alter the z component of the magnetization., M_z. the energy of the spin system must be changed by perturbing the spins with the radio frequency pulse. In order for the spin system to return to equilibrium, there must be an interaction between the spins and the surroundings, or lattice, leading to a loss of the excess energy. The rate at which the system returns to equilibrium will depend upon the ability of this interaction to convey energy into or out of the system. The return to equilibrium is not instantaneous, but usually occurs with a first order rate constant. R_1.
Since relaxation phenomena are usually studied by time dependance measurements, it is common to see the relaxation time constant, T_1, used rather than the relaxation rate constant.

$$R_1 = 1/T_1$$

For ^1H or ^{13}C nuclei in diamagnetic molecules in solution, R_1. is of the order of a few s^{-1} or less; it will therefore require a time of the order of seconds for the spin system to return to equilibrium. R_1 and T_1 are referred to as the spin-lattice relaxation rate constant or time constant respectively.

Once disturbed from equilibrium, the magnetization may have components in the xy plane and these will also relax to their equilibrium value of zero. The xy magnetization will decay at least as fast as spin-lattice relaxation returns the magnetization to the z axis. However, the xy magnetization can also be lost by additional processes which cause components of the xy magnetization to fan out or dephase, producing a net xy magnetization of zero. These additional processes do not necessarily require any change in energy, so the rate of xy relaxation may be faster than the rate of z

relaxation. The relaxation rate constant in the xy plane is denoted R_2 while the relaxation time constant is T_2

$$R_2 = 1/T_2$$

NOE's and relaxation rates are population effects. In the nmr experiment, excess spin population is moved from one energy level to another by electromagnetic radiation of the appropriate frequency. This is excitation. The radiationless return to equilibrium is called spin-lattice relaxation because the excess energy passes from the spins to the lattice (or surroundings in general) as heat. This relaxation requires magnetic fields which are fluctuating at the appropriate frequency. These can arise from many sources, but, for both protons and carbons in diamagnetic molecules, the dominant fields are due to the magnetic moments of protons in the same molecules as they tumble in solution. This is the dipole-dipole interaction.

The rate, or efficiency, of dipole-dipole relaxation depends on both the strength and frequency of the fluctuating magnetic fields. These, in turn, depend on three factors: (a) the distance between the nuclei involved, r_{1s}; (b) the effective correlation time, τc, of the vector which joins the nuclei (ie. the reciprocal of the rate of tumbling in solution of the relevant piece of the molecule); and (c) the nature of the nuclei themselves. Nuclear Overhauser enchancements and the rates at which they grow and decay, are also measures of the strengh of the dipole-dipole interaction between two spins, and are, therefore, dependent on interatomic distances and correlation times. Therein lies their great power as structural probes.

REFERENCES FOR CHAPTER 1

-1- J. Van Alpen, Rec. Trav. Chim. Pays-Bas (1936), 55, 835.

-2- R.P. Linstead and M. Whalley, J. Chem. Soc., (1952), 4839.

-3- G.E. Ficken and R.P. Lindstead, J. Chem. Soc., (1952), 4846.

-4- J.A. Elvidge and R.P. Lindstead, J. Chem. Soc., (1952), 5008.

-5- J.A. Elvidge and J.H. Golden, J. Chem. Soc., (1957), 700.

-6- N.F. Curtis, J. Chem. Soc., (1960), 4409.

-7- M.C. Thompson and D.H. Busch, J. Am. Chem. Soc., (1964), 86, 3651.

-8- C.J. Pederson, J. Am. Chem. Soc., (1967), 89, 2495,
ibid, 7017.

-9- A.C.L.Su and J.F. Weiher, Inorg. Chem., (1968), 7, 176.

-10- B. Dietrich, J.M. Lehn and J.P. Sauvage,
Tetrahedron Lett, (1969), 2885, 2889.

-11- J.M. Lehn, J. Simon and J. Wagner, Nouv. J. Chim., (1977), 1, 77

-12- E. Graaf and J.M. Lehn, J. Am. Chem.,Soc., (1975), 97, 5022.

-13- D.K. Cabbiness and D.W. Margerum, J. Am. Chem. Soc., (1970), 92, 2151

-14- D.H. Busch, K. Farmery, V. Goedken, V. Katovic, A.C. Melnyk,
C.R. Seperati, and N. Tokel in
"Bioinorganic Chemistry", Adv. Chem. Ser.,(1971), 100, 44

-15- D.K. Cabbiness and D.W Margerum, J. Am. Chem. Soc., (1969), 91, 6540

-16- F.P. Hinz and D.W. Margerum, J. Am. Chem. Soc., (1974), 96, 4993

-17- F.P. Hinz and D.W. Margerum, Inorg. Chem., (1974), 13, 294

-18- J.M. Lehn and J.P. Sauvage, J. Am. Chem. Soc., (1975), 97, 6700

-19- B.G. Cox, (I.C.I. Blackley U.K.) Macrocyclic meeting, Durham, 1989.

-20- H.J. Buschmann, Inorg. Chim. Acta., (1985), 108, 241.

-21- B. Dietrich, M.W. Hosseini, J.M. Lehn, and R.B. Sessions,
Helv. Chim. Acta., (1985), 68, 289.

-22- E.K. Barefield, Inorg. Chem., (1972), 11, 2273.

-23- E.K. Barefield and F. Wagner, Inorg. Chem., (1973), 12, 2435.

-24- J.E. Richman and T.J. Atkins, J. Am. Chem. Soc., (1974), 96, 2262

-25- S. Ogawa, T. Yamaguchi and N. Gotoh,
J. Chem. Soc., Chem. Commun., (1972), 557.

-26- J. Jurczak, R. Ostaszewski, M. Pietraszkiewicz, and P. Salanski,
J. Incl. Phenom., (1987), 5, 553.

-27- J. Jurczak and M. Pietraszkiewicz,
Top. Curr. Chem., (1985), 130, 183

-28- J. Jurczak, R. Ostaszewski, and P. Salanski,
J. Chem. Soc., Chem. Commun., (1989), 184.

-29- G.A. Melson. in "Coordination Chemistry of Macrocyclic Compounds."
Plenum Press, New York, (1979).

-30- S.M. Nelson, Pure Appl. Chem., (1980), 52, 2461.

-31- M.C. Thompson and D.H. Busch, J. Am. Chem. Soc., (1962), 84, 1762.

-32- L. Mandolini, Pure Appl. Chem., (1986), 58, 1485.

-33- D.E. Fenton, Pure Appl. Chem., (1986), 58, 1437.

-34- S.M. Nelson in "Copper Coordination Chemistry, Biochemical and
Inorganic Perspectives."
Ardenine Press, New York, (1983).

-35- J.M. Lehn, Structure and Bonding, (1973), 16, 1.

-36- F. Vogtle, Chem. Ber., (1973), 106, 1319.

-37- F. Vogtle and P. Neumann, J. Chem. Soc., Chem. Commun., (1970), 1464.

-38- M. Kanishi, J.I. Kunizaki, J. Inanaga, and M. Yamaguchi,
Bull. Chem. Soc. Jpn., (1981), 54, 3828.

-39- A. Ricci, R. Danieli, and S. Rossini,
J. Chem. Soc., Perkin Trans. (1976), 1, 1691.

-40- A.J. Hubert, J. Chem. Soc., (c) (1967), 6.

-41- F. Vogtle and G. Hohner, Agnew. Chem., (1975), 87, 522.

-42- P.L. Anelli, F. Montanari, and S. Quici,
J. Chem. Soc., Chem. Commun., (1983), 194.

-43- J.M. Lehn, S.H. Pine, E.I. Watanabe, and A.K. Willard,
J. Am. Chem. Soc., (1977), 99, 6766

-44- G.R. Newkome, V.K. Majestic, and F.R. Fronczek,
Tetrahedron Lett., (1981), 22, 3035.

-45- R.J. Geue, T.W. Hambley, J.M. Harrowfield, A.M. Sargeson, and M.R. Snow, J. Am. Chem. Soc., (1984), 106, 5478 (and references therein).

-46- J. Gabard and A. Collet, J. Chem. Soc., Chem. Commun., (1981), 1137.

-47- J. Canceill, A. Collet, J. Gabard, F. Kotzyba-Hibert, and J.M. Lehn, Helv. Chem. Acta., (1982), 65, 1894

-48- J.M. Lehn and J.B. Regnouf de Vains, Tetrahedron Lett., (1989), 30, 2209

-49- B. Alpha, J.M. Lehn and G. Mathis, Agnew. Chem. Int. Ed. Engl., (1987), 26, 266.

-50- B. Alpha, V. Balzani, J.M. Lehn, S. Perathoner and N. Sabbatini, Agnew. Chem. Int. Ed. Engl., (1987), 26, 1266.

-51- G.R. Newkome, J.D. Sauer, J.M. Roper and D.C. Hager, Chem. Rev., (1977), 77, 513.

-52- S. Patai, in "The Chemistry of the Carbon-Nitrogen Double Bond!". Interscience, New York, (1970).

-53- N.A. Bailey, M.M. Eddy, D.E. Fenton, G. Jones, S.Moss and J. Mukhopadhyay, J. Chem. Soc., Chem. Commun., (1981), 629.

-54- P.G. Owston, R. Peters, E. Ramaswany, P.A. Tasker, and J. Trotter, J. Chem. Soc., Chem. Commun., (1981), 1218.

-55- K.K. Abid and D.E. Fenton, Inorg. Chim. Acta., (1984),82,223

-56- U. Casellato, D. Fregona, S. Sitran, S. Tamburini, P.A. Vigato and P. Zanello, Inorg. Chim. Acta,. (1984),95, 309.

-57- L. De Cola, D.L. Smailes and L.M. Vallarino, Inorg. Chim. Acta., (1985), 110, LI.

-58- M.G.B. Drew, A. Rodgers, M. McCann, and S.M. Nelson, J. Chem. Soc., Chem. Commun. (1978), 415.

-59- D.H. Cook, D.E. Fenton, M.G.B. Drew, A. Rodgers, M. McCann, and S.M. Nelson, J. Chem. Soc., Dalton Trans., (1979), 414.

-60- M.G.B. Drew, S.G. McFall, S.M. Nelson and C.P. Waters. J. Chem. Res., (1979) (S) 16-17, (M) 0360-0378.

-61- J.L. Karn and D.H. Busch, Nature, (1966), 160, 211

-62- L.F. Lindoy and D.H. Busch. in "Preparative Inorganic Reactions", Ed. W. Jolly, Interscience, New York (1971), 6, 1.

-63- N.A. Bailey, D.E. Fenton, M.G. Williams and D.J. Winter, J. Chem. Soc., Dalton Trans., (1989). 1727.

References for Chapter 1

-64- K.A. Adam, A.J. Leong, L.F. Lindoy, B.J. McCool, A. Ekstrom, I. Liepa, P.A. Harding, K. Hendrick, M.McPartlin and P.A. Tasker, J. Chem. Soc., Dalton Trans., (1987), 2537.

-65- a. D.E. Fenton, Pure. Appl. Chem., (1989), 61, 1563.
b. C.J. van Staveren, D.E. Fenton, D.N. Reinhoudt, J. van Eerden, and S. Harkema, J. Am. Chem. Soc., (1987), 109, 3456.
c. C.T.Brewer and G.Brewer, J.Chem. Soc., Chem. Commun., (1988), 854.
d. N.W. Alcock, P. Moore, H.A.A. Omar and C.J. Reader, J. Chem. Soc. Dalton Trans (1987), 2643.
e. D.E. Fenton, B.P.Murphy, A.L. Leong, L.F. Lindoy, A.Bashall, and M.McPartlin, J. Chem. Soc., Dalton Trans.,(1987), 2543c

-66- a. S.M. Nelson, F.S. Esho and M.G.B. Drew, J. Chem. Soc. Dalton Trans., (1983),11857.
b. V. McKee and S.S. Tandon, J. Chem. Soc., Chem. Commun., (1988)
c. K.P. McKillop, S.M. Nelson, J. Nelson, and V. McKee., J. Chem. Soc., Chem. Commun., (1988), 387.

-67- V. McKee and W.B. Sheppard, J. Chem. Soc., Chem. Commun., (1985), 158.

-68- S. Brooker, V. McKee,W.B. Shepard and L.K. Pannell, J. Chem. Soc. Dalton Trans. (1987), 2555.

-69- P.D. Beer, J. Chem. Soc., Chem Commun., (1986), 1679.

-70- J. Rebek. Jr., Acc. Chem. Res., (1984), 17 258.

-71-U. Casellato, D. Fregona, S. Sitran, S. Tamburini and P.A. Vigato, Inorg. Chim. Acta., (1985), 110, 161.

-72- J. Jazwinski, J.M. Lehn, D. Lilenbaum, R. Ziessel, J. Guilhem, and C. Pascard J. Chem. Soc., Chem Commun., (1987) 1691.

-73- D. McDowell and J. Nelson. Tetrahedran Lett., (1988), 29, 385.

-74- L. Fabbrizzi, A. Perotti, A. Profumo, and T.Soldi. Inorg. Chem., (1986), 25, 4256.

-75- A. Buttafava, L. Fabbrizzi, A. Perotti, A. Poggi, G. Poli, and B. Seghi, Inorg. Chem., (1986), 25 1456.

-76- L. Fabrizzi, J. Chem. Soc., Chem. Commun., (1979), 1063.

-77- F.V.Lo Vecchio, E.S. Gore, and D.H. Busch, J. Am. Chem. Soc., (1974), 96, 3109.

-78- M. Ciampolini, L. Fabbrizzi, M. Licchelli, A. Perotti, F. Pezzini, and A. Poggi, Inorg. Chem. (1986), 25 4131.

-79- E. Zeigerson, I. Bar, J. Bernstein, L.J. Kirschenbaum and D. Meyerstein, Inorg. Chem., (1982), 21 73.

-80- L. Fabrizzi, T.A. Kaden, A. Perotti, B. Seghi and L. Siegfried,

Inorg. Chem., (1986), 25, 321.

-81- P. Moore, J. Sachinidis and G.R. Willey,
J. Chem. Soc., Chem. Commun., (1983) 522.

-82- S. F. Lincoln, J.H. Coates, A. Hadi and D.L. Pisaniello
Inorg. Chem. Acta., (1984), 81, L9.

-83- C.S. Kallianou and T.A. Kaden, Helv Chim. Acta., (1979), 62.
2562.

-84- C.M. Madeyski, J.P. Michael, and R.D. Hancock, Inorg. Chem.,
(1984), 23, 1487.

-85- S.P. Kasprizyk and R.G. Wilkins, Inorg. Chem., (1982), 21,3349.

-86- R.W. Hay, M.P. Pujari, W.T. Moodie, S. Craig, D.T. Richens,
A. Perotti. and L. Ungaretti,
J. Chem. Soc., Dalton Trans., (1987), 2605.

-87- P. Chaudhuri and K. Wieghardt, Prog. Inorg. Chem., (1987), 35,330.

-88- (a) M. Kodama and E. Kimura, J. Chem. Soc., Dalton Trans., (1978) 1081
(b) M. Kodama, T. Yatsunami and E. Kimura, Inorg. Chem.,
(1980),19,1600.
(c) R. Yang and L.J. Zompa, Inorg. Chem., (1976), 15, 1499
(d) L.J. Zompa, Inorg. Chem., (1978), 17, 2531
(e) R.D. Bereman, M.R. Churchill, P.M. Schaber, and M.E. Winkler,
Inorg. Chem. (1979), 18, 3122
(f) H. Gampp, M.M. Roberts, and S.J. Lippard,
Inorg. Chem., (1984), 23, 2793
(g) J.C.A. Bayens, A.G.S. Forbes, R.D. Hancock and K. Weighardt,
Inorg. Chem., (1985), 24, 2926

-89- N. Alcock, F. McLaren, P. Moore, G.A. Pike and S.M. Roe.
J. Chem. Soc., J. Chem. Commun., (1989), 629

-90- F. McLaren, P. Moore, and A.M. Wynn.,
J. Chem. Soc., Chem. Commun., (1989) 798

-91- N.W. Alcock, N. Gosal, F. McLaren, P. Moore, G.A. Pike, and S.M. Roe,
XIII Macrocyclic Symposium, Hamburg 1988.

-92- E. Kimura, M. Yamaoka, M. Morioka, and T. Koike.,
Inorg. Chem., (1986), 25, 3883

-93- A.S. Craig, I.M. Helps, K.J. Jankowski, D. Parker, N.R.A. Beeley, B.A.
Boyce, M.A.W. Eatom, A.T. Millican, K. Millar, A. Phipps, S.K.
Rhind, A.Harrison and C. Walker.,
J. Chem. Soc., Chem Commun., (1989), 794.

-94- M. Di. Vaira, F. Mani, and P. Stoppioni.,
J. Chem. Soc., Chem Commun, (1989), 127.

-95- H. Tsukube, K. Yamashita, T. Iwachido, and M. Zenki., Tetrahedron Lett. (1989), 30, 3983.

-96- E.K. Barefield, Inorg. Chem., (1972), 11, 2273.

-97- P. Paoletti, Pure Appl. Chem., (1980), 52, 2433.

-98- L. Fabbrizzi and L. Sabatini, Inorg. Chem., (1979), 18, 438.

-99- M. DiCasa, L. Fabbrizzi, A. Perotti, A. Poggi, and R. Riscassi., Inorg. Chem., (1986), 3984.

-100- L. Fabbrizzi., Pure Appl. Chem., (1989), 61, 1569.

-101- P.S. Pallavicini, A. Perotti, A. Poggi, B. Seghi, and L. Fabbrizzi., J. Am. Chem. Soc., (1987), 109, 5139.

-102- T.J. Lotz, and T.A. Kaden, J. Chem. Soc., Chem Commun., (1977), 15; , Helv. Chim. Acta., (1978), 61, 1376.

-103- R.W. Hay, M.P. Pujari, B. Korybut - Daszkiewicz z, G. Ferguson, and B.L. Ruhl, J. Chem. Soc, Dalton Trans., (1989), 85.

-104- R.W. Hay M.P. Pujari, W.T. Moodie, S. Craig, D.T. Richens, A. Perotti, and L. Ungaretti, J. Chem. Soc., Dalton Trans., (1987), 2605

-105- R.W. Hay and R. Bembi, Inorg. Chim. Acta., (1982), 65, L227.

-106- K.E. Krakowiak, J.S. Bradshaw, N.K. Dalley, W. Jiang and R.M. Izatt. Tetrahedron Lett., (1989), 30, 2897.

-107- E. Kimura, Pure Appl. Chem., (1989), 61, 823.

-108- E. Kimura, J. Coord. Chem., (1986), 15, 1.

-109- E. Kimura, M. Shionoya, M. Okamoto, and H. Nada., J. Am. Chem. Soc., (1988), 110, 3679.

-110- E. Kimura, T. Koike, K. Yenishi, M. Hediger, M. Kuramoto, S. Joko, Y. Arai M. Kodoma, and Y. Iitaka., Inorg. Chem., (1987), 26, 2975.

-111- E. Kimura, Pure Appl. Chem ., (1986), 58, 1461.

-112- E. Kimura, T. Koike, H. Nada, and Y. Iitaka., J. Chem. Soc., Chem Commun., (1986), 1322.

-113- E. Kimura, M. Shionoya, T. Mita, and Y. Iitaka., J. Chem. Soc., Chem Commun., (1987), 1712.

-114- E. Kimura and M. Kodama., J. Chem. Soc., Dalton Trans., (1981), 694.

-115- E. Kimura, and M. Kodama., ibid., (1979), 325.

-116- L. Fabbrizzi, T.A. Kaden, A. Perotti, B. Seghi, and L. Siegfried., Inorg. Chem., (1986), 25, 321.

-117- M.K. Moi, M. Yanuck, S.V. Deshpande, H. Hope, S.J. DeNardo, and C.F. Meares., Inorg. Chem., (1987), 26, 3458.

-118- D. Parker, J.R. Morphy, K. Janowski, and J. Cox., Pure Appl. Chem., (1989), 61, 1637.

-119- J.R. Morphy, D. Parker, R. Kataky, A. Harrison, M.A.W. Eaton, A. Millican, A. Phipps, and C. Walker., J. Chem. Soc., Chem Commun., (1989), 792.

-120- T.A. Kaden, D. Tschudin, M. Studer, and U. Brunner., Pure Appl. Chem., (1989), 61, 879.

-121- M. Ciampolini, M. Micheloni, N. Nardi, F. Vizza, A. Buttafava, L. Fabbrizzi, and A. Perotti., J. Chem. Soc., Chem Commun., (1984) 998.

-122- K. Weighardt, J. Tolksdorf, and W. Herman., Inorg. Chem., (1985), 24, 1230.

-123- R. Schneider, A. Riesen, and T.A. Kaden, Helv. Chim. Acta., (1985), 68, 53.

-124- a) M. Ciampolini, L. Fabbrizzi, A. Perotti, A. Poggi, B. Seghi, and F. Zanobini., Inorg. Chem., (1987), 26, 3527
b) I. Murase, S. Ueno, and S. Kido, Inorg. Chim. Acta., (1986), 57.

-125- E.K. Barefield, K.A. Foster, G. Freeman, and K.D. Hodges, Inorg. Chem., (1986), 25 4663.

-126- E.K. Barefield, D. Chueng, D.G. van Derveer, and F. Wagner, J. Chem. Soc., Chem Commun., (1981) 302.

-127- L. Fabrbizzi, L. Mortagne, A. Poggi, T.A. Kaden, L. Siegfried, Inorg. Chem. (1986), 25, 2671.

-128- L. Fabbrizzi, F. Forlini, A. Perotti, and B. Seghi. Inorg. Chem ., (1984), 23, 807.

-129- J. Jazwinski, J.M. Lehn, M.R. Vigneron, M. Cesario, J. Guilhem, and C. Pascard, Tetrahedron Lett., (1987), 28 3489.

-130- -a- M.C. Rakowski, M. Rycheck and D.H. Busch. Inorg. Chem., (1977), 14, 1194.
-b- N.A. Alcock, P. Moore, H.A.A. Omar, and J.C. Reader, J. Chem. Soc., Dalton Trans., (1987), 2643.
-c- R. Machida, E. Kimura, and K. Yoshihiko, Inorg, Chem., (1986), 25, 3461.

-d- S.G. Mc.Fall, S.M. Nelson, M.G.B.Drew and A.H. Bin Othman.
J. Chem. Soc., Chem. Commun., (1975), 818.

-131- -a- M.P. Suh, W. Shin. H. Kim, and C.H. Koo.,
Inorg. Chem., (1987) 26 1846.
-b- G.R. Newkome, F.A. Majestic, F. B. Fronczek.
Inorg. Chim. Acta., (1983) 77, L47.

-132- A. Bianchi, S. Mangani, M. Micheloni, V. Nanini, P. Orioli, P. Paoletti, and B. Seghi.
Inorg. Chem., (1985), 25, 1182.

-133- A. Bencini, A. Bianchi, E. Garcia - Espana, M. Giusti, M. Micheloni, and P. Paoletti.
Inorg. Chem., (1987) 26 681.

-134- ibid. 1243.

-135- A. Bencini. A. Bianchi, E. Garcia - Espana, G. Giusti, M. Micheloni, P. Paoletti, M. Stefano, and O. Pierluigi.
ibid 3902.

-136- A. Bencini, A. Bianchi, E. Garcia - Espana, M. Micheloni, and P. Paoletti,
Inorg. Chem., (1988), 27 176.

-137- A. Bianchi, M. Micheloni, S. Mangani, V. Nanini, P.Orioli, P. Paoletti and B. Seghi.
Inorg. Chem., (1985),24,1182.

-138- M. Micheloni, P. Paoletti, and A. Bianchi,
Inorg. Chem., (1985), 24, 3702.

-139- J. Malthete, P. Poupinet, R. Vilanove, and J.M. Lehn,
J. Chem. Soc., Chem. Commun., (1989) 1016.

-140- S.C. Rawle, R. Yagbasan, K. Prout and S.R. Cooper
J. Am. Chem. Soc., (1987), 109, 6181.

-141- A. Blake, A. Holder, T. Hyde, Y. Roberts, A. Lavery, and M. Schroder,
J. Org. Chem., (1987) 261.

-142- K. R. Adam, A. J. Leong, L.F. Lindoy, H.C. Lip, B.W. Skelton, and A. H. White.
J. Am. Chem. Soc., (1983), 105, 4645.

-143-a) L. F. Lindoy and D. S. Baldwin.
Pure Appl. Chem. (1989), 61, 909.
b) L. F. Lindoy, Pure Appl. Chem.(1989), 61, 1575

-144- K.R.Adam, C.W.G. Ansell, K.P. Dancey, L.A. Drummond, A.L. Leong, L.F. Lindoy and P.A. Tasker.
J. Chem. Soc., Chem., Commun., (1986), 1011.

-145- L.F. Lindoy, XIII, Macrocyclic Symposium, Hamburg, (1988).

-146- R.D. Hancock, Pure Appl. Chem., (1986), 58, 1445.

-147- S.M. Nelson, F.S. Esho and M.G.B. Drew,
J. Chem. Soc., Dalton Trans., (1983), 1857.

-148- K. Gu. K.B. Mertes, and M.P. Mertes,
Tetrahedron Lett. (1989) 30, 1323.

-149- N.A. Bailey, D.E. Fenton, S.J. Kitchen, and M.G. Williams,
XIII, Macrocyclic Symposium, Hamburg, (1988)

-150- K.E. Krakowiak, J.S. Bradshaw, and D.J. Zamecka-Krakowiak
Chem. Rev., (1989), 89, 929.

-151- N. Malhotra, H. Toftlund, G. Bojesen and J. Becher.
J. Chem. Soc., Chem. Commun., (1989), 1349.

-152- N. Atkinson, A.J. Blake, M.G.B. Drew, G. Forsyth, A.J. Lavery, G. Reid, and M. Schroder.
J. Chem., Soc., Chem. Commun., (1989), 984.

-153- A.J. Lavery and M. Schroder, XIII Macrocyclic Symposium, Hamburg, (1988).

-154- G. Markl and R. Vybiral, Tetrahedron Lett., (1989), 30, 2903.

-155- M. Ciampolini, M. Micheloni. F. Vizza, F. Zanobini, S. Chimichi, and P. Dapporto.
J. Chem. Soc., Dalton Trans., (1986), 505.

-156- A. Bianchi. E. Garcia-Espana, M. Micheloni, N. Nardi, and F. Vizza.
Inorg. Chem., (1986), 25, 4379.

-157- I.M. Help, K.E. Mathes, D. Parker, and G. Ferguson,
J. Chem. Soc., Dalton Trans., (1989), 915.

-158- A.S.Craig, D. Parker, and H.S. Buschmann.
XIII Macrocyclic Symposium, Hamburg, (1988).

-159- L. Bei, A. Bell, S. Warner, I.D. Williams, and S.J. Lippard.
J. Chem. Soc., (1986), 108, 8302.

-160- D.J. Cram, and J.M. Cram, Science, (1974), 183, 803.

-161- D.J. Cram. Science, (1983), 219, 1177.

-162- U. Luning, Liebigs. Ann. Chem., 1987, 949.

-163- R.E. Sheirdan and H.W. Whitlock,
J.Am. Chem. Soc., (1986). 108, 7120.

-164- S.P. Millar and H.W. Whitlock,
J.Am, Chem. Soc., (1984), 106, 1492.

-165- J. Rebek Jr., B. Askew, M. Killoran, D. Nemeth, and F.T. Lin.
J. Am. Chem. Soc.,(1987), 109, 2426.

-166- J. Wolfe, D. Nemeth, A. Costerno, and J. Rebek, Jr.,
J.Am. Chem. Soc., (1988), 110, 983.

-167- J. Rebek Jr., R.J. Duff, W.E. Gordon, and K. Parris.
J.Am. Chem. Soc., (1986), 108 6066.

-168- J.W.H. Smeets. R.P. Sijbesma, W. Drenth, and R.J.M. Nolte.
XIII Macrocyclic Symposium, Hamburg, (1988).

-169- W. Saegner, Angew. Chem.Int. Ed. Engl., (1980), 19, 344.

-170- I. Tabushi, Tetrahedron, (1984), 40, 269.

-171- R. Breslow, Biomimetric Chemistry., Adv. Chem. Ser., (1980), 1,191.

-172- R. Breslow, Chemistry in Britain, (1983), 128.

-173- R. M. Kellogg, Le Recherche, (1984), 15, 819..

-174- J.M. Lehn, Stuct. and Func. in Enzym. Catal. (1981) p24.

-175- J.M. Lehn, Pure Appl. Chem., (1980), 52, 2441.

-176- P. Potvin and J.M. Lehn.
Design of Cation & Anion Receptors, Catalysts and Carriers.

-177- M.L. Bender and M. Komoyama, "Cyclodextrin Chemistry"
Springer-Verlag, Berlin, (1978).

-178- Y. Inoue, T.Okuda, Y.M. Yata, and R. Chujo
Carbohydrate Res., (1984).65,125.

-179- T.J. Meade, C.M. Fendrick, P.A. Podolick, C.E. Cotterill, and D.H. Busch.
Inorg. Chem., (1987), 26. 4252.

-180- R.J. Mitchell Cyclophanes, vol II (P.M. Keehn,S.M. Rosenfeld eds.)
Academic Press, New York, (1983)

-181- I. Tabushi, Y. Kuroda and T. Mizirtari
Tetrahedron, (1984), 40, 545.

-182- I Tabushi, Y. Kuroda and H. Sasaki,
J. Am. Chem. Soc., (1976), 98, 5727

References for Chapter 1

-183- N.K. Dalley, "Synthetic Multidentate Macrocyclic Compounds" R.M. Izatt and J.J. Christenson Eds., Academic Press, New York, (1978)

-184- J.M. Lehn, Acc. Chem. Res., (1978), 11, 49.

-185- J.M. Lehn, J.Am. Chem Soc., (1970), 92, 2961.

-186- G.B. Cox, N. Vantroung and H. Schneider, J. Am. Chem. Soc., (1984), 106, 1273.

-187 L. Echegoye, A. Kaifer, H.D. Durst, and G.W. Gokel, J. Org. Chem. (1984), 49, 688.

-188- D.J. Cram and K.N. Trueblood, Topics in Curr. Chem., (1981), 98, 43.

-189- R.J. Motekaitis, A.E. Martell, J.M. Lehn and E. Watanabe Inorg. Chem., (1982), 21, 4253.

-190- J.M. Lehn, E. Sonveaux and A.J. Williard, J.Am. Chem. Soc., (1978), 100, 4911.

-191- R.J. Motekaitis, A.E. Martell, J.M. Lehn and E. Watanabe, Inorg. Chem., (1982), 21, 4253.

-192- R.J. Motekaitis, A.E. Martell, B. Dietrich and J.M. Lehn, Inorg. Chem., (1984), 23, 1588.

-193- R.J. Motekaitis and A.E. Martell, J.Am.Chem. Soc., (1988), 110, 7715.

-194- A.E. Martell, Acc. Chem. Res., (1982), 15, 155.

-195- R.J. Motekaitis, A.E.Martell and J. Murase, Inorg. Chem., (1986), 25, 938.

-196- R.J. Motekaitis, A.E. Martell, I. Murase, J.M. Lehn. and M.W. Hosseini, Inorg. Chem., (1988), 27, 3630.

-197- G.L. Woolery, L. Powers, M. Winkler, E.J. Solomon, and T.G. Spiro. J.Am. Chem. Soc., (1984), 106, 86.

-198- W.P.J. Gaykema, A. Volbeda, and W.G.J. Hol. J. Mol. Biol., (1985), 189, 255.

-199- J.M. Brown, L. Powers, B. Kincaid, J.A. Larrabee, and J.G. Spiro J. Am. Chem. Soc., (1980), 102, 4210.

-200- J.A. Tanier, E.D. Getzoff, K.M. Beem, J.S. Richardson, and D.C. Richardson, J.Mol. Biol., (1982), 106, 181.

-201- M.G. Basallote and A.E. Martell, Inorg. Chem., (1988), 27, 4219.

References for Chapter 1

-202- R.J. Motekaitis, A.E. Martell, J.M. Lehn and J.P. Lecomte.
Inorg. Chem., (1983), 22, 609.

-203- R.J. Motekaitis and A.E. Martell,
J. Chem. Soc., Chem. Commun., (1988), 1020.

-204- A.E. Martell and R.J. Motekaitis, ibid, 915.

-205- A.E. Martell and R.J. Motekaitis,
J. Am. Chem. Soc., (1988), 110, 8059.

-206- D. Chen and A.E. Martell, Inorg. Chem., (1987), 26, 1026.

-207- R.J. Motekaitis and A.E. Martell, Inorg. Chem., (1988). 27, 2718.

-208- I.T. Creaser, J. M. Harrowfield, A.J. Herlt, A. M. Sargeson,
J. Springborg, and M.R. Snow.
J.Am. Chem. Soc., (1977), 99, 3181.

-209- L.R. Gahen, T.W. Hambley, A.M. Sargeson, and M.R. Snow,
Inorg. Chem., (1982), 21, 2699.

-210- A.M. Sargeson, Pure Appl. Chem., (1984), 1603.

-211- P. Comba, N.F. Curtis, G.A. Lawrence, A.M. Sargeson,
B.W. Skelton, and A.H. White.
Inorg. Chem., (1986), 25, 4260.

-212- R.J. Geue, T.W. Hambley, J.M. Harrowfield, A.M. Sargeson,
and M.R. Snow.J.Am. Chem. Soc., (1984), 106, 0000.

--213- A.M. Bond, G.A. Lawrence, P.A. Lay and A.M. Sargeson,
Inorg. Chem., (1983), 22, 2010.

-214- A.M. Sargeson, Pure Appl. Chem., (1978), 50, 905.

-215- R.J. Geue, T.W. Hambley, J.M.B.Harrowfield,
A.M. Sargeson, and M.R. Snow.
J. Am. Chem. Soc., (1984), 5478.

-216- A.M. Sargeson, Pure Appl. Chem., (1986). 58, 1511.

-217- P. Bernhard and A.M. Sargeson, Inorg. Chem., (1987), 26, 4122.

-218- R.A. Marcus, Annu. Rev. Phys. Chem., (1964), 15, 155.

-219- N.S. Hush, Trans. Faraday. Soc., (1961) 57, 557.

-220- D.J. Bull, I.I. Creaser, A.M. Sargeson, B.W. Skelton, and
A.H. White, Inorg. Chem., (1987), 26, 3040.

-221- B. Korybut-Daszkiewiez, R.M. Hartshorn, and A.M. Sargeson.
J. Chem. Soc., Chem. Commun., (1989), 1375.

References for Chapter 1

-222- K. J. Takeuchi, N. Alcock and D.H. Busch.
J.Am. Chem. Soc., (1983), 105, 2421 :ibid 4261.

-223- J.H. Cameron, M. Kojima, B. Korybut-Daszkiewicz,, B.K. Coltrain, T.J. Meade, N.W. Alcock, and D.H. Busch.
Inorg. Chem., (1987), 26, 427.

-224- N.A. Alcock, W.K. Lin, A. Jircitana, J.D. Mokren, P.W.R. Corfield, G.Johnson, G. Novotnak, C. Cairns, and D.H. Busch.
Inorg. Chem., (1987), 26, 440.

-225-a) N.Herron and D.H. Busch, J.Am.Chem.Soc., (1981), 103, 1236.
b) N.Herron, W.P. Schammel, S.C. Jakels, J.J. Graybowski, L.L. Zimmer, and D.H. Busch, Inorg. Chem., (1983),22, 1433.
c) D.H. Busch, J.Am. Chem. Soc., (1983). 105,6585.
d) J.C. Stevens and D.H. Busch, J.Am. Chem. Soc., (1980),102, 3285.
e) J.C. Stevens, P.J. Jackson, W.P. Schammel, G.C. Christoph, and D.H. Busch, J.Am. Chem. Soc., (1980), 102, 3283.

-226- K.A. Goldsby, D.B. Beato, and D.H. Busch,
,Inorg. Chem., (1986), 25,2342.

-227- K.A. Goldsby, A.J. Jircitano, D.M. Minahan, D. Ramprasad, and D.H. Busch, Inorg. Chem., (1987), 26, 2651.

-228- P.J. Jackson, C. Cairns, W. Lin. N.W. Alcock, and D.H. Busch,
Inorg. Chem., (1986), 25, 4015.

-229- K.J. Takeuchi, N. Alcock, and D.H. Busch.
J.Am. Chem. Soc., (1981), 103, 2421.

-230- W.L. Kwik, N. Herron, K.J. Takeuchi, and D.H. Busch,
J.Chem. Soc., Chem. Commun., (1983), 409.

-231- T.J. Meade, W.L. Kwik, N. Herron, N.A. Alcock, and D.H. Busch.
J.Am. Chem. Soc., (1986), 108, 1954.

-232- E.Z. Jager, Z. Chem., (1968), 8, 392.

-233- R.Thomas, C.M. Fendrick, W.Lin, M.W. Glogowski, M.Y. Chavan, N.A. Alcock, and D.H. Busch,
Inorg. Chem., (1988),27, 2534.

-234- M.Y. Chavan, T.J. Meade, D.H. Busch, and T. Kuwana.
Inorg. Chem., (1986), 25, 314.

References for Chapter 1

-235- N. Hashino, A. Jircitano, and D.H. Busch.
Inorg. Chem., (1988), 27, 2292

-236- D.H. Busch, Pure Appl. Chem., (1980), 52, 2477.

-237- F.L. Weitl and K.N. Raymond, J.Org. Chem., (1981), 46, 5234

-238- F.L. Weitl,and K.N. Raymond, J.Am. Chem. Soc., (1980), 102,1252.

-239- F.L. Weitl, W.R. Harris, and K.N. Raymond, J.Med. Chem.,(1979), 1281.

-240- F.L. Weitl and K.N. Raymond, J.Am. Chem. Soc., (1979),101, 2728.

-241- W.R. Harris, F.L. Weitl, and K.N. Raymond,
J.Chem. Soc., Chem. Commun., (1979), 177.

-242- J.T. Rodgers, C.Y. Nu, and K.N. Raymond,
J.Am. Chem. Soc., (1985), 107, 4094.

-243- J.M. Lehn, Science, (1985), 227, 849.

-244- P.W.Durbin, N. Jeung, E. Jones, F.L. Weitl, and K.N. Raymond,
Radiat, Res., (1984), 99, 106.

-245- F.W. Weitl, K.N. Raymond, and P.W. Durbin.
J. Med. Chem., (1981), 26, 439.

-246- K. Wolfgang, and F. Vogtle. Angew. Chem. Int. Ed. Engl.,
(1984), 23,714

-247- T.J. Mc.Murray, S.J. Rodgers, and K.N. Raymond,
J. Am. Chem. Soc., (1987), 109, 3451.

-248- T.J. Mc.Murray, M.W. Hosseini, T.M. Garrett, E.F. Hahn, Z.E. Reyes,
and K.N. Raymond, J.Am. Chem. Soc., (1987), 109, 7196.

-249- B. Alpha, V.Balzini, J.M. Lehn, S. Perathoner, and S.Sabbatini,
Angew. Chem. Int. Ed. Engl., (1987), 26, 1266.

-250- V. Balzani, L. Maggi, and F. Scandola, in "Supramolecular
Photochemistry", V. Balzani, Ed., Reidel. Dordrecht, (1987): P1

-251- J.P. Knopelski, F. Kotzyba-Hibert, J.M. Lehn, J.P. Desvergne,
F.Fayes, A. Castellan, and H. Bouas-Laurent.
J. Chem. Soc., Chem. Commun., (1987), 433.

-252- C.W. Eigenbrot and K.N. Raymond, Inorg. Chem., (1982), 21, 2867

-253- P.H. Smith and K.N. Raymond, Inorg. Chem., (1985), 24, 3469.

-254- P.H. Smith, Z.E. Reyes, C.W. Lee and K.N. Raymond.
Inorg. Chem., (1988), 27, 4154.

-255- F. H. Kohnke and J.F. Stoddart, Pure Appl. Chem., (1989), 61, 1581

References for Chapter 1

-256- F.H. Kohnke, A.M. Slawin, J.F. Stoddart, and D.J. Williams,
Angew. Chem. Int. Ed. Engl., (1987), 26, 892.

-257- P.R. Ashton, N.S. Isaacs, F.H. Kohnke, A.M. Slawin, C.M. Spence,
J.F. Stoddart and D.J. Williams,
Angew. Chem, Int. Ed. Engl., (1988), 100, 981.

-258- J.F. Stoddart, Nature, (1988), 10, 334.

-259- J.M. Lehn, J. Simon, and J. Wagner.
Angew. Chem. Int. Ed. Engl., (1973), 12, 578.

-260-
(a) F.Vogtle, H. Sieger and W.M. Muller
Topics in Curr. Chem., (1981), 98, 107.
(b) J. Girodeau, J. M. Lehn and J. Sauvage,
Angew. Chem. Int. Ed. Engl., (1974), 14, 406.

-261- K. Freudenberg, F.Z. Cramer and B. Naturtotsch, Anorg.Chem. Org.Chem.
Biochem. Biophys. Biol. (1948), B3, 464.

-262- Z. Szejthi "Cyclodextrins and their Inclusion Complexes"
Akademiai Kiado, Budapest. (1982) p. 296.

-263- K. Harata, H. Udaura, and J. Tanaka.
Bull. Chem. Soc. Jpn. (1978), 51, 1627.

-264- I. Takahash, K. Odashima, and K. Koga,
Tetrahedron Lett., (1984), 7, 973.

-265- T. Takami, Chem. Lett., (1984), 53.

-266- Y. Matsui, Bull. Chem. Soc. Jpn., (1982), 55, 1246.

-267- I. Tabushi and Y. Kuroda, J. Am. Chem., Soc., (1984),106 4580.

-268- F. Franke and F. Vogtle, Topics in Curr. Chem. P135
"Complexation Of Organic Molecules in Water Solution"

-269- W. Saegner, M. Nolterneyer, P.C. Manor, B. Hingerty,and
B.Klar. Bioorg. Chem.,(1976). 5, 187.

-270- N. Kobayashi, J. Chem. Soc., Chem. Commun., (1989), 1126.

-271- H. Yonemura, H. Saito, S. Matsushima, H. Nakamura, and T. Matsyo
Tetrahedron Lett., (1989), 30, 3143,

-272- V.P. Rao and N.J. Turro, Tetrahedron Lett., (1989), 30, 4641.

-273-B.L. Poh, C.S. Lim, and K.S. Khoo,
Tetrahedron Lett, (1989), 30, 1005.

References for Chapter 1

-274-I. Tabushi, Pure Appl. Chem., (1986). 58, 1529.

-275- R.Breslow and L.E. Overman, J.Am. Chem. Soc., (1970), 92, 1076.

-276- I. Tabushi, N. Shimizu, T. Sugimoto, M. Shizuk, and K.Yamamura, J.Am. Chem. Soc., (1977), 99, 7100.

-277- I.Tabushi, N. Shimizu, and K.Yamamura, Jpn. Kokai Tokkyo. Koho, (1979), 79,61, 920.

-278- I. Tabushi, Y. Kuyosika, T. Sugimoto and K. Yamanina, J.Am. Chem. Soc., (1978), 100, 916.

-279- J.E. Baldwin, M.J. Crossley and J. Deberrands, Tetrahedron, (1982), 38, 685.

-280- J.P. Collman. Acc. Chem. Res., (1977), 10, 265.

-281- P.E. Ellis. Jr., J.E. Linard, T. Szymanski, R.D. Jones, J.R. Budge, and F. Basalo. J.Am. Chem. Soc., (1980), 102, 1889.

-282- S. Kamitori, K. Hirotsu, and T. Higushi, J. Chem. Soc., Chem. Commun, (1986), 690.

-283- S. Kamitori, K. Hirotsu, and T. Higushi. J.Am. Chem. Soc., (1987), 109, 2409.

-284- J.F. Stoddart and R. Zarzycki, X111 Macrocyclic Symposium, Hamburg, (1988).

-285- S. Shinkai, Pure Appl. Chem., (1986), 1523.

-286- I.Tabushi, Y. Kobuke, K. Ando, M. Kishimoto, and E. Ohara, J.Am. Chem. Soc., (1980), 102, 5947.

-287- S. Shinkai, H. Koreishi, K. Ueda, T. Arimura, and O. Manabe. J.Am. Chem. Soc., (1987), 109, 6371.

-288- T.Arimura, M. Kubota, K. Araki, S. Shinkai, and T. Matsuda. Tetrahedron. Lett., (1989), 30, 2563.

-289- M. Almi. A. Arduini, A. Casnati, A. Pochini, and R. Ungaro, Tetrahedron, (1989), 45, 2177.

-290- J.D. van Loon, A. Arduini, W. Verboom, R. Ungaro, G.J. van Hummel, S. Harkema, and D.N. Reinhoudt. Tetrahedron Lett., (1989), 30, 2681.

-291- D.N. Reinhoudt, P.J. Dijkstra, P.J.A. in't Veld, K.E. Bugge, S. Harkema, R. Ungaro and E. Ghidini. J.Am. Chem. Soc., (1987), 107, 4761.

References for Chapter 1

-292- V. Bohmer, H. Goldmann, W. Vogt, J. Vicens, and Z. Asfari.
Tetrahedron Lett. (1989) 30, 1391.

-293- J.M. Harrowfield, B.F. Furphy, M.I.Ogden, A.H. White, F.R. Wilner, and B. W. Skelton.
J.Chem. Soc., Dalton Trans., (1989), 2217.

-294- Y. Murakami, Topics in Curr. Chem., (1983), 115, 107.

-295- I.Tabushi and K. Yamanina, ibid (1983), 113, 145.

-296- F. Diederich, Angew. Chem. Int. Ed. Engl., (1988), 27, 362.

-297- K. Odashima, K.Koga, : Cyclophanes, Vol 11 (P.M. Keehn, S.M. Rosenfeld, eds.) Academic Press, New York, (1983) p 629ff.

-298- I.O. Sutherland : as ref 297, p679ff.

-299- Y. Murakami, M.K. Aoyama, and J. Kikuchi,
J. Chem. Soc., Perkin 1, (1981) 2809.

-300- Y. Murakami, M.K. Aoyama, and A. Nakana,
Bull. Chem. Soc. Jpn., (1977), 50, 3365.

-301- Y.Murakami, M.K. Aoyama, and J. Kikuchi, ibid, (1982), 55, 2898.

-302- L.Jimenez and F.Diederich, Tetrahedron Lett., (1989), 30, 2759.

-303- S.B.Ferguson, E.M.Seward, E.M.Sandford, M.Hester, M.Uyeki and F.Diederich, Pure Appl. Chem., (1989), 1523.

-304-
(a) J. Canceill, A.Collet, G.Gottarelli, and P.Palmieri,
J.Am. Chem., Soc., (1987),109, 6454.
(b) A.Renault, D.Talham, J.Canceill, P.Batail, A.Collet, and J.Lajzerowicz
Angew. Chem. Int. Ed. Engl., (1989), 28, 1249.
(c) J.Canceill, M.Cesarie, A.Collet, J. Guilhem, L.Lacombe, B.Lozach and C.Pascard.

-305- W.H.Watson, J.Galloy, D.A. Grossie, F.Vogtle, and W.M. Muller,
J.Org. Chem., (1984), 49, 347

-306-
(a) H.K.Yoo, H.Zhang, J.L. Atwood and G.W.Gokel,
Tetrahedron Lett., (1989), 30, 2489.
(b) M. Shirai and M. Tanaka, J. Chem. Soc., Chem. Commun., (1988) 381.
(c) K. Frensch and F. Vogtle, Liebigs. Ann. Chem., (1979), 858.
(d) N. Wester and F. Vogtle, Chem. Ber., (1980), 113, 1487.
(e) F.M. Menger, Topic Current Chem., (1986), 136, 1.
(f) A.R.van Doorn, A.R. Reichwein, W. Verboom and D.N. Reinhoudt,
X111 Macrocyclic Symposium, Hamburg, (1988).
(g) T.L. Tarnowski and D.J. Crown, J.Chem.Soc., Chem. Commun.,(1976) 661.
(h) F.Vogtle and H. Sieger, Angew Chem. Int. Ed. Engl., (1977), 17, 396.

References for Chapter 1

(i) C.Vincent and S.Penades, X111, Macrocyclic Symposium, Hamburg, (1988)

-307- D.R.Alston, A.M.Z.Slawin, J.F.Stoddart, D.J.Williams, and R.Zarzycki, Angew. Chem. Int. Ed. Engl., (1987), 26, 692.

-308- D.R.Alston, A.M.Z. Slawin, J.F. Stoddart, D.J. Williams, and R.Zarzycki. ibid, (1987), 26, 693.

-309- P.D.Beer and A.S.Rothin, Polyhedron, (1988), 7, 137.

-310- M.Pietraszkiewicz, X111, Macrocyclic Symposium, Hamburg, (1988)

-311- D.A.Buckingham, M.J.Gunter, and L.N. Mander, J.Am. Chem. Soc. (1978), 100, 2899.

-312- J.Almog, J.E. Baldwin, M.J. Crossley, J.F. Debenardis, R.L. Dyer, J.R. Huff and M.K. Peters, Tetrahedron, (1981), 37, 3589.

-313-
(a) T.G.Traylor, Acc. Chem. Res., (1981), 14, 102.
(b) A.R.Battersby and A.D. Hamilton, J.Chem. Soc., Chem. Commun., (1980), 117..
(c) J.Crosby, L.Cullen, J.F. Stoddart, and C. White, X111, Macrocyclic Symposium, Hamburg (1988).
(d) R.D. Hancock, J.S. Weaving and H.M. Marques, J.Chem.Soc.,Chem.Commun., (1989) 1176.
(e) M. Momenteau, Pure Appl.Chem., (1986), 58, 1493.

-314- J.E.Bennet, D.E.Wheeler, L.Czuchayowski, and T.Malinski. J.Chem.Soc.,Chem.Commun., (1989), 723..

-315-
(a) M.Meier, Y.Kobuke and S.Kugimiya. Tetrahedron Lett., (1989), 30, 5301.
(b) S. Chardon-Noblat, J.P. Sauvage, and P Mathis, Agnew. Chem. Int, Ed. Engl., (1989). 28, 592.

-316-
(a) J.P. Collman, A.O.Chong, G.B. Jameson, R.T. Oakley, E.Rose, E.R. Schmitton, and J.A. Ibers. J.Am. Chem. Soc., (1981), 103, 516.
(b) J.P. Collman, P.Denesevich, Y. Konai, M. Marrocco, C.Koval, and F.C.Anson. J.Am.Chem.Soc., (1980), 102, 6027.

-317- O.E.Sielcken, M.M van Tilborg, M.F.M.Roks, R.Hendriks, W.Drenth, and R.J.M. Nolte, J.Am. Chem. Soc., (1987), 109, 4261.

-318- O.Wennerstrom, H.Ericsson, I.Raston, S.Svensson, and W.Pimlott, Tetrahedron Lett., (1989), 30, 112229.

-319- H.L. Anderson, C.A. Hunter, and J.M. Sanders, J.Chem. Soc., Chem. Commun., (1989) 226.

References for Chapter 1

-320- C.O. Dietrich-Buchecker, J.P. Sauvage, and J.P. Kintzinger.
Tetrahedron Lett., (1983), 24, 5095.

-321- C.O. Dietrich-Buchecker and J.P. Sauvage.
J.Am. Chem. Soc., (1984), 106, 3043.

-322- C.O.Dietrich-Buchecker, J.Guilhem, A.K. Khemiss,
J.P. Kintzinger, C.Pascard, and J.P. Sauvage,
Angew. Chem. Int. Ed. Engl., (1987), 26, 661.

-323- D.J.Cram, I.B.Dicker, G.M.Lein, C.B. Knobler, and K.N. Trueblood,
J.Am. Chem. Soc., (1982), 104, 6827.

-324- D.J. Cram. Science, (1983), 219, 1177.

-325- D.J. Cram, H.E. Katz, and I.B. Dicker,
J.Am. Chem. Soc., (1984). 106, 4987.

-326- D.J. Cram, J. Weiss, R.C. Helgeson, C.B. Knobler,
A.E. Dorigo, and K.N. Houk,
J.Chem. Soc., Chem. Commun., (1988), 407.

-327- J.M. Lehn, in "Biomimetric Chemistry", Proc. 2nd. Int.
Kyoto Conf. on New Aspects of Organic Chemistry,
Kodansha, Tokyo (1983).

-328- C.O. Dietrich-Buchecker and J.P. Sauvage.
Angew. Chem. Int. Ed. Engl., (1989), 28, 189.

-329- J.M. Lehn and P. Vierling, Tetrahedron Lett., (1980), 1323.

-330- E.Graf, J.P. Kintzinger, J.M. Lehn, and J. Lemougne.
J.Am. Chem. Soc., (1982), 104, 1672.

-331- E. Graf, J.P. Kintzinger, J.M. Lehn, and L. Memougne,
J.Chem. Soc., Chem. Commun., (1982), 557.

-332- R. Mageswarin, S. Mageswarin, and I.O. Sutherland,
J.Chem. Soc., Chem. Commun., (1979), 722.

-333- N.F. Jones, A. Kumar, and I.O. Sutherland,
J.Chem. Soc. Chem. Commun, (1981). 991.

-334- M.R. Johnson, I.O. Sutherland, and R.F. Newton,
J.Chem. Soc., Chem. Commun., (1979), 309.

-335- A.D. Hamilton, J.M. Lehn, and J.L. Sessler,
J.Chem. Soc. Chem. Commun., (1984), 311.

-336- J. L. Pierre and P. Baret,
Bull. Soc. Chim. France 11., (1983), 367.

-337- B. Dietrich in "Inclusion Compounds", (J.L.Atwood, J.E.D. Davies and D.D. MacNicol, Eds.) Academic Press, London, (1984), 2, p97.

-338- H,.E.Simmons and C.H. Park, J.Am. Chem. Soc. (1968), 90, 2428.

-339- R.W. Alder and R.B. Sessions ibi.d (1979), 100, 3651.

-340- R.W. Alder and R.J. Arrowsmith, A. Carson, R.B. Sessions, E. Heilbronner, B. Kovac, H. Huber, and Taagepera ibid, (1981), 103, 6137.

-341- B.Dietrich, M.W.Hosseini, J.M.Lehn, and R.B.Sessions ibid, (1981), 103, 1282.

-342- M.W.Hosseini and J.M.Lehn, ibid,(1982), 104,3525.

-343- B. Dietrich, J.Guilhem, J.M. Lehn, C.Pascard, and E.Sonveaux, Helv. Chim. Acta., (1984), 67, 91.

-344- B.Dietrich, M.W.Hosseini, J.M.Lehn, and R.B.Sessions. Helv. Chim. Acta., (1985), 68, 289.

-345- B.Dietrich, M.W.Hosseini, J.M.Lehn, and R.B.Sessions. ibid. (1983), 66, 1262.

-346- J.Canceill, A.Collet, J.Gabard, F.Kotzyba-Hibert and J.M.Lehn. ibid. (1982), 65, 1894.

-347- J.M.Lehn and M.W.Hosseini, J.Am. Chem. Soc., (1982), 104, 3525.

-348- E.Graf and J.M.Lehn, J.Am. Chem. Soc., (1976), 98, 6403.

-349- F.R.Schmidtchen, Angew. Chem. Int. Ed. Engl., (1977), 16, 720.

-350- F.R.Schmidtchen, Chem. Ber., (1980), 113, 864.

-351- B.Dietrich, J.M.Lehn, J.Guilhem, and C.Pascard, Tetrahedron Lett., (1989), 30, 4125.

-352- M.W.Hosseini and J.M.Lehn, Helv. Chim. Acta., (1986),69, 587.

-353- J.M.Lehn, E.Sonveaux, and A.K.Willard. J.Am. Chem. Soc., (1978), 100, 4914.

-354- M.W. Hosseini and J.M.Lehn, Helv. Chim. Acta., (1988),71, 749.

-355- D.Heyer and J.M. Lehn,Tetrahedron Lett., (1986), 27, 5869.

-356- T.Fujita and J.M.Lehn, ibid, (1988),29, 1709.

-357- P.D.Beer and A.D.Keefe, X111 Macrocyclic Symposium, Hamburg, (1988).

References for Chapter 1

-358- M.Newcomb, A.M.Madonik, M.J.Blanda, and J.K. Judice
Organometallics, (1984), 3, 9

-360- M.T.Blanda, M. Newcomb, J.H. Horner, and J.Squattrito,
Tetrahedron Lett., (1989), 30, 3501.

-361- J.M.Lehn, Angew. Chem. Int. Ed. Engl., (Nobel Lecture) (1988) 27, 89.

-362- M.W.Hosseini and J.M. Lehn, Helv. Chim. Acta., (1987), 70, 1312.

-363- M.W.Hosseini, J.M.Lehn, L.Maggiora, K.B.Mertes, and M.P.Mertes,
J.Am. Chem. Soc., (1987), 109, 537.

-364- G.M.Blackburn, G.R.J. Thatcher, M.W.Hosseini, and J.M.Lehn,
Tetrahedron Lett., (1987), 28, 2779.

-365- M.W.Hosseini, A.J.Blacker, and J.M.Lehn,
J.Chem. Soc., Chem. Commun., (1988), 596.

-366- M.W.Hosseini and J.M.Lehn,
J.Am. Chem. Soc., (1987), 109, 7047.

-367- A.D.Hamilton and D.van. Engen, ibid, (1987), 109, 5035.

-368- J.Rebek Jr., B.Askew, P.Ballester, C.Buhr, A.Costero,
S.Jones, and K.Williams, J.Am. Chem. Soc., (1987), 109, 6866.

-369- J.Rebek Jr., B.Askew, P.Ballester, C.Buhr, S.Jones,
D.Nemeth, and K.Williams. ibid. 5033.

-370- M.H.Colquhoun, E.P.Goodings, J.M.Maud, J.F.Stoddart,
J.B.Wolstenholme, and D.J.Williams.
J.Chem. Soc., Perkin Trans.2. (1985), 607.

-371- G.J.Moody, R.K.Owusu, and J.D.R. Thomas,
Analyst, (1987), 112, 121.

-372- P.R.Ashton, E.J.T.Chrystal, J.P.Mathias, K.P.Parry,
A.M.Z. Slawin, N.Spencer, J.F.Stoddart, and D.J.Williams.
Tetrahedron Lett., (1987), 28, 6367.

-373- S.B.Ferguson, E.M. Seward, E.M.Sandford, M.Hester,
M.Uyeki, and F.Diederich, X111 Macrocyclic Symposium,
Hamburg, (1988).

REFERENCES FOR CHAPTER 2.

-1- D.Jerchel, Ann., (1958), 180, 613.

-2- O.Mancera, G.Rosenkranz, and F.Sandheimer, J.Chem. Soc., (1953), 2189.

-3- R.J.Highet and W.C.Wildman, J.Am.Chem. Soc., (1955), 77, 4399.

-4- P.Hemmerich and C.Sigwart, Experimenta, (1963), 19, 448.

-5- J.M.Griffing and L.F.Salisburg, J.Am.Chem.Soc., (1948),70, 3416.

-6- T.Stone, Bull. Chem.Soc. Jpn., (1964), 37, 1197.

-7- as ref 10 Chapter 1.

REFERENCES FOR CHAPTER 3.

-1- H.Beinhart, Coord. Chem. Rev., (1980), 55, 33.

-2- J.P.Collman, C.M.Elliot, T.R.Halbert and B.S.Tourage, Proc. Natl. Acad. Sci. USA., (1977), 74,18.

-3- D.E.Fenton and R.L.Lindvedt, J.Am. Chem. Soc., (1978), 100, 6367.

-4- R.Malkin and B.G.Malstrom, Adv. Enzym, (1970), 33, 177.

-5- E.I.Solomon, J.W.Hare, and H.B.Gray. Proc. Natl. Acad. Sci. USA, (1970), 73, 1389.

-6- E.R.Amudsen, J.Whelan, and B.Bosnich, J.Am. Chem. Soc., (1977), 99, 6730.

-7- J.M.Gussand and H.C.Freeman, J.Mol. Biol., (1983), 169, 521.

-8- J.S.Richardson, K.A.Thomas, B.H.Rubin and D.C.Richardson, Proc. Natl. Acad. Sci. USA. (1975), 72, 1349.

-9- W.P.J.Gaykema, W.G.J.Hoi, J.M.Verijken, N.M.Soeter,H.J.Bak, and J.J.Beintenia, Nature. (1984), 23, 309.

-10- N.C.Eickmann, E.I.Solomon, J.A.Larrabee, T.G.Spiro, and K.Lerch, J.Am. Chem. Soc., (1978), 100, 6529.

-11- D.J.Spira-Solomon, M.D.Allendorf, and E.I.Solomon, J.Am.Chem. Soc., (1986), 108, 5318.

-12- J.A.Fee, Struct. Bonding,(1975), 23,1.

-13- R.W.Hay, "Bioinorganic Chemistry", Ellis Harwood, Chichester (1984).

-14- J.Deinum and T.Vanngard, Biochim, Biophys. Acta., (1973), 310, 321.

-15- R.Huber, Agnew. Chem. Int. Ed. Engl., (1989), 28, 84.

-16- A.Messerschmidt, A.Rossi, R.Ladenstein, R.Huber, M.Bolognesi, G.Gatti, A.Marchesini, T.Petruzzelli and A.Finazzi-Agra. J.Mol. Biol., (1989), 206, 513.

-17- L.Holm, M.Sarastre, and M.Wikstrom, EMBO. J.b. (1987) 2819.

-18- "Magneto-Structural Correlations in Exchanged Coupled Systems," R.D.Willet, D.Gatteschi, O.Kahn, (Eds.) Reidel: Dordrecht, The Netherlands, 1985.

-19- D.Gatteschi and A.Bencini, (in Ref. 18, p241.)

-20- M.L.Boillot, O.Kahn, C.J.O'Connor, J.Gouteron, S.Jeanin, and Y.Jeanin. J.Chem. Soc., Chem. Commun., (1985), 178.

References for Chapter 3

-21- T.Mallah, O.Kahn, M.L.Boillot, J.Gouteron, S.Jeannin, and Y.Jeannin. Inorg. Chem., (1986), 25, 3058.

-22- T.Mallah, O.Kahn, J.Gouteron, J.Jeannin, Y.Jeannin, and C.J.O'Connor. Inorg. Chem., (1987), 26, 1357.

-23- O.Kahn, T.Mallah, J.Gouteron, S.Jeannin, and Y.Jeannin. J.Chem. Soc., Dalton Trans., (1989), 1117.

-24- C.J.Cairns and D.H.Busch, Coord. Chem. Rev., (1986), 69. 1.

-25- S.S.Tandon and V.Mc.Kee, J.Chem. Soc., Dalton Trans., (1989), 19.

-26- S.Brooker and V.Mc.Kee, J.Chem. Soc., Chem. Commun., (1989). 619.

-27- S.Brooker, V.Mc.Kee, and W.B.Sheppard, J.Chem. Soc., Dalton Trans., (1987), 2555.

-28-
(a) K.Wieghardt, U.Bossek, and W.Gebert, Agnew.Chem., Int. Ed. Engl. (1983), 22, 328.
(b) R.Bhule, G.J.Gainsford, and D.C.WeatherBurn, J.Am. Chem. Soc., (1988), 110, 7550.

-29- G.C.Dismukes, Photochem. Photobiol., (1986), 43, 99.

-30- J.B.Vincent and G.Christou, Inorg. Chim. Acta., (1987), 136, L41.

-31- W.Micklitz and S.J.Lippard, Inorg. Chem., (1988), 27, 3069.

-32- E.I.Solomon, in "Copper Proteins", T.G.Spiro (Ed)., John Wiley and Sons. Incl., (1981) 41.

-33- D.E.Fenton, Pure and Appl. Chem., (1989), 61, 903.

-34- J.Lorosch, W.Haase, and P.V.Huong, J.Inorg. Biochem., (1986), 27, 53.

-35- W.P.J.Gaykema, A.Volbeda, and W.G.J.Hol, J.Mol. Biol., (1985), 189, 255.

-36- K.D.Karlin, R.W.Cruse, Y.Gultneh, J.C.Hayes, and J.Zubieta. J.Am. Chem., Soc., (1984), 106, 3372.

-37- K.D.Karlin, R.Cruse, Y.Gultneh, A.Farooq, J.C.Hayes, and J.Zybieta, J.Am. Chem. Soc., (1987), 109,2668.

-38- R.W.Cruse, S.Kaderli, K.D.Karlin, and A.D.Zuberbuhler, J.Am.Chem. Soc., (1988), 110, 6882.

-39- H.P.Beremds and D.W.Stephan, Inorg. Chem., (1987), 26, 749.

-40- T.N.Sorrell, D.L.Jameson, and C.J.O'Connor, Inorg. Chem., (1984), 23, 190.

References for Chapter 3

-41- K.Bertoncello, G.D.Fallon, J.H.Hodgkin, and K.S.Murray, Inorg. Chem., (1988), 27, 4750.

-42- A.Benzekri, P.Dubourdeaux, J-M.Latour, J.Laugier, and P.Rey, Inorg. Chem., (1988), 27, 3710.

-43-
(a) H.Adams, N.A.Bailey, D.E.Fenton, R.J.Good, R.Moody,and C.O.Rodriquez de Barbarin, J.Chem. Soc., Dalton Trans., (1987), 207.
(b) D.E.Fenton and R.Moody, J.Chem. Soc., Dalton Trans., (1987), 219.
(c) N.A.Bailey, D.E.Fenton, P.B.Roberts, and A.M.Walford. J.Chem. Soc., Dalton Trans., (1987), 1865.
(d) N.A.Bailey, D.E.Fenton, R.Moody, O.Rodriquez de Barbarrin, I.N. Sciamberella, J.M.Latour, D.Limosin, and V.Mc.Kee, J.Chem.Soc., Dalton Trans.,
(e) D.E. Fenton, S.J.Kitchen, C.M.Spencer, S. Tamburini, and P.A.Vigato, J.Chem.Soc., Dalton Trans., (1988), 685
(f) N.A.Bailey, D.E.Fenton, R.Moody, P.J.Scrimshire, E.Beloritzky, P.H.Fries, and J.M.Latour, J.Chem Soc., Dalton Trans., (1988), 2817.
(g) N.A.Bailey, D.E.Fenton, M.G.Williamson, and D.J.Winter, J.Chem.Soc., Dalton Trans., (1989), 1727.
(h) N.A.Bailey, D.E.Fenton, and D.J.Winter, J.Chem.Soc., Dalton Trans., (1990), 15.

-44- U.Casellato, M.Vidali, and P.A.Vigato, Inorg. Nucl. Chem. Lett., (1974), 10 437

-45- M.Vidali, P.A.Vigato, U.Casellato, E.Tondello, and O.Traverso, J. Inorg., Nucl. Chem., (1975), 37, 1715

-46- D.E.Fenton, P.A.Vigato, U.Casselato, R.Graziani, and M.Vidali, Inorg. Chim Acta., (1981), 51, 159

-47- U.Casellato, S.Sitran, S.Tamburini, P.A.Vigato, and R.Graziani, Inorg. Chim. Acta., (1984), 95 37.

-48- D.E.Fenton, V.Castellato, D,Fregona, S.Sitran, S.Tamburini, and P.A.Vigato, Inorg. Chim. Acta., (1985), 110, 181.

-49- T.Tanube, "Electron Transfer Reactions of Complex Ions in Solution" Acad. Press. New York, (1970).

-50- K.Takamura, M.Sakamoto, and S.Ohashi, Chem. Pharm. Bull., (1980),28, 2318.

-51- N.Oishi, Y.Nishida, K.Kida, and S.Kida, Bull. Chem. Soc. Jpn., (1980), 53, 2318.

References for Chapter 3

-52- K.Wolfgang and F.Vogtle,
Angew. Chem. Int. Ed. Engl., (1984), 23, 714

-53- S.J.Rodgers, C.Y.Ng, and K.N,Raymond,
J.Am. Chem.Soc., (1985), 107, 4094.

-54- Y.Sun, A.E.Martell, and R.J.Motekaitis,
Inorg. Chem., (1986), 25, 4780.

-55- D.D.Cox and L.Que, Jr. J.Am.Chem. Soc., (1988), 110, 8085.

-56- C.J.van Staveren, U.M.L.J.Aarts, P.D.J.Grootenhuis,W.H.J.Droppers, J.van Eerden, S.Harkema, and D.N.Reinhoudt,
J.Am. Chem. Soc.,(1988), 110, 8134.

-57- F.C.J.M. van Veggel, S.Harkema, M.Bos, W.Verboom, C.J.van Staveren, G.J.Gerritsma, and D.N.Reinhoudt,
Inorg. Chem., (1989), 28, 1133.

-58- E.Kimura, Y.Kimura, T.Yatsunami, M.Shionoya, and T.Koike,
J.Am. Chem. Soc., (1987), 109, 6212.

-59- M.Julve, M.Verdaguer, O.Kahn, A.Gleizes, and M.Philoches-Levisalles,
Inorg. Chem., (1984), 23, 3808.

-60- M.F.Charlot, M.Verdaguer, Y.Journeaux, P.de Loth, and J.P. Daudey,
Inorg. Chem., (1984), 23, 3802.

-61- M.Verdauger, O.Kahn, M.Julve, and A.Gleizes,
Nouv. J.Chim., (1985),9, 325.

-62- Y.Journeau, J.Sletter, and O.Kahn,
Inorg. Chem., (1985), 24, 4063.

-63- R.Veit, J.J.Girerd, O.Kahn, F.Robert, Y. Jeannin, and N.Elmurr,
Inorg. Chem., (1984),23, 4448.

-64- F.Tinti, M.Verdaguer, O.Kahn, and J.Savariault,
Inorg. Chem., (1987),26, 2380.

-65- R.E. Coffman and G.R. Buettner, J.Phys. Chem., (1979), 83, 2387.

-66- M.Julve, M.Verdaguer, J.Faus, F.Tinti, J.Moratal, A.Monge, and E.Gutierrez-Puebla. Inorg. Chem., (1987), 26, 3520.

-67- S.M.Nelson, Inorg. Chim. Acta., (1982), 62, 39.

-68- S,M.Nelson, "Copper Coordination Chemistry: Biochemical and Inorganic Perspectives."
Eds. Karlin and Zubieta, Adenine Press Inc., (1983).

-69- C.Akers, S.W.Peterson, and R.P.Willet,
Acta. Cryst. (1968), B24, 1125.

References for Chapter 3

-70- G.A. Melson and D.H. Busch, Proc. Chem. Soc., (1963), 223.

-71- S.M.Nelson and F.S.Esho, J.Chem. Soc., Chem. Commun.,(1981), 388.

-72- L.M. Engelbert, B.M. Furphy, J.Mac. Harrowfield, J.M. Patrick, B.W. Skelton, and A.A. White,
J. Chem. Soc., Dalton Trans., (1989), 595

-73- F.A. Cotton, A. Davidson, W.H. Ilsley, and H.S. Trop,
Inorg. Chem., (1979), 18,2719.

-74- M.G.B. Drew, F.S. Esho, and S.M. Nelson,
Inorg. Chim. Acta., (1983), 76, L269.

-75- L.R. Groenveld, G. Vos, G.C. Verschar, and J. Reedijk,
J.Chem. Soc., Chem. Commun., (1982), 620.

-76- P. Harding, K. Hendrick, L.F. Lindoy, M. Mc.Partlin, and P.A. Tasker, J.Chem. Soc., Chem. Commun., (1983), 1300.

-77- J.L. Burmeister, in "Chemistry and Biochemistry of Thiocyanic Acid and its Derivates"
A.A.Newman, Ed., Academic Press, 1975.

-78- S. Raghunathan, C. Stevenson, C. Harding, D. Mc.Dowell, J. Nelson M.G.B. Drew and P. Yates, J.Chem. Soc., Dalton Trans., (in Press).

-79- J. Nelson, B. Murphy, M.G.B. Drew, P. Yates, and S.M. Nelson,
J.Chem. Soc., Dalton Trans., (1988), 1001
and refs. therin.

-80- B.P. Murphy, J. Nelson, M.G.B. Drew, P. Yates, and S.M. Nelson,
J.Chem. Soc., Dalton Trans., (1987), 123.

-81- K.R. Adam, A.J. Leong, L.F. Lindoy, B.J. Mc.Cool, A. Ekstrom, L.Liepa, P.A. Harding, K. Hendrick, M.Mc.Partlin, and P.A.Tasker.
J.Chem. Soc., Dalton Trans., (1987) 2537.

-82- S.Raghunathan, C.Stevenson, J.Nelson, and V.Mc.Kee.
J.Chem. Soc., Chem. Commun., (1989), 5.

-83- R.A.Bailey, S.L.Kozak, T.W.Michelson, and W.N.Mills.
Coord. Chem. Rev., (1971), 6, 407.

-84- F.A.Cotton, W.R.Robinson, R.A.Walton, and R.Whyman,
Inorg. Chem., (1967), 929.

-85- Y.Agnus, R.Louis, and R.Weiss,
J.Am. Chem. Soc., (1979),101, 3381.

-86- M.G.B.Drew, M.Mc.Cann, and S.M.Nelson,
J.Chem. Soc., Chem. Commun., (1979), 481.

References for Chapter 3

-87- J.Comarmond, P.Plumere, J.M.Lehn, Y.Agnus, R.Louis, R.Weiss. O.Kahn, and E.Morgenstern-Badarau, J.Am. Chem. Soc., (1982), 104, 6330.

-88- J.Z.Pickardt and B.Naturforsch, Anorg. Chem. Org. Chem., (1982), 37, 110.

-89- M.G.B.Drew, J.Nelson, F.Esho, V.Mc.Kee, and S.M.Nelson, J.Chem. Soc., Dalton Trans., (1982), 1837.

-90- P.Chaudhuri, K.Oder, K.Weighardt, B.Nuber, and J.Weiss, Inorg. Chem., (1986), 25, 2818.

-91-
(a) V.Mc.Kee, J.V.Dadigan, R.Ball and C.A.Reed, J.Am. Chem. Soc., (1981), 103, 7000.
(b) V.Mc.Kee, M.Zuagulis, J.V.Dadigian, M.G.Patch and C.A.Reed, J.Am. Chem. Soc., (1984), 106, 4765.

-92- T.N.Sorrell, C.J.O'Connor, O.P.Anderson, and J.H.Reiber, J.Am. Chem. Soc., (1985), 107, 4199.

-93- T.R.Felthouse and D.N.Hendrickson, Inorg. Chem., (1978), 17, 444.

-94- E.I.Solomon, K.W.Penfield, and D.E.Wilcox, Struct. Bonding, (Berlin), (1983), 53, 1-77.

-95- ref. 68 p1-22.

-96- K.D.Karlin, A.Farooq, J.C.Hayes, B.I.Cohen, and J.Zubieta, Inorg. Chem., (1987). 26, 147.

-97- K.D.Karlin, J.C.Hayes, J.P.Hutchinson, and J.Zubita J.Chem. Soc., Chem. Commun., (1983), 376.

-98- K.D.Karlin, and B.I.Cohen, Inorg. Chim. Acta., (1983), 107, L17.

-100- K.D.Karlin, A.Farooq, J.A.Hayes, B.Cohen, J.M.Rowe, E.Sinn and J.Zubita, Inorg. Chem., (1987), 26, 1271.

-101- M.Suzuki, H.Kanatomi, Y.Demura and I.Murase. Bull. Chem. Soc. Jpn., (1984), 57, 1003.

-102- M.G.B.Drew, J.Nelson, F.S.Esho, V.Mc.Kee and S.M.Nelson. J.Chem. Soc., Dalton Trans., (1982), 1837.

-103- V.Mc.Kee, PhD Thesis., Q.U.B. (1978).

-104- I.Bkouche-Waksman,, M.L.Boillot, O.Kahn, and S.S.Korav, Inorg. Chem., (1984), 23, 4445.

-105- O.Kahn, Inorg. Chim. Acta., (1982), 62, 3.

References for Chapter 3

-106- C.B.Barraclough, R.W.Brooks, and R.L.Martin,
Aust. J.Chem., (1974), 27, 1843.

-107- O.Kahn, S.Sikorov, and I.Bkouche-Waksman,
Inorg.Chem., (1984), 23, 490.

-108- O.Kahn, Comment Inorg. Chem., (1984) 3, 105.

-109- M.F.Charlot, O.Kahn, M.Chaillet, and C.Larrieu,
J.Am. Chem. Soc., (1986), 108, 2574.

-110- J.F.Wyatt, I.H.Hillier, V.R.Saunders, J.A.Connor, and M.Barber.
J.Chem. Phys., (1971), 54, 5311.

-111- W.H.Crawford, W.H.Richardson, J.R.Wasson, D.J.Hodgson,
and W.E.Hatfield, Inorg. Chem., (1976), 15, 2107.

-112- J.P. Hay, J.C.Thibeault, and R.Hoffmann,
J.Am. Chem. Soc., (1975), 97, 4884.

-113- O.Kahn and M.F.Charlot, Nouv. J.Chim., (1980), 4, 567.

-114- M.F.Charlot, S.Jeannin, Y.Jeannin, O.Kahn, J.Lucree-Abaul,
and J.Martin-Frere. Inorg. Chem., (1979), 18, 1675.

-115- M.G.B.Drew, J.Nelson, F,S,Esho, V.McKee and S.M.Nelson,
J.Chem. Soc., Dalton Trans., (1982), 1837.

-116- L.K.Thompson, F.W.Hartstock, P.Robichaud, and A.W.Hanson.
Can. J.Chem., (1984),62, 2755.

-117- P.L.Burk, J.A.Osborn, M.T.Youinow, Y.Agnus, R.Louis, and R.Weiss,
J.Am.Chem.Soc.,(1981), 103, 1273.

-118- P.K.Coughlin and S.J.Lippard,
J.Am.Chem.Soc., (1981), 103, 1273.

-119- L.K.Thompson, F.L.Lee, and E.J.Gabe,
Inorg. Chem., (1987), 27, 39.

-120- D.N.Hendrickson and D.M.Duggen, "Exchange Interactions in
Nickel (11), Copper (11) and Cobalt (11) Dimers Bridged
by Small Anions".

-121- R.L.Martin in "New Pathways in Inorganic Chemistry" Chapter 9.

-122- N.L.Allinger and Y.H.Huh, MM2 Program. Q.C.P.E. Program.No.423.
Quantum Chemistry Program Exchange, Indianna University Chemistry
Department, Indianna U.S.A. (1977) m., modified version 1980.

-123- M.G.B.Drew and P.C.Yates,
J.Chem. Soc., Chem. Commun., (1987), 2563.

-124- V.McKee, private communication.

References for Chapter 3

-125- F.Lions, I.G.Dance and J.Lewis,
J.Chem. Soc., A, (1967), 565.

-126- A.Earnshaw, "Introduction to Magnetochemistry"
Academic Press, London, (1968).

-127- C.J.Harding, J.Nelson, C.Stevenson, and M.G.B.Drew to be published.

-128- M.G.B.Drew, F.S.Esho, A.Lavery, and S.M.Nelson,
J.Chem. Soc., Dalton Trans., (1984), 545.

-129- J.E.Wertz and J.R.Bolton, "Electron Spin Resonance",Chap.10.,
Chapman and Hall, London 1986.

-130- T.R.Felthouse, E.J.Laskowski, and D.N.Hendricckson,
Inorg. Chem., (1977), 16, 1077.

-131- T.N.Sorrell, in "Biological and Inorganic Copper Chemistry,"
(Karlin and Zubieta, Eds.,)
Adenine Press Inc., (1986), Vol.II, p41-57.

-132- V.Mc.Kee, PhD. Thesis, Q.U.B. (1978).

-133- P.K.Coughlin and S.J.Lippard,
J.Am. Chem. Soc., (1981), 103, 3228.

-134- M.S.Haddad, S.R.Wilson, D.J.Hodgson and D.N.Hendrickson,
J.Am. Chem. Soc., 1981, 103, 384.

-135- M.G.B.Drew, P.C.Yates, F.S.Esho, J.T.Grimshaw, K.P.Mc.Killop,
S.M.Nelson and J.Nelson,
J.Chem. Soc., Dalton Trans., (1988), 2995
and references therein.

-136- H.Beinhart, Coord. Chem. Rev., (1980), 55, 33.

-137- L.Antolini, G.Marcotrigiano, L.Menabue, and G.C.Pellacanti,
J.Am.Chem. Soc., (1980), 102, 1303.

-138- G.C.Allen and N.S.Hush,
Inorg. Chem., (1967), 6, 4.

-139- T.D.Smith and J.R.Pilbrow, Coord. Chem. Rev., (1974),13, 178.

-140- R.R.Adams and J.B.Raynor, Adv. Inorg. Radiochem., (1970), 13, 135.

-141- A.Longo and T.Buch, Inorg. Chem., (1967), 6, 556.

-142- P.J.M.Birker, J.Hedler, G.Henkel, B.Krebs, and J.Reedijk,
Inorg. Chem., (1982), 21, 2637.

-143- A.W.Addison, H.M.J.Hendricks, J.Reedijk, and L.K.Thompson,
Inorg. Chem., (1981), 20, 103.

References for Chapter 3

-144- B.J.Hathaway and D.E.Billing,
Coord.Chem. Rev., (1970), 5, 231.

-145- M.F.Charlot, Y.Journaux, O.Kahn, A.Bencini, D.Gatteschi, and C.Zanchini, Inorg. Chem., (1986), 25, 1060.

-146- W.M.Davis and S.J.Lippard,
Inorg. Chem., (1985), 24, 3688.

-147- F.A.Cotton and G.Wilkinson, "Advanced Inorganic Chemistry," 4th Edn., New York, Wiley Interscience, (1980), p800.

-148- B.Bleaney and K.B.Bowers, Proc. Roy.Soc., Ser.A.(London), (1952), 214, 451.

REFERENCES FOR CHAPTER 4.

-1- D.L.Pavia, G.M.Lampman, and G.S.Kriz.Jr., "Introduction to Spectroscopy" Saunders Golden Sunburst Series, 1979.

-2- M.Carson, B.M.Foxman, and P.M.Keehn, Tetrahedron, (1979),34, 1641.

-3- G.Binsch and H.Kessler, Agnew. Chem. Int. Ed. Engl. (1980), 19, 411.

-4- I.O.Sutherland, in "Annual Reports on NMR Spectroscopy" (E.F.Mooney, Ed.) Vol.4, pp71. Academic Press, New York (1971).

-5- R.H.Mitchell : Cyclophanes, Vol.11 (P.M.Keehn, S.M.Rosenfeld, Eds) Academic Press, New York (1983).

-6- H.Kessler, Agnew. Chem. Int. Ed. Engl., (1970), 9, 219.

-7- C.S.Johnson, Advances Magnetic Resonance, (1965), 1, 33.

-8- H.S. Gutowsky and C.H.Holm, J.Chem. Phys. (1956).25 1228.

-9- J.A.Pople, W.G. Schneider and H.J. Bernstein, High Resolution Nuclear Magnetic Resonance. McGraw-Hill.New York. (1959).

-10- F.R.Jensen, D.S.Noyce, C.H. Sederholm, and A.J.Berlin, J.Am. Chem. Soc., (1960), 82 1256.

-11- R.U.Lemieux, R.K.Kullnig, H.J.Bernstein, and W.G.Schneider, J.Am. Chem. Soc., (1958), 80, 6098.

-12- L.W. Reeves and K.O.Stromme, Can. J.Chem., (1960), 38, 1241.

-13- L.W. Reeves and K.O.Stromme, Faraday Trans, (1961), 390.

-14- F.A. Bovey, E.W. Anderson. F.P. Hood, and R.L. Kornegay, J.Chem. Phys., (1964), 40, 3099.

-15- L.W. Reeves and K.O. Stromme, J. Chem. Phys., (1961), 34, 1711.

-16- F. Vogtle and P. Neuman, Angew. Chem. Int. Ed. Engl., (1972). 11, 73.

-17- N.L. Allinger, B.J. Gordon, S.E. Hill, and R.A. Ford, J. Org. Chem., (1969) 32, 2272.

-18- C.E. Johnson and F.A. Bovey, J.Chem. Phys., (1958), 29, 1012.

-19- R.A. Pascal, C.G. Winans and D.van Engen, J.Am. Chem. Soc., (1989), 111, 3007.

-20- M. Tashiro and T. Yamoto, Chem. Lett., (1979), 595

References for Chapter 4

-21- W.S. Lindsay, P. Stokes, L.G. Hunter, and V. Boekelheide, J.Am. Chem. Soc., (1961), 83, 943.

-22- D. Krois, E. Langer, and H. Lehner, Tetrahedron, (1980), 36, 1345.

-23- K. Bockmann and F. Vogtle, Chem. Ber., (1981), 114, 1048.

-24- R.H. Mitchell and V. Boekelheide, Tetrahedron Lett., (1970), 1197.

-25- H. Blasche, C.E. Ramey, I. Calder, and V. Boekelheide, J. Am. Chem. Soc., (1970), 92, 3675.

-26- A. W. Hanson and M. Rohrl, Acta. Crystallogr., Sect, B, B28, (1972), 2032.

-27- T. Umento, T. Otsuho, and S. Misumi, Tetrahedron Lett., (1973), 593.

-28- I. Tabushi, H. Yamada and Y. Kuroda, J. Org. Chem., (1975), 40, 1946.

-29- S.P. Adams and H.W. Whitlock Jr., (1981), 46, 3474.

-30- E.T. Jarui and H.W. Whitlock Jr., J.Am. Chem. Soc., (1980), 102, 657.

-31- I. Tabushi and H. Yamada, Tetrahedron, 1977, 33, 1101.

-32- D. Tanner, B. Thulin, and O, Wennerstrom, Acta. Chem. Scand., Sect B. B33 (1979), p443 and p464.

-33-I.D. Reingold, W. Schmidt, and V. Boekelheide, J.Am. Chem. Soc., (1979), 101, 2121.

-34- V. Boekelheide, K. Galusko and K.S. Szeto J.Am, Chem. Soc., (1974), 96, 1579.

-35- T. Olsson, T. Tanner, B. Thulin, and O. Wennerstrom, Tetrahedron, (1981),37, 3485.

-36- R.H. Mitchell and Y.H. Lai, Tetrahedron Lett., (1980), 21, 2633.

-37- F.E. Elhadi, W.D. Ollis, J.F. Stoddart, D.J. Williams and K.A. Woode, ibid 4215.

-38- G.R. Newkome, Y.K. Majestic, and F.R. Fronczek, Tetrahedron Lett., (1981), 32, 3055.

-39- N.A. Bailey, M.M. Eddy, D.E. Fenton, G.Jones, S. Moss, and A. Mukhopadhyay, J.Chem. Soc., Chem. Commun., (1981), 628.

-40- P.G. Owston, R. Peters, E. Ramsammy, P.A. Tasker, and J. Trotter, J. Chem. Soc., Chem. Commun., (1980), 1218.

References for Chapter 4

-41- H. Adams, G. Candeland, J.D. Crane, D.E. Fenton, and A.J. Smith, J. Chem. Soc., Chem. Commun., (1990). 93.

-42- N.W. Alcock, R.G. Kingston, P. Moore, and C. Pierpoint, J.Chem. Soc., Dalton Trans., (1984), 1937.

-43- N.A. Bailey, D.E. Fenton, M.G. Williams, and D.J. Winter, J.Chem. Soc., Dalton Trans., (1989), 1727.

-44- I.Tabushi and K. Yamamura, Top. Curr. Chem., (1983), 113, 145.

-45- T. Sato, S. Akabori, M. Kainosha, and K. Hata, Bull. Chem., Soc. Jpn., (1968), 41 218.

-46- T. Sato, S. Akabori, S. Muto, and K. Hata, Tetrahedron, (1968), 24, 5557.

-47- F.A. Cotton and G. Wilkinson, Advanced Inorganic Chemistry, 5th Edition, Wiley Interscience, (1988).

-48- S.K. Mandal and K. Nag, J.Chem. Soc., Dalton Trans., (1984), 2141.

-49- J.J. Gryzbowski, P.H. Merrill, and F.L. Urbach, Inorg. Chem., (1978), 17, 3078.

-50- R.R. Gagne, R.P. Kerh, and J.A. Dodge, J. Am. Chem. Soc., (1979), 101, 6917.

-51- C.J. O'Connor, P. Firmin, A.K. Pan, B.R. Babu, and E.D. Stevens, Inorg. Chem., (1986), 25, 2300.

-52- E.E. Edouk and C.J. O'Connor, Inorg. Chim. Acta., (1984), 88, 229.

-53- K. Mc.Killop, PhD Thesis, Q.U.B. (1987)..

-54- L. Casella and L. Rigoni, J. Chem. Soc., Chem. Commun., (1985) 1668.

-55- L. Casella and M. Gullotti, J.Am. Chem. Soc., (1981), 103, 6338.

-56- P. Sharma and G.S. Vigee, Inorg. Chim. Acta., (1984), 88, 29.

-57- R. Menif and A.E. Martell, J.Chem. Soc., Chem. Commun., (1989), 1521

-58- T.N. Sorrell, D.L. Tameson, and C.J. O'Connor, Inorg. Chem., (1984), 23, 190.

-59- P.F. Rodesiler and E.L. Amma, Inorg. Chem., (1972), 11, 388.

-60- As Ref 72 Chapter.1.

-61- D.E. Fenton, "Biological and Inorganic Copper Chemistry," (K.D. Karlin and J.Zubieta, Eds.,) Adenine Press, New York, (1985).

References for Chapter 4

-62- S.M. Nelson, F.S. Esho, and M.G,B. Drew,
J.Chem. Soc., Dalton Trans., (1983), 1857.

-63- W.J. Geary, Coord. Chem. Rev., (1971), 7, 81.

-64- D.Mc.Dowell and J. Nelson, Tetrahedron Lett., (1988), 29, 385.

-65- G.R. Newkome, V. Majestic, F.Fronczek, and J.L. Atwood,
J.Am. Chem., Soc., (1979), 101, 1047.

-66- as Ref. 10. in Chapter 1.

-67- W.W. Paudler and D.M. Bezoari, as Ref. 5.

-68- A.B.P. Lever, "Inorganic Electronic Spectroscopy"
Elsevier Publishing Co. Ltd., The Netherlands (1968) p329-331.

-69- A.S. Craig. R. Kataky, D. Parker, H.Adams, N. Bailey, and H. Schneider,
J.Chem. Soc., Chem. Commun., (1989), 1870.

-70- J.M. Lehn and F. Montavon, Helv. Chim. Acta., (1978), 61, 67.